

JAERI - M
84-131

REPORT ON REFLOOD EXPERIMENT
OF GRID SPACER EFFECT

July 1984

Jun SUGIMOTO and Yoshio MURAO

日本原子力研究所
Japan Atomic Energy Research Institute

JAERI-Mレポートは、日本原子力研究所が不定期に公刊している研究報告書です。
入手の問合わせは、日本原子力研究所技術情報部情報資料課（〒319-11茨城県那珂郡東海村）あて、お申しこしてください。なお、このほかに財団法人原子力弘済会資料センター（〒319-11茨城県那珂郡東海村日本原子力研究所内）で複写による実費頒布をおこなっております。

JAERI-M reports are issued irregularly.

Inquiries about availability of the reports should be addressed to Information Section, Division of Technical Information, Japan Atomic Energy Research Institute, Tokai-mura, Naka-gun, Ibaraki-ken 319-11, Japan.

©Japan Atomic Energy Research Institute, 1984

編集兼発行 日本原子力研究所
印刷 いらき印刷株

Report on Reflood Experiment of Grid Spacer Effect

Jun SUGIMOTO and Yoshio MURAO

Department of Nuclear Safety Research
Tokai Research Establishment, JAERI

(Received June 28, 1984)

Experiments were performed in order to clarify the effect of grid spacers on reflood heat transfer in PWR-LOCA. The flow pattern, the thermal responses and the water accumulation near the grid spacer were investigated by shifting the grid spacer at the midplane of the simulated core. Also tested is the effect of the thickness of the grid spacer wall on the reflood behavior.

The heat transfer coefficient before the quenching was about 20 to 50 percent higher just above the grid spacer than just below the grid spacer. The decrease of the droplet diameter due to the grid spacer was observed in the droplet dispersed flow regime. In the slug flow regime, the grid spacer was rewetted early in the reflood transient and the increased water accumulation near the grid spacer was observed. Hence, the heat transfer enhancement due to the grid spacer is mainly attributed to the increased interfacial surface area of droplets in the dispersed flow and also to the increased film boiling heat transfer in the slug flow. The heat transfer enhancement tended to be larger with the larger thickness of the grid spacer.

The simple model was developed for both the dispersed flow and slug flow regimes based on the present experimental results. The thermo-hydraulic behavior near the grid spacer was well calculated with the developed model. The further detailed information, however, is required for the improvement and the verification of the grid spacer model.

Keywords : Reactor Safety, PWR, LOCA, Reflood Heat transfer, Grid Spacer, Two-phase Flow, Droplet Dispersed Flow, Slug Flow, Breakups, Thermohydraulic Behavior

再冠水グリッドスペーサ効果実験報告

日本原子力研究所東海研究所安全工学部

杉本 純・村尾良夫

(1984年6月28日受理)

PWR-LOCA時再冠水熱伝達に及ぼすグリッドスペーサの影響を明らかにするため、 6×6 本模擬燃料体を用いた再冠水実験を行った。模擬炉心中央部のグリッドスペーサを移動させることにより、グリッドスペーサ近傍での流動様式、熱的応答および蓄水の変化を調べた。再冠水挙動に及ぼすグリッドスペーサ板厚の影響も同時に調べた。

クエンチ前の熱伝達率は、グリッドスペーサの直上では直下に比べて約20～50%増加した。液滴分散流領域ではグリッドスペーサ上方での液滴の細分化が観測された。スラグ流領域ではグリッドスペーサの早期リウエットおよびグリッドスペーサ近傍への蓄水の増加が観測された。このためグリッドスペーサによる熱伝達率の増加は、液滴分散流領域での液滴表面積の増加と、スラグ流領域での膜沸騰熱伝達の増加が主な原因と推察された。この熱伝達の増加は、グリッドスペーサ板厚の増加と共に増大する傾向が認められた。

本実験結果に基づいて、液滴分散流およびスラグ流両領域に対する簡単なモデルを開発した。本モデルにより、グリッドスペーサ近傍での熱水力挙動が良く予測されることがわかった。ただし、グリッドスペーサ効果モデルの改良と検証のためには、より詳細な実験的知見が今後必要である。

目 次

1. 序	1
2. 試験装置	2
2.1 テスト部	2
2.2 グリッドスペーサ	3
2.3 計測	3
2.4 データ処理	5
2.5 試験方法	6
2.6 試験条件	6
3. 試験結果	24
3.1 基準試験の結果	24
3.2 グリッドスペーサからの距離の影響	25
3.3 グリッドスペーサ板厚の影響	29
4. 解析と議論	46
4.1 解析モデル	46
4.2 計算結果	50
4.3 議論	50
5. 結論	52
謝 辞	53
記号表	54
参考文献	56
付録 主要データ	58

Contents

1. Introduction	1
2. Test description	2
2.1 Test facility	2
2.2 Grid spacer	3
2.3 Instrumentation	3
2.4 Data processing	5
2.5 Test procedure	6
2.6 Test conditions	6
3. Test results	24
3.1 Description of base case test	24
3.2 Effect of distance from grid spacer	25
3.3 Effect of thickness of grid spacer	29
4. Analysis and discussion	46
4.1 Model description	46
4.2 Calculation	50
4.3 Discussion	50
5. Conclusions	52
Acknowledgments	53
Nomenclature	54
References	56
Appendix Selected data	58

List of tables

Table 2.1	Main specification of small scale reflood test facility
Table 2.2	Main specification of test section
Table 2.3	Comparison of grid spacers
Table 2.4	Summary of measurement and accuracy
Table 2.5	List of measurement
Table 2.6	Density of heater rod material
Table 2.7	Characteristics of heater rod
Table 2.8	Summary of test conditions

List of figures

- Fig. 2.1 Schematic of test apparatus
- Fig. 2.2 Schematic of test section and heater rod
- Fig. 2.3 Details of grid spacer
- Fig. 2.4 Configuration of grid spacers
- Fig. 2.5 Location and elevation of the instrumented rod
- Fig. 2.6 Differential pressure measurement in core
- Fig. 2.7 Noding diagram of heater rod
- Fig. 2.8 Specific heat of heater rod material
- Fig. 2.9 Thermal conductivity of heater rod material
- Fig. 3.1 Clad temperature histories in lower half of core
(Run 8107)
- Fig. 3.2 Clad temperature histories in upper half of core
(Run 8107)
- Fig. 3.3 Sectional differential pressures in lower half of core
(Run 8107)
- Fig. 3.4 Sectional differential pressures in upper half of core
(Run 8107)
- Fig. 3.5 Void fractions in lower half of core (Run 8107)
- Fig. 3.6 Void fractions in lower half of core (Run 8107)
- Fig. 3.7 Grid spacer wall and fluid temperatures (Run 8107)
- Fig. 3.8 Comparison of axial temperature distribution between Case
A and Case B
- Fig. 3.9 Comparison of temperature histories and heat transfer
coefficients at midplane between Case A and Case B
- Fig. 3.10 Comparison of quench envelopes between Case A and Case B
- Fig. 3.11 Effect of distance from quench front on heat transfer
coefficients
- Fig. 3.12 Effect of distance from grid spacer on heat transfer
coefficient in the highest power region
- Fig. 3.13 Comparison of droplet diameter distributions between Case
A and Case B
- Fig. 3.14 Comparison of differential pressures near central grid
spacer between Case A and Case B
- Fig. 3.15 Parameter effect on difference of heat transfer coefficients
between Case A and Case B at midplane

List of figures (cont)

- Fig. 3.16 Comparison of clad temperatures at midplane among Case A, B and C
- Fig. 3.17 Comparison of heat transfer coefficients at midplane as function of distance from quench front among Case A, B and C
- Fig. 3.18 Comparison of clad temperatures at midplane between Case B and Case C
- Fig. 3.19 Comparison of heat transfer coefficients at midplane as function of distance from quench front between Case B and Case D
- Fig. 3.20 Comparison of differential pressure near central grid spacer between Case B and Case D
- Fig. 3.21 Comparison of droplet diameter distributions between Case B and Case D
- Fig. 3.22 Flow model near grid spacer in dispersed and slug flows
- Fig. 3.23 Comparison of calculated and measured heat transfer coefficients at midplane for Case A and Case B
- Fig. 3.24 Comparison of calculated and measured temperature histories at midplane above grid spacer
- Fig. 3.25 Comparison of calculated and measured axial temperature distributions

Photo

- Photo 3.1 Comparison of flow pattern between below and above grid spacers observed at midplane

1. Introduction

In the safety analysis of loss-of-coolant accident (LOCA) of water reactors, one of the most important items is to evaluate the peak clad temperature during the reflood phase. Many experimental⁽¹⁾⁽²⁾ and analytical⁽³⁾⁽⁴⁾ works have been conducted in order to investigate the thermo-hydraulic behavior during LOCA.

The effect of the grid spacers on the reflood heat transfer has recently been pointed out.⁽⁵⁾ The grid spacers, used to maintain a relative rod position in a fuel bundle, are supposed to act as flow disturbers to reduce the peak clad temperature in the reflood phase. The pressure drop and the heat transfer enhancements of the grid spacers in a single phase flow have been studied for the design requirement.⁽⁶⁾ In the reflood two-phase flow condition, however, the effect of the grid spacers on the heat transfer has not been studied in detail.

In FLECHT⁽⁷⁾ and FEBA⁽⁸⁾ experiments, the heat transfer enhancement due to the grid spacers has been observed in the dispersed flow region. Lee et al.⁽⁹⁾ has measured the distribution of the water droplet diameter near the grid spacers in the air-water flow conditions. In these works, the governing heat transfer mechanisms in the typical reflood conditions have not been fully identified.

In the previous preliminary analysis⁽¹⁰⁾, the possible heat transfer enhancement due to the grid spacer was pointed out for the slug flow region by the increased water accumulation near above the grid spacer. However, the flow observation near the grid spacer was not made in the typical reflood conditions.

The objective of the present study is to experimentally clarify the effect of grid spacers on the reflood heat transfer. The flow observation near the grid spacer and the temperature measurement of the grid spacer wall are effectively utilized for that purpose.

Presented in this report are the test description, test results and analytical model developed with the present test. The analytical calculation are then compared with the experiments. Also included is the selected data in Appendix.

2. Test description

2.1 Test facility

The experimental apparatus is designed to investigate the thermo-hydraulic behavior during reflood phase of a PWR-LOCA. Several series of reflood experiments have already been conducted and the results have been issued.⁽¹¹⁾⁽¹²⁾⁽¹³⁾⁽¹⁴⁾⁽¹⁵⁾

The apparatus is called a small scale reflood test facility in comparison with large scale reflood test facilities⁽¹⁶⁾⁽¹⁷⁾ at JAERI. The scaling ratio based on the core flow area is about 1/1,130 of a 1,000 MWe class PWR. The schematic of the test section is shown in Fig. 2.1. The main specification of the facility is summarized in Table 2.1. As shown in Fig. 2.1, the facility consists of a test section, an exhaust line (primary loop) with a pressure regulating system, and a coolant injection system.

(1) Test section

The schematic of the test section and the heater rod are shown in Fig. 2.2. The main specification of the test section is summarized in Table 2.2. The test section consists of a 6 × 6 heater rod bundle, a lower and an upper plenums and a flow channel housing. The axial power distribution is a 7 step cosine profile with a peaking factor of 1.6. The sectional differential pressures and the rod surface temperatures are measured along the test section as shown in Fig. 2.2. The outer diameter and the heated length of the heated rod are 10.7 mm and 3.6 m, respectively. Four rods at the corner of the array are non-heated rods. The heated region of the rods is supported with seven grid spacers. The flow housing is equipped with the viewing windows of 50 mm diameter to observe the flow inside the rod bundle as shown in Fig. 2.2. A water separator in the upper plenum removes the entrained water from the two-phase mixture from the core and drains the separated water into a tank to measure the entrainment rate.

(2) Primary loop

Two-phase mixture from the core exit is separated by the separator in the upper plenum, and the fluid is exhausted to the atmosphere via the simulated primary loop. The primary loop consists of the simulated hot leg, the orifice plate to measure the mass flow rate, Containment 1,

Containment 2 tanks, and the exhaust pipings. The flow area of the hot leg is 23.67 cm^2 . The pressure in the containment tank 2 is kept constant during the test with the pressure regulating system.

(3) Coolant injection system

The coolant injection water is preheated in the 0.691 m^3 storage tank 1. The capacity of the main pump for the coolant injection is $3,600 \text{ m}^3/\text{hr}$ maximum. The coolant is recirculating prior to the test through the storage tank, the lower plenum, the overflow nozzle at the lower plenum, and the storage tank. The constant flow rate is injected into the core by quickly opening the magnetic valve attached to the injection line.

2.2 Grid spacers

The structure of the grid spacer is shown in Fig. 2.3. The grid spacer is an egg crate type made of Hasteloy with dimples to hold the heater rod. The height of the grid spacer is 40 mm.

In order to investigate the effect of the grid spacers, the tests were conducted with four different configurations concerning the central grid spacer, named case A, B, C, and D as shown in Fig. 2.4. This allowed an easy comparison of the flow pattern and heat transfer just below and above the central grid spacer with minimum modification of the existing reflood test section. The comparison of the grid spacers used in four cases is summarized in Table 2.3. The elevations of the upper edge of totally seven grid spacers are 0.36, 0.86, 1.36, 1.86 (or 1.78), 2.36, 2.86, and 3.36 m from the bottom of the core.

The case A has the basic configuration of the grid spacers, which was almost the same as the 15×15 type rod bundles of a reference PWR. In case B, the location of the central grid spacer was shifted 8 cm downward as shown in Fig. 2.4. In case C, the central grid spacer was removed from the rod bundle. The thickness of the grid spacer wall is 0.8 mm in cases A through C, whereas the grid spacers were all exchanged to those with 0.4 mm thickness in case D to investigate the effect of the blocking ratio of the grid spacers.

2.3 Instrumentation

Instrumentation for the present tests include heater rod thermocouples, fluid temperature thermocouples, structure wall thermocouples,

absolute and differential pressure transducers, flow meters and supplied power transducers.

Table 2.4 summarizes the measurement and the accuracy of the instruments. Table 2.5 shows the list of the specific instrument, location, and tag identification symbols. The signals from detectors were recorded on a magnetic tape for data reduction by the central computer.

(1) Heater rod thermocouples

The thermocouple for measuring the clad surface temperature is buried in grooves on the outside surface of the heater rod. Figure 2.5 shows the location of the instrumented rods and the elevation of the thermocouples. The thermocouple is an ungrounded type and the diameter is 0.5 mm. The thermocouples near the top of the heated length are intended to supply the information on the top quenching phenomena.

(2) Superheated steam probe

The location of the superheated steam probes is also shown in Fig. 2.5. The superheated steam probes are all connected to the non-heated rods via guide plates. The superheated steam probe consists of a bare thermocouple of 0.5 mm diameter. The leading lines of the thermocouples are all buried on the surface of the non-heated rods.

(3) Grid spacer wall temperature

Two thermocouples are attached in the wall of the central grid spacer in case B and C as already shown in Fig. 2.3. The tip of the thermocouple is buried inside the wall of the grid spacer to avoid the influence of the water droplet flow. The leading lines of the thermocouples are buried on the surface of the non-heated rods. The grid spacer wall temperature can be utilized to evaluate the radiation heat transfer from the heater rod to the grid spacer. The timing of the rewetting of the grid spacer is compared with the initiation of the heat transfer augmentation near the grid spacer.

(4) Differential pressures and pressures

Figure 2.6 shows the schematic of the core differential pressure measurement in the core. The differential pressure transducer is a strain-gauge type and the maximum range is 0.5 kg/cm² or 0.1 kg/cm². The pressure is measured at upper and lower plenums and in the containment tank with the same strain-gauge type pressure transducers. The maximum

range of the transducer is 10 kg/cm².

(5) Motion picture

Motion pictures were taken by the 16 mm camera through the housing view windows to identify the flow patterns near the grid spacers for some selected runs. The time interval of the strobe light varies from ~1 μsec to ~10 μs, and the frequency of the motion pictures was 16 frames per second coincident with the strobe light.

2.4 Data processing

(1) Calibration method

Temperatures were measured with Chromel-Alumel thermocouples calibrated with the standard thermoelectro-motive force table. The linearity of the output is so good that the simplified linear transformation was utilized for the temperature conversion.

The pressure and differential pressure transducers were first calibrated with the in-situ test either by pressurizing the system or by filling the test vessel with water. The sectional core differential pressures were carefully checked each day before the test by filling the water in the test section.

The magnetic flow meters were calibrated by reading the water filling rate with the water level indicator at the test sections. The flooding rate was measured each time before the test by reading the water filling rate in the test section.

(2) Heat flux calculation method

The heat flux from the heated rod can be evaluated using the measured clad temperature and the supplied power to the heated rod by considering the heat balance in the rod. The heat conduction in the rod is numerically calculated with REFLQH code, which is based on the finite element heat conduction code HETRAP⁽¹⁸⁾.

The noding diagram of the heated rod is shown in Fig. 2.7. The code calculates the temperature distribution in the rod using the clad temperature measurement, which is located about 0.25 mm from the outer clad surface. The heat transfer coefficient h is defined as,

$$h = q / (T_w - T_{sat}),$$

where q is the heat flux, T_w the surface temperature, and T_{sat} the

saturation temperature.

The physical properties of the rod materials are based on either the reported values or the measured value by the rod manufacturer. The density of the rod materials is summarized in Table 2.7, the specific heat and the thermal conductivity are shown in Fig. 2.8 and Fig. 2.9, respectively. The comparison of the physical property between the fuel rod of a typical PWR and the heater rod used in the present experiment is shown in Table 2.7.

2.5 Test procedure

The test procedure is as follows:

- (1) The coolant circulates through the lower plenum to the overflow line before the test. The flow rate and the coolant temperature are adjusted to the specified values during this period. The housing of the test section is heated up to nearly the saturation temperature.
- (2) The electric power is supplied to the heated rods and the data recording to the magnetic tape is initiated. The recording of the visual flow data is also initiated.
- (3) The coolant injection into the test section is initiated by closing the overflow valve when a clad temperature reaches a pre-set value. This time is defined as 0 s in the reflood transient or the start of the test. The supplied power is kept constant during the test.
- (4) As the coolant advances up in the rod bundle, the two-phase flow develops along the test section. The pressure in the containment tank is maintained constant by exhausting the generated vapor using the pressure regulator.
- (5) When all the clad temperatures show cooled conditions, the power supply and the data recording are turned off, terminating the test.

2.6 Test conditions

The test conditions of the present grid spacer effect tests are listed in Table 2.8. The base case test was selected as the principal reference data. The parametric effect tests were run with basically one parameter varied from the base case test. The test parameters are considered to cover the typical reflood conditions of a PWR-LOCA.

The range of the parameters is listed below. The underlined values indicate the base case test conditions.

System pressure	: P_{sys} (MPa)	<u>0.1</u> , 0.2, 0.4
Linear peak power	: P_p (kW/m)	<u>1.6</u> , 1.8, 2.0
Flooding rate	: U_{in} (m/s)	0.03, <u>0.04</u> , 0.06
Initial peak clad temperature	: T_{win} (°C)	400, <u>550</u> , 650
Inlet subcooling	: ΔT_{sub} (°C)	<u>20</u> , 40, 60

Table 2.1 Specification of small scale reflood test facility

<u>Loop</u>	
Maximum operating pressure	0.5 MPa
Maximum operating temperature	423K(Water) 623K(Steam)
Water storage tank	0.691 m ³
Volume of containment tank	1.0 m ³
Power of preheater for water in storage tank	30 kW
Cooling capacity for water in storage tank	5 kW
Volume of upper plenum	0.49 m ³
Main piping	1 inch pipe
Material of loop	Stainless steel type 304
 <u>Test section</u>	
Maximum operating pressure	0.5 MPa
Maximum operating temperature	1473K (Heater rod)
Power/Voltage of power supplied to heater rods	300kW/400V

Note: Other specification of test section are shown in Table 2.2.

Table 2.2 Main specification of test section

<u>Rod bundle</u>	
Arrangement of heater rods	6 × 6 (square pitch)
Pitch	14.3 mm
Number of heated rod	32
Number of non-heated rod	4
Power supply	3 phase star connection (30 rods) and single phase (2 rod)
Material of grid spacer	Hasteloy
Material of flow housing	Stainless steel type 304
Core flow area	$4.68 \times 10^{-3} \text{ m}^2$
<u>Heater rod</u>	
Type	Indirect heating
Effective heated length	3.6 m
Outer diameter of heated rod	10.7 mm
Maximum heating power per rod	7.2 kW
Maximum linear power	3.2 kW/m
Power distribution	7 step chopped cosine
Cladd thickness	1.0 mm
Cladding material	Inconel 600
Isolating material	Magnesium oxide
Outer diameter of heating element	6.4 mm
Material of heating element	Nichrome

Table 2.3 Comparison of grid spacers

Case	Thickness (mm)	Blocking ratio (%)	Elevation of upper edge of central grid spacer (m)
A	0.8	19.4	1.86
B	0.8	19.4	1.86
C	0.8	19.4	—
D	0.4	9.8	1.78

Table 2.4 Summary of measurement

Clad surface temperature	0.5 mm dia. Ungrounded, sheathed type chromel-alumel thermocouple 0.75 class (JIS CI602-1974)
Core differential pressure	Strain-gauge type differential pressure transducer, full scale 0.5 kg/cm ² or 0.1 kg/cm ²
Pressure	Strain-gauge type pressure transducer, 5 kg/cm ² G full scale
Power supplied to heater rods	Hall-element type power transducers one unit for 3 phases power and one unit for single phase power
Flow rate	Turbine flow meter 0 to 1200 l/h ±1.0 % Error
Differential pressure across orifice for measuring steam generated in core (installed in exhaust line)	Strain-gauge type differential pressure transducer 1 kg/cm ² full scale, Linearity 0.5 % FS Hysteresis 0.5 % FS

Table 2.5 List of measurement

Ch. No.	Symbol	Item	Location
1	TE1L	Clad surface temperature	E-rod 3.35 m
2	TE4U		E-rod 2.1 m
3	TE4M		E-rod 1.8 m
4	TE4L		E-rod 1.5 m
5	TE7		E-rod 0.25 m
6	TS1L		S-rod 3.35 m
7	TS4U		S-rod 2.1 m
8	TS4M		S-rod 1.8 m
9	TS4L		S-rod 1.5 m
10	TS7		S-rod 0.25 m
11	TF2		F-rod 2.875 m
12	TF3		F-rod 2.425 m
13	TF4M		F-rod 1.8 m
14	S2A	Super heated steam temperature	2.875 m
15	S2B		2.875 m
16	S3A		2.425 m
17	S3B		2.425 m
18	S4UA		2.1 m
19	S4UB		2.1 m
20	S4MA		1.8 m
21	S4MB		1.8 m
22	S4LA		1.5 m
23	S4LB		1.5 m
24	TGSA	Grid spacer wall temperature	1.765 m (Case B,D)
25	TGSB		
26	DPT6A	Differential pressure	1.5 - 1.8 m
27	—		
28	DPT8A		2.1 - 2.4 m
29	DPTSA		-0.35 - 3.6 m
30	DPPMA		Pump orifice
31	VST	Water injection signal	Overflow line valve pressure regulation valve Water supply tank outlet
32	VPR	Valve action signal	
33	FM	Flow rate	
34	—		
35	VLMP	Movie action signal	16 mm movie camera
36	TA2	Clad surface temperature	A-rod 2.875 m
37	TA3		A-rod 2.425 m
38	TA4M		A-rod 1.8 m
39	TA5		A-rod 1.175 m
40	TA6		A-rod 0.725 m
41	TQ2		Q-rod 2.875 m
42	TQ3		Q-rod 2.425 m
43	TQ4M		Q-rod 1.8 m
44	TQ5		Q-rod 1.175 m
45	TQ6		Q-rod 0.725 m
46	TB2		B-rod 2.875 m
47	TB3		B-rod 2.425 m
48	TB4M		B-rod 1.8 m
49	TB5		B-rod 1.175 m
50	TB6		B-rod 0.725 m

Table 2.5 List of measurement (cont.)

Ch. No.	Symbol	Item	Location
51	TR2	Clad surface temperature	R-rod 2.875 m
52	TR3		R-rod 2.425 m
53	TR4M		R-rod 1.8 m
54	TR5		R-rod 1.175 m
55	TR6		R-rod 0.725 m
56	TD4U		D-rod 2.1 m
57	—		
58	TD4M		D-rod 1.8 m
59	—		
60	TD4L		D-rod 1.5 m
61	TK1U	Clad surface temperature	K-rod 3.55 m
62	TK1M		K-rod 3.45 m
63	TY1U		Y-rod 3.55 m
64	TY1M		Y-rod 3.45 m
65	TT5		T-rod 1.175 m
66	TC1L		C-rod 3.35 m
67	TC4U		C-rod 2.1 m
68	TC4M		C-rod 1.8 m
69	TC4L		C-rod 1.5 m
70	TC7		C-rod 0.25 m
71	TI2		I-rod 2.875 m
72	TI3		I-rod 2.425 m
73	TI4M		I-rod 1.8 m
74	TI5		I-rod 1.175 m
75	TI6		I-rod 0.725 m
76	TV2		V-rod 2.875 m
77	TV3		V-rod 2.425 m
78	TH11	Flow fousing wall temperature	3.85 m
79	TH16		3.65 m
80	TH17		3.55 m
81	TH1		3.6 m
82	TH2		2.7 m
83	TH4U		2.1 m
84	TH4M		1.8 m
85	TH4L		1.5 m
86	TH6	0.9 m	
87	TL1	Fluid temperature	3.45 m
88	TL2		2.7 m
89	TL3		2.1 m
90	—		
91	TL5	Fluid temperature	1.5 m
92	TL6		0.9 m
93	TUG		Upper plenum
94	TUL		Upper plenum
95	TPMW	Structure wall temperature	Pump orifice
96	TDHW		Hold-up tank
97	TSGW		Primary loop pipe
98	TSGG	Fluid temperature	Primary loop pipe
99	TPIG		Containment tank
100	TIN		Core inlet

Table 2.5 List of measurement (cont.)

Ch. No.	Symbol	Item	Location
101	DPT2	Differential pressure in core	-0.35 - 0.6 m
102	DPT4		0.6 - 1.2 m
103	DPT5		1.2 - 1.5 m
104	DPT6B		1.5 - 1.8 m
105	DPT7		1.8 - 2.1 m
106	DPT8B		2.1 - 2.4 m
107	DP10		2.4 - 3.0 m
108	DP12		3.0 - 3.6 m
109	DPTA		3.6 - 3.73 m
110	DPTB		3.73 - 3.845 m
111	DPTC		3.845 - 5.175 m
112	DPTSB		-0.35 - 3.6 m
113	DPUL		-0.35 - 5.175 m
114	DPR4		1.2 m (horizontal)
115	DPR8		2.4 m (horizontal)
116	DP12		3.6 m (horizontal)
117	PUP	Pressure	Upper plenum
118	PLP		Lower plenum
119	PPT		Containment tank
120	DPHT	Differential pressure	Hold-up tank
121	DPPMB		Pump orifice
122	DPL		Primary loop
123	DPDN		Downcomer
124	DPDO		Downcomer overflow tank
125	V1	Supplied voltage	3-phase power
126	V2		single-phase power
127	W11	Supplied power	3-phase power (1)
128	W12		3-phase power (2)
129	W13		3-phase power (3)
130	W2		single-phase power

Table 2.6 Density of heater rod material

Material	Density (kg/m ³)
Inconel 600	6100
Magnesium oxide	3040
Nichrome-V	8400

Table 2.7 Characteristics of heater rod

Rod type	Clad diameter (mm)	Clad thickness (mm)	Volume per unit length ($\times 10^{-5}$ m ³ /m)	Heat capacity per unit volume ($\times 10^3$ kJ/m ³ K)	Thermal conductivity (W/m·K)	Total heat capacity per unit length ($\times 10^{-3}$ kJ/m K)
Heater rod	10.7	1.0	Inconel	3.54	20.9	3.36
			MgO	3.65	1.4	
			Nichrome	4.79	20.1	
Fuel rod (15×15 type)	10.72	0.62 (gap) (0.12)	Zircaloy 4	2.26	19.6	2.53
			UO ₂	3.11	4.0	

(Note) Referred temperature: ~873 K

Table 2.8 Summary of test conditions

Grid spacer Configuration	Run No.	Pressure (MPa)	Linear peak power (kW/m)	Flooding rate (cm/s)	Initial peak clod temperature (°C)	Injected water temperature (°C)	Flow housing temperature (°C)	Reflow initiation time (s)
Case A	8007	0.2	2.0	3.9	400	100	120	23.0
	8008	0.2	1.6	3.9	400	100	120	41.0
	8009	0.2	2.0	3.9	550	100	120	51.0
	8011	0.1	1.6	4.0	550	80	100	26.5
	8012	0.1	1.8	4.1	550	80	100	40.0
	8017	0.1	1.6	3.8	550	80	100	55.0
Case B	8109	0.1	1.8	3.8	550	80	100	32.0
	8113	0.1	1.8	3.8	550	80	100	35.0
	8116	0.2	1.6	3.8	550	100	120	50.0
	8117	0.2	2.0	3.8	400	100	120	54.0
	8118	0.2	2.0	3.8	550	104	120	41.0
	8120	0.2	1.8	5.8	550	100	120	64.0
	8121	0.2	1.8	3.9	400	100	120	38.0
	8122	0.2	1.8	3.9	550	100	120	25.0
	8123	0.2	1.8	3.9	650	100	120	53.0
	8124	0.2	1.8	3.0	550	100	120	41.0
	8126	0.2	1.8	3.9	550	60	120	22.5
	8127	0.2	1.8	3.9	550	80	120	31.0
	8131	0.4	1.8	3.9	550	120	140	34.0
	Case C	8202	0.2	1.8	3.9	400	100	120
8203		0.2	1.8	3.9	550	100	120	27.0
8205		0.2	1.8	5.8	550	100	120	56.5
8207		0.2	1.8	3.9	550	60	120	35.0
8210		0.2	1.6	3.9	550	100	120	42.0

Table 2.8 Summary of test conditions (cont.)

Grid spacer configuration	Run No.	Pressure (MPa)	Linear peak power (kW/m)	Flooding rate (cm/s)	Initial peak clad temperature (°C)	Injected water temperature (°C)	Flow housing temperature (°C)	Reflood initiation time (s)
Case D	8308	0.1	1.6	4.0	550	80	100	47.0
	8309	0.1	1.8	4.0	550	80	100	38.5
	8311	0.2	1.8	4.0	550	80	120	40.5
	8312	0.2	1.6	4.0	550	100	120	38.0
	8313	0.2	1.8	3.9	550	100	120	35.0
	8314	0.2	2.0	3.9	550	100	120	33.5
	8316	0.2	1.8	4.1	550	100	120	33.0
	8317	0.2	1.8	6.0	550	100	120	40.0
	8318	0.2	1.8	3.1	550	100	120	37.5

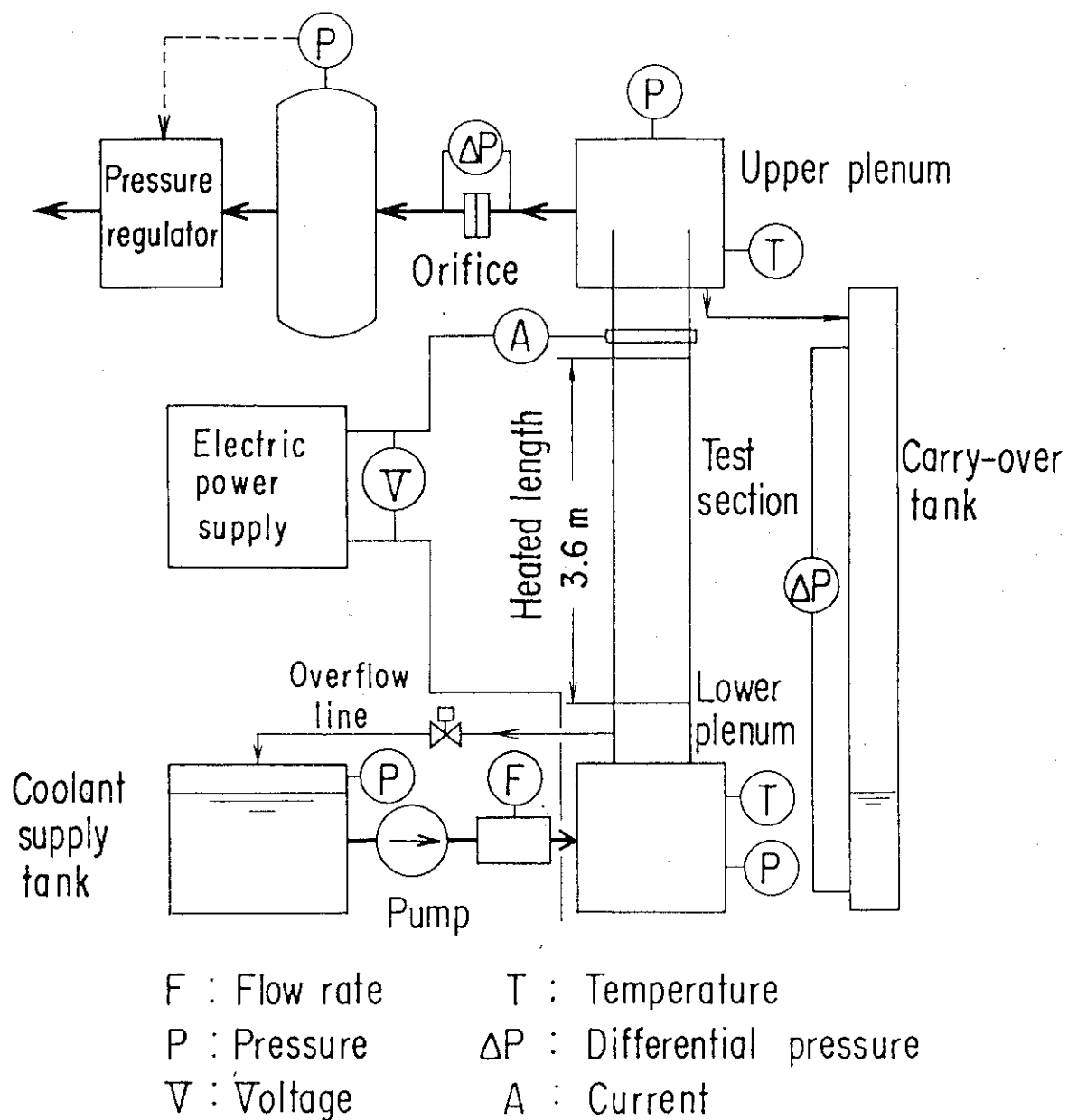


Fig. 2.1 Schematic of test apparatus

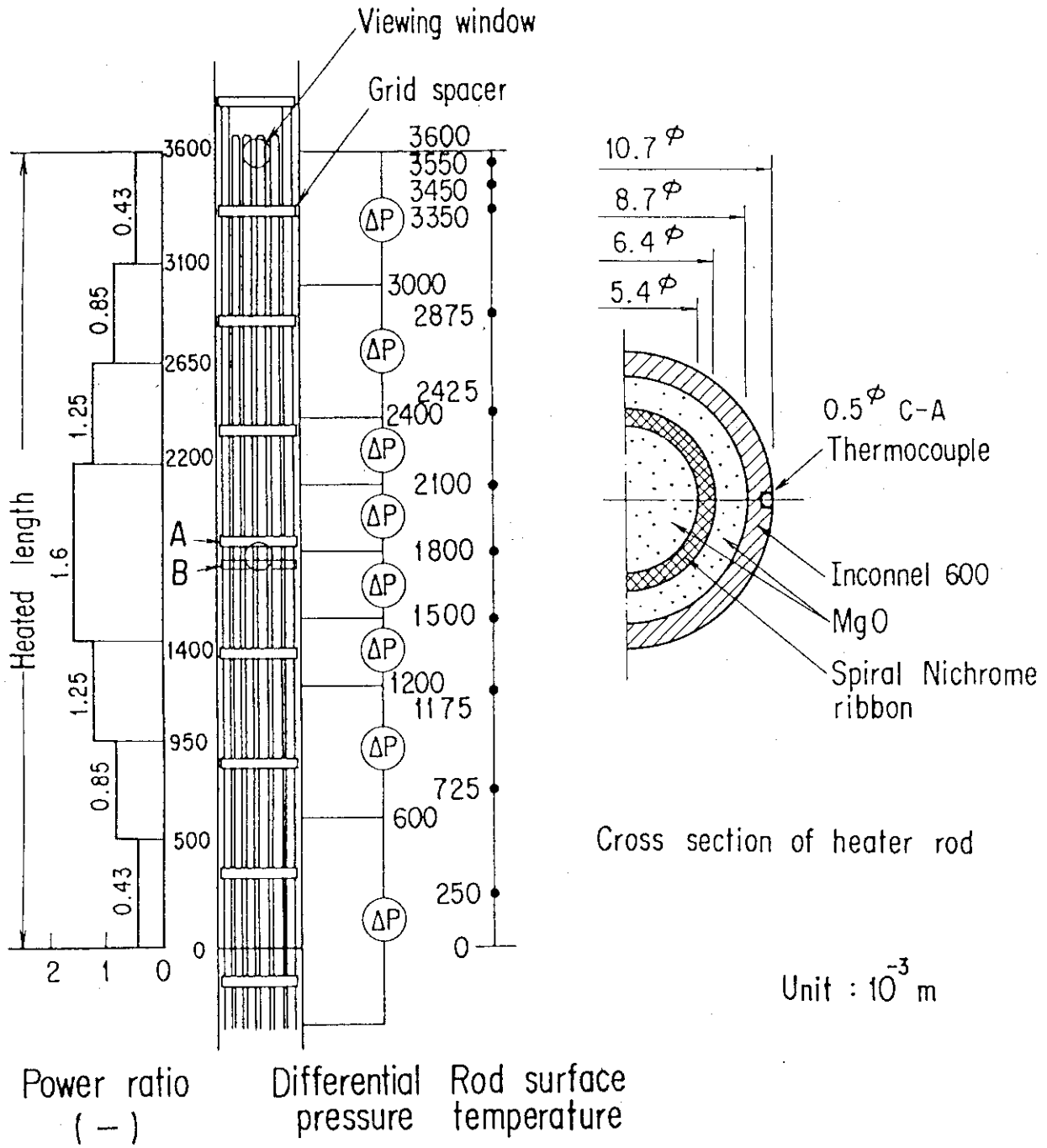
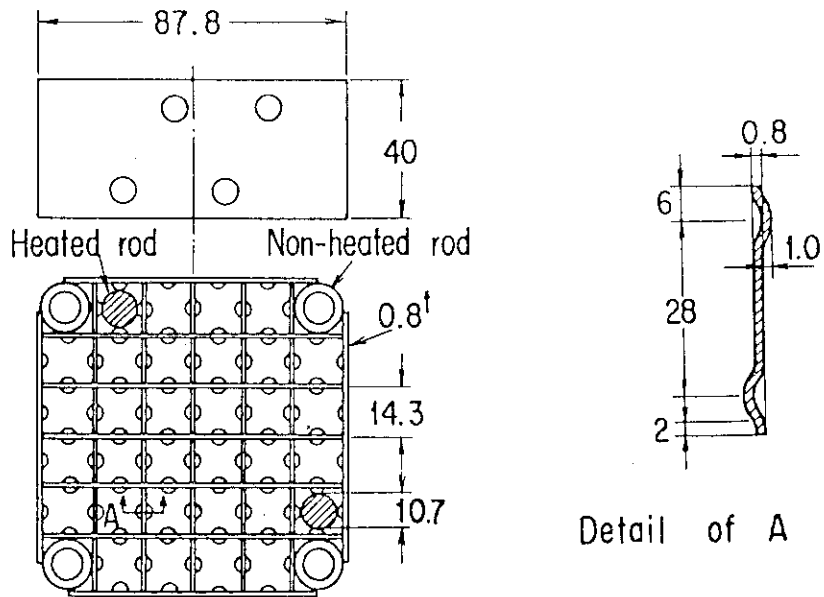


Fig. 2.2 Schematic of test section and heater rod



Grid spacer

Fig. 2.3 Details of grid spacer

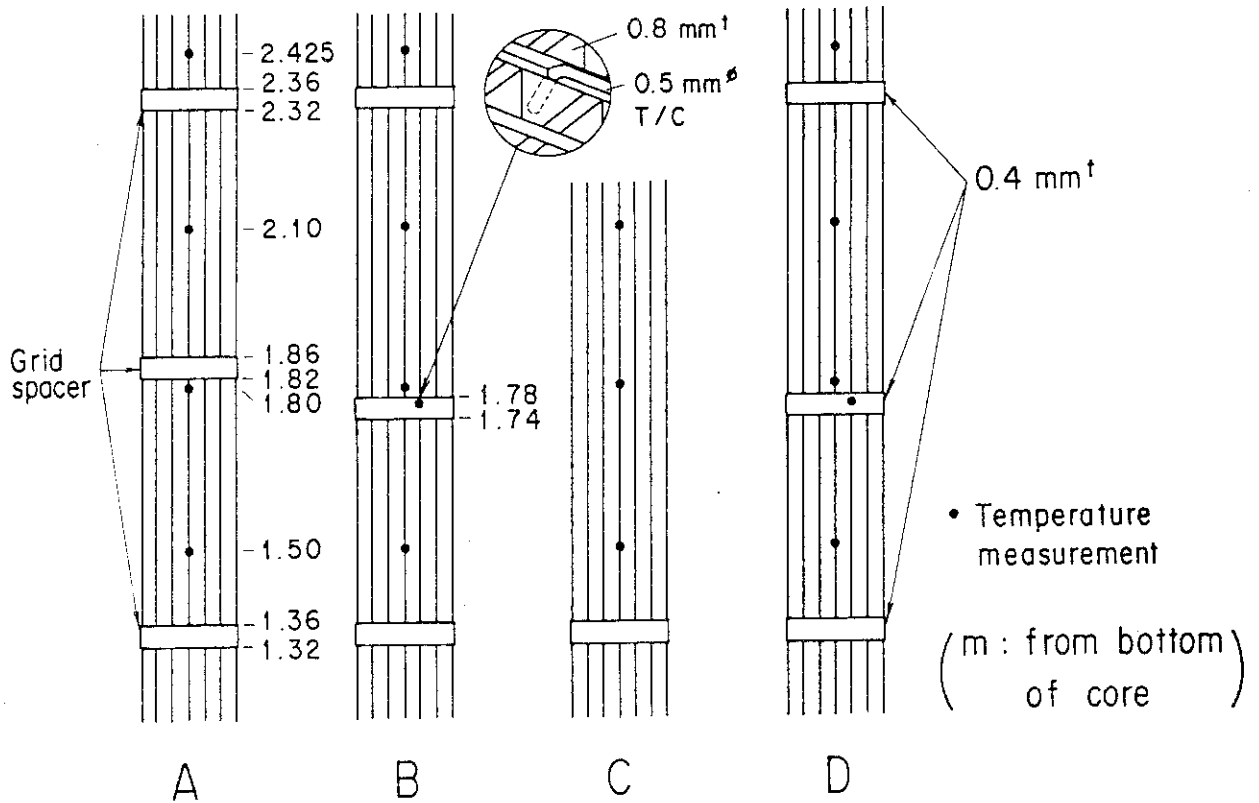


Fig. 2.4 Configuration of grid spacers

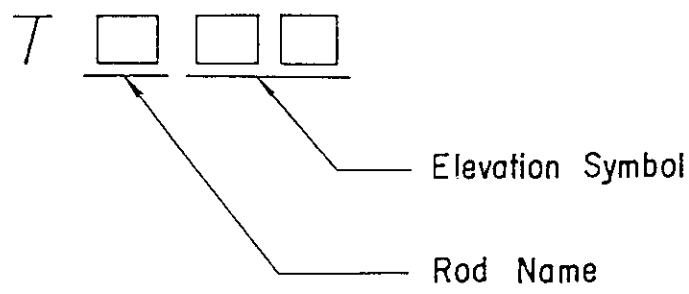
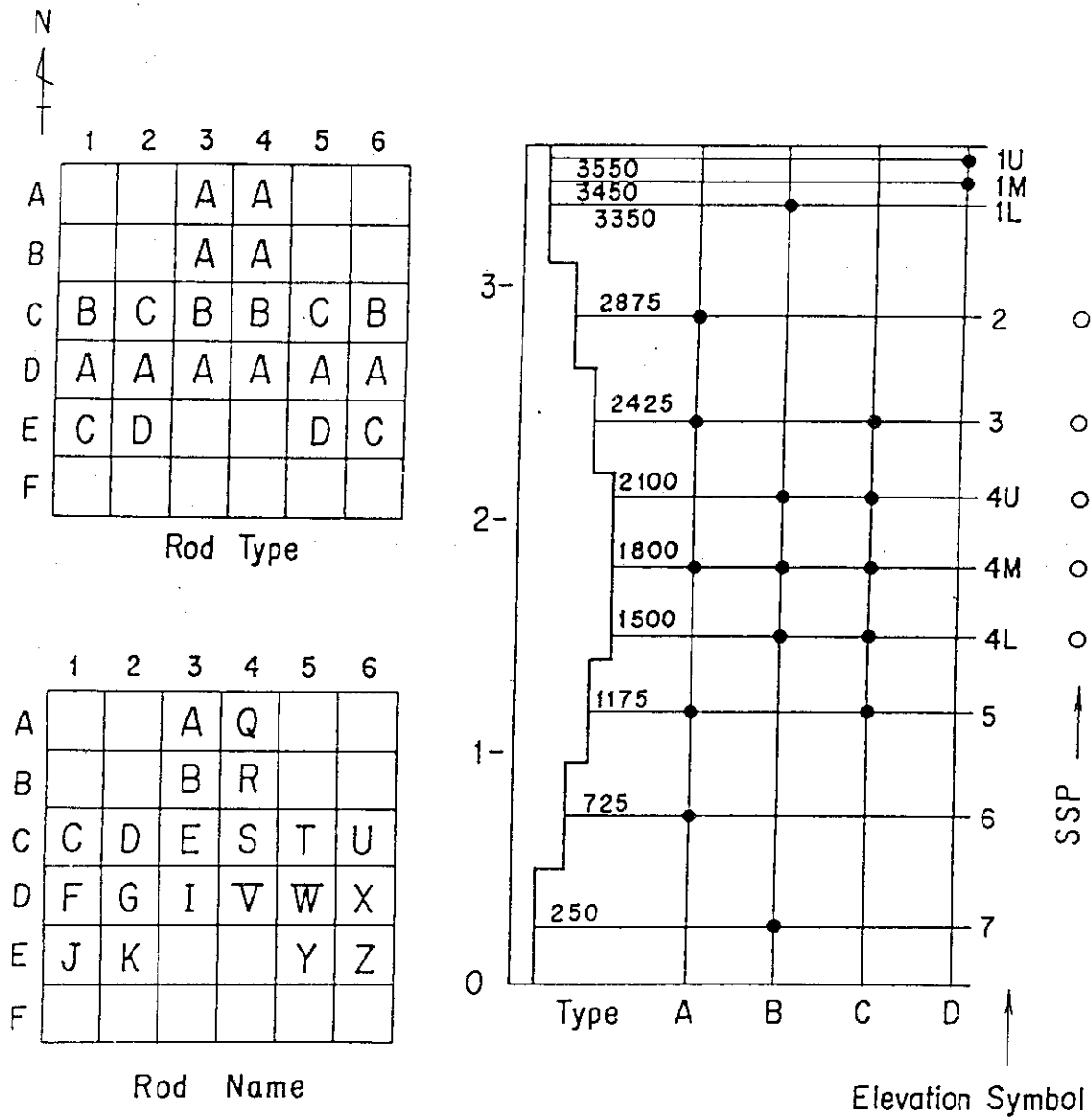


Fig. 2.5 Location and elevation of the instrumented rod

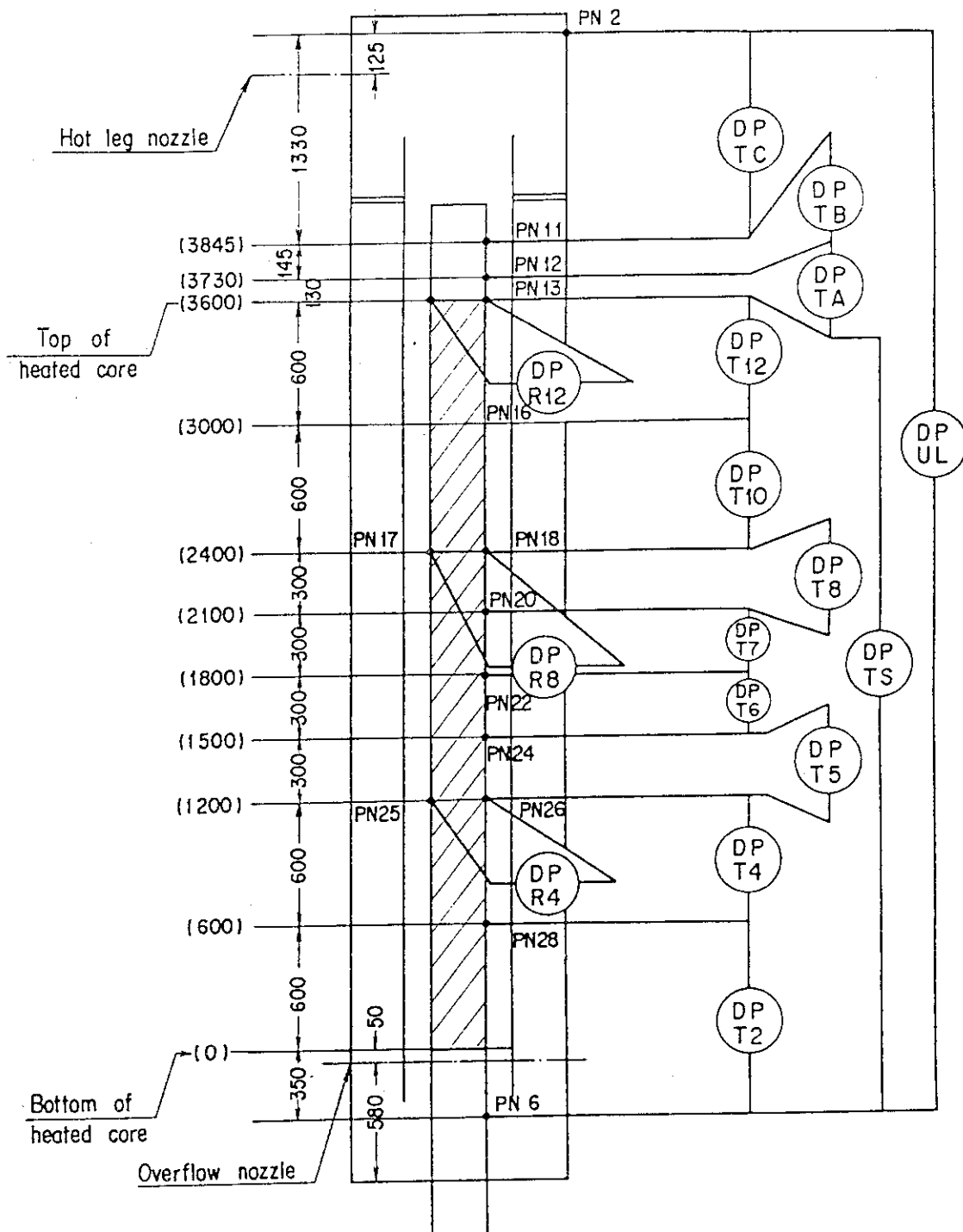


Fig. 2.6 Differential pressure measurement in core

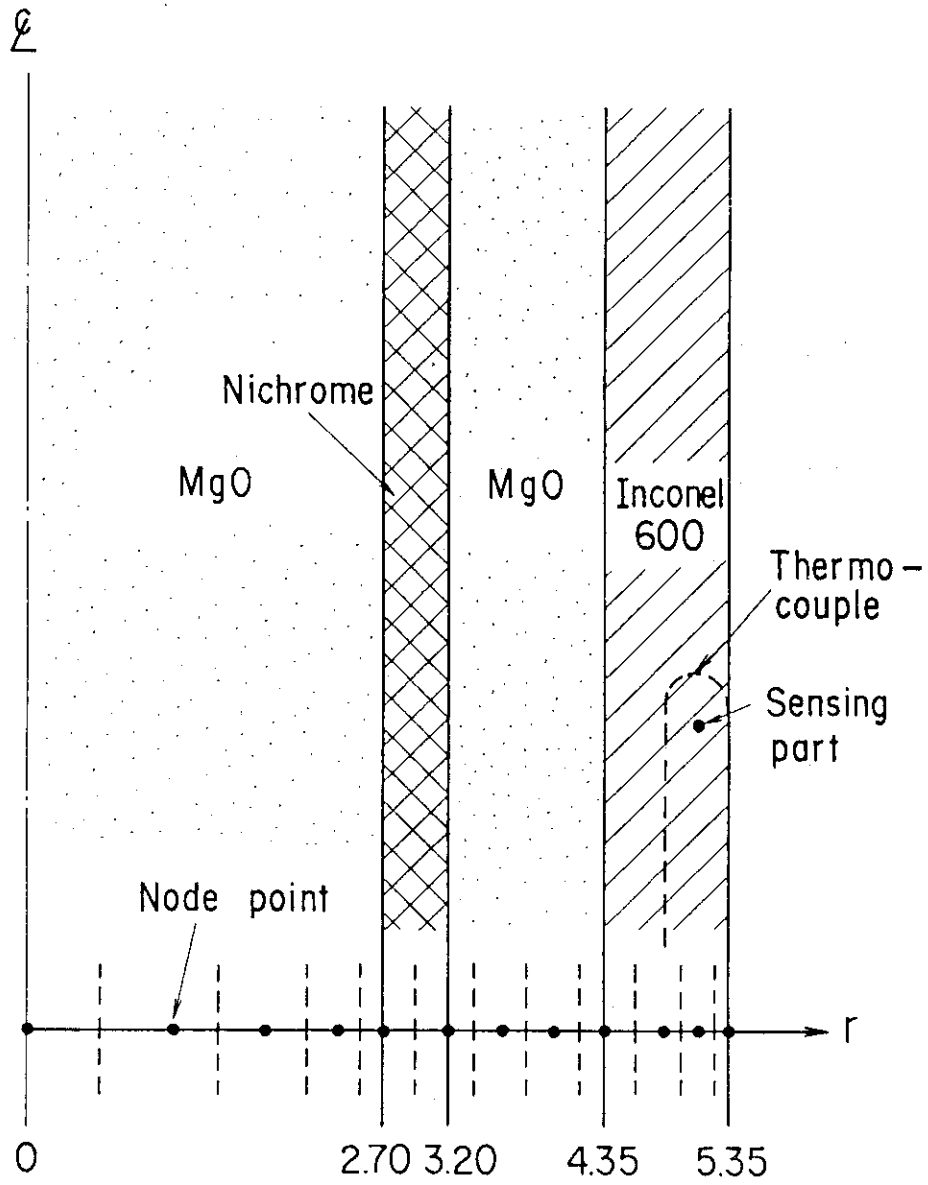


Fig. 2.7 Noding diagram of heater rod

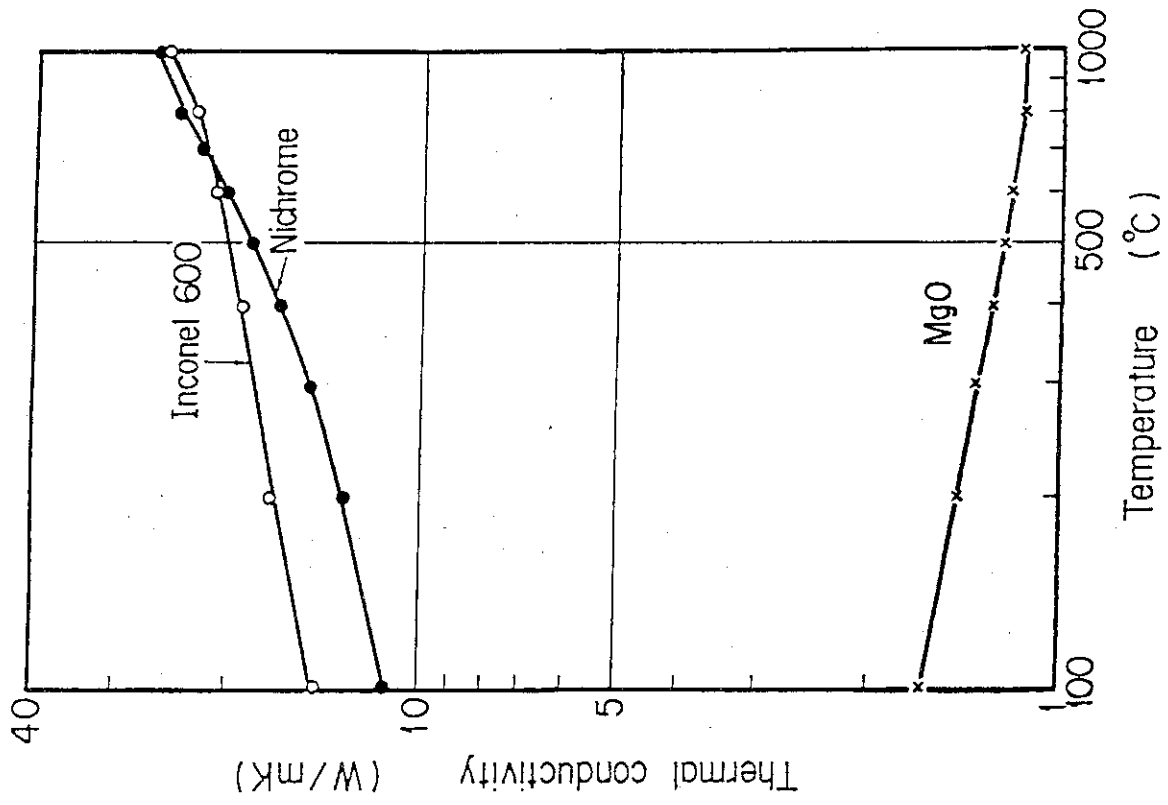


Fig. 2.9 Thermal conductivity of heater rod material

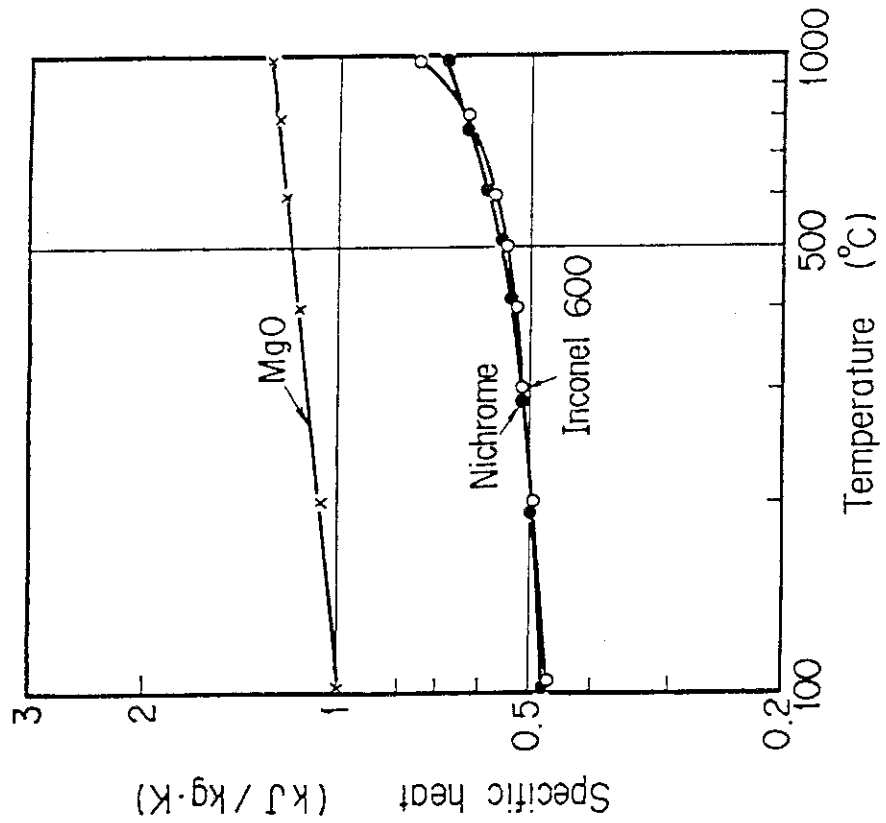


Fig. 2.8 Specific heat of heater rod material

3. Test result

3.1 Description of base case test

(1) Clad temperature of heated rod

Figure 3.1 through 3.2 show an example of the temperature histories of the cladding of the heated rod obtained in Run 8107. The reflood initiation i.e., the water injection time into the core is 26.5 s after the test.

The clad temperature increases after the reflood initiation to a turnaround point, and it then gradually decreases to a quench point where it rapidly drops to nearly a saturation temperature.

The cooling of the heated rod above 1.5 m elevation in the core was initiated simultaneously at about 26 s after the reflood initiation as shown in Fig. 3.2. This indicates that the two-phase flow was fully developed along the core at about 26 s after the reflood initiation.

The maximum clad temperature was realized at 2.1 m from the bottom of the core. The quench front gradually moved from the bottom to 2.875 m elevation of the core. At the 3.35 m elevation, however, the quench occurred early at about 27 s after the reflood initiation. This is caused by the top down quenching, since the temperature was relatively low at the top part of the core due to the low heat generation rate.

(2) Core differential pressure

The sectional core differential pressures are shown in Figs. 3.3 through 3.4. The sectional differential pressures increase simultaneously right after the reflood initiation. This indicates that the water accumulation was initiated along the whole core after the reflood initiation.

The lowest differential pressure reached early a saturated value, which almost corresponds to the static head of a single-phase water. The differential pressures at upper part of the core gradually increased until the supposed quench front reached the upper location of the differential pressure measurement section as indicated in the figures.

(3) Void fraction

Figures 3.5 through 3.6 show void fractions in the core. The void fractions are converted from the core sectional differential pressure shown in Figs. 3.3 through 3.4 by neglecting the frictional and

accelerational pressure losses. This assumption is reportedly valid for the typical reflood conditions⁽¹⁹⁾.

The void fraction tends to decrease as the propagation of the quench front, which corresponds to the increase of the sectional differential pressure described above. The void fraction in the upper part of the core is in the range from 0.8 to 0.9 above the quench front.

(4) Grid spacer and fluid temperatures

The grid spacer wall and the fluid temperatures are shown in Fig. 3.7. The tip elevation of the thermocouple in the grid spacer wall is estimated to be 1.765 m from the bottom of the core. The clad surface temperature at 1.8 m elevation is also shown in the figure for the comparison.

As shown in the figure, the grid spacer wall is soon quenched at about 30 s after the reflood initiation, when the heated rod begins to be cooled. The fluid temperatures from 0.8 and 2.1 m also show an early quenching. It is therefore considered that two phase flow in the upper part of the core contains water slug or large droplets soon after the reflood initiation. The low heat capacity of the grid spacer wall could also contribute to the early quenching of the grid spacer.

3.2 Effect of distance from grid spacer

(1) Thermal responses

Figure 3.8 shows the comparison of the axial temperature distribution of the heated rod between Case A and Case B under the base case test conditions. The temperature at the midplane (1.8 m above the bottom of the heated length) just above the grid spacer in Case B is lower than just below the grid spacer in Case A for both 50 and 100 s after the reflood initiation. The temperatures at other locations, however, are nearly the same between two cases. This shows that the heat transfer is locally enhanced by the grid spacers in the downstream region of the grid spacer.

The temperature histories of the heated rod and the grid spacer wall at the midplane are shown in Fig. 3.9. The rod surface temperature in Case A is about 170 K higher than Case B before the quench time. According to the quench envelope shown in Fig. 3.10, the quench time is nearly the same between two cases even though the location of the central grid spacer is different. This shows that the quench front movement is

not much affected by the location of the grid spacer. The heat transfer coefficient are also compared between the two cases in Fig. 3.9. The heat transfer coefficient before the quench time is about 20 to 50 percent higher just above the grid spacer (Case B) than just below the grid spacer (Case A) as shown in the figure.

According to the flow observation at the midplane of the core, three flow patterns were identified as indicated in Fig. 3.9. They are single phase vapor, a droplet dispersed flow and a slug flow. The wall temperature of the grid spacer at the midplane, measured in Case B, indicates an early rewetting in the slug flow region as already shown in Fig. 3.7. The heat transfer enhancement is significant in the slug flow region compared with the dispersed flow region as shown in Fig. 3.9.

Figure 3.11 compares the heat transfer coefficients at the midplane between Case A and Case B as a function of the distance from the quench front. The distance from the quench front is linearly interpolated using the quench envelope shown in Fig. 3.10. The heat transfer coefficient is again much higher just above the grid spacer than just below the grid spacer. However, this heat transfer enhancement is not dominant in the regions very close or very far from the quench front. This implies that the heat transfer enhancement due to the grid spacer may not be effective in the vicinity of the quench front or in the dilute dispersed flow region.

Figure 3.12 shows the heat transfer coefficient in the slug flow region as a function of the distance from the upper edge of the grid spacer. The data were obtained at the highest power level (shown in Fig. 2.2) in both case A and B experiments. The heat transfer coefficient is higher with the shorter distance from the grid spacer and also from the quench front. As shown in Fig. 3.12, the characteristic length representing the heat transfer enhancement due to the grid spacer in the slug flow is in the order of 0.15 m.

(2) Flow observations

An example of the observed flow at the midplane is shown in Photo 3.1. The number in the circle of Photo 3.1 corresponds to the number indicated in Fig. 3.9. Before about 10 s of the reflood transient, the flow is identified as a single phase vapor. The water droplets begin to appear in the vapor flow at about 10 s of the transient as shown in

Photo 3.1. This droplet dispersed flow continues up to about 30 s. The water droplets become larger, and the united droplets can sometimes be observed in the later part of the dispersed flow region. The flow then becomes a slug flow with the large oscillating water slug as shown in ④ in Photo 3.1 through the end of the transient.

Figure 3.13 shows the distribution of the water droplet diameter in the dispersed flow region. The droplet diameter was calibrated with the rod diameter of 10.7 mm. The distribution just below the grid spacer is shown by a solid line, while the distribution just above the grid spacer is shown by a broken line. The droplet diameter tends to be smaller just above the grid spacer (Case B) than below the grid spacer (Case A). It is considered that this decrease of the droplet diameter is primarily due to the breakup of the impinging droplets by the edge of the grid spacer.

The distribution of the droplet diameter can well be described with a Γ -distribution function shown in a smoothed line in Fig. 3.13. The Γ -distribution is written as

$$\frac{\Delta N}{N} = \frac{\tau^\tau}{\Gamma(\tau)} \left(\frac{d}{\bar{d}} \right)^{\tau-1} \exp\left(-\tau \frac{d}{\bar{d}}\right) \frac{\Delta d}{\bar{d}}, \quad (1)$$

where

$$\tau = \frac{\bar{d}^2}{\sigma_n^2}$$

ΔN : number of droplets with diameter from $\bar{d} - \frac{\Delta d}{2}$ to $\bar{d} + \frac{\Delta d}{2}$,

N : total number of droplets, $\Gamma(\tau)$: gamma function,

\bar{d} : average droplet diameter, and σ_n : standard deviation.

(3) Water accumulation

Figure 3.14 shows the comparison of the differential pressure between 1.5 and 1.8 m elevations. The differential pressure in Case B includes the grid spacer in the measurement section, whereas it does not include in Case A. The differential pressure is higher in Case B than in Case A before the quench time of 1.8 m elevation, but the differential pressures are nearly identical with each other after the quench front passed the 1.8 m elevation.

This indicates that the water accumulation is larger just above the grid spacer than below the grid spacer, since the frictional pressure loss is not significant compared with the pressure loss of the static head in a typical reflood condition.⁽¹⁹⁾ Also the flow observation revealed the larger amount of water slug just above the grid spacer than below the grid spacer in the slug flow as suggested by Photo 3.1. This larger water accumulation can be attributed to the water stagnation above the grid spacer and to the counter-current flow limitation (CCFL) due to the reduced flow area of the grid spacer.

(4) Parametric effect

Figure 3.15 shows the parametric effect on the heat transfer enhancement due to the grid spacers. The difference of the heat transfer coefficients between Case A and Case B at the midplane (1.8 m), $\Delta h = h_B - h_A$, is plotted against the distance from the quench front. The parameter tested were the system pressure, the peak power, the flooding rate and the initial clad temperature at the midplane. The location of the quench front was estimated by the linear interpolation of the measured quench times along the rod bundles.

The larger heat transfer enhancement due to the grid spacer is obtained with the higher flooding rate. The heat transfer enhancement occurs earlier, i.e., at the longer distance from the quench front with the lower pressure, the higher flooding rate and the higher initial clad temperature. The effect of the peak power on the heat transfer enhancement is not clear in the present experiment.

It is considered that the heat transfer enhancement is strongly affected by the vapor flow rate and the entrained liquid flow rate. With the lower pressure, since the vapor density is lower, the vapor flow is higher causing the larger amount of entrained liquid flow. The sooner vaporization and liquid entrainment can also be attributed to the higher flooding rate and the higher initial clad temperature, because the inlet coolant contacts earlier with the hot surface of the heater rod. These parametric effects, therefore, can be analytically treated by providing the reasonable grid spacer model.

(5) Experiments with no central grid spacer

In case C experiment, the central grid spacer was removed from the rod bundle as already shown in Fig. 2.4. This is to investigate the

effect of the existence of the grid spacer itself on the reflood behavior by comparing the test results with Case A or Case B,

Figure 3.16 shows the clad temperatures of the heated rod at the midplane of Case A, B and C experiments. The clad temperature just below the grid spacer (Case A) is higher than other two cases. The clad temperature with no central grid spacer (Case C) is similar to Case A, but it is lower than Case A near the quench point. The clad temperature just above the grid spacer (Case B) is the lowest among three, due to the heat enhancement effect of the grid spacer.

The heat transfer coefficients of the three cases are shown in Fig. 3.17(a) as a function of the distance from the quench front. The heat transfer coefficient with no central grid spacer (Case C) is close to Case A when the distance from the quench front is greater than 0.5 m. This shows that the heat transfer is not much affected by the grid spacer in the region far from the quench front.

The heat transfer coefficient of Case C almost agrees with that of Case B when the distance from the quench front is less than 0.2 m as shown in Figs. 3.17(a) and (b). This may indicate the CCFL (Counter current flow limitation) effect due to the grid spacer in the region near above the quench front, causing less water suspension just below the grid spacer. This will then result in the higher heat transfer coefficient of Case C than Case A, but similar to Case B, when the void fraction is relatively low.

It should be noted, however, that the local flow blockage might have occurred near the midplane due to the bending of the heated rods since there was no central grid spacer in Case C. This is because the partial bending of the heated rods was observed through the viewing window at the midplane. The local flow blockage could result in the heat transfer enhancement near the quench front in the similar manner as the grid spacer. It is therefore considered that the test with no central grid spacer may not be suitable to experimentally clarify the direct effect of grid spacers due to the probable flow blockage.

3.3 Effect of thickness of grid spacer

In Case D experiment, the grid spacer of 0.4 mm thick was used in order to investigate the effect of the thickness of grid spacers on reflood behavior. The thickness of grid spacer was 0.8 mm in Cases A, B

and C experiments. The flow blocking ratio was almost one half in Case D as already shown in Table 2.3.

(1) Thermal responses

The clad temperatures at the midplane (just above grid spacer) are shown in Fig. 3.18. The quench time of Case D with thin grid spacer is a little sooner than Case B with thick grid spacer. However, overall temperature responses are quite similar between the two cases. This shows that the effect of the thickness of the grid spacers is not significant on the reflood behavior in the thickness range tested in the present experiments.

The heat transfer coefficients are shown in Fig. 3.19 as a function of the distance from the quench front. The heat transfer coefficients of Case D with 0.4 mm thick spacer near the quench front (less than 0.5 m) are slightly higher than Case B with 0.8 mm thick spacer. This is not understood well, however, it is considered that the residual rod bending during Case C experiment might have still caused the heat transfer enhancement in the following Case D experiment.

The heat transfer coefficients of Case D tends to be smaller than Case B in the region far from the quench front as shown in Fig. 3.19. This shows that the heat transfer in the slug flow with relatively high void fraction or in the droplet dispersed flow could be more enhanced by the thicker grid spacer.

(2) Water accumulation

Figure 3.20 shows the comparison of the differential pressure between 1.5 and 1.8 m elevations. The differential pressures are similar with each other as shown in Fig. 3.20. This implies that the water accumulation behavior near the grid spacer is not much affected by the thickness of the grid spacer. It is noted, however, the accuracy of the differential pressure measurement could not be enough to identify the difference between the two differential pressures. The axially fine measurement of the pressure distribution is therefore required for the modeling of the water accumulation near the grid spacers with various thickness.

(3) Droplet diameter in dispersed flow

Figure 3.21 shows the comparison of water droplet diameter distribution between Case B and Case D. The distribution of the water droplet diameter in Case D is again similar to Case B, showing small

effect of the thickness of the grid spacer wall. However, the average droplet diameter in Case D tends to be larger than Case B as shown in Fig. 3.21. It is considered that this is due to the smaller probability of the droplet breakup, since the thickness of the spacer wall is smaller in Case D than Case B.

RUN8107

○--TC4M (11) △--TC4L (11) +--TR5 (11)
 X--TR6 (11) ◇--TC7 (11)

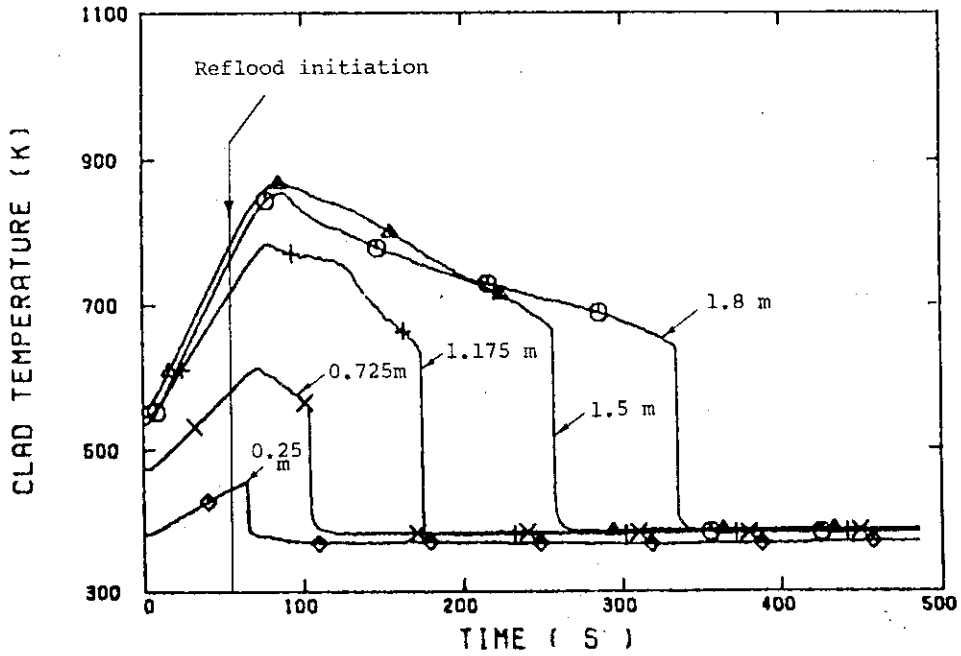


Fig. 3.1 Clad temperature histories in lower half of core (Run 8107)

RUN8107

○--TC1L (11) △--TA2 (11) +--TA3 (11)
 X--TC4U (11)

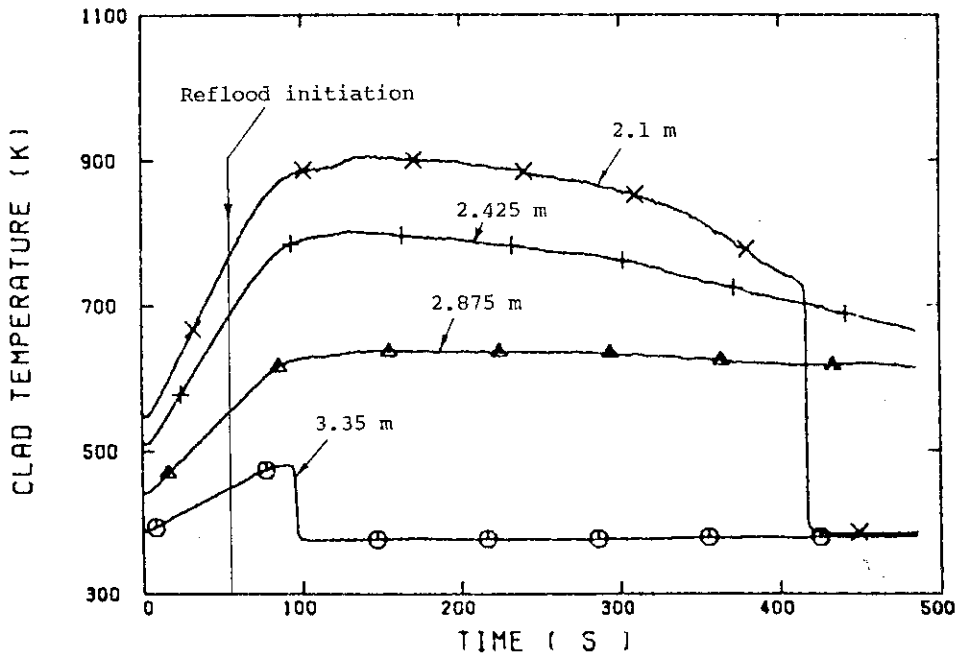


Fig. 3.2 Clad temperature histories in upper half of core (Run 8107)

RUN8107

○--DPT2 (11) △--DPT4 (11) +--DPT5 (11)
 X--DPT6B (11)

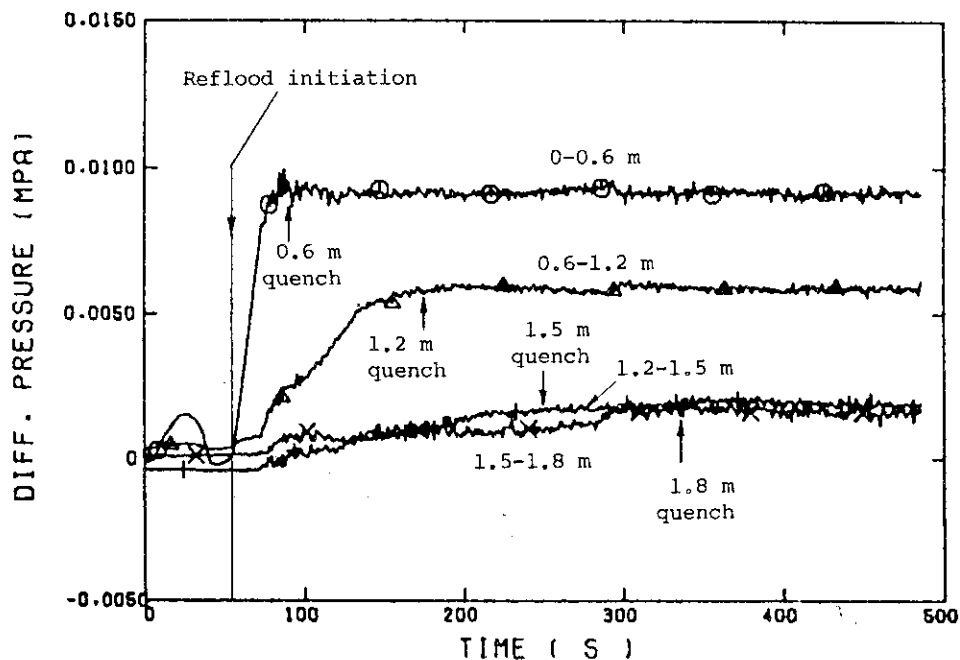


Fig. 3.3 Sectional differential pressures in lower half of core (Run 8107)

RUN8107

○--DPT7 (11) △--DPT8B (11) +--DP10 (11)
 X--DP12 (11)

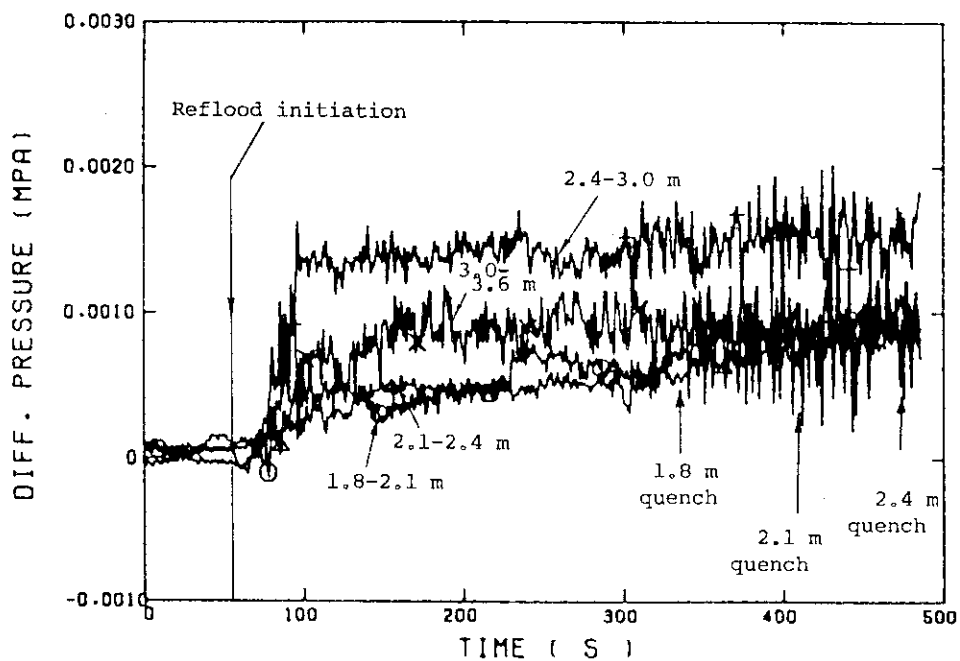


Fig. 3.4 Sectional differential pressures in upper half of core (Run 8107)

RUN8107

○--DPT2 (11) △--DPT4 (11) +--DPT5 (11)
 X--DPT6B (11)

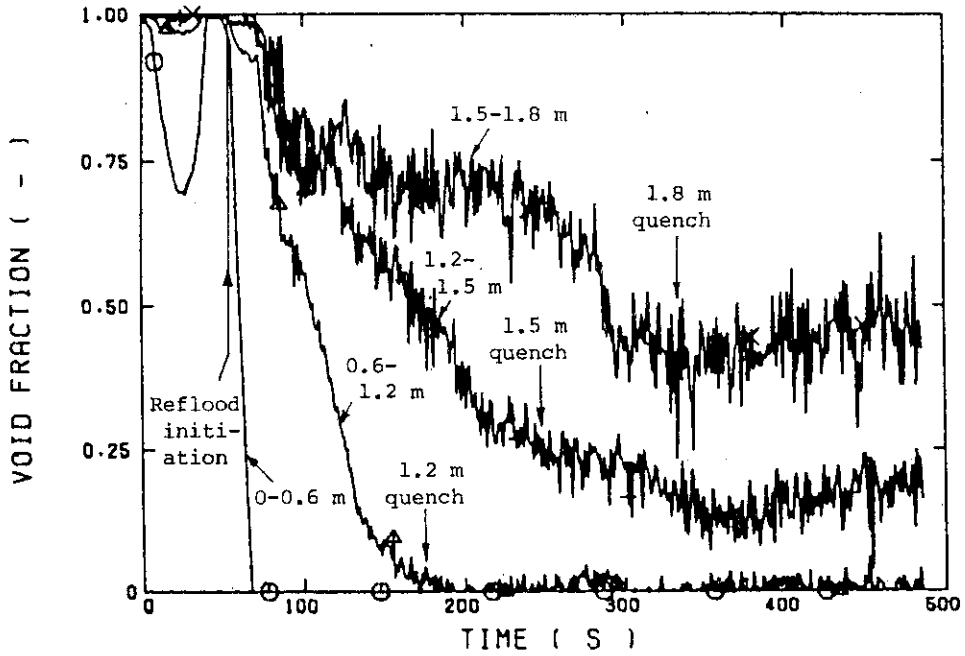


Fig. 3.5 Void fractions in lower half of core (Run 8107)

RUN8107

○--DPT7 (11) △--DPT8B (11) +--DP10 (11)
 X--DP12 (11)

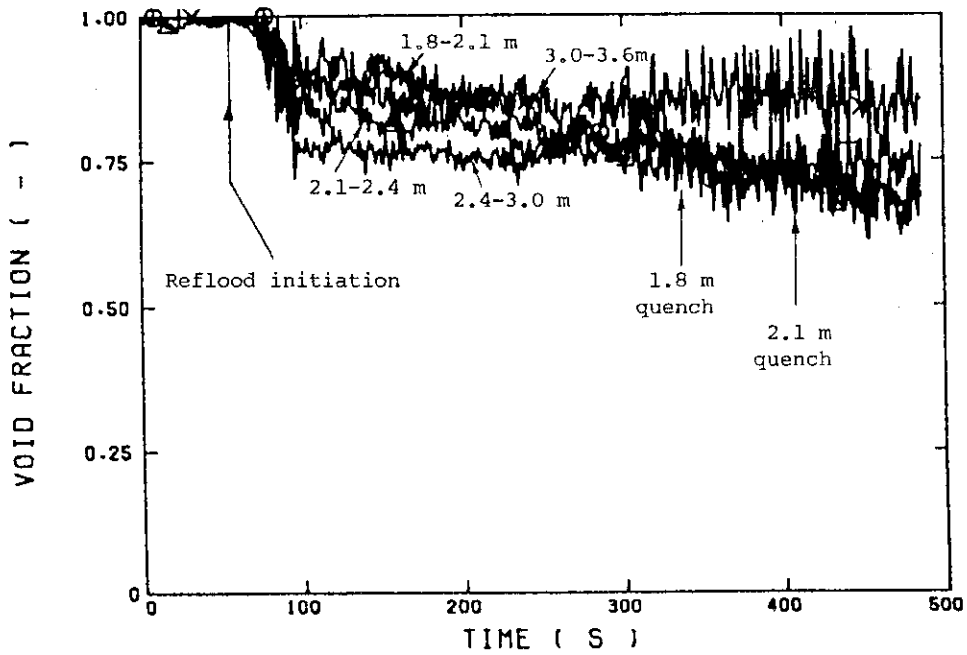


Fig. 3.6 Void fractions in lower half of core (Run 8107)

RUN8107

○--TGSB (11) △--S4MR (11) +--TC4M (11)

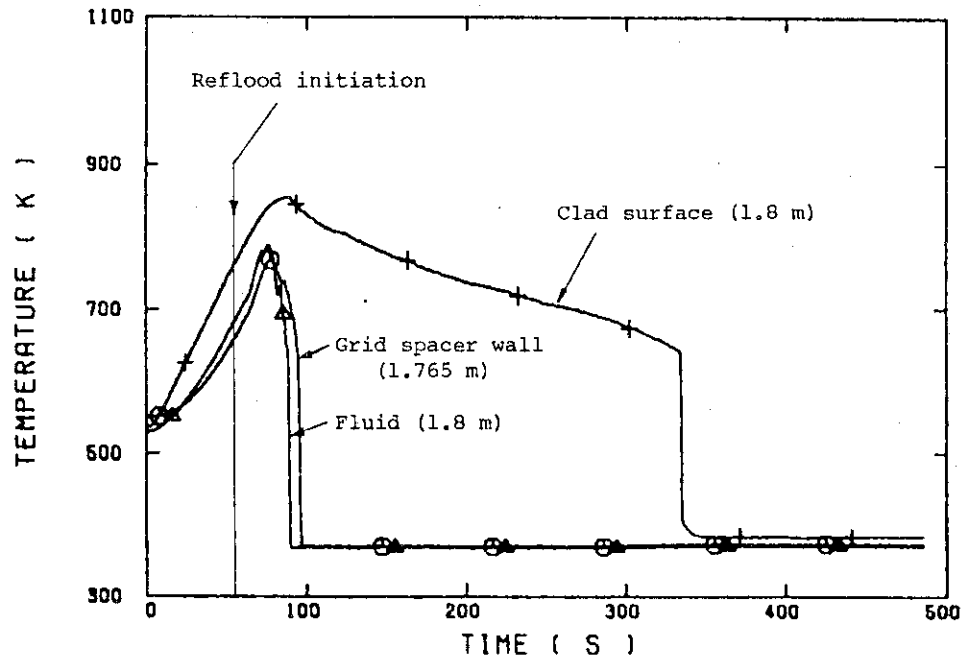


Fig. 3.7 Grid spacer wall and fluid temperatures (Run 8107)

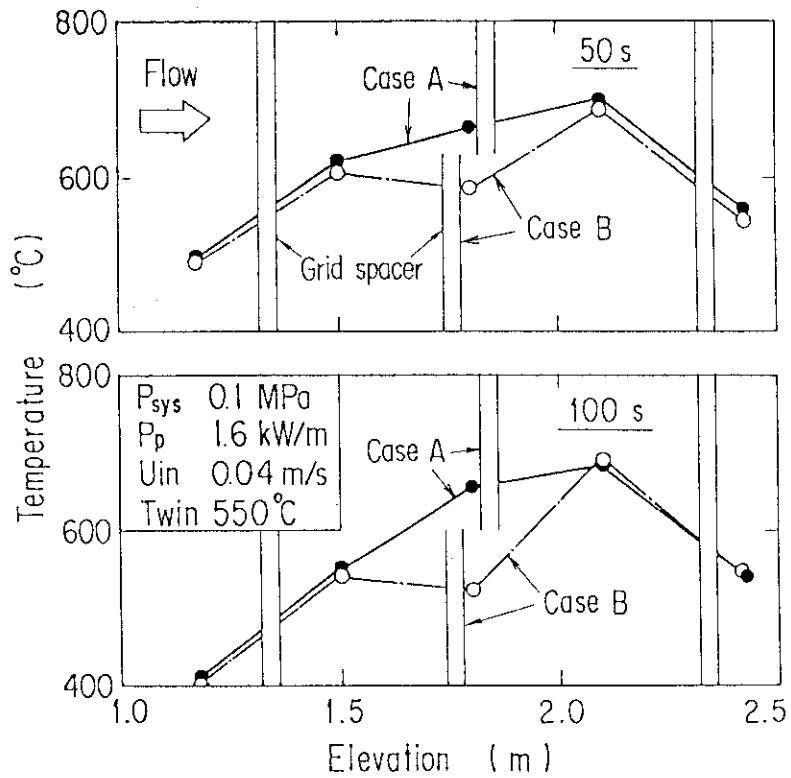


Fig. 3.8 Comparison of axial temperature distribution between Case A and Case B

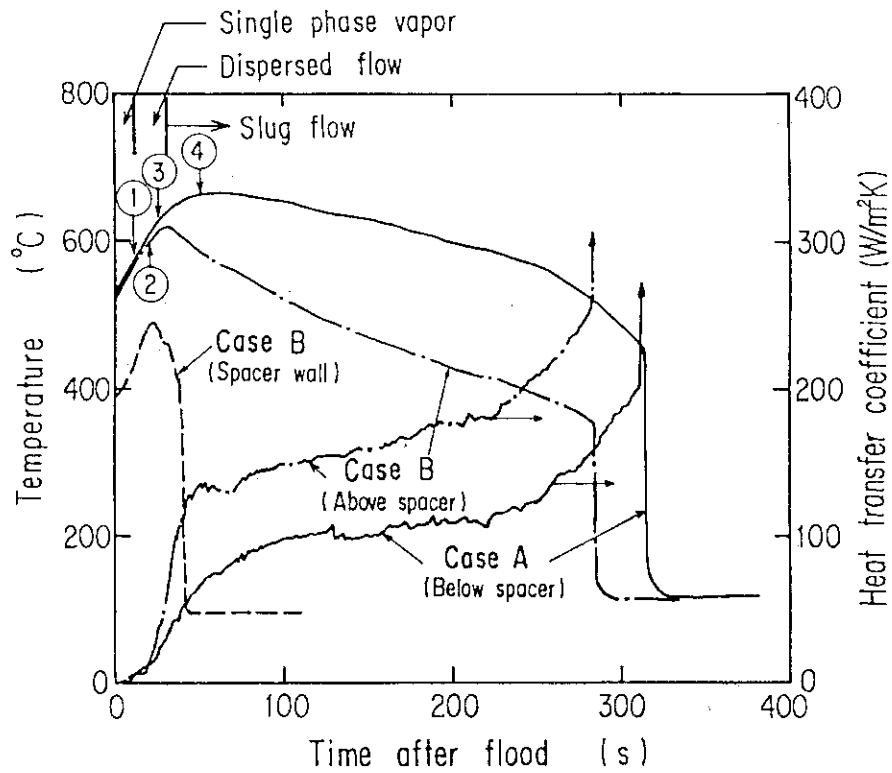


Fig. 3.9 Comparison of temperature histories and heat transfer coefficients at midplane between Case A and Case B

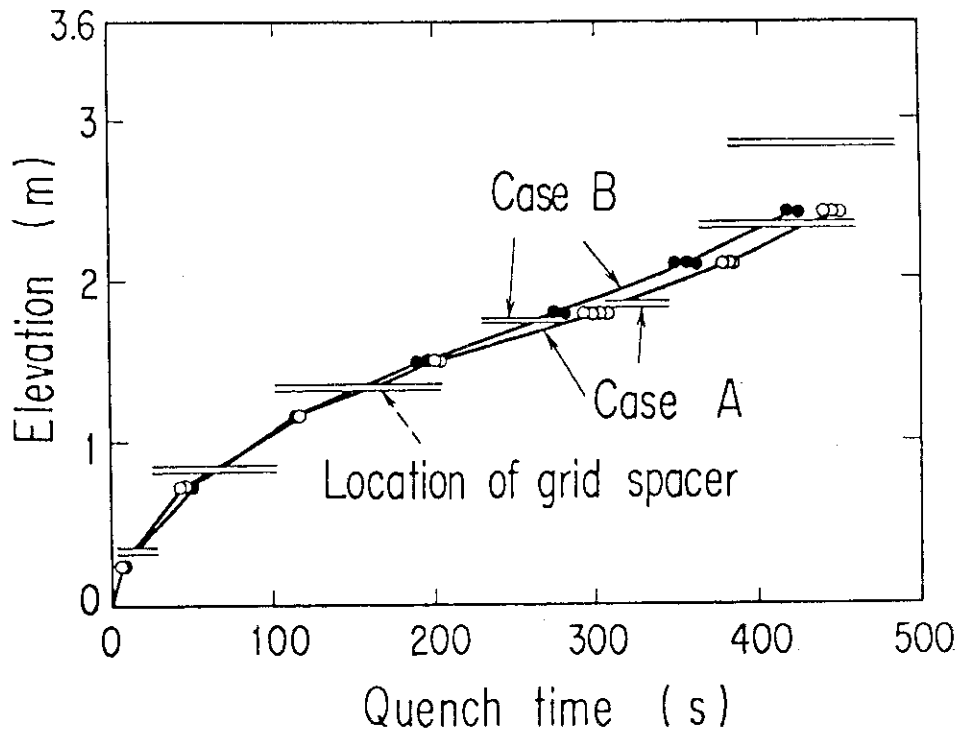


Fig. 3.10 Comparison of quench envelopes between Case A and Case B

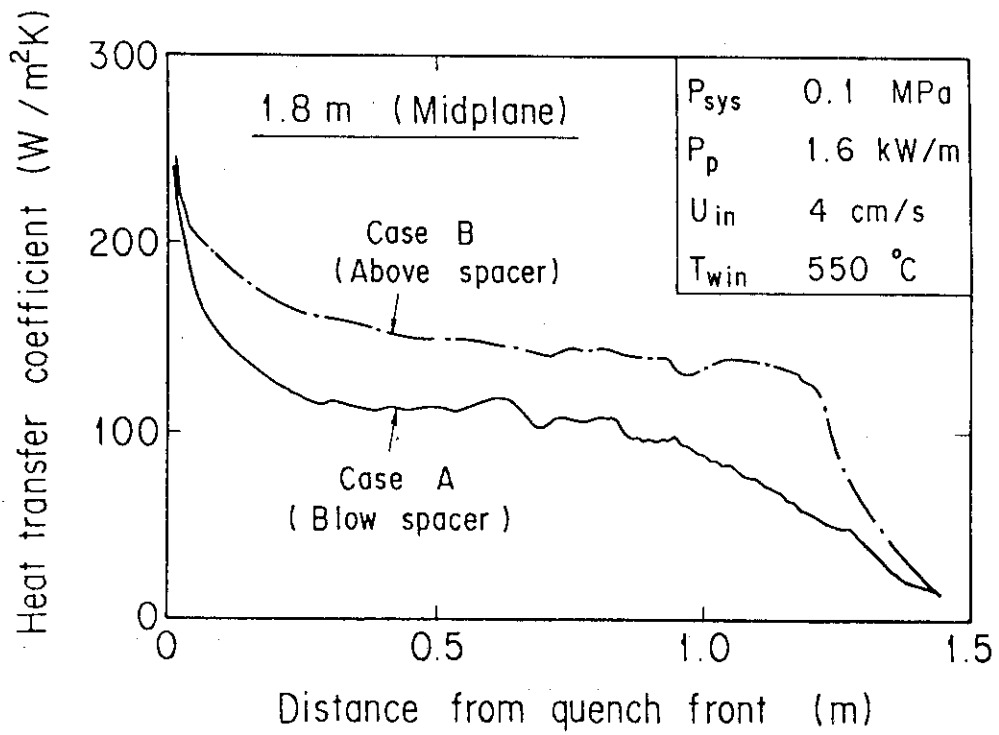


Fig. 3.11 Effect of distance from quench front on heat transfer coefficients

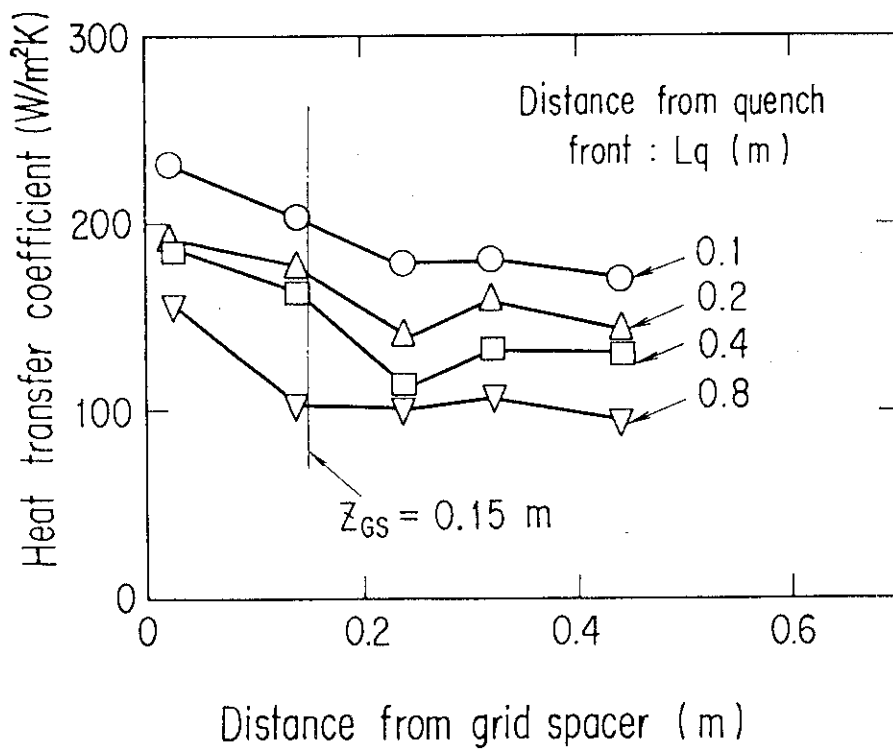


Fig. 3.12 Effect of distance from grid spacer on heat transfer coefficient in the highest power region

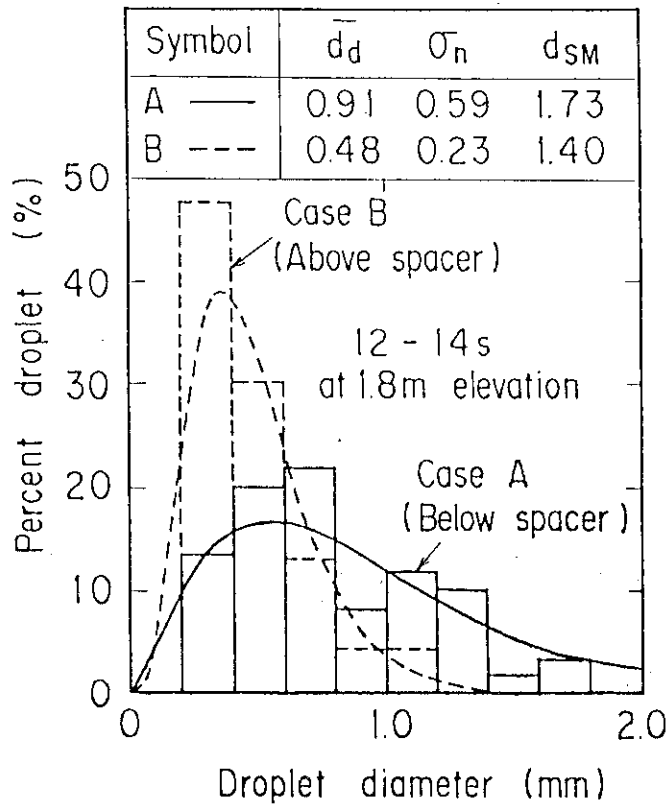


Fig. 3.13 Comparison of droplet diameter distributions between Case A and Case B

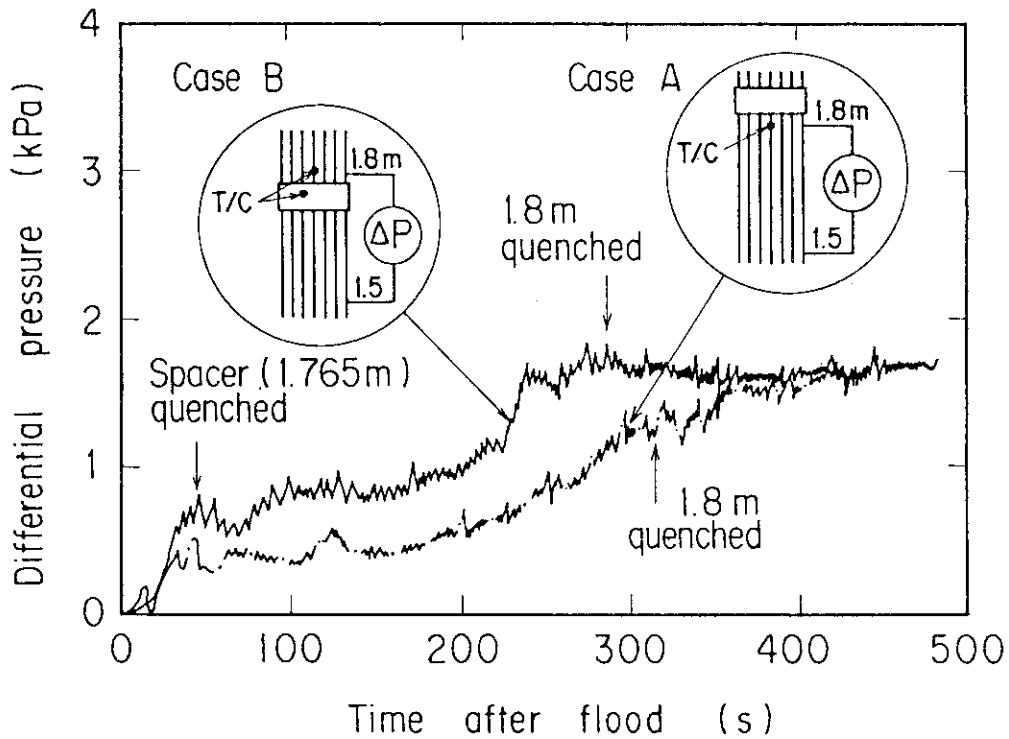


Fig. 3.14 Comparison of differential pressures near central grid spacer between Case A and Case B

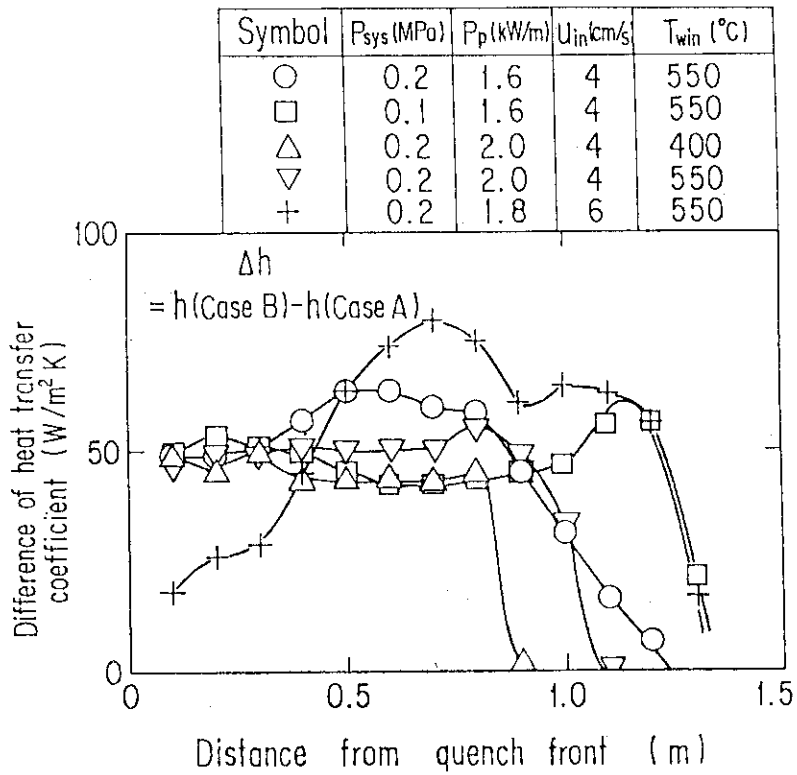


Fig. 3.15 Parameter effect on difference of heat transfer coefficients between Case A and Case B at midplane

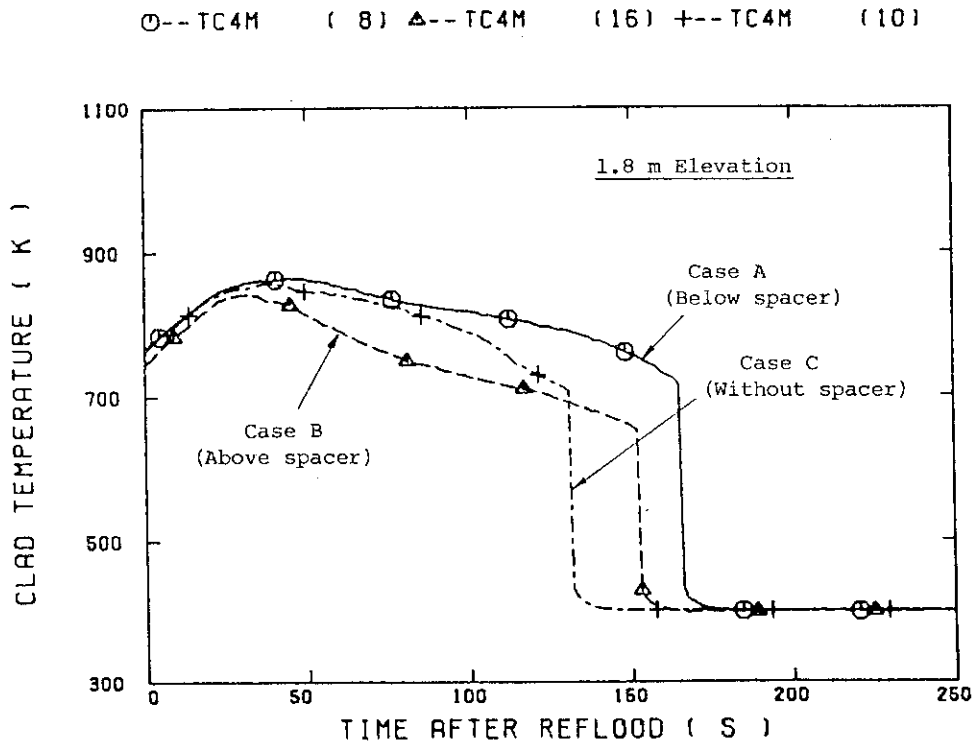


Fig. 3.16 Comparison of clad temperatures at midplane among Case A, B and C

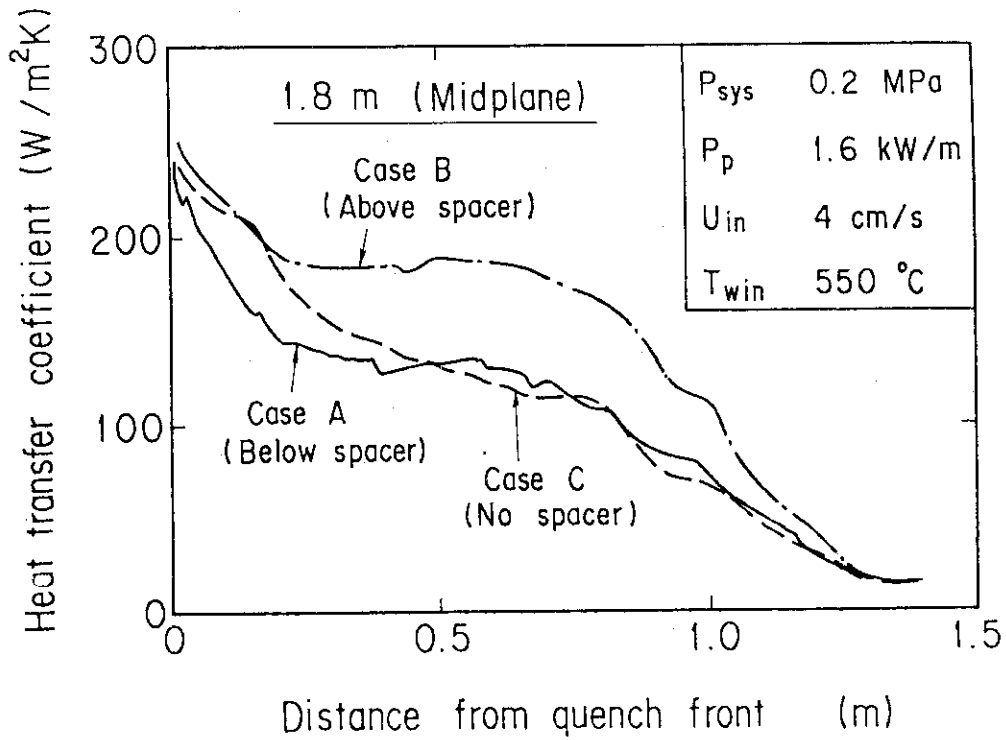


Fig. 3.17 Comparison of heat transfer coefficients at midplane as function of distance from quench front among Case A, B and C

RUN 8122-8313

○--TC4M (22) ▲--TC4M (13)

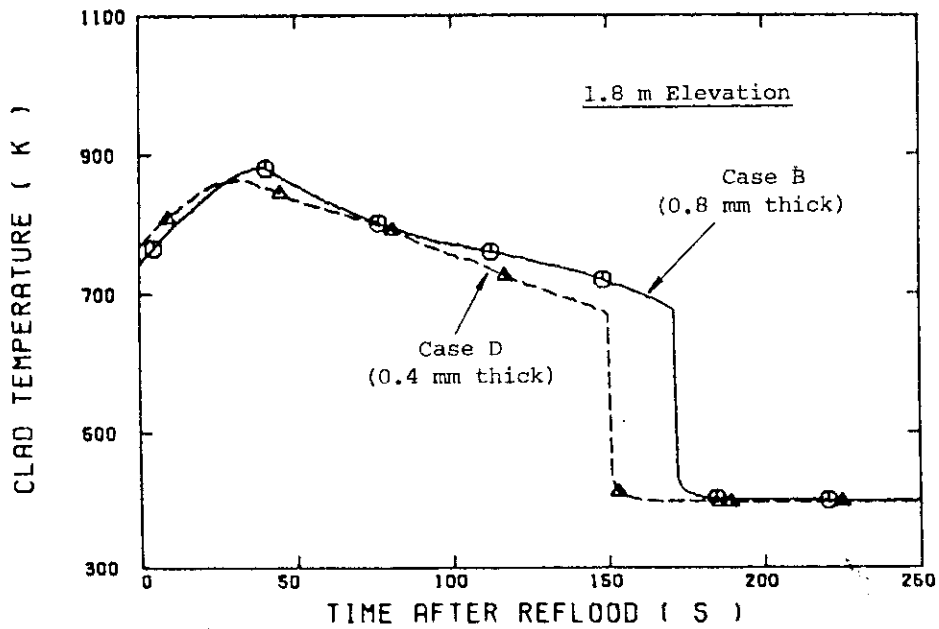


Fig. 3.18 Comparison of clad temperatures at midplane between Case B and Case C

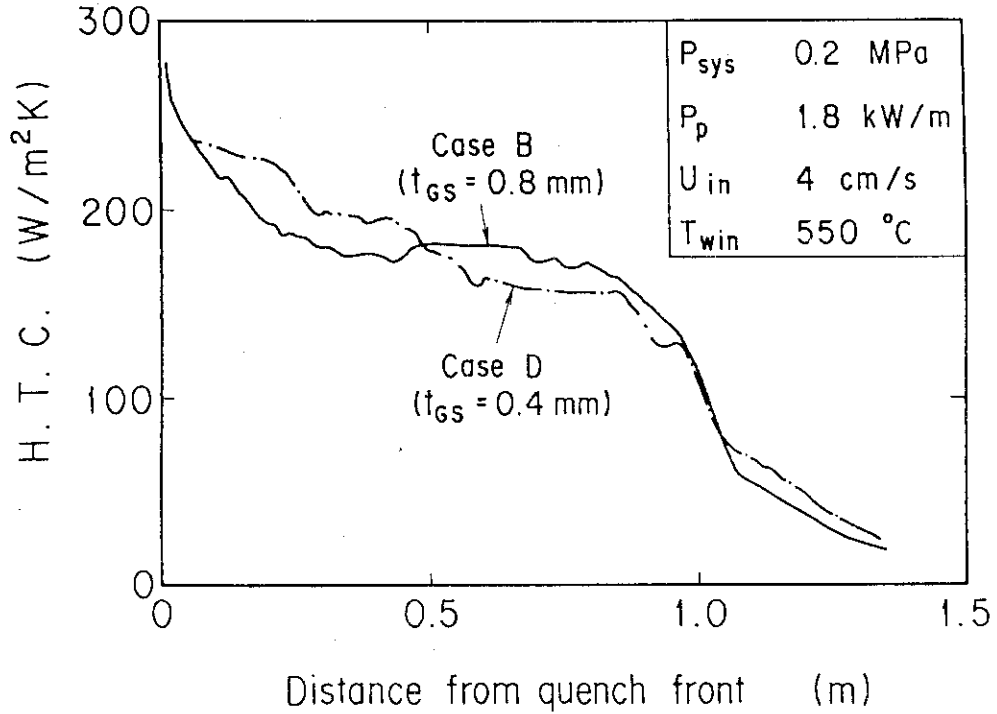


Fig. 3.19 Comparison of heat transfer coefficients at midplane as function of distance from quench front between Case B and Case D

RUN 8122-8313

○--DPT6B (22) △--DPT6B (13)

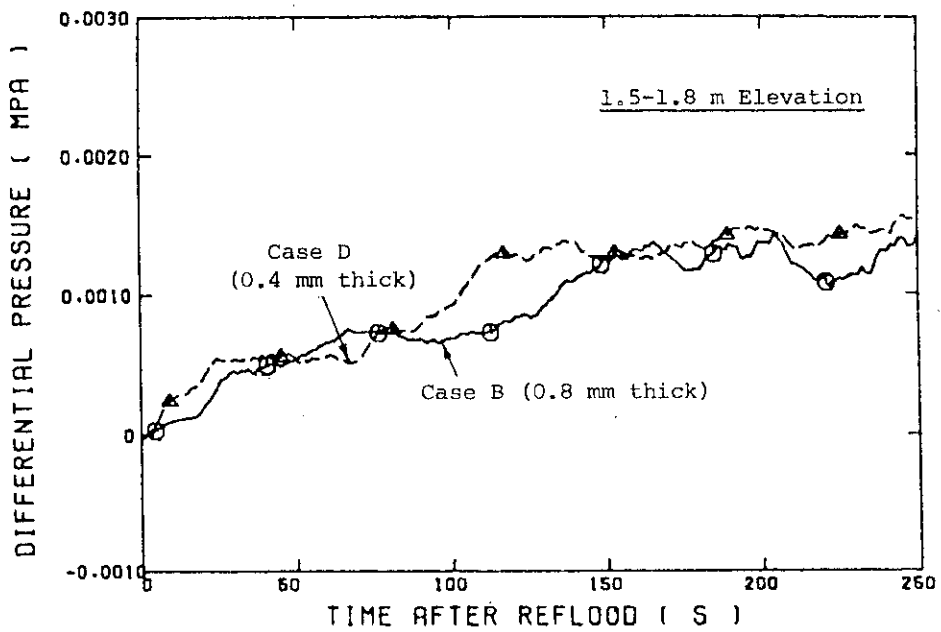


Fig. 3.20 Comparison of differential pressure near central grid spacer between Case B and Case D

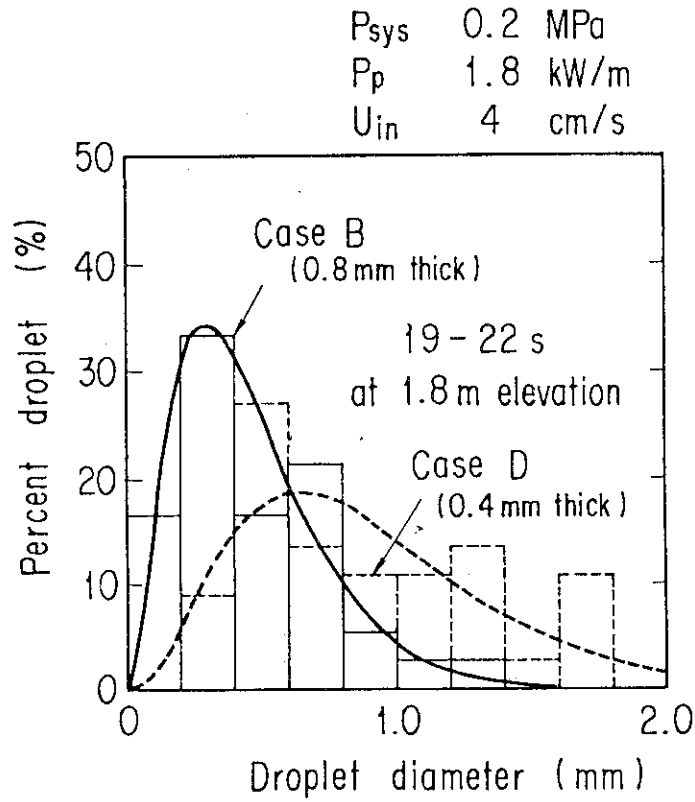


Fig. 3.21 Comparison of droplet diameter distributions between Case B and Case D

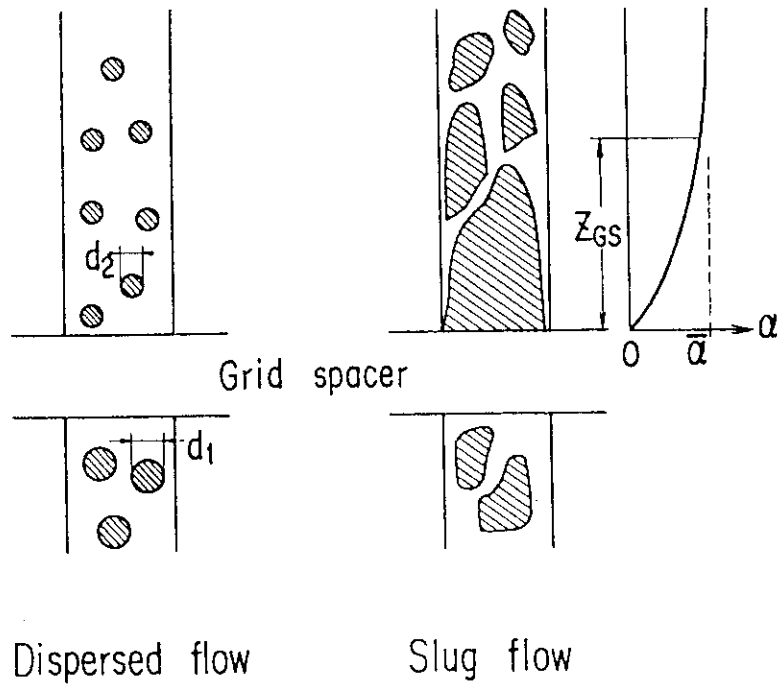


Fig. 3.22 Flow model near grid spacer in dispersed and slug flows

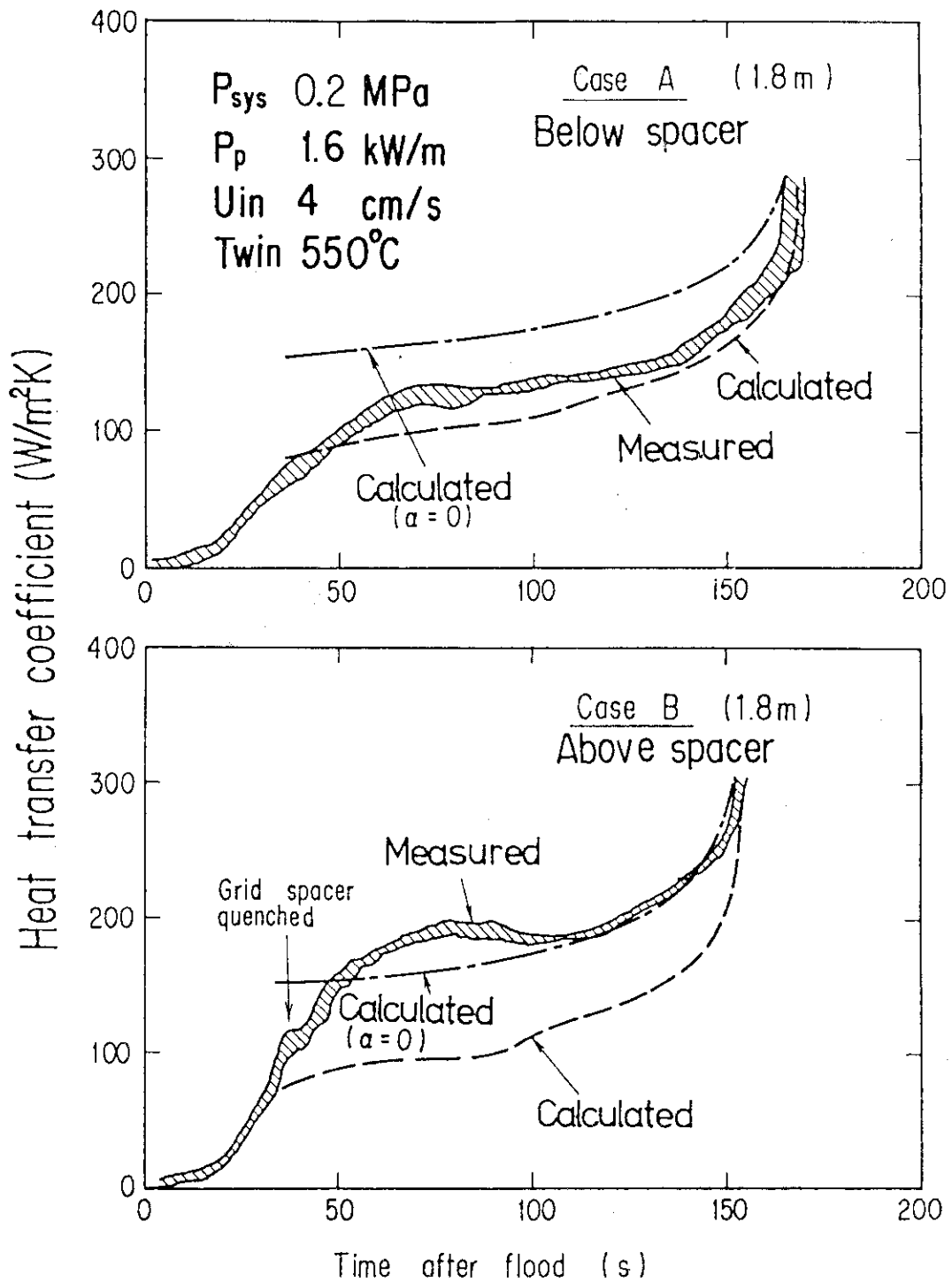


Fig. 3.23 Comparison of calculated and measured heat transfer coefficients at midplane for Case A and Case B

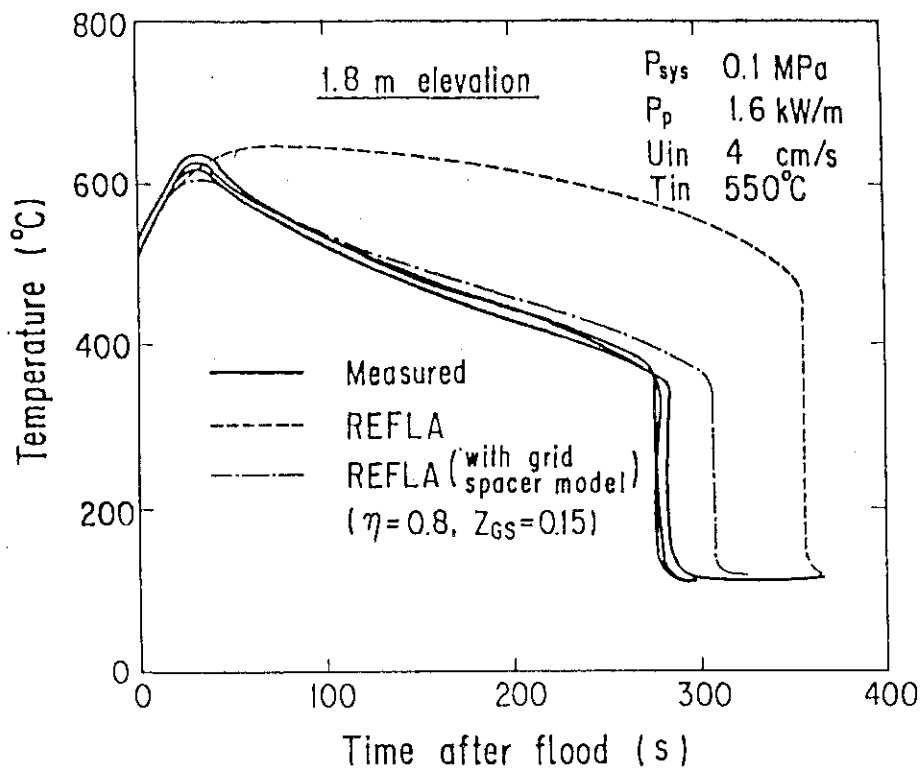


Fig. 3.24 Comparison of calculated and measured temperature histories at midplane above grid spacer

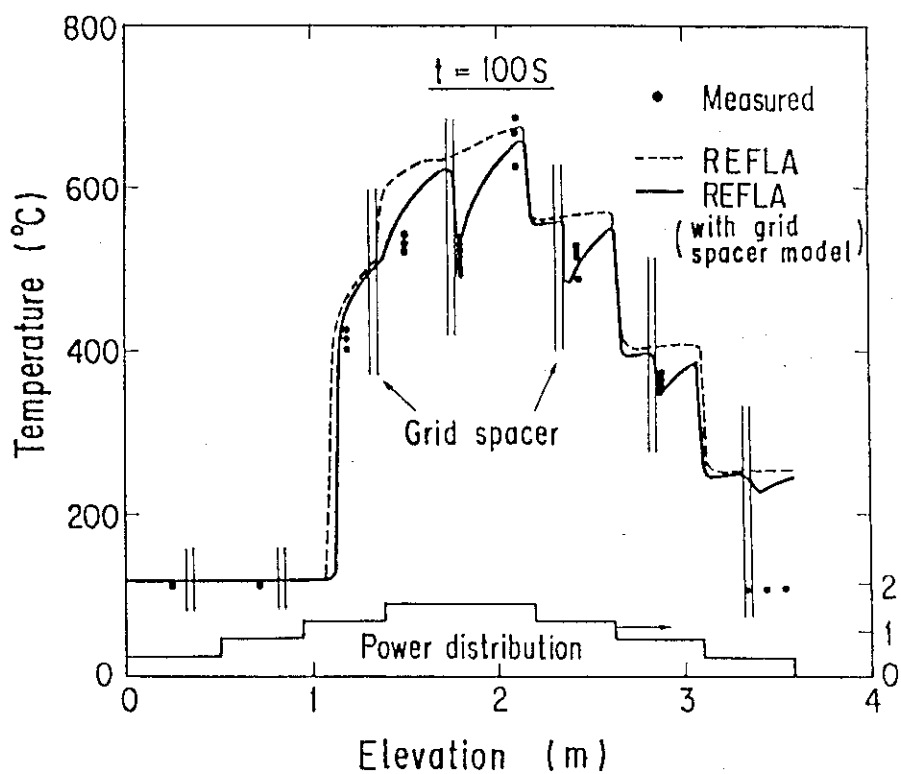


Fig. 3.25 Comparison of calculated and measured axial temperature distributions

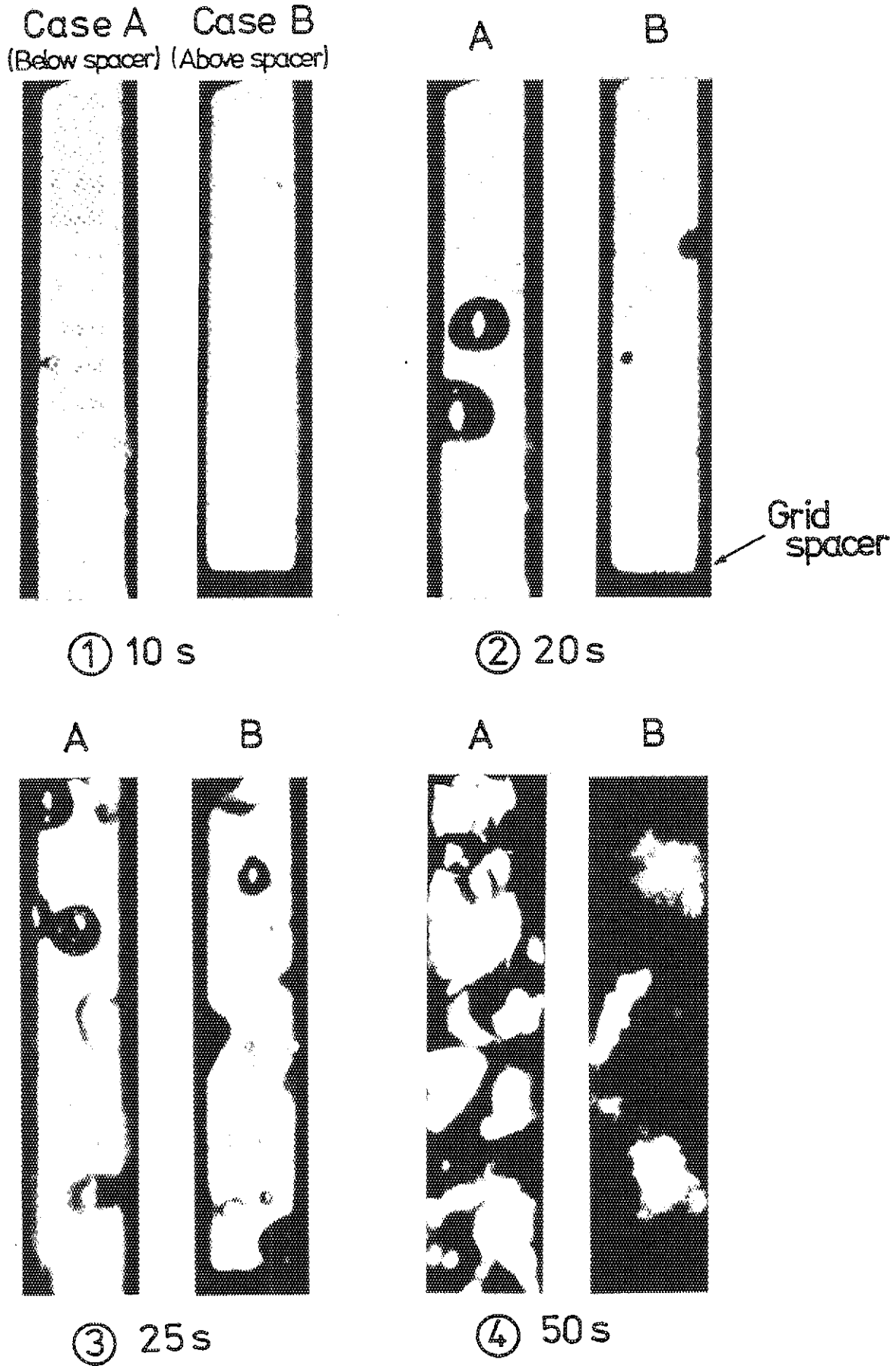


Photo 3.1 Comparison of flow pattern between below and above grid spacers observed at midplane

4. Analysis and discussion

4.1 Model description

The simple model for describing the effect of the grid spacers on reflood thermohydraulics was developed based on the present experimental results⁽²⁰⁾. The present model is primarily based on the results of Case A and Case B experiments to avoid the possible flow blockage during the process of Case C and D experiments. The model consists of the grid spacer model in the dispersed flow and that in the slug flow, since the two flow regimes are dominant and typical in the reflood transient. The schematic of the present grid spacer model is illustrated in Fig. 3.22.

(1) Grid spacer model in dispersed flow

a. Decrease of droplet diameter

The average droplet diameter above the grid spacer was found to be smaller than that below the grid spacer as already shown in Fig. 3.13. In the present modeling, this is assumed to be caused by the breakup of the water droplet when it collides with the blocking surface of the grid spacer as shown in Fig. 3.22.

The effective atomization factor η due to the grid spacer is defined as,

$$\eta = d_{SM2} / d_{SM1} \quad , \quad (2)$$

using Sauter mean diameter d_{SM} , which is the thermo-hydraulic mean diameter conserving the void fraction and the surface area, given by

$$d_{SM} = \overline{d^3} / \overline{d^2} \quad . \quad (3)$$

In Eq. (2), suffixes 1 and 2 denote the droplet just below and above the grid spacer, respectively. The mathematical mean diameter \bar{d} is expressed as,

$$\bar{d} = \frac{1}{N} \sum_{i=1}^N d_i = \frac{1}{N} \sum_{j=1}^M v_j d_j \quad , \quad (4)$$

where N is the total number of the droplet in the concerning volume, d_i the i -th droplet diameter and v_j the number of droplet of the j -th

diameter class in totally M diameter classes.

In order to estimate the effective atomization factor η , it is assumed that the probability of the droplet breakup is equal to the blocking ratio, a , of the flow channel and the water droplet is split into n smaller droplets with same diameters. First, the mass conservation across the grid spacer requires the following for the collided droplet:

$$d_{2j} = n^{-\frac{1}{3}} d_{1j} \quad . \quad (5)$$

Since the total number of droplets after breakup is $(1-a)N + anN$, therefore,

$$\overline{d_2^2} = \frac{1}{(1-a)N + anN} \sum_{j=1}^M \{ (1-a)v_j d_{1j}^2 + anv_j d_{2j}^2 \} \quad . \quad (6)$$

Using Eq. (5),

$$\overline{d_2^2} = \frac{1 + (n^{\frac{1}{3}} - 1)a}{1 + (n-1)a} \overline{d_1^2} \quad . \quad (7)$$

Similarly,

$$\overline{d_2^3} = \frac{1}{1 + (n-1)a} \overline{d_1^3} \quad . \quad (8)$$

Therefore, η in Eq. (2) is written as,

$$\eta = \frac{1}{1 + (n^{\frac{1}{3}} - 1)a} \quad . \quad (9)$$

The value of η in Eq. (9) is in the order of 0.89 ~ 0.97 for the typical value of a (0.1 ~ 0.2) and for the supposed value of n (2 ~ 4).

b. Disturbance

The wall-to-vapor heat transfer enhancement due to the disturbance of the vapor flow by the grid spacer has been correlated by Yao et al.⁽²¹⁾ using the results of the single phase experiments. The correlation is written as,

$$h = h_0(1 + 5.55 a^2 e^{-z/7.7De}) \quad , \quad (10)$$

where h_0 is the heat transfer coefficient without grid spacers, z the distance from the upper edge of the grid spacer and De the equivalent diameter of the flow channel. Equation (10) is adopted for the wall-to-vapor heat transfer enhancement due to grid spacers in the present modeling for both in the dispersed flow and also in the single phase vapor flow.

(2) Grid spacer model in slug flow

In the slug flow region, the grid spacer is rewetted by the impinging water slug in a very short time. The rewetted grid spacer then tends to accumulate the water near above the grid spacer due to CCFL as already described in the previous section. The upper edge of the grid spacer acts like a quench front as shown in Fig. 3.22. It is considered that the vapor film is disturbed by the existence of the grid spacer to cause the increased film boiling heat transfer just above the grid spacer.

Figure 3.23 shows the comparison of the calculated and measured heat transfer coefficients. The calculation is based on the heat transfer correlation⁽²²⁾ of the saturated film boiling:

$$h = 0.94(1 - \alpha)^{1/4} [\lambda_g^3 \rho_g \rho_l H_{fg} g / L Q \mu_g (T_w - T_s)]^{1/4} \quad (11)$$

$$+ \epsilon E(1 - \alpha)^{1/2} (T_w^4 - T_s^4) / (T_w - T_s).$$

As shown in the figure, the heat transfer coefficient just below the grid spacer is well approximated with Eq. (11). The heat transfer coefficient just above the grid spacer, on the contrary, is much larger than the prediction of Eq. (11). However, it agrees well to the calculation by Eq. (11) when the void fraction α is set to zero. This indicates that the heat transfer correlation in the slug flow should be modified near above the grid spacer.

Based on the above consideration, the following are assumed in the present model for the slug flow region.

- 1) The void fraction α increase exponentially to the saturated value with the distance from the upper edge of the grid spacer as

$$\alpha = \bar{\alpha} (1 - e^{-z/z_{GS}}) \quad (12)$$

where $\bar{\alpha}$ is the average void fraction, z the distance from the upper edge of the grid spacer and z_{GS} the characteristic length for the effect of the grid spacer.

- 2) The heat transfer coefficient h is expressed by Eq. (11) using the modified void fraction expressed by Eq. (12).
- 3) The average void fraction $\bar{\alpha}$ in the slug flow is expressed by the method proposed by Murao et al.⁽¹⁹⁾ using the modified Cunningham-Yeh and Lockhart-Martinelli correlations:

$$\bar{\alpha} = [1 + (U_{go} + U_{lo})/\Delta U - \{1 + 2(U_{lo} - U_{go})/\Delta U + (U_{go} + U_{lo})^2/\Delta U^2\}^{1/2}]/2 \quad , \quad (13)$$

where

$$\Delta U = U_{go}/\min(\alpha_{CY}, \alpha_{LM})$$

$$\alpha_{CY} = 0.925(\rho_g/\rho_l)^{0.239} (U_{go}/U_{bcr})^a$$

$$U_{bcr} = 1.53(\sigma \cdot g/\rho_l)^{0.25}$$

$$a = \begin{cases} 0.67 & (U_{go}/U_{bcr} < 1) \\ 0.47 & (U_{go}/U_{bcr} \geq 1) \end{cases}$$

$$\alpha_{LM} = 1 + 0.84(U_{lo}/U_{go})^{0.64}(\rho_l/\rho_g)^{0.28}(\mu_l/\mu_g)^{0.07}.$$

4.2 Calculation

The grid spacer model described in the previous sections was implemented into REFLA code⁽⁴⁾ in order to evaluate the model by comparing the calculation with the experiments. The basic thermo-hydraulic relations in the dispersed flow regime are based on the two step model which assumes the heat transfers from wall-to-vapor, vapor-to-droplet and wall-to-droplet. The heat transfer enhancement due to the grid spacer in the dispersed flow is realized by the increased interfacial surface area calculated using Eq. (2) for the increased vapor-to-droplet heat transfer and also by the increased wall-to-vapor heat transfer described with Eq. (10). The heat transfer enhancement in the slug flow is described with Eqs. (11) through (13). In the present calculation, the effective atomization factor $\eta (=d_{SM B}^3/d_{SM A}^3)$ in Eq. (2) was set to 0.8 and the characteristic length z_{GS} in Eq. (12) was set to 0.15 (m) based on the experimental results shown in Figs. 3.12 and 3.13, respectively.

Figure 3.24 shows the measured and the calculated temperature histories at the midplane just above the grid spacer. Although the peak clad temperature is slightly underestimated, the overall temperature transient is better predicted with the present grid spacer model than the calculation without the model. It is noticed that the sooner quench time and the lower quench temperature are also well predicted with the present model.

The axial temperature distribution at 100 s along the test section is shown in Fig. 3.25. The calculation without the grid spacer model tends to overestimate the temperature in the region of the high power level. The early quenching observed above 3.3 m elevation is not predicted by the codes due to the lack of the top-down quenching model. The calculation with the grid spacer model, however, gives better agreement with the experiment, especially in the region near above the grid spacer.

4.3 Discussion

The proposed grid spacer model reasonably gives the qualitative thermo-hydraulic behavior near the grid spacer especially in the slug flow region. The measured and calculated heat transfer enhancements due to the grid spacers in the dispersed flow region are not large as in the

slug flow region. This is due to the short duration of the dispersed flow in the present experimental condition.

The calculated radiative heat transfer estimated with the second term in Eq. (11) in the slug flow region is small compared with the convection term. However, it can be enhanced by the rewetted or cooled grid spacer when the rod surface temperature is extremely high. Hence, the experimental information at higher clad temperature would be required for the verification of the present grid spacer model both in the dispersed and slug flow regions.

The observed decrease of the droplet diameter above the grid spacer could also be related to the de-entrainment or the re-entrainment from the grid spacer surface, not only to the droplet breakups. The smaller droplet diameter less than 0.01 mm could not be identified with the present photo method. It is recommended to conduct a simple droplet breakup test to observe a local droplet behaviors.

According to the present experiments, the heat transfer enhancement tends to be larger with the blocking ratio of the grid spacer. It is, therefore, expected that the heat transfer enhancement will be larger with the grid spacers having mixing vanes which are currently being used in PWRs. Several types of grid spacers should be tested concerning the heat transfer enhancement.

The existing experimental information on the local effect of grid spacers is still limited. Highly required is axially finer instrumentation of the clad temperature and the pressure distribution near the grid spacer. The more mechanistic model can then be developed for the wider range of the LOCA conditions.

5. Conclusions

The effect of the grid spacers on the reflood heat transfer was experimentally investigated. The following conclusions were obtained.

- (1) The flow regimes identified at the core midplane were a single phase vapor, a dispersed flow and a slug flow in the reflood transient. The heat transfer coefficient just above the grid spacer was found to be 20~50 percent higher than that just below the grid spacer in the slug flow region, which lasted most of the transient before the quench time.
- (2) The observed average droplet diameter was smaller just above the grid spacer than that below the grid spacer in the dispersed flow regime. This decrease of the droplet diameter due to the grid spacer is supposed to contribute to the increased heat transfer from the vapor to droplets.
- (3) In the slug flow regime, the grid spacer was rewetted early in the transient and the increased water accumulation near above the grid spacer was observed. Hence, it is considered that the increased heat transfer in the slug flow is the result of the better film boiling heat transfer due to the rewetted grid spacer.
- (4) The heat transfer coefficient above the grid spacer tends to be smaller with thinner spacer wall in the region far from the quench front. It is, however, rather larger near the quench front, probably due to the partial flow blockage occurred in the later period of the experiment.
- (5) A simple analytical model of the grid spacer effect was developed based on the present experimental results for both in the dispersed and slug flows. Model was implemented into the reflood analysis code REFLA and the thermo-hydraulic behavior near the grid spacer was qualitatively well predicted with the present model.
- (6) It was found that further experimental information is required on the detailed axial distributions of the clad temperatures and the differential pressures. The need of the mechanistic modeling of the heat transfer enhancement is also emphasized.

Acknowledgment

The authors are much grateful to Dr. M. Nozawa and Dr. K. Hirano for their hearty suggestions and encouragement. They are deeply indebted to Mr. T. Iguchi, Mr. T. Sudoh, Mr. K. Okabe Dr. H. Akimoto and Mr. T. Okubo for their experimental and analytical supports. They would like to express their thanks to Mr. Y. Niitsuma for the test conduction and to Mr. T. Mimura for the data processing.

[Nomenclature]

a	: Blocking ratio of grid spacer	
D_e	: Equivalent hydraulic diameter	(m)
d	: Droplet diameter	(m)
E	: Stefan Boltzmann constant	(W/m ² ·K ⁴)
g	: Acceleration of gravity	(m/s ²)
H_{fg}	: Latent heat of evaporation	(J/kg)
h	: Heat transfer coefficient	(W/m ² ·K)
L_Q	: Distance from quench front	(m)
$\min(A,B)$: Smaller value of A or B	
N	: Total number of droplets	
n	: Average number of droplets after breakup	
P_p	: Peak linear power	(kW/m)
P_{sys}	: System pressure	(MPa)
T	: Temperature	(K)
T_{win}	: Initial peak clad temperature	(°C)
U_{in}	: Flooding rate	(m/s)
U_o	: Superficial velocity	(m/s)
z	: Distance from upper edge of grid spacer	(m)
z_{GS}	: Characteristic length for the grid spacer effect in slug flow	(m)
α	: Void fraction	
ϵ	: Emissivity	
Δ	: Difference	
ΔT_{sub}	: Inlet subcooling of coolant	(°C)
λ	: Thermal conductivity	(W/m·K)
η	: Effective atomization factor	
μ	: Dynamic viscosity	(Pa·s)

ρ : Density (kg/m³)

σ : Surface tension (kg/m)

(Subscripts)

A : Case A

B : Case B

g : Gas phase

l : Liquid phase

s : Saturated

w : Wall

1 : Below grid spacer

2 : Above grid spacer

References

- (1) Rosal, E.R., et al.: FLECHT low flooding rate cosine test series evaluation report, WCAP-8838, (1977).
- (2) Murao, Y., et al.: Experimental study of system behavior during reflood phase of PWR-LOCA using CCTF, J. Nucl. Sci. Technol., 19[9], 705 ~ 719 (1982).
- (3) Liles, D., et al.: TRAC-PD2, An advanced best-estimate computer program for pressurized water reactor loss-of-coolant accident analysis, LA-8709-MS, NUREG/CR-2054, (1981).
- (4) Murao, Y.: Analytical study of thermo-hydrodynamic behavior of reflood-phase during LOCA, J. Nucl. Sci. Technol., 16 [11], 803 ~ 817 (1979).
- (5) Ihle, P.: FEBA recent results and future plans, presented at Eighth Water Reactor Research Information Meeting (1980).
- (6) Rehme K.: Pressure drop correlations for fuel element spacers, Nucl. Technol., 17 [15], 15 ~ 23 (1973).
- (7) Conway, C.E. et al.: PWR FLECHT SEASET program plan, NRC/EPRI Report No.1 (1977).
- (8) Ihle, P., et al.: Experimental investigation of reflood heat transfer in the wake of grid spacers, Int. Meeting on Thermal Nuclear Reactor Safety (1982).
- (9) Lee, S.L., et al.: An LDA in situ study of droplet hydrodynamics across grid spacers in PWR-LOCA reflood, presented at Tenth Water Reactor Safety Information Meeting (1982).
- (10) Sugimoto, J., et al.: Preliminary analysis of the effect of the grid spacers on the reflood heat transfer, JAERI-M9992, (1982).
- (11) Murao, Y., et al.: Report on Series 4 Reflood Experiment, JAERI-M 6982, (1977).
- (12) Murao, Y., et al.: Report on series 5 reflood experiment, JAERI-M 7383, (1977).
- (13) Iguchi, T., et al.: Data report on series 6 reflood experiment (Constant flooding rate experiment data), JAERI-M 8161, (1979).
- (14) Sudoh, T., et al.: Data report on reflood experiment VII (Series 6, Intermittent flow rate core forced injection tests and system effect tests), JAERI-M 8162, (1979).
- (15) Sugimoto, J., et al.: Data report on reflood experiment VIII (Series 6, heat transfer data), JAERI-M 8169, (1979).

- (16) Murao, Y., et al.: CCTF Core I test results, JAERI-M 82-073, (1982).
- (17) Adachi, H., et al.: SCTF Core I test results, JAERI-M 82-075, (1982).
- (18) Malang, S.: HETRAP: A heat transfer analysis program, ORNL-TM-4555, (1974).
- (19) Murao, Y., et al.: Experimental modeling of hydrodynamics in reflood phase of PWR-LOCA, J. Nucl. Sci. Technol., 19 [8], 613 ~ 627 (1982).
- (20) Sugimoto, J., et al.: Effect of grid spacers on reflood heat transfer in PWR-LOCA, J. Nucl. Sci. Technol., 21 [2], 103 ~ 114 (1984).
- (21) Yao, Y., et al.: Heat transfer augmentation in rod bundles near grid spacers, ASME paper 80-WA/HI-62, (1980).
- (22) Murao, Y., et al.: Correlation of heat transfer coefficient for saturated film boiling during reflood phase prior to quenching, J. Nucl. Sci. Technol., 18 [4], 275 ~ 284 (1981).

Appendix Selected Data

A.1 Contents

Selected data are compiled in this appendix. Data of one experimental run consist of 1) Test conditions, 2) Temperature profile, 3) Quench envelope, 4) Clad temperature history, 5) Heat transfer coefficient, 6) Core sectional differential pressure, and 7) Void fraction in core.

A.2 Tag identification

Tag IDs or symbols of each instrument are indicated in Figs. 2.5 and 2.6 for clad temperatures and core sectional differential pressures, respectively. The heat transfer coefficient (HT---) is calculated using the clad temperature according to the scheme shown in section 2.4. The void fraction (VDP--) is converted from the core sectional differential pressure neglecting the accelerational and frictional pressure losses.

 * RUN NO. 8007 *

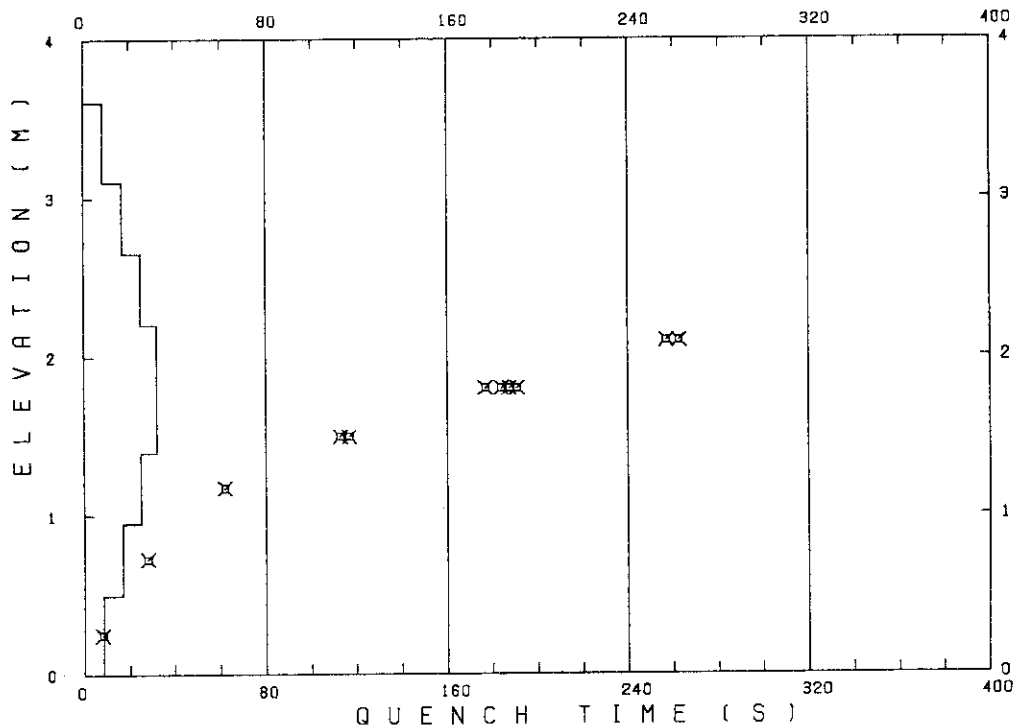
 TEST CONDITIONS

LINEAR PEAK POWER 2.0 KW/M
 SYSTEM PRESSURE 0.2 MPA
 INLET WATER TEMPERATURE 100 .C
 INJECTED WATER VELOCITY 3.9 CM/S

 TEMPERATURE PROFILE

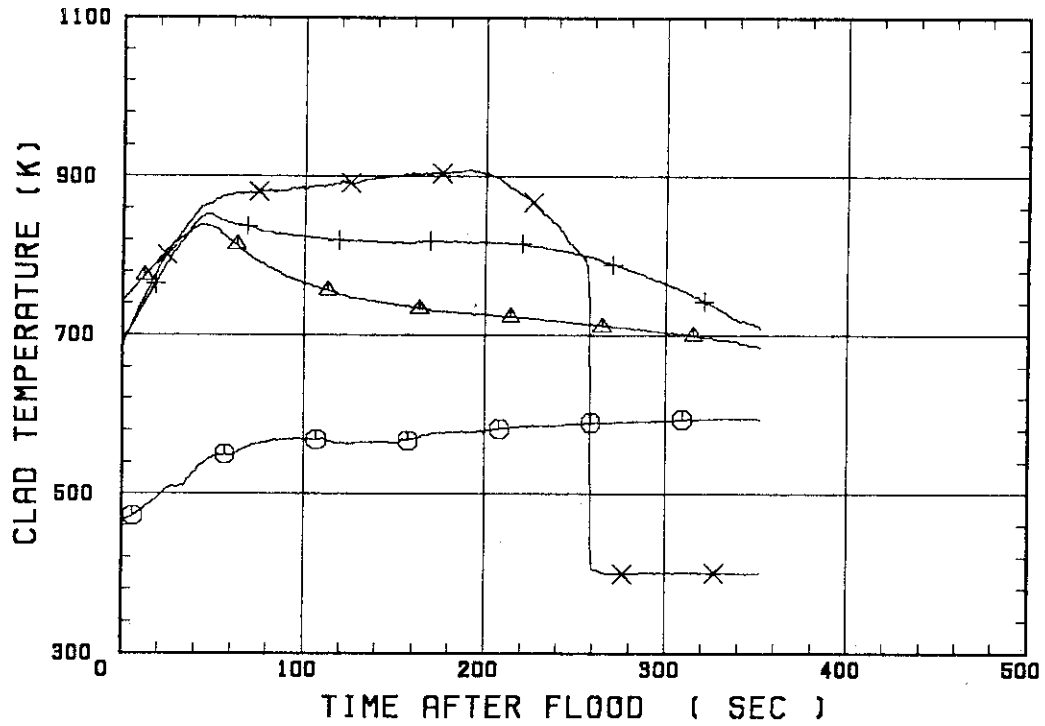
CH.NO.	SYMBOL	INITIAL TEMP. (.C)	TURNAROUND TIME (S)	TURNAROUND TEMP. (.C)	QUENCH TIME (S)	QUENCH TEMP. (.C)
66	TC1L	190	346.0	322		
51	TR2	468	44.0	566		
52	TR3	415	47.0	579		
67	TC4U	410	191.0	636	257.0	513
7	TS4U	413	173.0	641	262.5	470
53	TR4M	387	86.0	597	191.0	488
68	TC4M	388	87.0	574	184.0	482
8	TS4M	381	87.0	585	187.5	468
48	TB4M	395	86.0	596	177.0	508
69	TC4L	394	41.0	524	117.0	449
9	TS4L	390	38.0	525	113.0	440
54	TR5	337	42.0	427	62.0	389
55	TR6	253	17.0	296	28.0	279
70	TC7	183	6.0	191	8.0	189

RUN NO. 8007



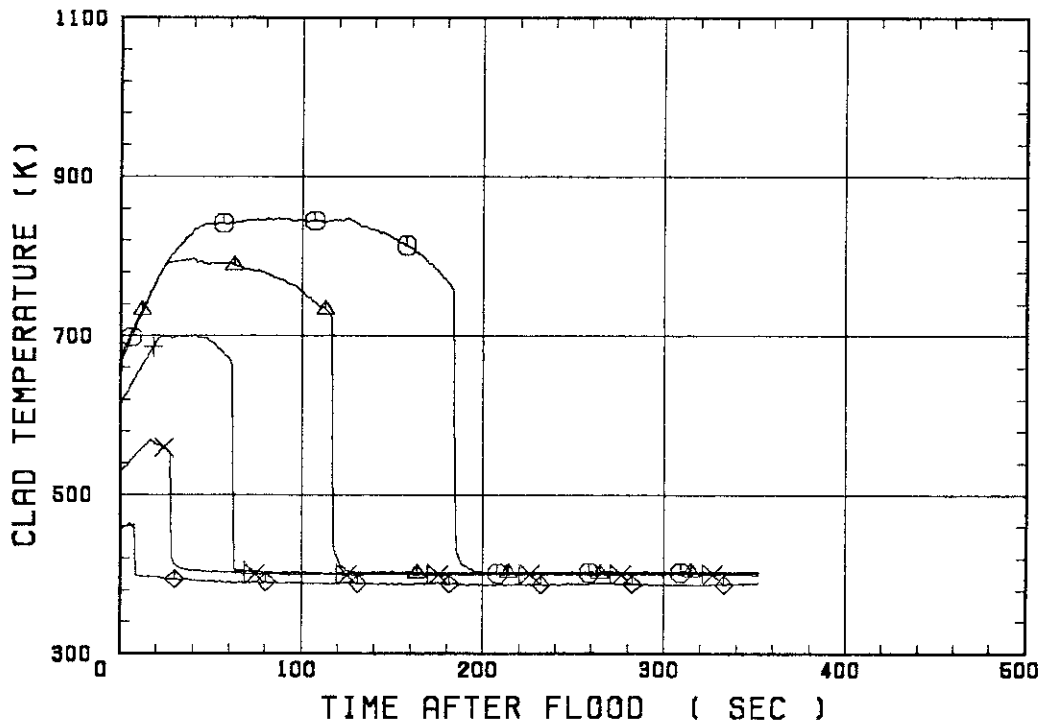
SMALL SCALE REFLOOD TEST
RUN 8007

○--- TC1L △--- TR2 +--- TR3
X--- TC4U

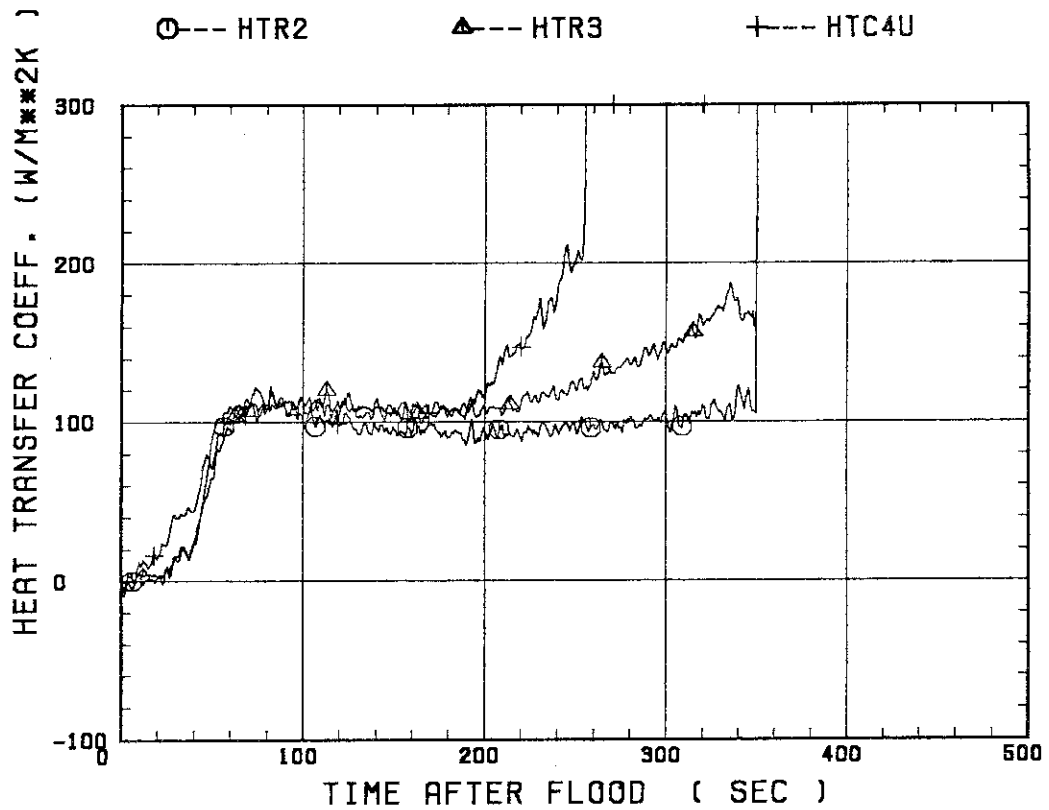


SMALL SCALE REFLOOD TEST
RUN 8007

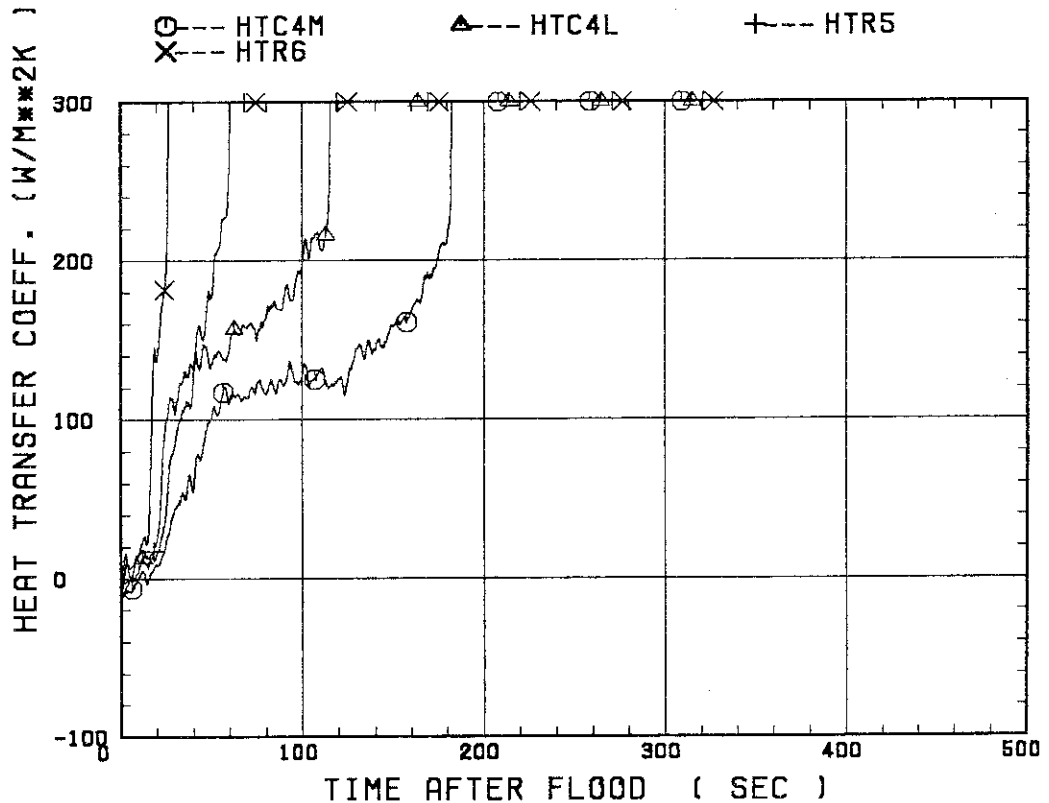
○--- TC4M △--- TC4L +--- TR5
X--- TR6 ◆--- TC7



SMALL SCALE REFLOOD TEST
RUN 8007

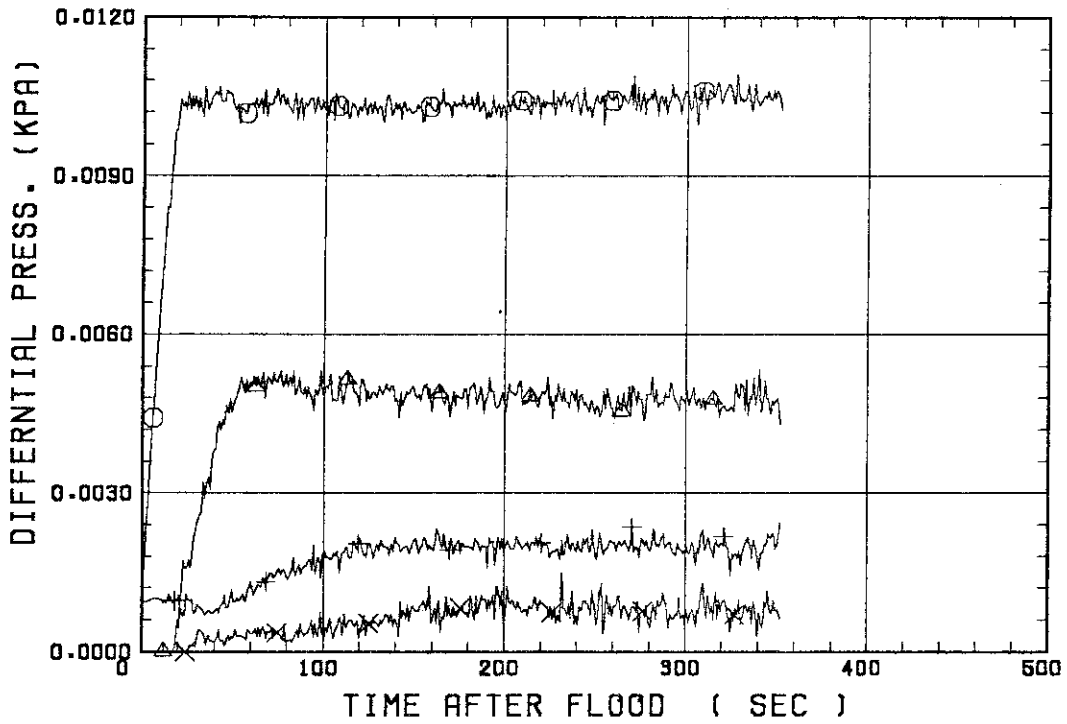


SMALL SCALE REFLOOD TEST
RUN 8007



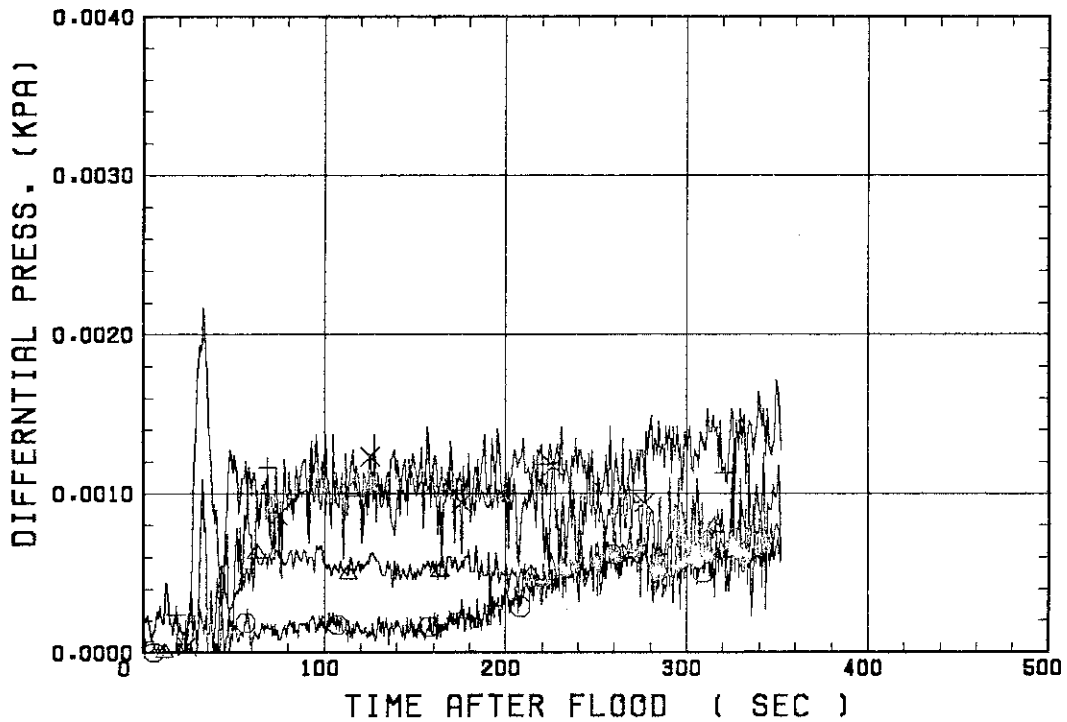
SMALL SCALE REFLOOD TEST
RUN 8007

○--- DPT2 ▲--- DPT4 +--- DPT5
X--- DPT6B



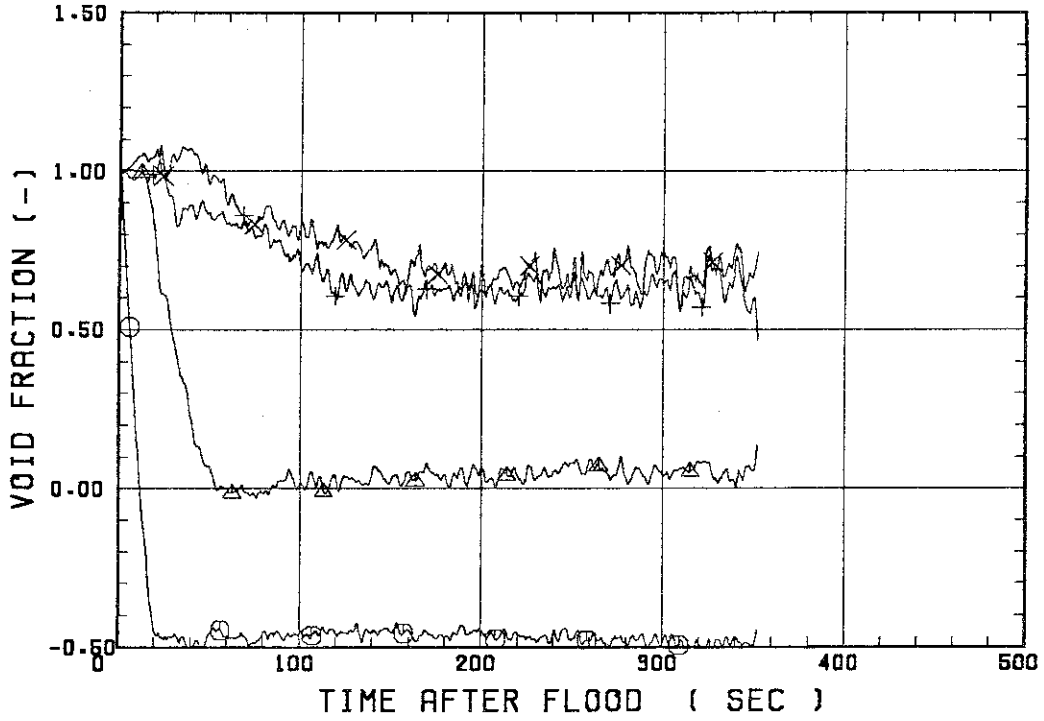
SMALL SCALE REFLOOD TEST
RUN 8007

○--- DPT7 ▲--- DPT8B +--- DP10
X--- DP12



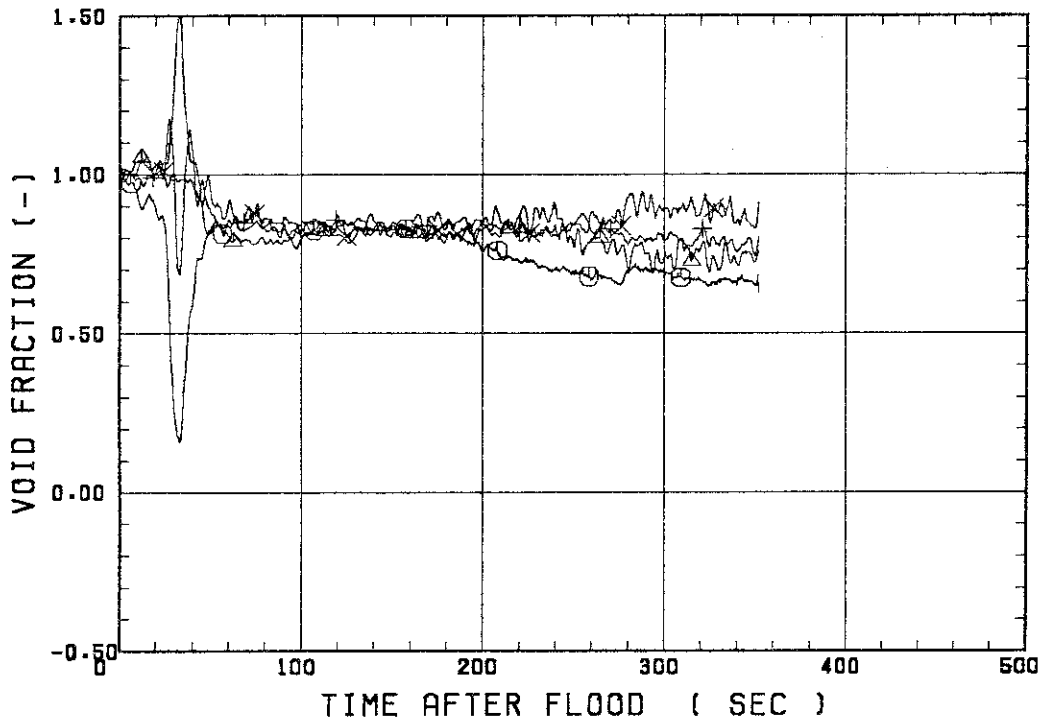
SMALL SCALE REFLOOD TEST
RUN 8007

○--- VDPT2 △--- VDPT4 +--- VDPT5
X--- VDPT6B



SMALL SCALE REFLOOD TEST
RUN 8007

○--- VDPT7 △--- VDPT8B +--- VDP10
X--- VDP12



 * RUN NO. 8008 *

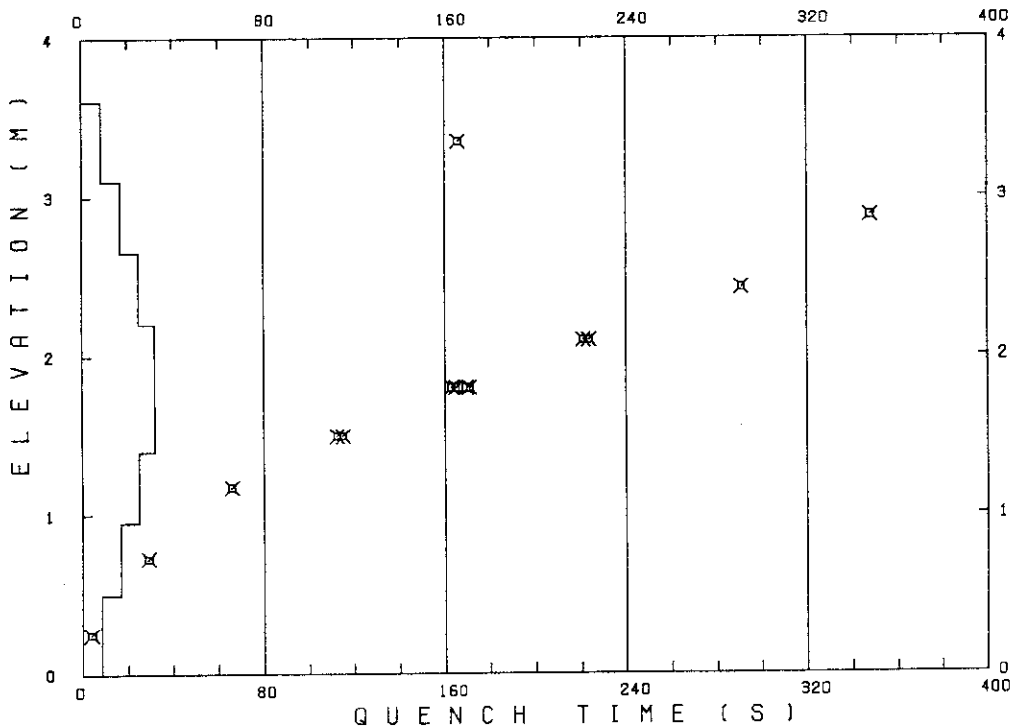
 TEST CONDITIONS

LINEAR PEAK POWER 1.6 KW/M
 SYSTEM PRESSURE 0.2 MPA
 INLET WATER TEMPERATURE 100 .C
 INJECTED WATER VELOCITY 3.9 CM/S

 TEMPERATURE PROFILE

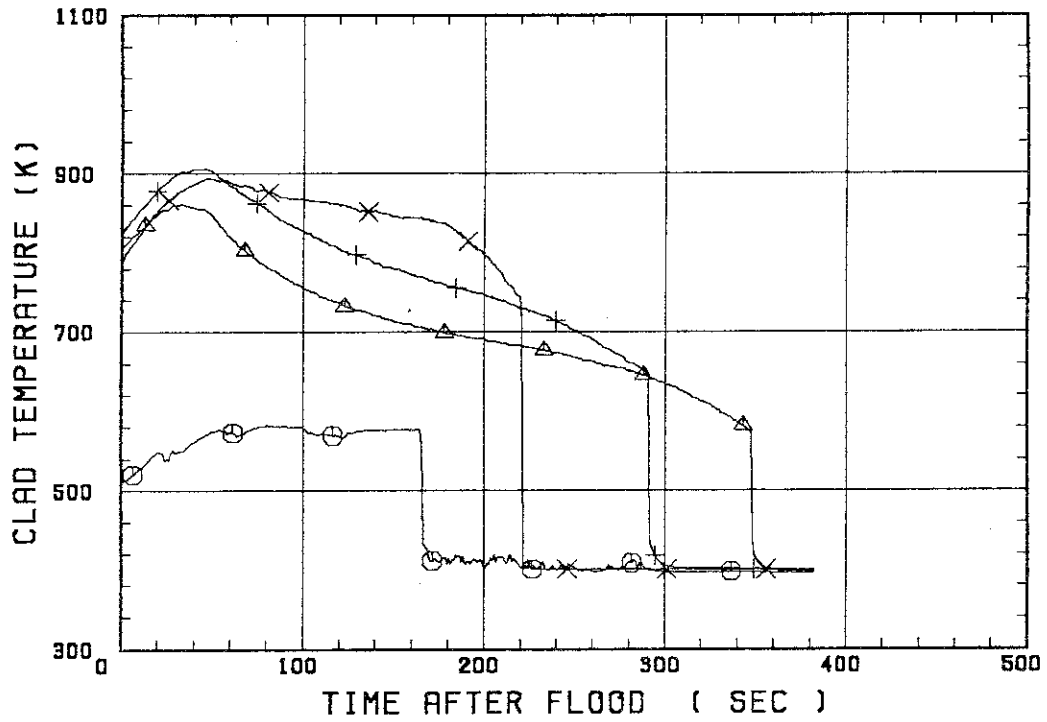
CH.NO.	SYMBOL	INITIAL TEMP. (.C)	TURNAROUND TIME (S)	TURNAROUND TEMP. (.C)	QUENCH TIME (S)	QUENCH TEMP. (.C)
66	TC1L	238	81.0	310	166.0	283
51	TR2	532	34.0	588	348.0	301
52	TR3	550	46.0	633	291.0	371
67	TC4U	513	48.0	621	221.0	440
7	TS4U	544	48.5	669	223.5	458
53	TR4M	505	47.0	624	171.0	457
68	TC4M	492	45.0	592	165.0	441
8	TS4M	500	47.0	612	169.5	440
48	TB4M	514	41.0	627	163.0	465
69	TC4L	489	24.0	559	115.0	387
9	TS4L	507	25.5	583	112.5	420
54	TR5	433	20.0	483	66.0	388
55	TR6	316	11.0	338	29.0	303
70	TC7	217	3.0	220	4.0	219

RUN NO. 8008



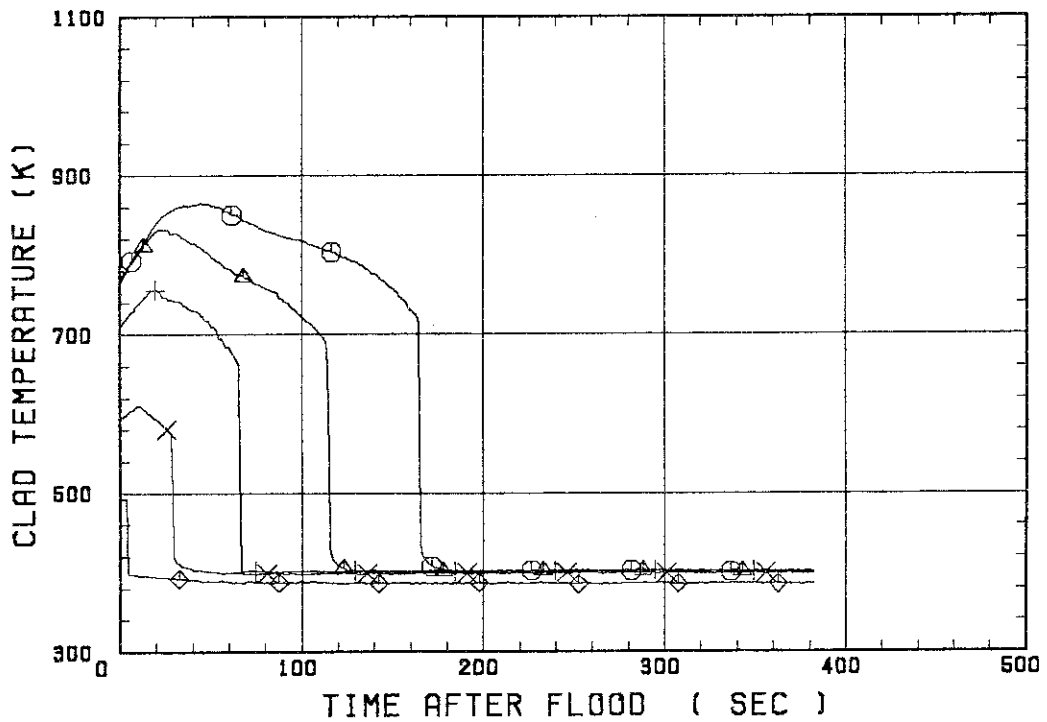
SMALL SCALE REFLOOD TEST
 RUN 8008

○--- TC1L △--- TR2 +--- TR3
 X--- TC4U

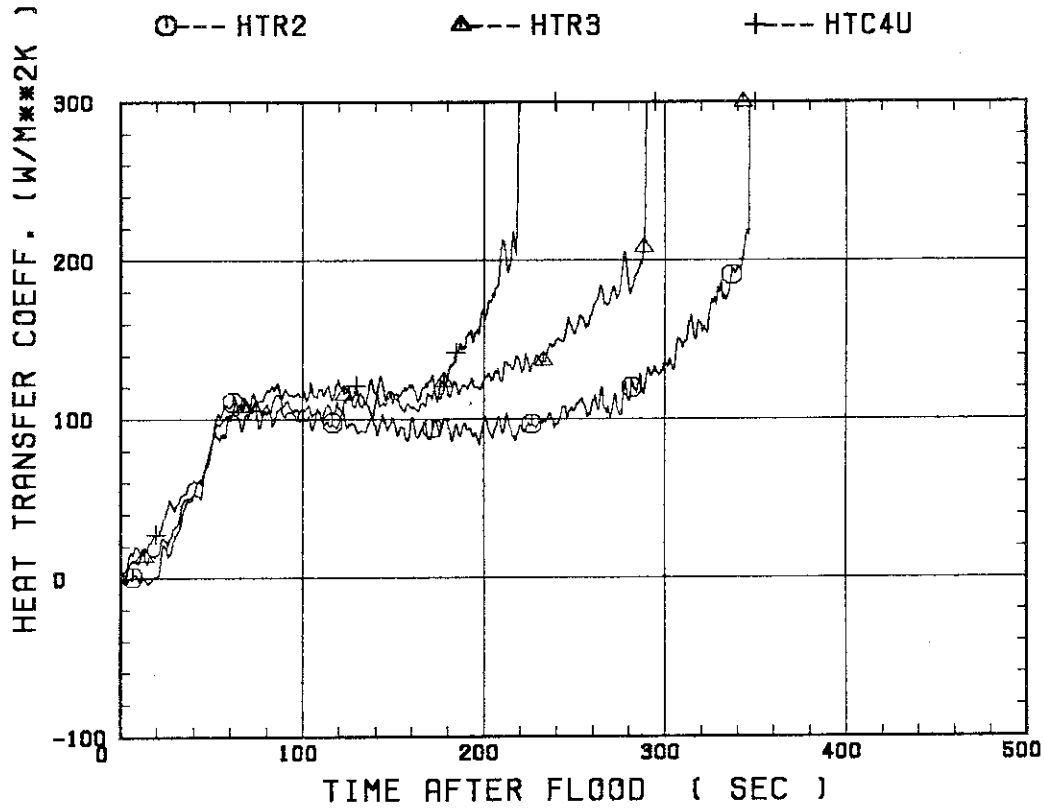


SMALL SCALE REFLOOD TEST
 RUN 8008

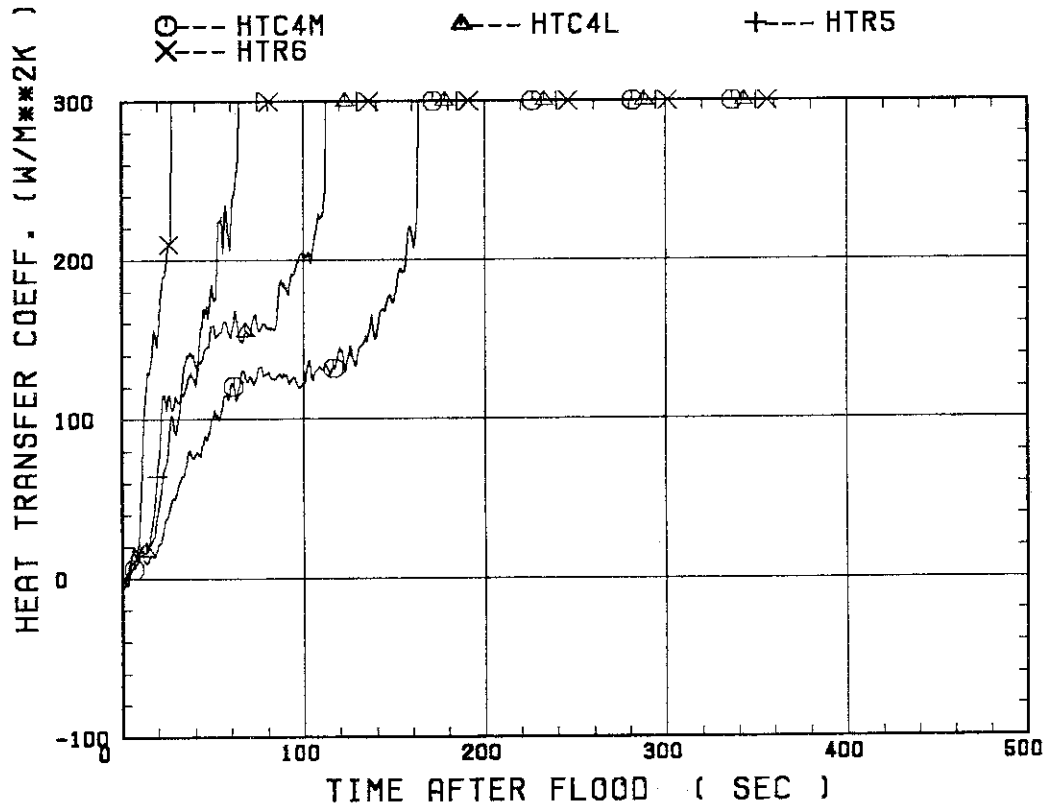
○--- TC4M △--- TC4L +--- TR5
 X--- TR6 ◇--- TC7



SMALL SCALE REFLOOD TEST
 RUN 8008

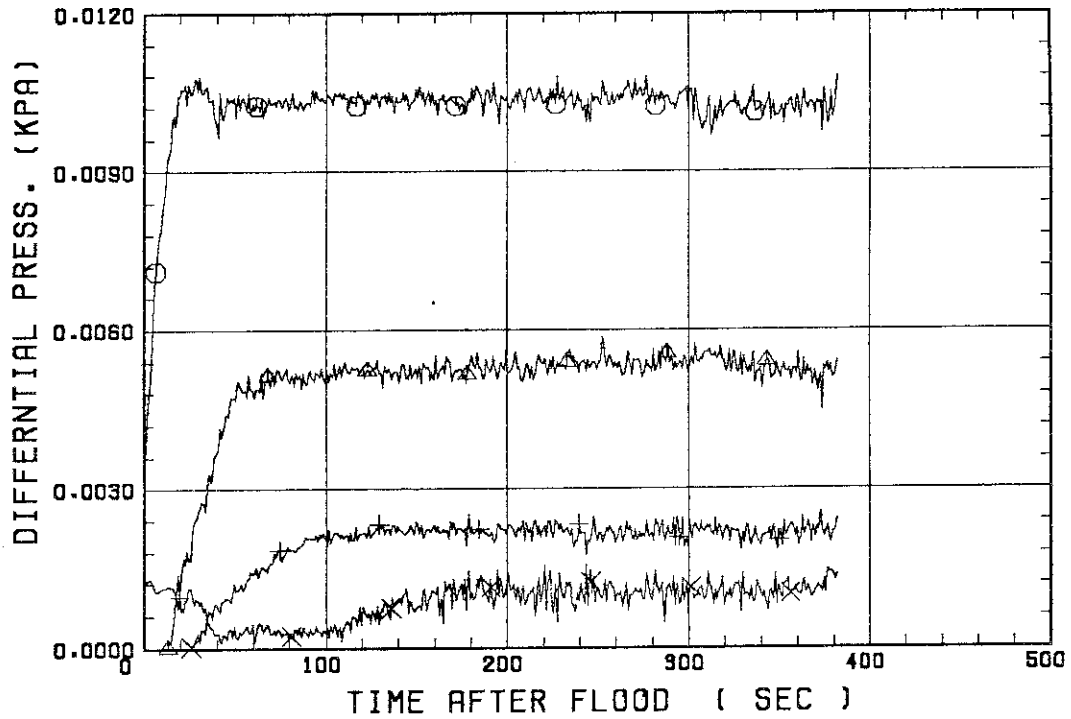


SMALL SCALE REFLOOD TEST
 RUN 8008



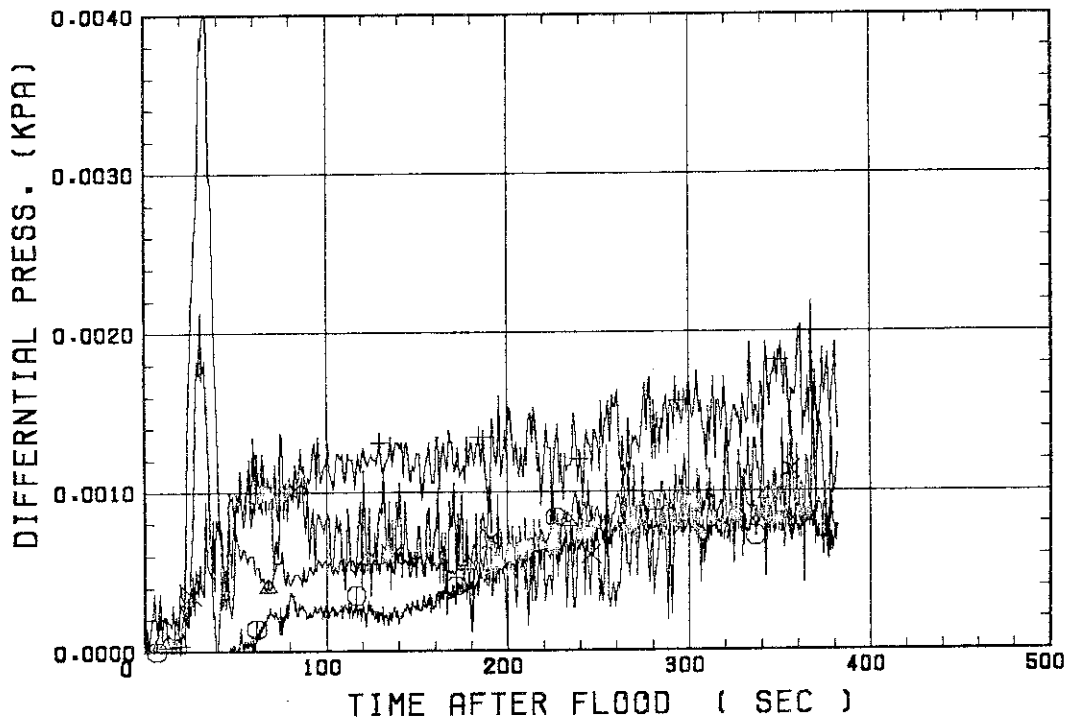
SMALL SCALE REFLOOD TEST
RUN 8008

○ --- DPT2 ▲ --- DPT4 + --- DPT5
X --- DPT6B



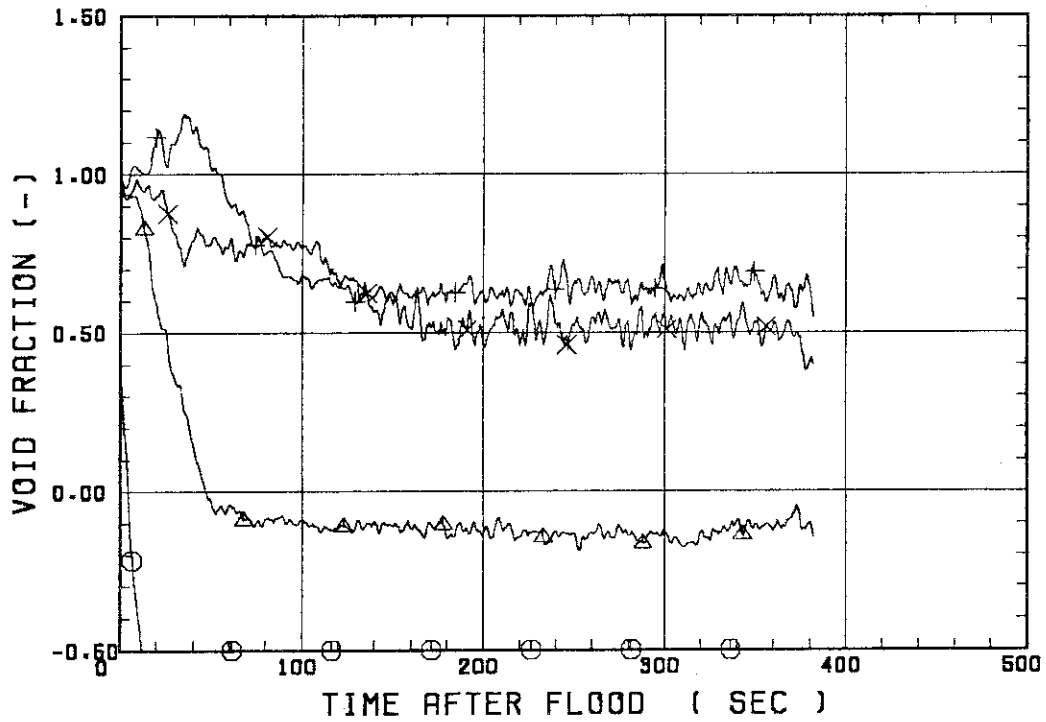
SMALL SCALE REFLOOD TEST
RUN 8008

○ --- DPT7 ▲ --- DPT8B + --- DP10
X --- DP12



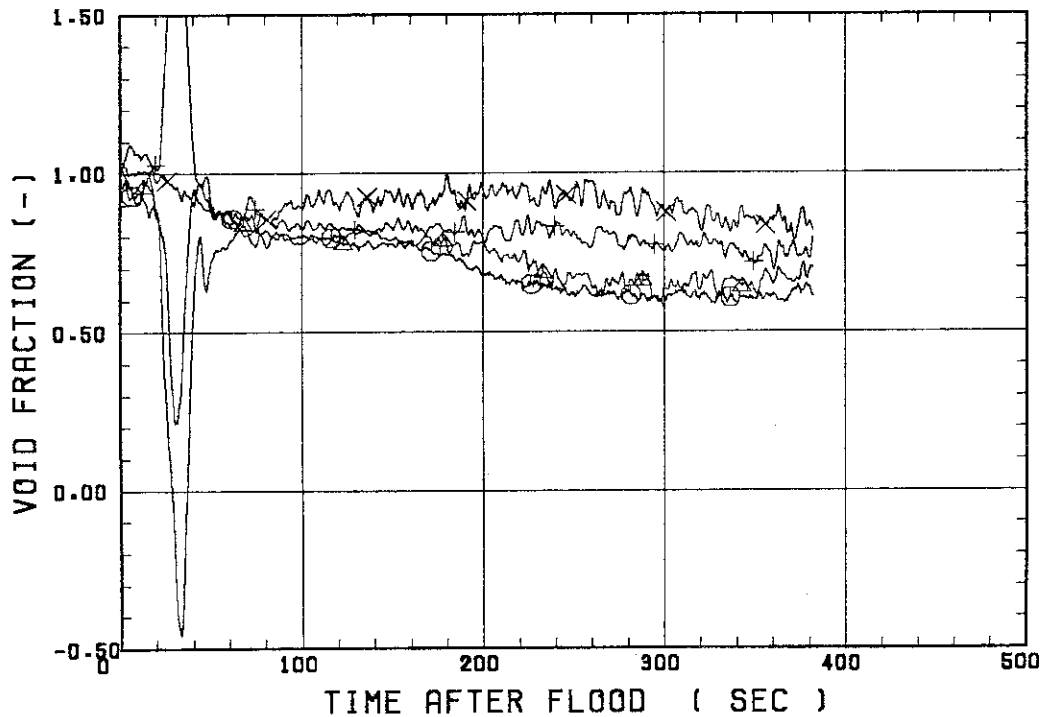
SMALL SCALE REFLOOD TEST
RUN 8008

○--- VDPT2 △--- VDPT4 +--- VDPT5
X--- VDPT6B



SMALL SCALE REFLOOD TEST
RUN 8008

○--- VDPT7 △--- VDPT8B +--- VDP10
X--- VDP12



 * RUN NO. 8009 *
 * *****

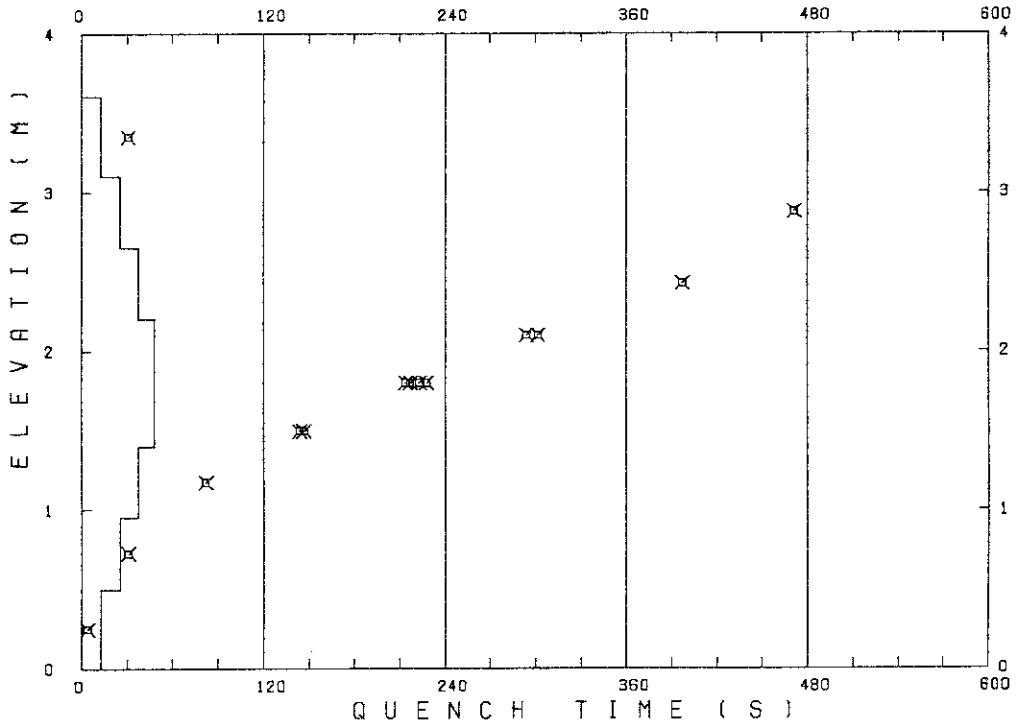
 TEST CONDITIONS

LINEAR PEAK POWER 2.0 KW/M
 SYSTEM PRESSURE 0.2 MPA
 INLET WATER TEMPERATURE 100 .C
 INJECTED WATER VELOCITY 3.9 CM/S

 TEMPERATURE PROFILE

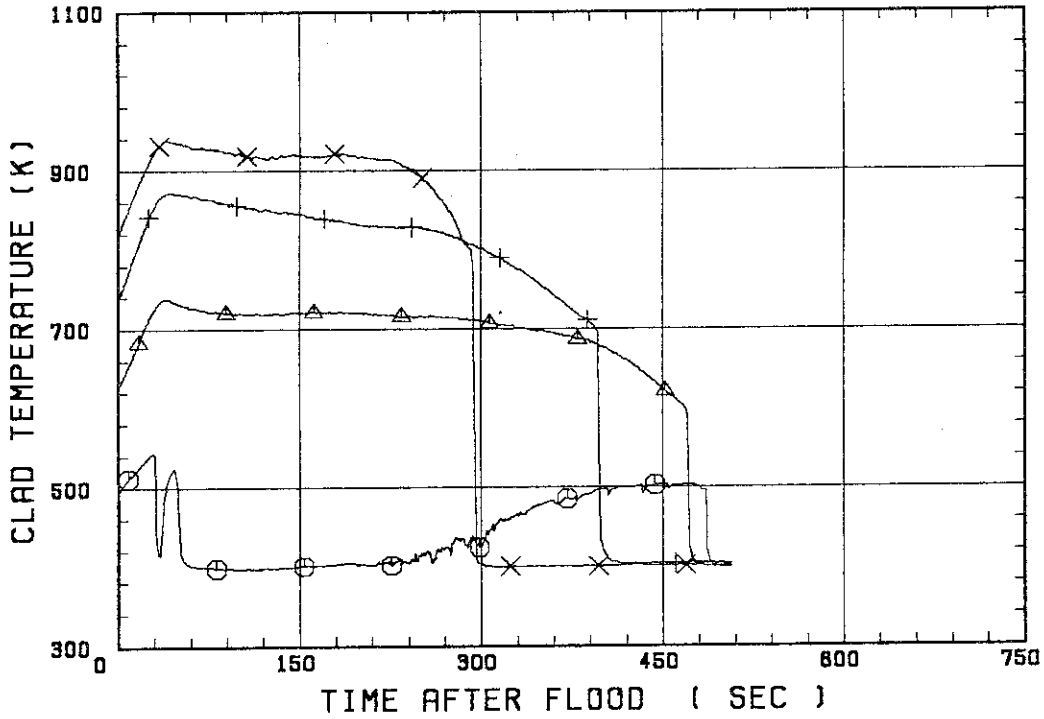
CH.NO.	SYMBOL	INITIAL TEMP. (.C)	TURNAROUND TIME (S)	TURNAROUND TEMP. (.C)	QUENCH TIME (S)	QUENCH TEMP. (.C)
66	TC1L	222	30.0	270	31.0	268
51	TR2	352	43.0	465	471.0	317
52	TR3	461	44.0	600	397.0	420
67	TC4U	538	40.0	666	294.0	492
7	TS4U	562	39.5	713	301.5	486
53	TR4M	547	50.0	690	228.0	486
68	TC4M	541	49.0	660	217.0	489
8	TS4M	538	50.0	685	223.0	461
48	TB4M	557	51.0	693	214.0	508
69	TC4L	539	23.0	622	147.0	458
9	TS4L	551	25.0	641	144.0	462
54	TR5	460	19.0	524	82.0	421
55	TR6	329	12.0	354	31.0	289
70	TC7	223	4.0	227	4.0	227

RUN NO. 8009



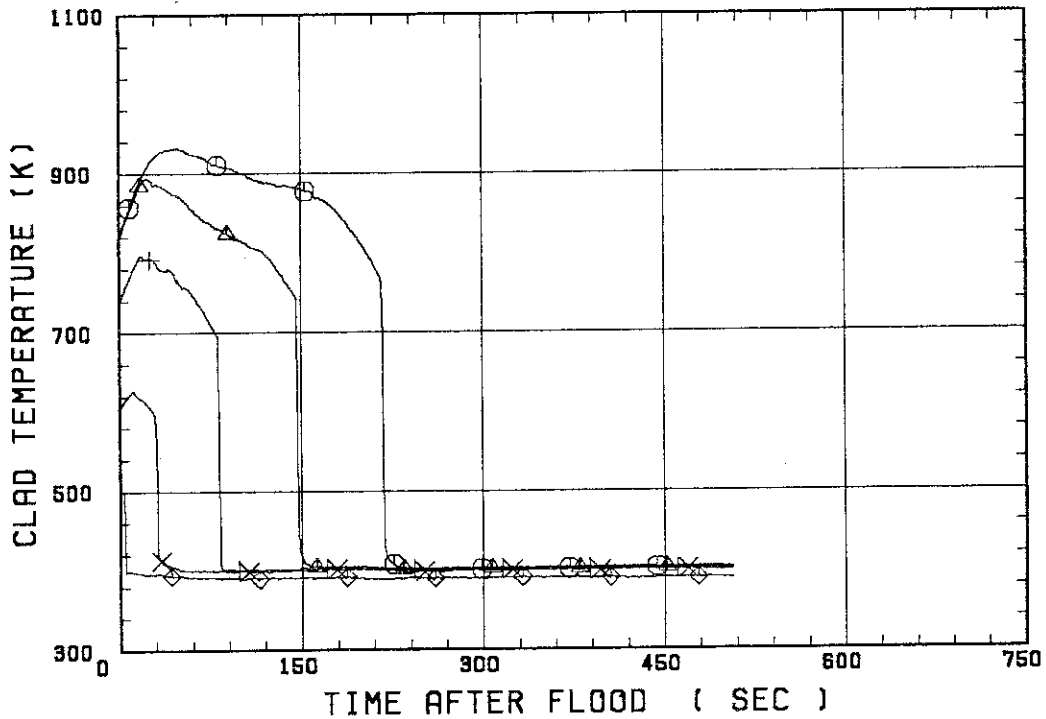
SMALL SCALE REFLOOD TEST
 RUN 8009

○--- TC1L △--- TR2 +--- TR3
 X--- TC4U

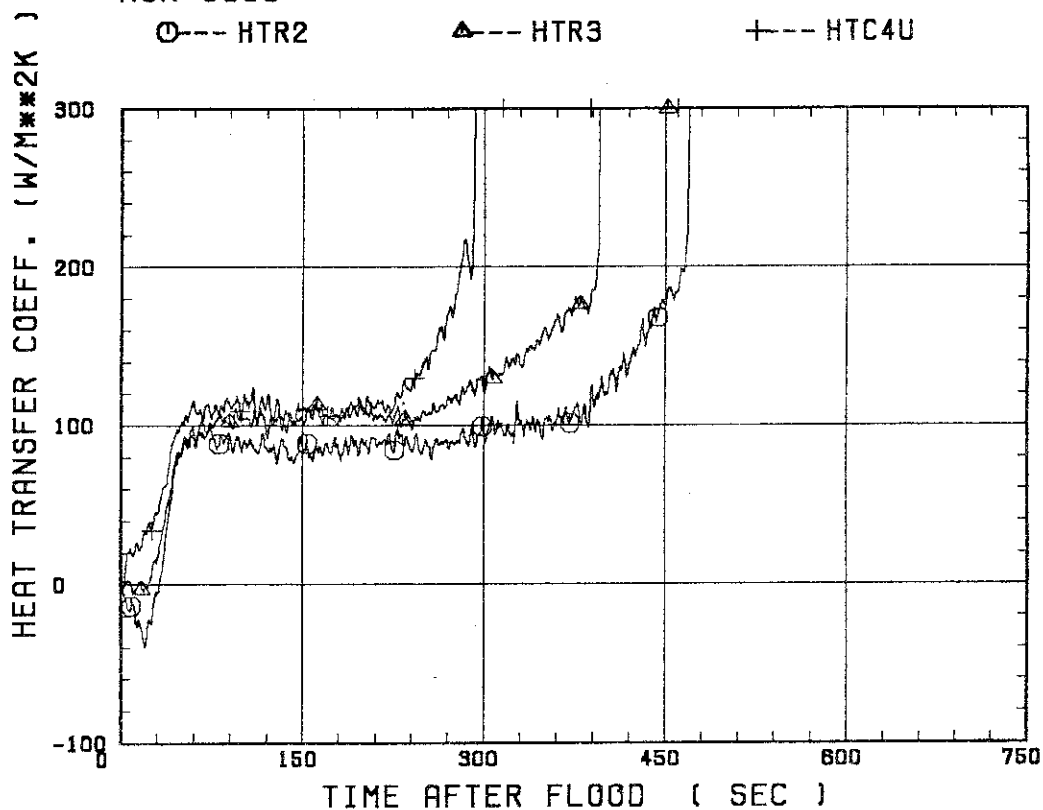


SMALL SCALE REFLOOD TEST
 RUN 8009

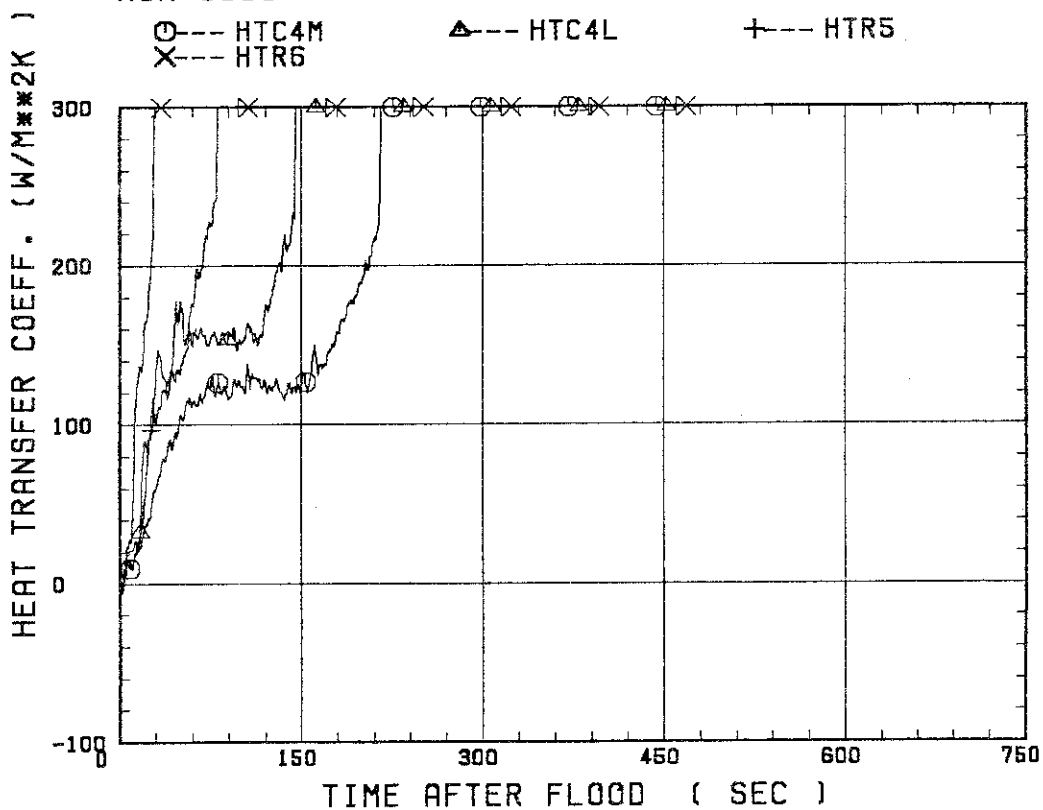
○--- TC4M △--- TC4L +--- TR5
 X--- TR6 ◇--- TC7



SMALL SCALE REFLOOD TEST
RUN 8009

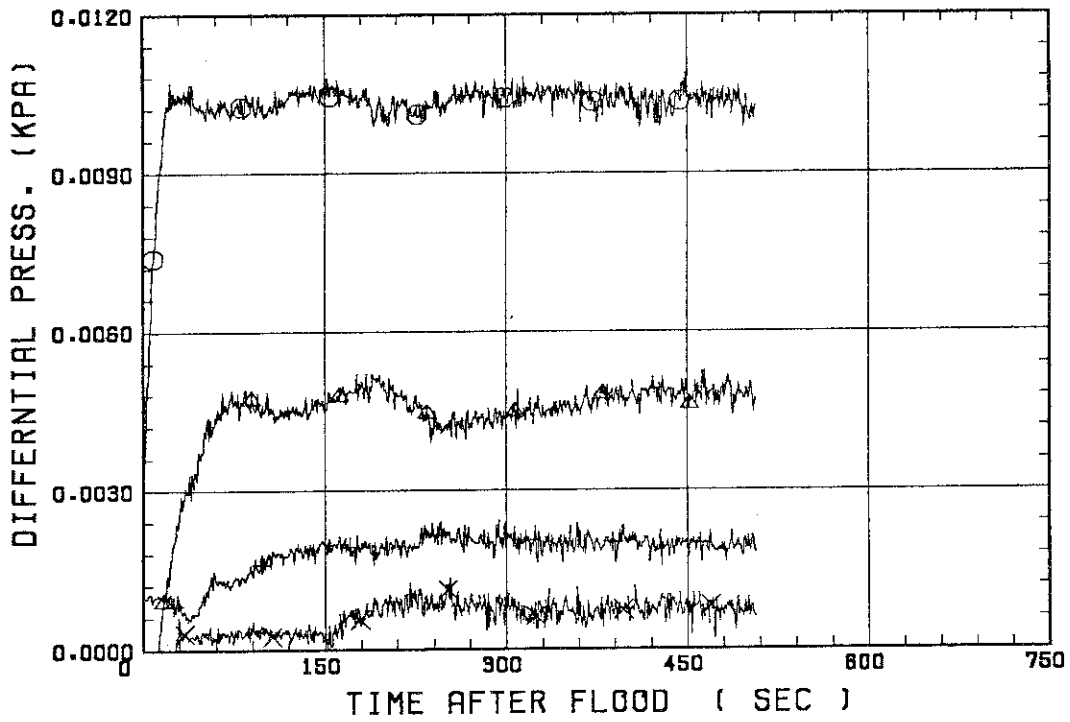


SMALL SCALE REFLOOD TEST
RUN 8009



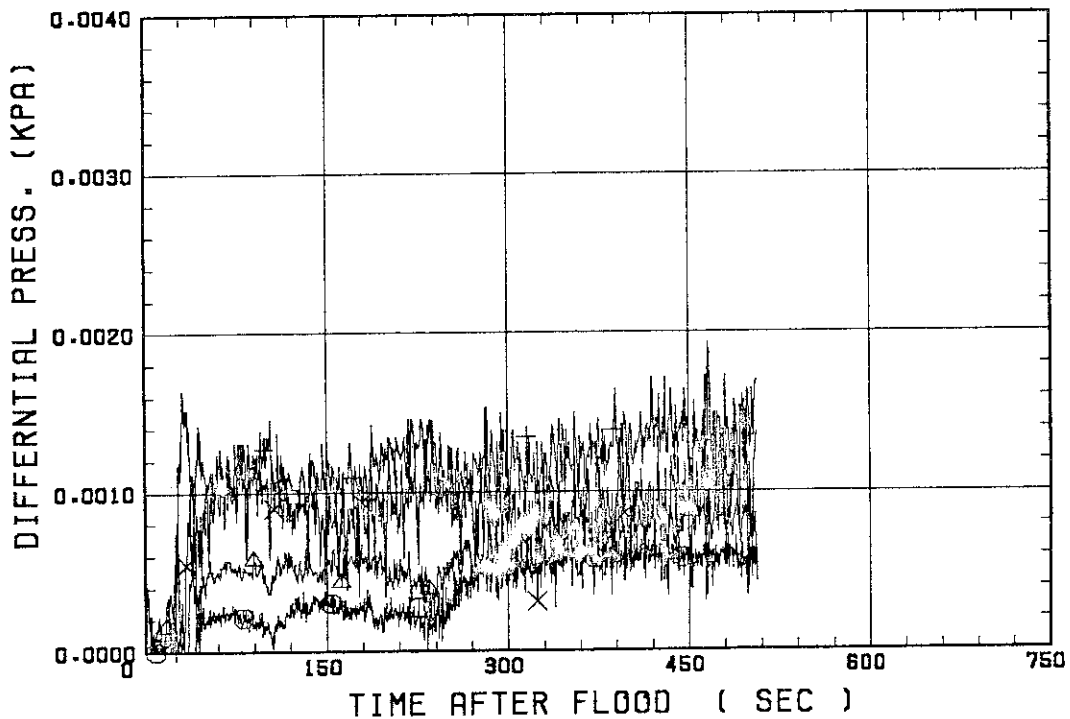
SMALL SCALE REFLOOD TEST
RUN 8009

○ --- DPT2 △ --- DPT4 + --- DPT5
X --- DPT6B



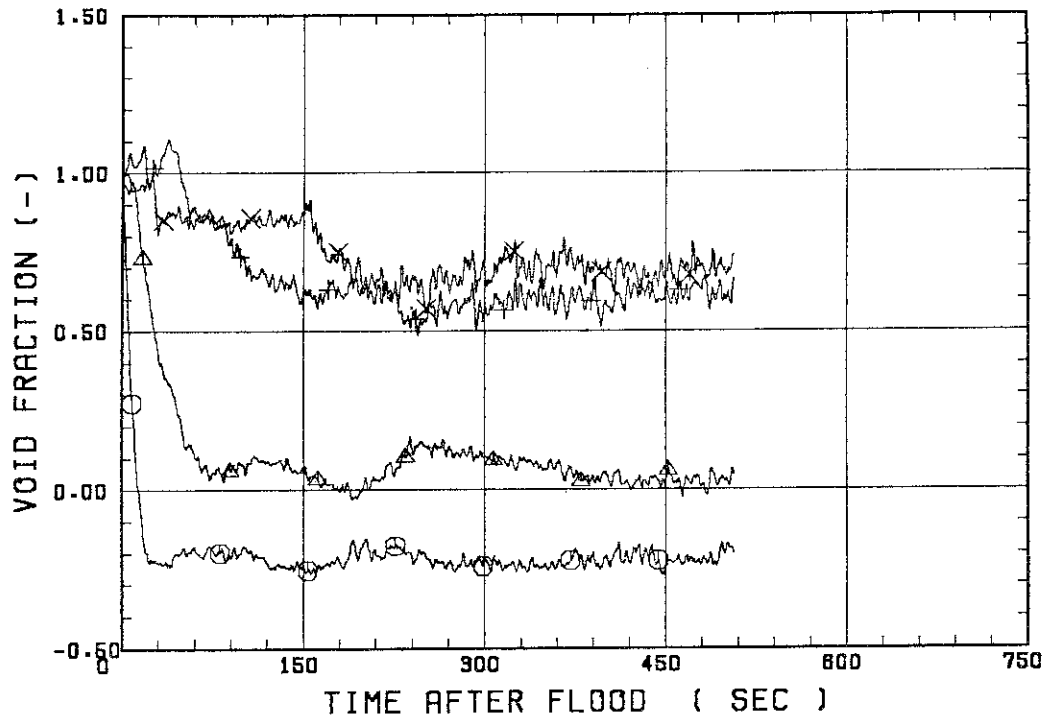
SMALL SCALE REFLOOD TEST
RUN 8009

○ --- DPT7 △ --- DPT8B + --- DP10
X --- DP12



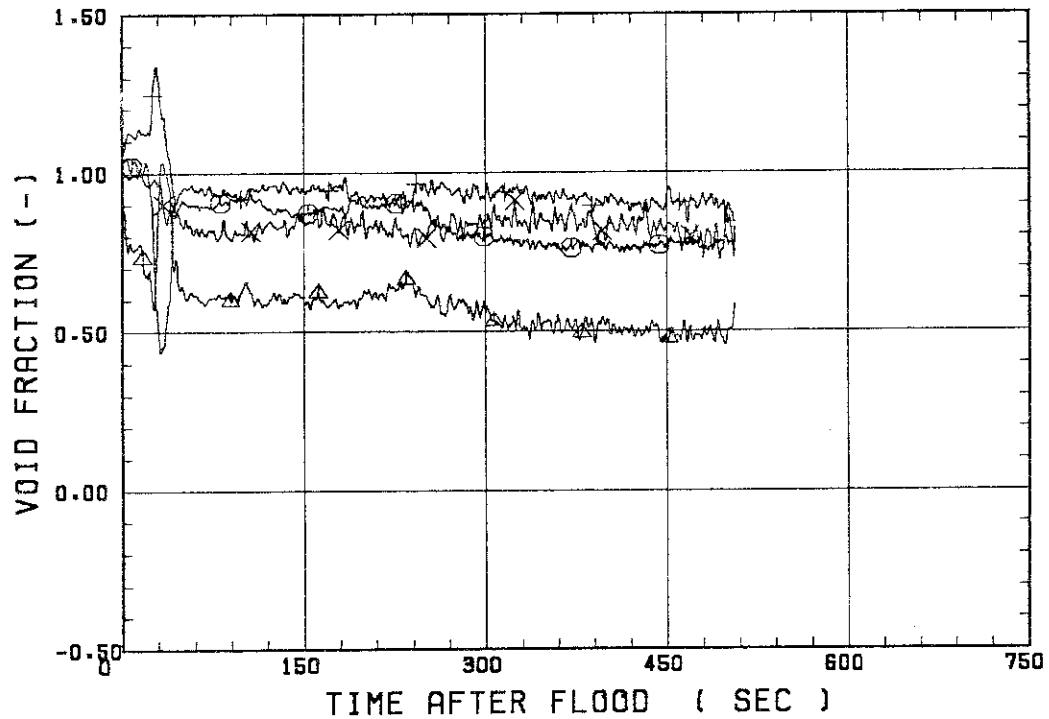
SMALL SCALE REFLOOD TEST
RUN 8009

○--- VDPT2 △--- VDPT4 +--- VDPT5
X--- VDPT6B



SMALL SCALE REFLOOD TEST
RUN 8009

○--- VDPT7 △--- VDPT8B +--- VDP10
X--- VDP12



 * RUN NO. 8011 *
 *

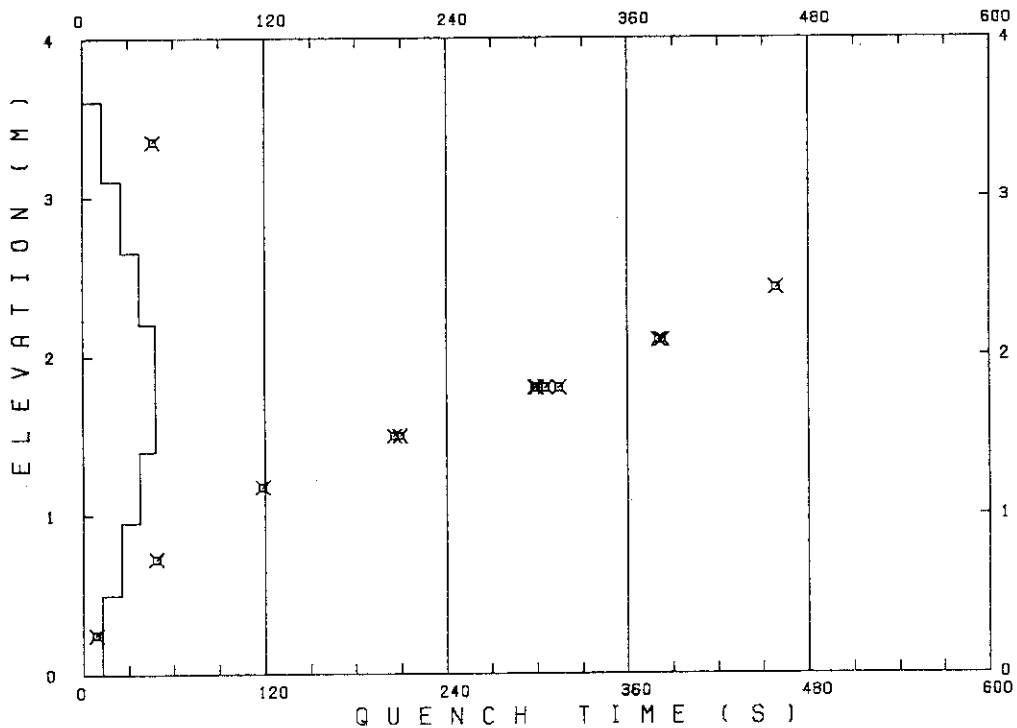
 TEST CONDITIONS

LINEAR PEAK POWER 1.6 KW/M
 SYSTEM PRESSURE 0.1 MPA
 INLET WATER TEMPERATURE 80 -C
 INJECTED WATER VELOCITY 4.0 CM/S

 TEMPERATURE PROFILE

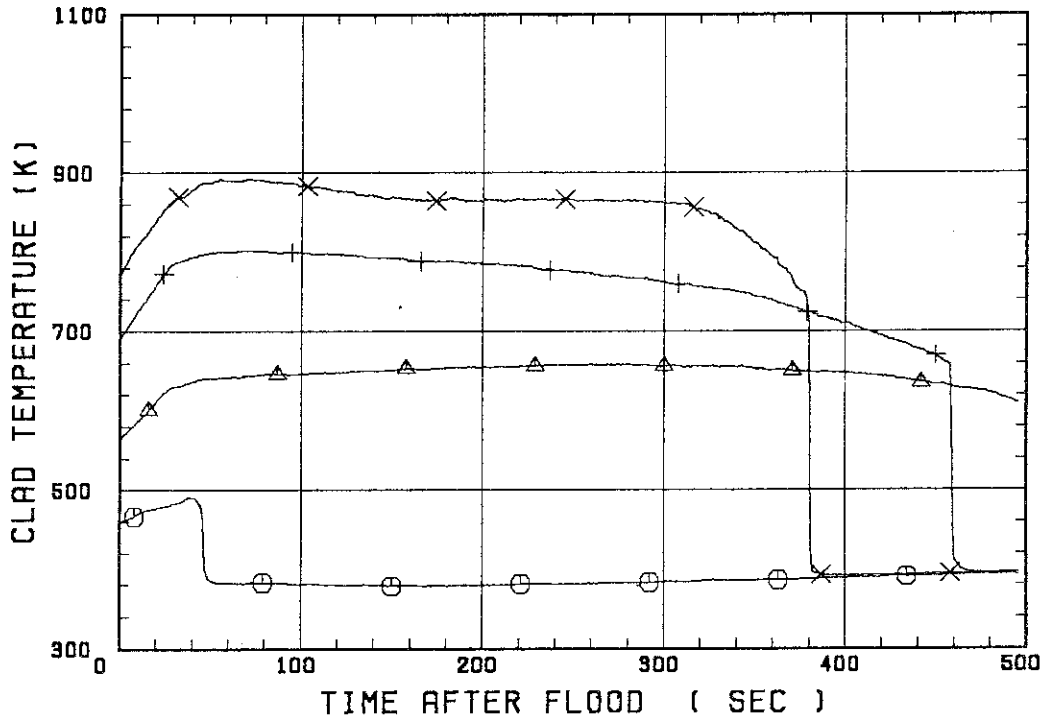
CH.NO.	SYMBOL	INITIAL TEMP. (.C)	TURNAROUND TIME (S)	TURNAROUND TEMP. (.C)	QUENCH TIME (S)	QUENCH TEMP. (.C)
66	TC1L	185	38.5	218	46.5	189
36	TA2	290	280.5	385		
37	TA3	415	69.5	529	458.5	384
67	TC4U	495	71.5	619	380.5	435
7	TS4U	548	55.0	688	383.0	433
53	TR4M	528	66.5	669	314.5	422
68	TC4M	494	66.5	623	299.5	435
8	TS4M	522	56.0	656	305.5	427
48	TB4M	533	50.5	668	298.5	465
69	TC4L	505	39.5	595	209.5	390
9	TS4L	541	33.5	637	205.5	412
54	TR5	458	29.5	522	118.5	361
55	TR6	325	15.5	350	48.5	298
70	TC7	200	7.5	207	8.5	207

RUN NO. 8011



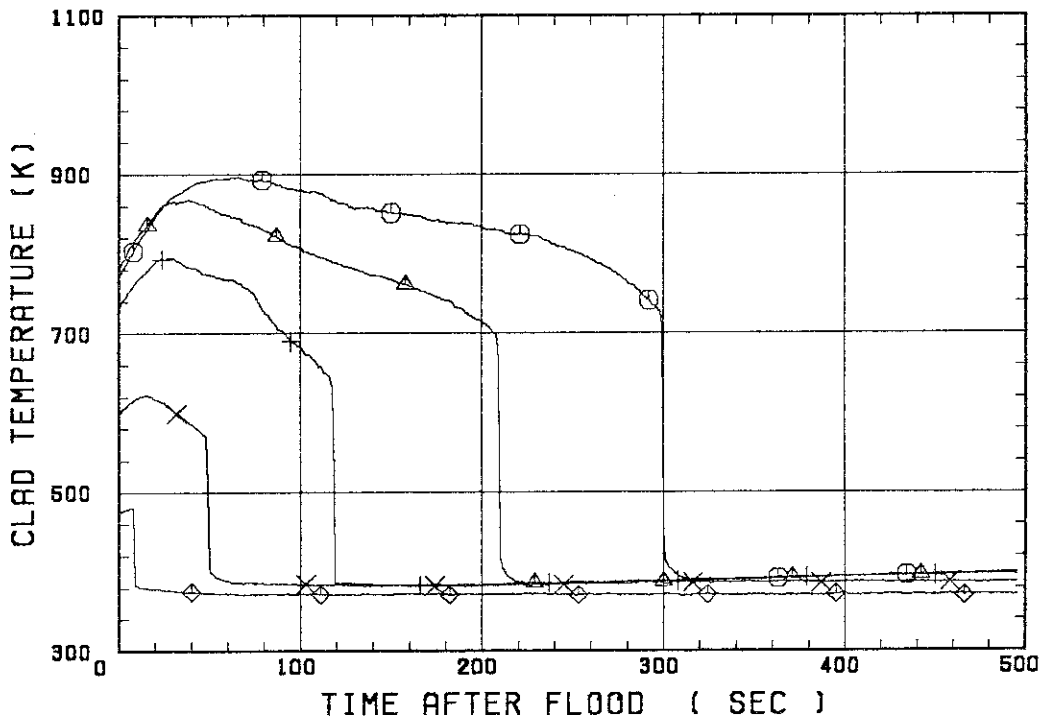
SMALL SCALE REFLOOD TEST
RUN 8011

○--- TC1L ▲--- TA2 +--- TA3
X--- TC4U

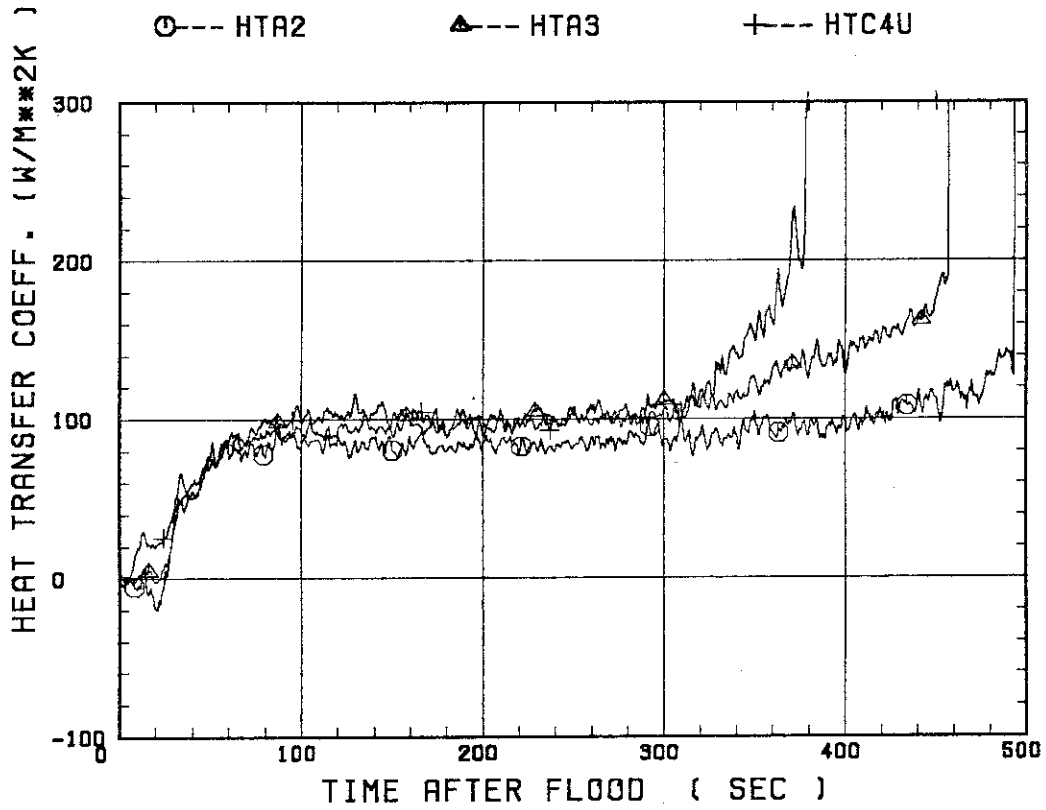


SMALL SCALE REFLOOD TEST
RUN 8011

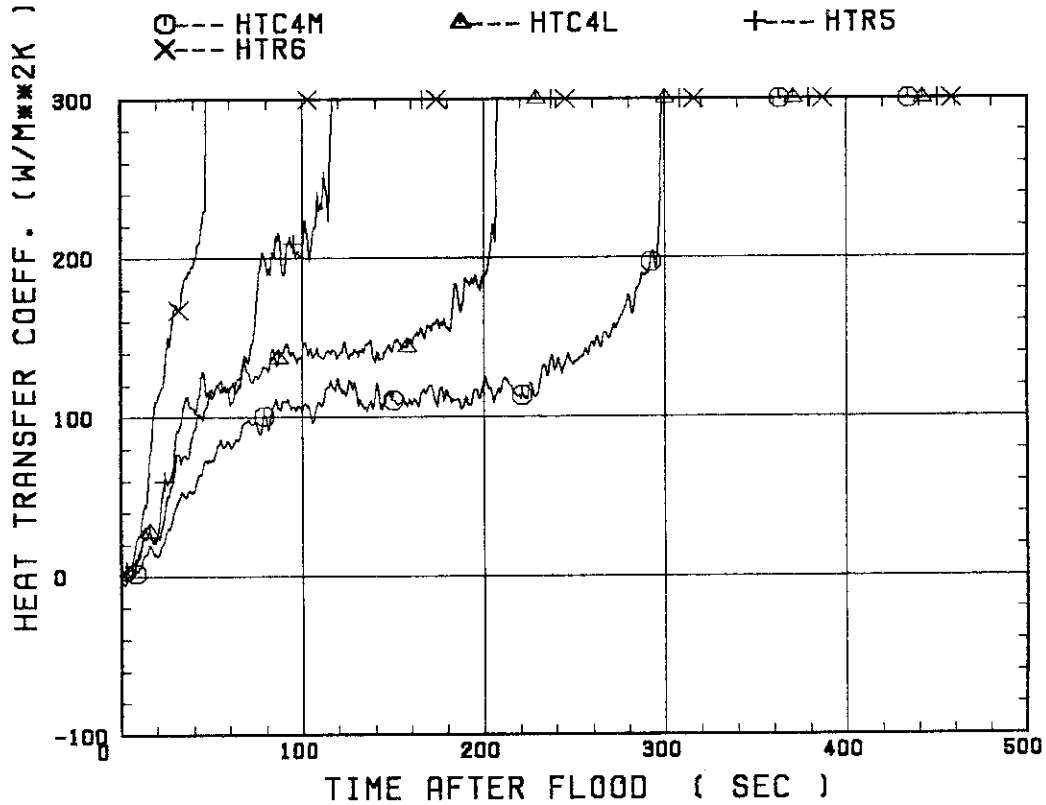
○--- TC4M ▲--- TC4L +--- TR5
X--- TR6 ◆--- TC7



SMALL SCALE REFLOOD TEST
RUN 8011

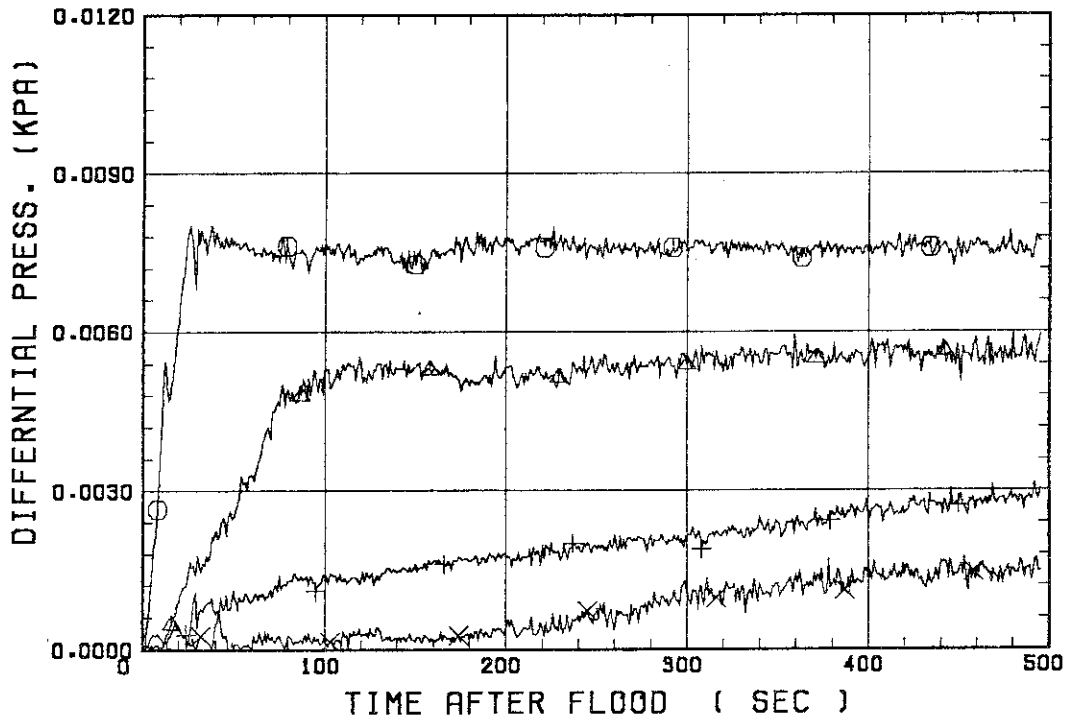


SMALL SCALE REFLOOD TEST
RUN 8011



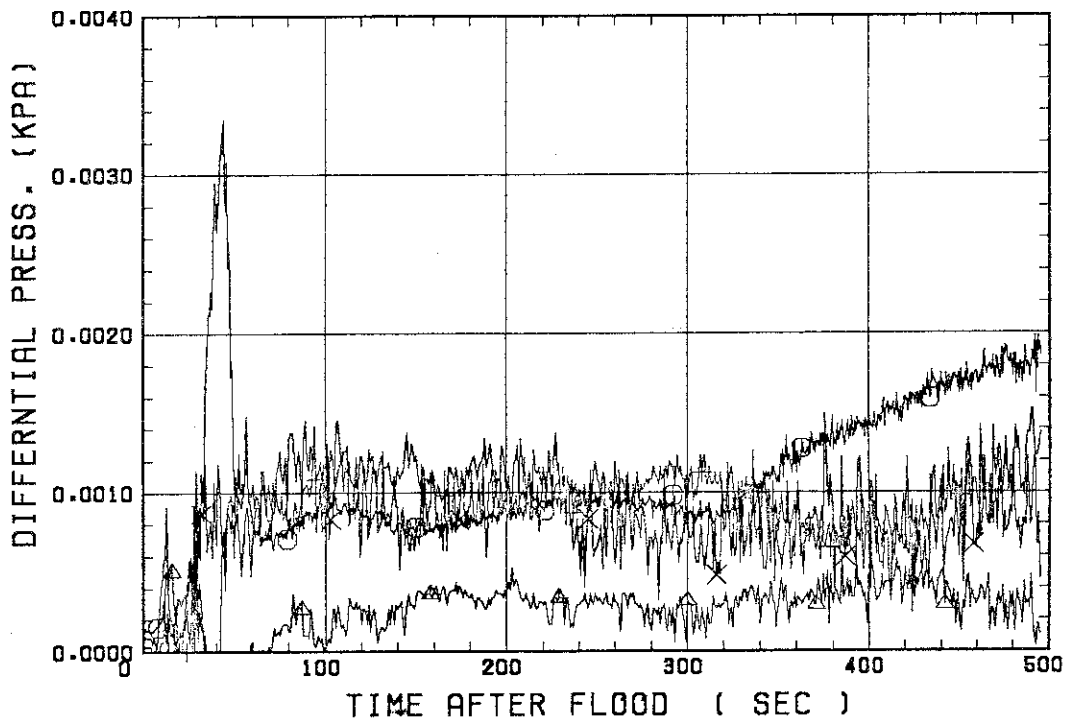
SMALL SCALE REFLOOD TEST
 RUN 8011

○ --- DPT2 ▲ --- DPT4 + --- DPT5
 X --- DPT6B



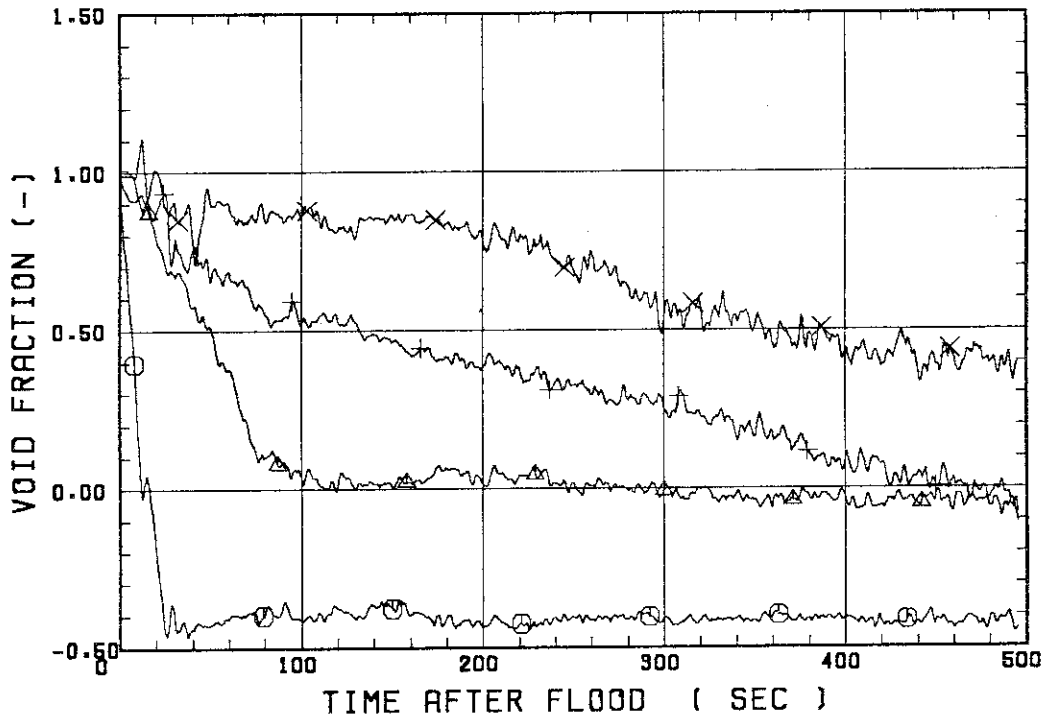
SMALL SCALE REFLOOD TEST
 RUN 8011

○ --- DPT7 ▲ --- DPT8B + --- DP10
 X --- DP12



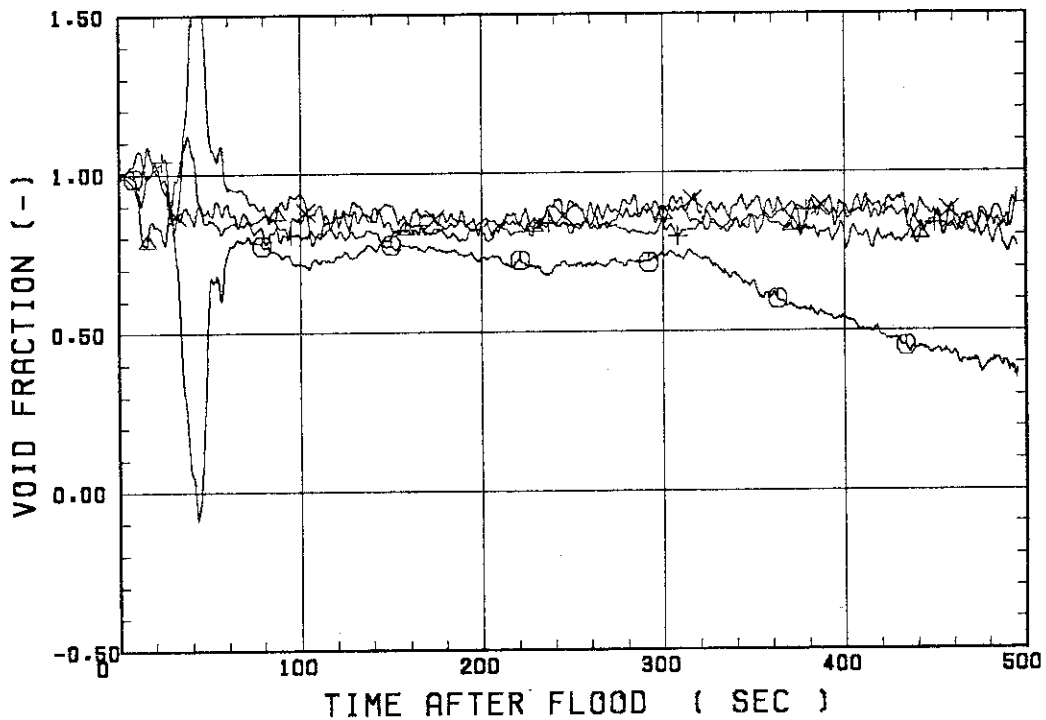
SMALL SCALE REFLOOD TEST
RUN 8011

○--- VDPT2 △--- VDPT4 +--- VDPT5
X--- VDPT6B



SMALL SCALE REFLOOD TEST
RUN 8011

○--- VDPT7 △--- VDPT8B +--- VDP10
X--- VDP12



 * RUN NO. 8012 *

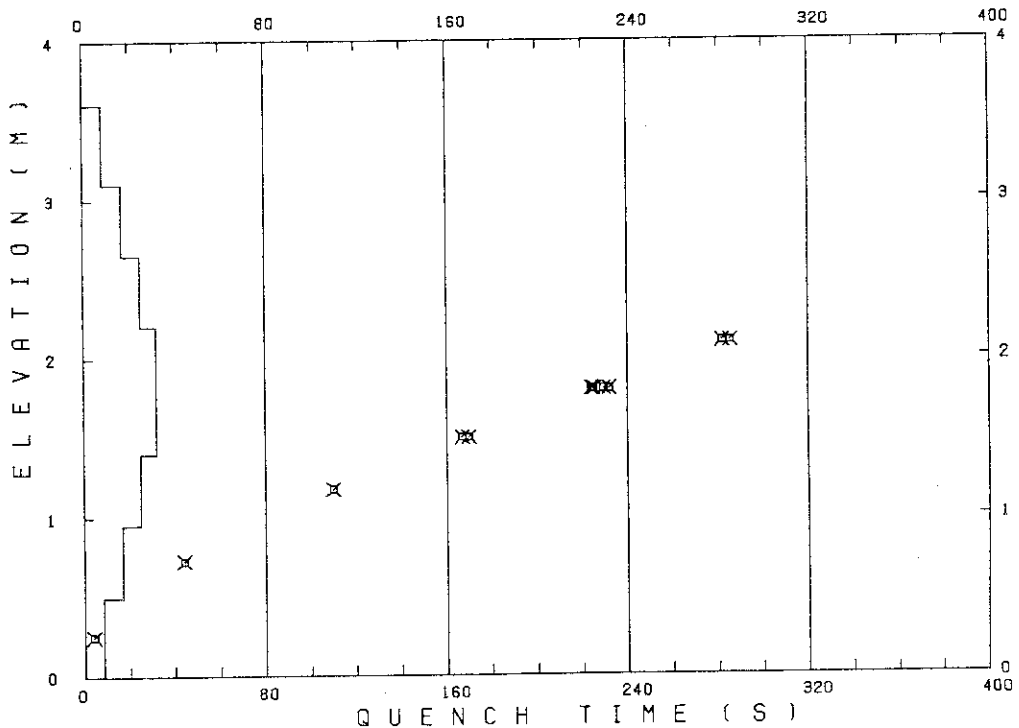
 TEST CONDITIONS

LINEAR PEAK POWER 1.8 KW/M
 SYSTEM PRESSURE 0.1 MPA
 INLET WATER TEMPERATURE 80 .C
 INJECTED WATER VELOCITY 4.1 CM/S

 TEMPERATURE PROFILE

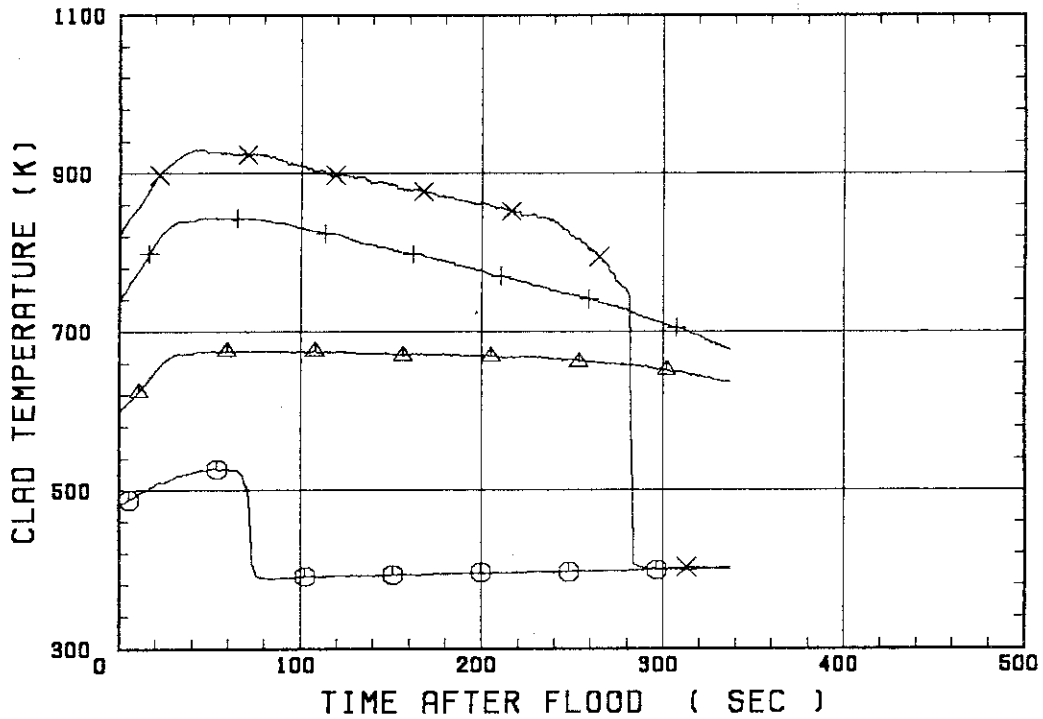
CH.NO.	SYMBOL	INITIAL TEMP. (.C)	TURNAROUND TIME (S)	TURNAROUND TEMP. (.C)	QUENCH TIME (S)	QUENCH TEMP. (.C)
66	TC1L	206	53.0	255		
36	TA2	323	108.0	403		
37	TA3	463	54.0	571		
67	TC4U	545	45.0	657	282.0	471
7	TS4U	574	44.5	708	285.5	444
53	TR4M	552	67.0	691	232.0	455
68	TC4M	539	56.0	654	225.0	452
8	TS4M	547	52.0	681	229.5	449
48	TB4M	561	69.0	691	224.0	464
69	TC4L	552	27.0	630	170.0	427
9	TS4L	569	28.0	654	167.0	424
54	TR5	469	22.0	530	110.0	387
55	TR6	329	12.0	349	44.0	304
70	TC7	215	3.0	219	4.0	218

RUN NO. 8012



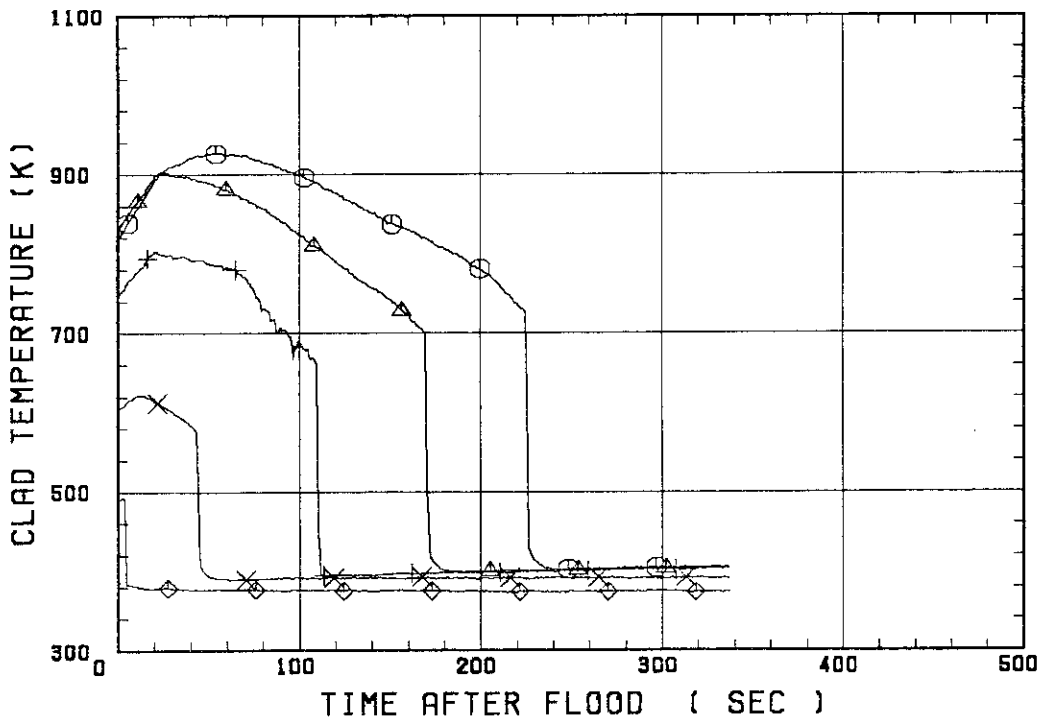
SMALL SCALE REFLOOD TEST
RUN 8012

○--- TC1L ▲--- TA2 +--- TA3
X--- TC4U

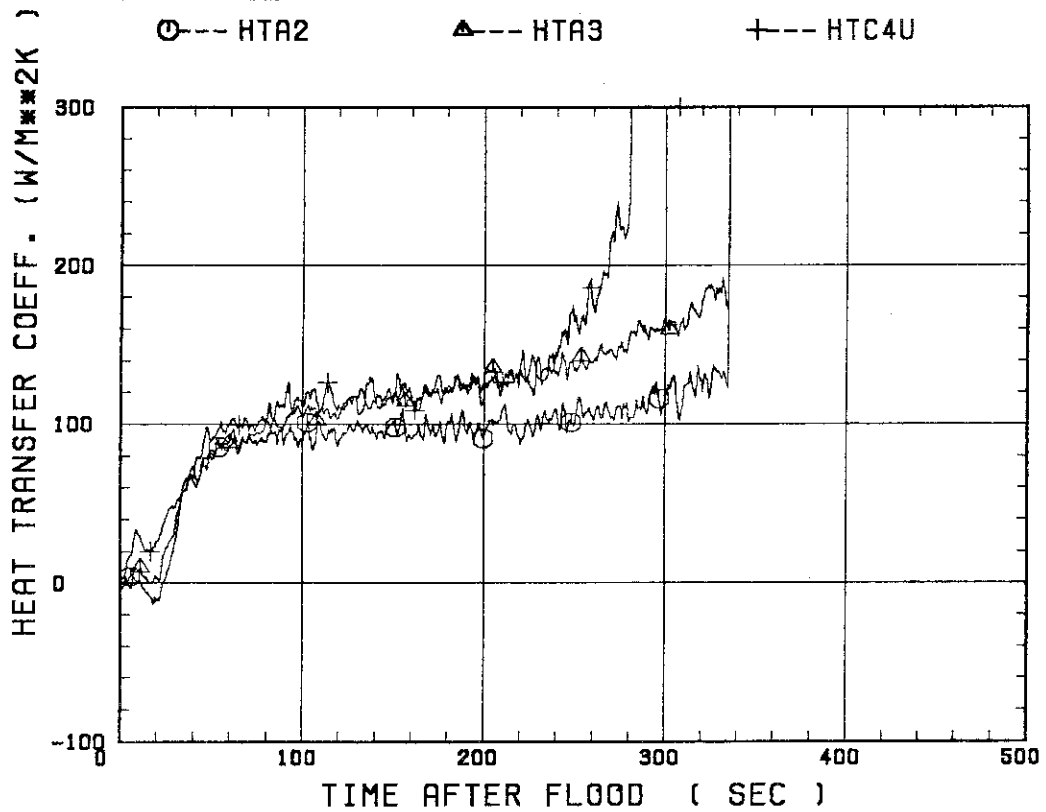


SMALL SCALE REFLOOD TEST
RUN 8012

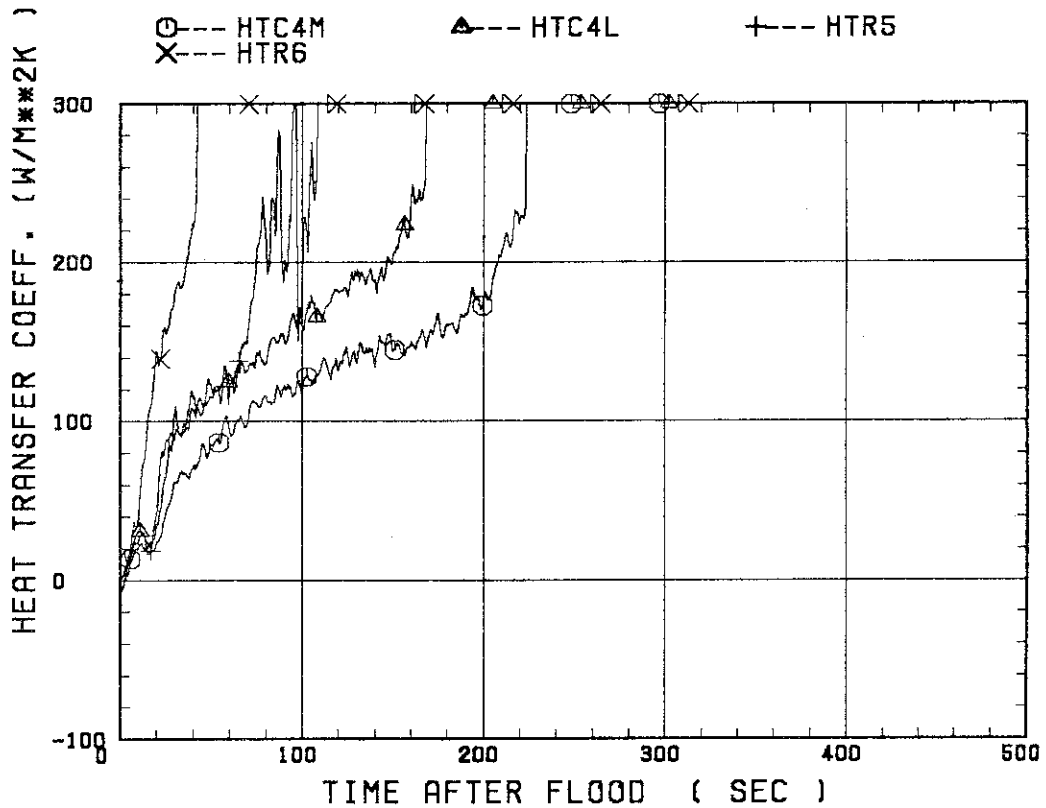
○--- TC4M ▲--- TC4L +--- TR5
X--- TR6 ◆--- TC7



SMALL SCALE REFLOOD TEST
RUN 8012

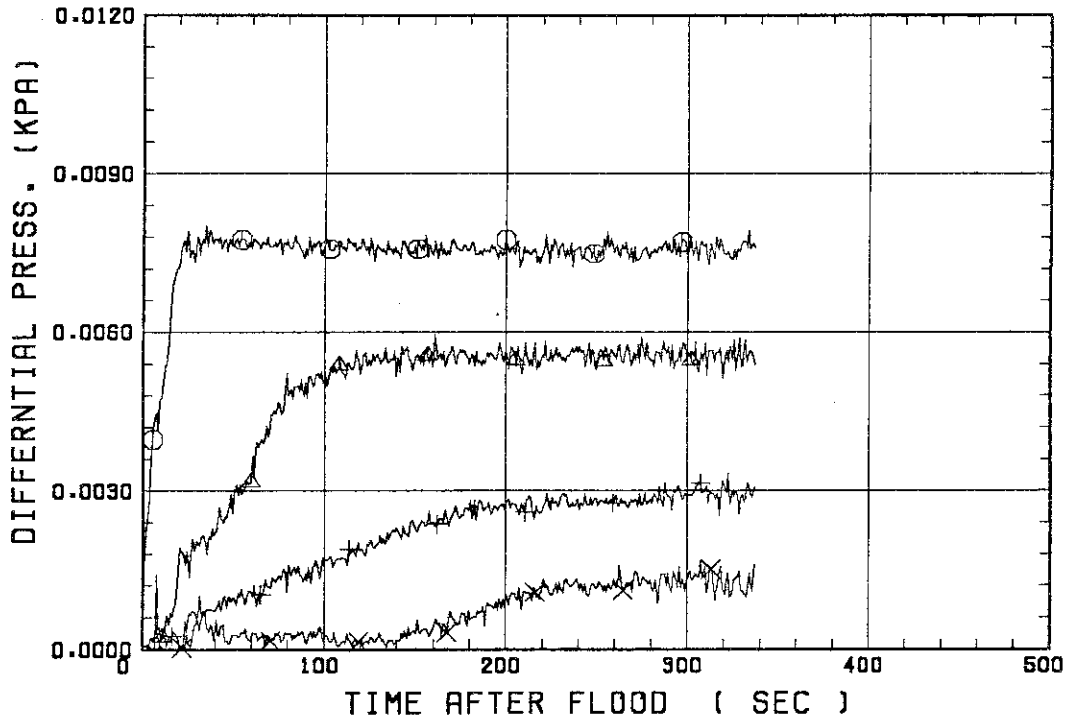


SMALL SCALE REFLOOD TEST
RUN 8012



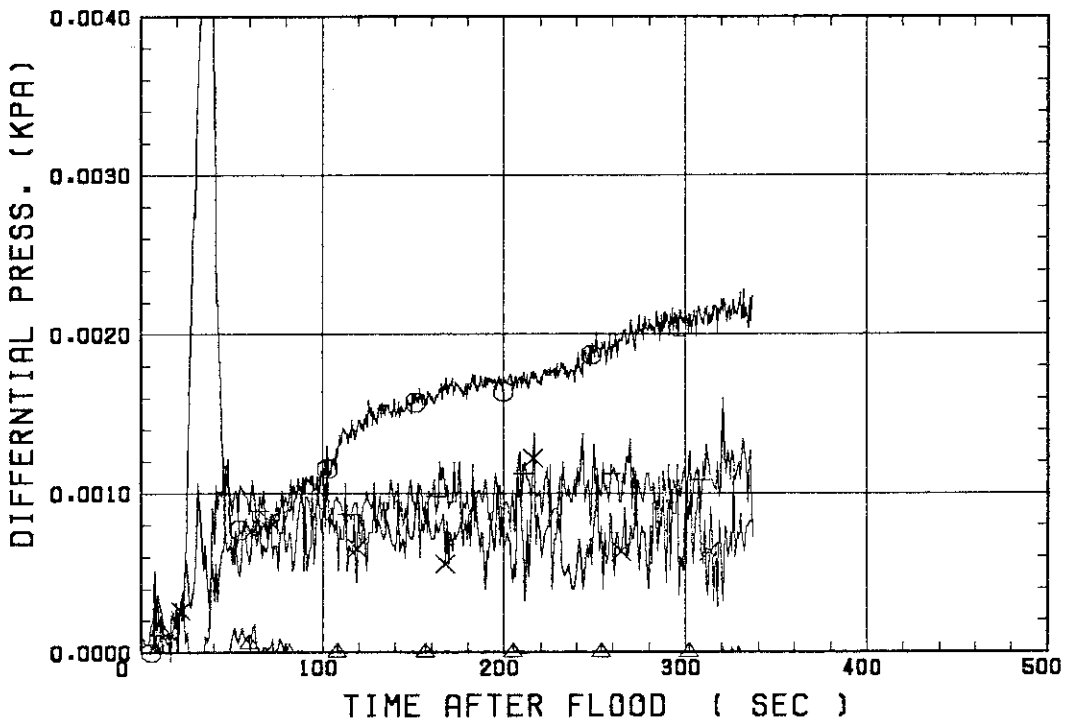
SMALL SCALE REFLOOD TEST
RUN 8012

○--- DPT2 △--- DPT4 +--- DPT5
X--- DPT6B



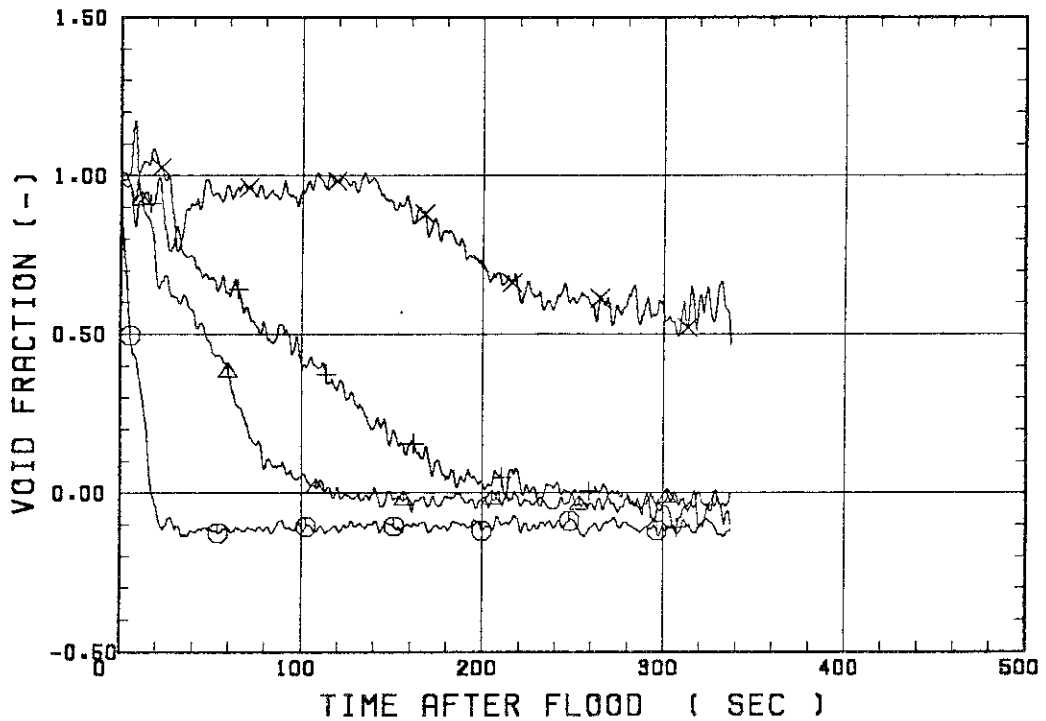
SMALL SCALE REFLOOD TEST
RUN 8012

○--- DPT7 △--- DPT8B +--- DP10
X--- DP12



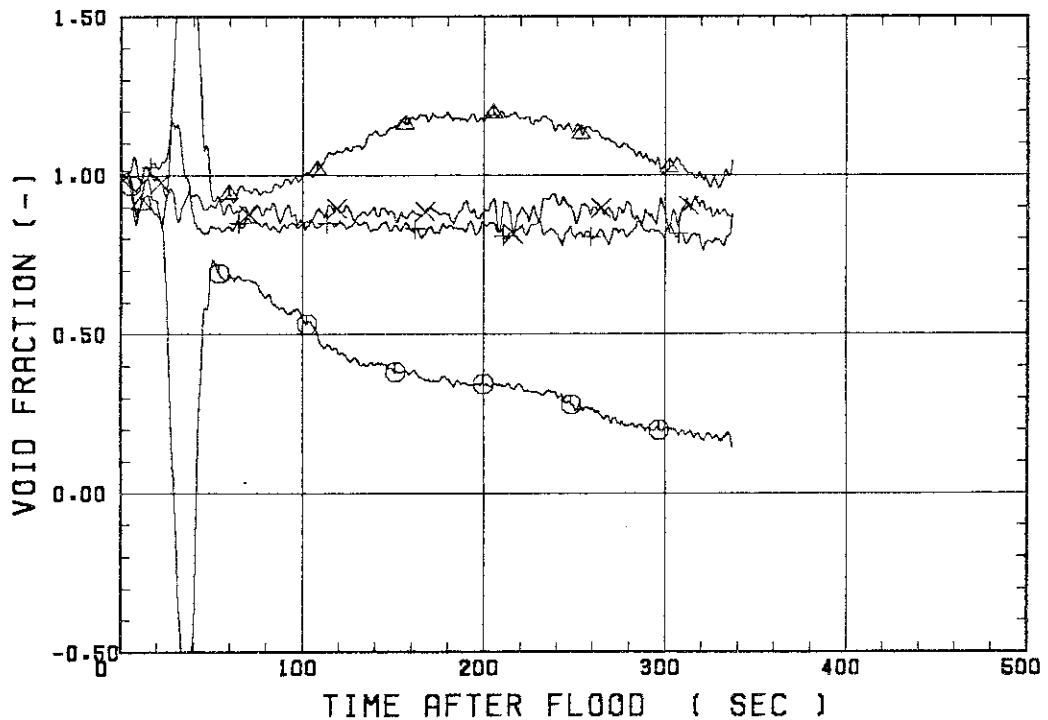
SMALL SCALE REFLOOD TEST
RUN 8012

○--- VDPT2 ▲--- VDPT4 +--- VDPT5
X--- VDPT6B



SMALL SCALE REFLOOD TEST
RUN 8012

○--- VDPT7 ▲--- VDPT8B +--- VDP10
X--- VDP12



 * RUN NO. 8107 *

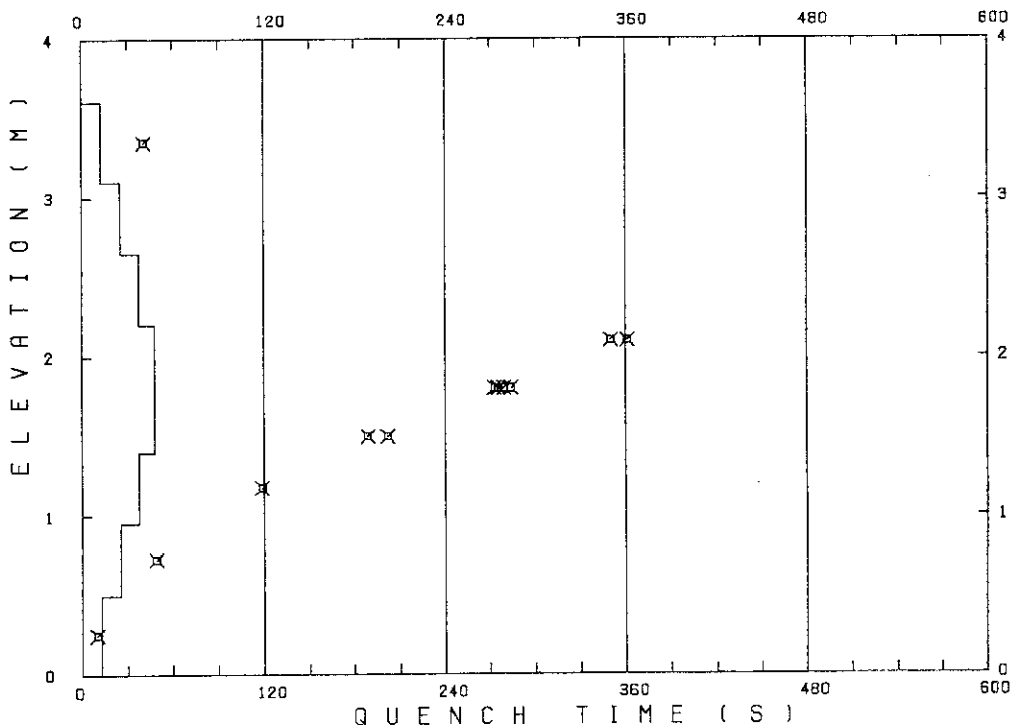
 TEST CONDITIONS

LINEAR PEAK POWER 1.6 KW/M
 SYSTEM PRESSURE 0.1 MPA
 INLET WATER TEMPERATURE 80 .C
 INJECTED WATER VELOCITY 3.8 CM/S

 TEMPERATURE PROFILE

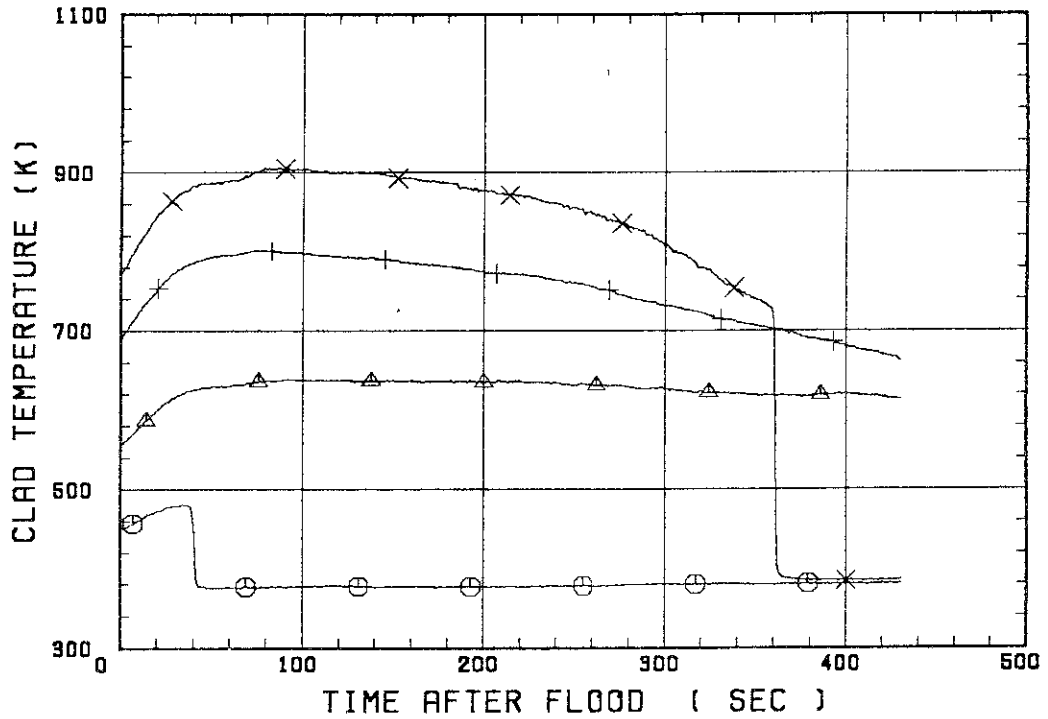
CH.NO.	SYMBOL	INITIAL TEMP. (.C)	TURNAROUND TIME (S)	TURNAROUND TEMP. (.C)	QUENCH TIME (S)	QUENCH TEMP. (.C)
66	TC1L	176	35.0	208	41.0	165
36	TA2	281	125.0	365		
37	TA3	414	79.0	528		
67	TC4U	494	87.0	634	361.0	417
7	TS4U	548	74.5	684	350.0	426
53	TR4M	518	33.0	620	284.0	354
68	TC4M	489	34.0	582	279.0	364
8	TS4M	521	34.5	620	275.5	360
48	TB4M	524	34.0	630	273.0	372
69	TC4L	509	33.0	595	202.0	392
9	TS4L	535	30.0	627	189.0	397
54	TR5	444	23.0	511	119.0	361
55	TR6	309	17.0	341	49.0	287
70	TC7	172	9.0	181	10.0	181

RUN NO. 8107



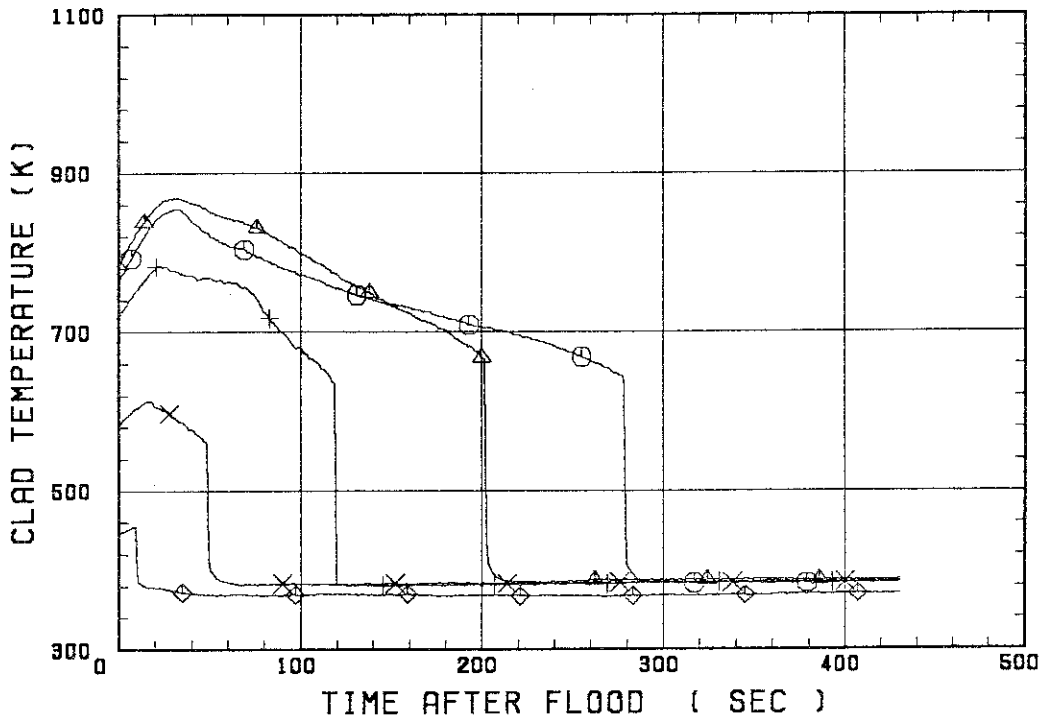
SMALL SCALE REFLOOD TEST
 RUN 8107

○--- TC1L ▲--- TR2 +--- TR3
 X--- TC4U

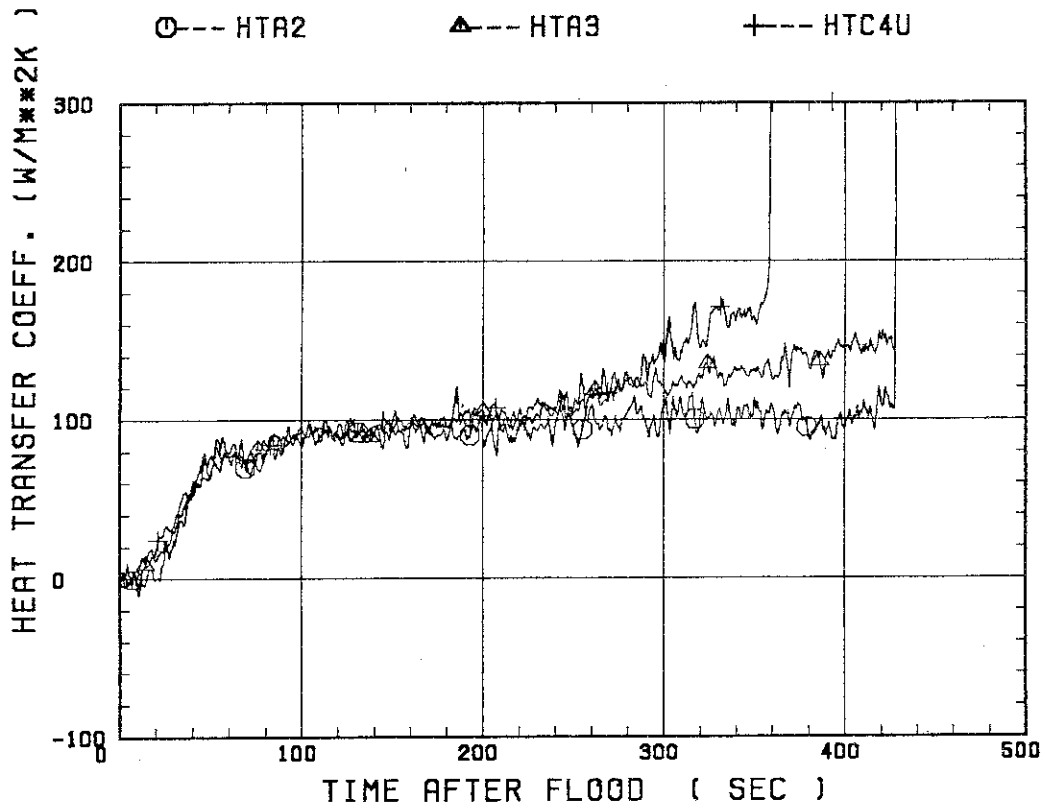


SMALL SCALE REFLOOD TEST
 RUN 8107

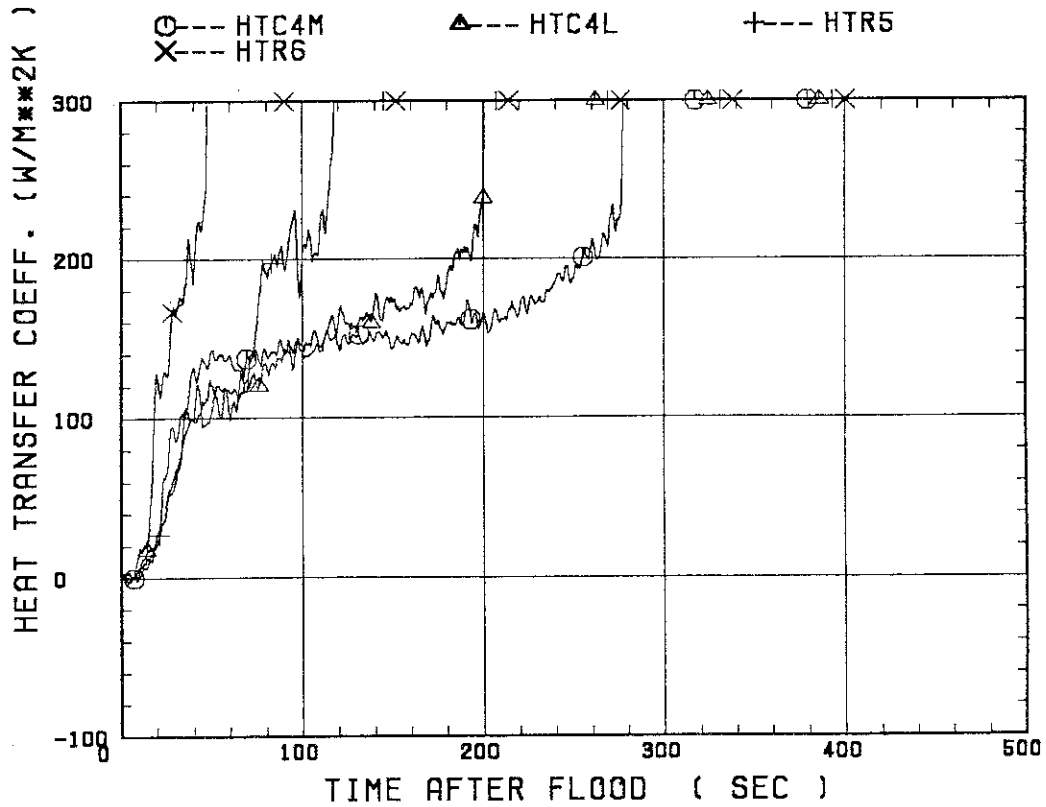
○--- TC4M ▲--- TC4L +--- TR5
 X--- TR6 ◆--- TC7



SMALL SCALE REFLOOD TEST
 RUN 8107

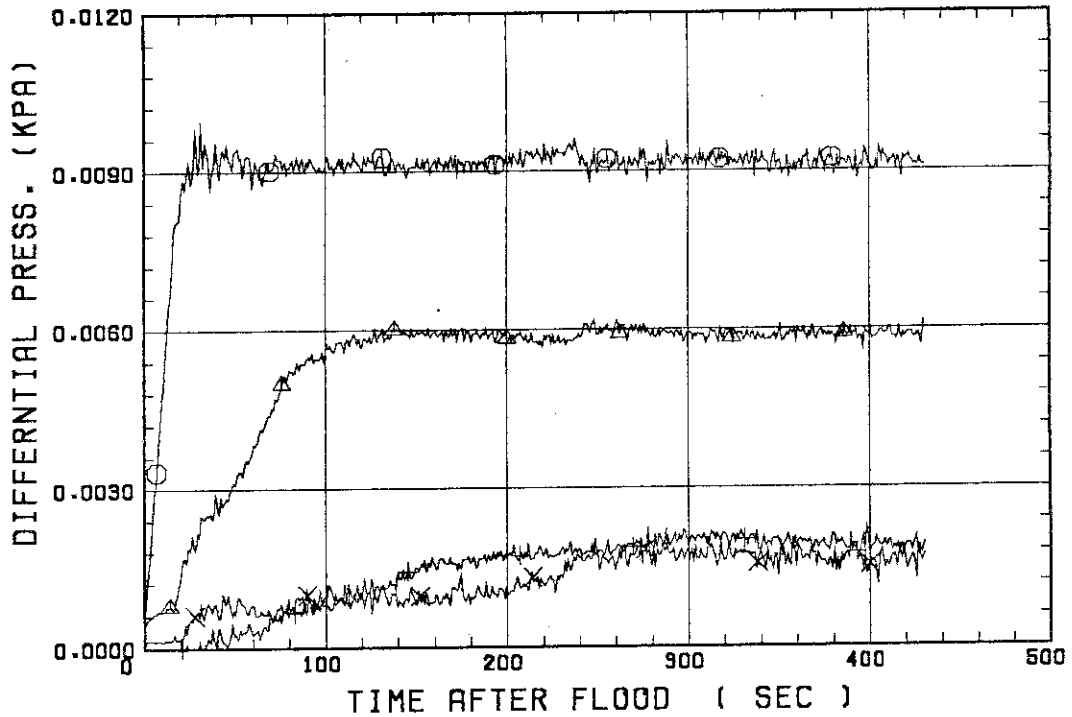


SMALL SCALE REFLOOD TEST
 RUN 8107



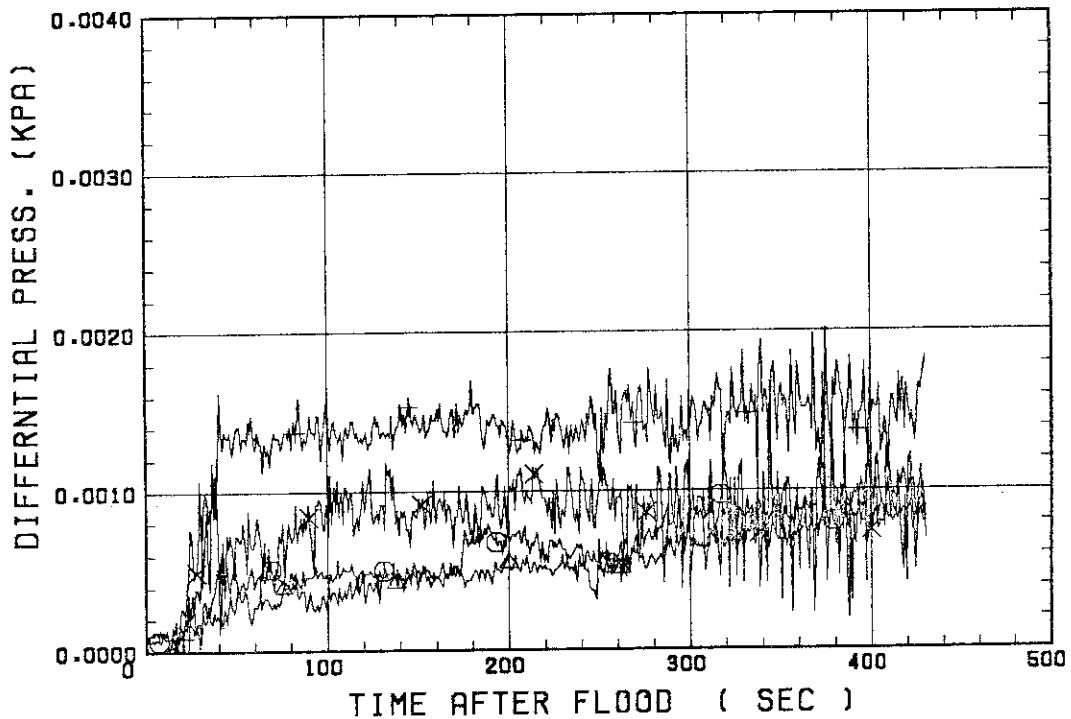
SMALL SCALE REFLOOD TEST
RUN 8107

○ --- DPT2 ▲ --- DPT4 + --- DPT5
X --- DPT6B



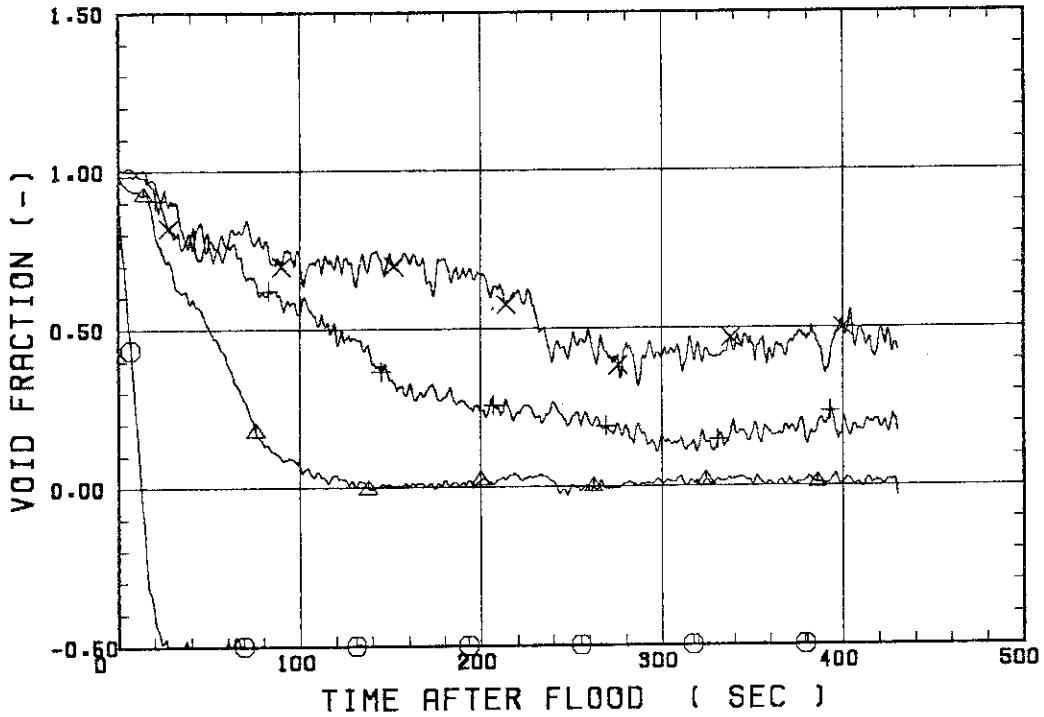
SMALL SCALE REFLOOD TEST
RUN 8107

○ --- DPT7 ▲ --- DPT8B + --- DP10
X --- DP12



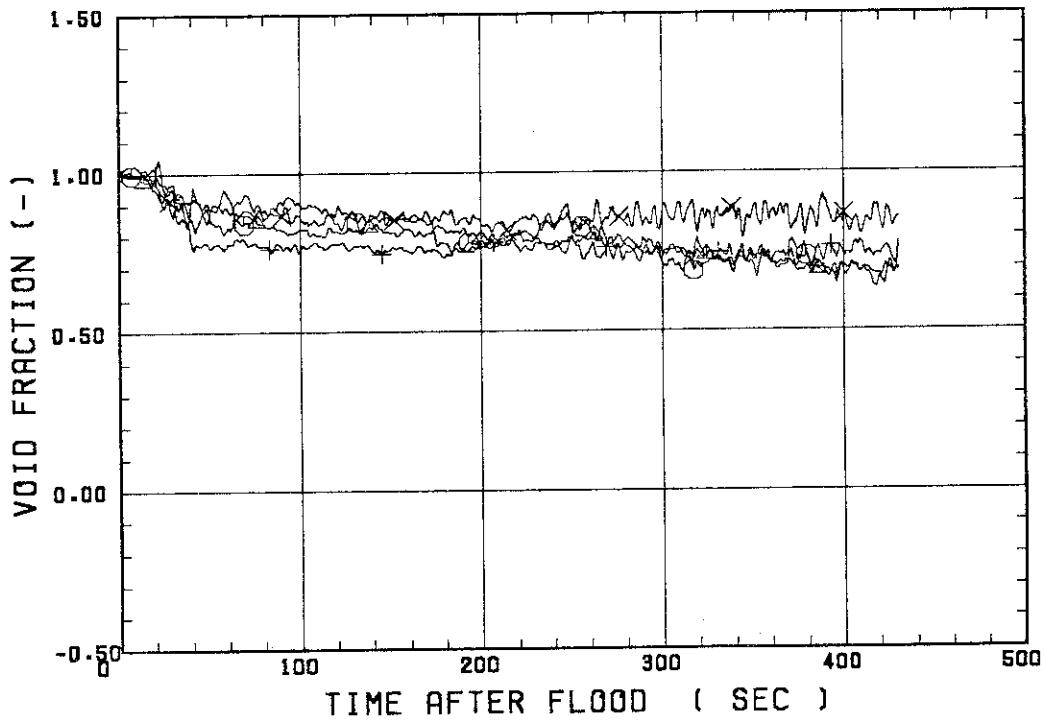
SMALL SCALE REFLOOD TEST
RUN 8107

○--- VDPT2 △--- VDPT4 +--- VDPT5
X--- VDPT6B



SMALL SCALE REFLOOD TEST
RUN 8107

○--- VDPT7 △--- VDPT8B +--- VDP10
X--- VDP12



 * RUN NO. 8109 *

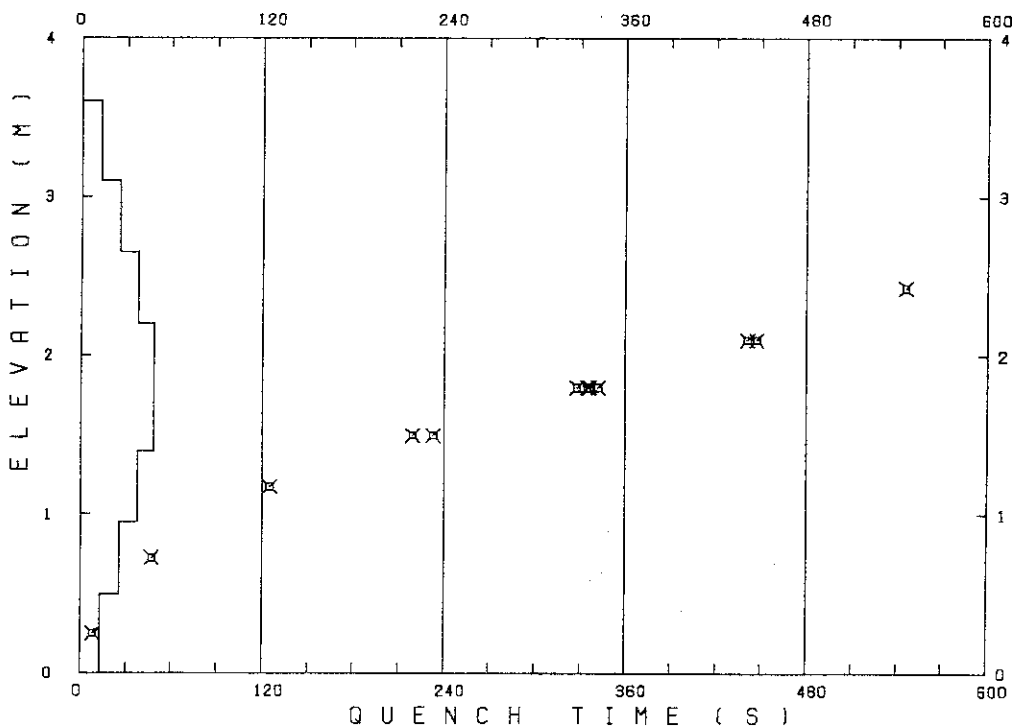
 TEST CONDITIONS

LINEAR PEAK POWER 1.8 KW/M
 SYSTEM PRESSURE 0.1 MPA
 INLET WATER TEMPERATURE 80 .C
 INJECTED WATER VELOCITY 3.8 CM/S

 TEMPERATURE PROFILE

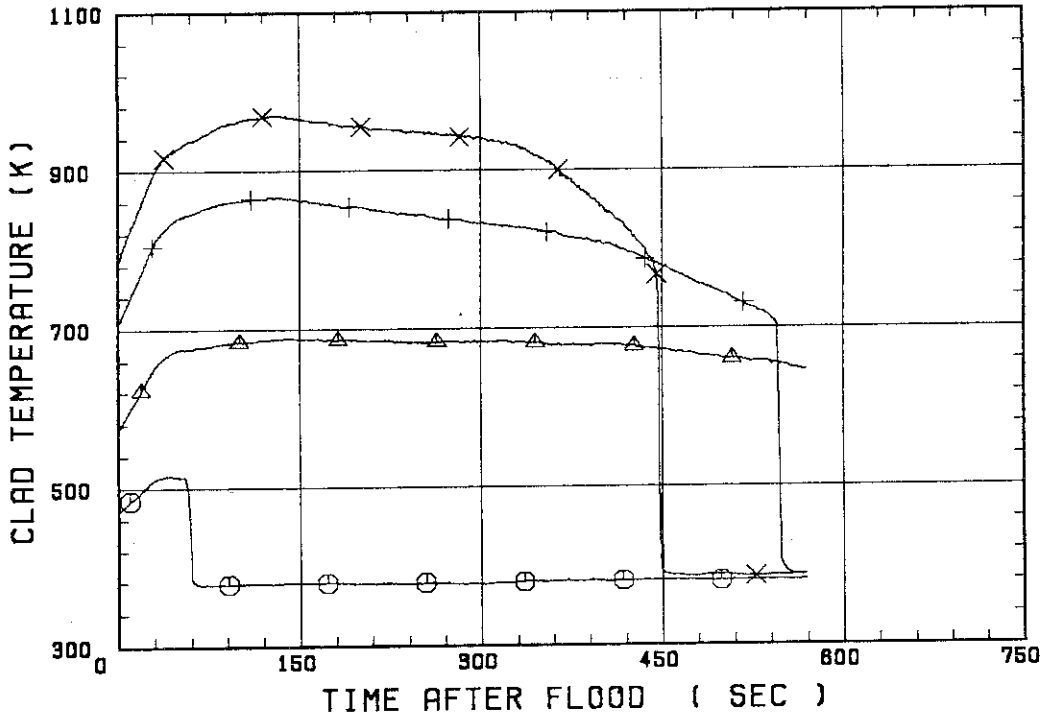
CH.NO.	SYMBOL	INITIAL TEMP. (.C)	TURNAROUND TIME (S)	TURNAROUND TEMP. (.C)	QUENCH TIME (S)	QUENCH TEMP. (.C)
66	TC1L	198	44.0	243		
36	TA2	299	144.0	416		
37	TA3	430	128.0	595	546.0	430
67	TC4U	508	134.0	697	447.0	464
7	TS4U	540	119.5	741	441.0	455
53	TR4M	518	42.0	653	342.0	397
68	TC4M	492	41.0	618	335.0	407
8	TS4M	520	42.5	660	336.5	395
48	TB4M	524	43.0	664	328.0	407
69	TC4L	511	35.0	619	233.0	409
9	TS4L	527	31.5	637	219.5	432
54	TR5	435	26.0	510	125.0	401
55	TR6	309	17.0	337	47.0	304
70	TC7	202	7.0	211	8.0	167

RUN NO. 8109



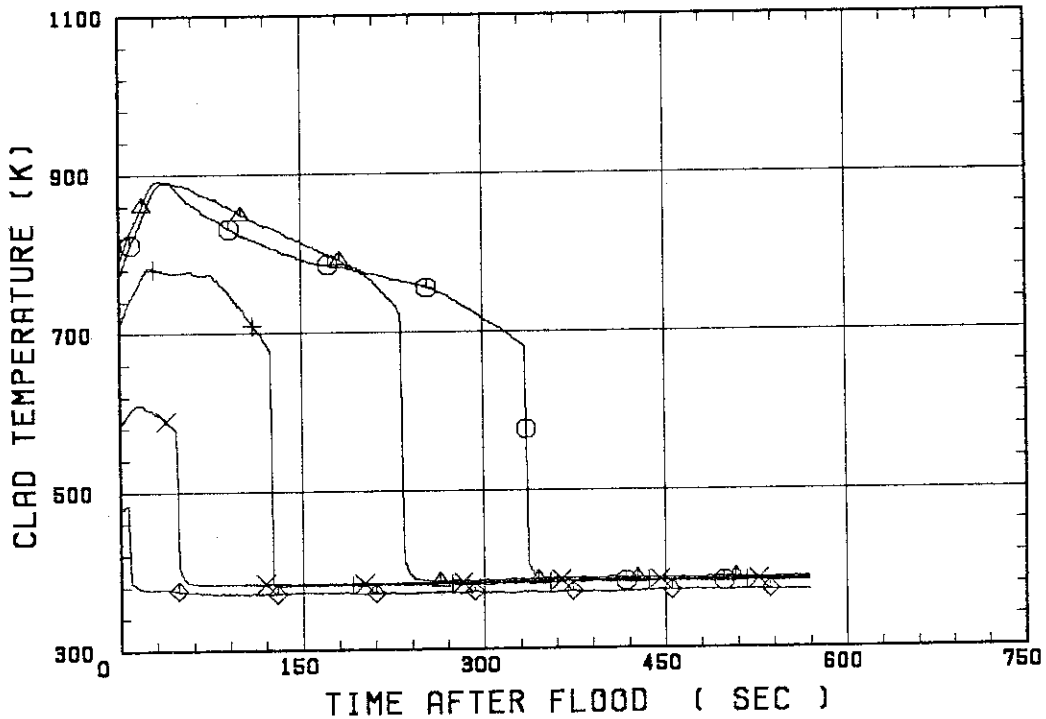
SMALL SCALE REFLOOD TEST
 RUN 8109

○--- TC1L ▲--- TA2 +--- TA3
 X--- TC4U

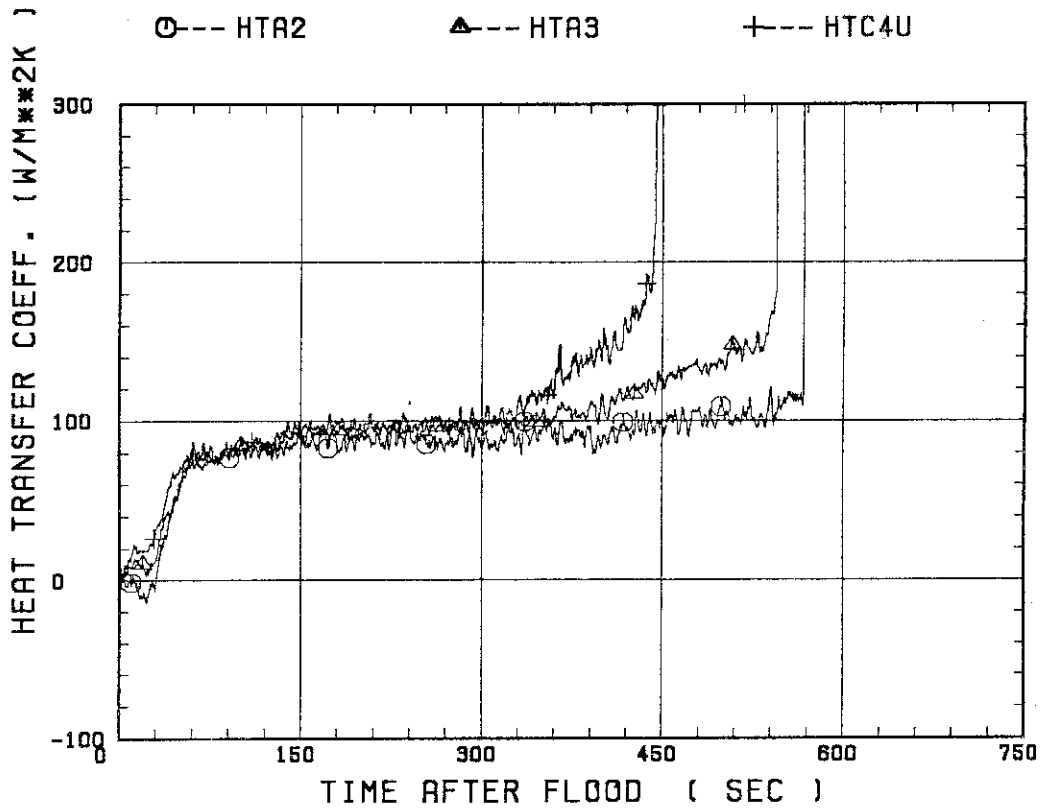


SMALL SCALE REFLOOD TEST
 RUN 8109

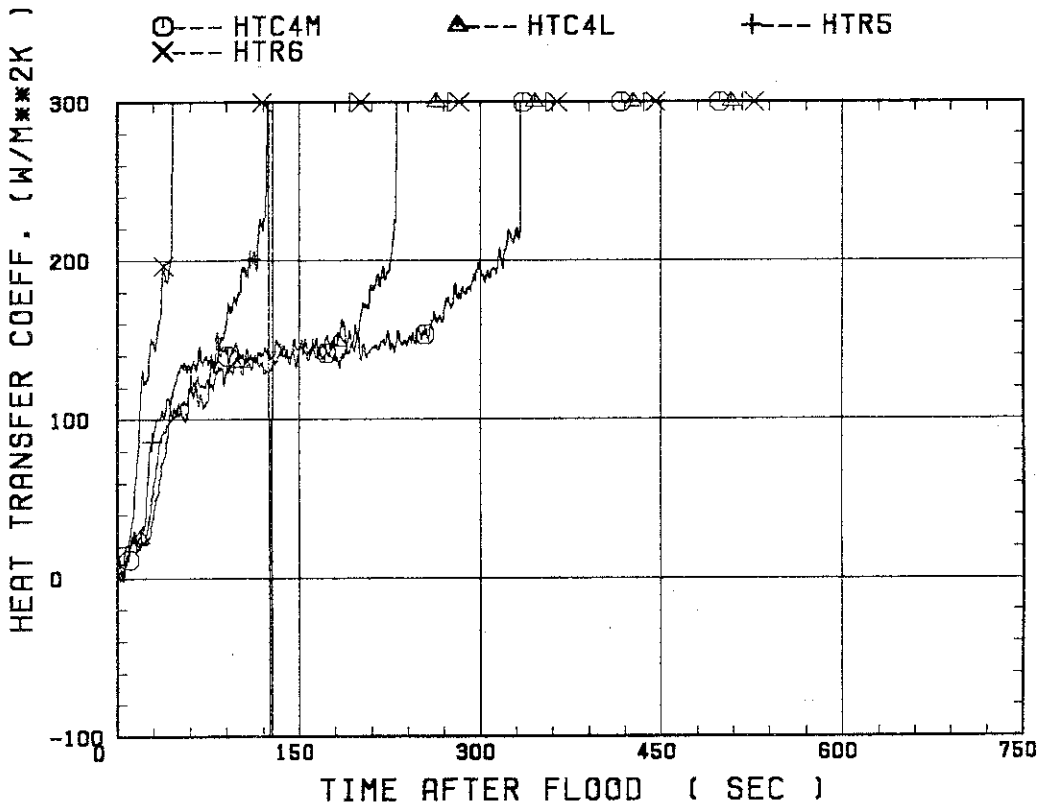
○--- TC4M ▲--- TC4L +--- TR5
 X--- TR6 ◆--- TC7



SMALL SCALE REFLOOD TEST
 RUN 8109

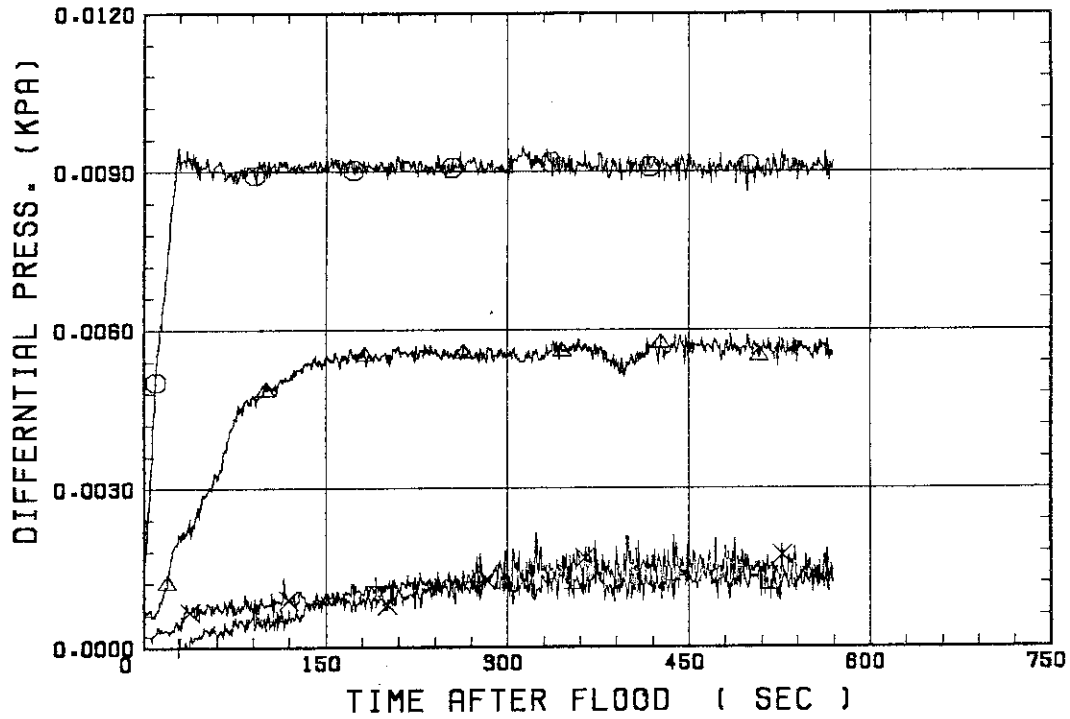


SMALL SCALE REFLOOD TEST
 RUN 8109



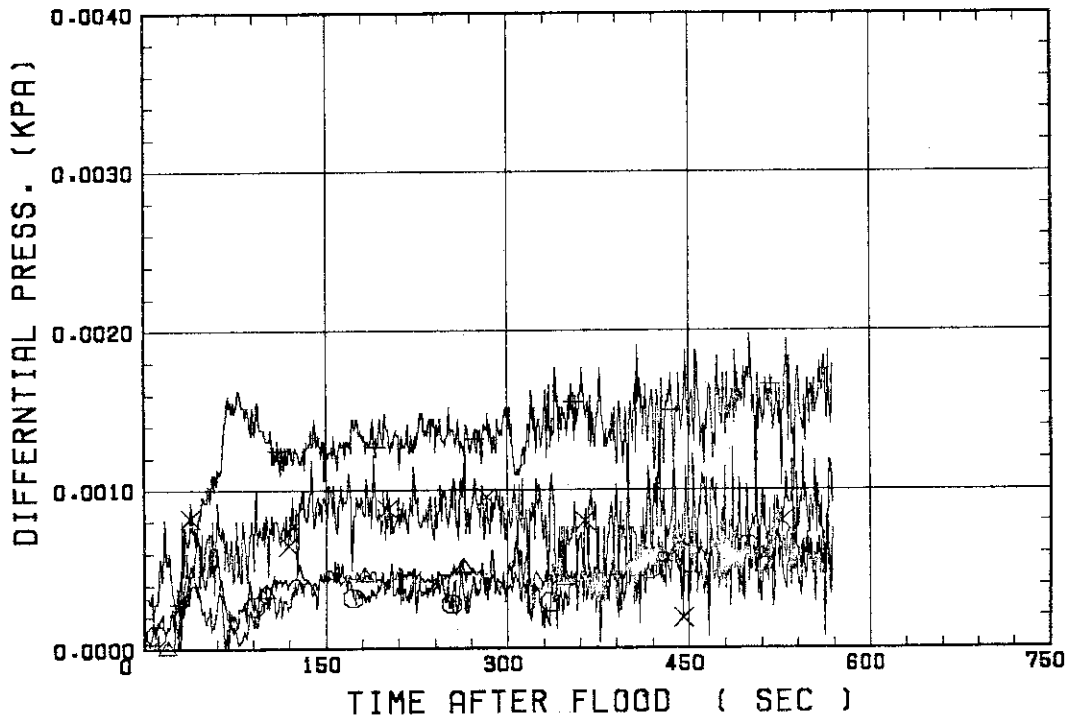
SMALL SCALE REFLOOD TEST
RUN 8109

○ --- DPT2 ▲ --- DPT4 + --- DPT5
X --- DPT6B



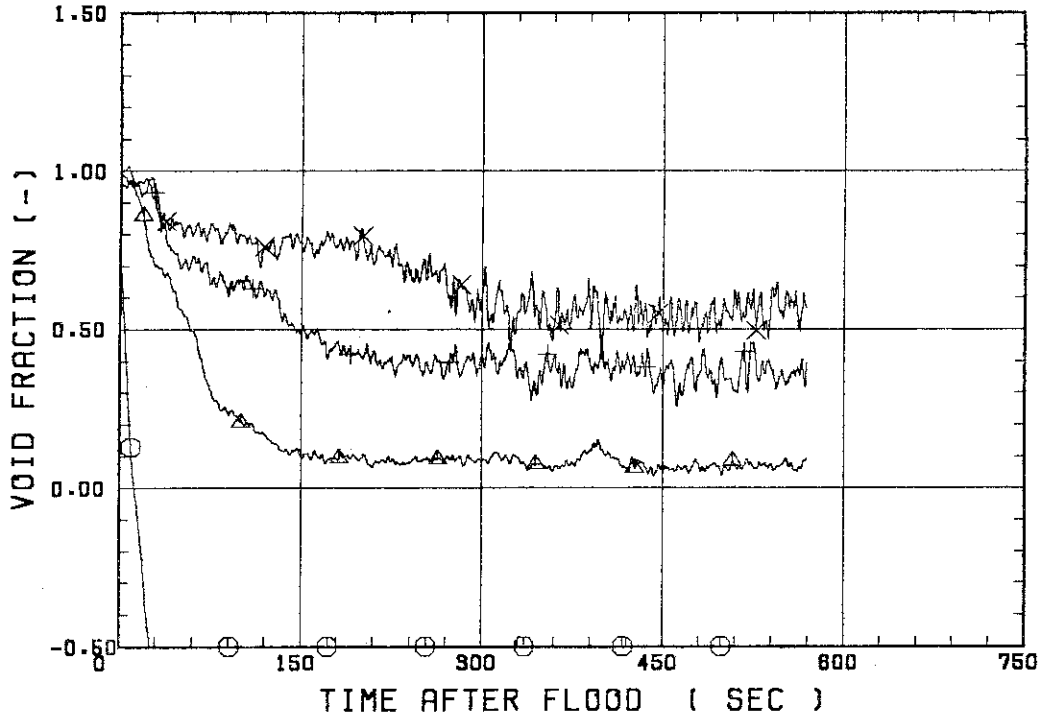
SMALL SCALE REFLOOD TEST
RUN 8109

○ --- DPT7 ▲ --- DPT8B + --- DP10
X --- DP12



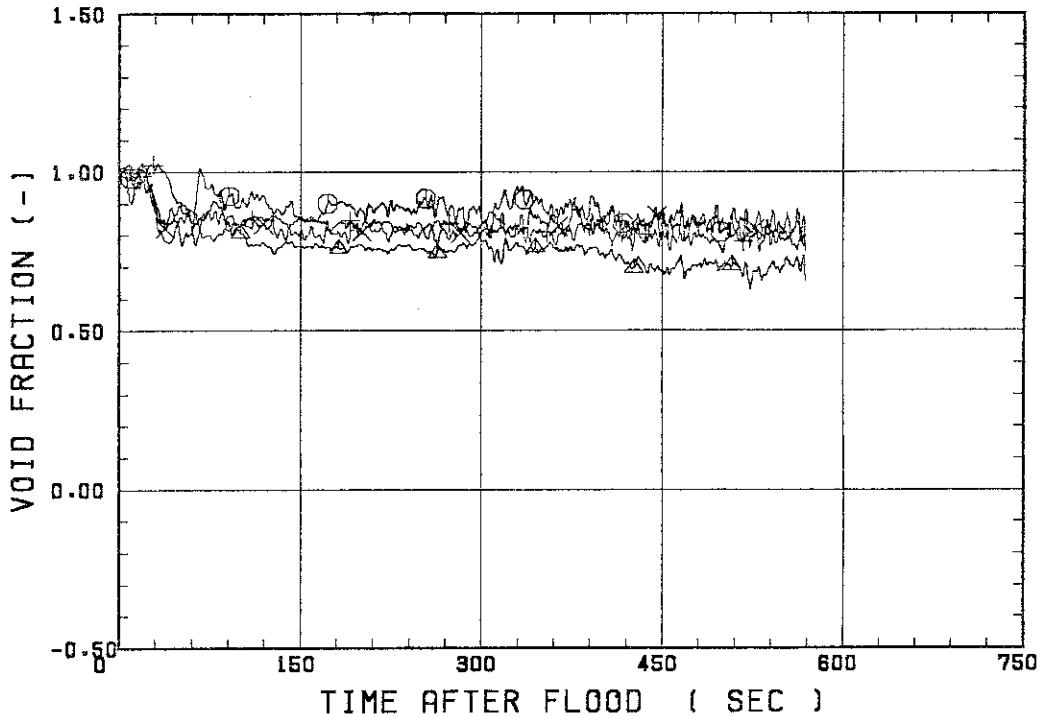
SMALL SCALE REFLOOD TEST
RUN 8109

○--- VDPT2 △--- VDPT4 +--- VDPT5
X--- VDPT6B



SMALL SCALE REFLOOD TEST
RUN 8109

○--- VDPT7 △--- VDPT8B +--- VDP10
X--- VDP12



 * RUN NO. 8113 *
 * *****

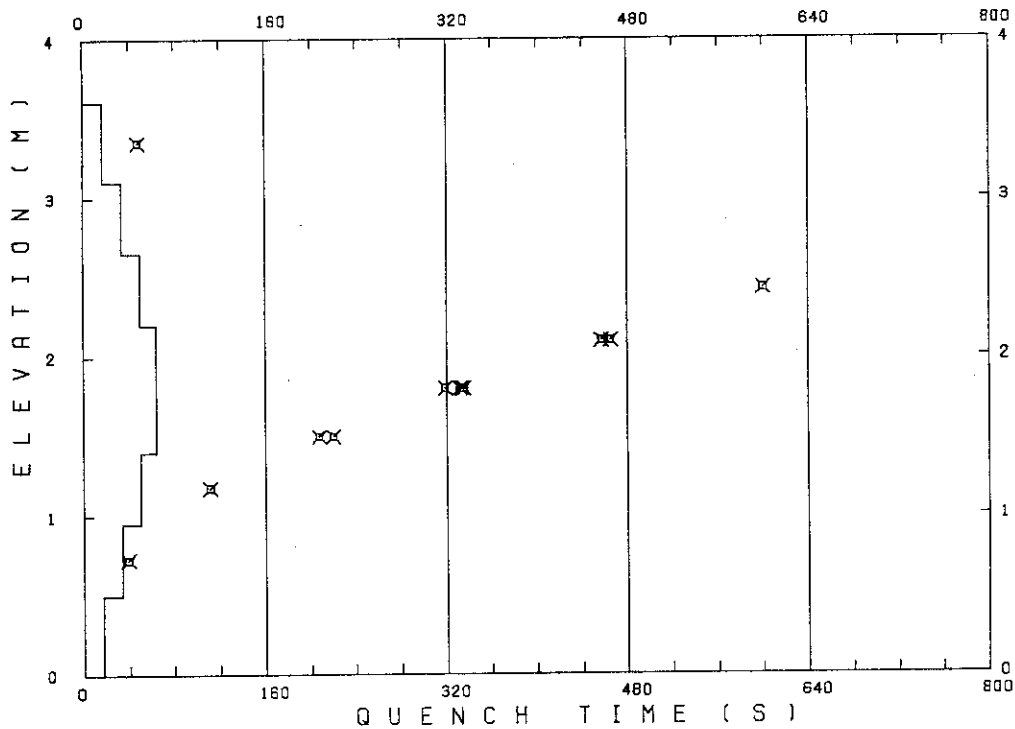
 TEST CONDITIONS

LINEAR PEAK POWER 1.8 KW/M
 SYSTEM PRESSURE 0.1 MPA
 INLET WATER TEMPERATURE 80 .C
 INJECTED WATER VELOCITY 3.8 CM/S

 TEMPERATURE PROFILE

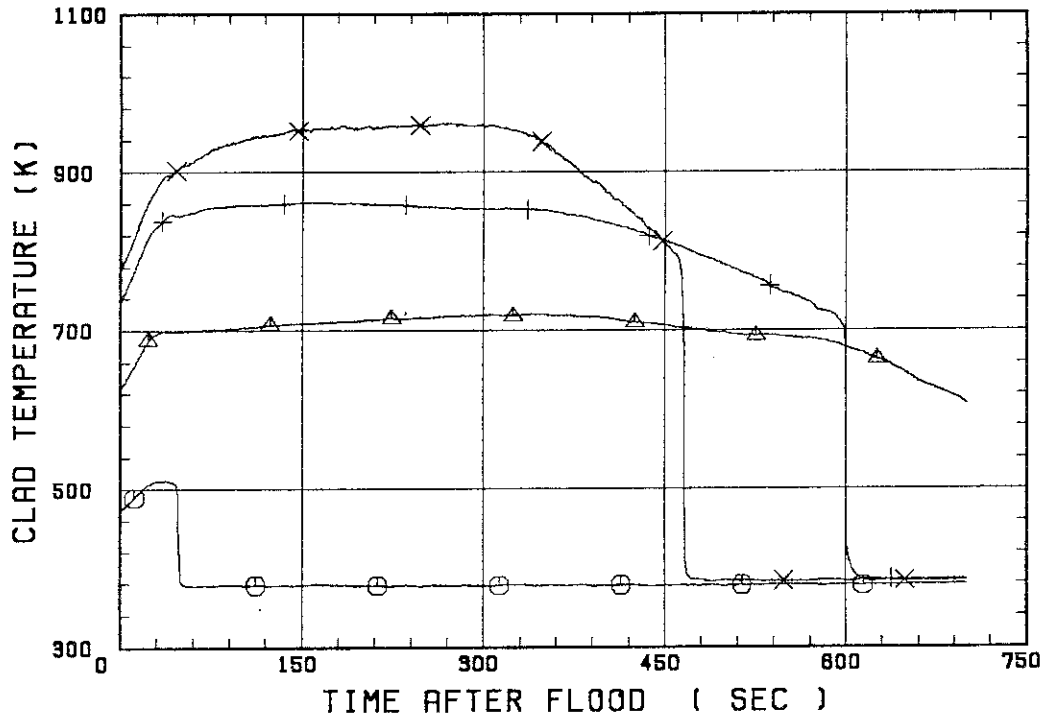
CH.NO.	SYMBOL	INITIAL TEMP. (.C)	TURNAROUND TIME (S)	TURNAROUND TEMP. (.C)	QUENCH TIME (S)	QUENCH TEMP. (.C)
66	TC1L	199	38.0	238	48.0	219
51	TR2	351	340.0	448		
52	TR3	459	166.0	590	600.0	408
67	TC4U	498	273.0	689	465.0	462
7	TS4U	547	100.5	714	457.0	437
53	TR4M	516	35.0	626	334.0	405
68	TC4M	488	33.0	594	332.0	383
8	TS4M	521	35.5	636	335.5	400
48	TR4M	521	38.0	638	319.0	385
69	TC4L	508	35.0	595	220.0	460
9	TS4L	532	28.0	625	207.5	438
54	TR5	442	25.0	504	111.0	403
55	TR6	313	16.0	330	39.0	292
70	TC7	203	2.0	205		

RUN NO. 8113



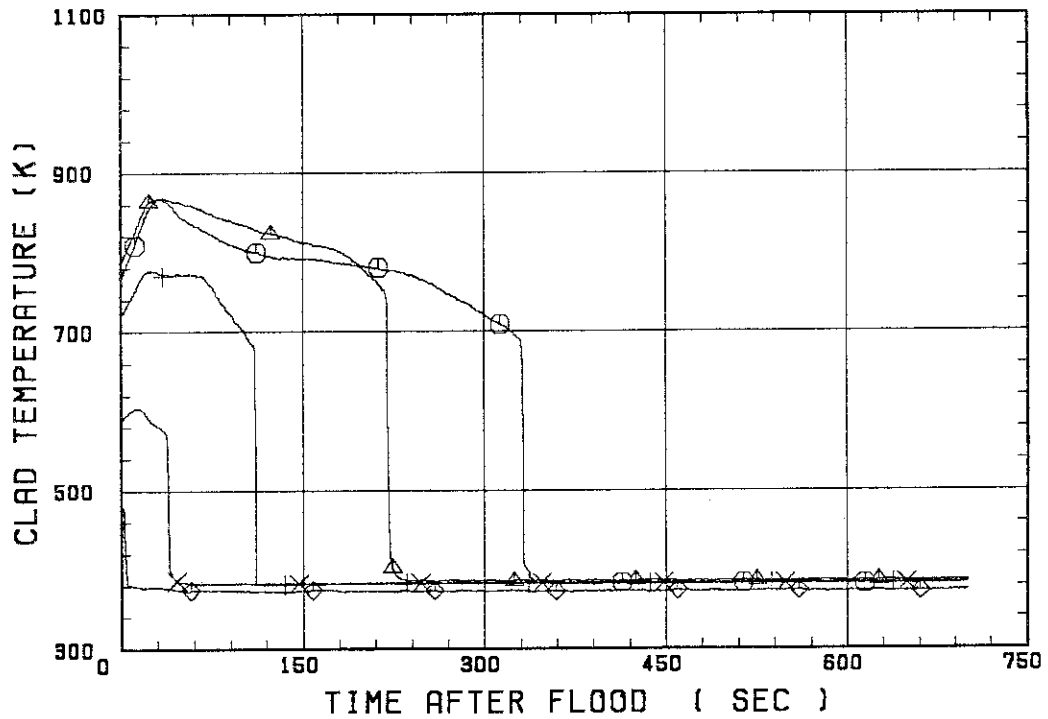
SMALL SCALE REFLOOD TEST
 RUN 8113

○--- TC1L △--- TR2 +--- TR3
 X--- TC4U

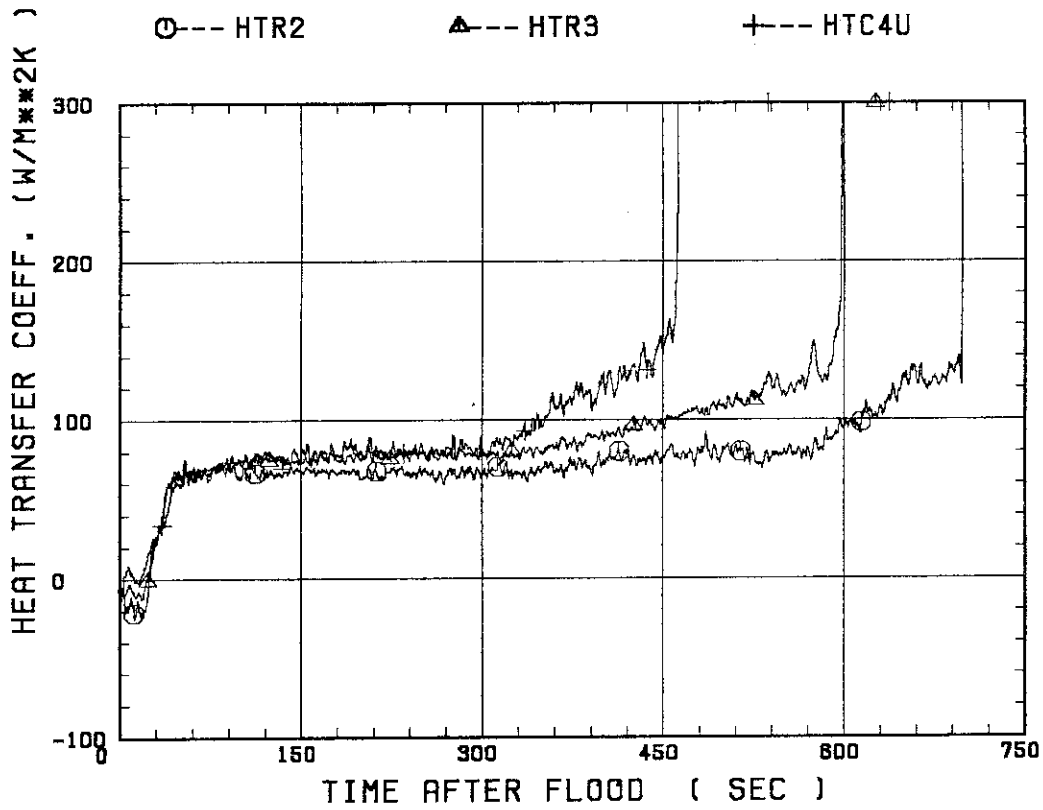


SMALL SCALE REFLOOD TEST
 RUN 8113

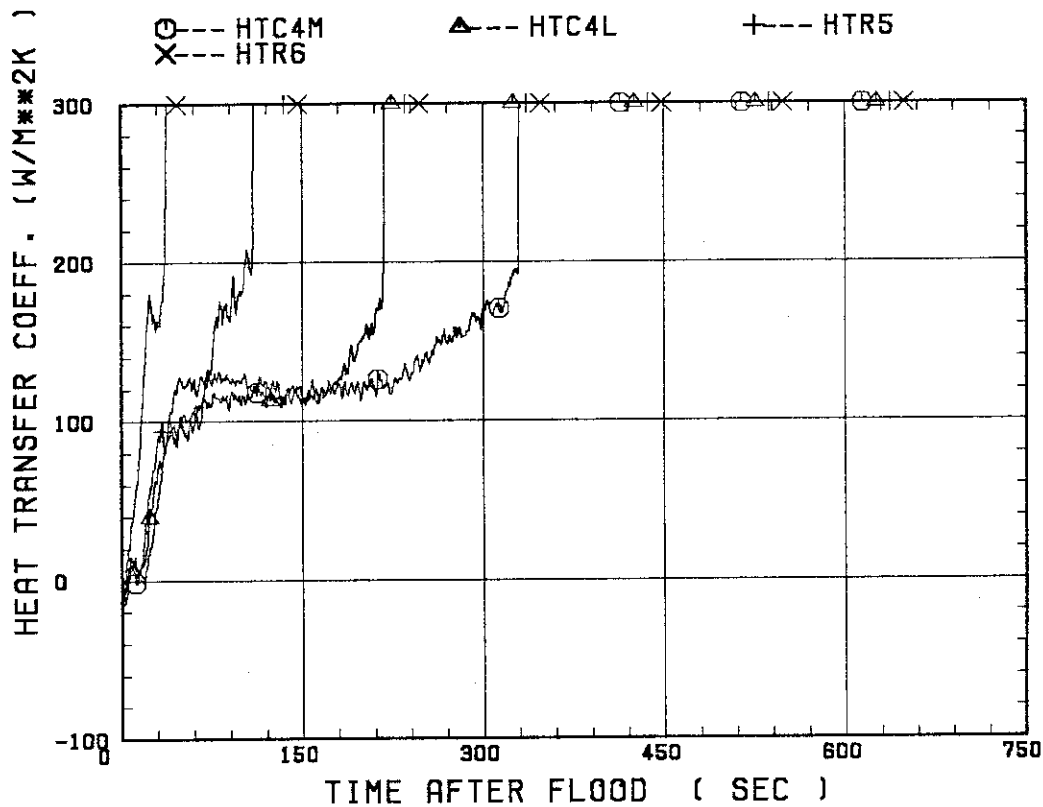
○--- TC4M △--- TC4L +--- TR5
 X--- TR6 ◇--- TC7



SMALL SCALE REFLOOD TEST
 RUN 8113

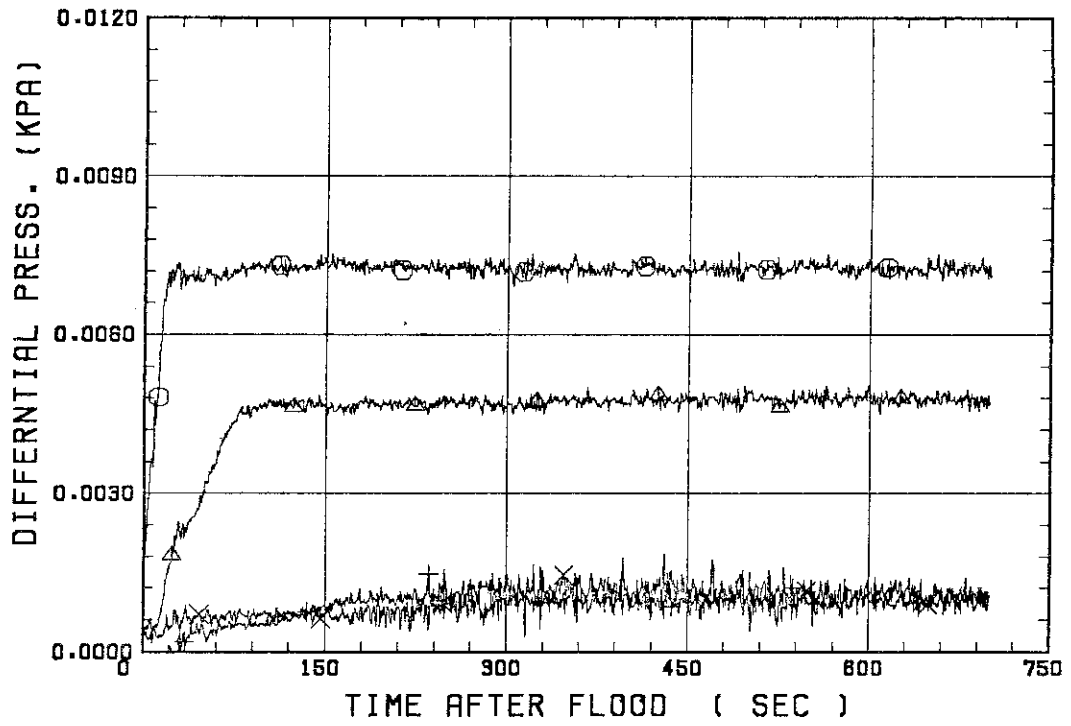


SMALL SCALE REFLOOD TEST
 RUN 8113



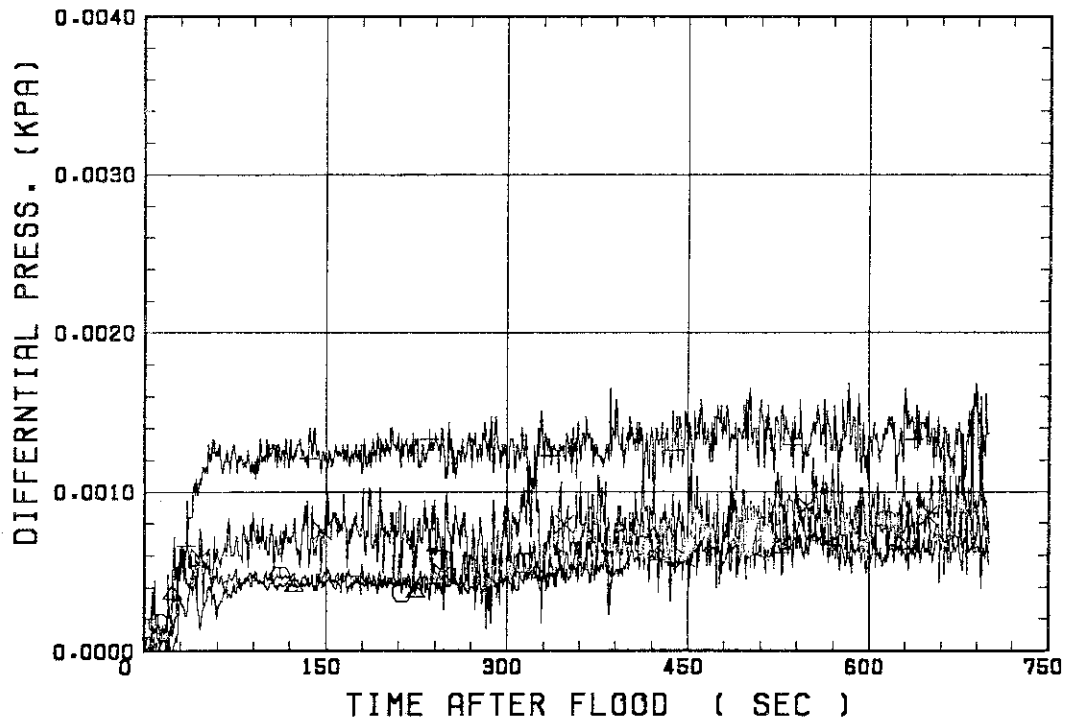
SMALL SCALE REFLOOD TEST
 RUN 8113

○ --- DPT2 ▲ --- DPT4 + --- DPT5
 X --- DPT6B



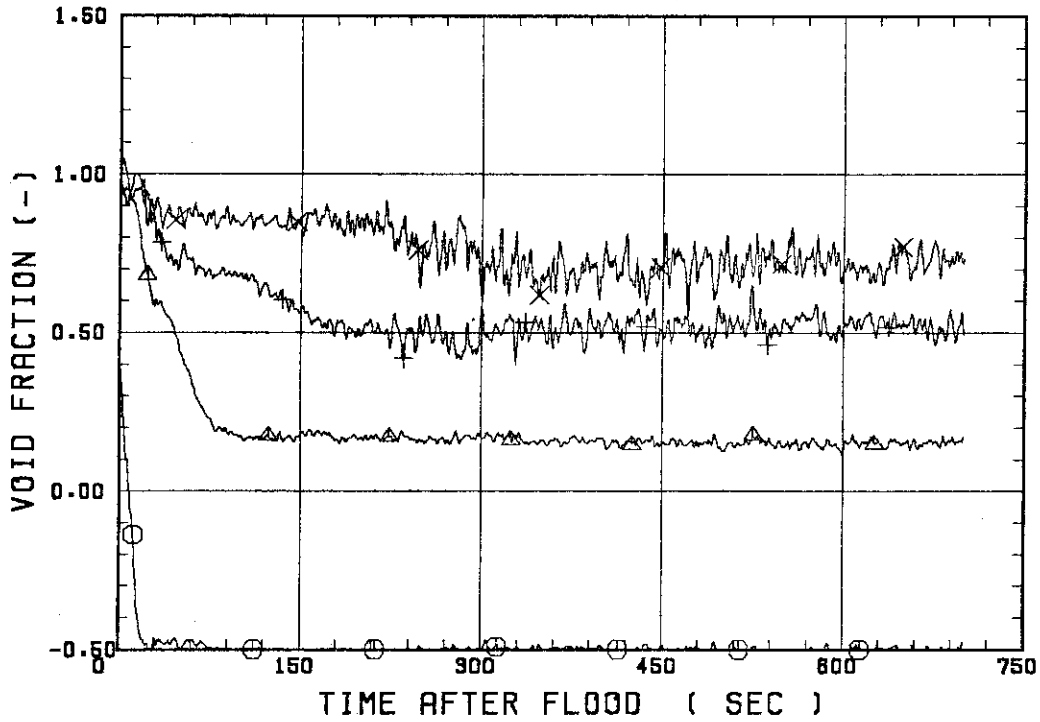
SMALL SCALE REFLOOD TEST
 RUN 8113

○ --- DPT7 ▲ --- DPT8B + --- DP10
 X --- DP12



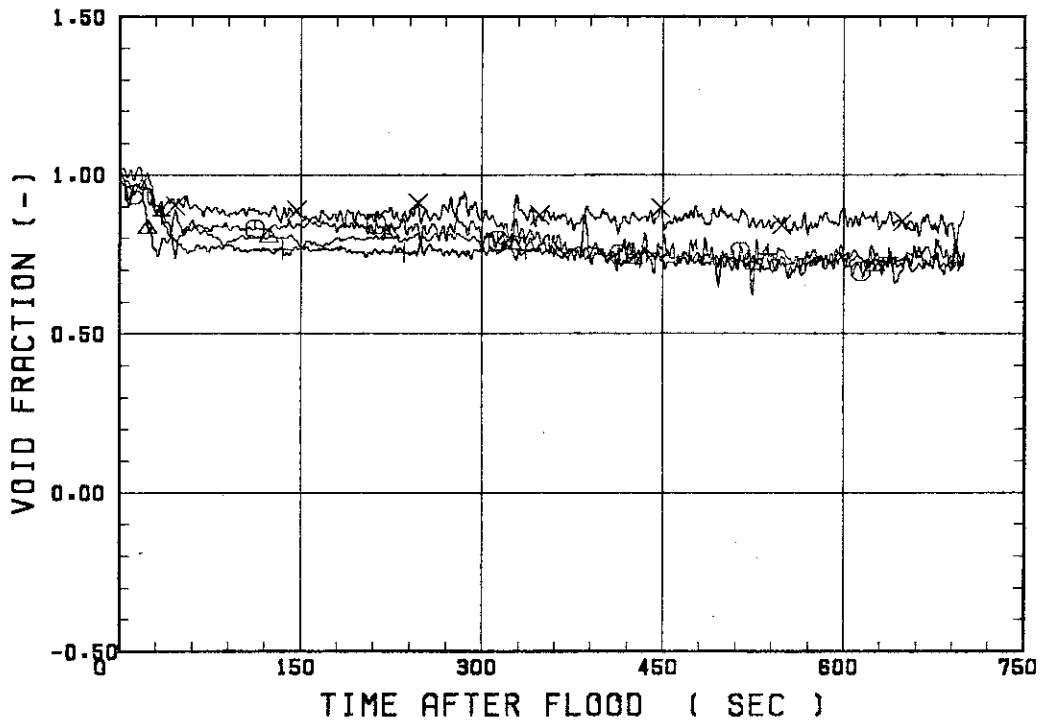
SMALL SCALE REFLOOD TEST
RUN 8113

○--- VDPT2 △--- VDPT4 +--- VDPT5
X--- VDPT6B



SMALL SCALE REFLOOD TEST
RUN 8113

○--- VDPT7 △--- VDPT8B +--- VDP10
X--- VDP12



 * RUN NO. 8116 *
 * *****

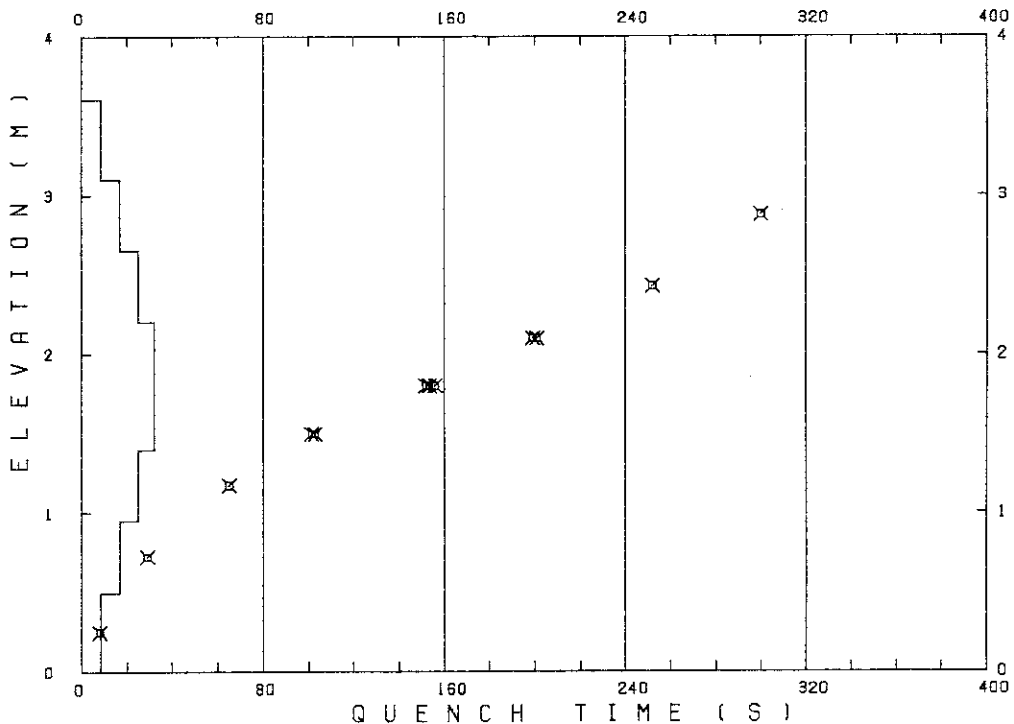
 TEST CONDITIONS

LINEAR PEAK POWER 1.6 KW/M
 SYSTEM PRESSURE 0.2 MPA
 INLET WATER TEMPERATURE 100 .C
 INJECTED WATER VELOCITY 3.8 CM/S

 TEMPERATURE PROFILE

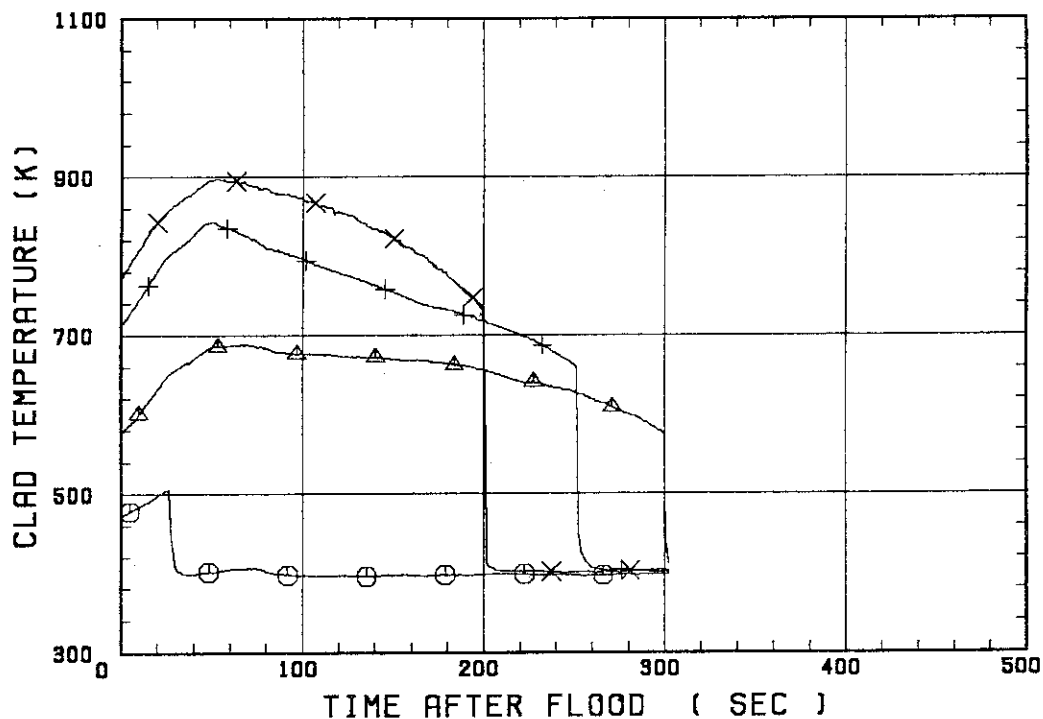
CH.NO.	SYMBOL	INITIAL TEMP. (.C)	TURNAROUND TIME (S)	TURNAROUND TEMP. (.C)	QUENCH TIME (S)	QUENCH TEMP. (.C)
66	TC1L	198	27.0	232		
51	TR2	303	70.0	416	300.0	302
52	TR3	436	52.0	570	252.0	386
67	TC4U	495	54.0	624	201.0	417
7	TS4U	550	48.5	689	199.0	491
53	TR4M	505	35.0	610	156.0	378
68	TC4M	471	33.0	569	152.0	380
8	TS4M	516	36.5	620	153.5	375
48	TB4M	512	35.0	618	152.0	391
69	TC4L	502	26.0	582	103.0	438
9	TS4L	526	26.0	611	101.5	426
54	TR5	452	24.0	514	65.0	393
55	TR6	324	17.0	354	29.0	323
70	TC7	214	7.0	222	8.0	216

RUN NO. 8116



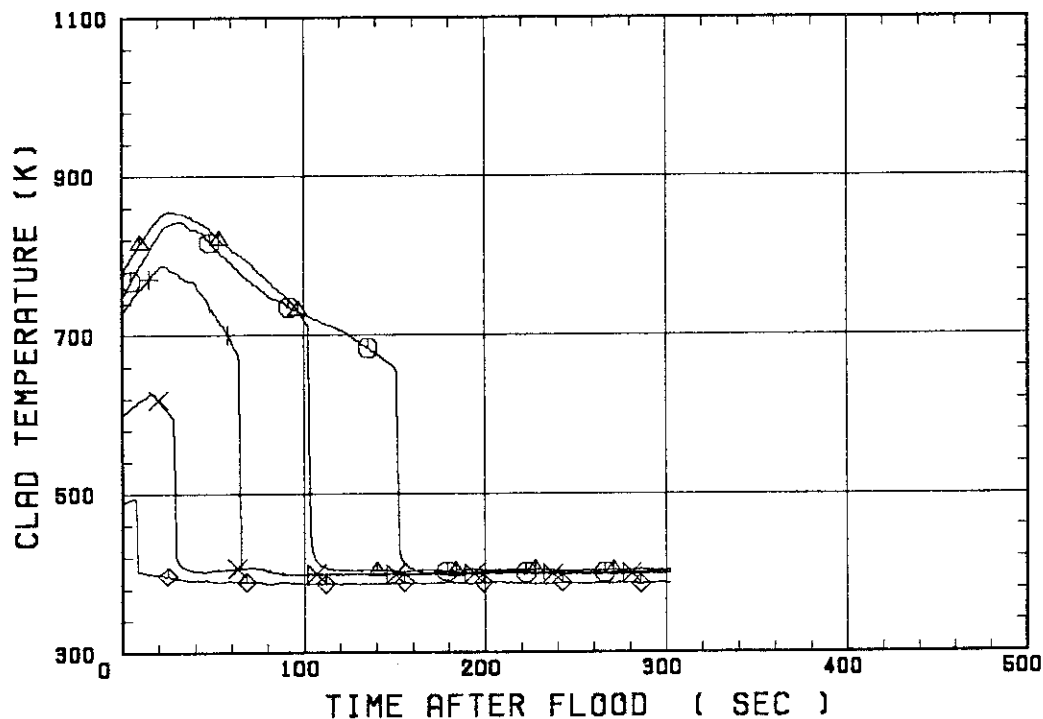
SMALL SCALE REFLOOD TEST
 RUN 8116

○--- TC1L ▲--- TR2 +--- TR3
 X--- TC4U

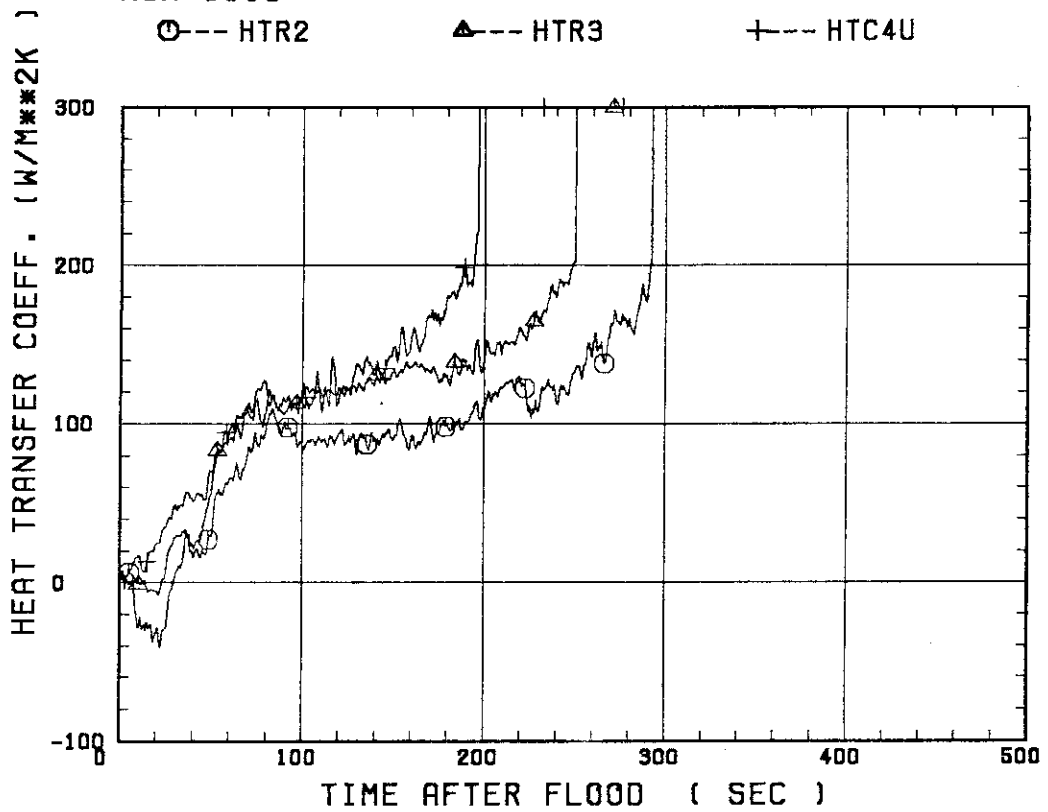


SMALL SCALE REFLOOD TEST
 RUN 8116

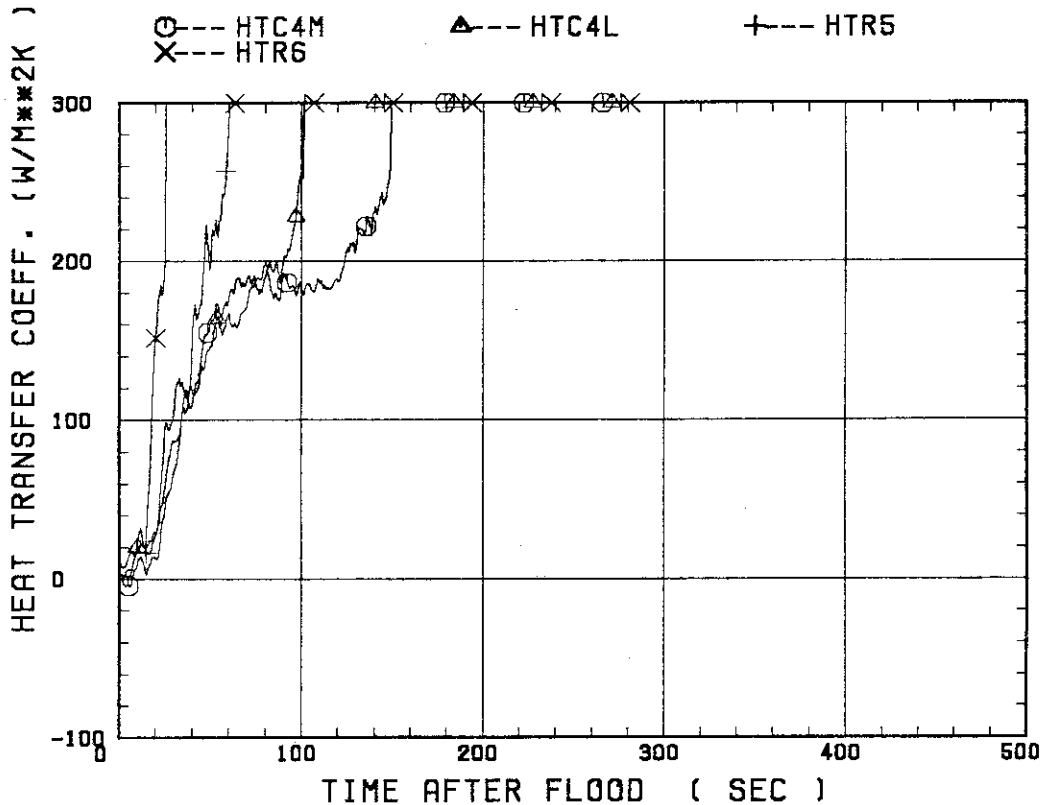
○--- TC4M ▲--- TC4L +--- TR5
 X--- TR6 ◆--- TC7



SMALL SCALE REFLOOD TEST
 RUN 8116

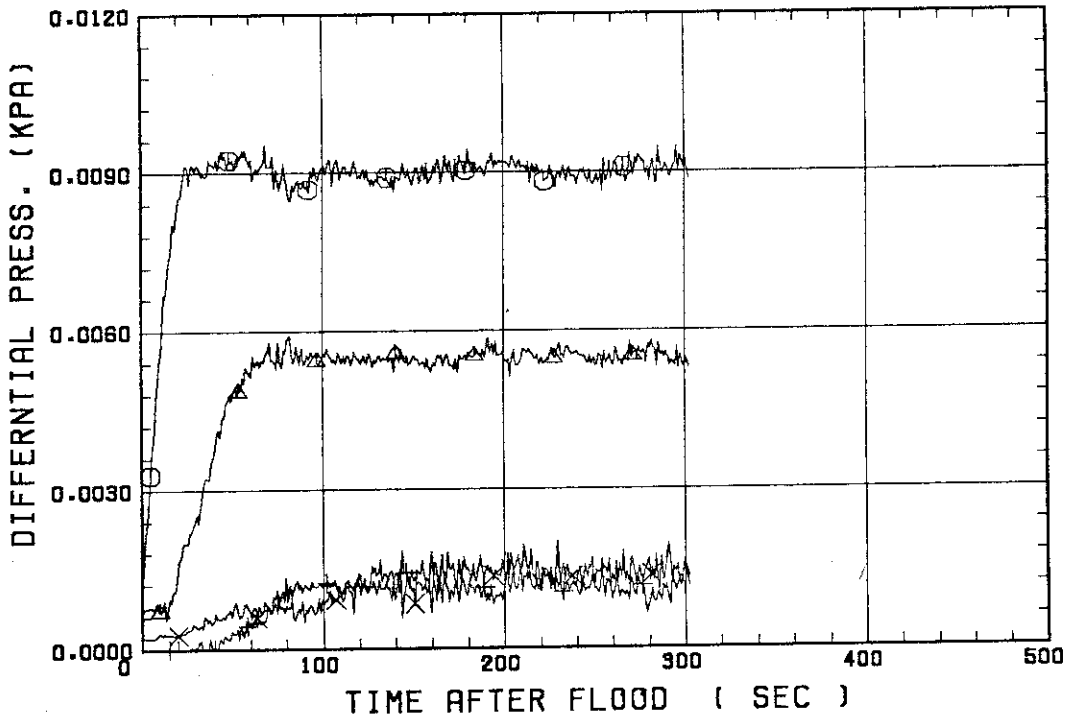


SMALL SCALE REFLOOD TEST
 RUN 8116



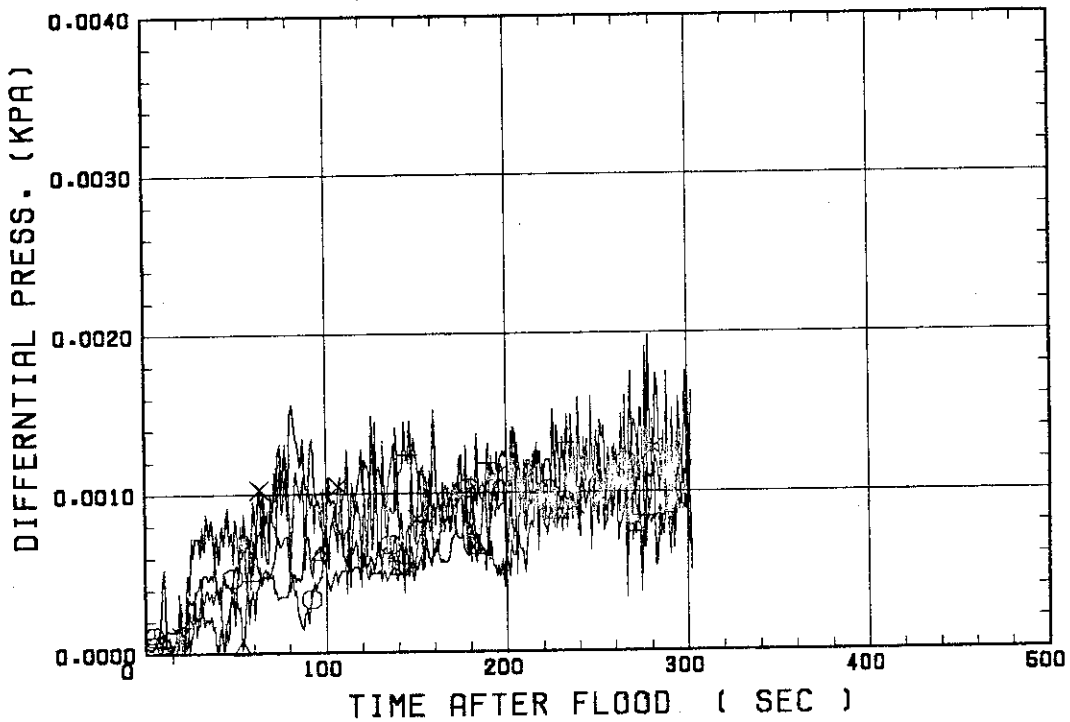
SMALL SCALE REFLOOD TEST
RUN 8116

○ --- DPT2 ▲ --- DPT4 + --- DPT5
X --- DPT6B



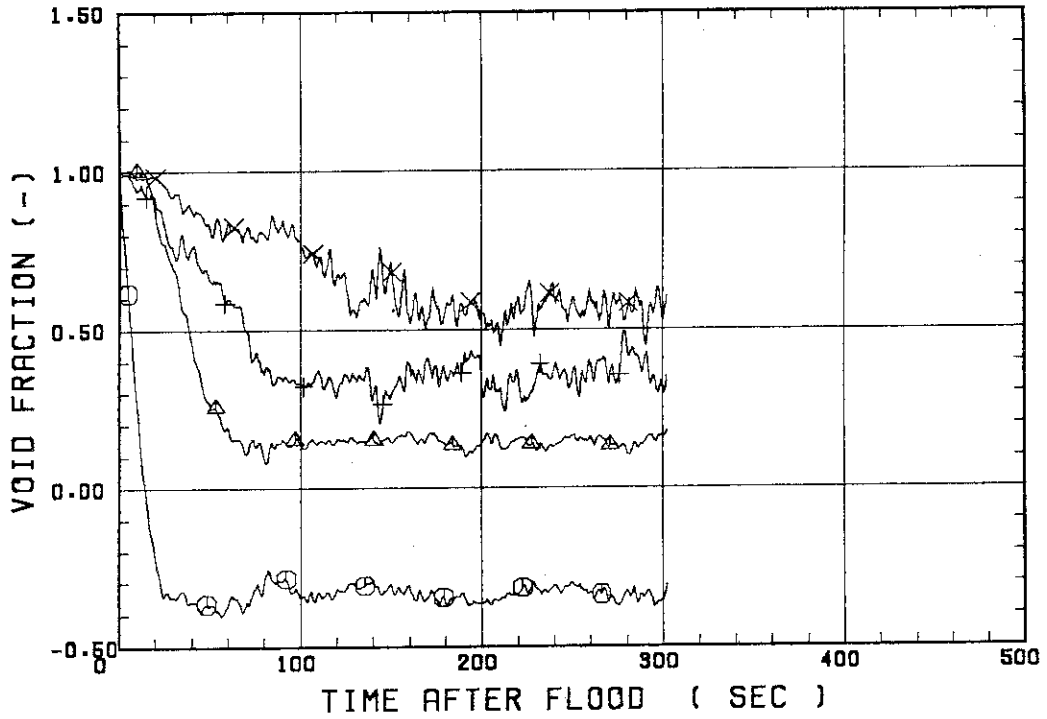
SMALL SCALE REFLOOD TEST
RUN 8116

○ --- DPT7 ▲ --- DPT8B + --- DP10
X --- DP12



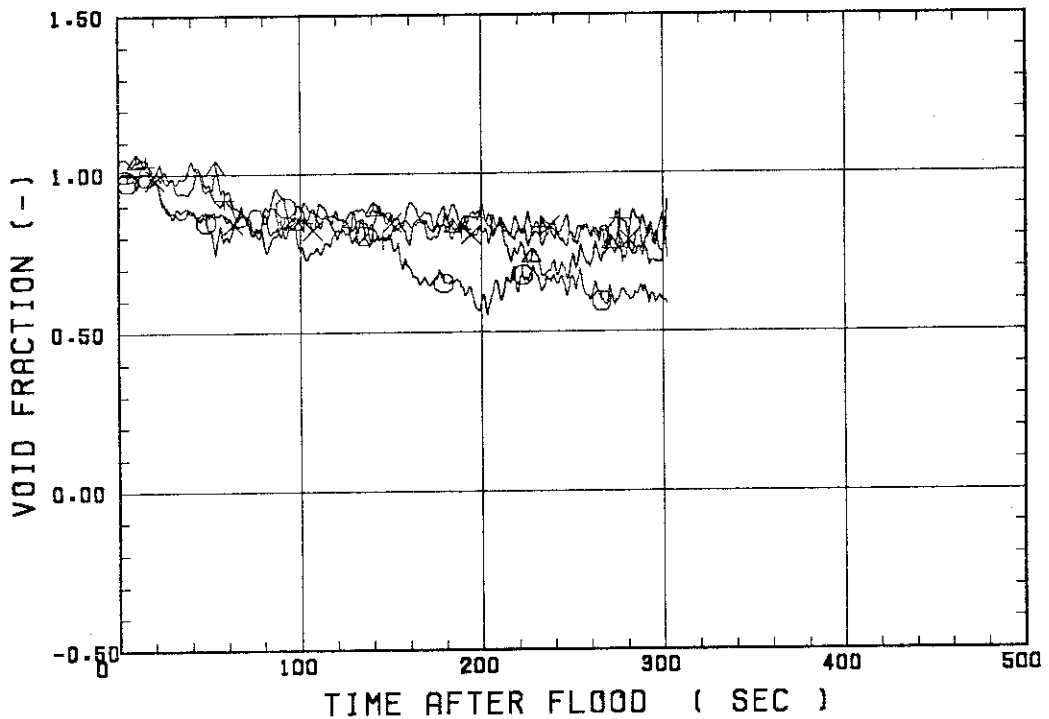
SMALL SCALE REFLOOD TEST
RUN 8116

○--- VDPT2 ▲--- VDPT4 +--- VDPT5
X--- VDPT6B



SMALL SCALE REFLOOD TEST
RUN 8116

○--- VDPT7 ▲--- VDPT8B +--- VDP10
X--- VDP12



 * RUN NO. 8117 *

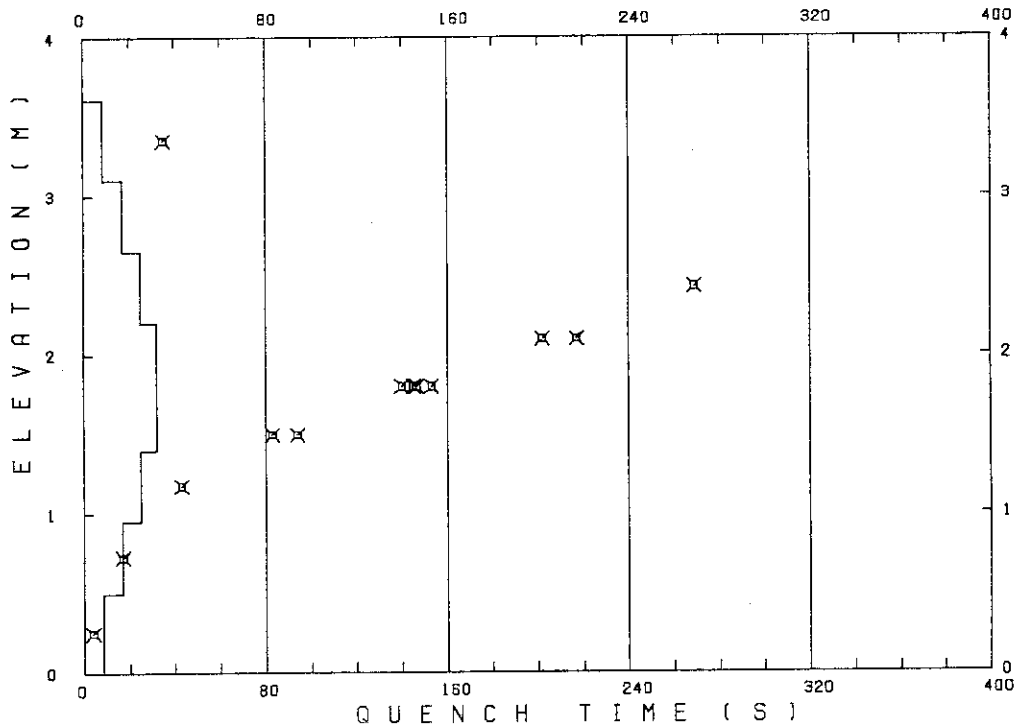
 TEST CONDITIONS

LINEAR PEAK POWER 2.0 KW/M
 SYSTEM PRESSURE 0.2 MPA
 INLET WATER TEMPERATURE 100 .C
 INJECTED WATER VELOCITY 3.8 CM/S

 TEMPERATURE PROFILE

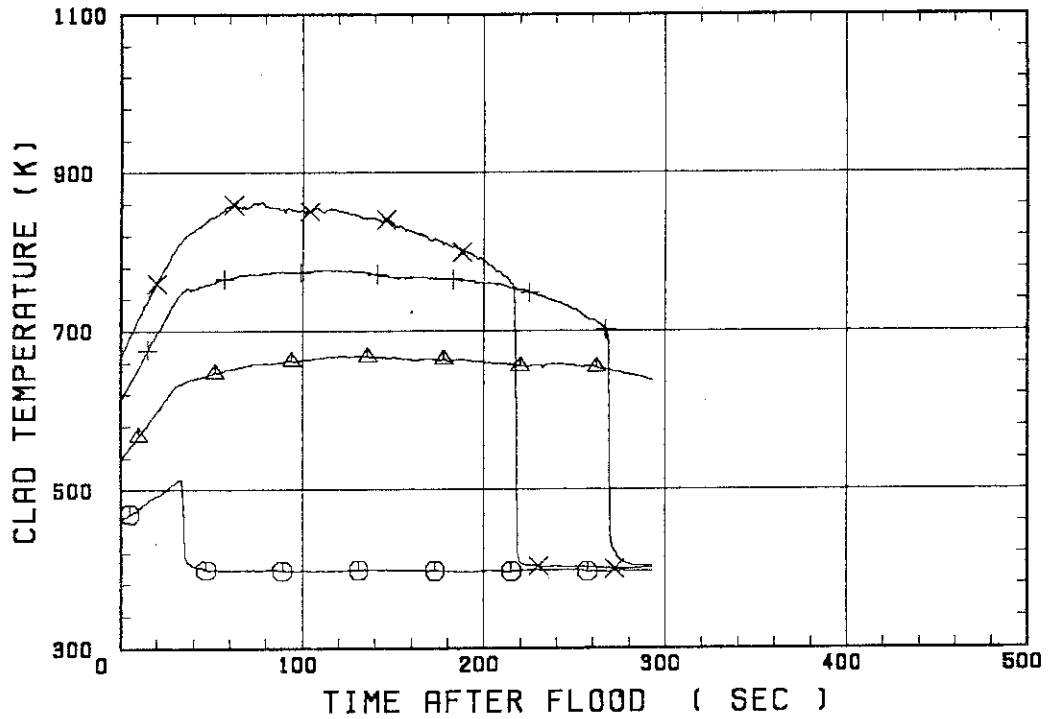
CH.NO.	SYMBOL	INITIAL TEMP. (.C)	TURNAROUND TIME (S)	TURNAROUND TEMP. (.C)	QUENCH TIME (S)	QUENCH TEMP. (.C)
66	TC1L	189	33.0	240	35.0	211
51	TR2	265	132.0	395		
52	TR3	339	115.0	504	269.0	410
67	TC4U	390	78.0	590	217.0	481
7	TS4U	393	62.0	589	202.0	443
53	TR4M	378	33.0	524	145.0	410
68	TC4M	381	31.0	609	153.0	407
8	TS4M	373	33.5	523	146.5	402
48	TB4M	383	33.0	529	140.0	422
69	TC4L	383	59.0	503	94.0	452
9	TS4L	376	30.0	504	83.0	458
54	TR5	323	27.0	405	43.0	381
55	TR6	241	13.0	272	17.0	262
70	TC7	181	4.0	185	4.0	185

RUN NO. 8117



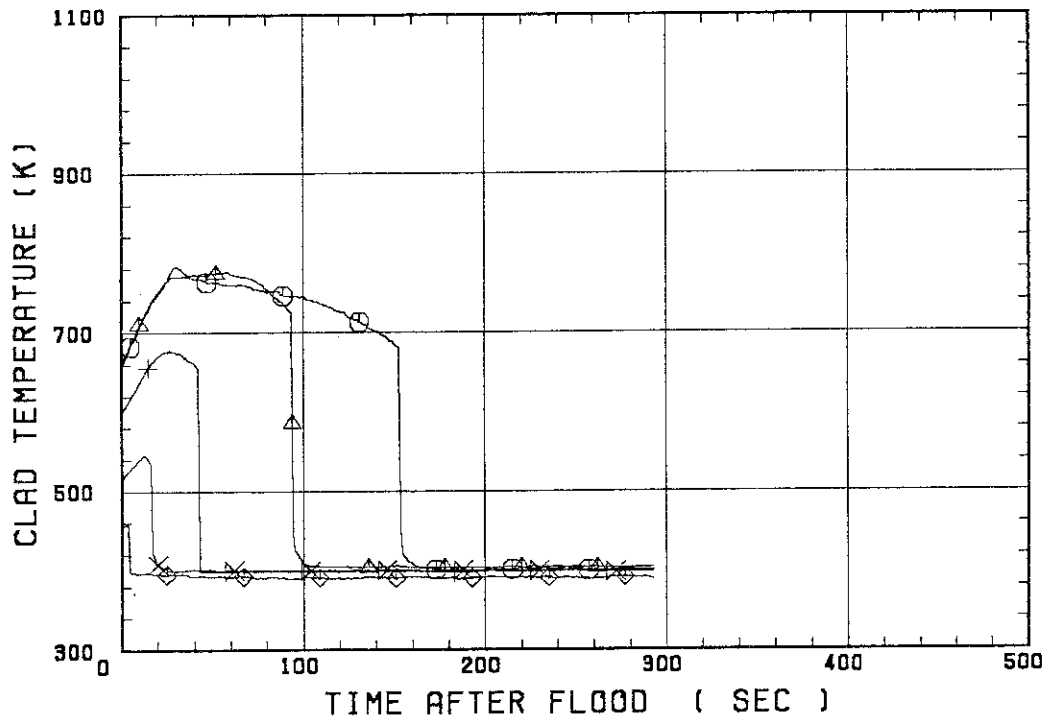
SMALL SCALE REFLOOD TEST
RUN 8117

○--- TC1L △--- TR2 +--- TR3
X--- TC4U

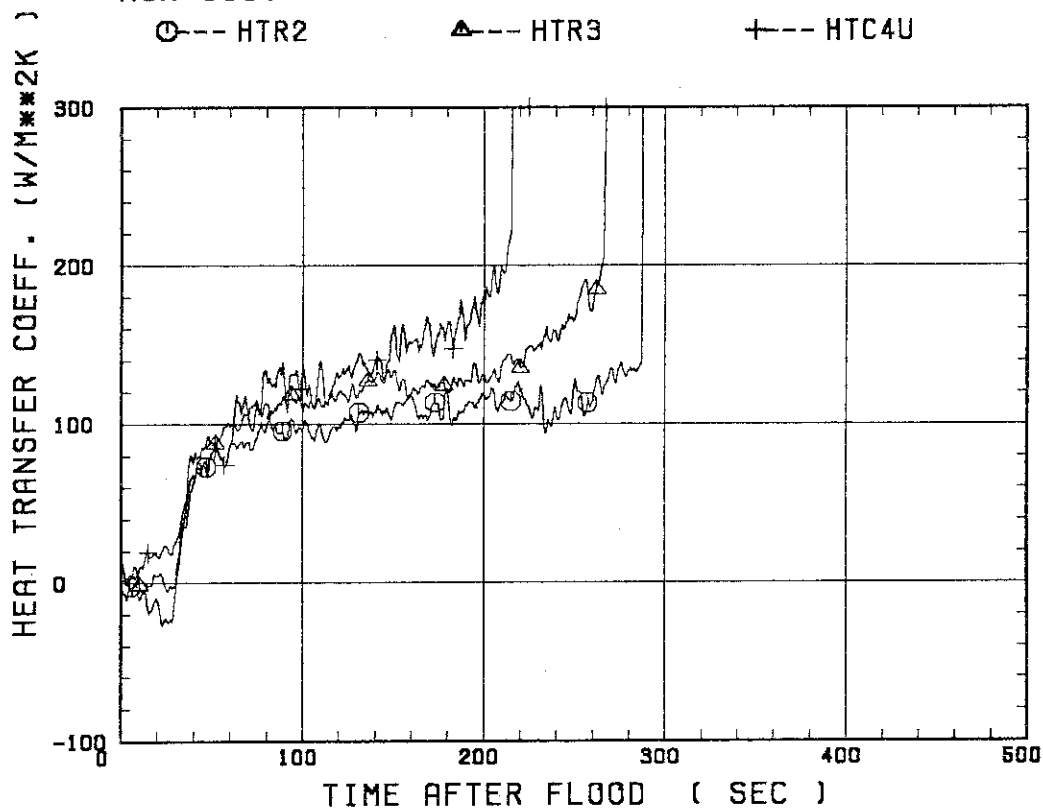


SMALL SCALE REFLOOD TEST
RUN 8117

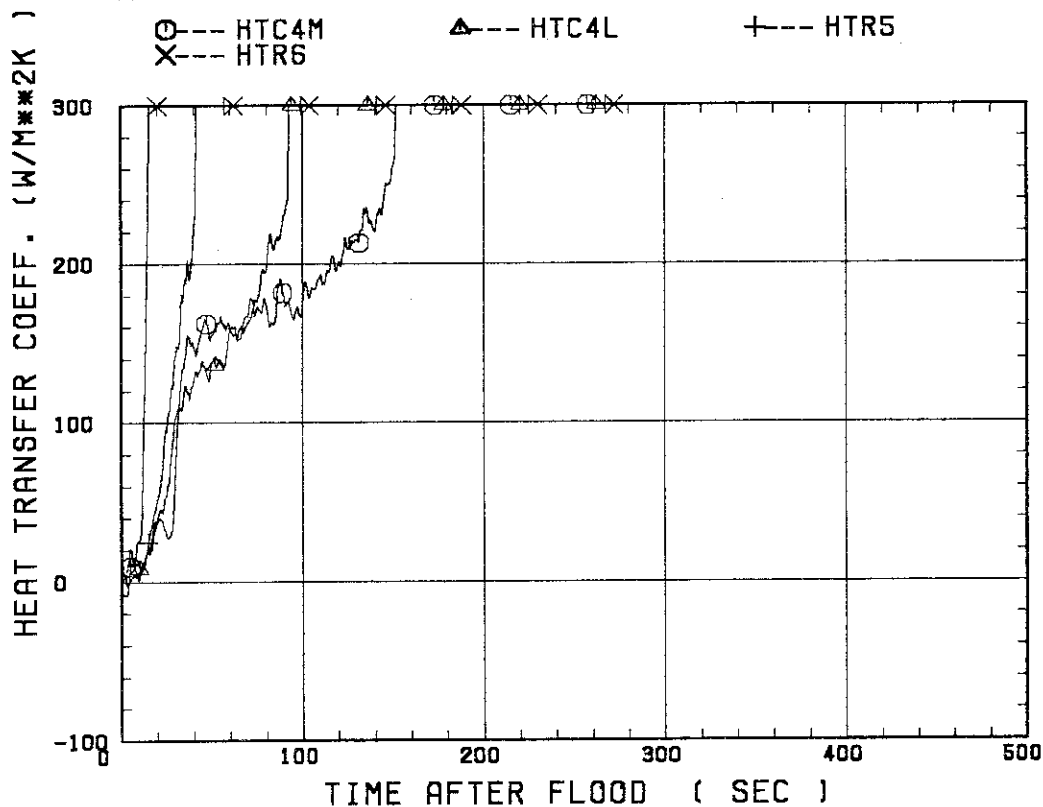
○--- TC4M △--- TC4L +--- TR5
X--- TR6 ◇--- TC7



SMALL SCALE REFLOOD TEST
 RUN 8117

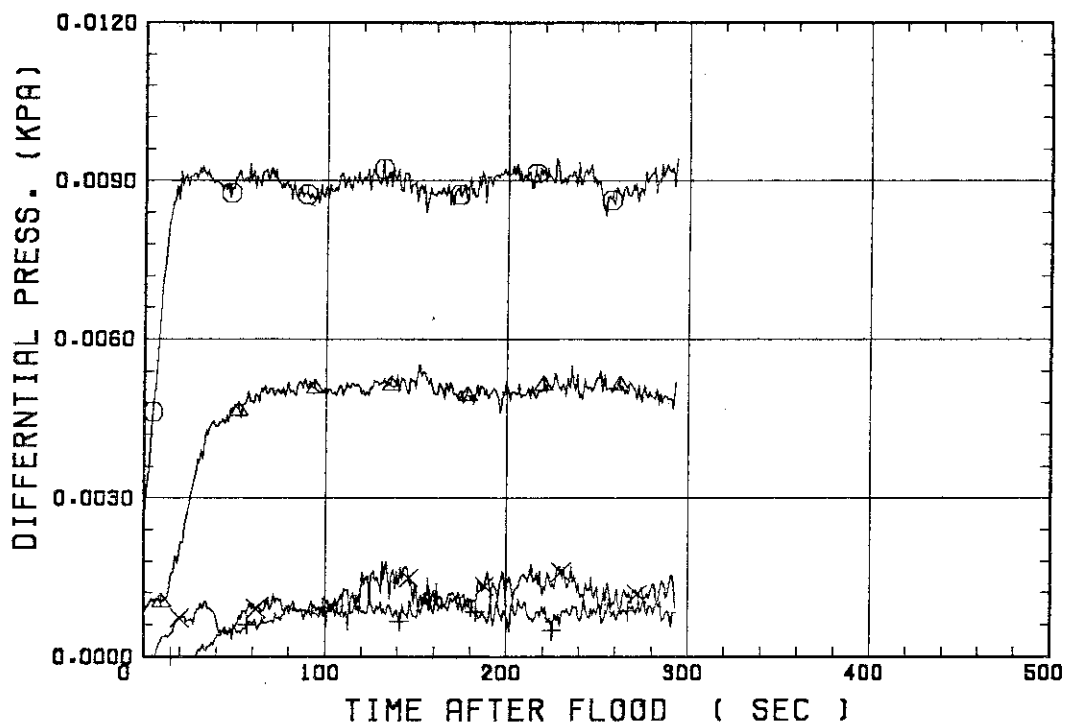


SMALL SCALE REFLOOD TEST
 RUN 8117



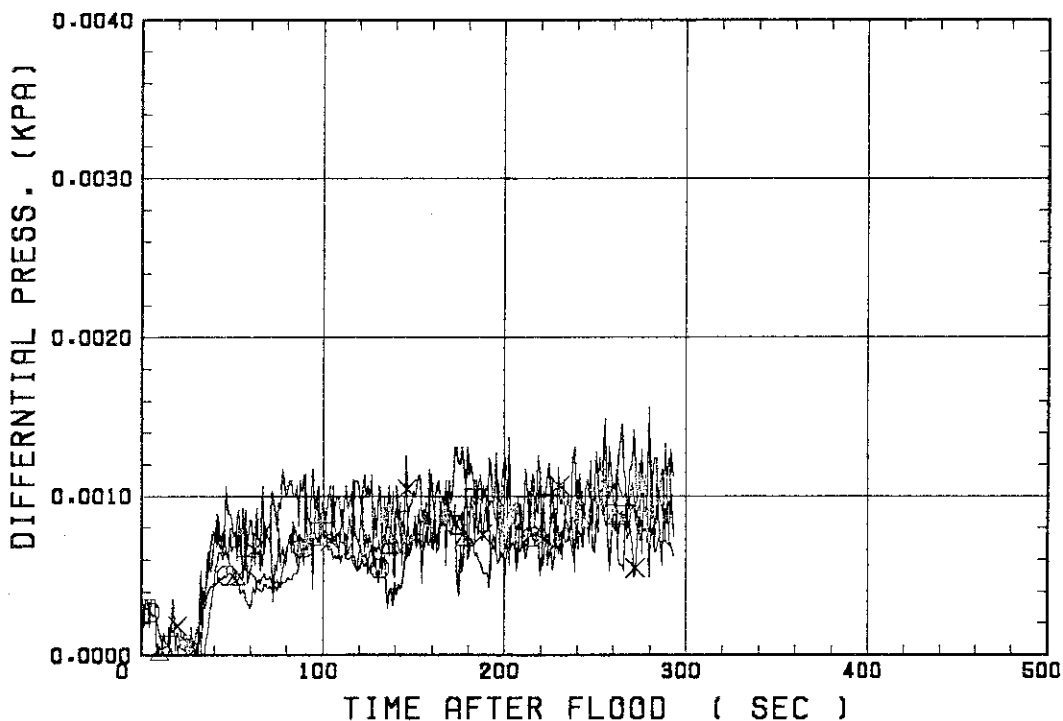
SMALL SCALE REFLOOD TEST
RUN 8117

○ --- DPT2 △ --- DPT4 + --- DPT5
X --- DPT6B



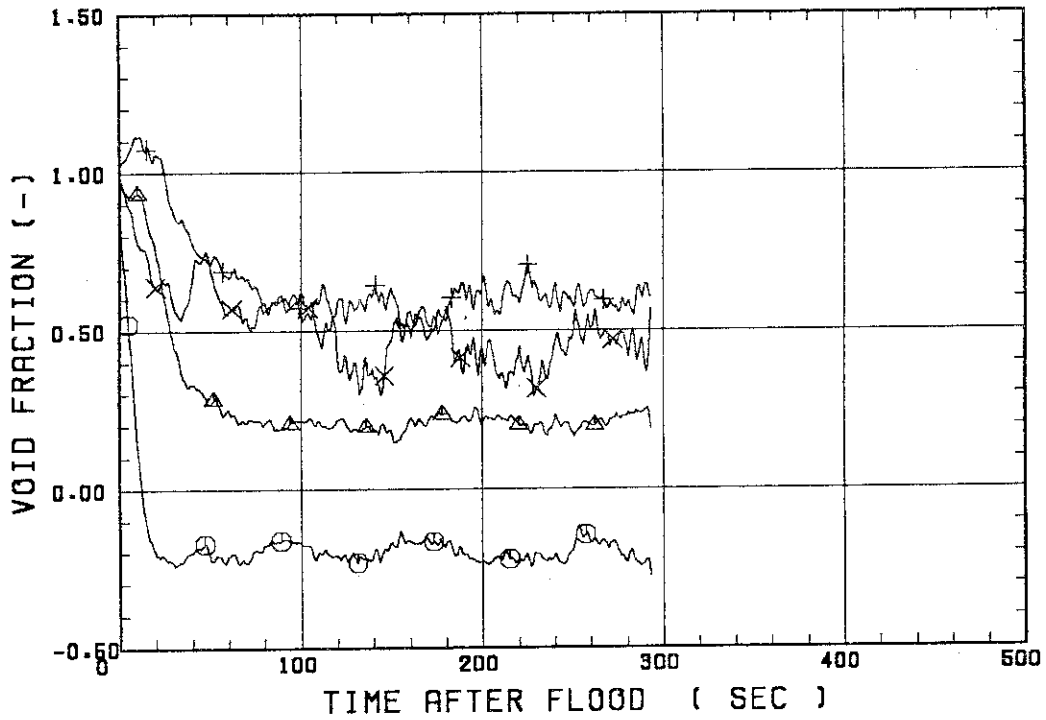
SMALL SCALE REFLOOD TEST
RUN 8117

○ --- DPT7 △ --- DPT8B + --- DP10
X --- DP12



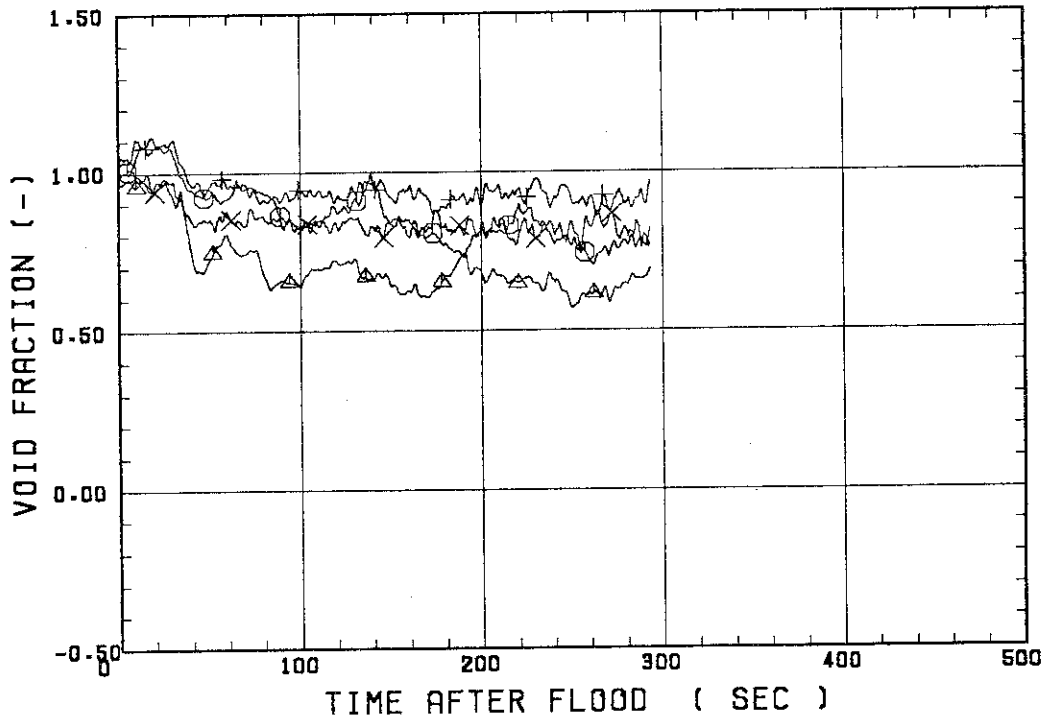
SMALL SCALE REFLOOD TEST
RUN 8117

○ --- VDPT2 ▲ --- VDPT4 + --- VDPT5
X --- VDPT6B



SMALL SCALE REFLOOD TEST
RUN 8117

○ --- VDPT7 ▲ --- VDPT8B + --- VDP10
X --- VDP12



 * RUN NO. 8118 *
 * *****

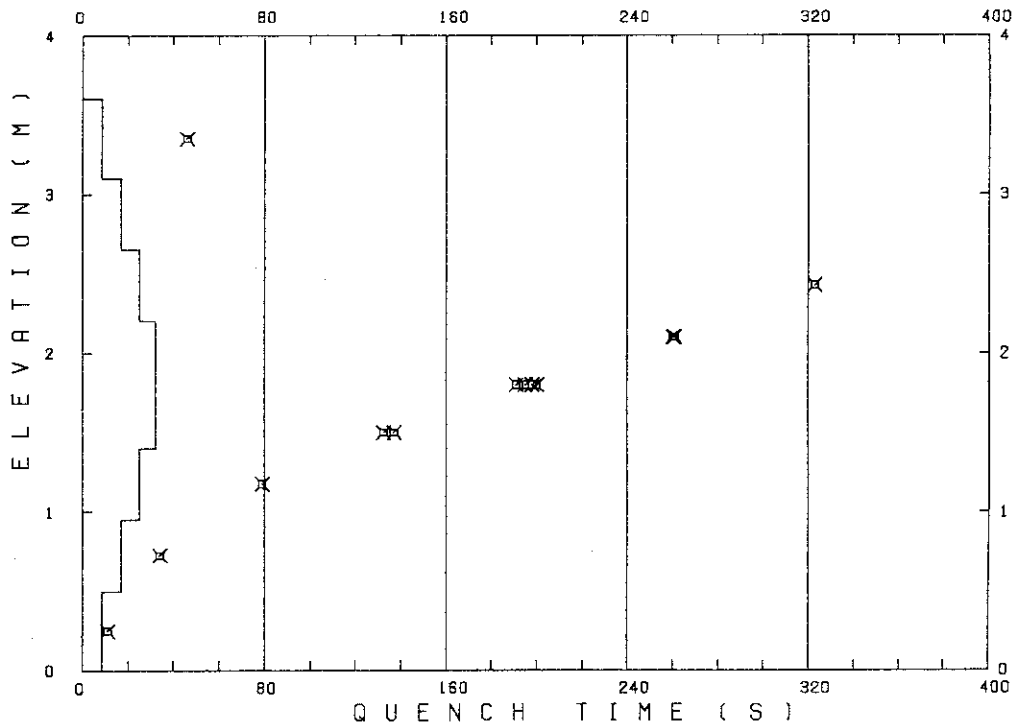
 TEST CONDITIONS

LINEAR PEAK POWER 2.0 KW/M
 SYSTEM PRESSURE 0.2 MPA
 INLET WATER TEMPERATURE 104 .C
 INJECTED WATER VELOCITY 3.8 CM/S

 TEMPERATURE PROFILE

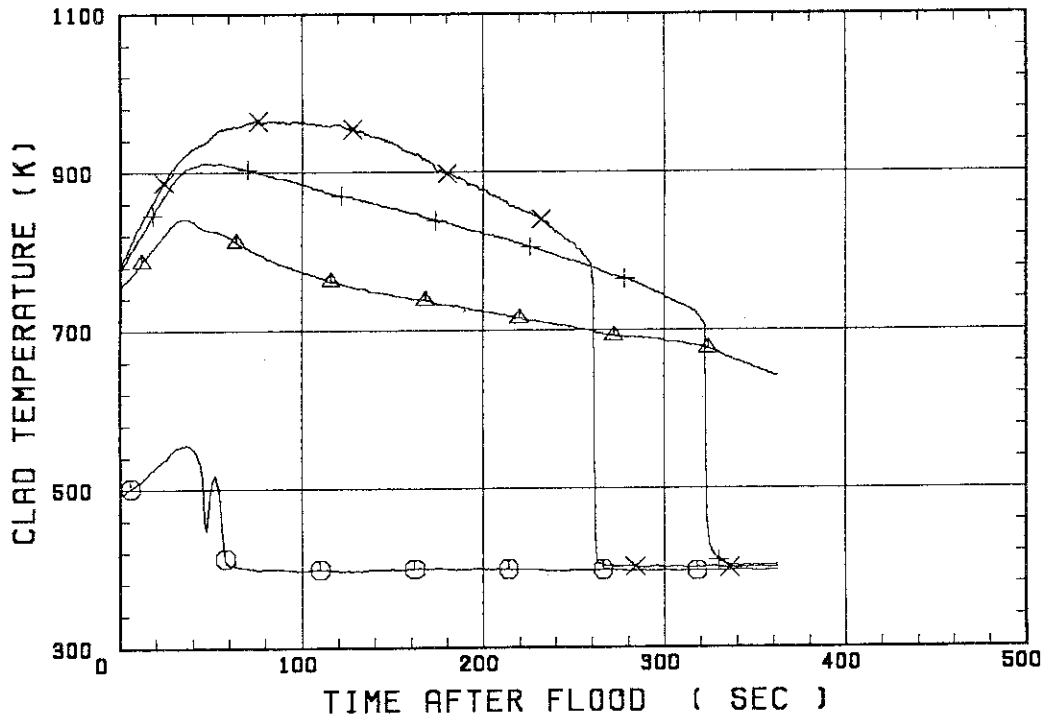
CH.NO.	SYMBOL	INITIAL TEMP. (.C)	TURNAROUND TIME (S)	TURNAROUND TEMP. (.C)	QUENCH TIME (S)	QUENCH TEMP. (.C)
66	TC1L	219	38.0	283	46.0	239
51	TR2	480	37.0	568		
52	TR3	498	55.0	639	323.0	432
67	TC4U	505	76.0	692	261.0	482
7	TS4U	548	59.0	737	260.0	470
53	TR4M	509	40.0	663	195.0	412
68	TC4M	483	40.0	627	198.0	404
8	TS4M	517	41.0	672	200.0	388
48	TB4M	515	40.0	673	191.0	432
69	TC4L	510	35.0	635	137.0	488
9	TS4L	528	35.5	663	132.5	483
54	TR5	448	28.0	541	79.0	437
55	TR6	327	21.0	368	34.0	338
70	TC7	223	10.0	234	11.0	193

RUN NO. 8118



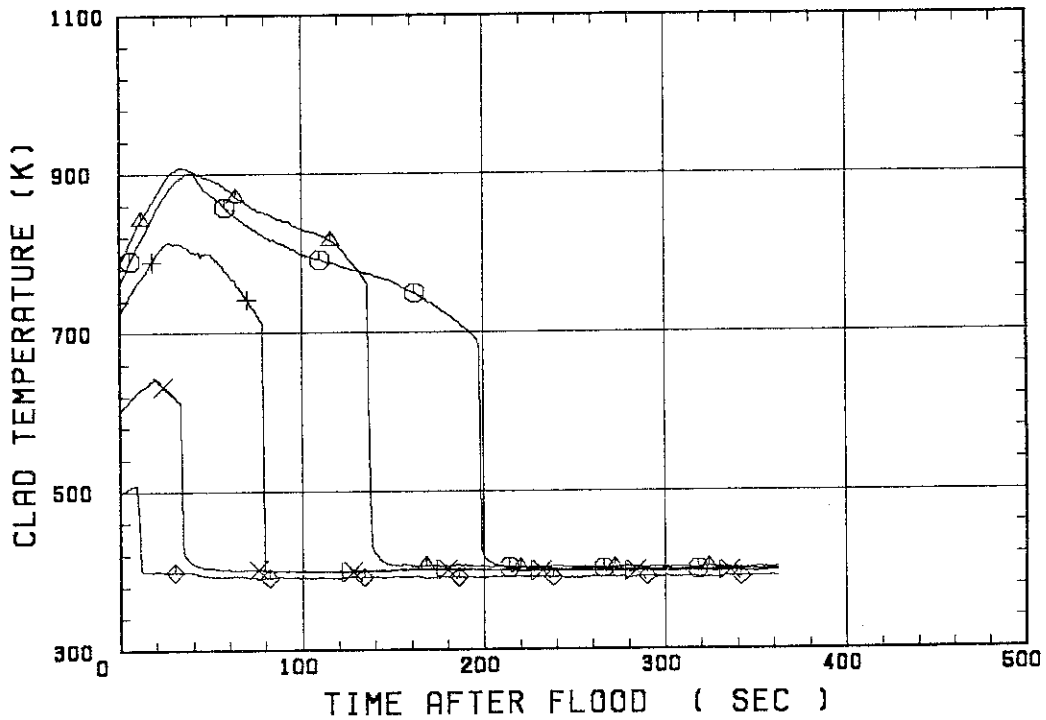
SMALL SCALE REFLOOD TEST
RUN 8118

○--- TC1L △--- TR2 +--- TR3
X--- TC4U

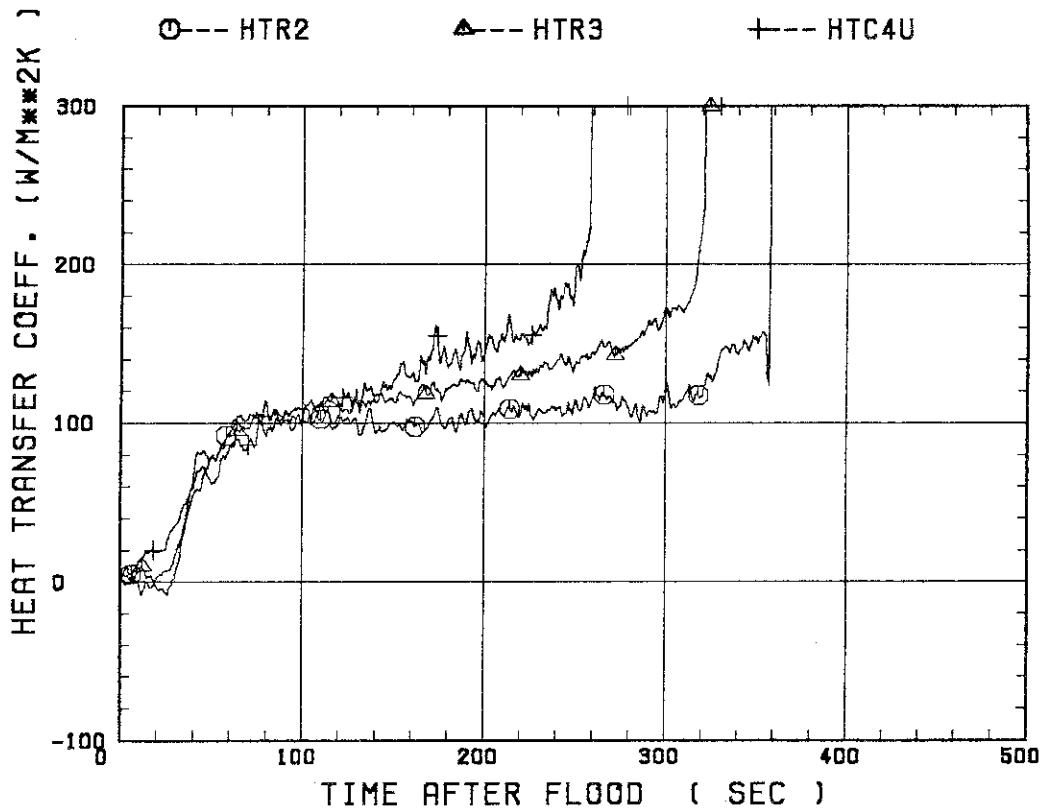


SMALL SCALE REFLOOD TEST
RUN 8118

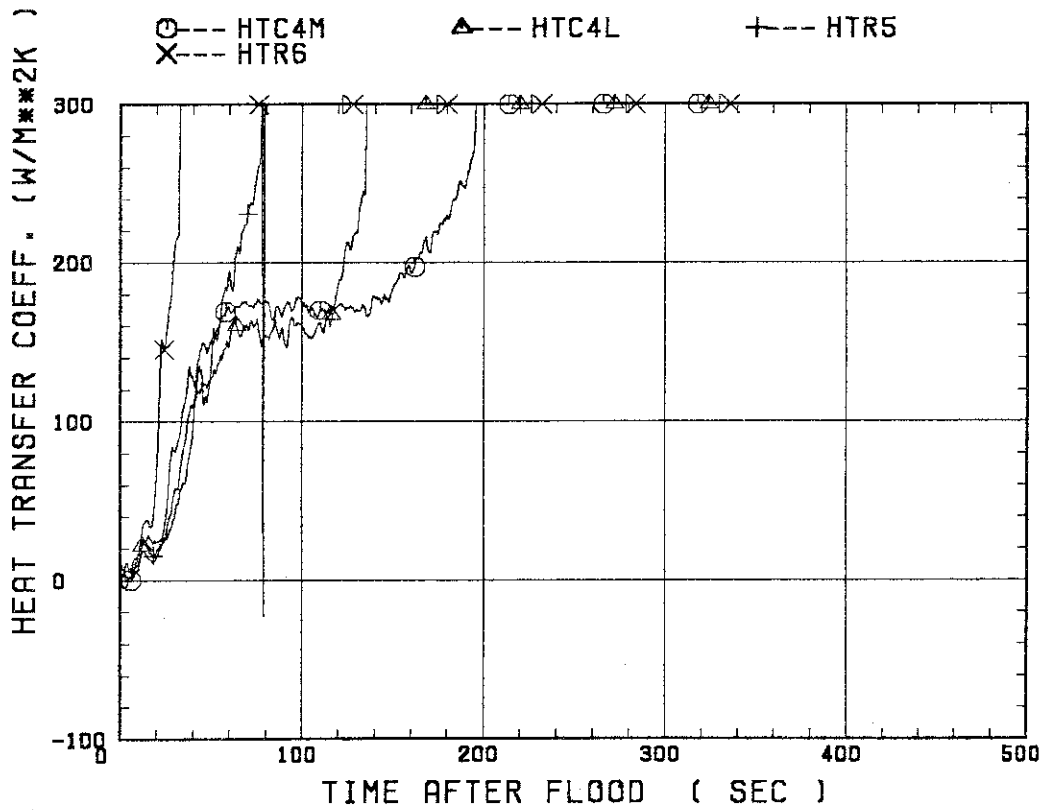
○--- TC4M △--- TC4L +--- TR5
X--- TR6 ◇--- TC7



SMALL SCALE REFLOOD TEST
 RUN 8118

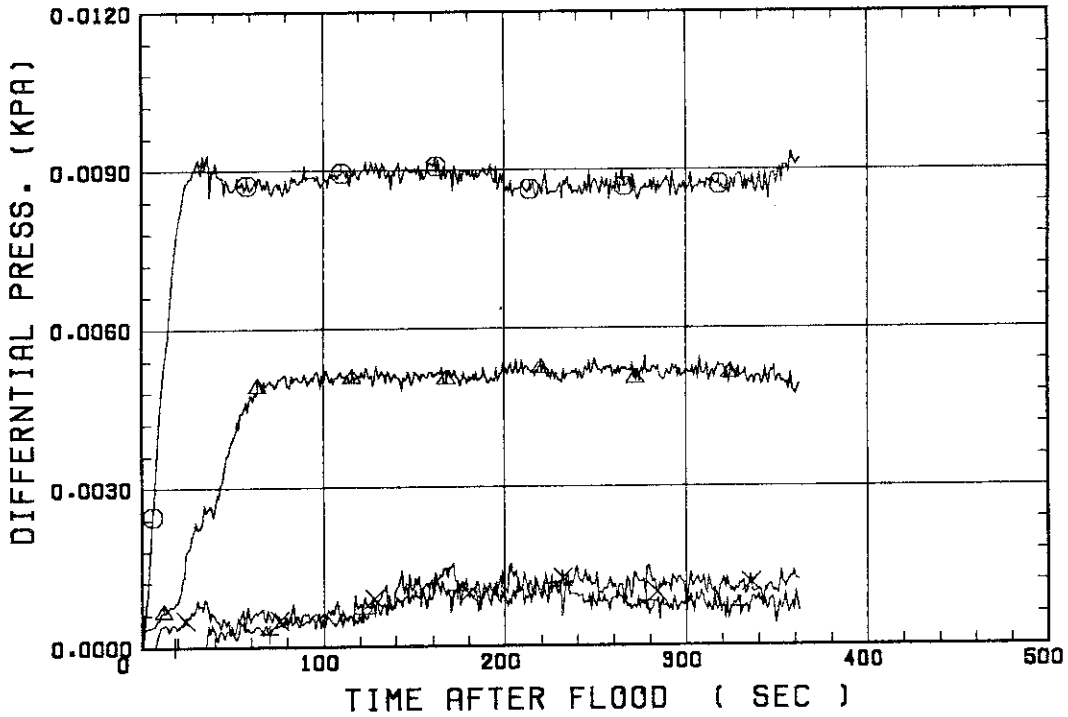


SMALL SCALE REFLOOD TEST
 RUN 8118



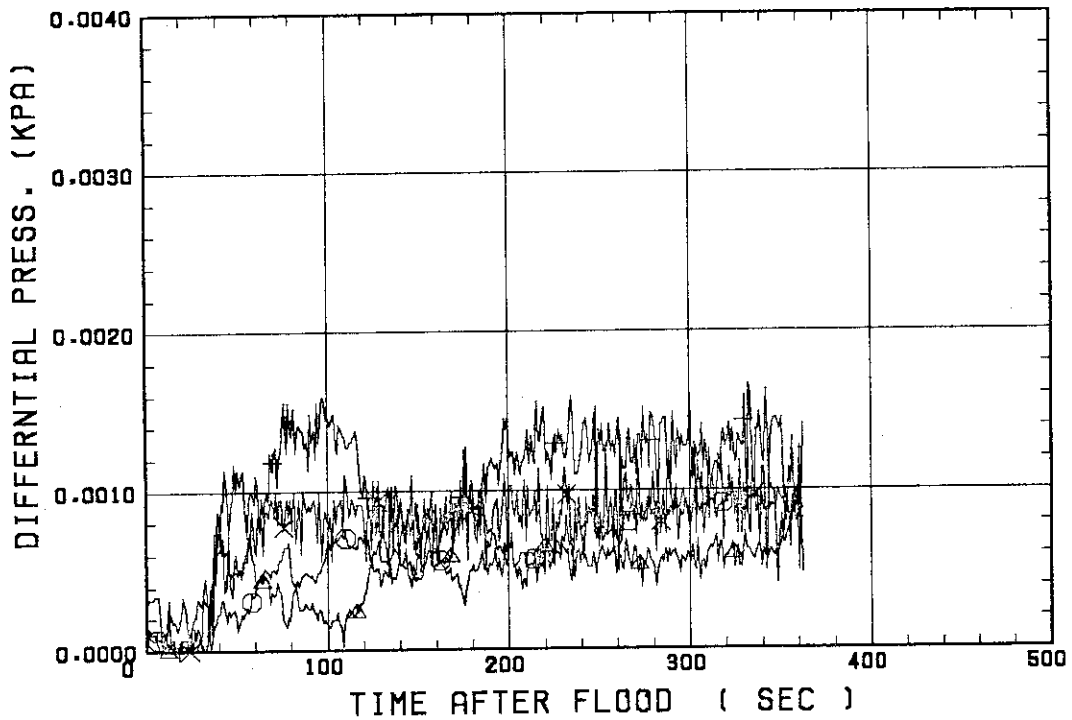
SMALL SCALE REFLOOD TEST
RUN 8118

○ --- DPT2 △ --- DPT4 + --- DPT5
X --- DPT6B



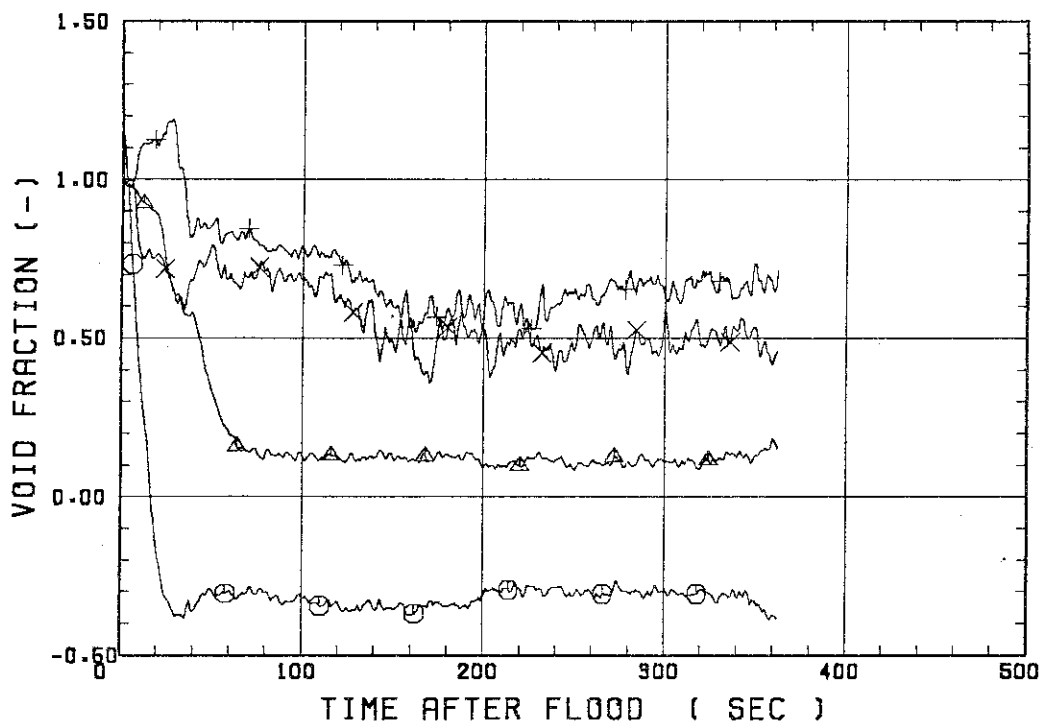
SMALL SCALE REFLOOD TEST
RUN 8118

○ --- DPT7 △ --- DPT8B + --- DP10
X --- DP12



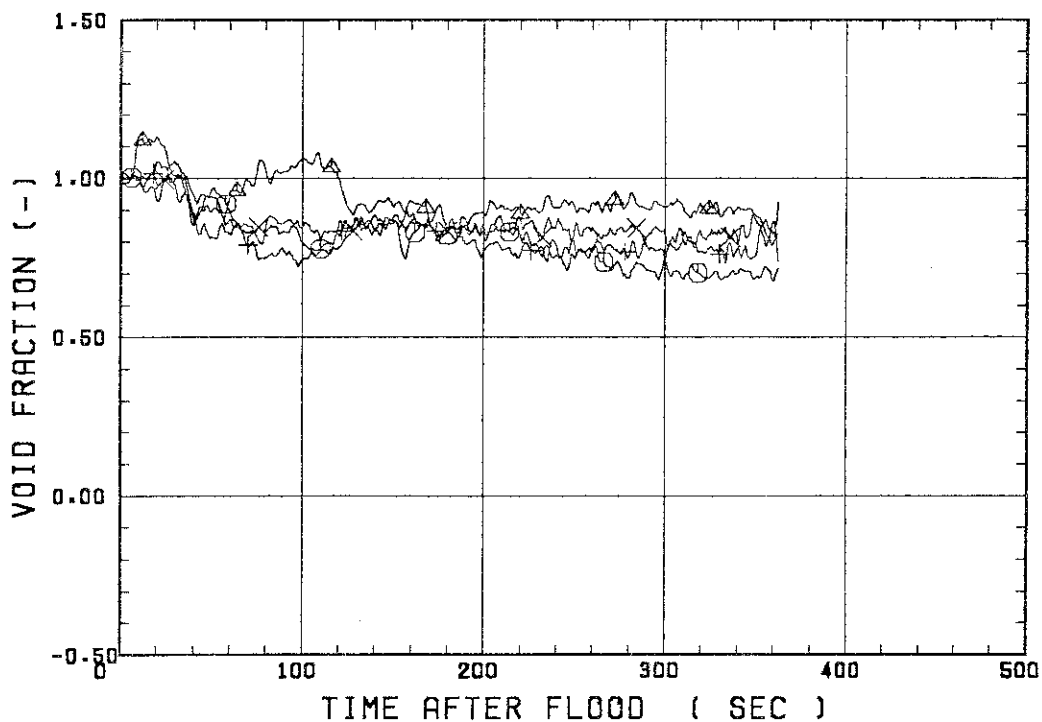
SMALL SCALE REFLOOD TEST
RUN 8118

○--- VDPT2 △--- VDPT4 +--- VDPT5
X--- VDPT6B



SMALL SCALE REFLOOD TEST
RUN 8118

○--- VDPT7 △--- VDPT8B +--- VDP10
X--- VDP12



 * RUN NO. 8120 *

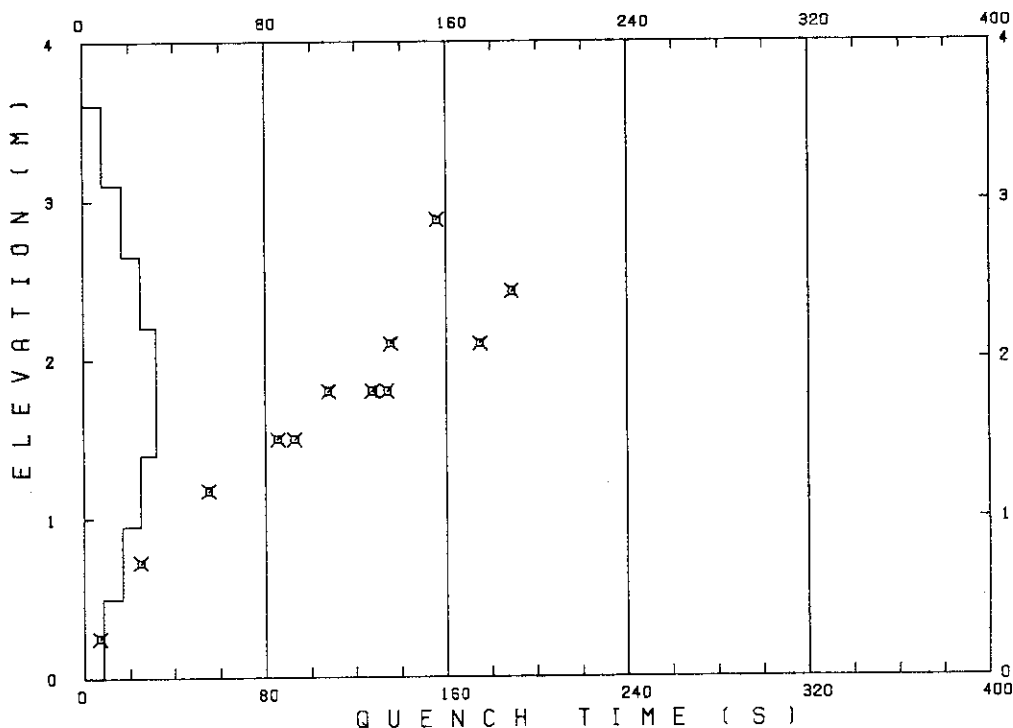
 TEST CONDITIONS

LINEAR PEAK POWER 1.8 KW/M
 SYSTEM PRESSURE 0.2 MPA
 INLET WATER TEMPERATURE 100 .C
 INJECTED WATER VELOCITY 5.8 CM/S

 TEMPERATURE PROFILE

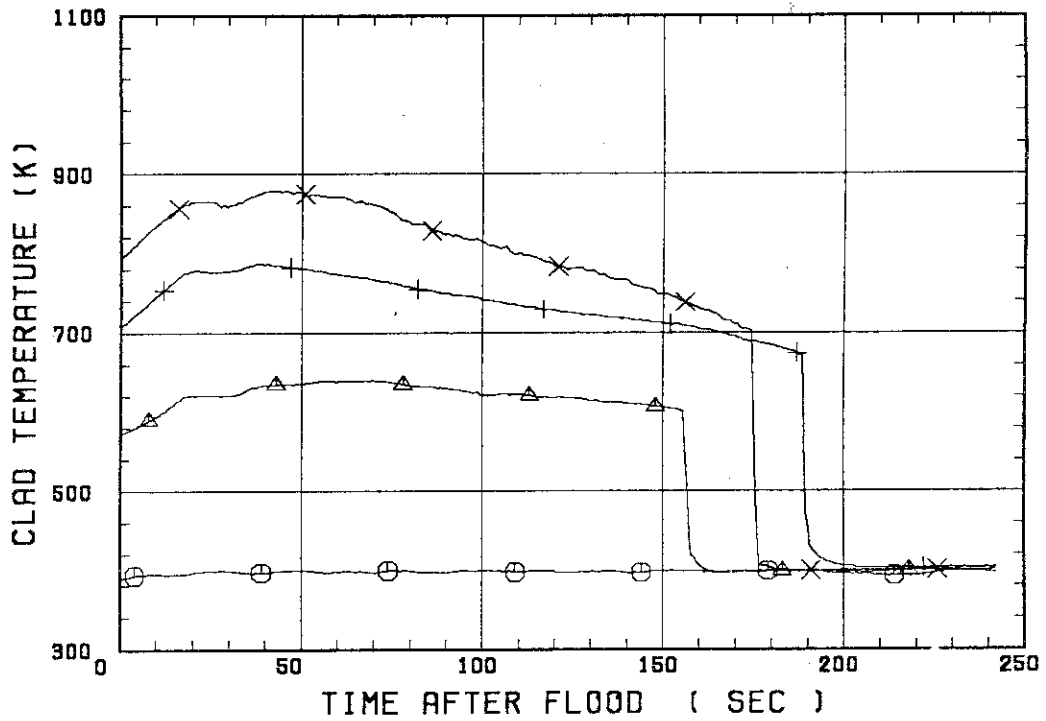
CH.NO.	SYMBOL	INITIAL TEMP. (.C)	TURNAROUND TIME (S)	TURNAROUND TEMP. (.C)	QUENCH TIME (S)	QUENCH TEMP. (.C)
66	TC1L	115	102.0	127		
51	TR2	298	70.0	367	156.0	327
52	TR3	432	39.0	514	189.0	398
67	TC4U	517	43.0	606	175.0	429
7	TS4U	541	37.5	639	135.5	468
53	TR4M	519	20.0	599	108.0	417
68	TC4M	504	20.0	577	134.0	380
8	TS4M	517	18.5	598	127.5	377
48	TB4M	526	21.0	605	127.0	392
69	TC4L	530	18.0	597	93.0	420
9	TS4L	535	18.0	606	85.5	426
54	TR5	448	16.0	500	55.0	416
55	TR6	317	13.0	343	25.0	316
70	TC7	213	7.0	221	7.0	221

RUN NO. 8120



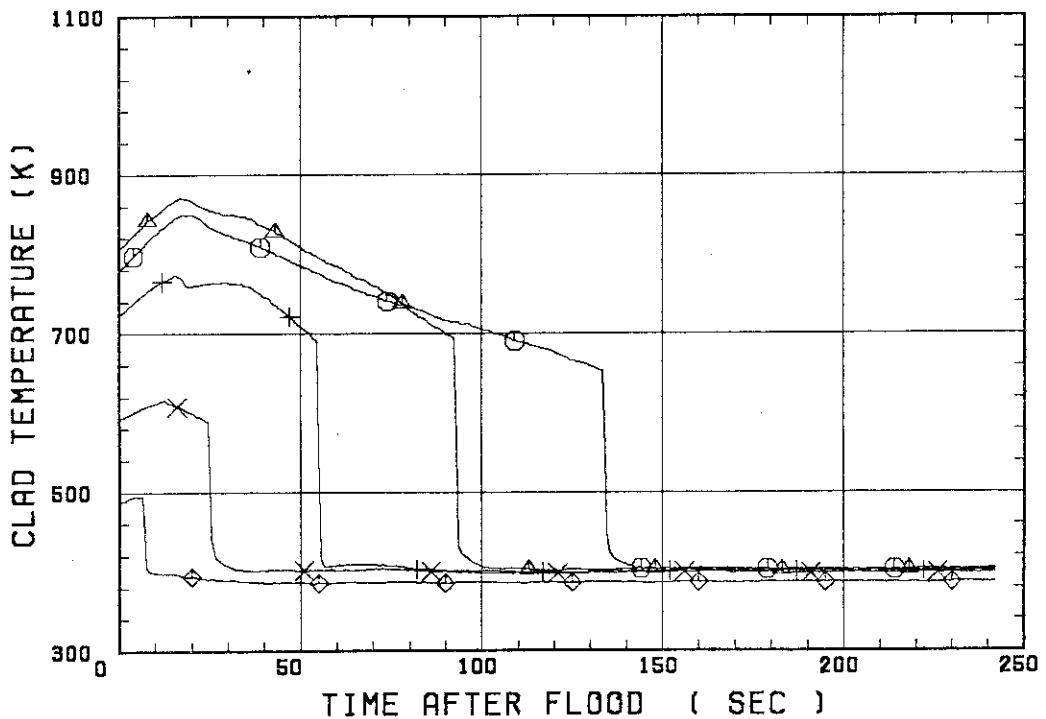
SMALL SCALE REFLOOD TEST
 RUN 8120

○--- TC1L ▲--- TR2 +--- TR3
 X--- TC4U

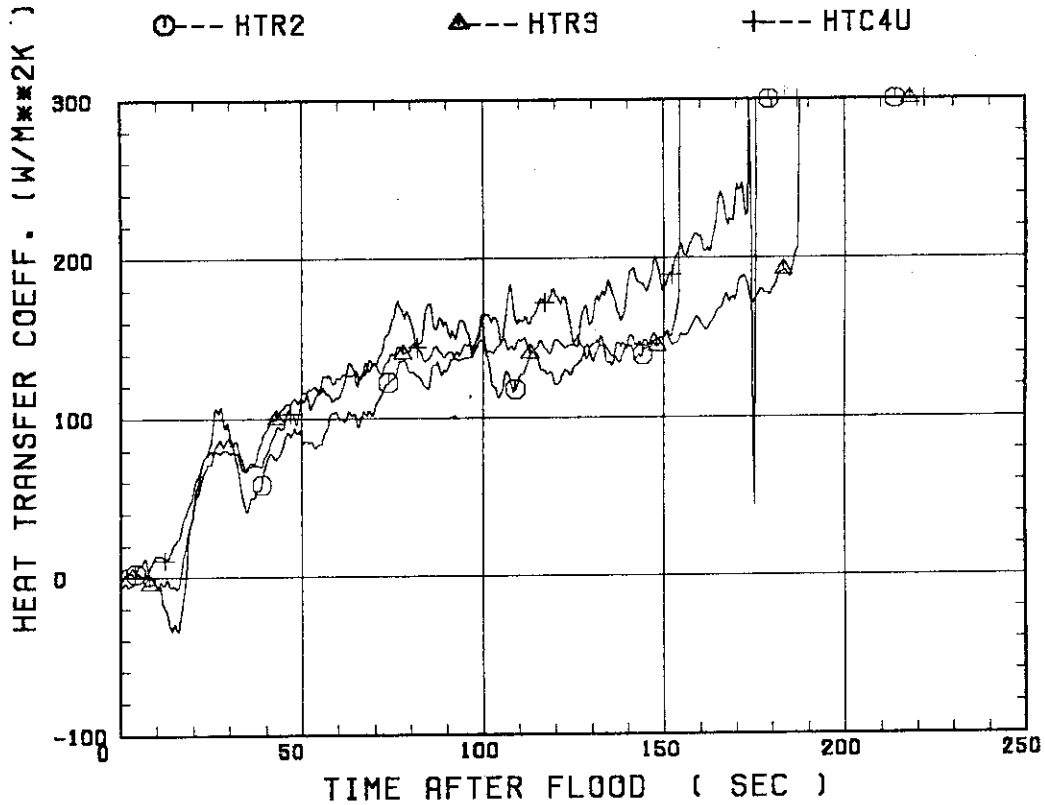


SMALL SCALE REFLOOD TEST
 RUN 8120

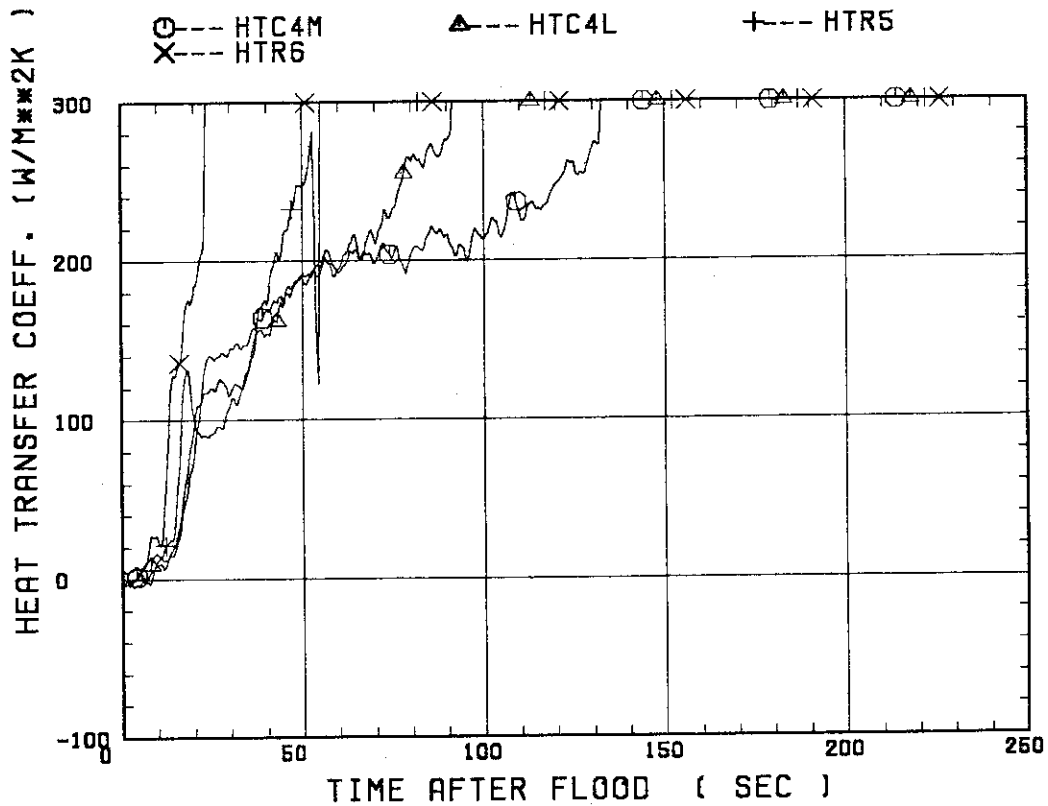
○--- TC4M ▲--- TC4L +--- TR5
 X--- TR6 ◆--- TC7



SMALL SCALE REFLOOD TEST
RUN 8120

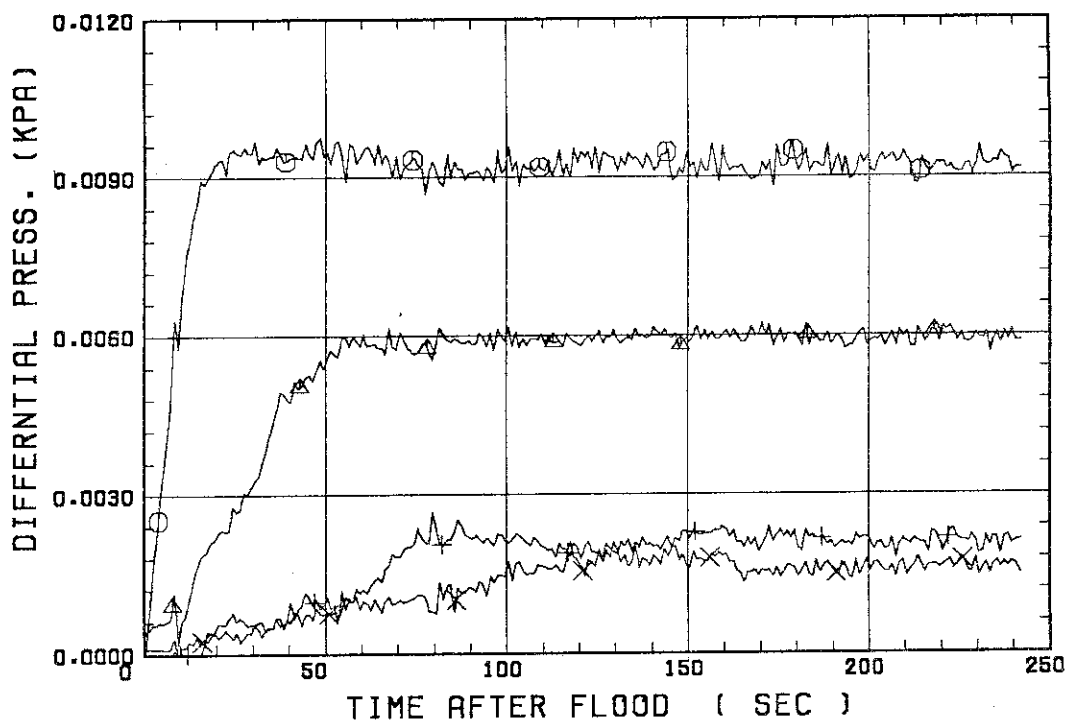


SMALL SCALE REFLOOD TEST
RUN 8120



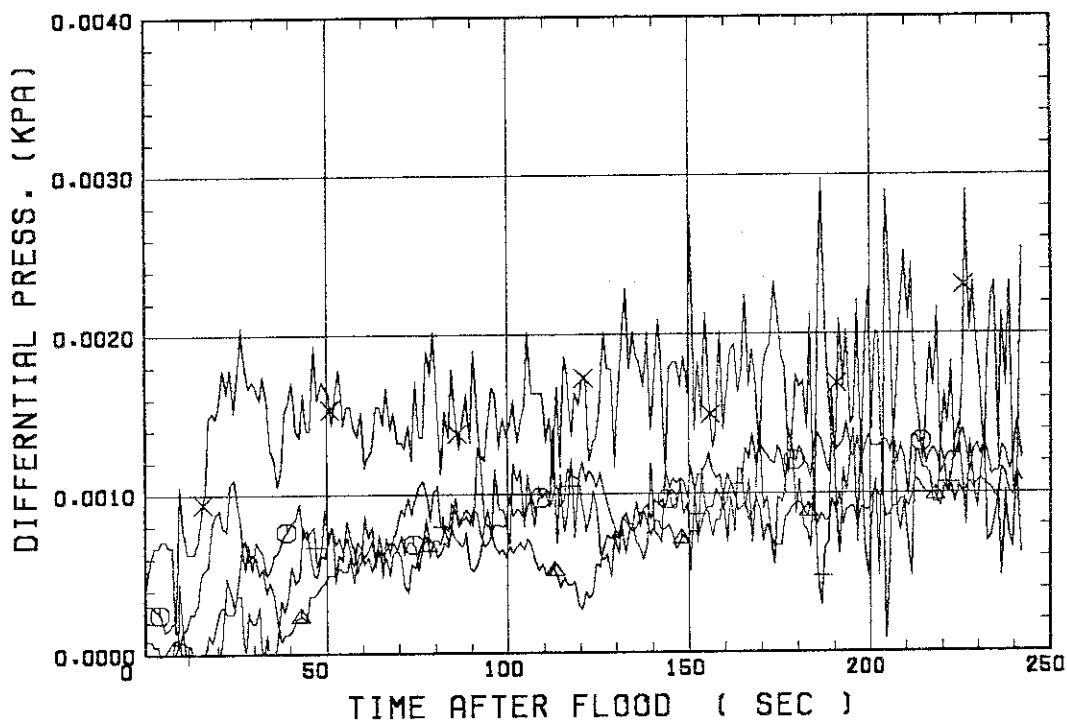
SMALL SCALE REFLOOD TEST
RUN 8120

○ --- DPT2 ▲ --- DPT4 + --- DPT5
X --- DPT6B



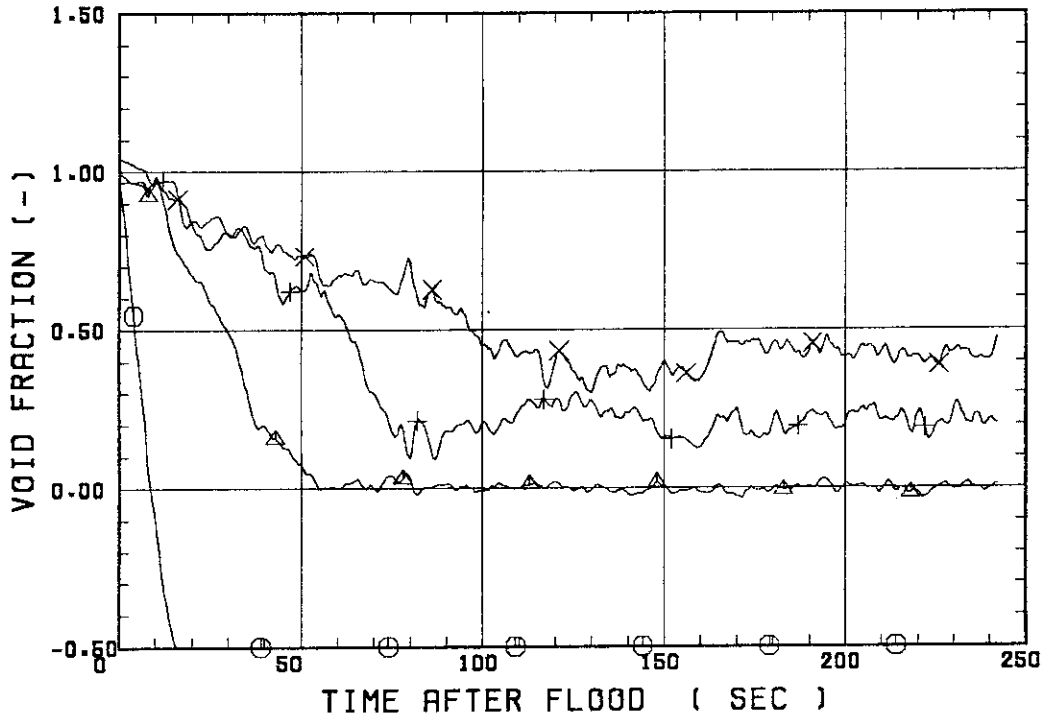
SMALL SCALE REFLOOD TEST
RUN 8120

○ --- DPT7 ▲ --- DPT8B + --- DP10
X --- DP12



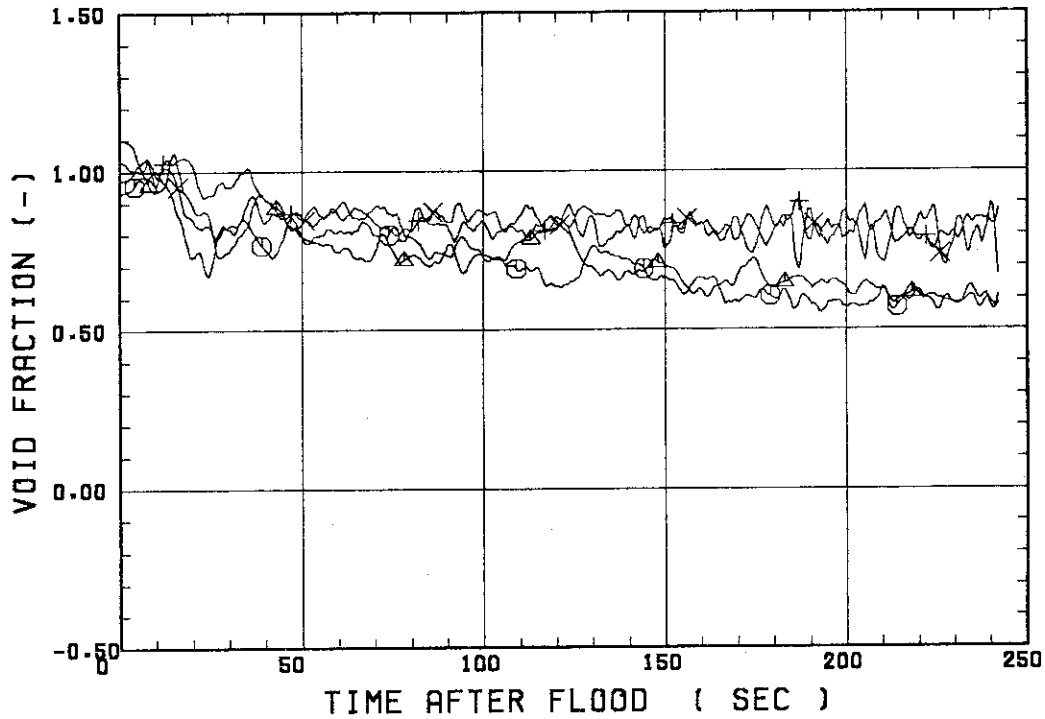
SMALL SCALE REFLOOD TEST
RUN 8120

○--- VDPT2 ▲--- VDPT4 +--- VDPT5
X--- VDPT6B



SMALL SCALE REFLOOD TEST
RUN 8120

○--- VDPT7 ▲--- VDPT8B +--- VDP10
X--- VDP12



 * RUN NO. 8121 *

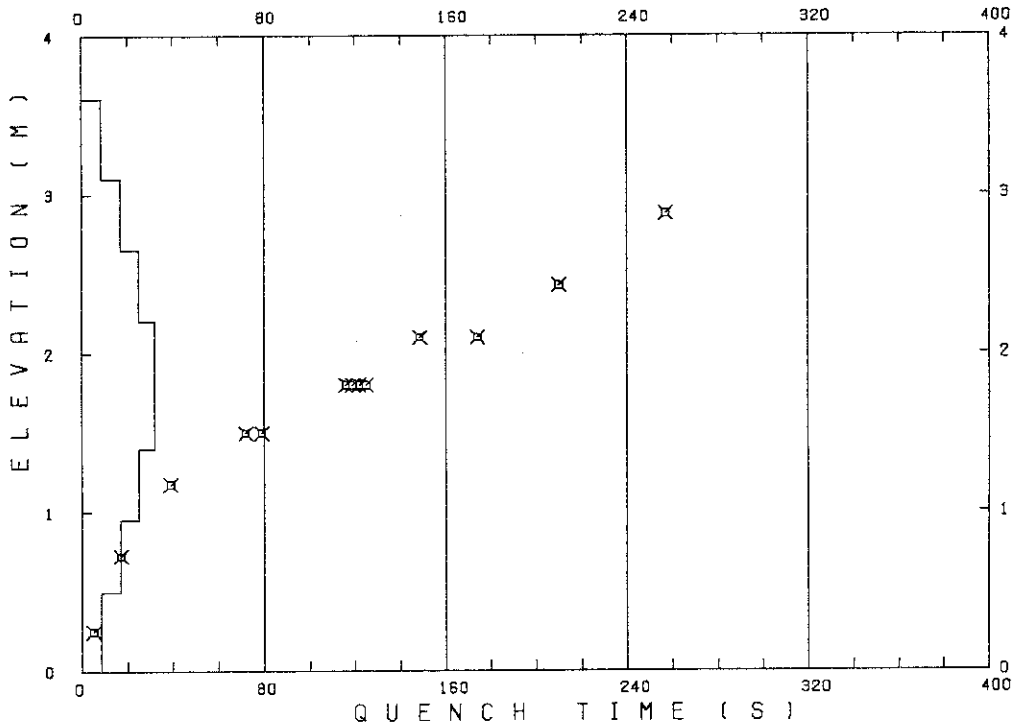
 TEST CONDITIONS

LINEAR PEAK POWER 1.8 KW/M
 SYSTEM PRESSURE 0.2 MPA
 INLET WATER TEMPERATURE 100 .C
 INJECTED WATER VELOCITY 3.9 CM/S

 TEMPERATURE PROFILE

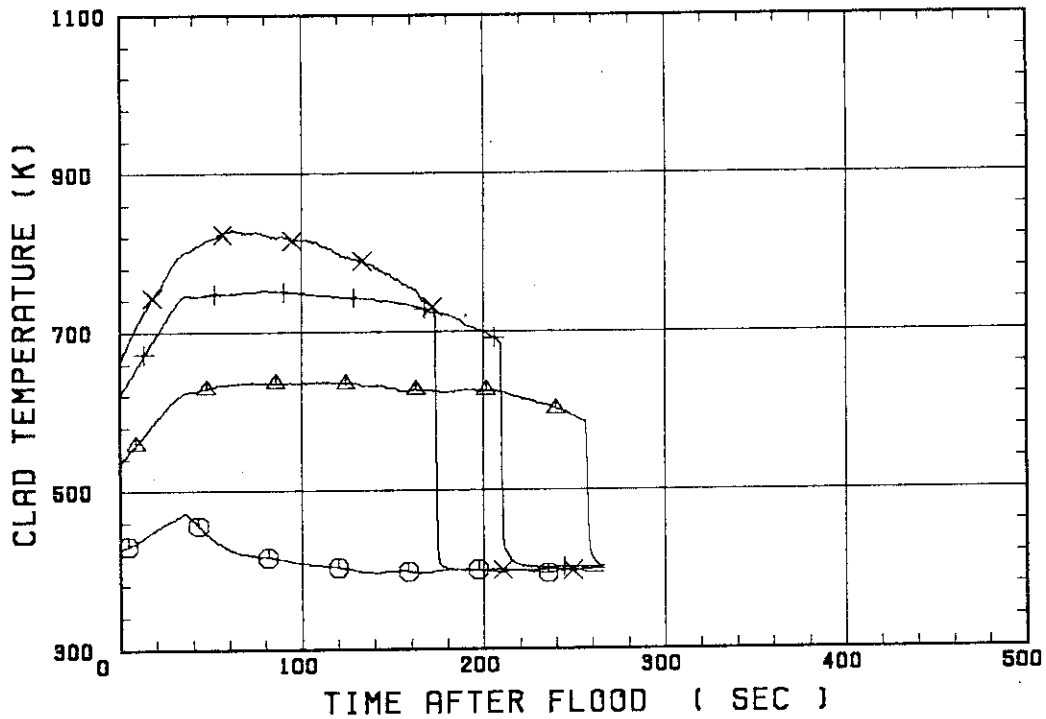
CH.NO.	SYMBOL	INITIAL TEMP. (.C)	TURNAROUND TIME (S)	TURNAROUND TEMP. (.C)	QUENCH TIME (S)	QUENCH TEMP. (.C)
66	TC1L	153	36.0	199		
51	TR2	261	115.0	364	257.0	312
52	TR3	345	81.0	479	210.0	410
67	TC4U	387	63.0	555	174.0	442
7	TS4U	393	61.0	558	148.5	457
53	TR4M	371	32.0	492	119.0	392
68	TC4M	374	30.0	481	125.0	390
8	TS4M	369	31.0	493	122.0	385
48	TB4M	377	30.0	498	116.0	405
69	TC4L	378	34.0	479	79.0	408
9	TS4L	372	28.0	485	72.0	438
54	TR5	319	29.0	392	39.0	372
55	TR6	239	14.0	268	17.0	262
70	TC7	177	4.0	182	5.0	181

RUN NO. 8121



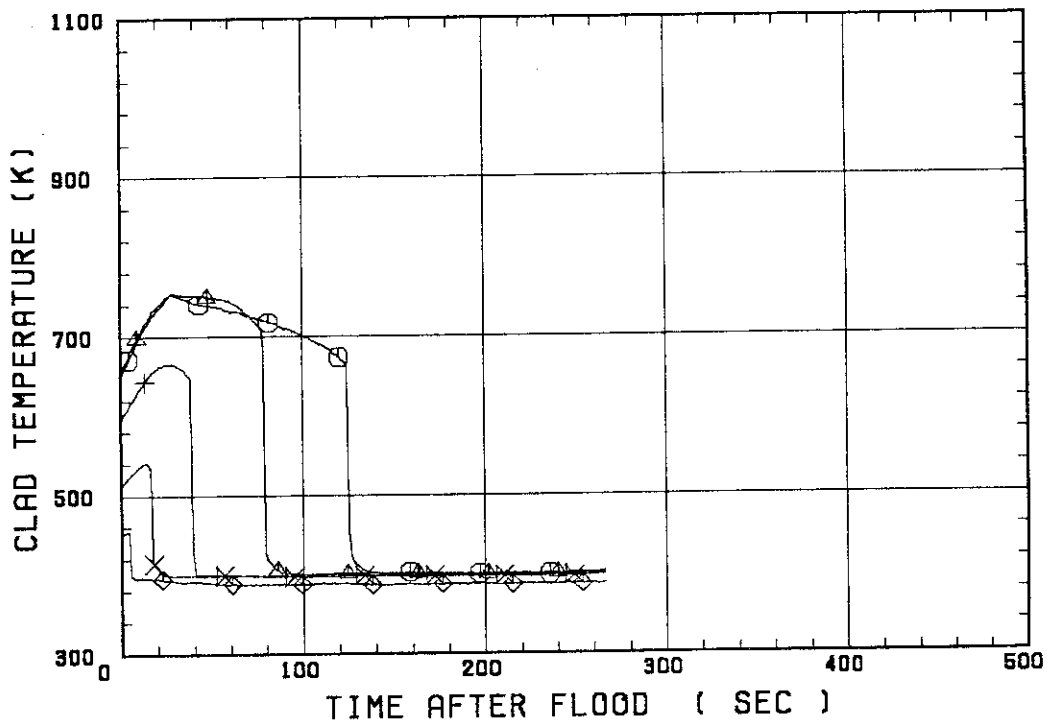
SMALL SCALE REFLOOD TEST
 RUN 8121

○--- TC1L △--- TR2 +--- TR3
 X--- TC4U

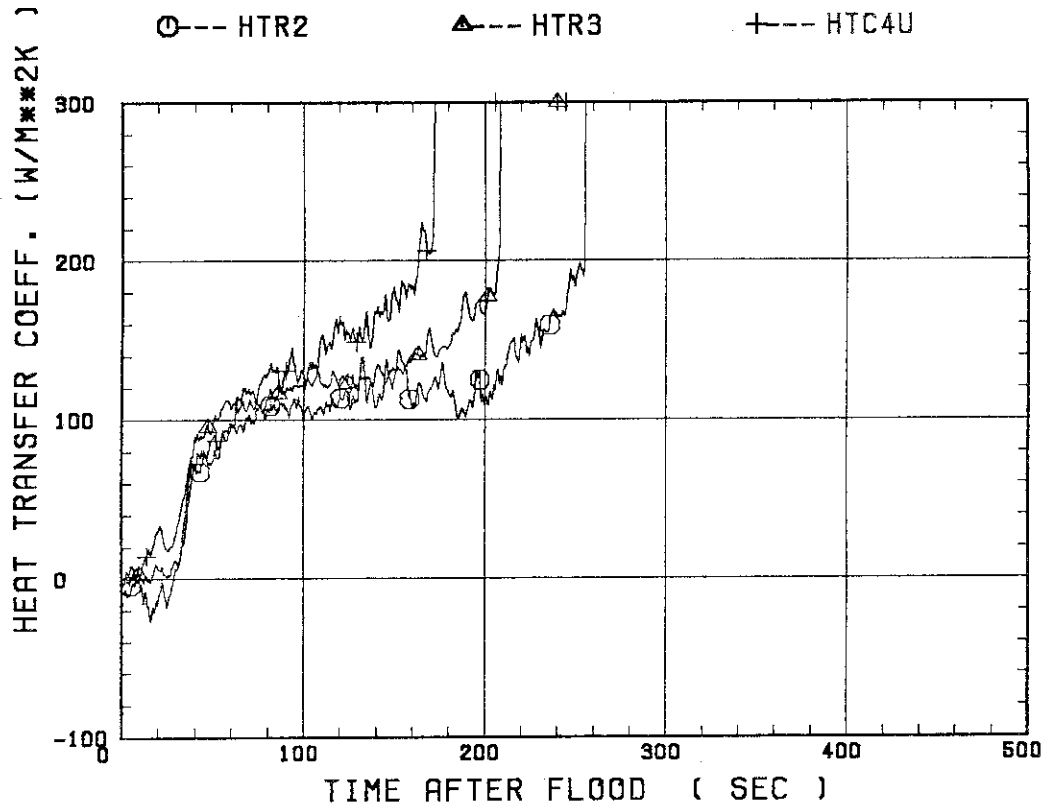


SMALL SCALE REFLOOD TEST
 RUN 8121

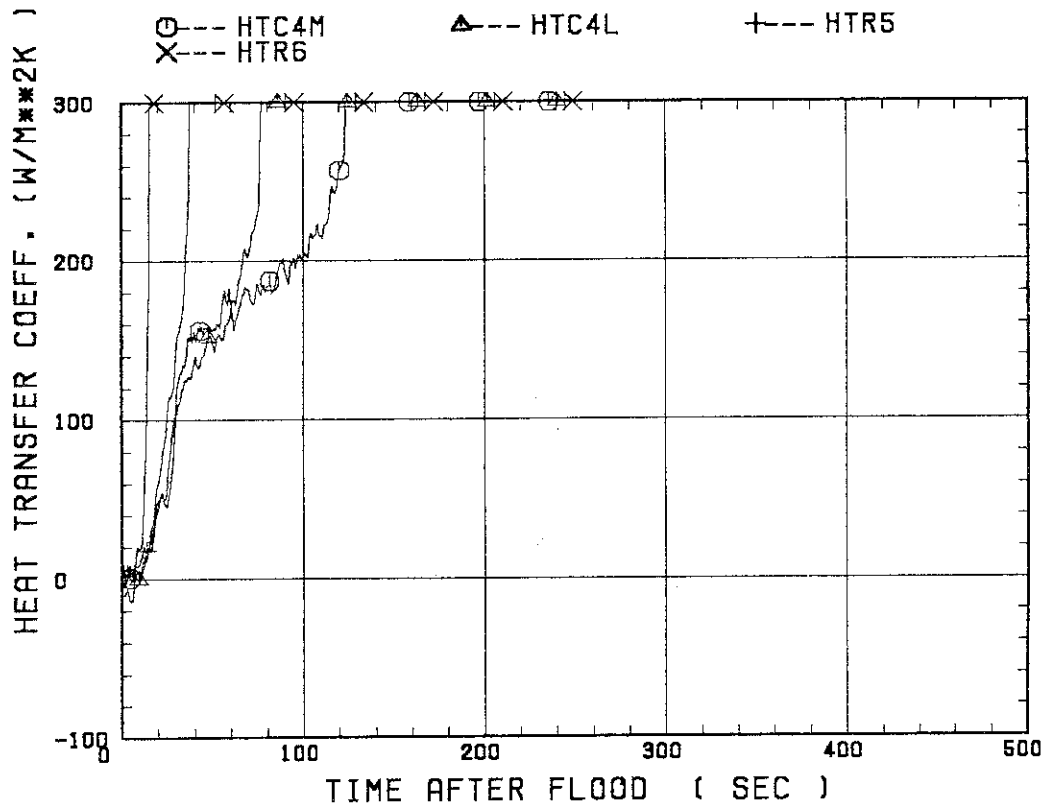
○--- TC4M △--- TC4L +--- TR5
 X--- TR6 ◇--- TC7



SMALL SCALE REFLOOD TEST
RUN 8121

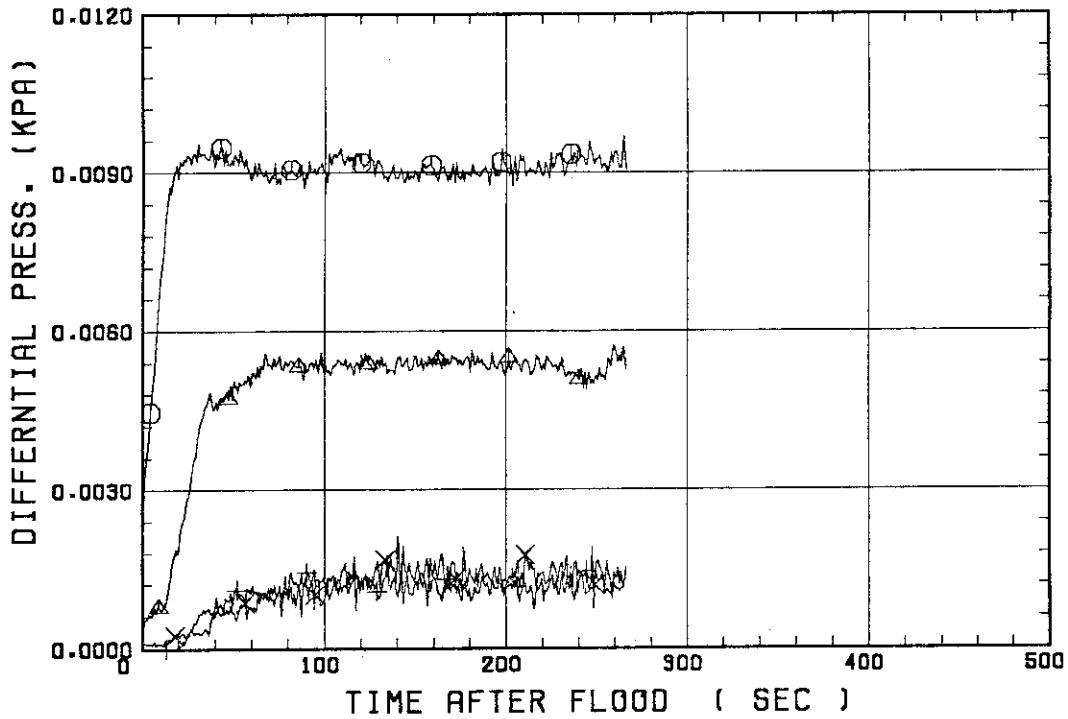


SMALL SCALE REFLOOD TEST
RUN 8121



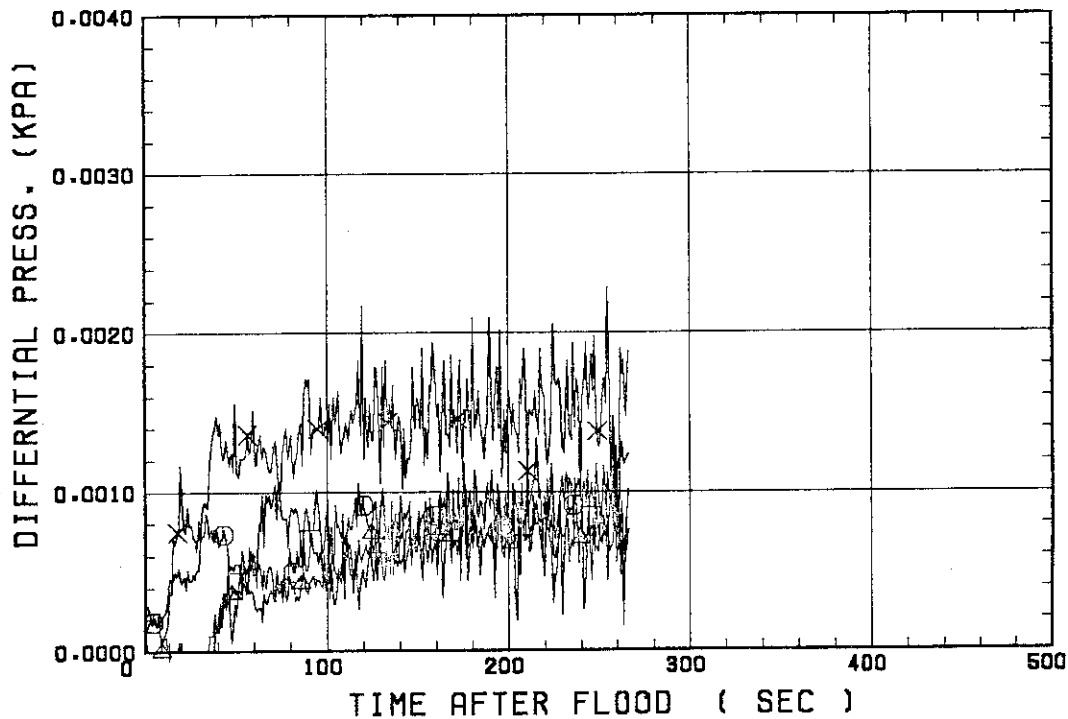
SMALL SCALE REFLOOD TEST
RUN 8121

○--- DPT2 △--- DPT4 +--- DPT5
X--- DPT6B



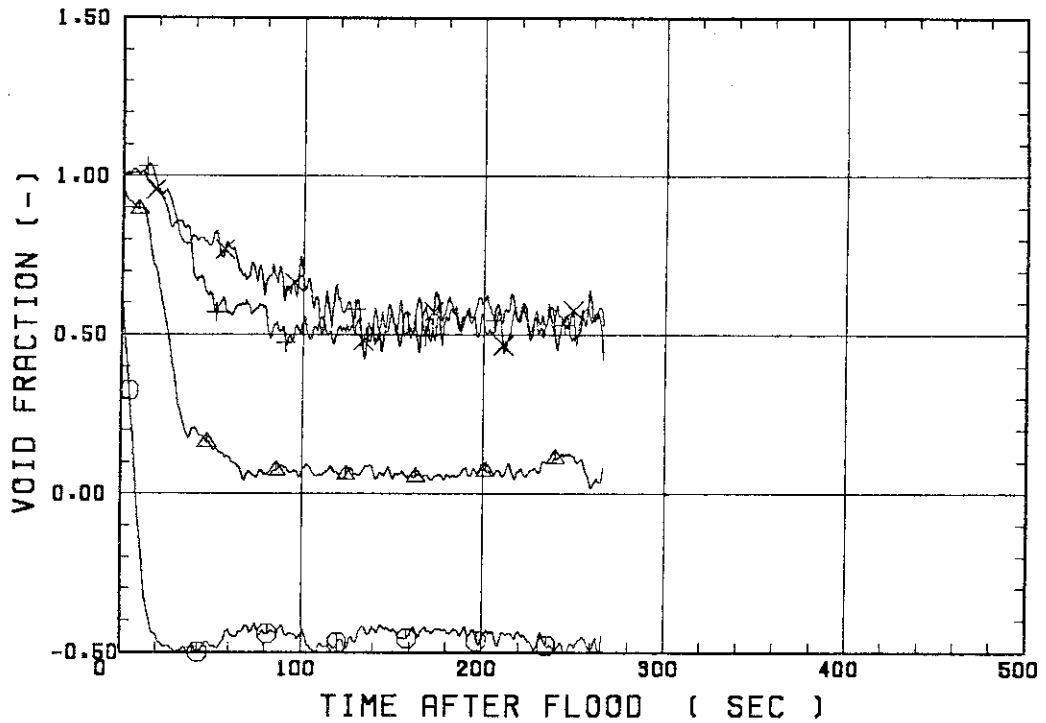
SMALL SCALE REFLOOD TEST
RUN 8121

○--- DPT7 △--- DPT8B +--- DP10
X--- DP12



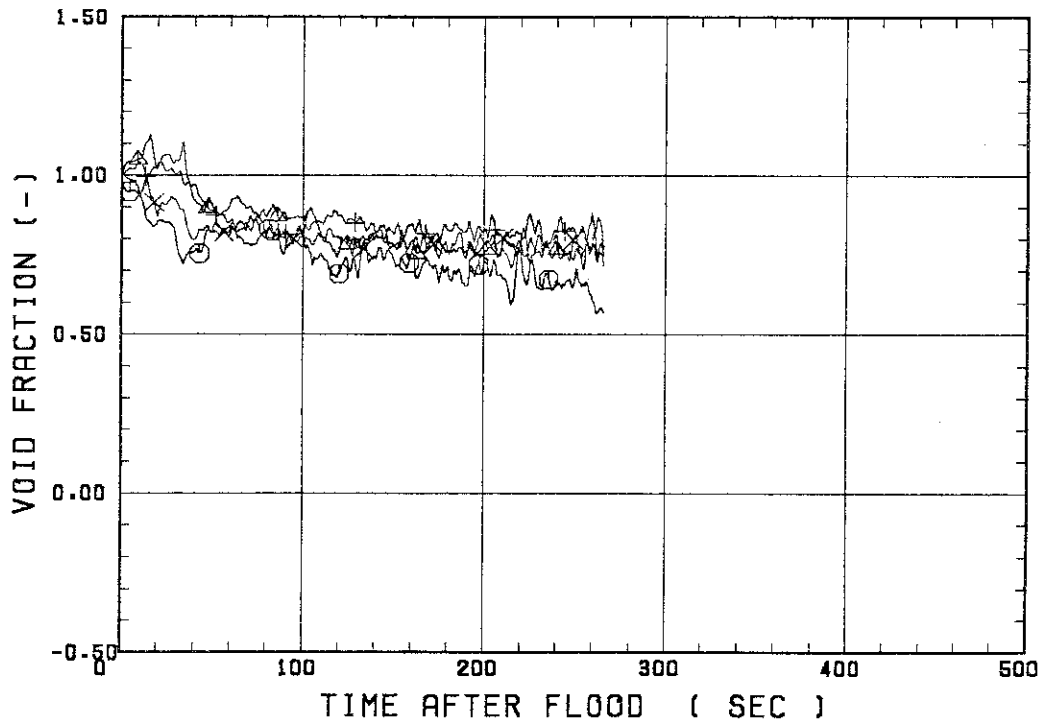
SMALL SCALE REFLOOD TEST
RUN 8121

○--- VDPT2 △--- VDPT4 +--- VDPT5
X--- VDPT6B



SMALL SCALE REFLOOD TEST
RUN 8121

○--- VDPT7 △--- VDPT8B +--- VDP10
X--- VDP12



 * RUN NO. 8122 *

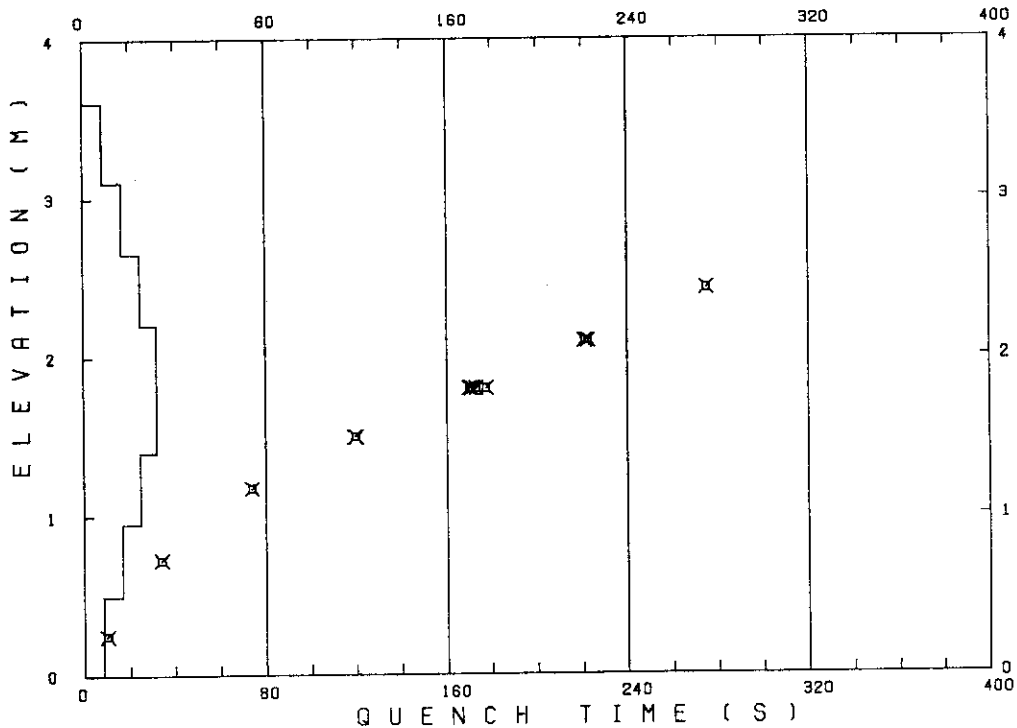
 TEST CONDITIONS

LINEAR PEAK POWER 1.8 KW/M
 SYSTEM PRESSURE 0.2 MPA
 INLET WATER TEMPERATURE 100 -C
 INJECTED WATER VELOCITY 3.9 CM/S

 TEMPERATURE PROFILE

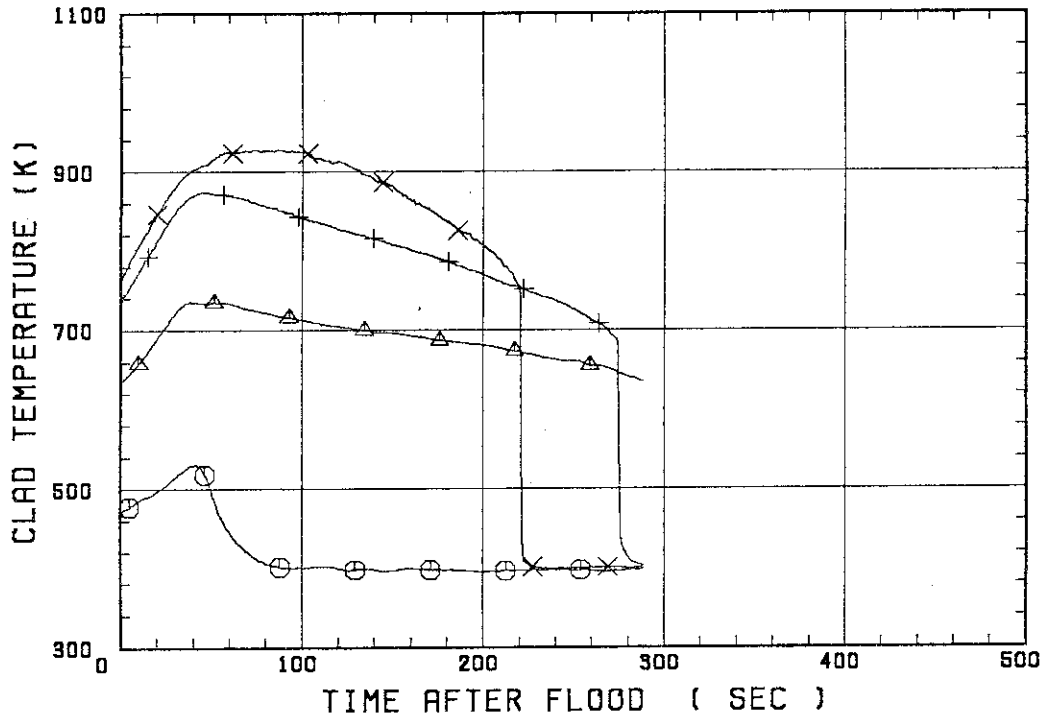
CH.NO.	SYMBOL	INITIAL TEMP. (.C)	TURNAROUND TIME (S)	TURNAROUND TEMP. (.C)	QUENCH TIME (S)	QUENCH TEMP. (.C)
66	TC1L	199	42.0	258		
51	TR2	359	39.0	463		
52	TR3	461	45.0	603	275.0	410
67	TC4U	486	87.0	655	221.0	471
7	TS4U	552	57.5	722	222.5	457
53	TR4M	516	40.0	659	173.0	399
68	TC4M	470	40.0	609	171.0	403
8	TS4M	526	41.5	670	177.5	394
48	TB4M	524	42.0	667	170.0	416
69	TC4L	500	38.0	618	120.0	449
9	TS4L	533	36.0	656	119.5	465
54	TR5	461	32.0	541	74.0	440
55	TR6	335	20.0	373	34.0	339
70	TC7	222	9.0	234	10.0	234

RUN NO. 8122



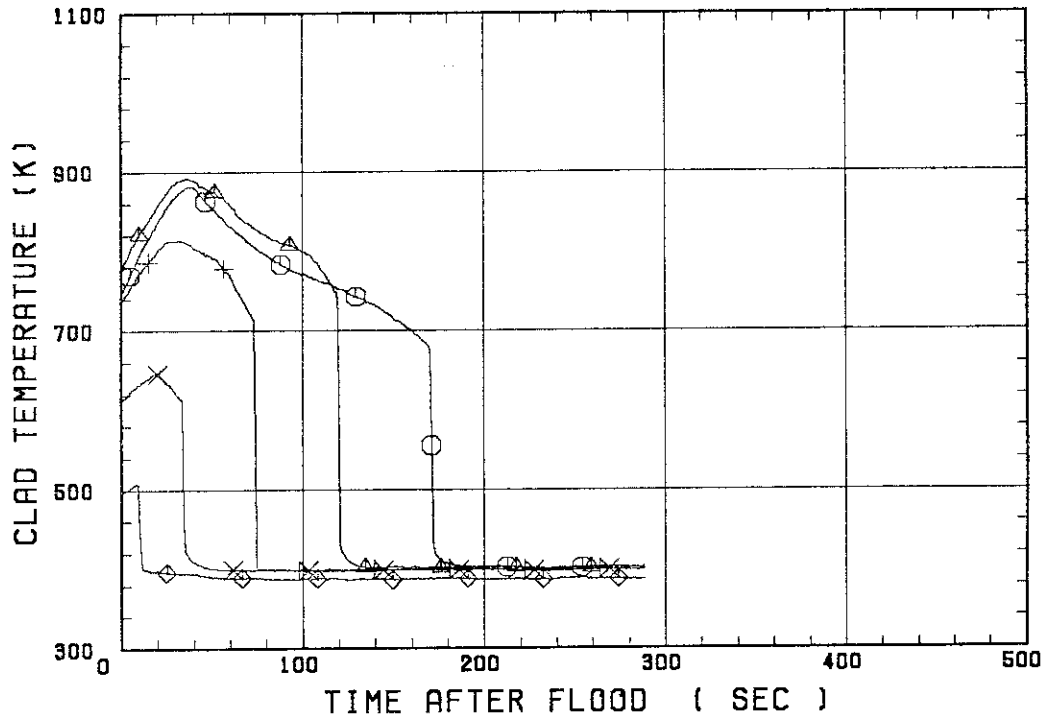
SMALL SCALE REFLOOD TEST
RUN 8122

○--- TC1L △--- TR2 +--- TR3
X--- TC4U

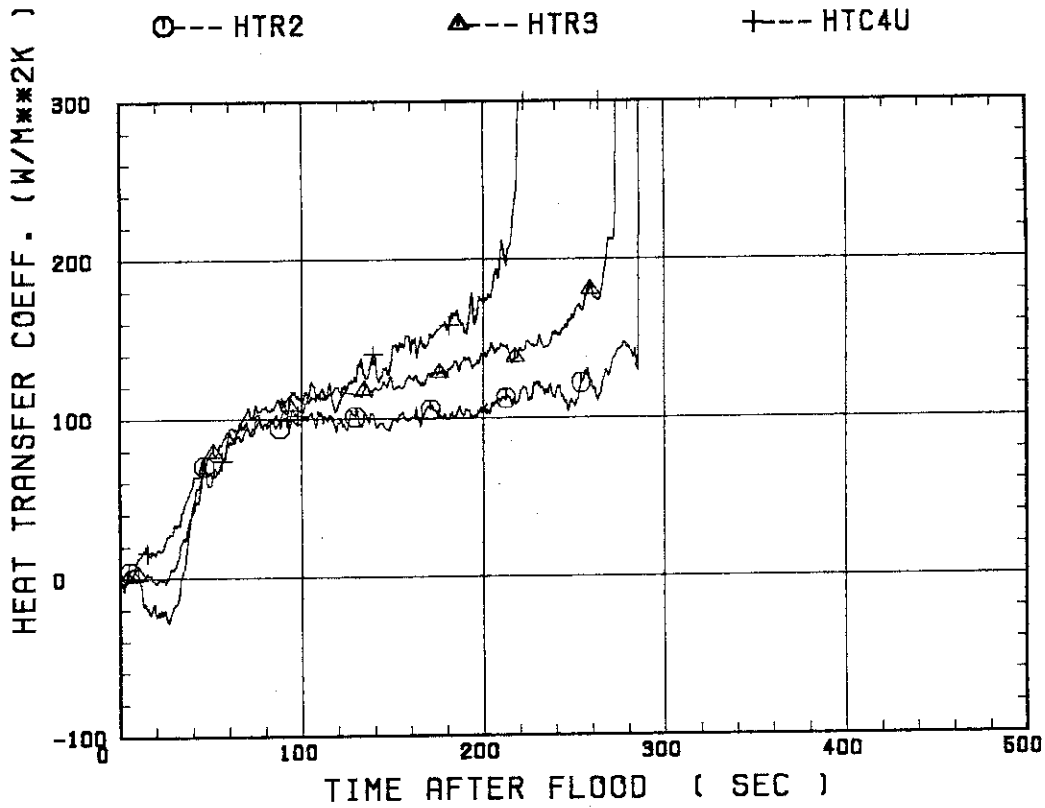


SMALL SCALE REFLOOD TEST
RUN 8122

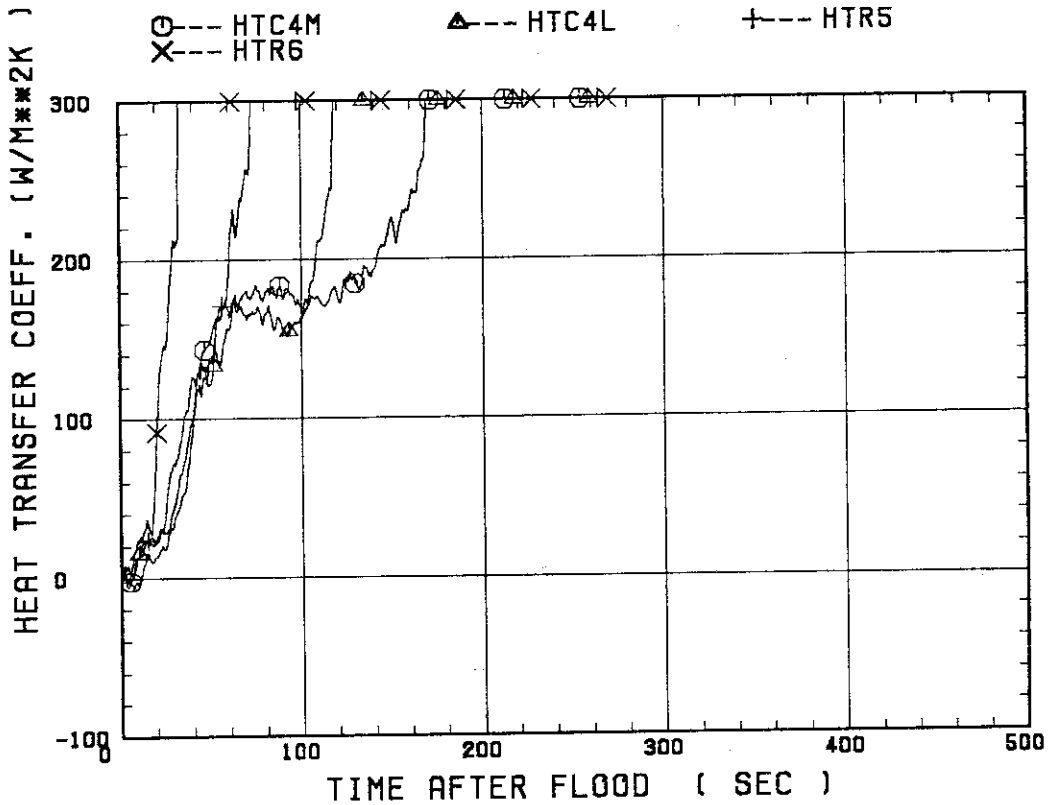
○--- TC4M △--- TC4L +--- TR5
X--- TR6 ◇--- TC7



SMALL SCALE REFLOOD TEST
 RUN 8122

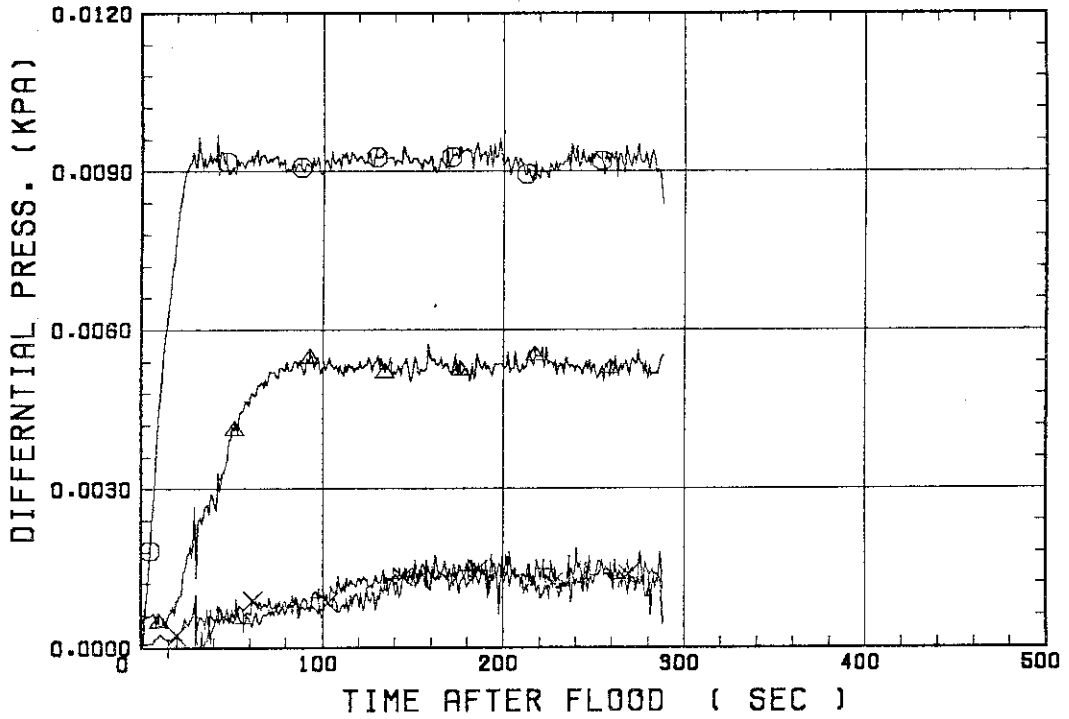


SMALL SCALE REFLOOD TEST
 RUN 8122



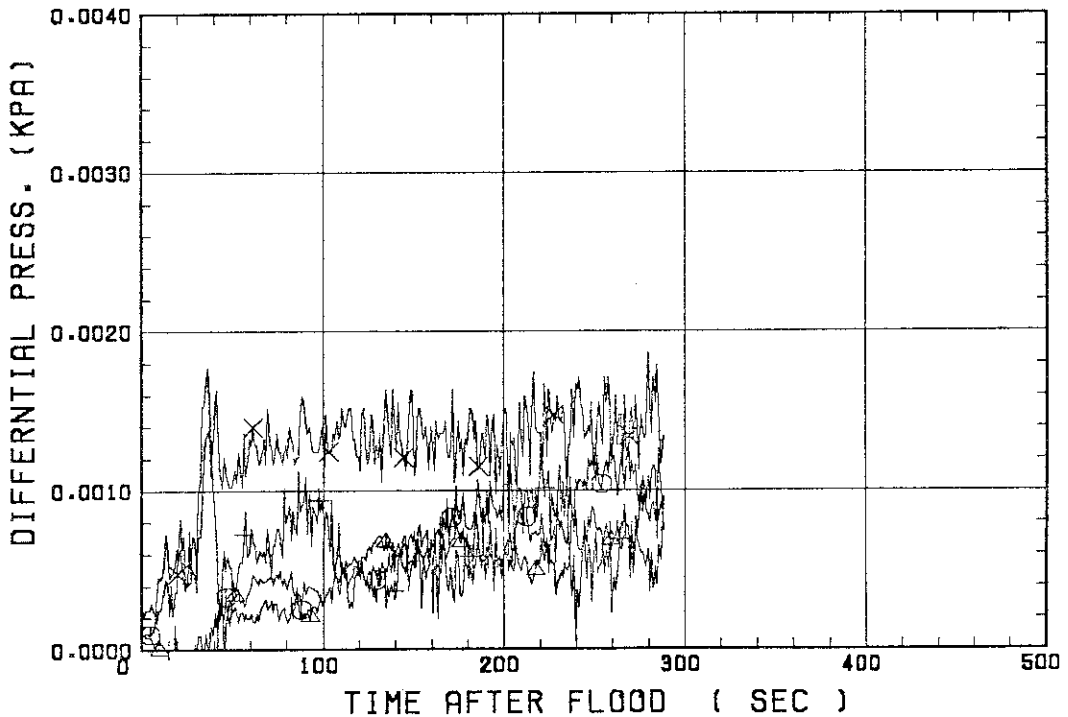
SMALL SCALE REFLOOD TEST
RUN 8122

○ --- DPT2 ▲ --- DPT4 + --- DPT5
X --- DPT6B



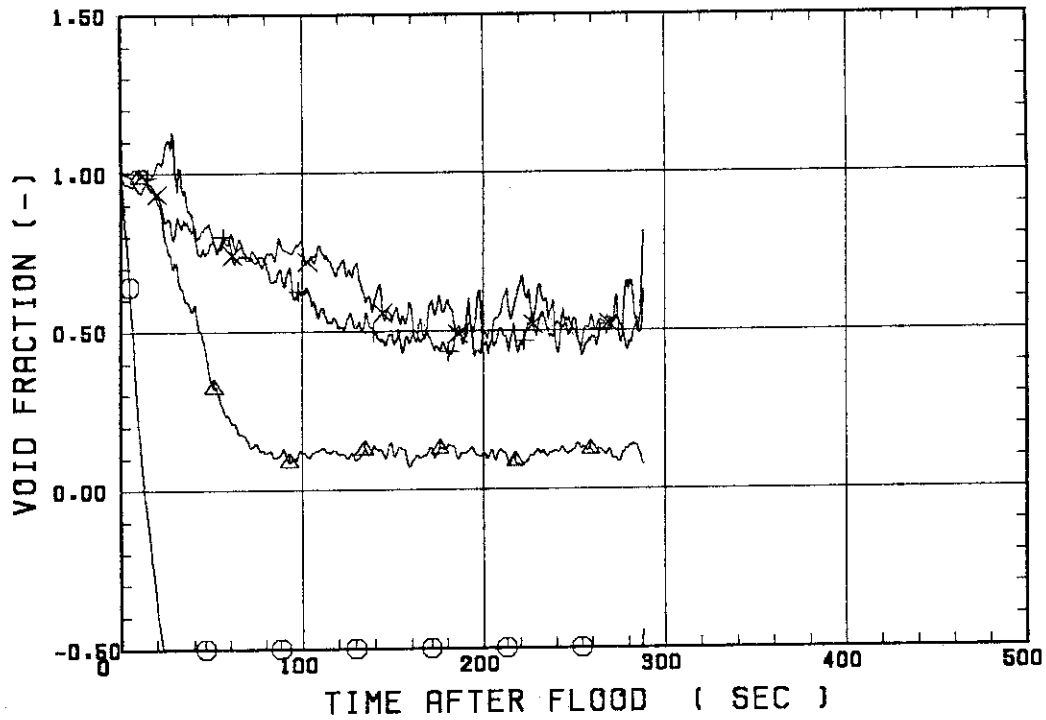
SMALL SCALE REFLOOD TEST
RUN 8122

○ --- DPT7 ▲ --- DPT8B + --- DP10
X --- DP12



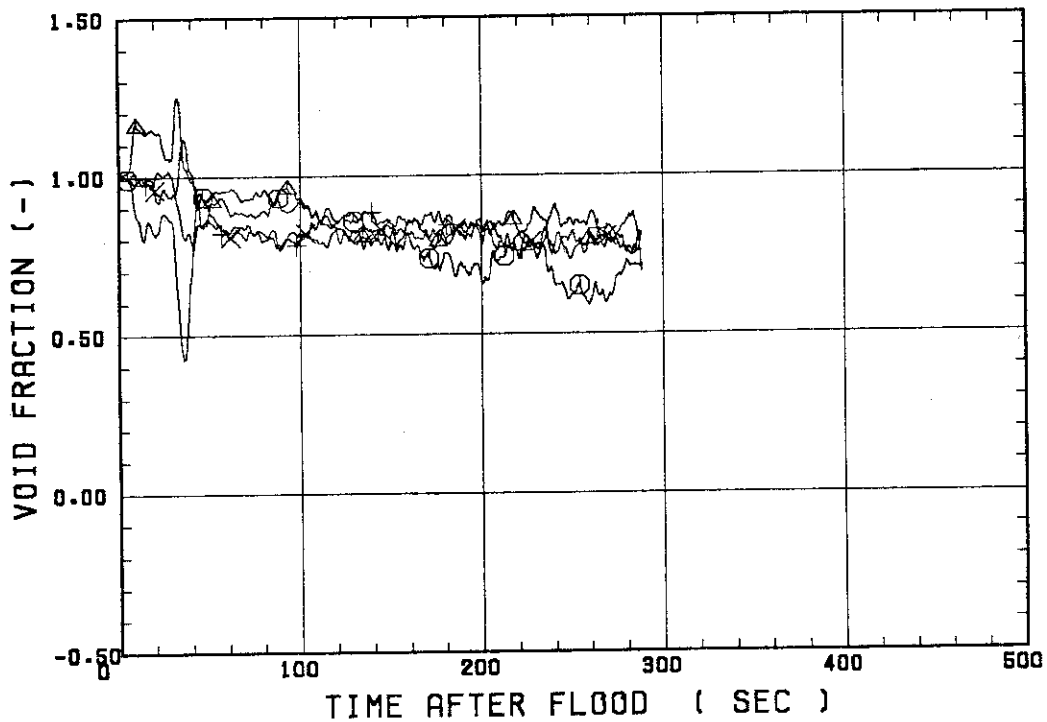
SMALL SCALE REFLOOD TEST
RUN 8122

○--- VDPT2 △--- VDPT4 +--- VDPT5
X--- VDPT6B



SMALL SCALE REFLOOD TEST
RUN 8122

○--- VDPT7 △--- VDPT8B +--- VDP10
X--- VDP12



```

*****
*   RUN NO. 8123   *
*   *****   *
    
```

 TEST CONDITIONS

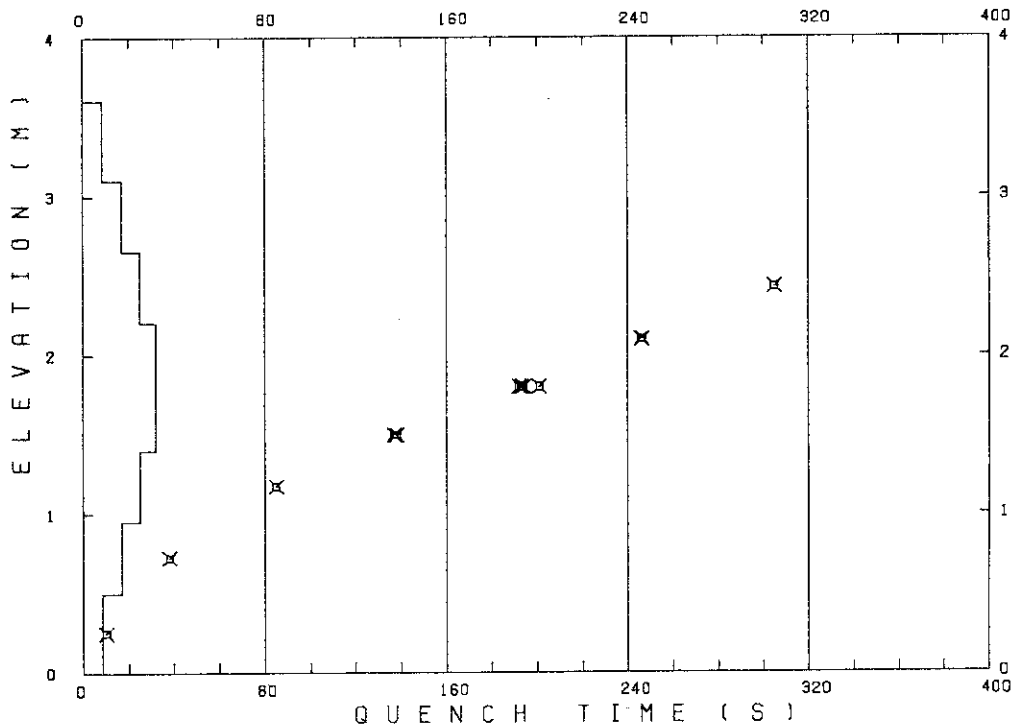
```

          LINEAR PEAK POWER      1.8  KW/M
          SYSTEM PRESSURE        0.2  MPA
          INLET WATER TEMPERATURE 100  .C
          INJECTED WATER VELOCITY 3.9  CM/S
    
```

 TEMPERATURE PROFILE

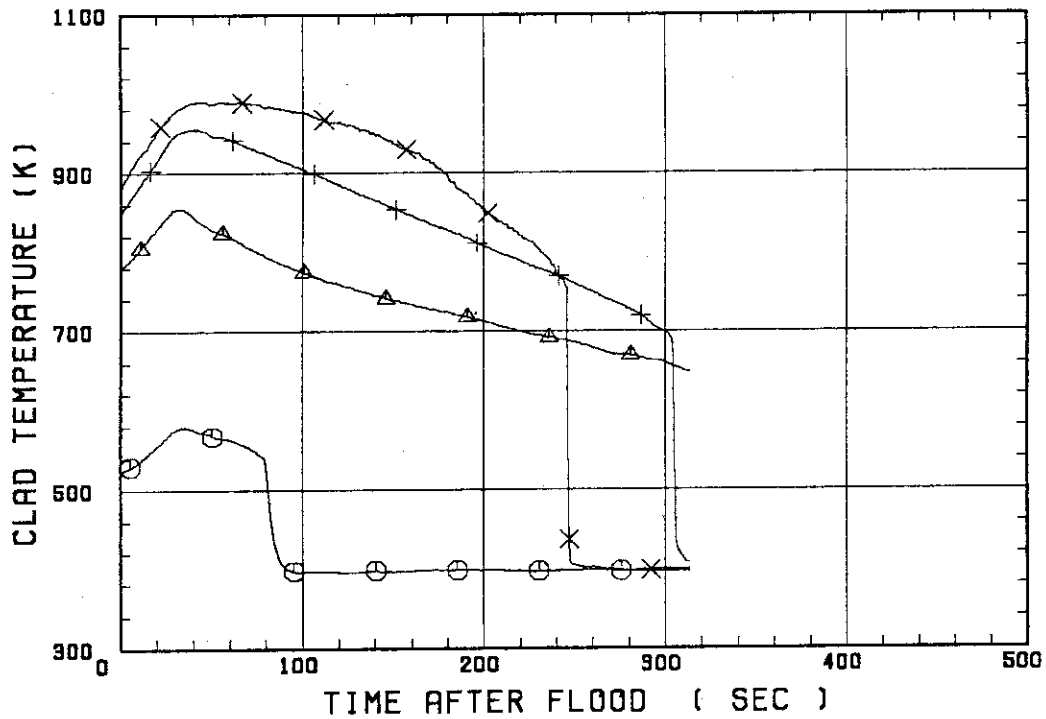
CH.NO.	SYMBOL	INITIAL TEMP. (.C)	TURNAROUND TIME (S)	TURNAROUND TEMP. (.C)	QUENCH TIME (S)	QUENCH TEMP. (.C)
66	TC1L	250	36.0	306		
51	TR2	503	34.0	582		
52	TR3	574	43.0	682	305.0	394
67	TC4U	606	46.0	717	245.0	480
7	TS4U	649	58.5	785	246.5	459
53	TR4M	617	34.0	732	194.0	405
68	TC4M	594	34.0	690	193.0	406
8	TS4M	622	33.0	736	201.0	392
48	TB4M	624	38.0	740	192.0	417
69	TC4L	618	32.0	703	138.0	481
9	TS4L	634	33.0	731	137.0	474
54	TR5	534	25.0	610	85.0	441
55	TR6	380	19.0	411	38.0	360
70	TC7	256	9.0	264	10.0	229

RUN NO. 8123



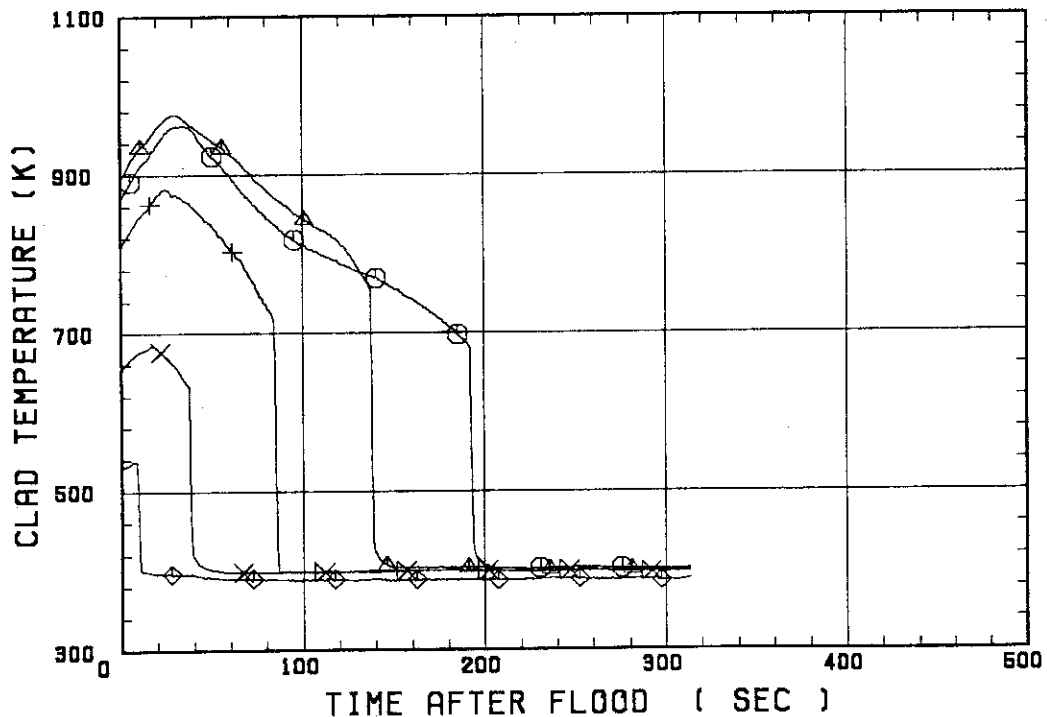
SMALL SCALE REFLOOD TEST
 RUN 8123

○--- TC1L △--- TR2 +--- TR3
 X--- TC4U

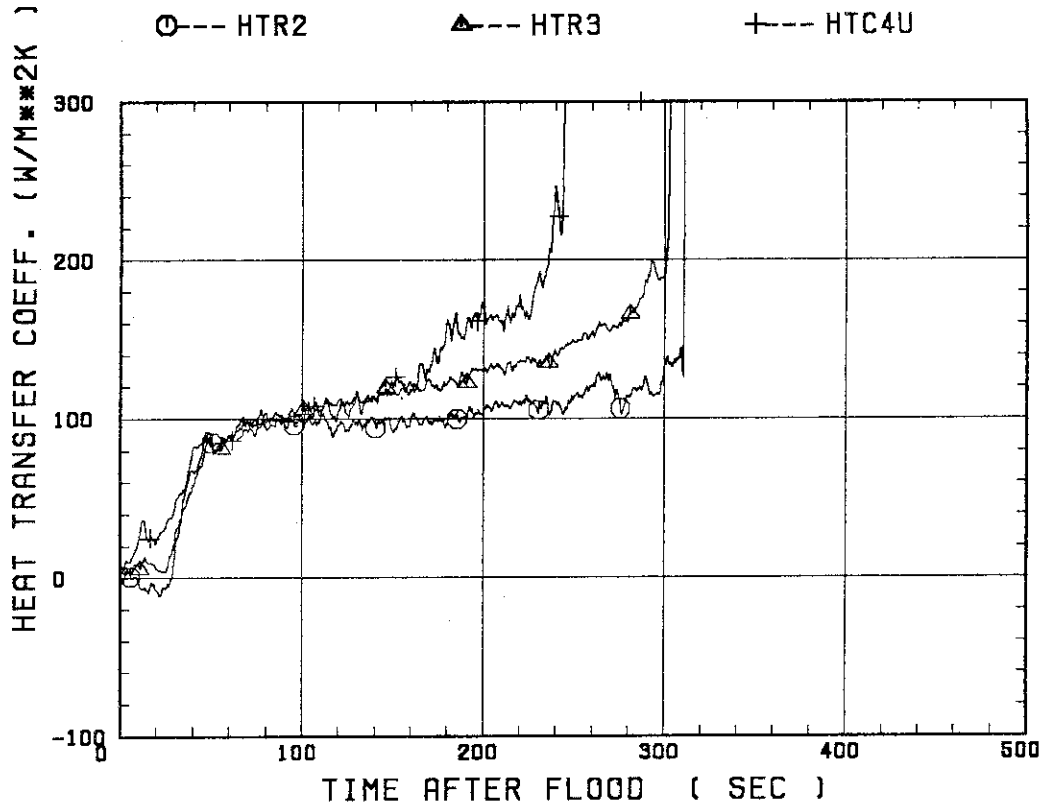


SMALL SCALE REFLOOD TEST
 RUN 8123

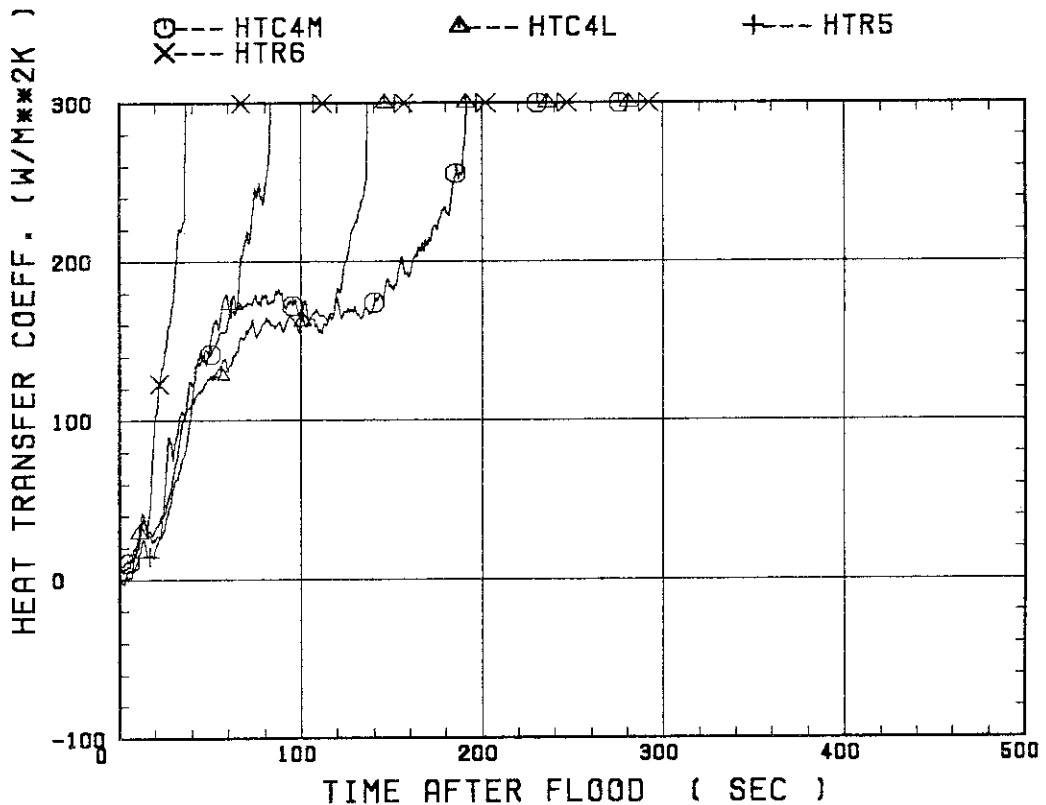
○--- TC4M △--- TC4L +--- TR5
 X--- TR6 ◇--- TC7



SMALL SCALE REFLOOD TEST
RUN 8123

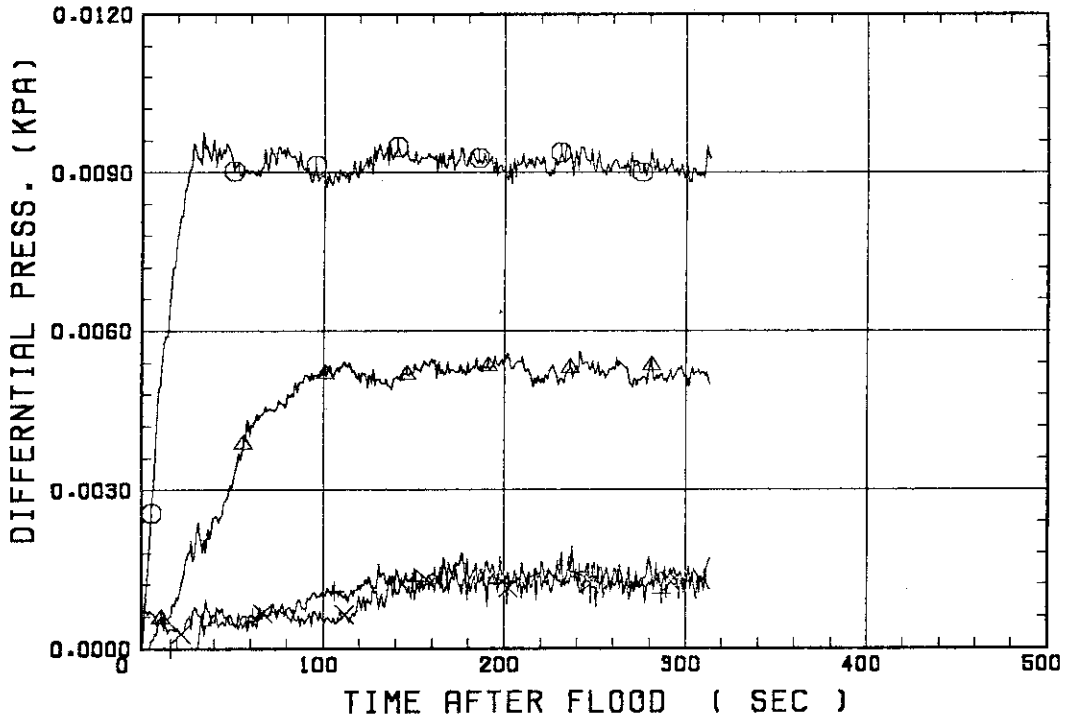


SMALL SCALE REFLOOD TEST
RUN 8123



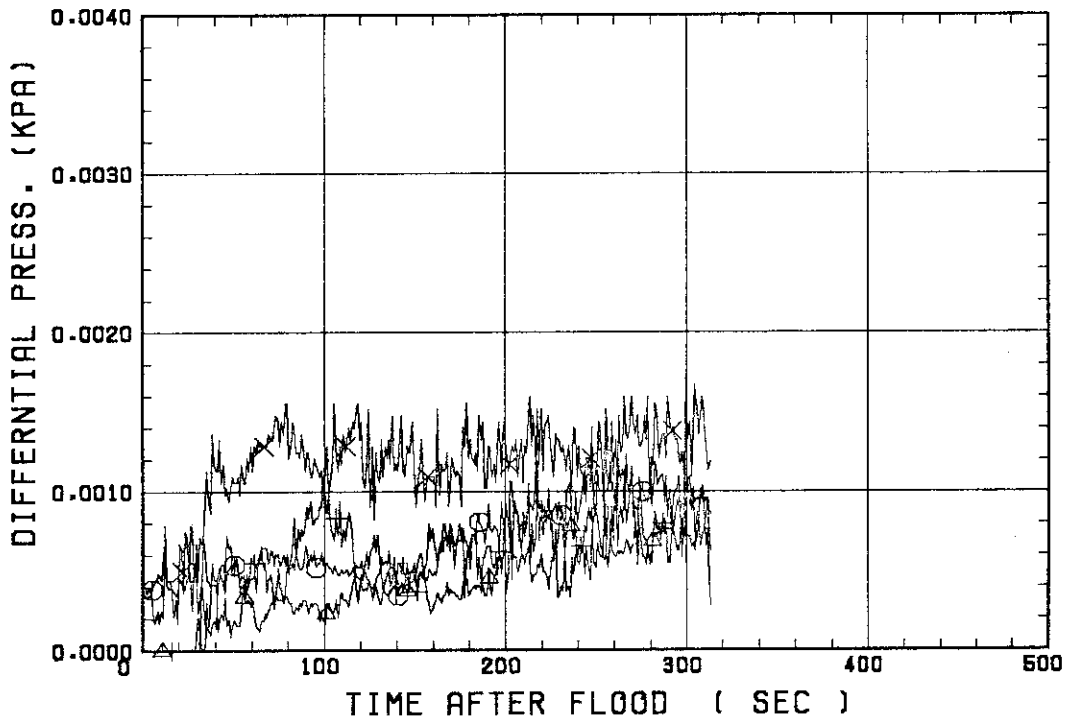
SMALL SCALE REFLOOD TEST
RUN 8123

○ --- DPT2 ▲ --- DPT4 + --- DPT5
X --- DPT6B



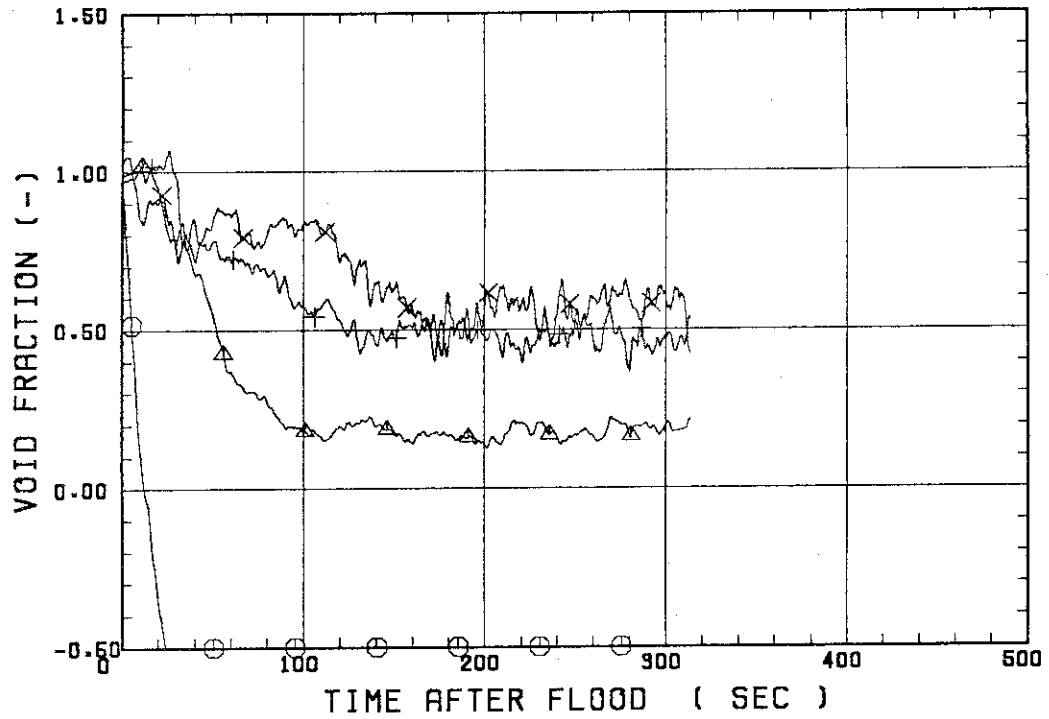
SMALL SCALE REFLOOD TEST
RUN 8123

○ --- DPT7 ▲ --- DPT8B + --- DP10
X --- DP12



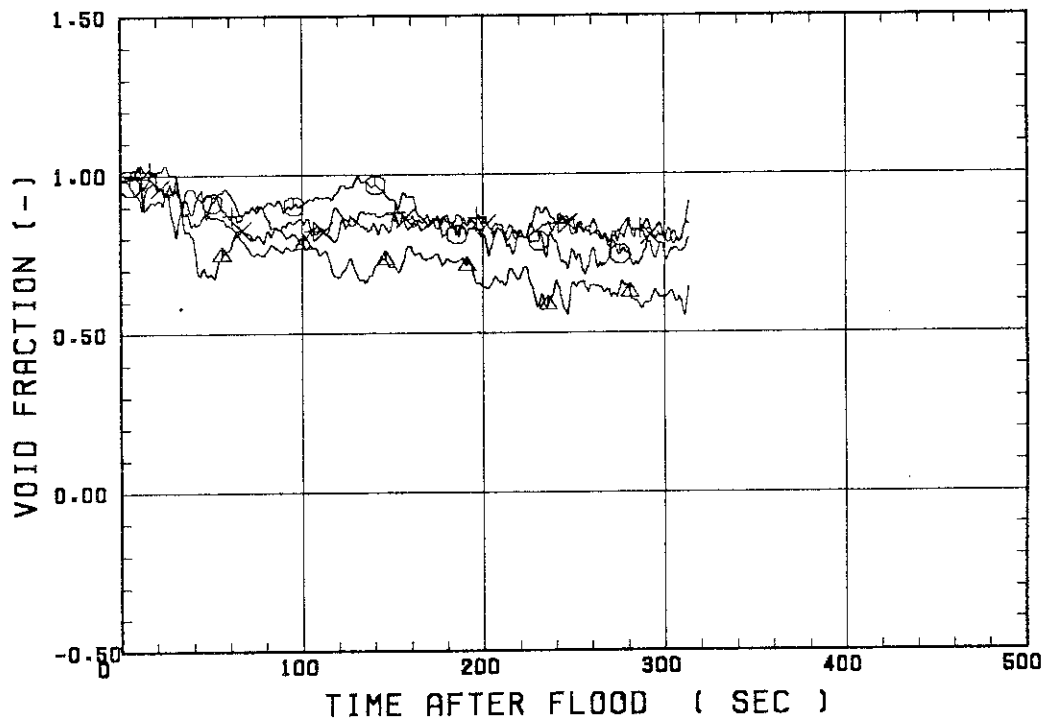
SMALL SCALE REFLOOD TEST
RUN 8123

○ --- VDPT2 ▲ --- VDPT4 + --- VDPT5
X --- VDPT6B



SMALL SCALE REFLOOD TEST
RUN 8123

○ --- VDPT7 ▲ --- VDPT8B + --- VDP10
X --- VDP12



 * RUN NO. 8124 *
 *

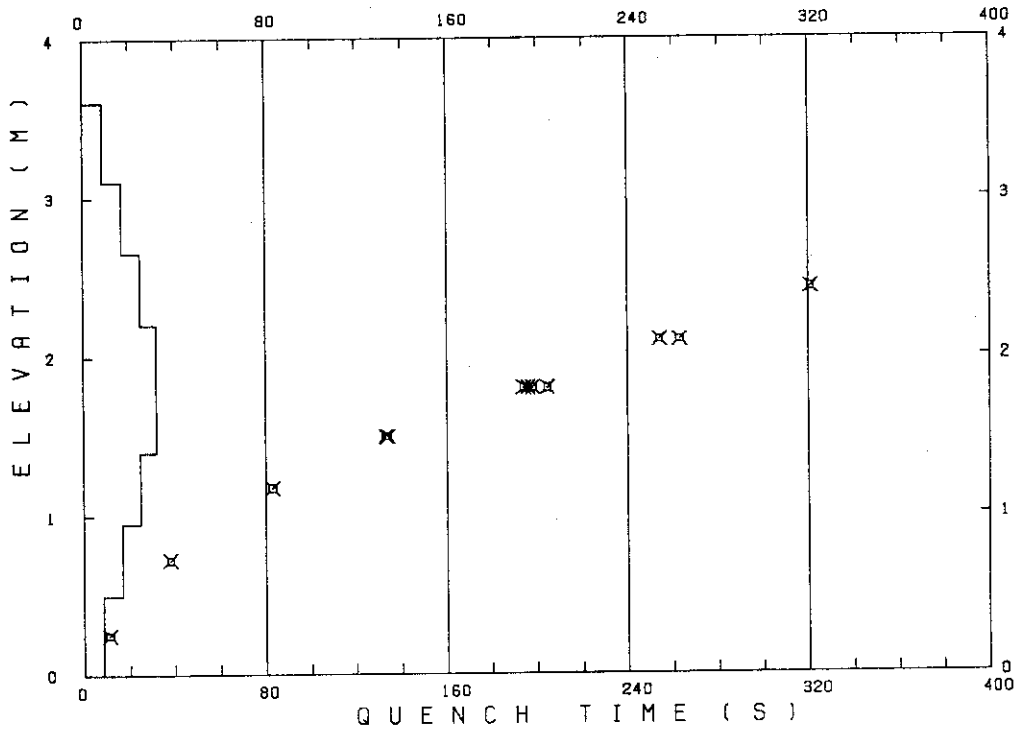
 TEST CONDITIONS

LINEAR PEAK POWER 1.8 KW/M
 SYSTEM PRESSURE 0.2 MPA
 INLET WATER TEMPERATURE 100 °C
 INJECTED WATER VELOCITY 3.0 CM/S

 TEMPERATURE PROFILE

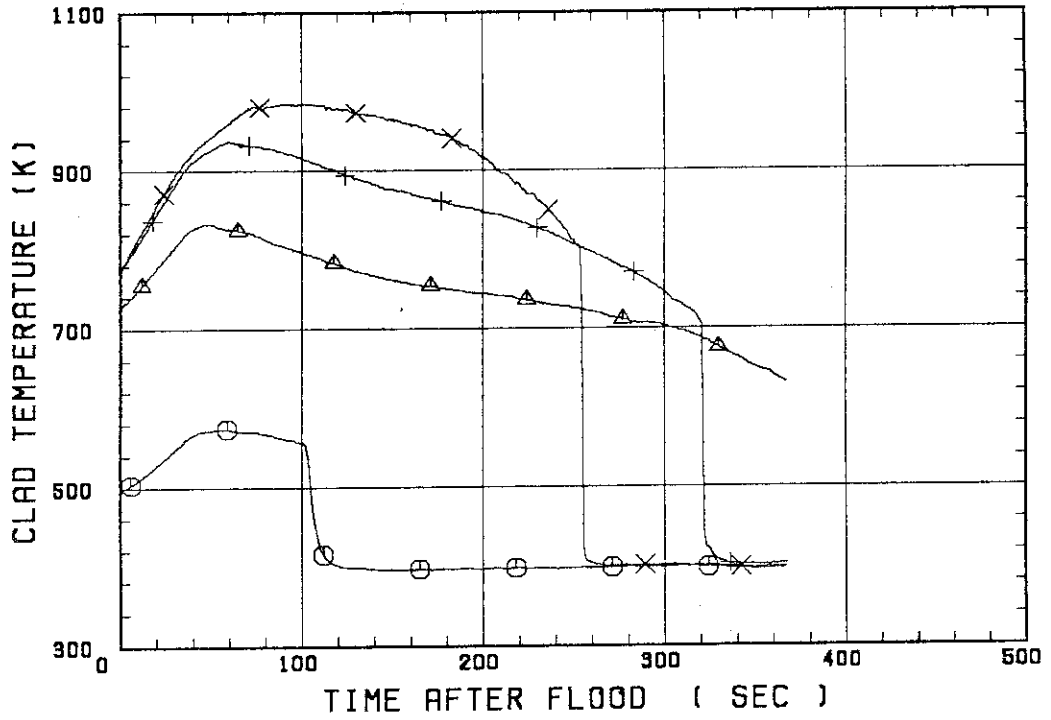
CH.NO.	SYMBOL	INITIAL TEMP. (°C)	TURNAROUND TIME (S)	TURNAROUND TEMP. (°C)	QUENCH TIME (S)	QUENCH TEMP. (°C)
66	TC1L	223	60.0	301		
51	TR2	452	49.0	560		
52	TR3	497	60.0	665	321.0	431
67	TC4U	495	101.0	712	254.0	525
7	TS4U	554	84.0	769	253.0	472
53	TR4M	514	52.0	689	198.0	412
68	TC4M	479	47.0	639	196.0	416
8	TS4M	525	53.0	701	204.5	401
48	TB4M	520	53.0	700	194.0	431
69	TC4L	500	46.0	643	134.0	492
9	TS4L	528	44.0	679	133.0	483
54	TR5	457	36.0	564	83.0	438
55	TR6	334	25.0	378	38.0	341
70	TC7	218	8.0	228	11.0	199

RUN NO. 8124



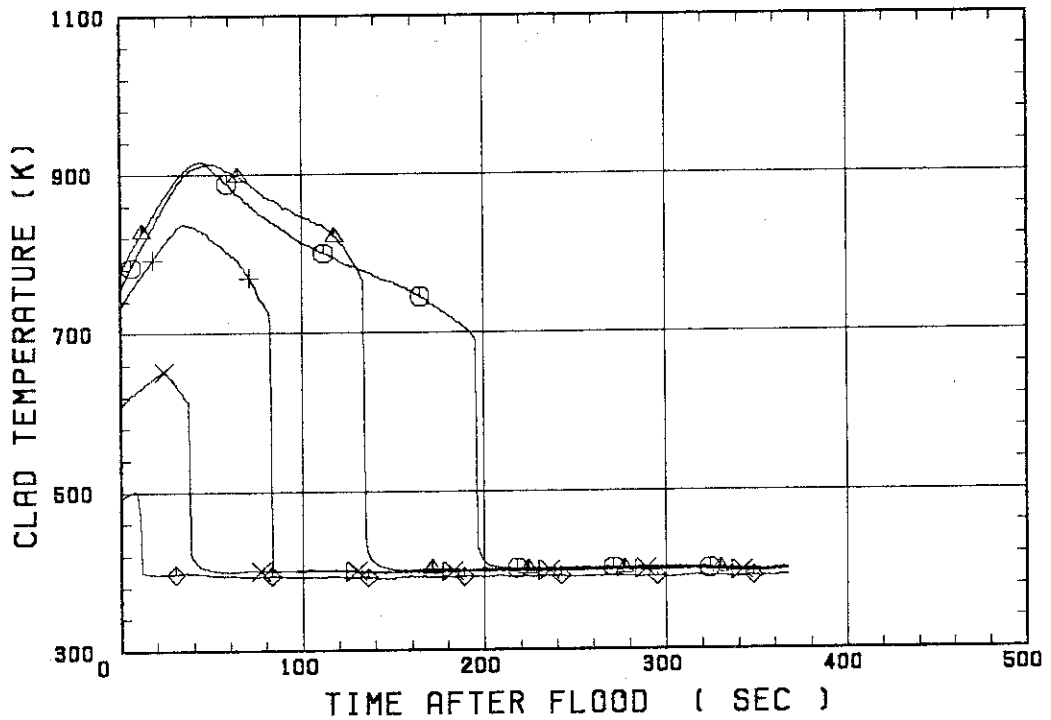
SMALL SCALE REFLOOD TEST
 RUN 8124

○--- TC1L △--- TR2 +--- TR3
 X--- TC4U

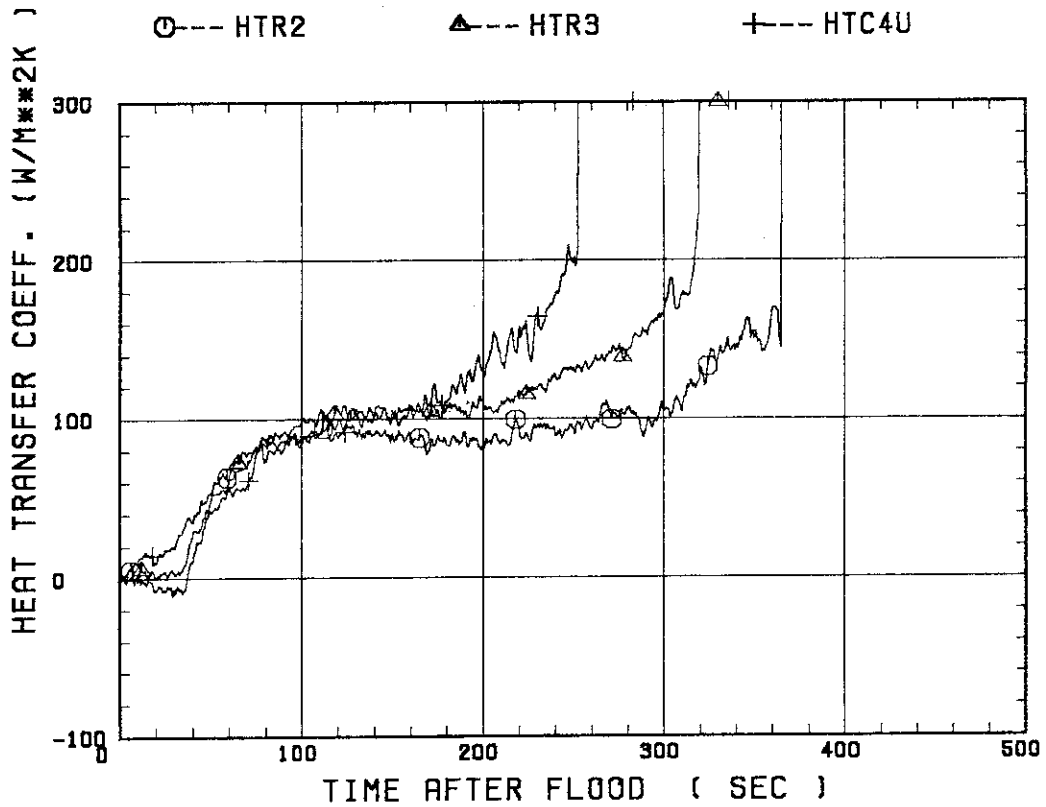


SMALL SCALE REFLOOD TEST
 RUN 8124

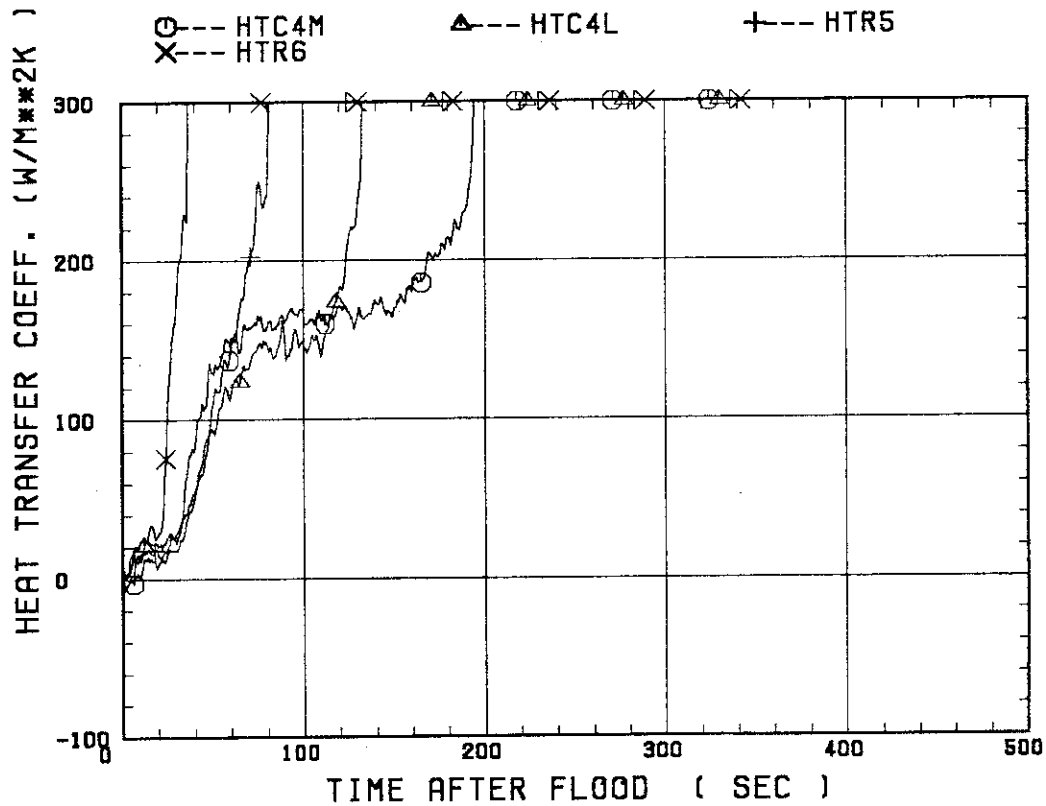
○--- TC4M △--- TC4L +--- TR5
 X--- TR6 ◇--- TC7



SMALL SCALE REFLOOD TEST
RUN 8124

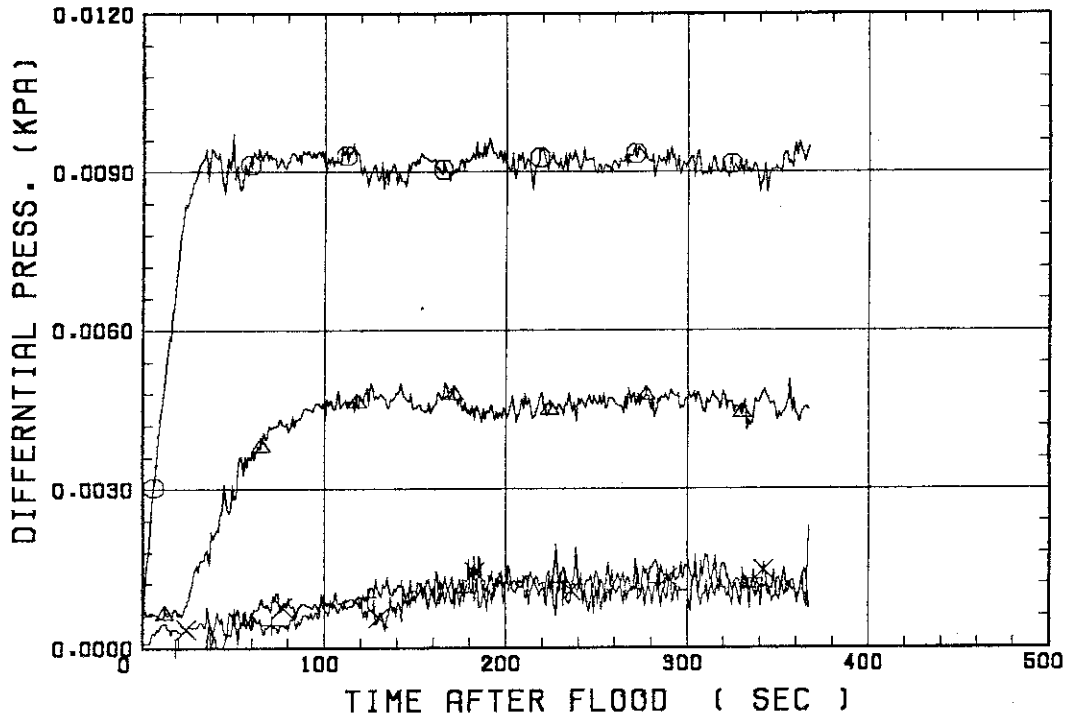


SMALL SCALE REFLOOD TEST
RUN 8124



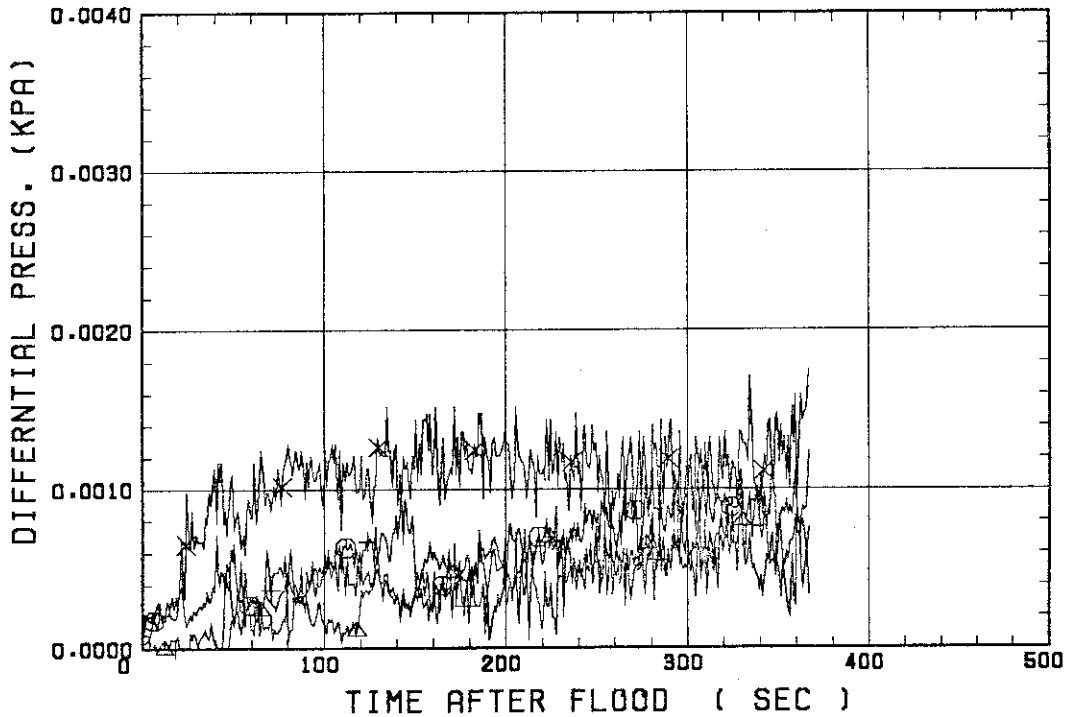
SMALL SCALE REFLOOD TEST
RUN 8124

○--- DPT2 ▲--- DPT4 +--- DPT5
X--- DPT6B



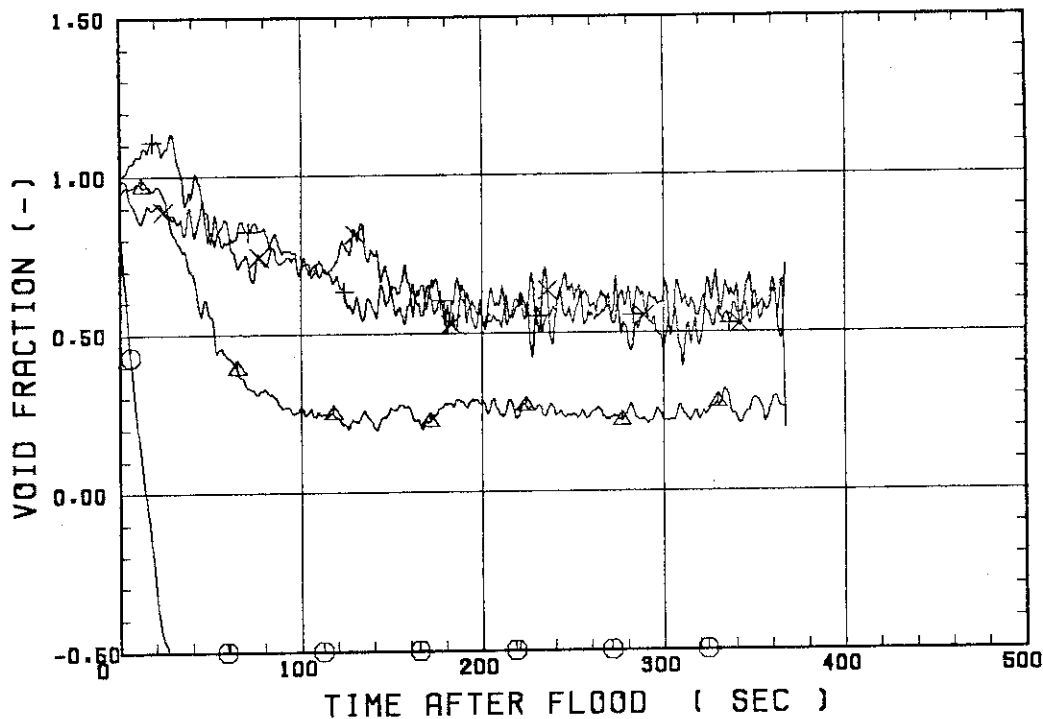
SMALL SCALE REFLOOD TEST
RUN 8124

○--- DPT7 ▲--- DPT8B +--- DP10
X--- DP12



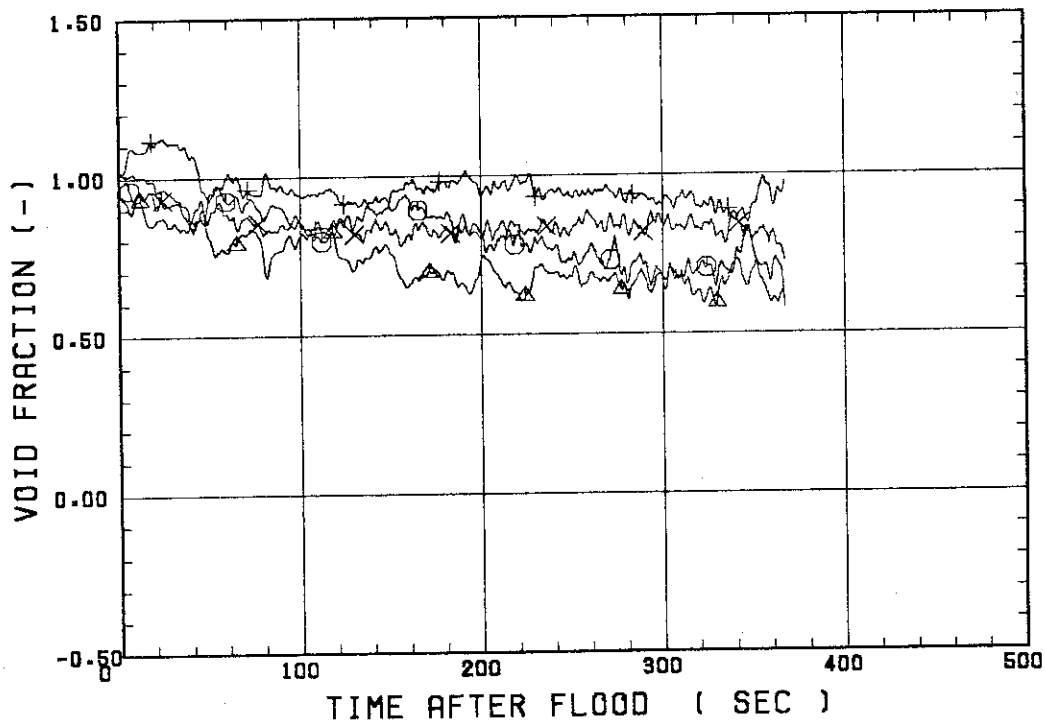
SMALL SCALE REFLOOD TEST
RUN 8124

○--- VDPT2 △--- VDPT4 +--- VDPT5
X--- VDPT6B



SMALL SCALE REFLOOD TEST
RUN 8124

○--- VDPT7 △--- VDPT8B +--- VDP10
X--- VDP12



 * RUN NO. 8126 *

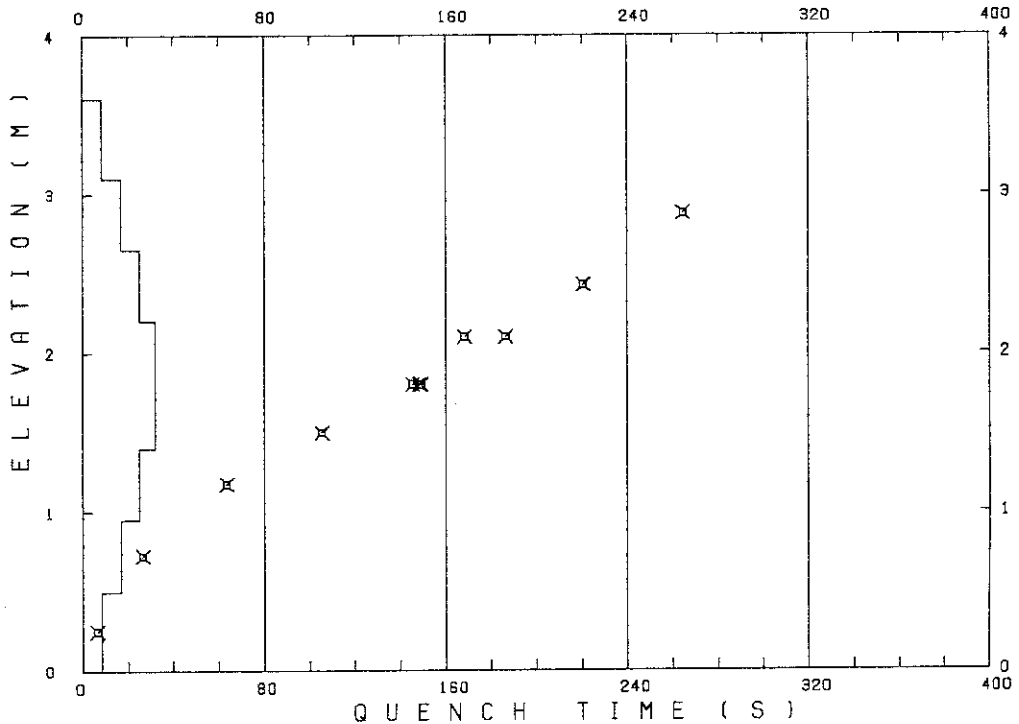
 TEST CONDITIONS

LINEAR PEAK POWER 1.8 KW/M
 SYSTEM PRESSURE 0.2 MPA
 INLET WATER TEMPERATURE 60 °C
 INJECTED WATER VELOCITY 3.9 CM/S

 TEMPERATURE PROFILE

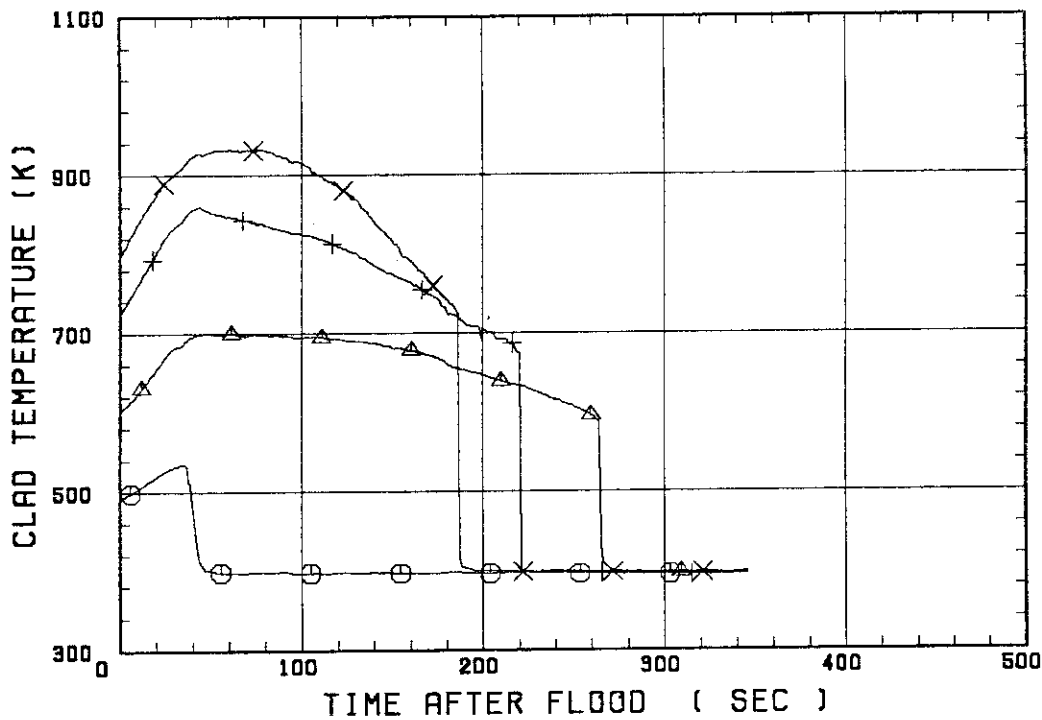
CH.NO.	SYMBOL	INITIAL TEMP. (°C)	TURNAROUND TIME (S)	TURNAROUND TEMP. (°C)	QUENCH TIME (S)	QUENCH TEMP. (°C)
66	TC1L	217	35.5	262		
46	TB2	327	47.5	427	264.5	314
47	TB3	449	44.5	587	220.5	401
67	TC4U	520	78.5	659	186.5	450
56	TD4U	569	47.5	726	168.5	450
38	TA4M	510	33.5	621	148.5	400
68	TC4M	513	32.5	619	145.5	395
58	TD4M	546	36.5	666	149.5	401
48	TB4M	538	37.5	662	145.5	406
69	TC4L	531	27.5	623	105.5	448
60	TD4L	553	29.5	652	105.5	455
54	TR5	456	22.5	526	63.5	418
55	TR6	307	16.5	340	26.5	316
70	TC7	204	5.5	210	6.5	208

RUN NO. 8126



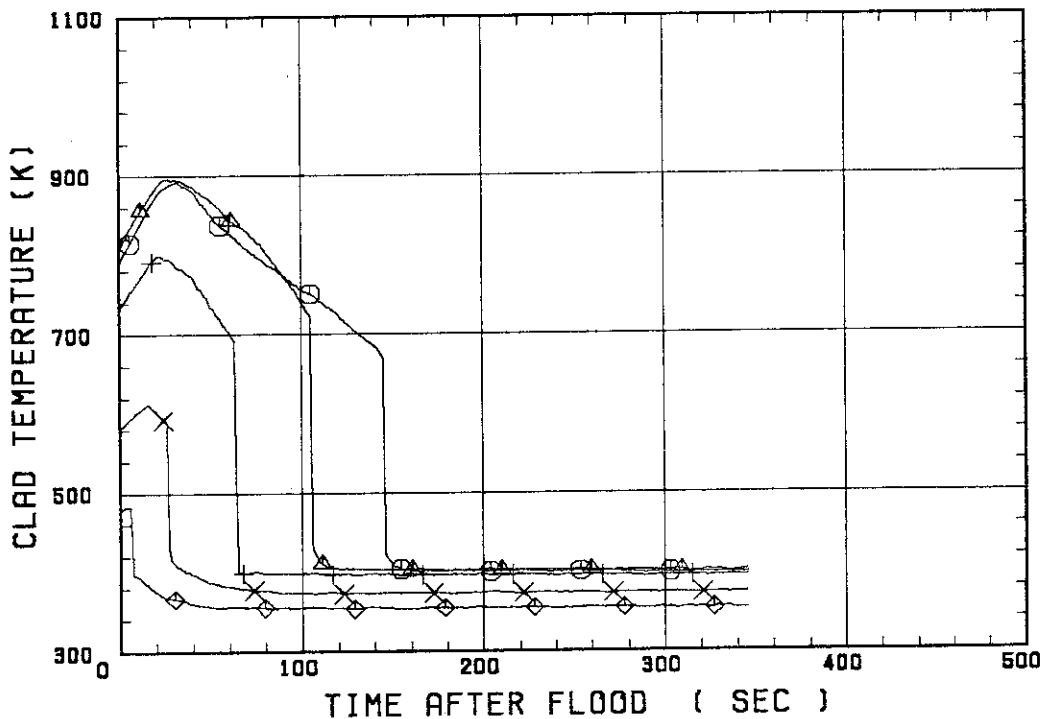
SMALL SCALE REFLOOD TEST
 RUN 8126

○--- TC1L △--- TB2 +--- TB3
 X--- TC4U

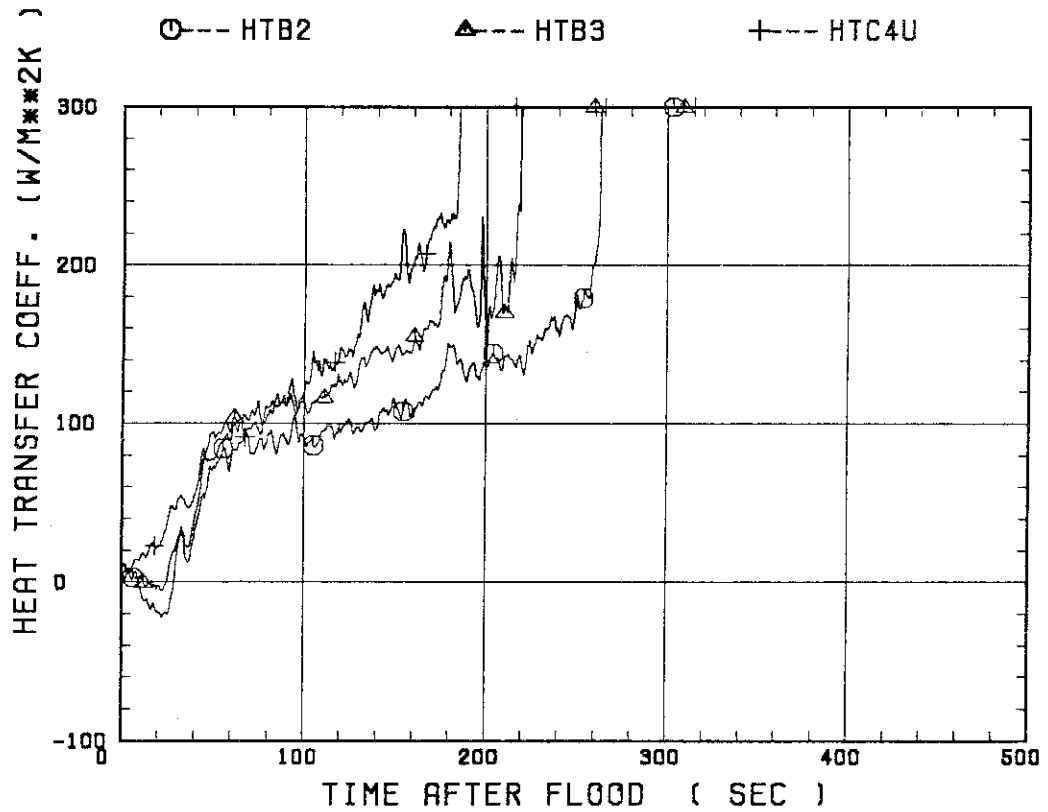


SMALL SCALE REFLOOD TEST
 RUN 8126

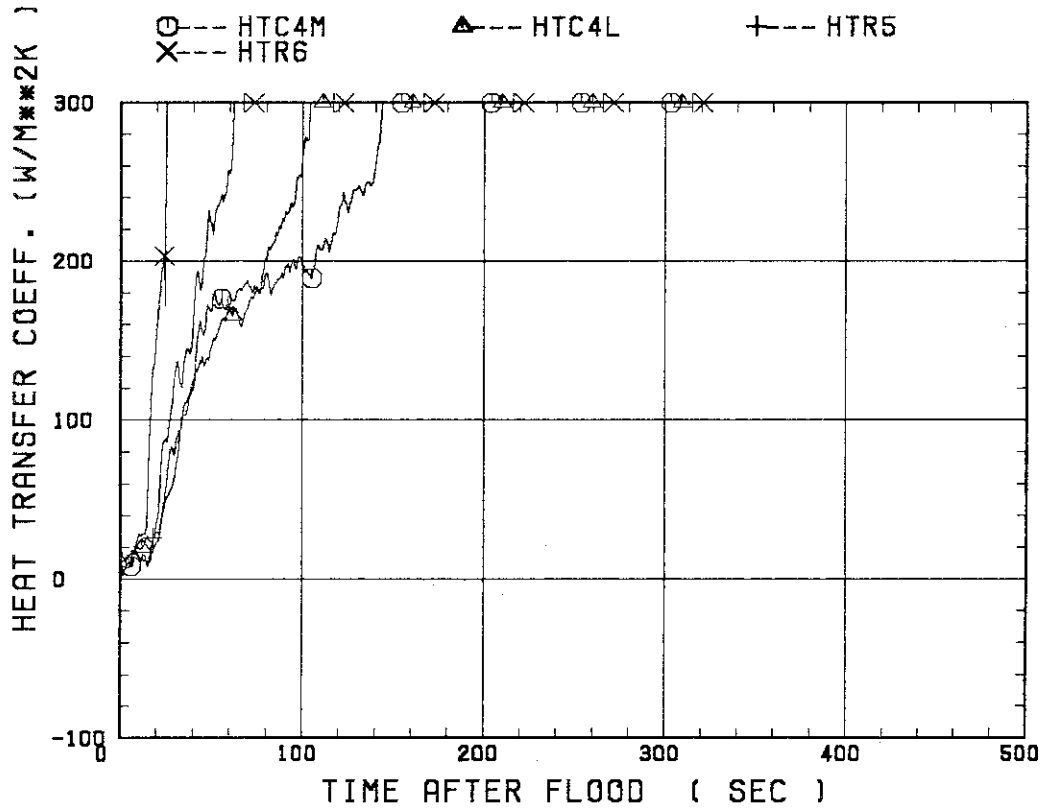
○--- TC4M △--- TC4L +--- TR5
 X--- TR6 ◇--- TC7



SMALL SCALE REFLOOD TEST
 RUN 8126

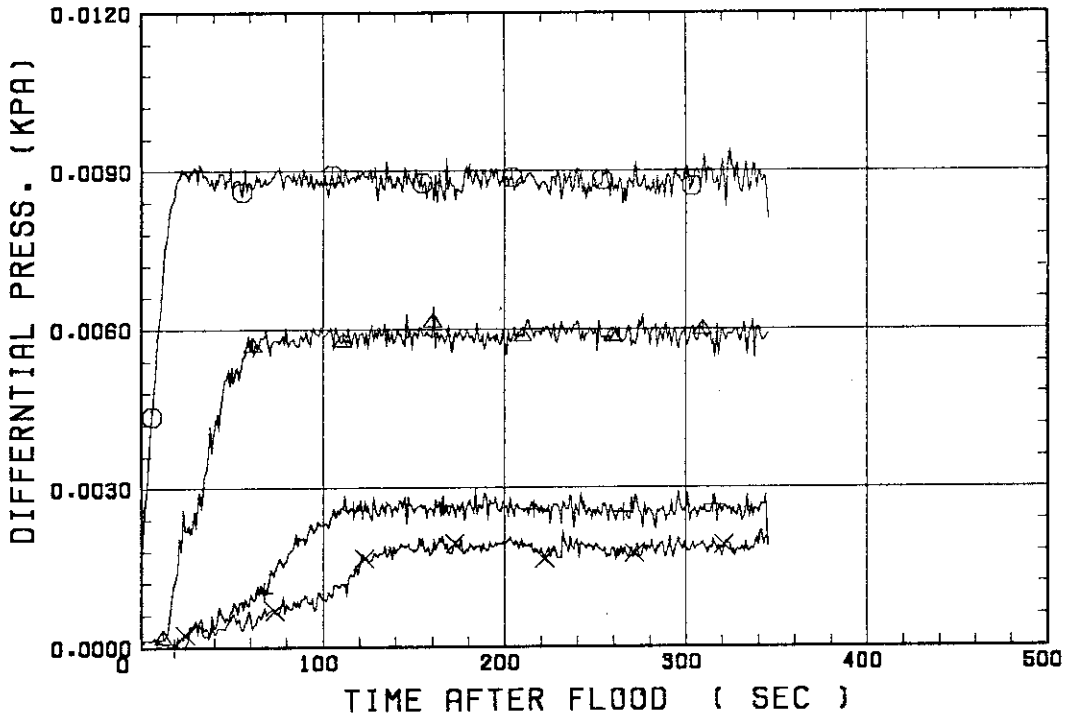


SMALL SCALE REFLOOD TEST
 RUN 8126



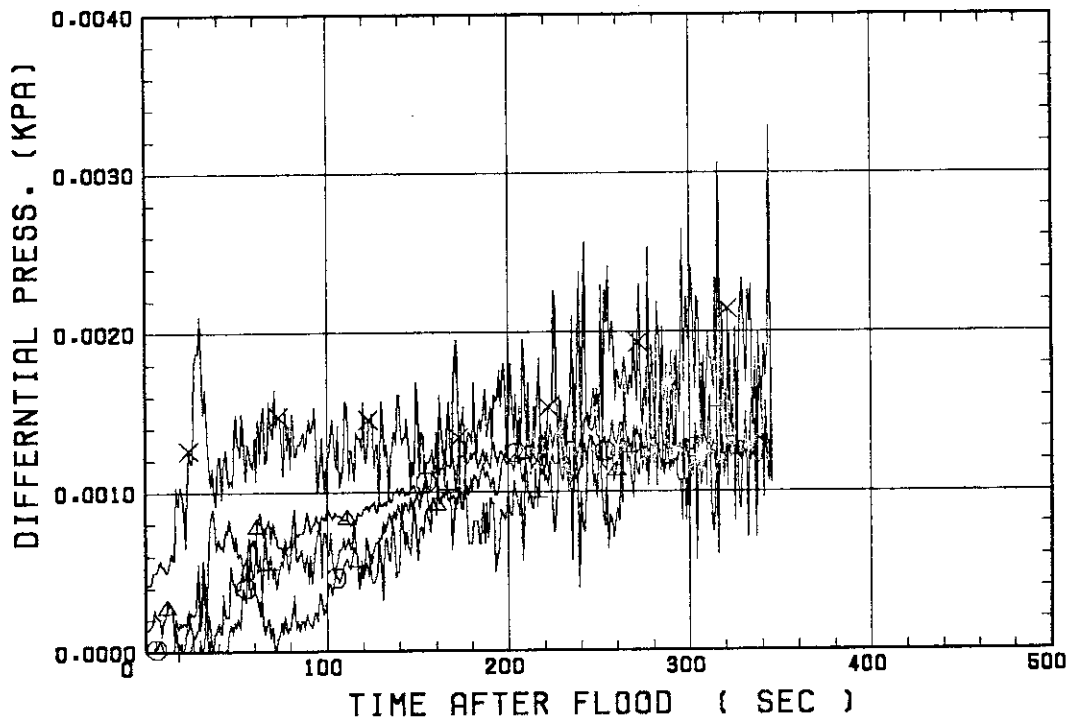
SMALL SCALE REFLOOD TEST
RUN 8126

○ --- DPT2 ▲ --- DPT4 + --- DPT5
X --- DPT6B



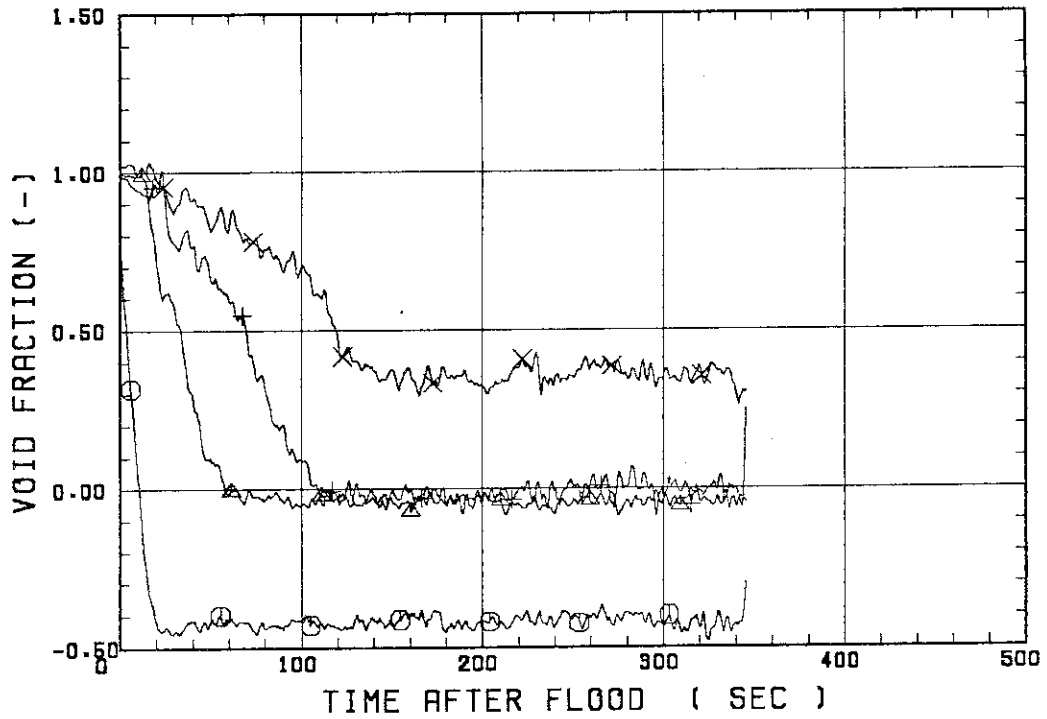
SMALL SCALE REFLOOD TEST
RUN 8126

○ --- DPT7 ▲ --- DPT8B + --- DP10
X --- DP12



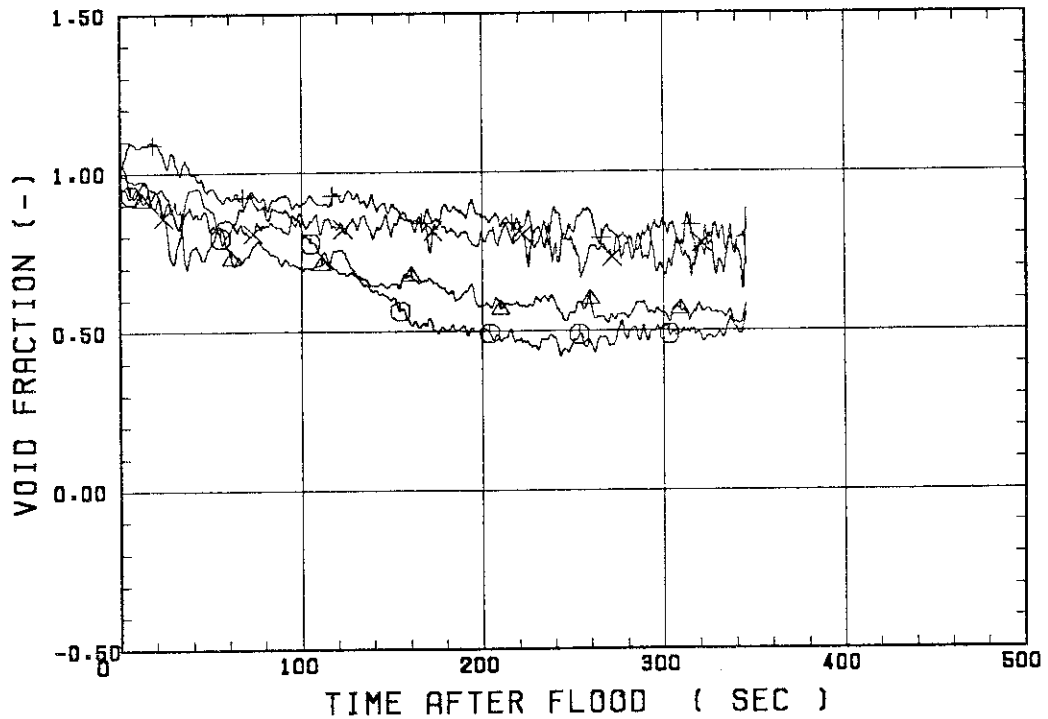
SMALL SCALE REFLOOD TEST
RUN 8126

○--- VDPT2 △--- VDPT4 +--- VDPT5
X--- VDPT6B



SMALL SCALE REFLOOD TEST
RUN 8126

○--- VDPT7 △--- VDPT8B +--- VDP10
X--- VDP12



 * RUN NO. 8127 *

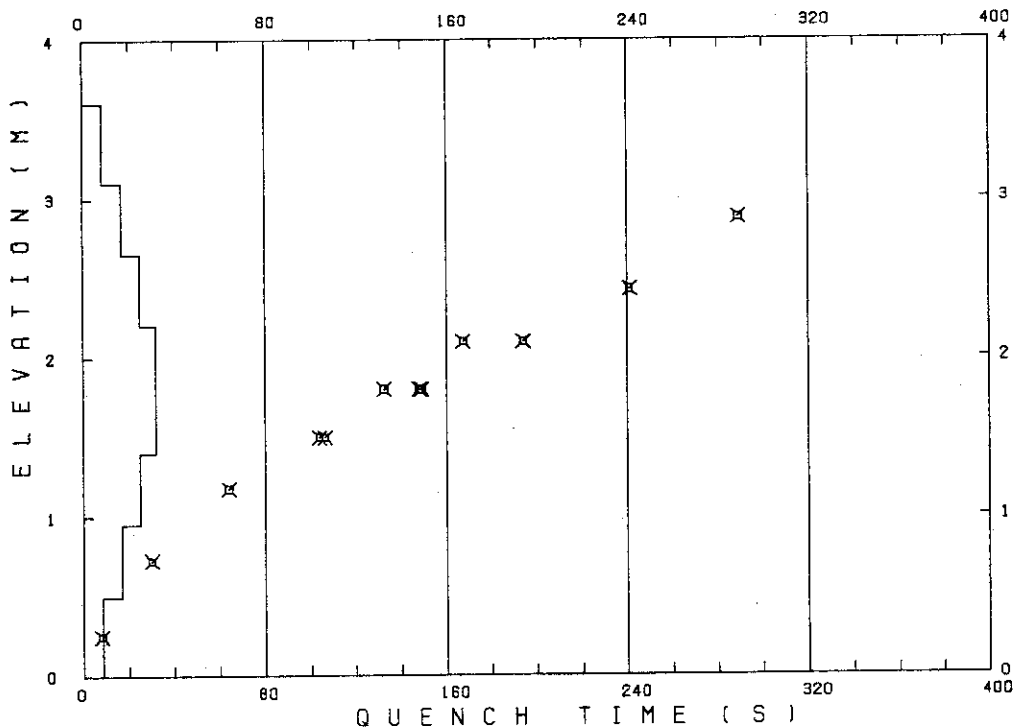
 TEST CONDITIONS

LINEAR PEAK POWER 1.8 KW/M
 SYSTEM PRESSURE 0.2 MPA
 INLET WATER TEMPERATURE 80 .C
 INJECTED WATER VELOCITY 3.9 CM/S

 TEMPERATURE PROFILE

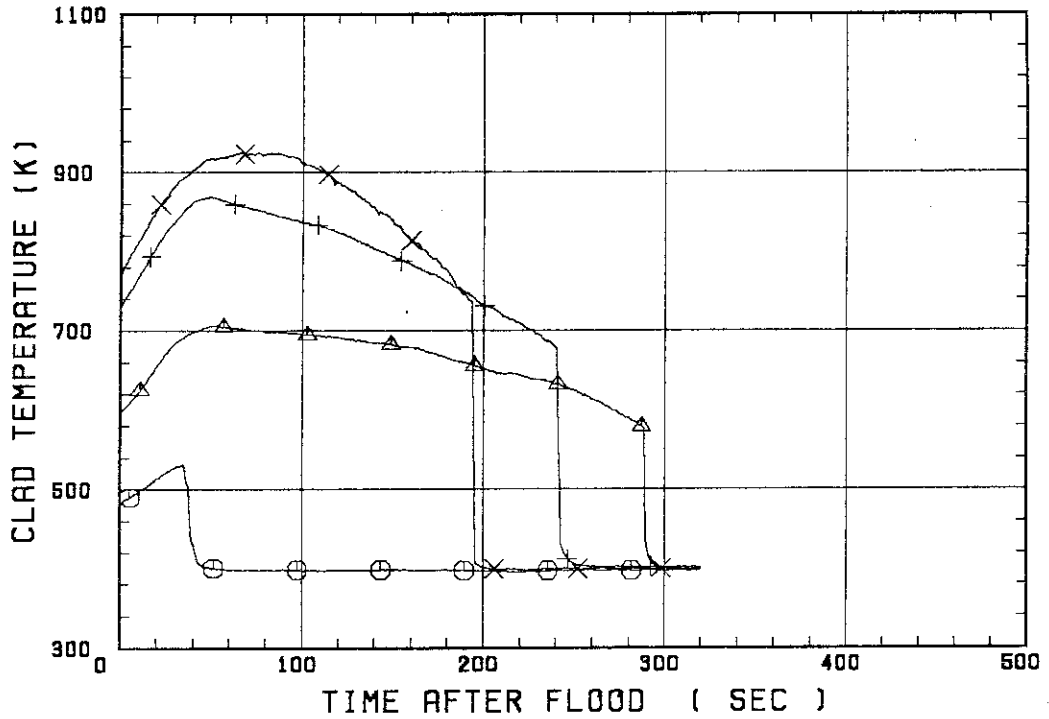
CH.NO.	SYMBOL	INITIAL TEMP. (.C)	TURNAROUND TIME (S)	TURNAROUND TEMP. (.C)	QUENCH TIME (S)	QUENCH TEMP. (.C)
66	TC1L	209	35.0	258		
51	TR2	323	54.0	433	289.0	303
52	TR3	455	50.0	596	241.0	403
67	TC4U	495	87.0	651	194.0	463
7	TS4U	560	51.0	728	167.5	483
53	TR4M	519	38.0	648	149.0	401
68	TC4M	482	35.0	601	148.0	403
8	TS4M	534	39.0	662	132.5	405
48	TB4M	527	39.0	657	148.0	373
69	TC4L	514	31.0	611	104.0	465
9	TS4L	545	34.5	653	106.5	458
54	TR5	467	24.0	533	64.0	433
55	TR6	341	16.0	371	30.0	336
70	TC7	225	6.0	232	8.0	214

RUN NO. 8127



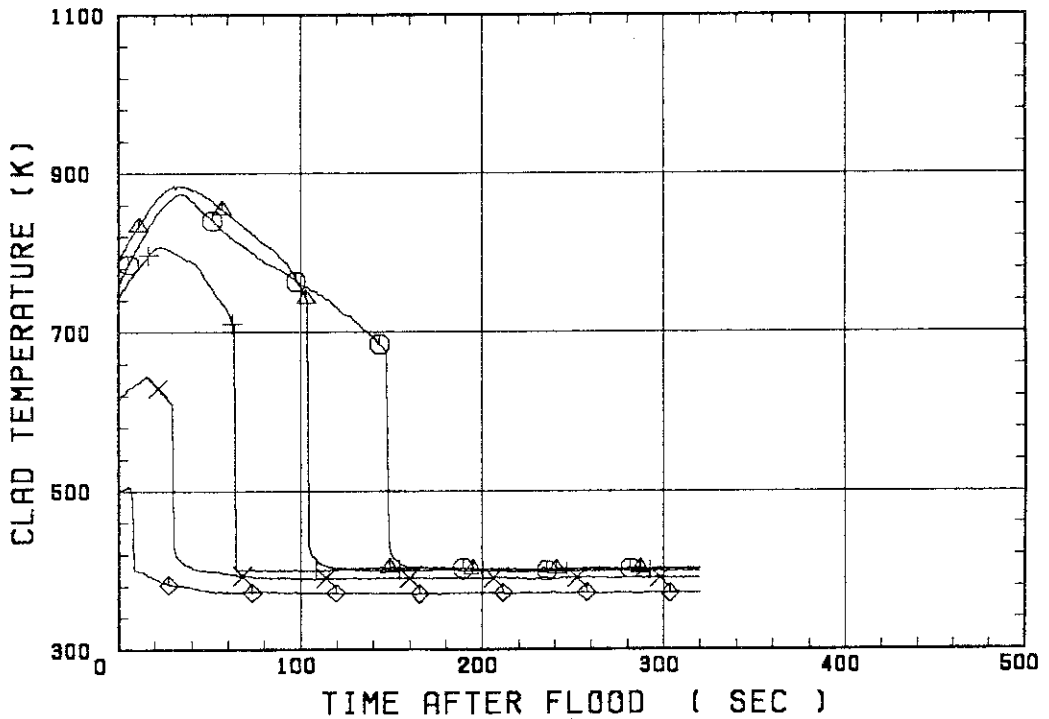
SMALL SCALE REFLOOD TEST
RUN 8127

○--- TC1L △--- TR2 +--- TR3
X--- TC4U

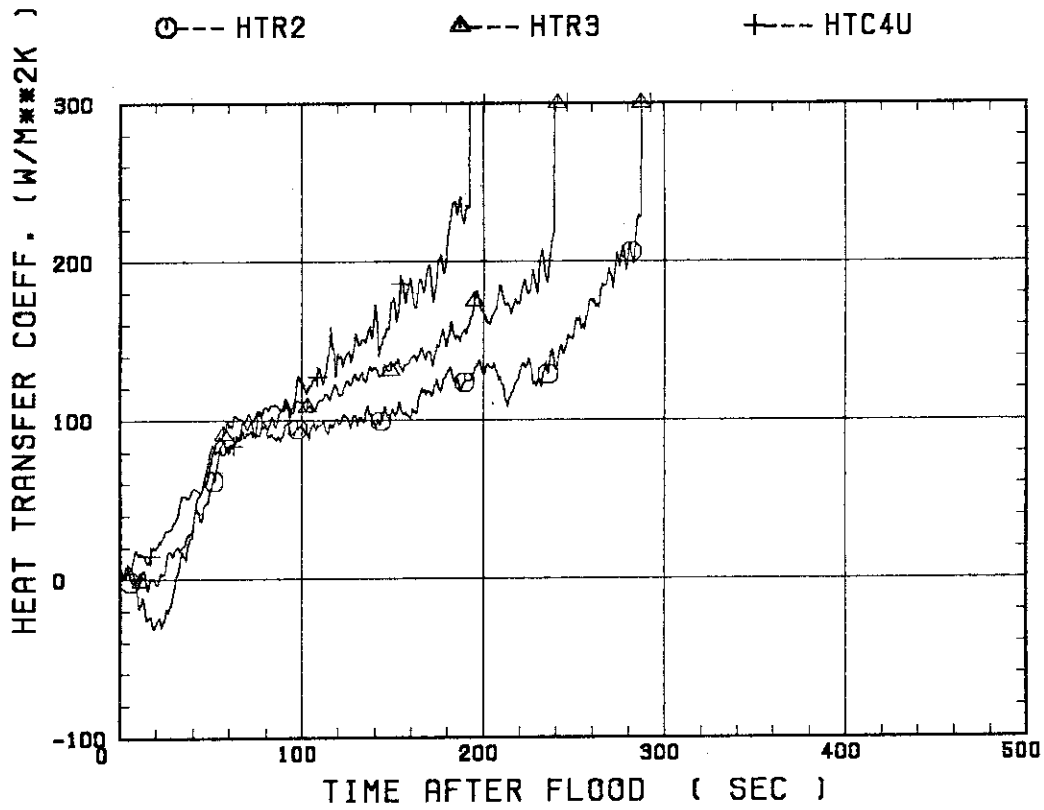


SMALL SCALE REFLOOD TEST
RUN 8127

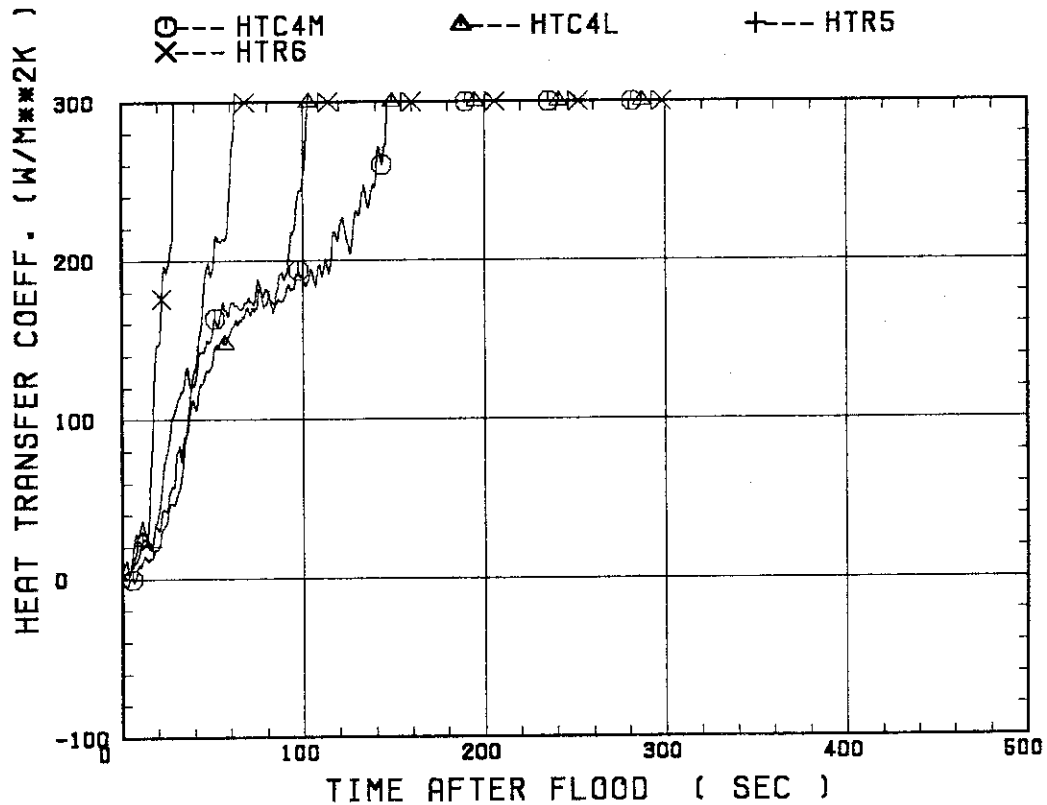
○--- TC4M △--- TC4L +--- TR5
X--- TR6 ◇--- TC7



SMALL SCALE REFLOOD TEST
 RUN 8127

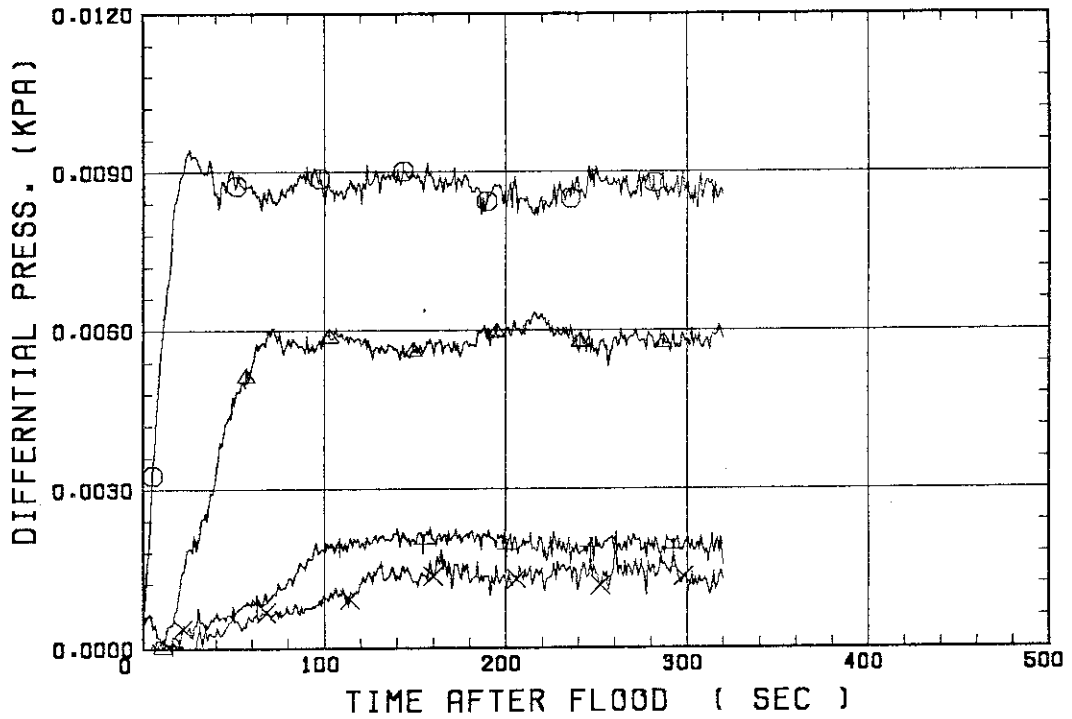


SMALL SCALE REFLOOD TEST
 RUN 8127



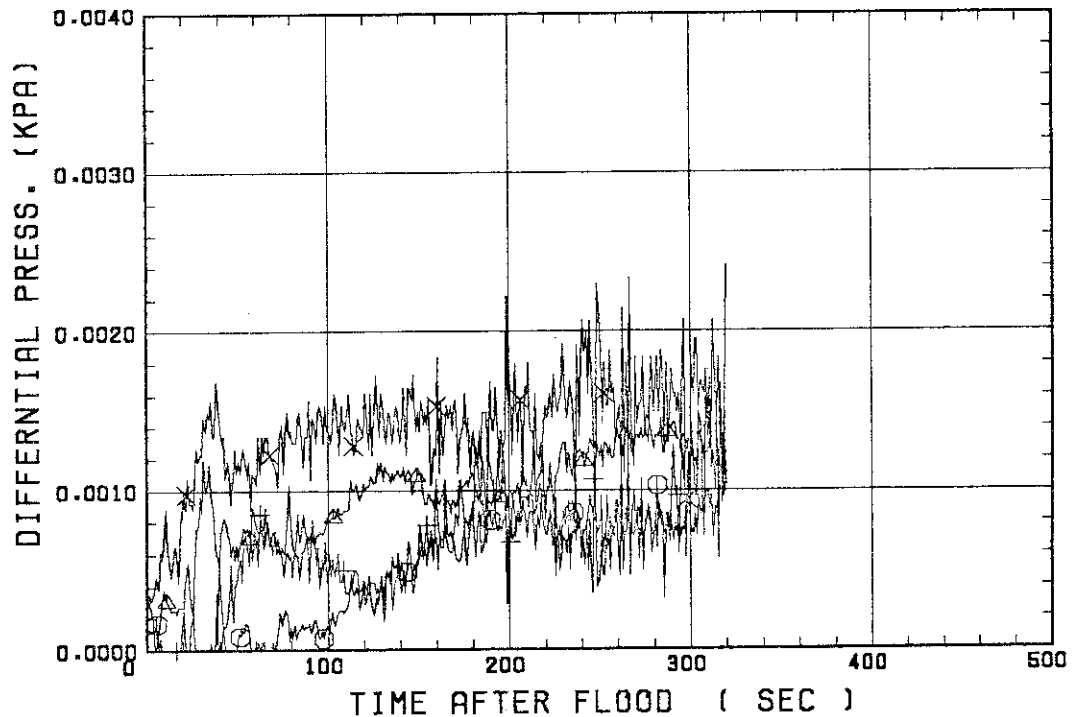
SMALL SCALE REFLOOD TEST
RUN 8127

○--- DPT2 △--- DPT4 +--- DPT5
X--- DPT6B



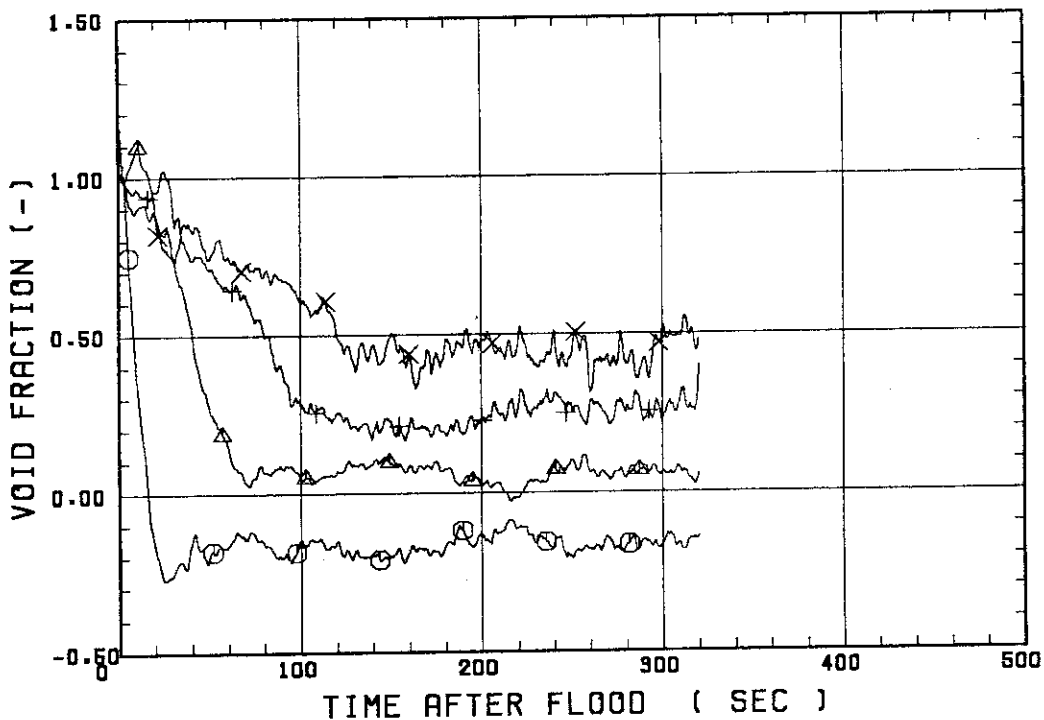
SMALL SCALE REFLOOD TEST
RUN 8127

○--- DPT7 △--- DPT8B +--- DP10
X--- DP12



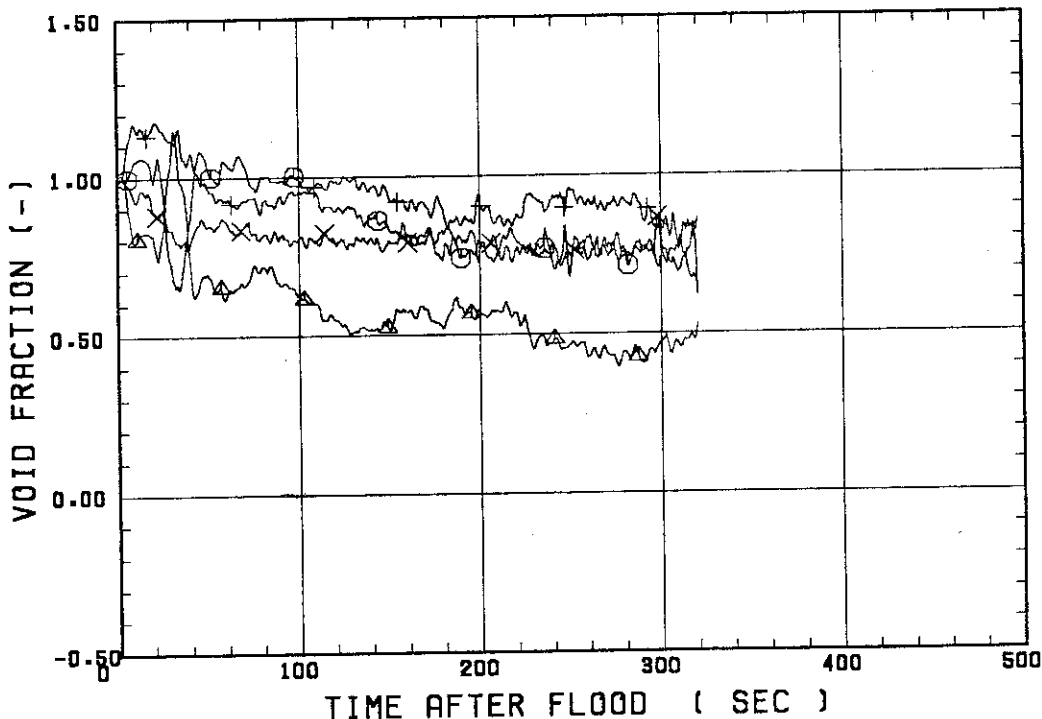
SMALL SCALE REFLOOD TEST
RUN 8127

○--- VDPT2 △--- VDPT4 +--- VDPT5
X--- VDPT6B



SMALL SCALE REFLOOD TEST
RUN 8127

○--- VDPT7 △--- VDPT8B +--- VDP10
X--- VDP12



 * RUN NO. 8131 *

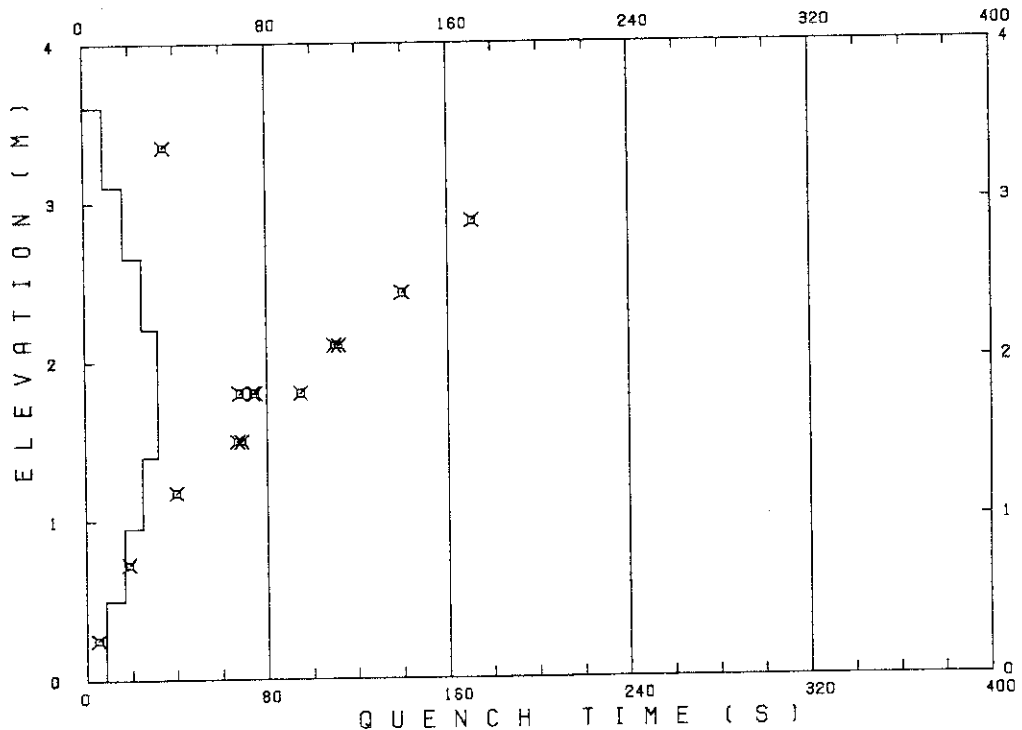
 TEST CONDITIONS

LINEAR PEAK POWER 1.8 KW/M
 SYSTEM PRESSURE 0.4 MPA
 INLET WATER TEMPERATURE 120 .C
 INJECTED WATER VELOCITY 3.9 CM/S

 TEMPERATURE PROFILE

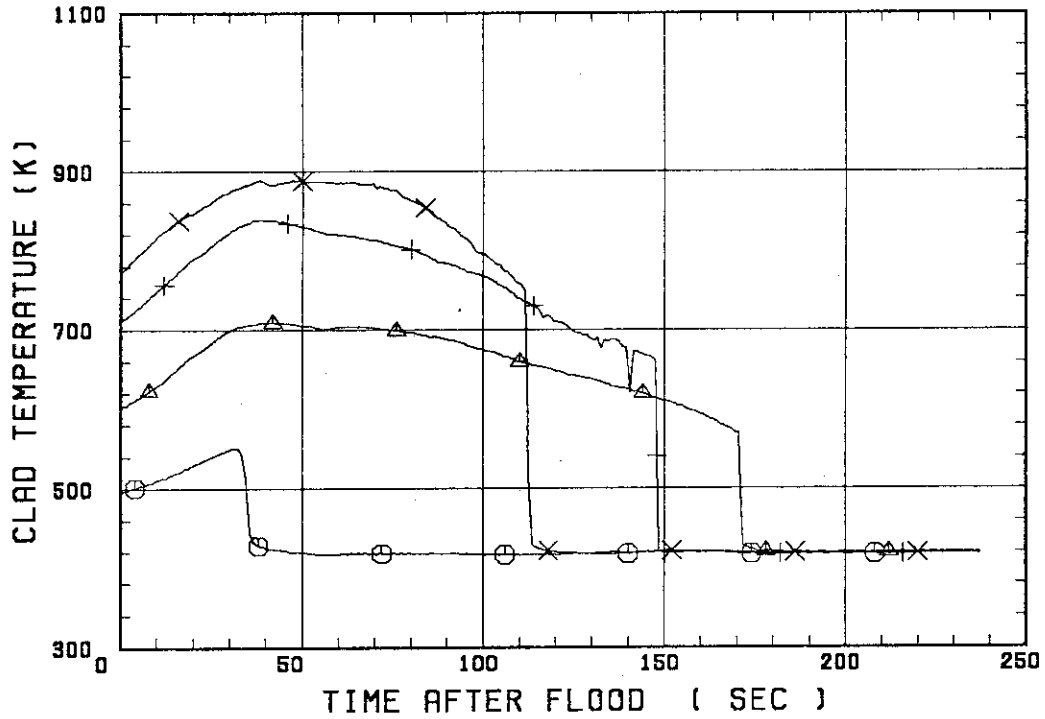
CH.NO.	SYMBOL	INITIAL TEMP. (.C)	TURNAROUND TIME (S)	TURNAROUND TEMP. (.C)	QUENCH TIME (S)	QUENCH TEMP. (.C)
66	TC1L	223	33.0	278	35.0	241
46	TB2	327	45.0	435	171.0	296
47	TB3	435	39.0	566	140.0	404
67	TC4U	496	50.0	616	112.0	476
7	TS4U	559	42.0	695	110.0	480
38	TA4M	460	31.0	563	68.0	457
68	TC4M	459	30.0	563	75.0	453
8	TS4M	513	32.5	625	74.0	461
48	TB4M	498	33.0	616	95.0	412
69	TC4L	492	29.0	572	67.0	461
9	TS4L	513	26.0	600	69.0	458
54	TR5	452	19.0	508	40.0	439
55	TR6	334	14.0	360	19.0	342
70	TC7	225	5.0	231	5.0	231

RUN NO. 8131



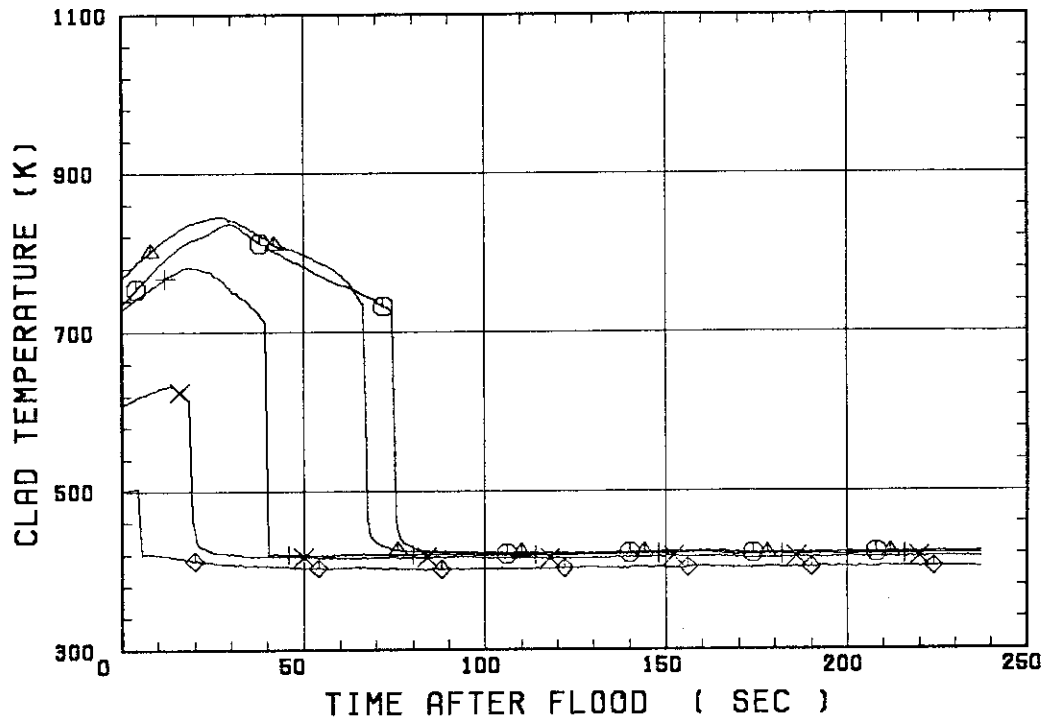
SMALL SCALE REFLOOD TEST
 RUN 8131

○--- TC1L ▲--- TB2 +--- TB3
 X--- TC4U

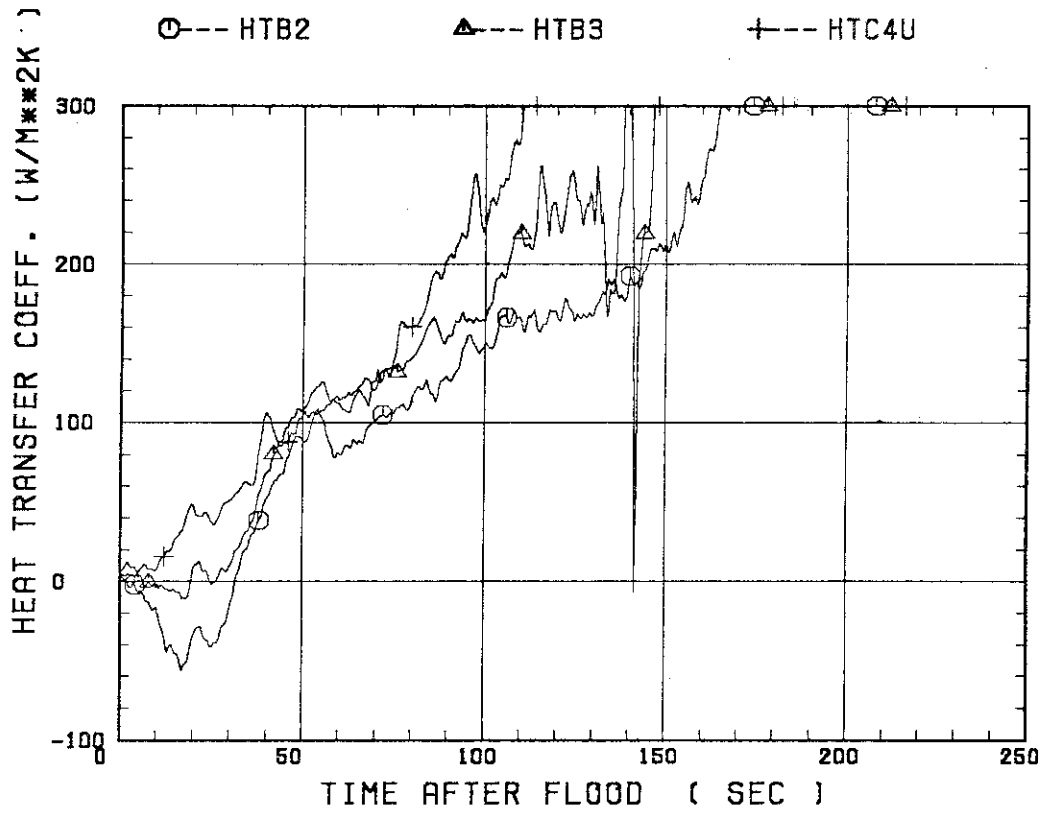


SMALL SCALE REFLOOD TEST
 RUN 8131

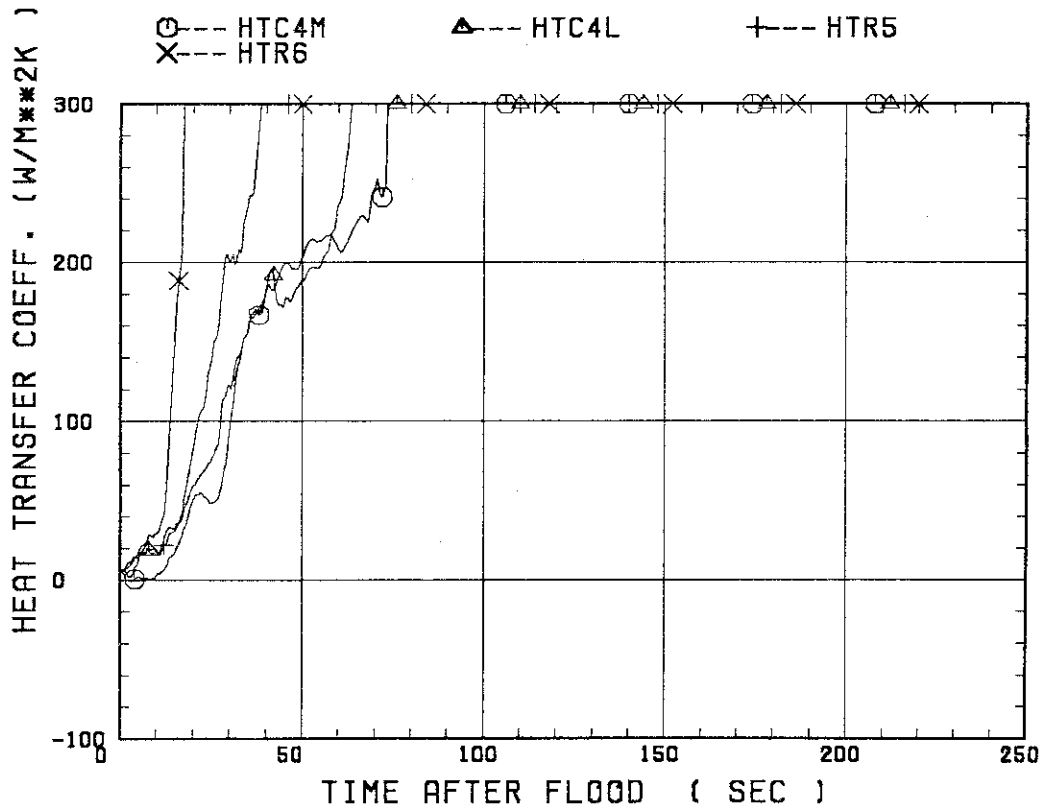
○--- TC4M ▲--- TC4L +--- TR5
 X--- TR6 ◆--- TC7



SMALL SCALE REFLOOD TEST
RUN 8131

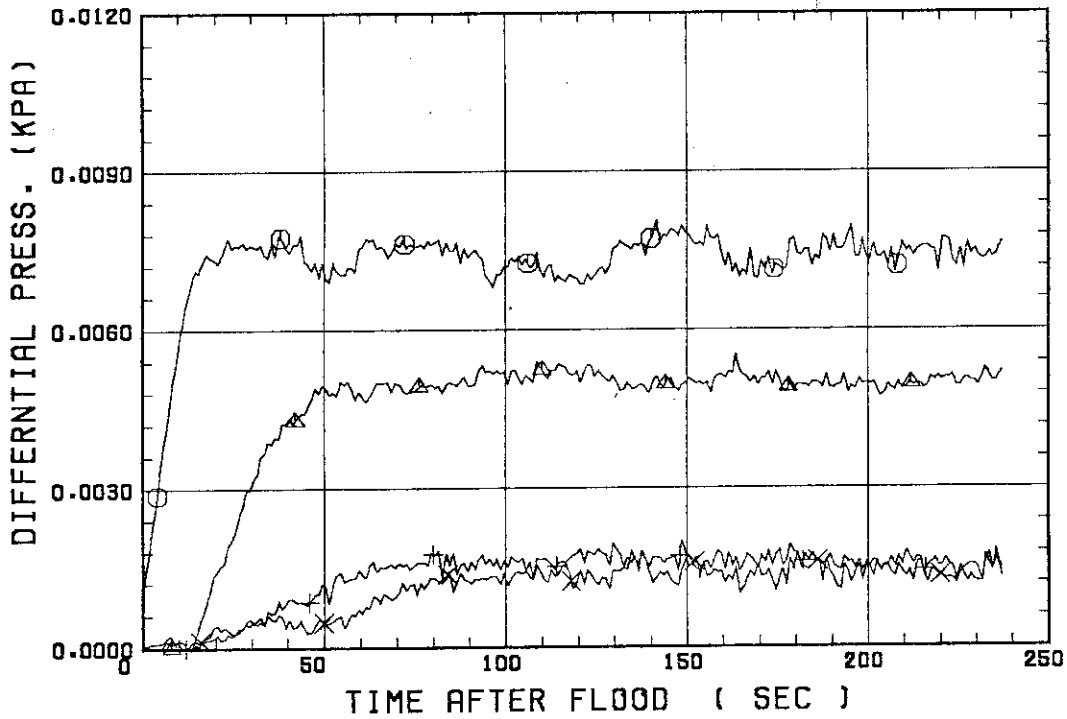


SMALL SCALE REFLOOD TEST
RUN 8131



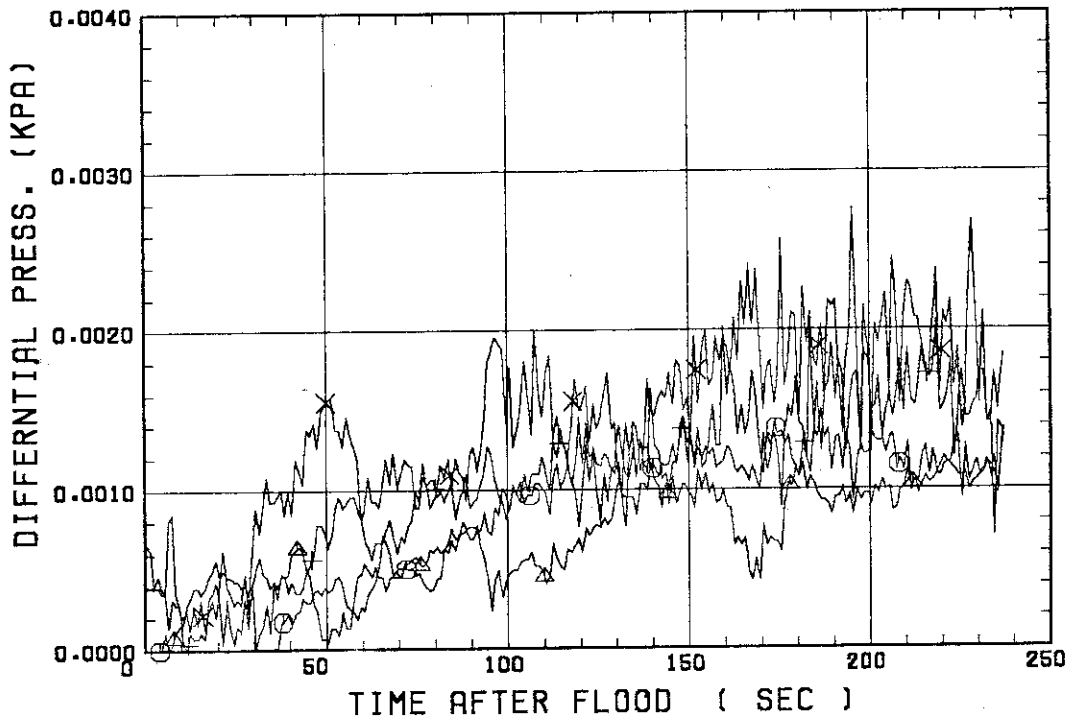
SMALL SCALE REFLOOD TEST
RUN 8131

○ --- DPT2 ▲ --- DPT4 + --- DPT5
X --- DPT6B



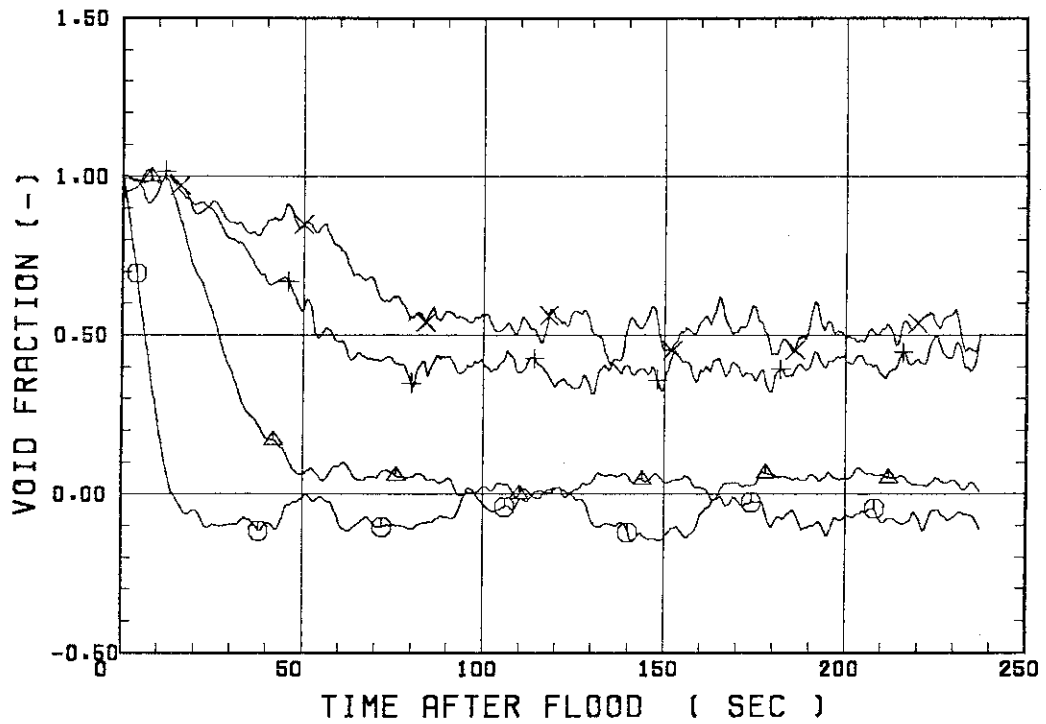
SMALL SCALE REFLOOD TEST
RUN 8131

○ --- DPT7 ▲ --- DPT8B + --- DP10
X --- DP12



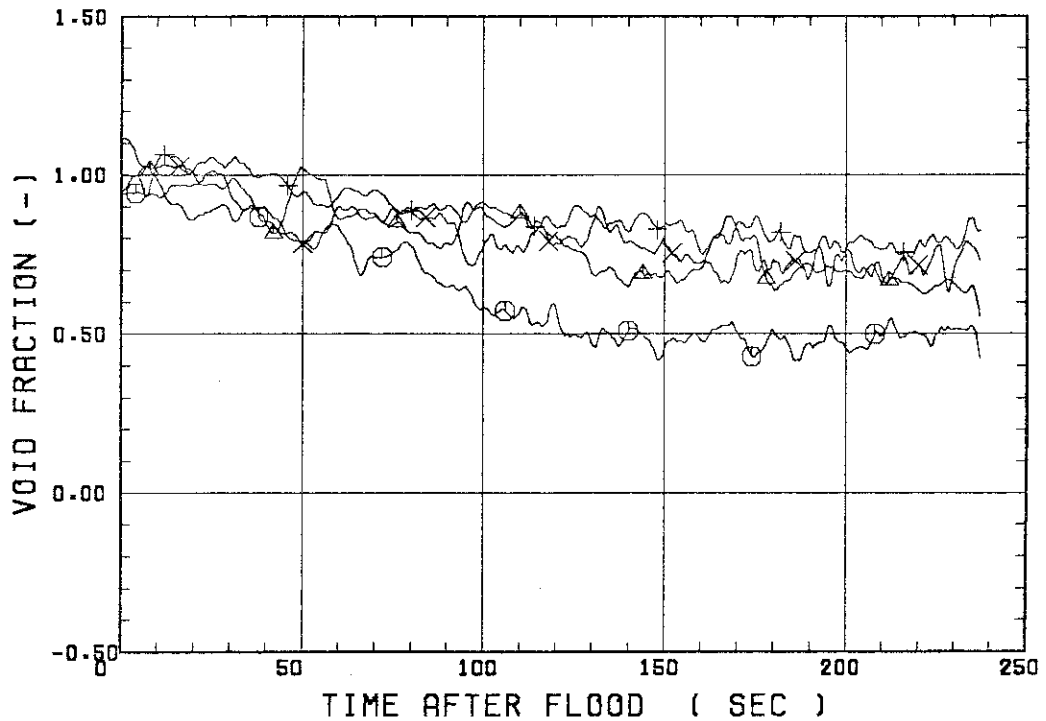
SMALL SCALE REFLOOD TEST
 RUN 8131

○ --- VDPT2 ▲ --- VDPT4 + --- VDPT5
 X --- VDPT6B



SMALL SCALE REFLOOD TEST
 RUN 8131

○ --- VDPT7 ▲ --- VDPT8B + --- VDP10
 X --- VDP12



 * RUN NO. 8202 *

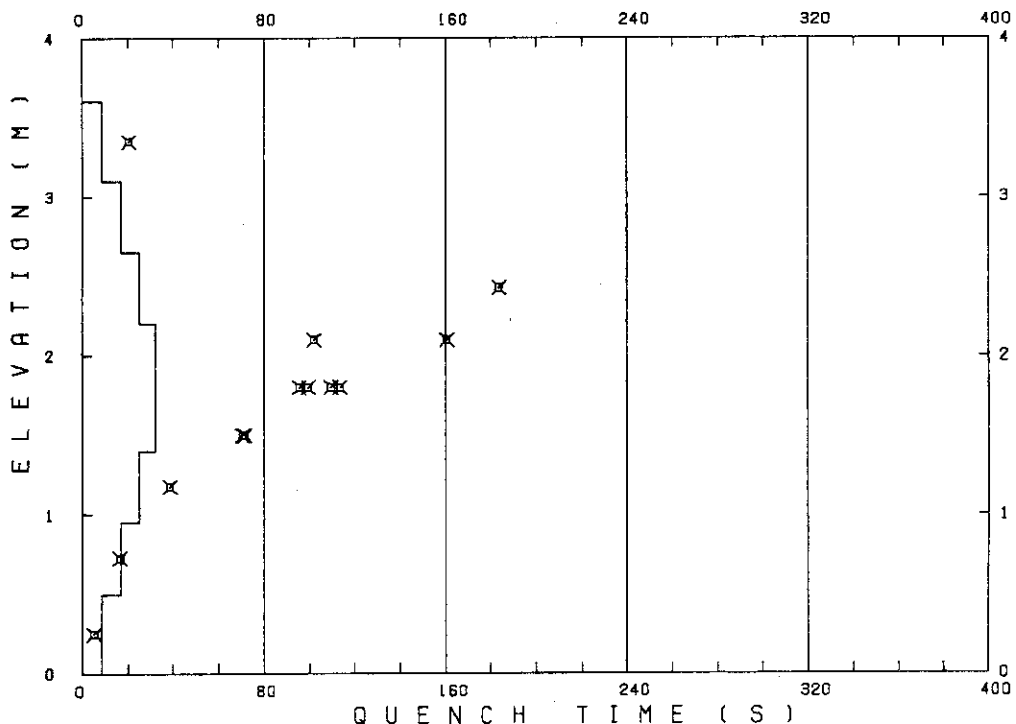
 TEST CONDITIONS

LINEAR PEAK POWER 1.8 KW/M
 SYSTEM PRESSURE 0.2 MPA
 INLET WATER TEMPERATURE 100 .C
 INJECTED WATER VELOCITY 3.9 CM/S

 TEMPERATURE PROFILE

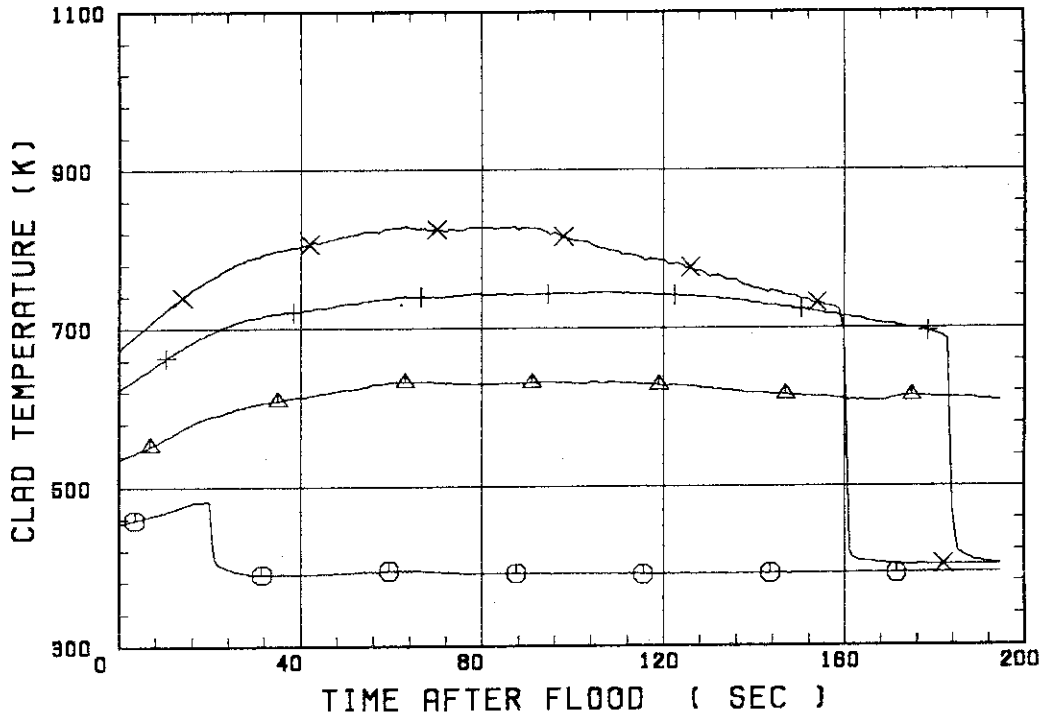
CH.NO.	SYMBOL	INITIAL TEMP. (.C)	TURNAROUND TIME (S)	TURNAROUND TEMP. (.C)	QUENCH TIME (S)	QUENCH TEMP. (.C)
1	TE1L	181	20.0	210	20.5	207
51	TR2	261	66.5	359		
37	TR3	348	108.5	472	183.5	412
67	TC4U	398	87.5	555	160.5	422
7	TS4U	423	65.0	594	102.0	483
38	TR4M	408	58.5	545	109.5	432
68	TC4M	391	54.5	513	113.5	428
8	TS4M	406	50.5	543	95.5	386
48	TB4M	416	47.5	552	99.5	461
69	TC4L	391	34.5	482	70.5	436
9	TS4L	400	28.0	493	71.5	434
54	TR5	343	24.5	405	38.5	385
55	TR6	256	12.5	284	16.5	273
5	TE7	177	4.0	182	5.0	179

RUN NO. 8202



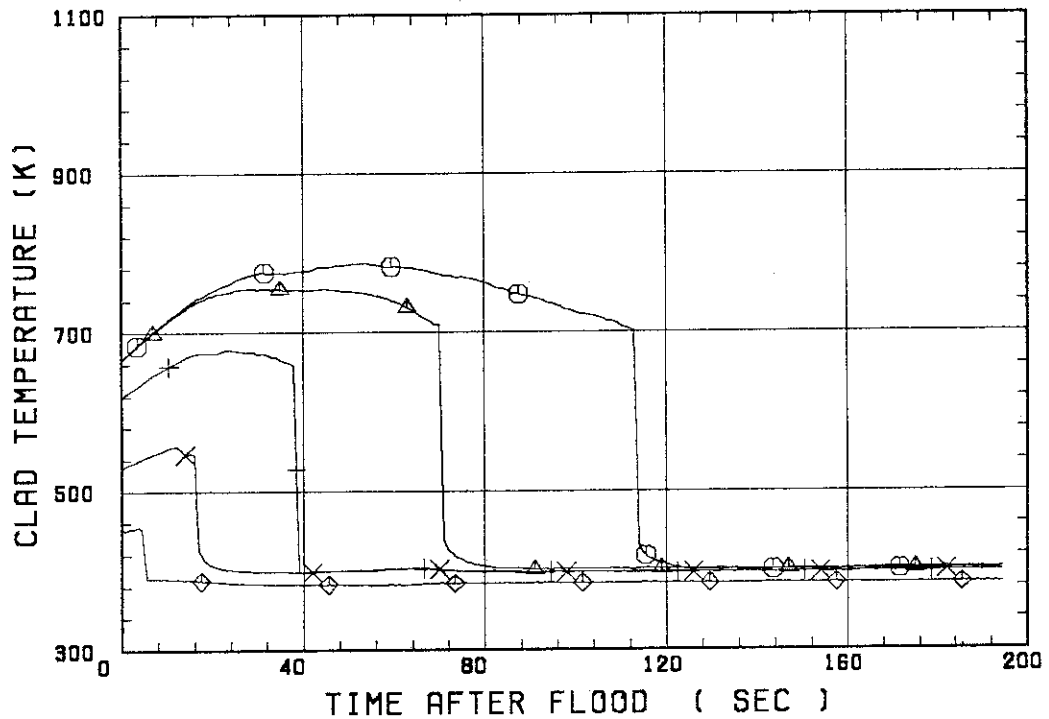
SMALL SCALE REFLOOD TEST
RUN 8202

○ --- TE1L △ --- TR2 + --- TR3
X --- TC4U

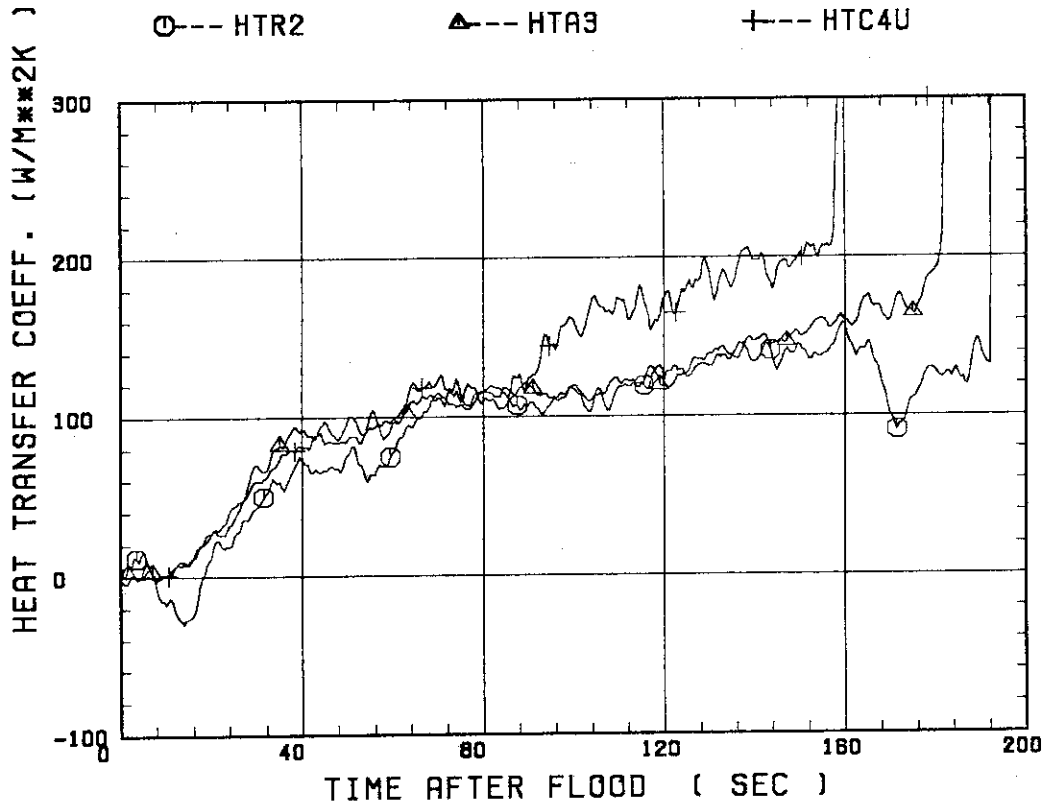


SMALL SCALE REFLOOD TEST
RUN 8202

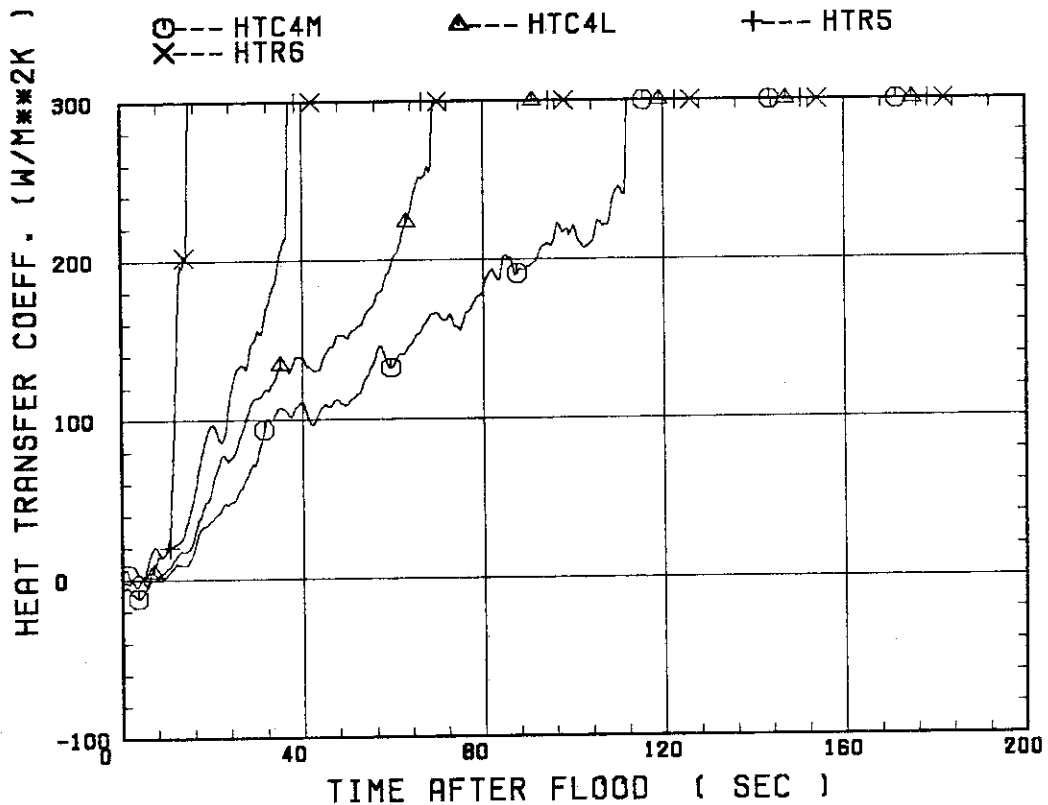
○ --- TC4M △ --- TC4L + --- TR5
X --- TR6 ◇ --- TE7



SMALL SCALE REFLOOD TEST
RUN 8202

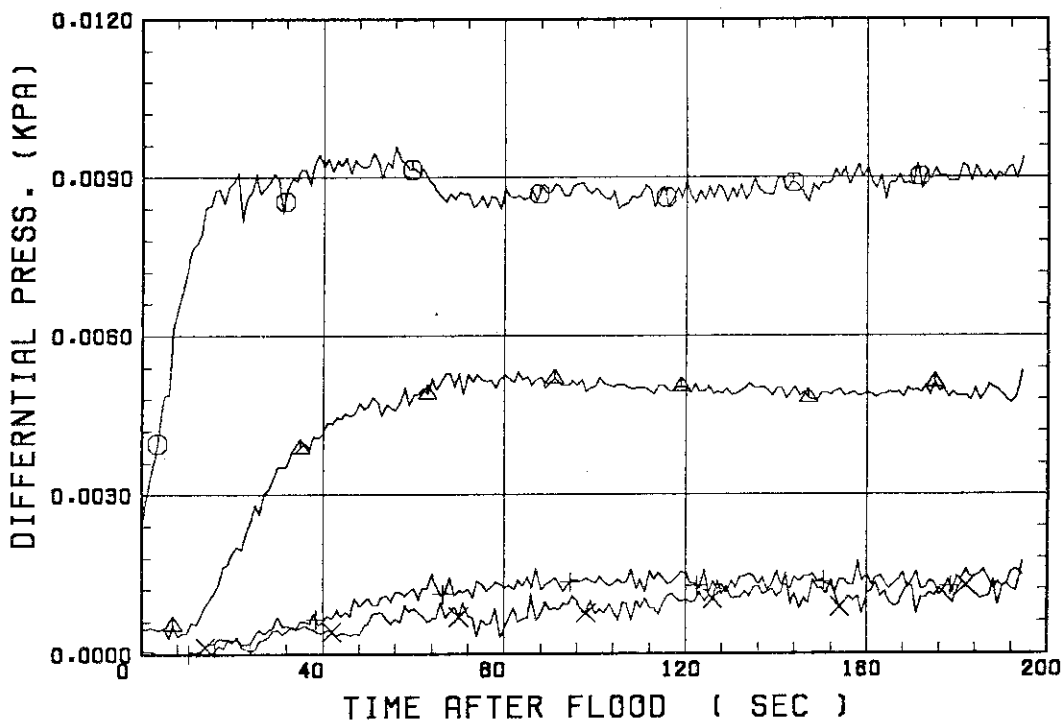


SMALL SCALE REFLOOD TEST
RUN 8202



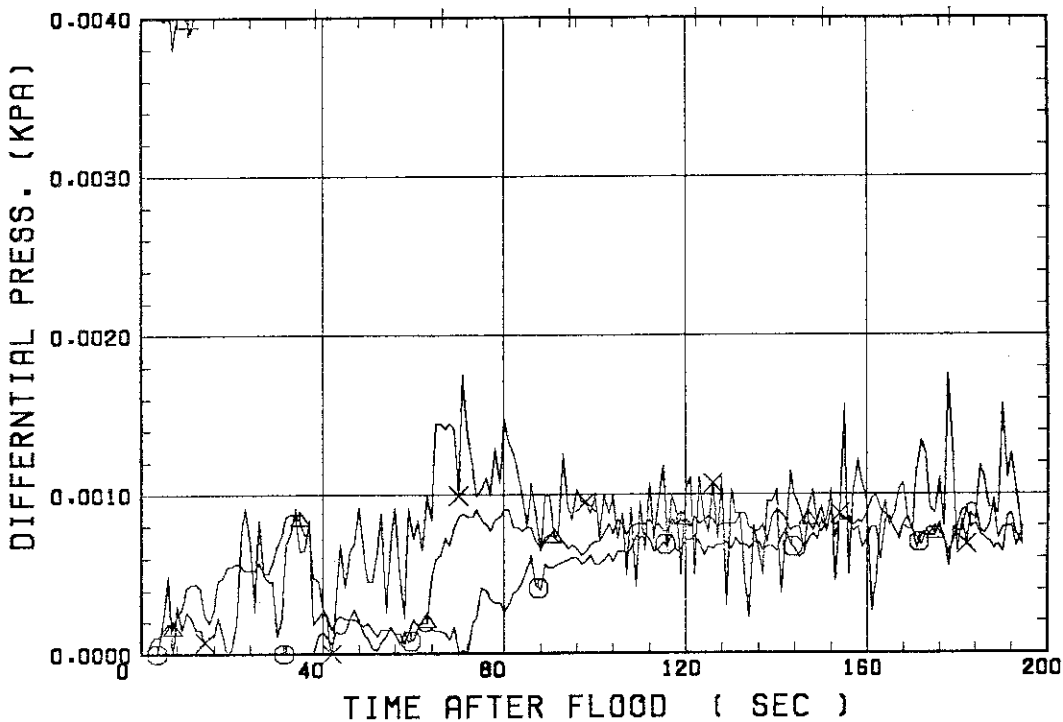
SMALL SCALE REFLOOD TEST
 RUN 8202

○ --- DPT2 ▲ --- DPT4 + --- DPT5
 X --- DPT6B



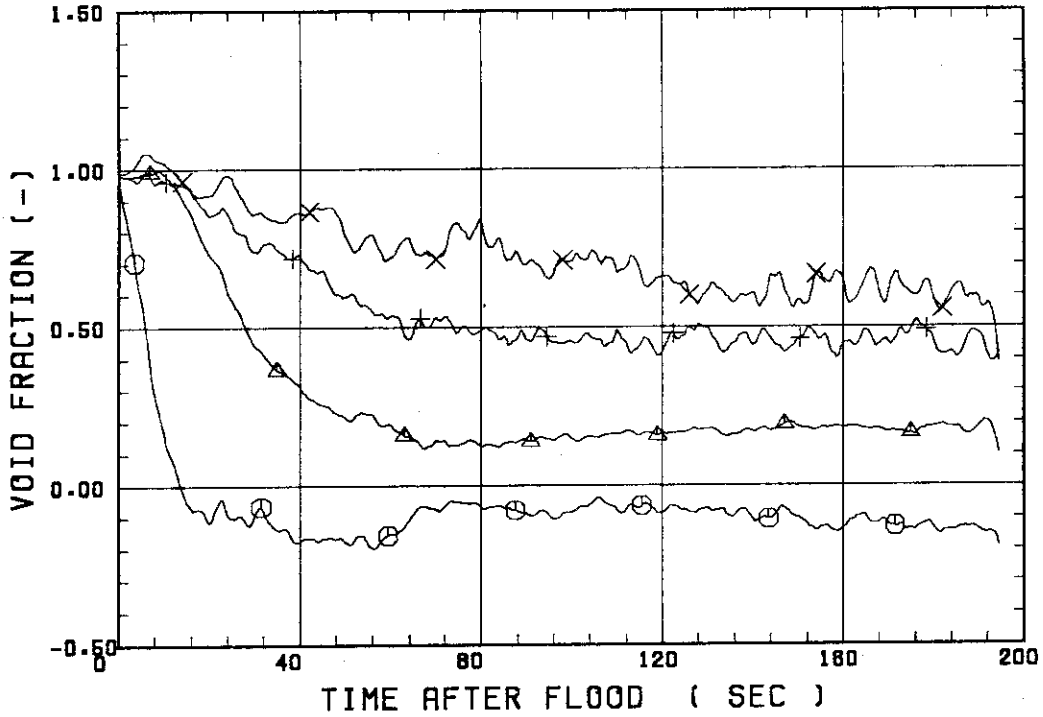
SMALL SCALE REFLOOD TEST
 RUN 8202

○ --- DPT7 ▲ --- DPT8B + --- DP10
 X --- DP12



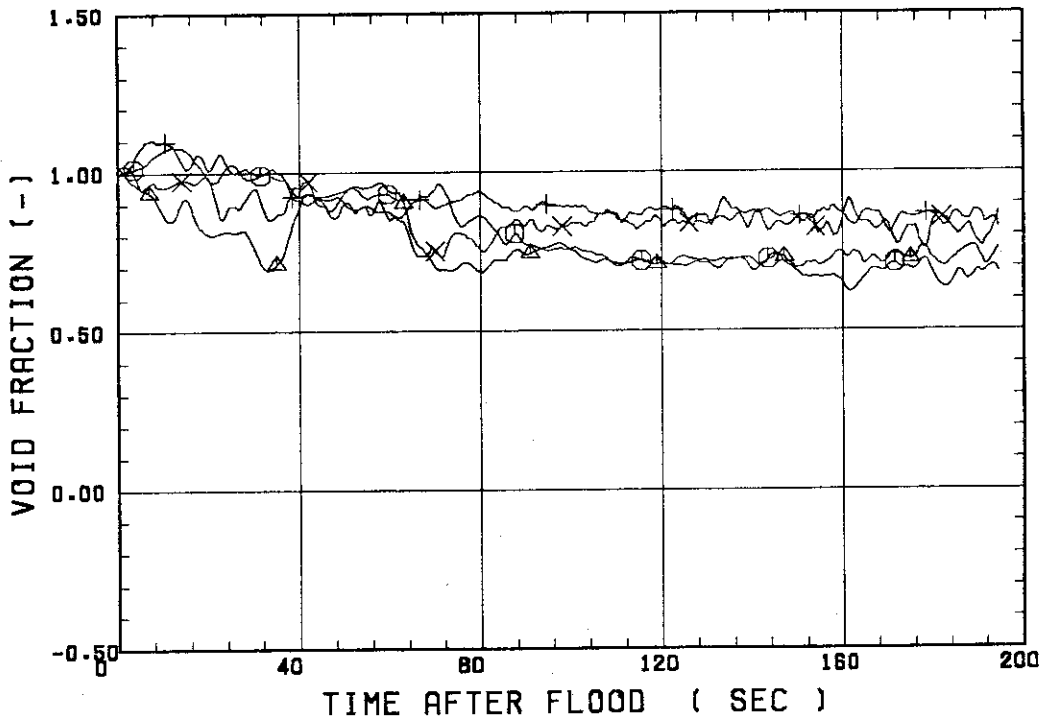
SMALL SCALE REFLOOD TEST
RUN 8202

○ --- VDPT2 △ --- VDPT4 + --- VDPT5
X --- VDPT6B



SMALL SCALE REFLOOD TEST
RUN 8202

○ --- VDPT7 △ --- VDPT8B + --- VDP10
X --- VDP12



 * RUN NO. 8203 *
 * *****

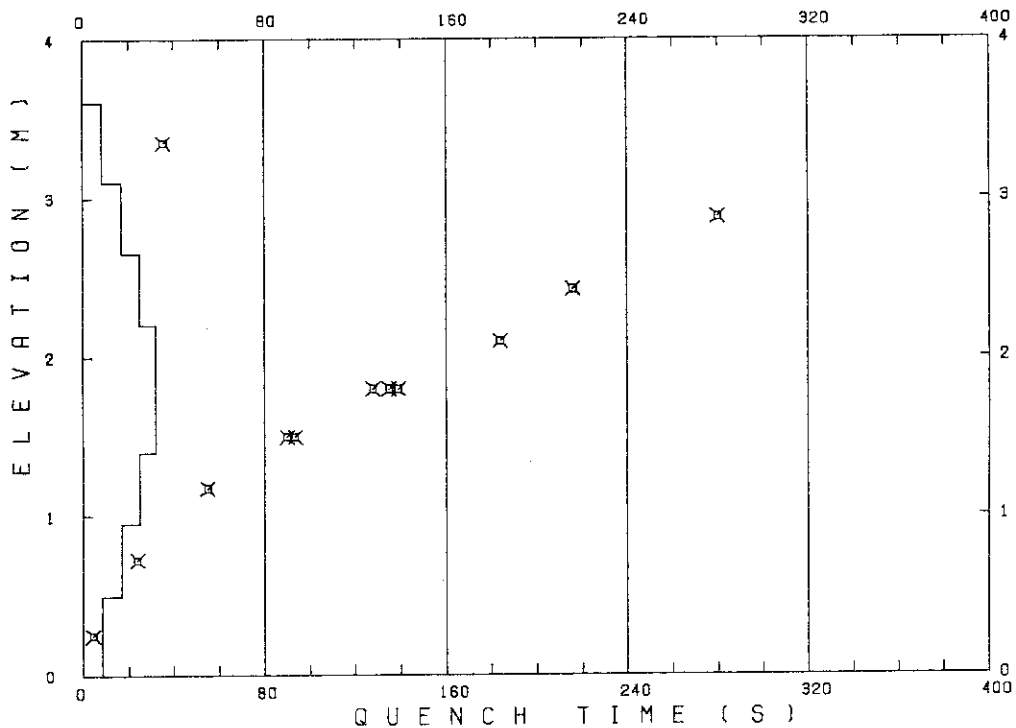
 TEST CONDITIONS

LINEAR PEAK POWER 1.8 KW/M
 SYSTEM PRESSURE 0.2 MPA
 INLET WATER TEMPERATURE 100 .C
 INJECTED WATER VELOCITY 3.9 CM/S

 TEMPERATURE PROFILE

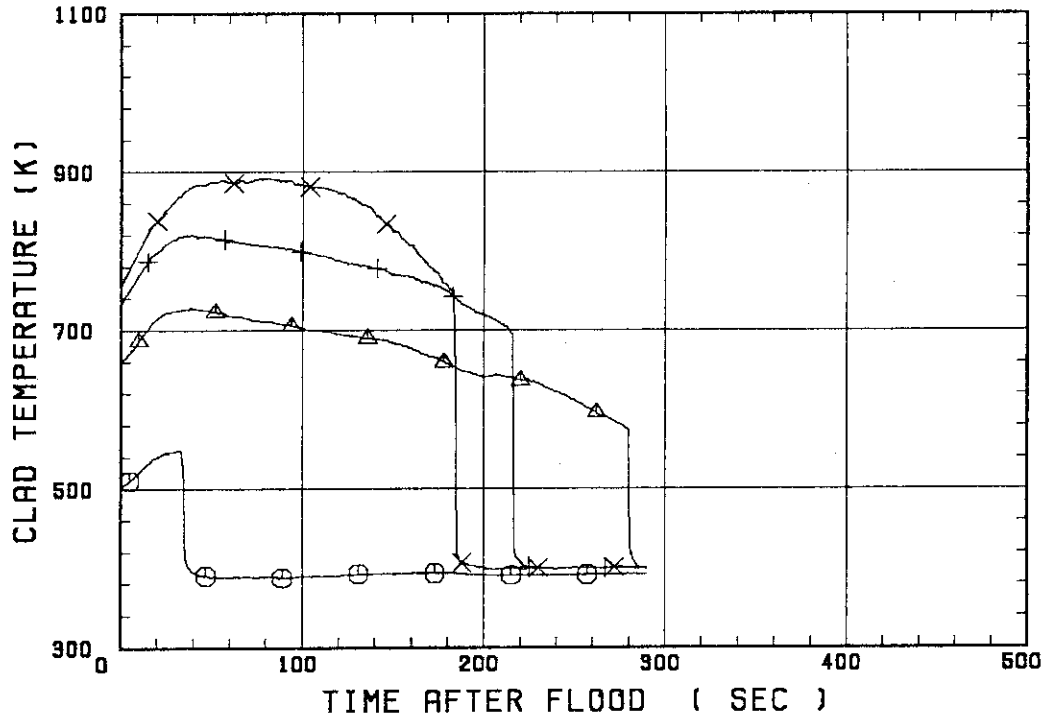
CH.NO.	SYMBOL	INITIAL TEMP. (.C)	TURNAROUND TIME (S)	TURNAROUND TEMP. (.C)	QUENCH TIME (S)	QUENCH TEMP. (.C)
1	TE1L	229	32.5	276	35.5	234
51	TR2	385	39.0	456	280.0	300
37	TA3	458	40.0	546	216.0	422
67	TC4U	478	82.0	620	184.0	471
7	TS4U	553	65.0	694	184.0	417
38	TA4M	498	41.0	616	135.0	471
68	TC4M	474	42.0	584	135.0	453
8	TS4M	532	41.5	657	139.0	456
48	TB4M	535	41.0	649	128.0	488
69	TC4L	470	32.0	556	90.0	457
9	TS4L	516	28.0	600	93.5	445
54	TR5	446	19.0	499	55.0	423
55	TR6	325	14.0	351	24.0	325
5	TE7	212	2.5	215	4.5	205

RUN NO. 8203



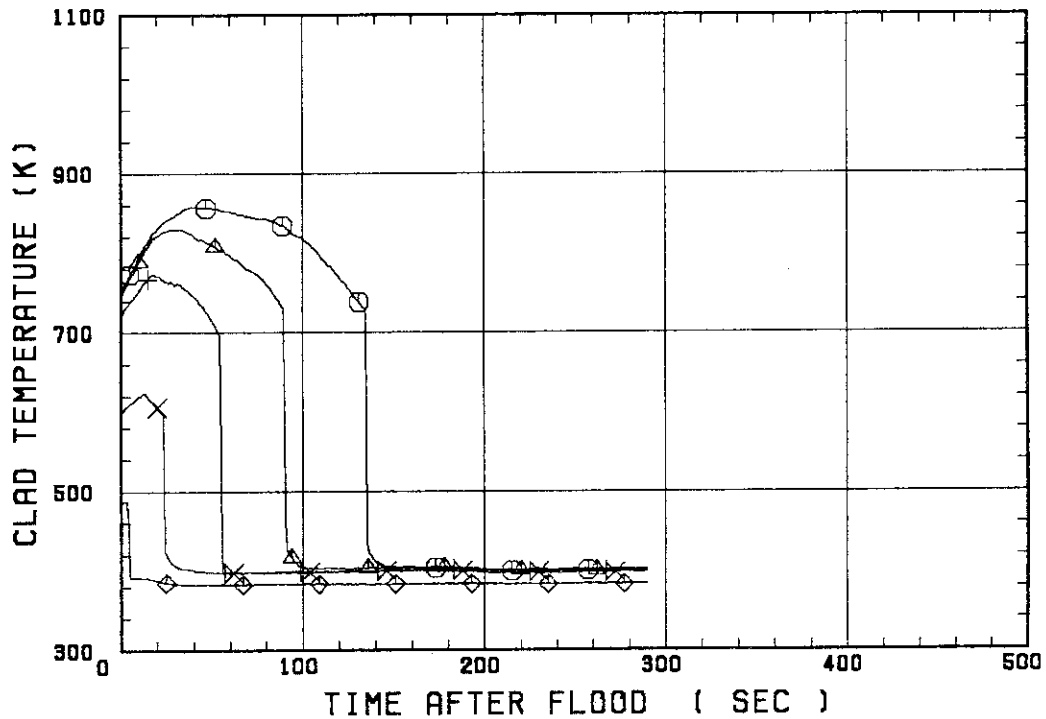
SMALL SCALE REFLOOD TEST
 RUN 8203

○--- TE1L △--- TR2 +--- TA3
 X--- TC4U

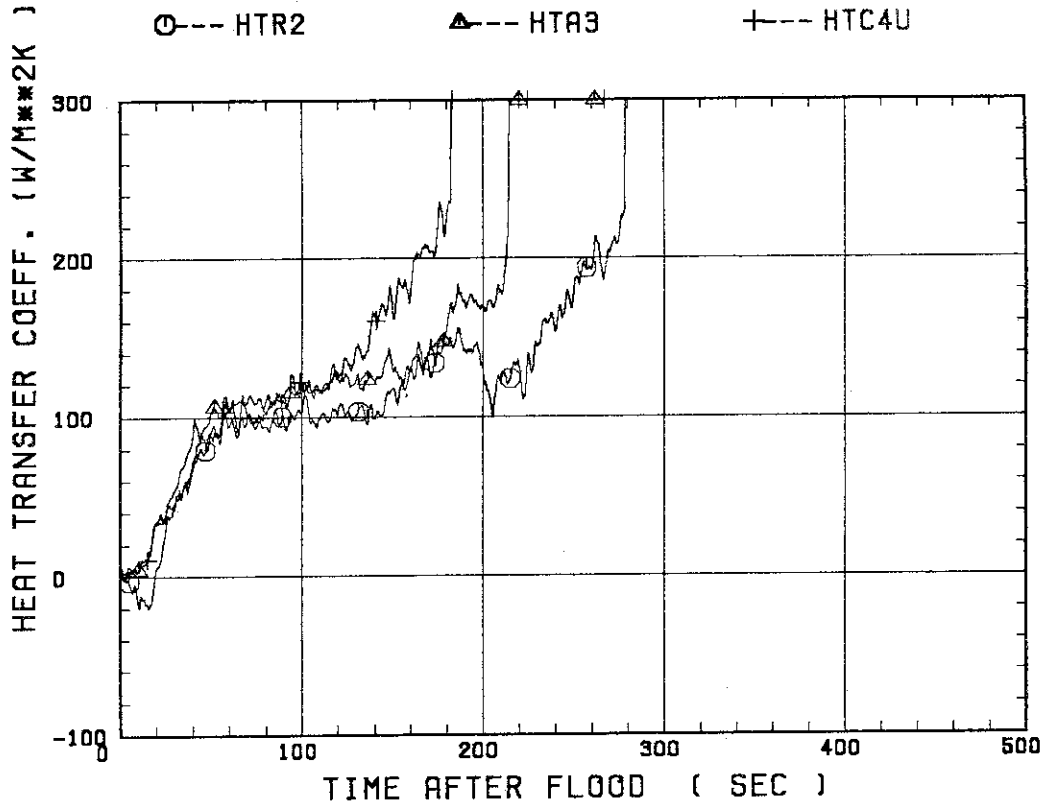


SMALL SCALE REFLOOD TEST
 RUN 8203

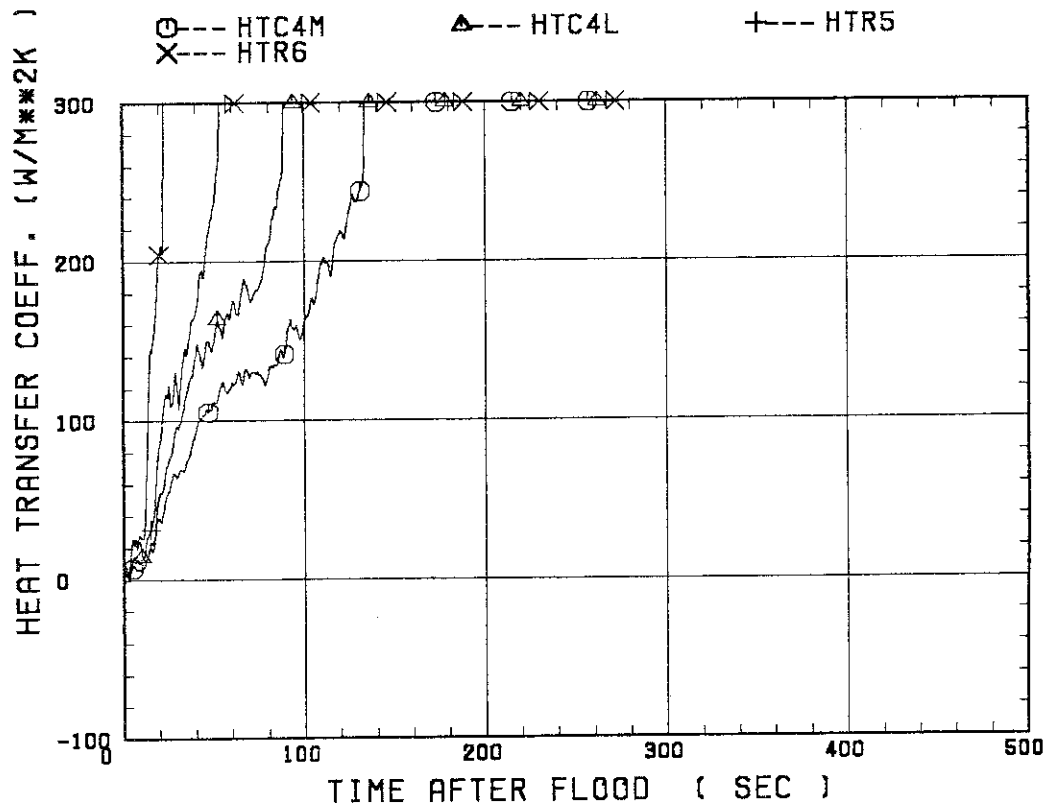
○--- TC4M △--- TC4L +--- TR5
 X--- TR6 ◇--- TE7



SMALL SCALE REFLOOD TEST
 RUN 8203

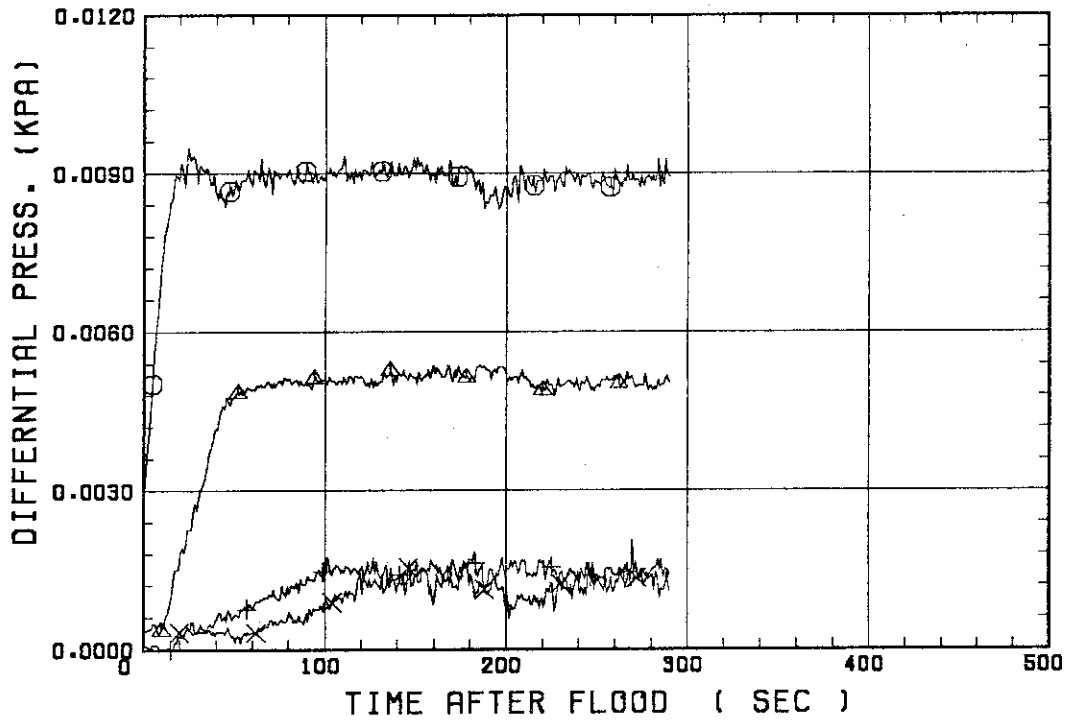


SMALL SCALE REFLOOD TEST
 RUN 8203



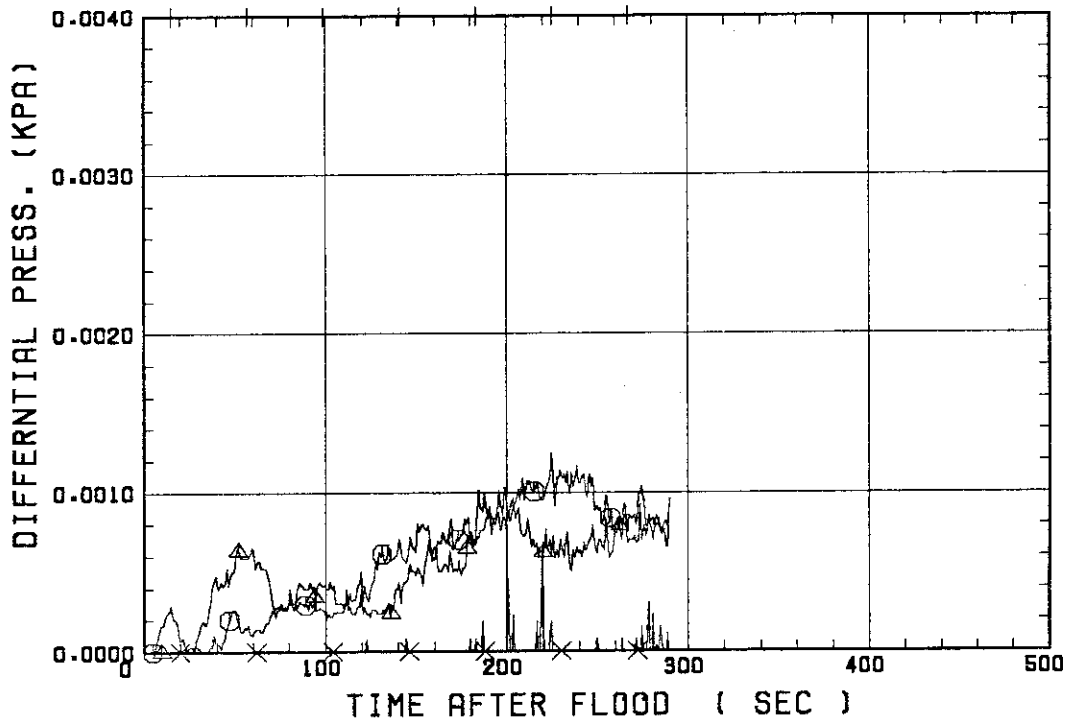
SMALL SCALE REFLOOD TEST
RUN 8203

○ --- DPT2 △ --- DPT4 + --- DPT5
X --- DPT6B



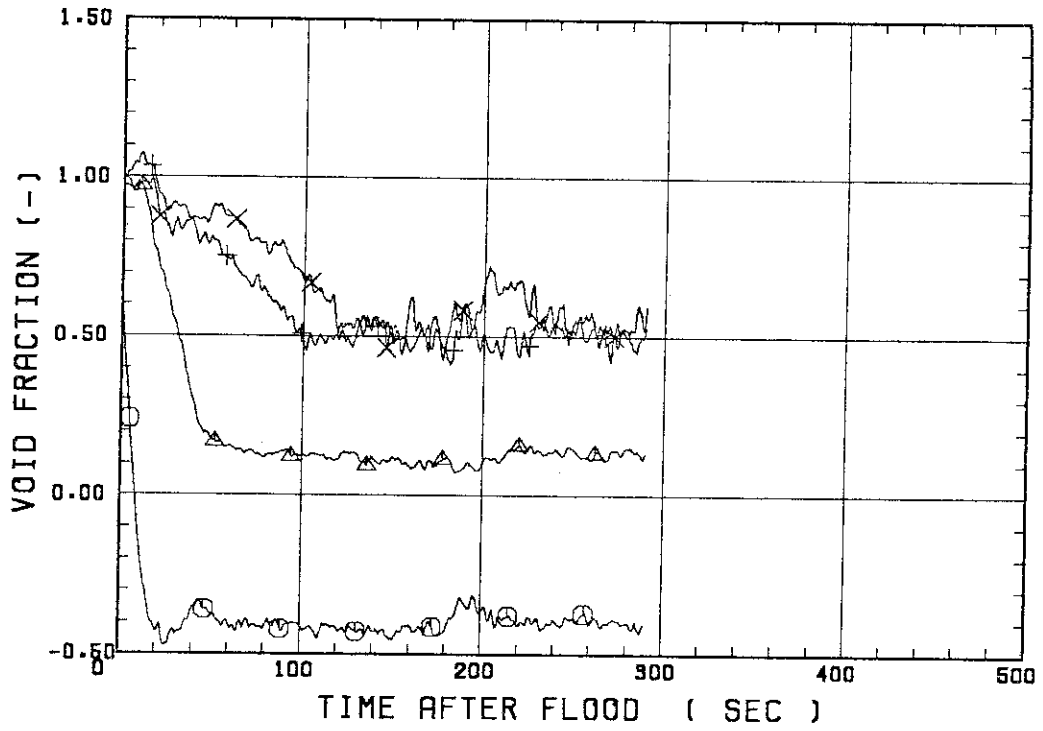
SMALL SCALE REFLOOD TEST
RUN 8203

○ --- DPT7 △ --- DPT8B + --- DP10
X --- DP12



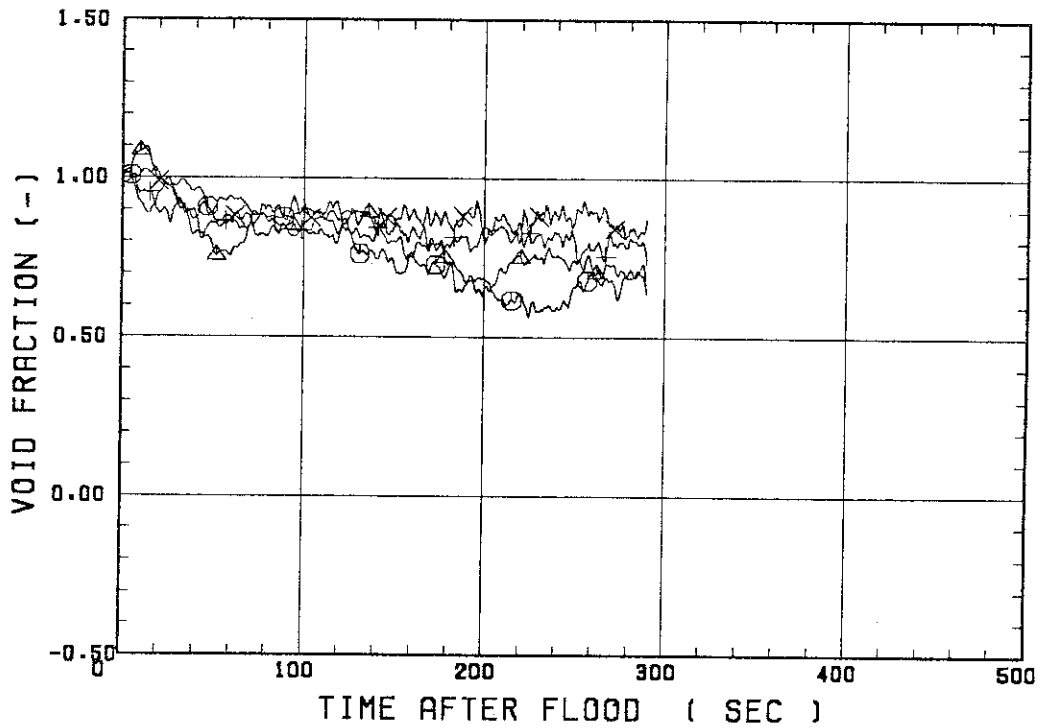
SMALL SCALE REFLOOD TEST
RUN 8203

○--- VDPT2 △--- VDPT4 +--- VDPT5
X--- VDPT6B



SMALL SCALE REFLOOD TEST
RUN 8203

○--- VDPT7 △--- VDPT8B +--- VDP10
X--- VDP12



 * RUN NO. 8205 *

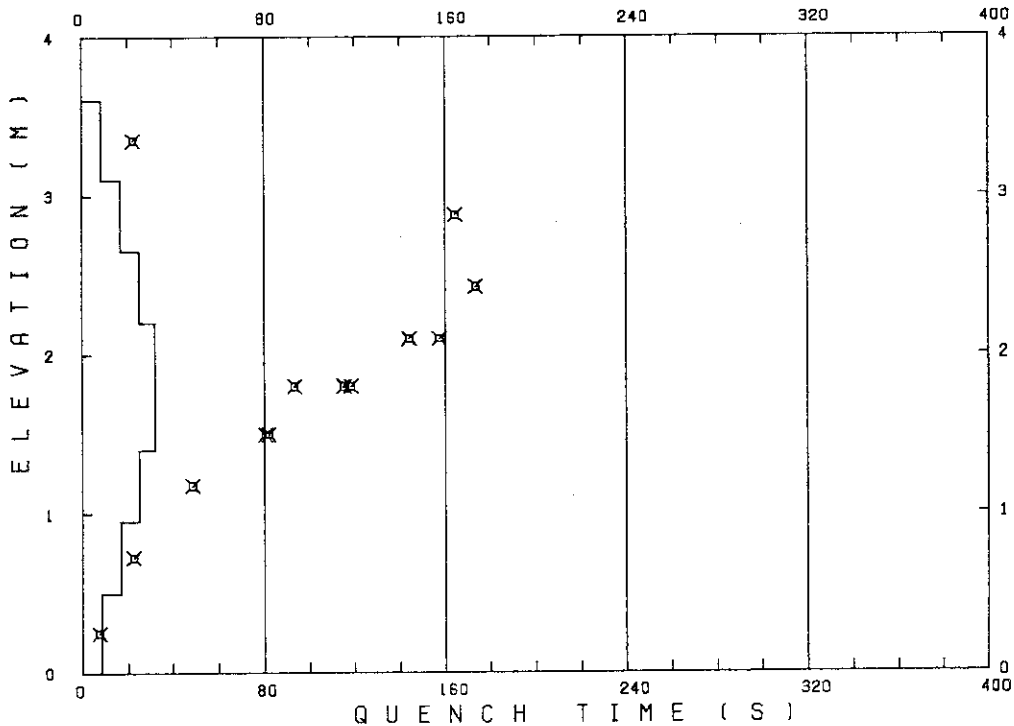
 TEST CONDITIONS

LINEAR PEAK POWER 1.8 KW/M
 SYSTEM PRESSURE 0.2 MPA
 INLET WATER TEMPERATURE 100 .C
 INJECTED WATER VELOCITY 5.8 CM/S

 TEMPERATURE PROFILE

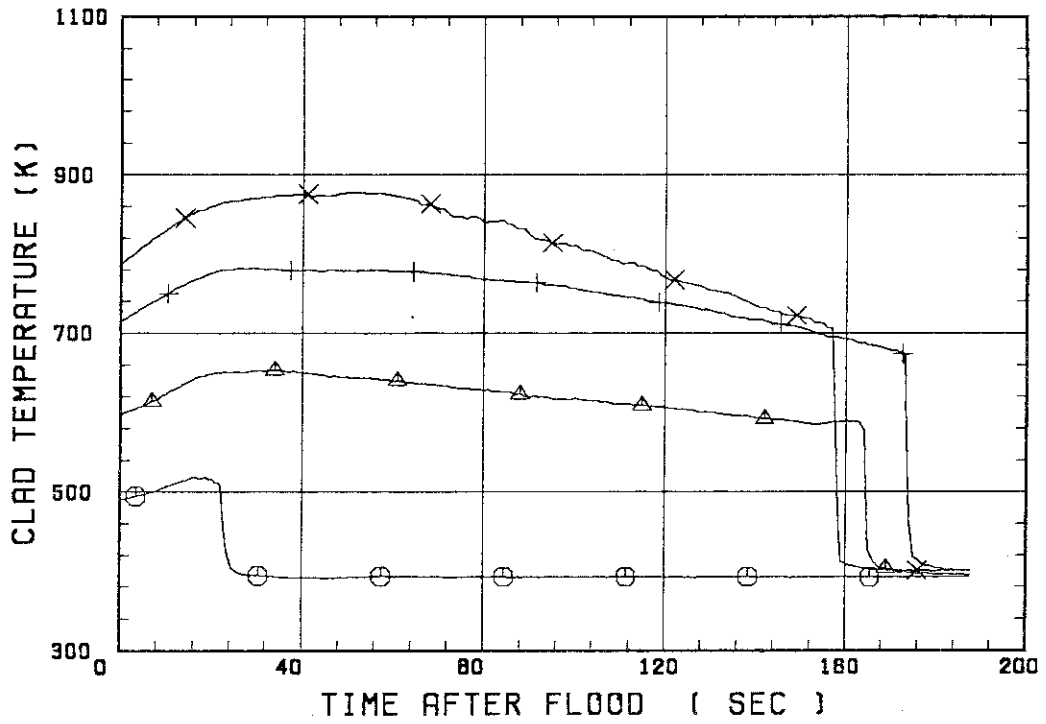
CH.NO.	SYMBOL	INITIAL TEMP. (.C)	TURNAROUND TIME (S)	TURNAROUND TEMP. (.C)	QUENCH TIME (S)	QUENCH TEMP. (.C)
1	TE1L	216	16.5	246	22.5	234
51	TR2	323	34.5	380	164.5	303
37	TA3	439	30.5	508	173.5	400
67	TC4U	511	50.5	605	157.5	433
7	TS4U	543	42.0	646	144.0	446
38	TA4M	524	32.5	609	115.5	445
68	TC4M	514	23.5	587	118.5	425
8	TS4M	529	23.5	615	115.0	432
48	TB4M	536	32.5	623	93.5	513
69	TC4L	513	22.5	577	80.5	443
9	TS4L	527	19.5	595	82.0	443
54	TR5	438	16.5	488	48.5	411
55	TR6	317	13.5	344	22.5	321
5	TE7	210	5.5	217	7.5	204

RUN NO. 8205



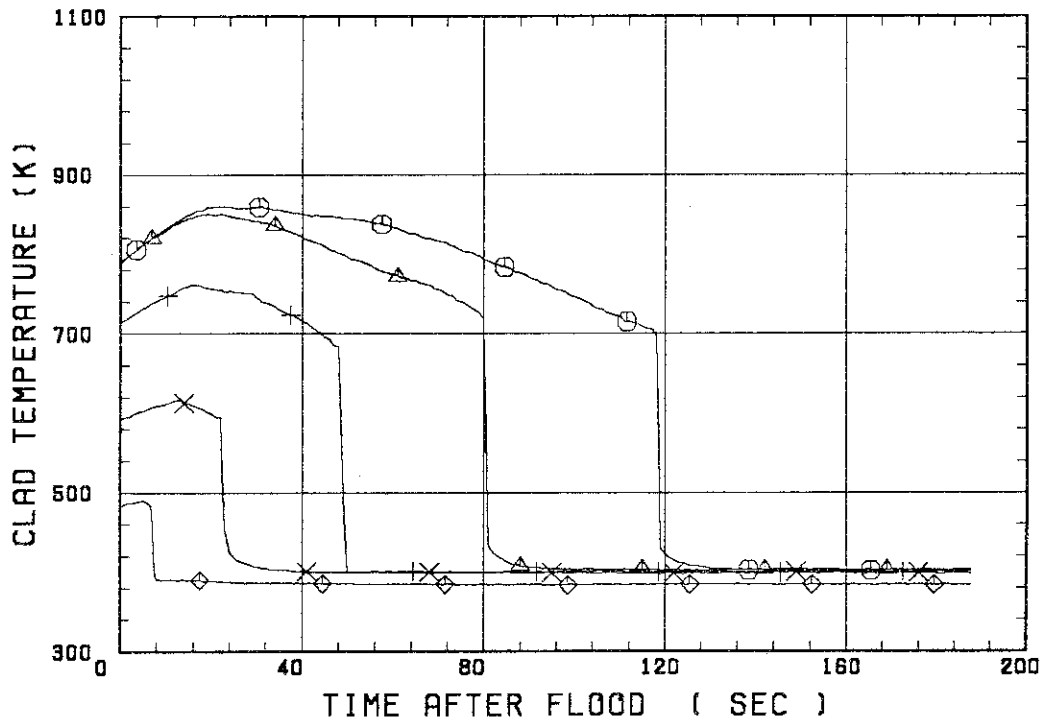
SMALL SCALE REFLOOD TEST
 RUN 8205

○ --- TE1L ▲ --- TR2 + --- TR3
 X --- TC4U

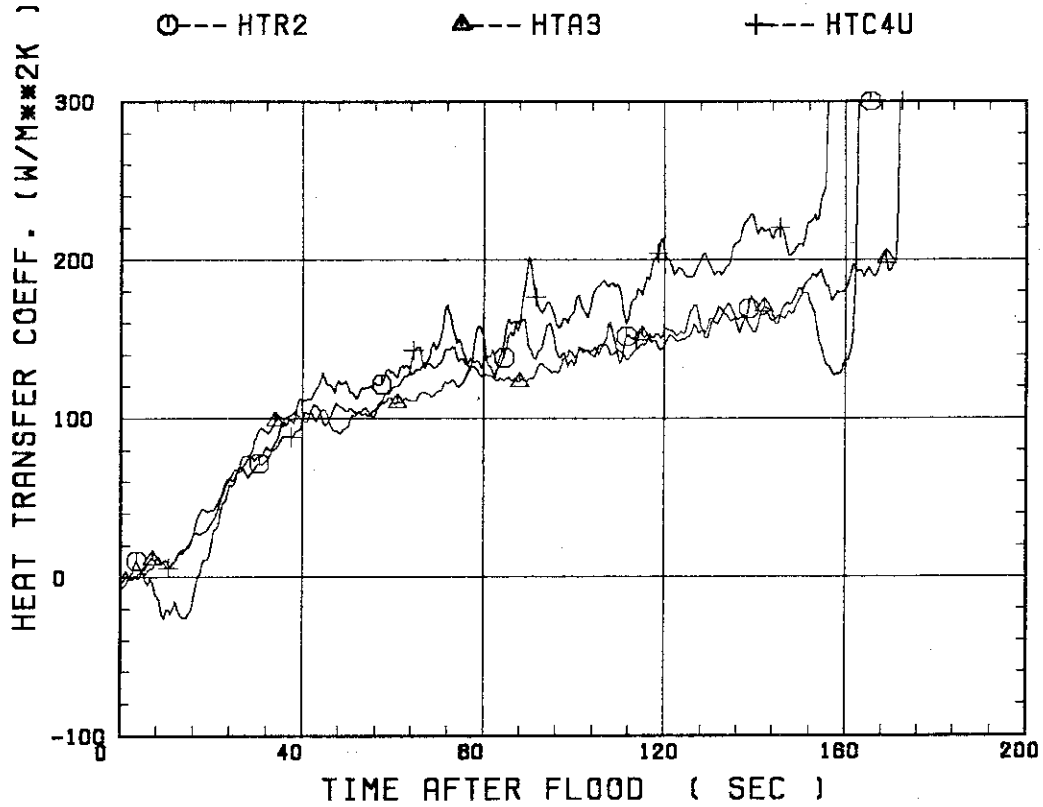


SMALL SCALE REFLOOD TEST
 RUN 8205

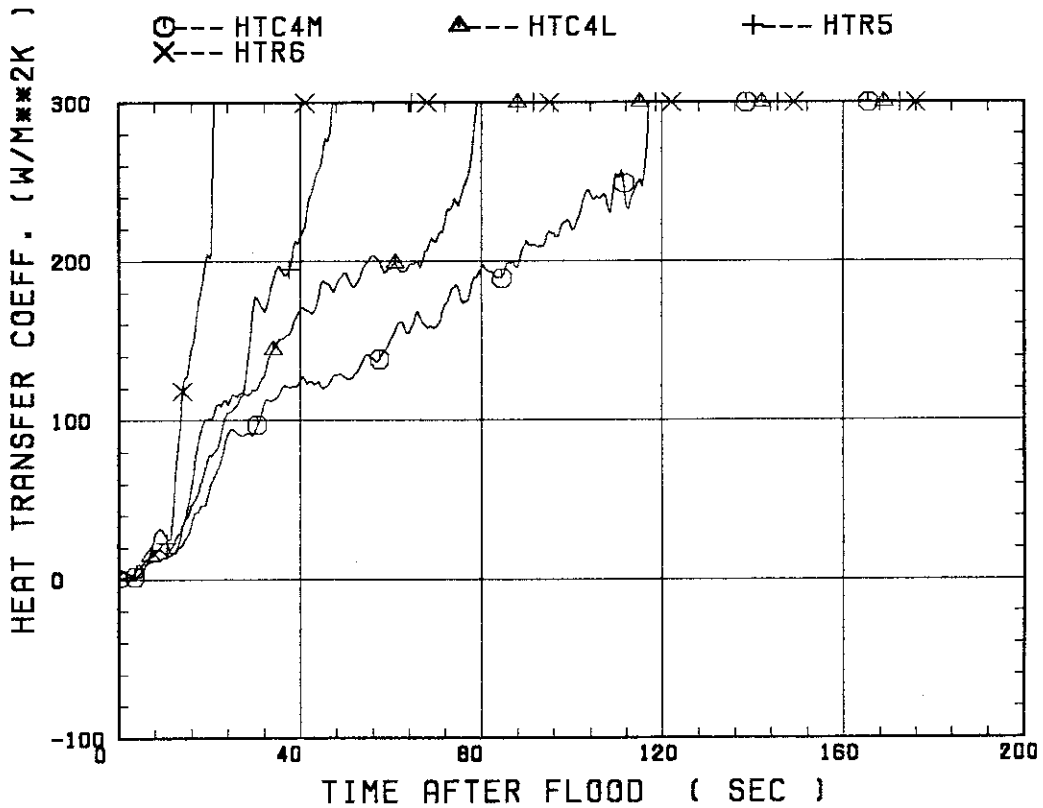
○ --- TC4M ▲ --- TC4L + --- TR5
 X --- TR6 ◆ --- TE7



SMALL SCALE REFLOOD TEST
RUN 8205

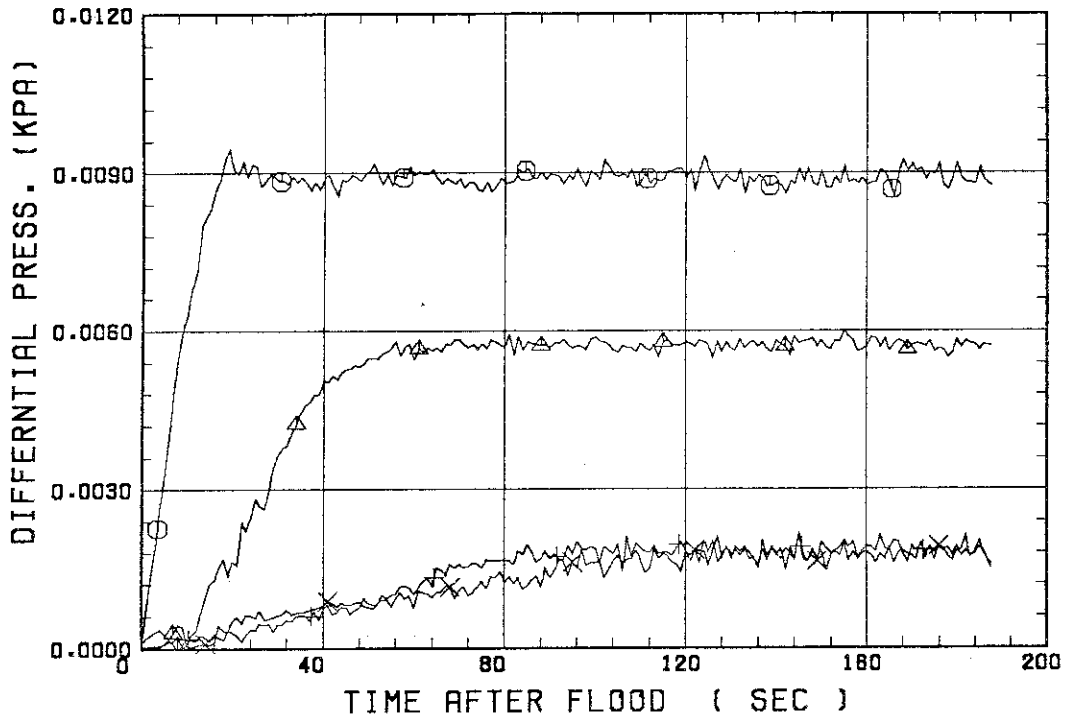


SMALL SCALE REFLOOD TEST
RUN 8205



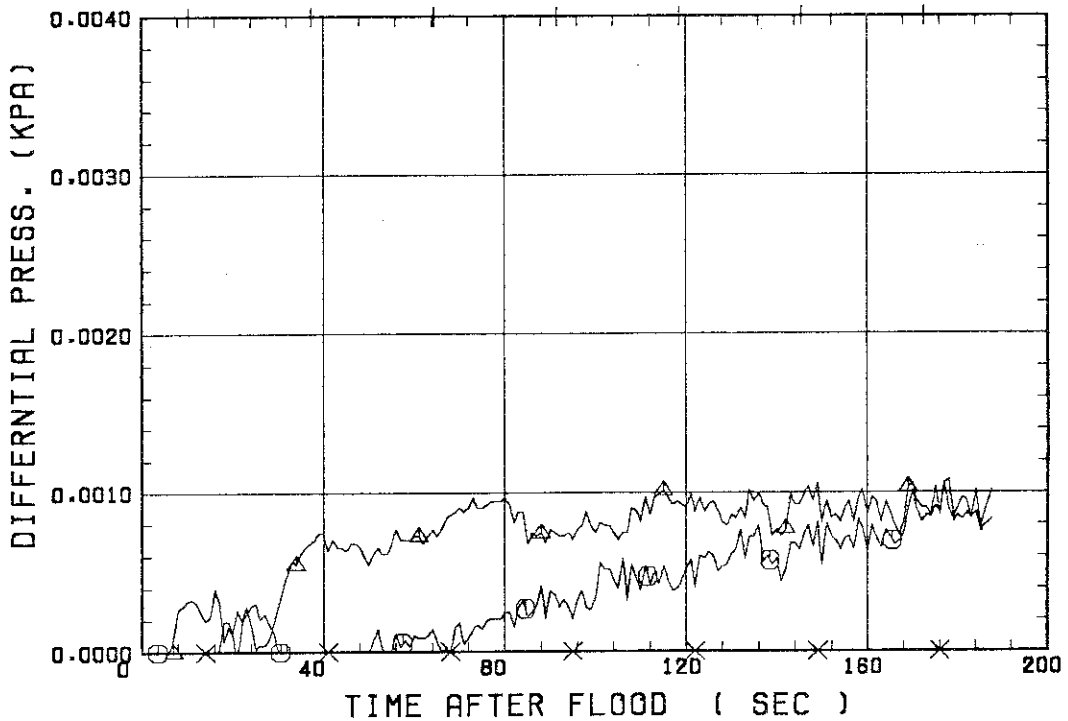
SMALL SCALE REFLOOD TEST
RUN 8205

○ --- DPT2 ▲ --- DPT4 + --- DPT5
X --- DPT6B



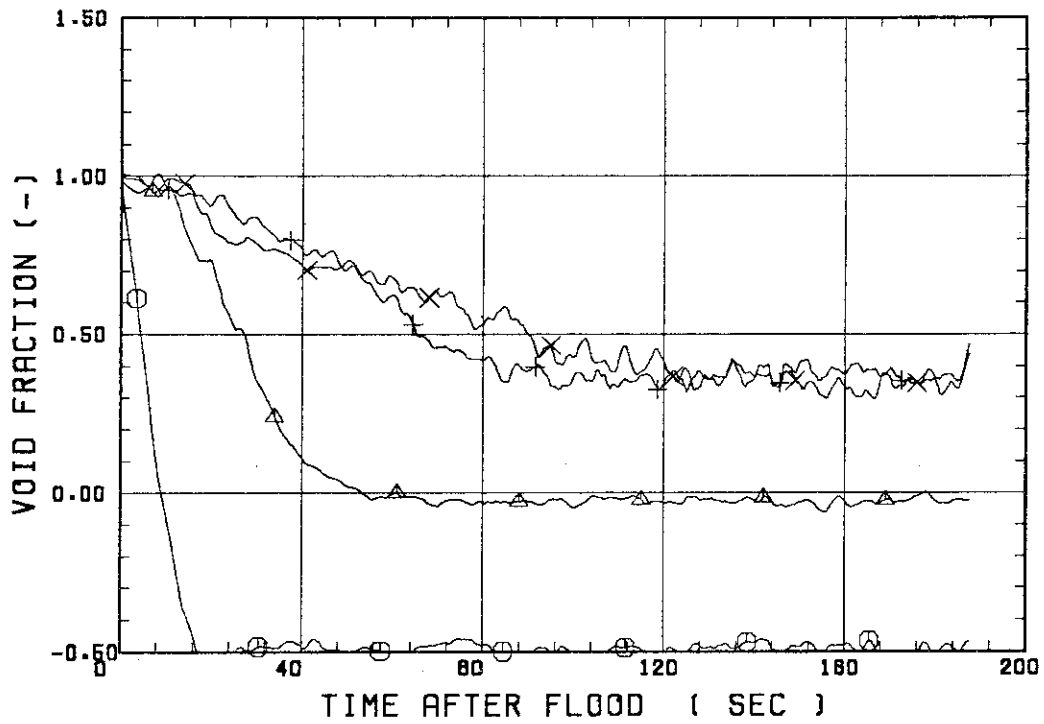
SMALL SCALE REFLOOD TEST
RUN 8205

○ --- DPT7 ▲ --- DPT8B + --- DP10
X --- DP12



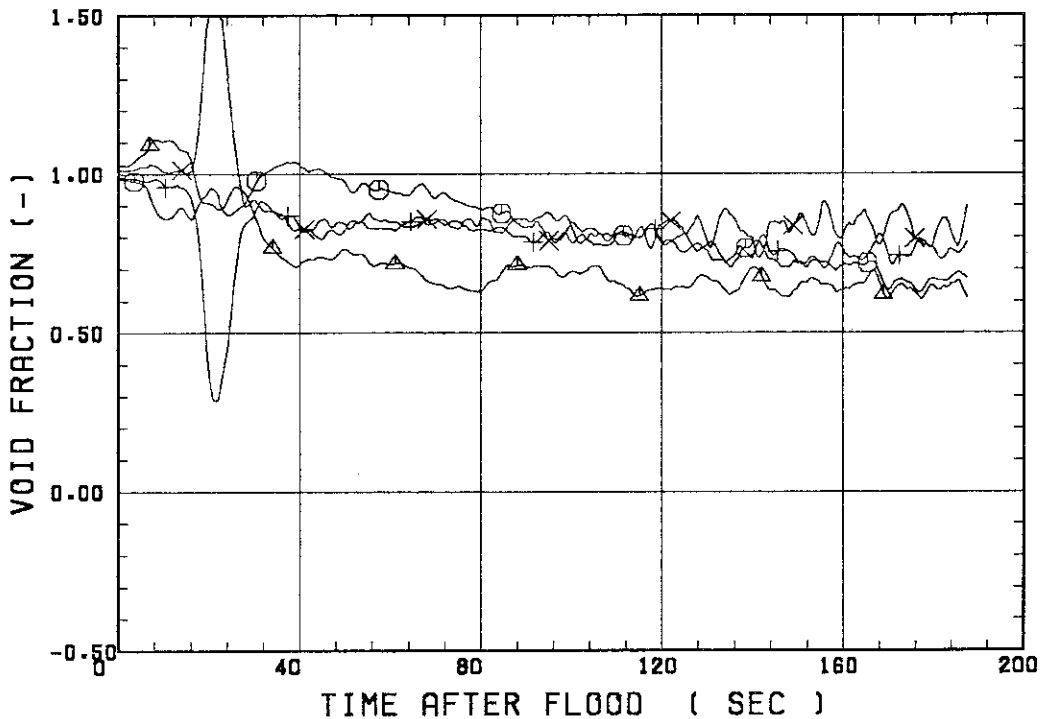
SMALL SCALE REFLOOD TEST
RUN 8205

○--- VDPT2 ▲--- VDPT4 +--- VDPT5
X--- VDPT6B



SMALL SCALE REFLOOD TEST
RUN 8205

○--- VDPT7 ▲--- VDPT8B +--- VDP10
X--- VDP12



 * RUN NO. 8207 *
 * *****

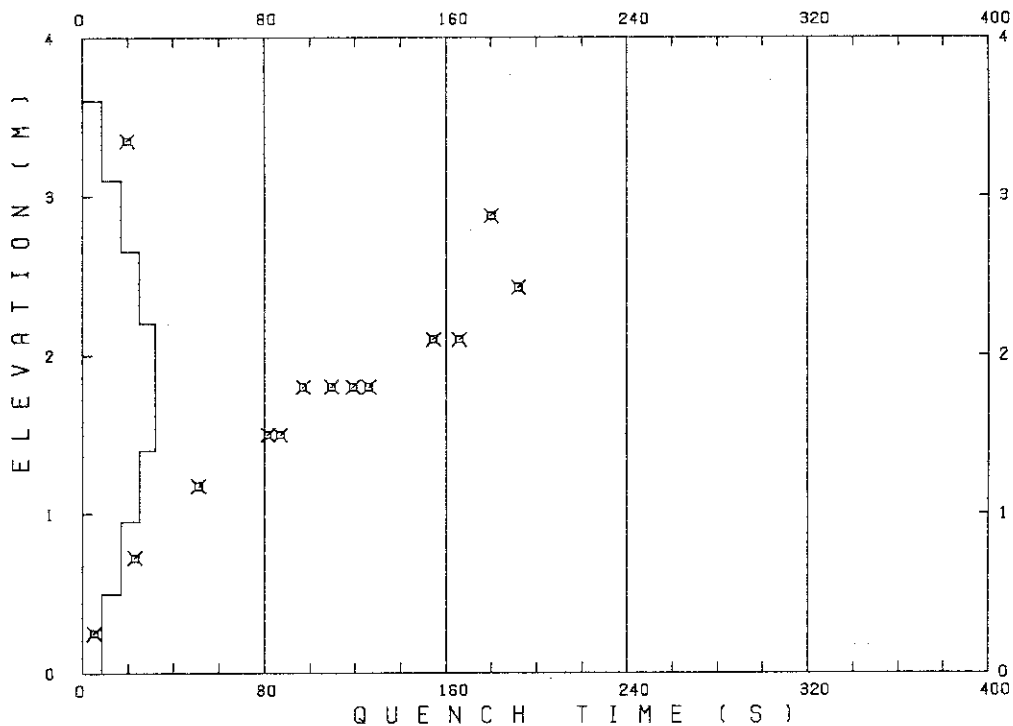
 TEST CONDITIONS

LINEAR PEAK POWER 1.8 KW/M
 SYSTEM PRESSURE 0.2 MPA
 INLET WATER TEMPERATURE 60 °C
 INJECTED WATER VELOCITY 3.9 CM/S

 TEMPERATURE PROFILE

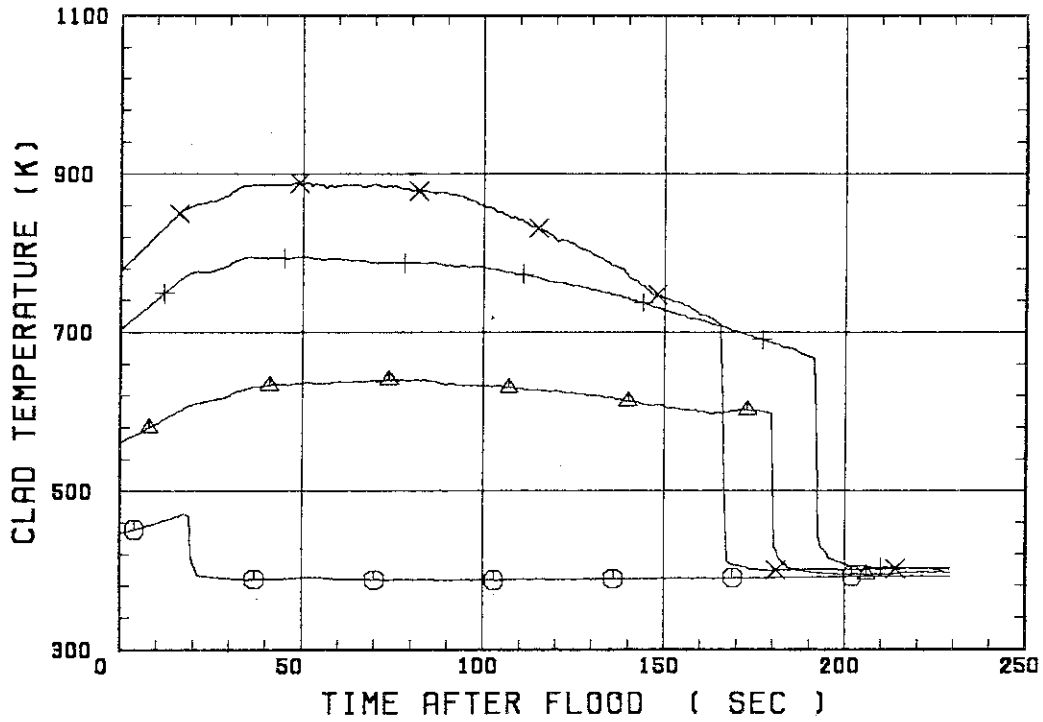
CH.NO.	SYMBOL	INITIAL TEMP. (°C)	TURNAROUND TIME (S)	TURNAROUND TEMP. (°C)	QUENCH TIME (S)	QUENCH TEMP. (°C)
1	TE1L	173	18.5	198	19.5	195
51	TR2	287	76.0	367	180.0	324
52	TR3	428	49.0	522	192.0	393
67	TC4U	502	52.0	617	166.0	435
7	TS4U	542	43.0	669	154.5	448
38	TA4M	523	34.0	630	119.0	443
68	TC4M	501	34.0	597	126.0	420
8	TS4M	534	37.0	643	109.5	461
48	TB4M	539	33.0	643	97.0	522
69	TC4L	506	20.0	582	87.0	436
9	TS4L	531	18.5	610	81.5	434
54	TR5	437	17.0	499	51.0	411
55	TR6	302	14.0	334	23.0	309
5	TE7	184	4.0	189	5.0	189

RUN NO. 8207



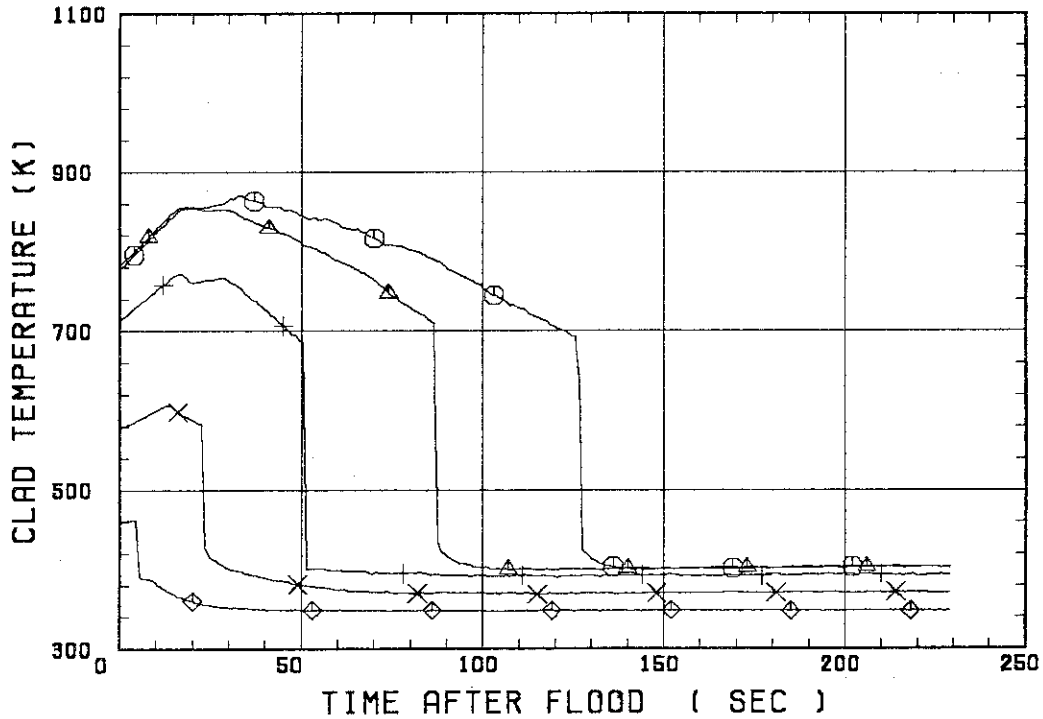
SMALL SCALE REFLOOD TEST
 RUN 8207

○--- TE1L △--- TR2 +--- TR3
 X--- TC4U

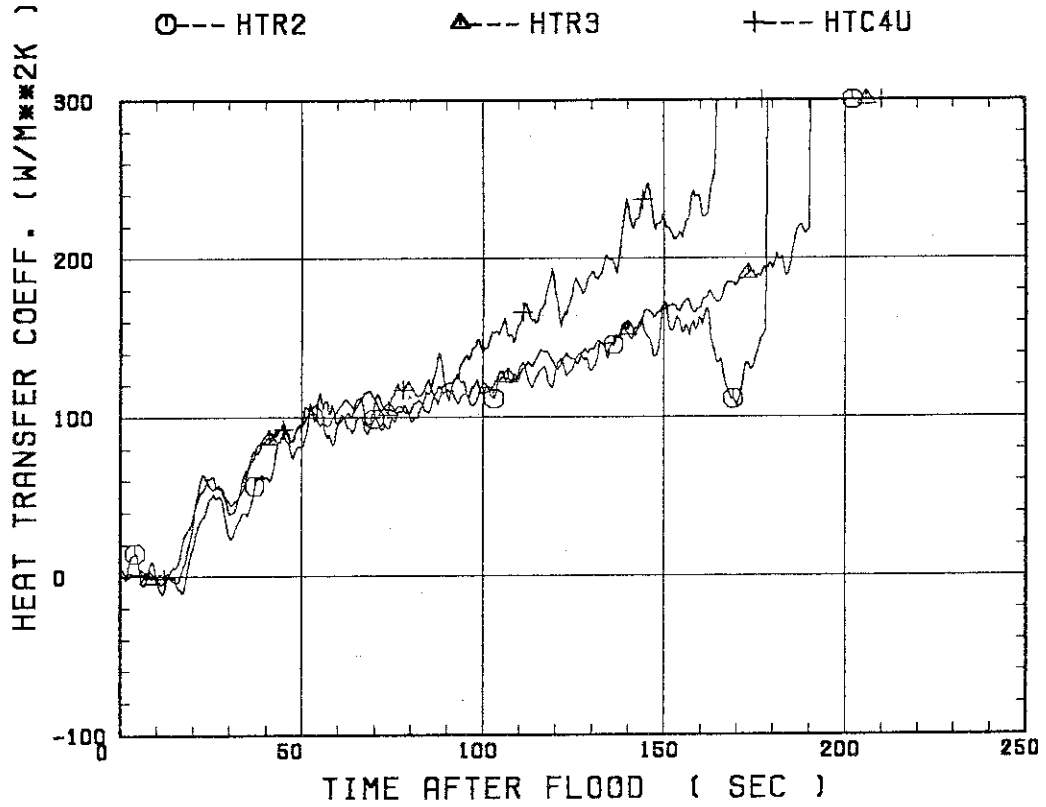


SMALL SCALE REFLOOD TEST
 RUN 8207

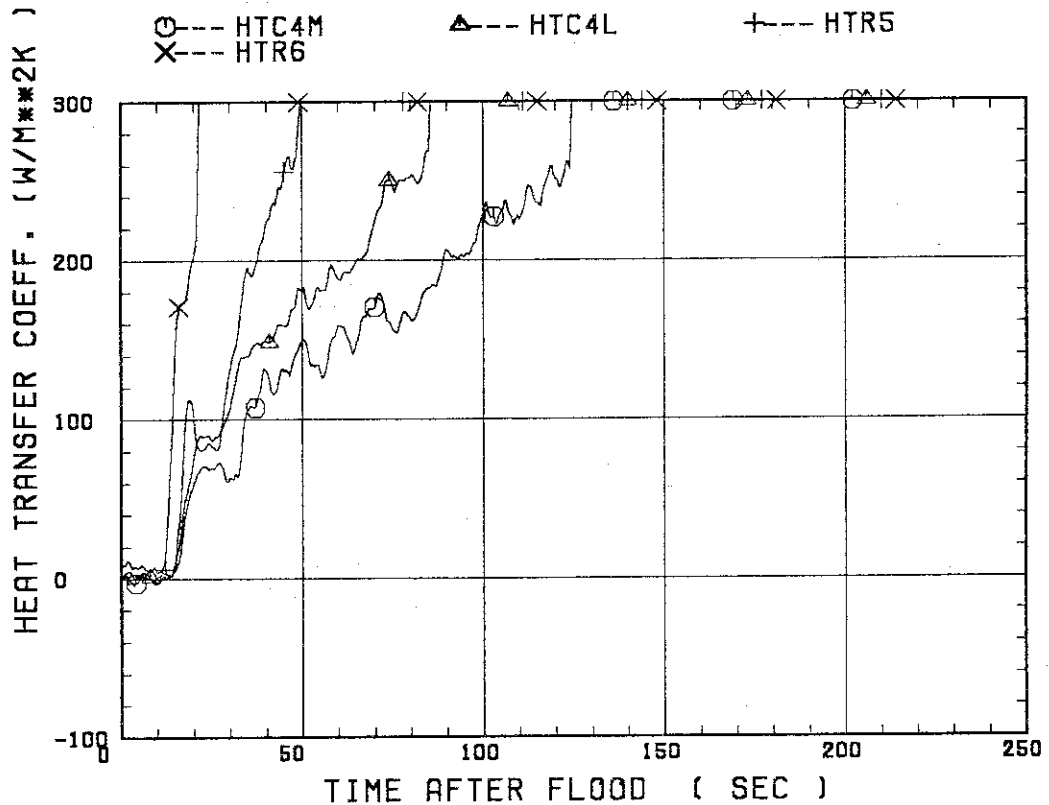
○--- TC4M △--- TC4L +--- TR5
 X--- TR6 ◇--- TE7



SMALL SCALE REFLOOD TEST
RUN 8207

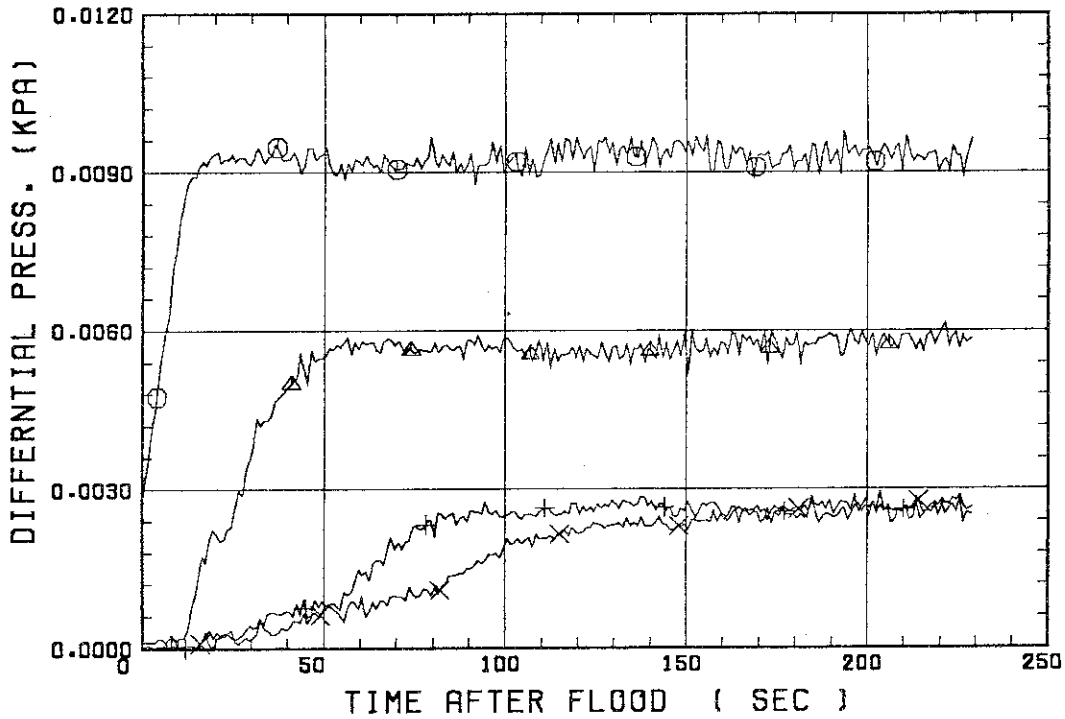


SMALL SCALE REFLOOD TEST
RUN 8207



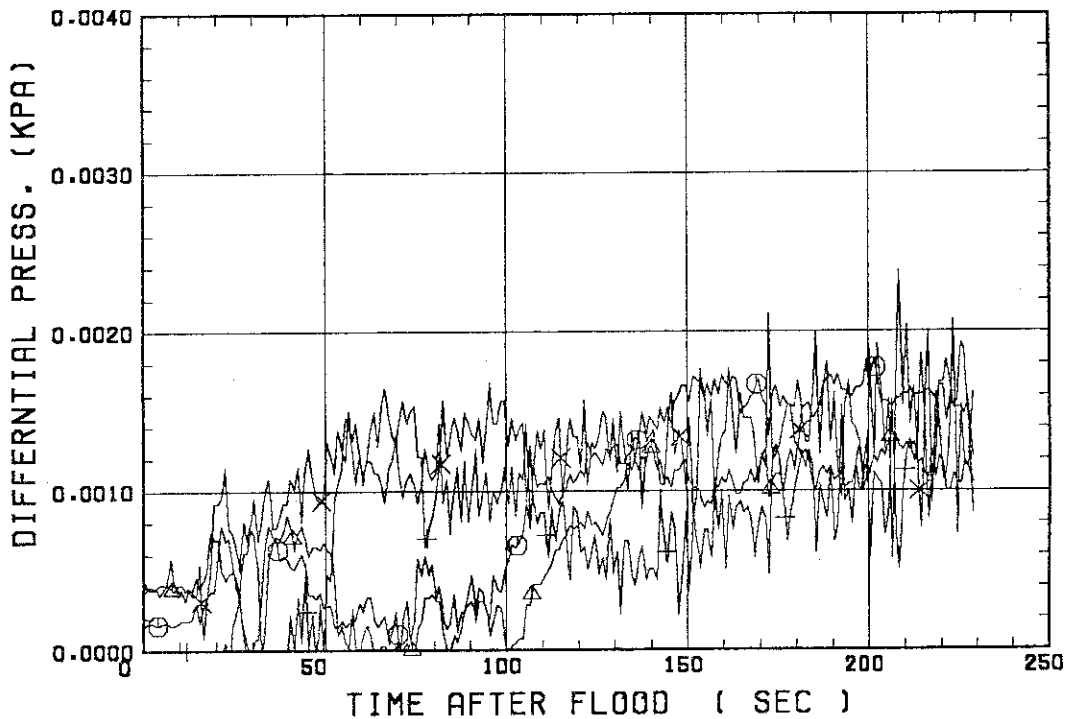
SMALL SCALE REFLOOD TEST
RUN 8207

○--- DPT2 △--- DPT4 +--- DPT5
X--- DPT6B



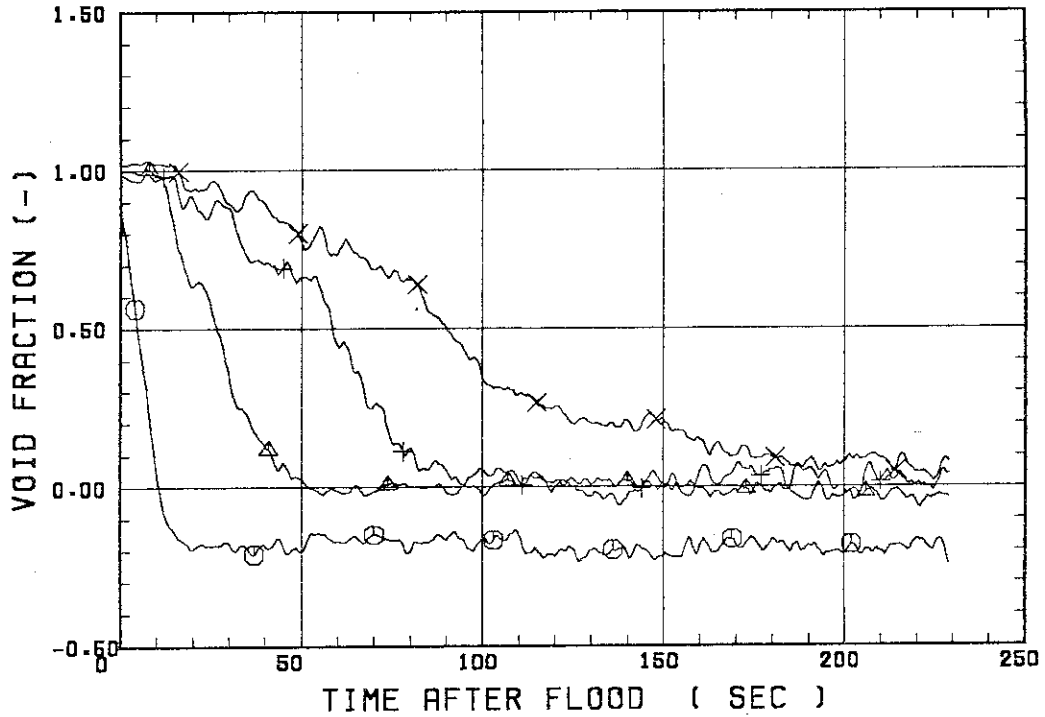
SMALL SCALE REFLOOD TEST
RUN 8207

○--- DPT7 △--- DPT8B +--- DP10
X--- DP12



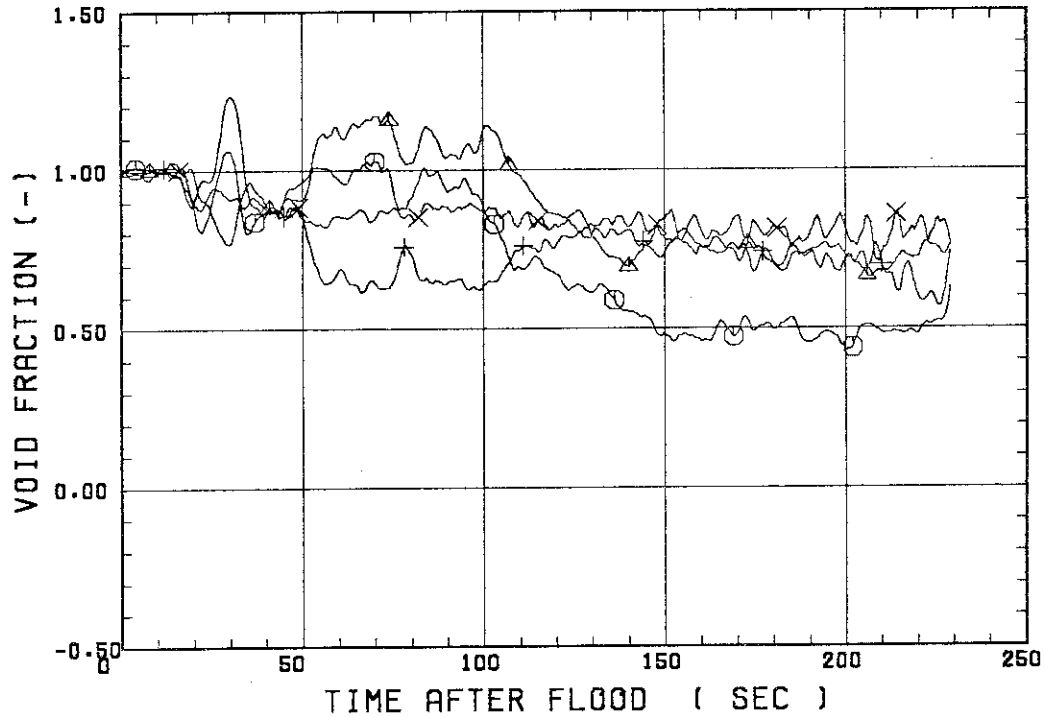
SMALL SCALE REFLOOD TEST
RUN 8207

○ --- VDPT2 △ --- VDPT4 + --- VDPT5
X --- VDPT6B



SMALL SCALE REFLOOD TEST
RUN 8207

○ --- VDPT7 △ --- VDPT8B + --- VDP10
X --- VDP12



 * RUN NO. 8210 *
 *

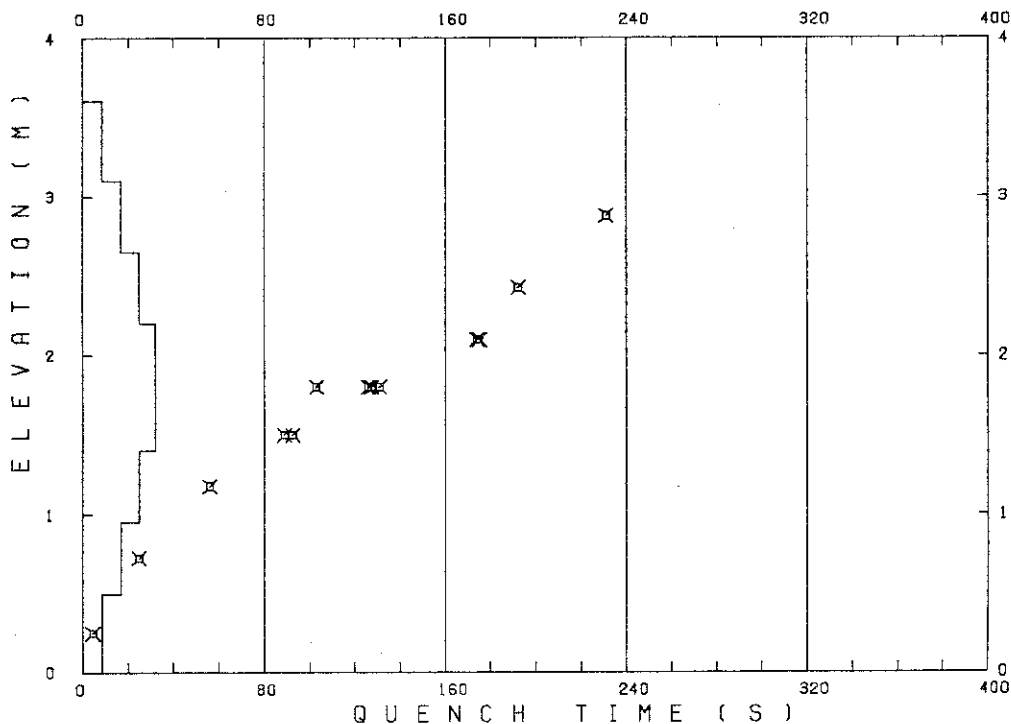
 TEST CONDITIONS

LINEAR PEAK POWER 1.6 KW/M
 SYSTEM PRESSURE 0.2 MPA
 INLET WATER TEMPERATURE 100 °C
 INJECTED WATER VELOCITY 3.9 CM/S

 TEMPERATURE PROFILE

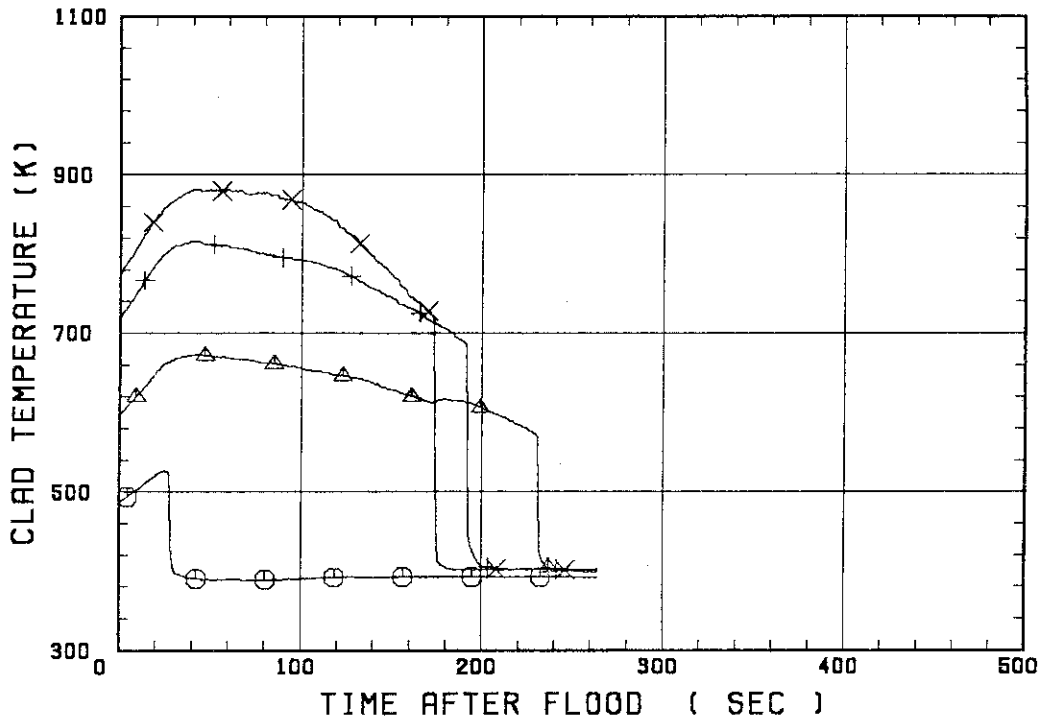
CH.NO.	SYMBOL	INITIAL TEMP. (°C)	TURNAROUND TIME (S)	TURNAROUND TEMP. (°C)	QUENCH TIME (S)	QUENCH TEMP. (°C)
66	TC1L	209	29.0	246		
51	TR2	323	44.0	400	231.0	296
52	TR3	444	43.0	543	192.0	410
67	TC4U	497	50.0	608	174.0	442
7	TS4U	546	49.5	676	175.0	433
38	TA4M	520	40.0	623	126.0	452
68	TC4M	490	39.0	585	131.0	433
8	TS4M	538	42.5	661	127.5	468
48	IB4M	543	40.0	646	103.0	532
69	TC4L	502	29.0	577	89.0	458
9	TS4L	533	28.5	607	92.5	452
54	TR5	453	22.0	506	56.0	417
55	TR6	333	14.0	354	25.0	290
5	TE7	219	2.0	221	4.5	214

RUN NO. 8210



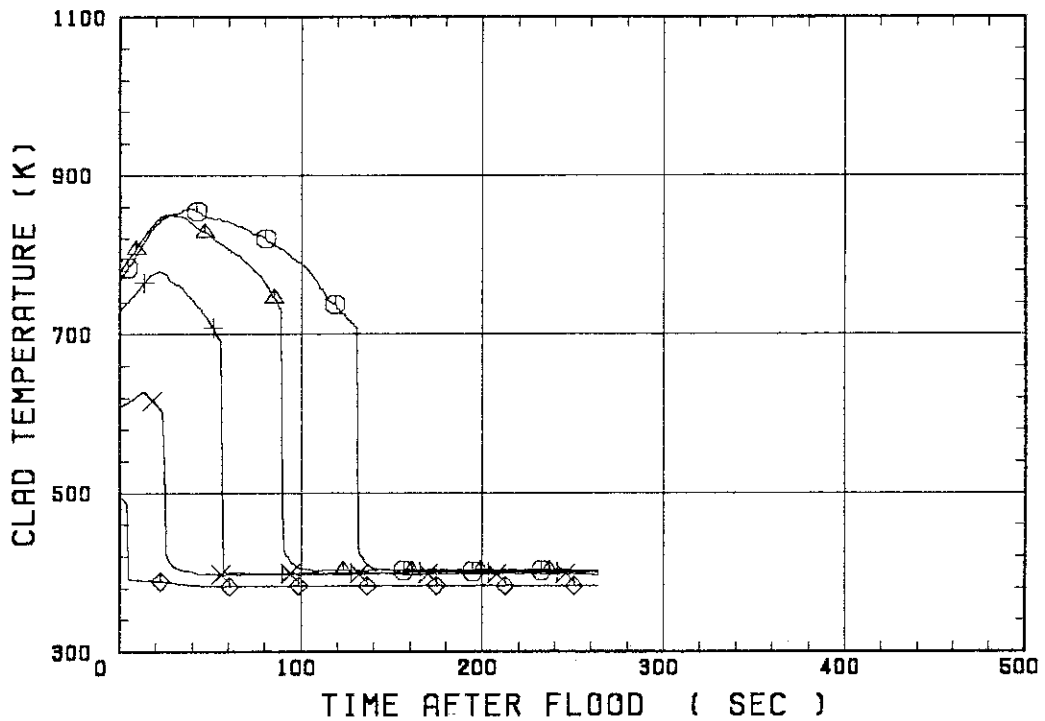
SMALL SCALE REFLOOD TEST
 RUN 8210

○--- TE1L ▲--- TR2 +--- TR3
 X--- TC4U

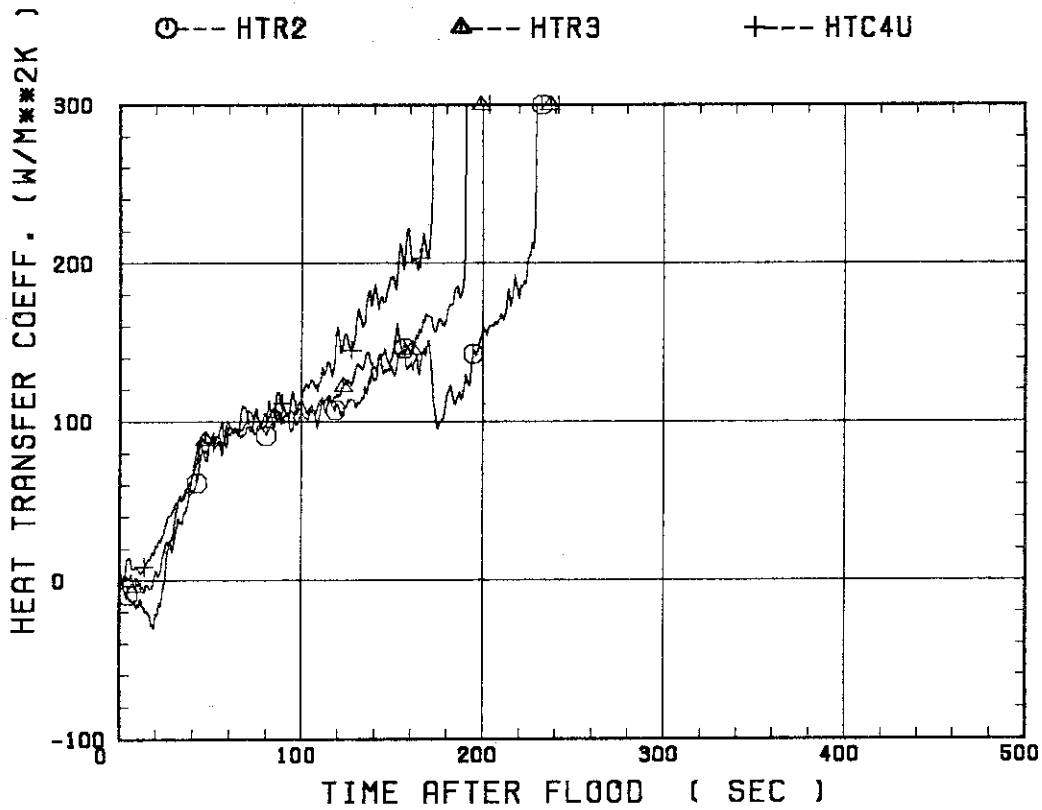


SMALL SCALE REFLOOD TEST
 RUN 8210

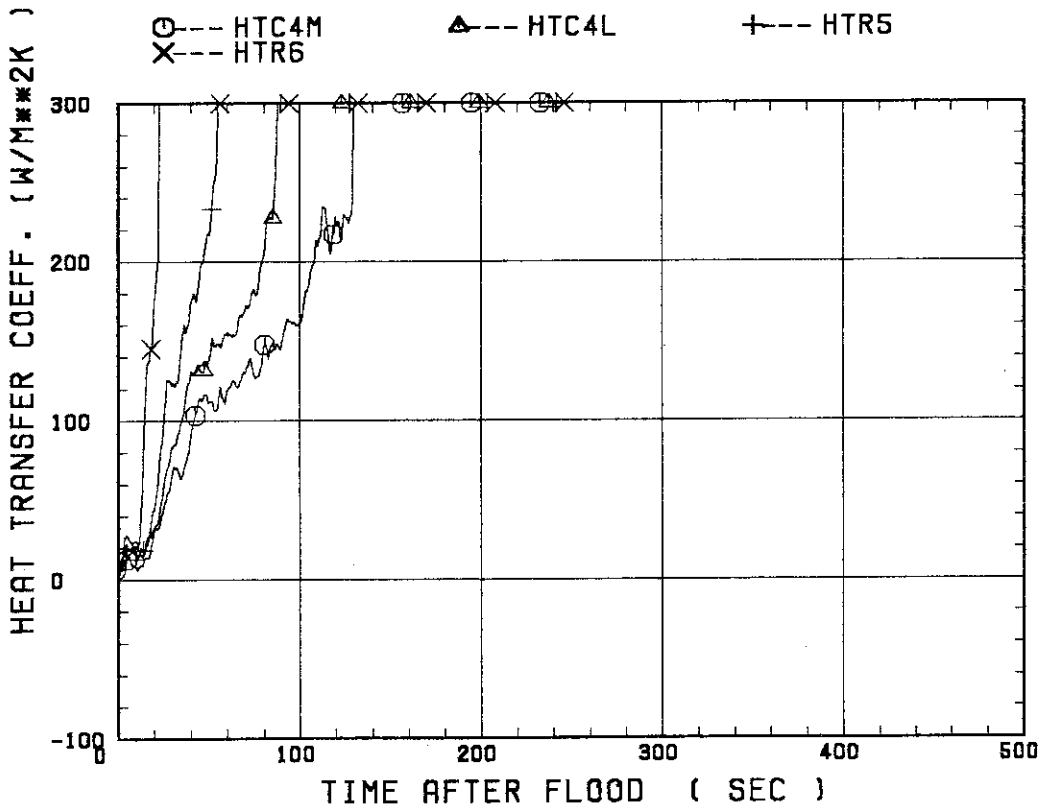
○--- TC4M ▲--- TC4L +--- TR5
 X--- TR6 ◆--- TE7



SMALL SCALE REFLOOD TEST
 RUN 8210

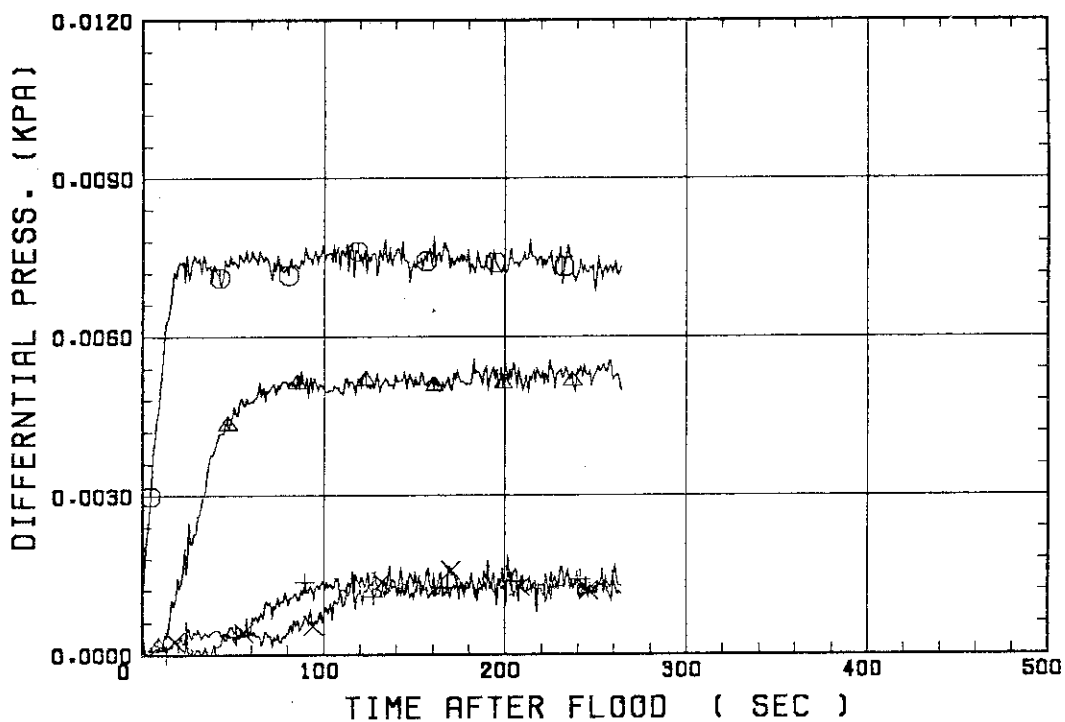


SMALL SCALE REFLOOD TEST
 RUN 8210



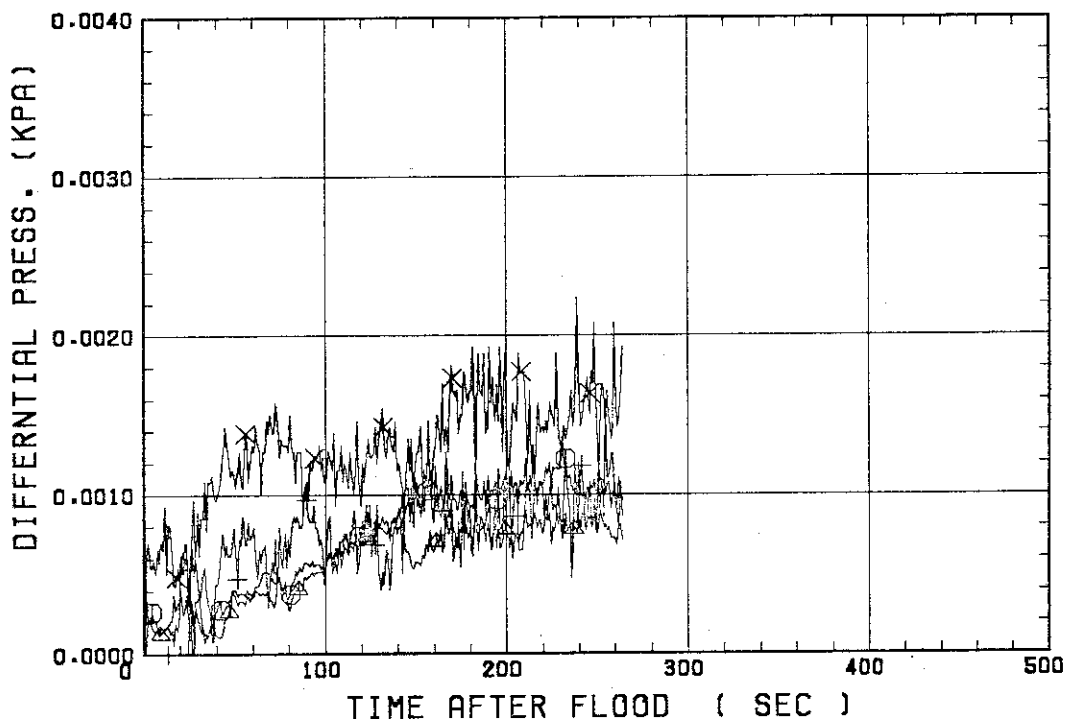
SMALL SCALE REFLOOD TEST
RUN 8210

○ --- DPT2 ▲ --- DPT4 + --- DPT5
X --- DPT6B



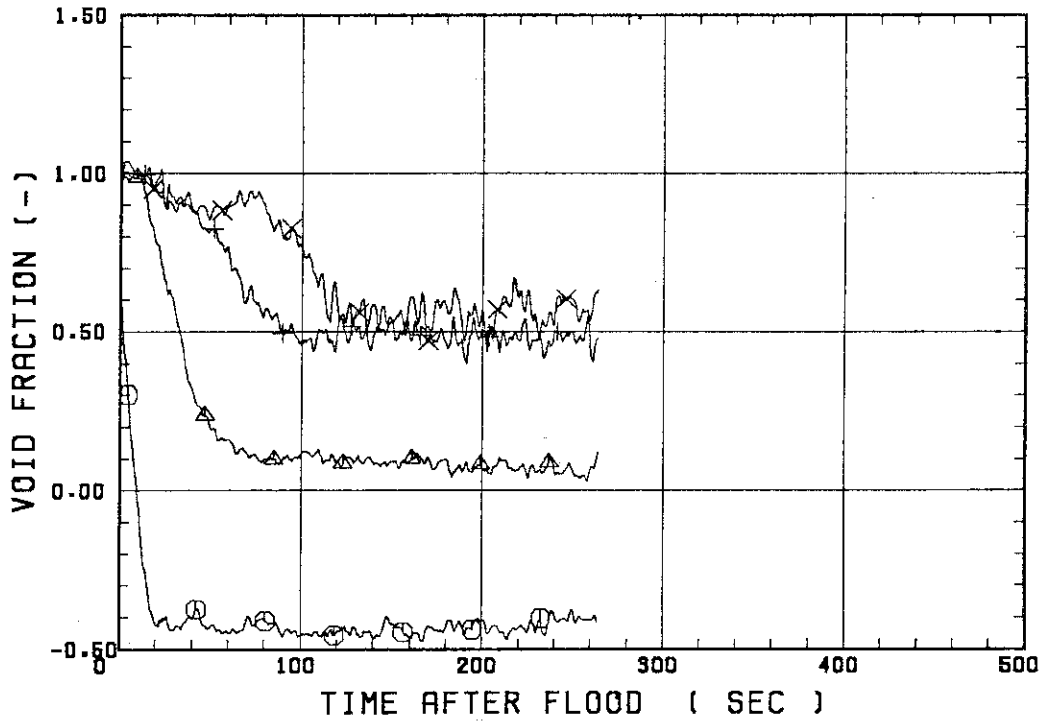
SMALL SCALE REFLOOD TEST
RUN 8210

○ --- DPT7 ▲ --- DPT8B + --- DP10
X --- DP12



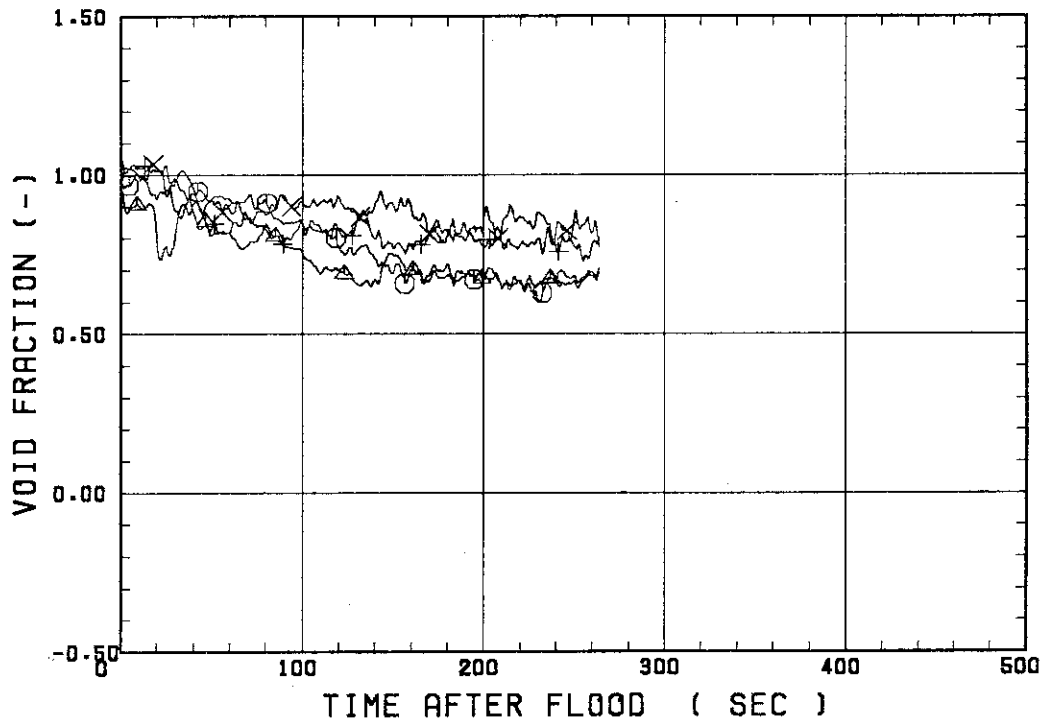
SMALL SCALE REFLOOD TEST
RUN 8210

○--- VDPT2 △--- VDPT4 +--- VDPT5
X--- VDPT6B



SMALL SCALE REFLOOD TEST
RUN 8210

○--- VDPT7 △--- VDPT8B +--- VDP10
X--- VDP12



 * RUN NO. 8308 *

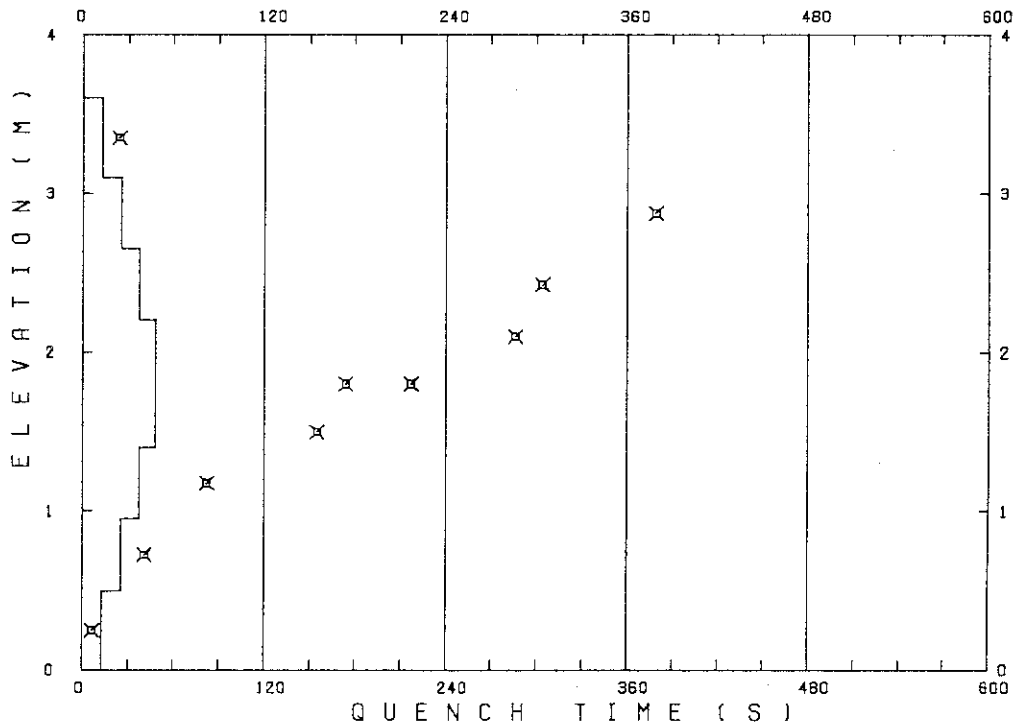
 TEST CONDITIONS

LINEAR PEAK POWER 1.6 KW/M
 SYSTEM PRESSURE 0.1 MPA
 INLET WATER TEMPERATURE 80 .C
 INJECTED WATER VELOCITY 4.0 CM/S

 TEMPERATURE PROFILE

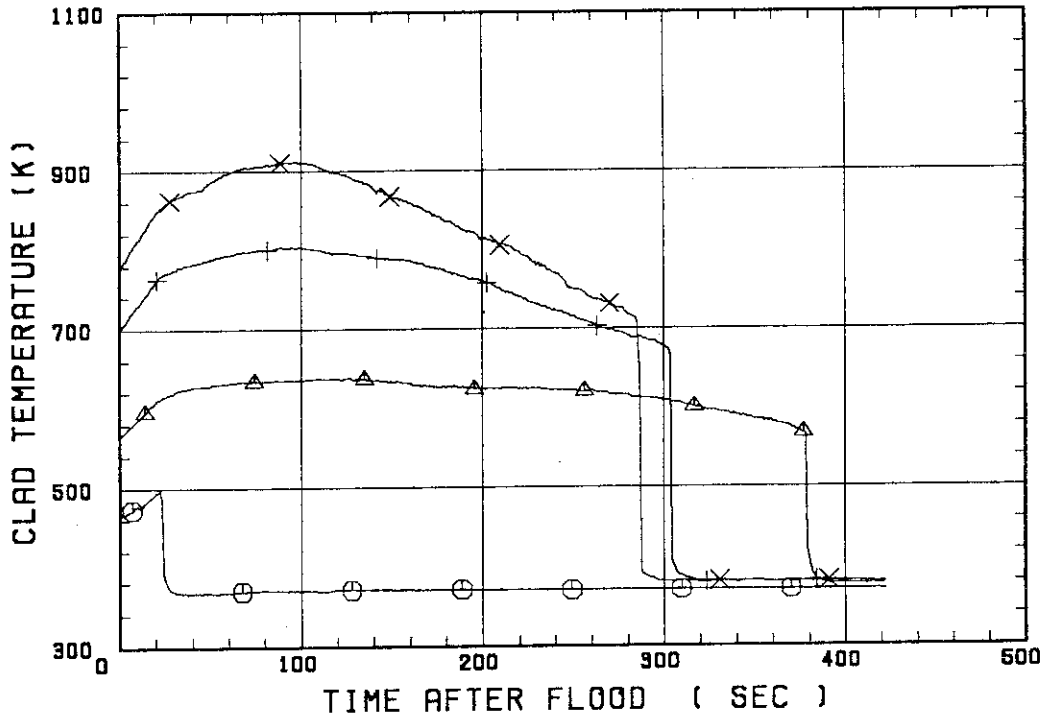
CH.NO.	SYMBOL	INITIAL TEMP. (.C)	TURNAROUND TIME (S)	TURNAROUND TEMP. (.C)	QUENCH TIME (S)	QUENCH TEMP. (.C)
1	TE1L	191	22.5	225	24.0	213
36	TA2	291	128.0	365	379.0	292
37	TA3	424	100.0	531	304.0	392
67	TC4U	499	97.0	639	286.0	432
68	TC4M	511	28.0	584	217.0	387
8	TS4M	549	25.5	635	174.0	389
69	TC4L	529	26.0	599	155.0	383
39	TA5	449	47.0	525	82.0	357
40	TA6	314	18.0	342	41.0	294
5	TE7	205	4.5	210	6.5	189

RUN NO. 8308



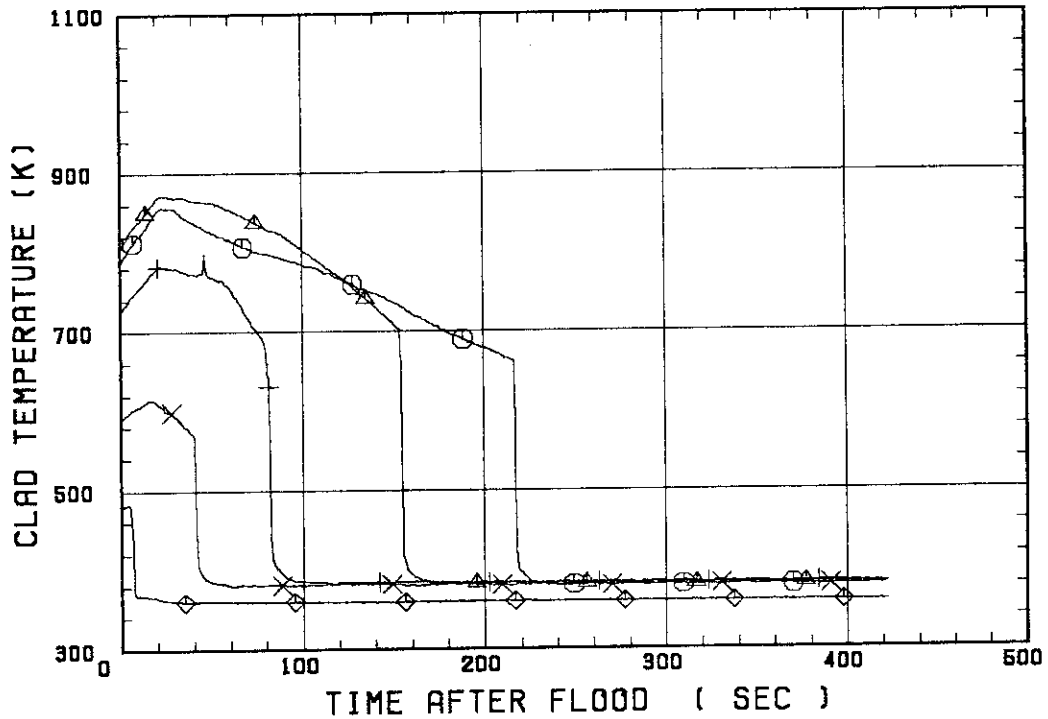
SMALL SCALE REFLOOD TEST
 RUN 8308

○ --- TE1L △ --- TA2 + --- TA3
 X --- TC4U

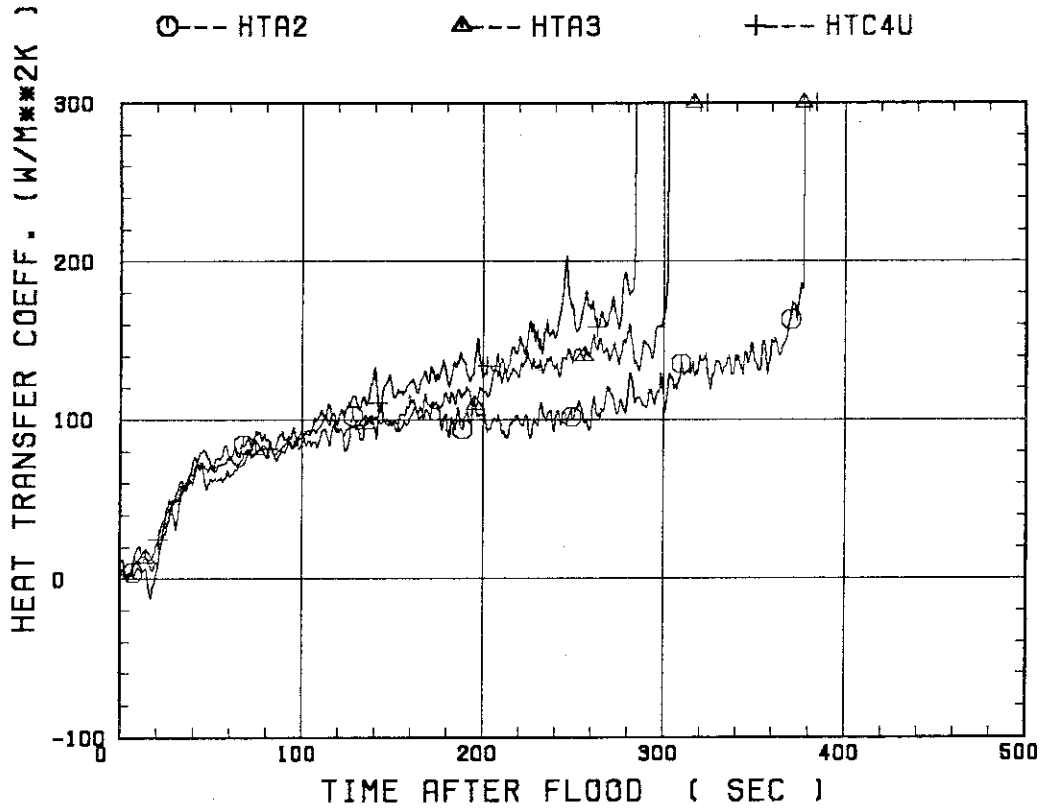


SMALL SCALE REFLOOD TEST
 RUN 8308

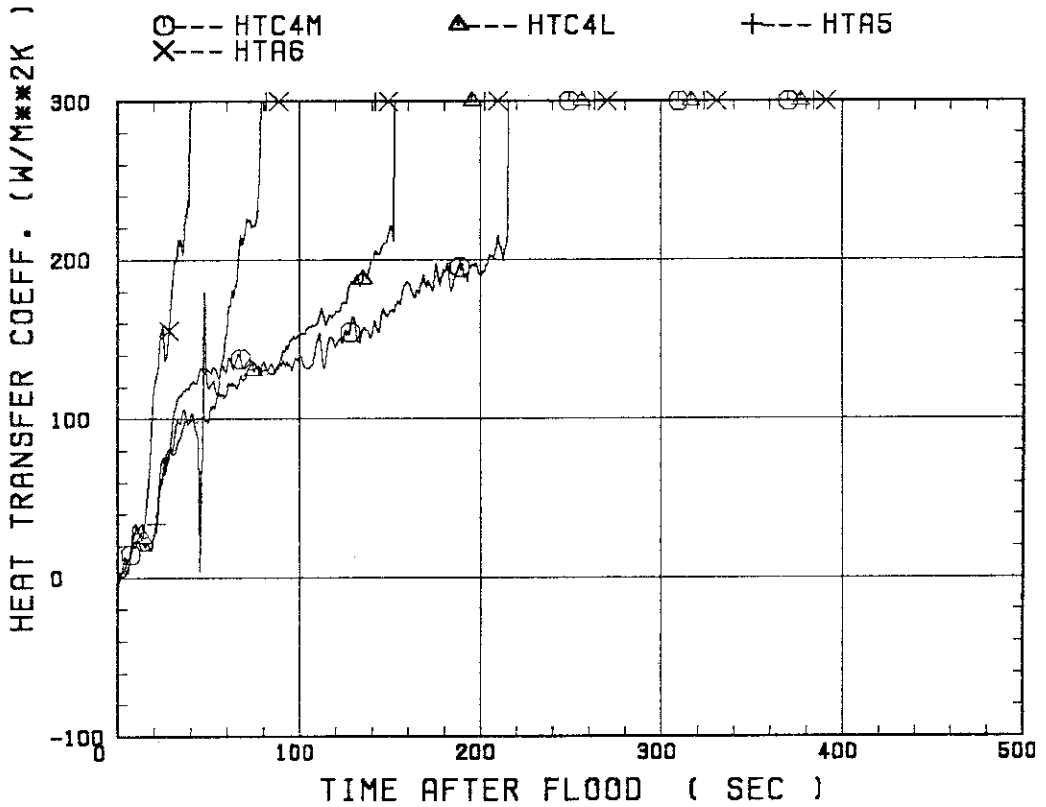
○ --- TC4M △ --- TC4L + --- TA5
 X --- TA6 ◇ --- TE7



SMALL SCALE REFLOOD TEST
 RUN 8308



SMALL SCALE REFLOOD TEST
 RUN 8308

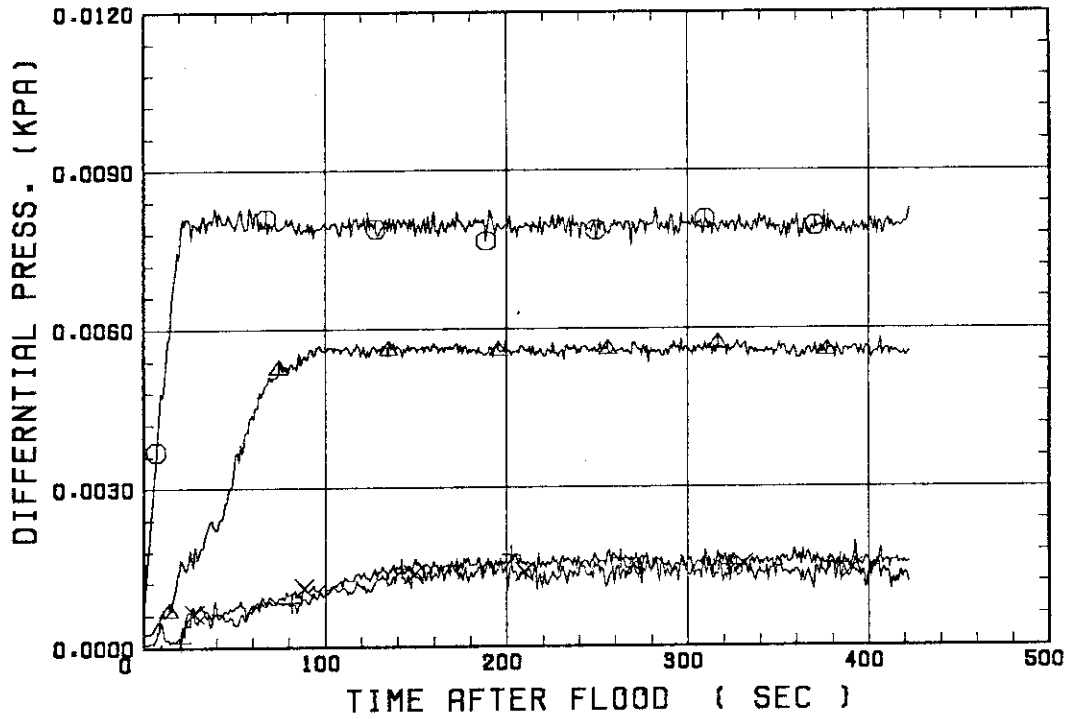


SMALL SCALE REFLOOD TEST
RUN 8308

○--- DPT2
X--- DPT6B

△--- DPT4

+--- DPT5

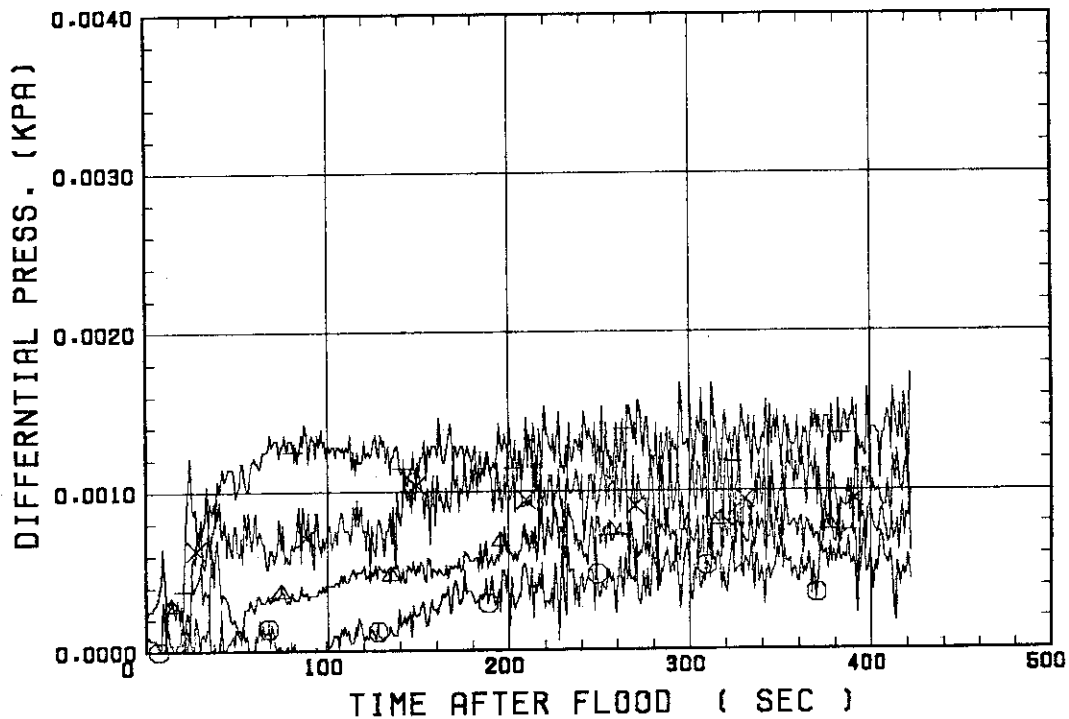


SMALL SCALE REFLOOD TEST
RUN 8308

○--- DPT7
X--- DP12

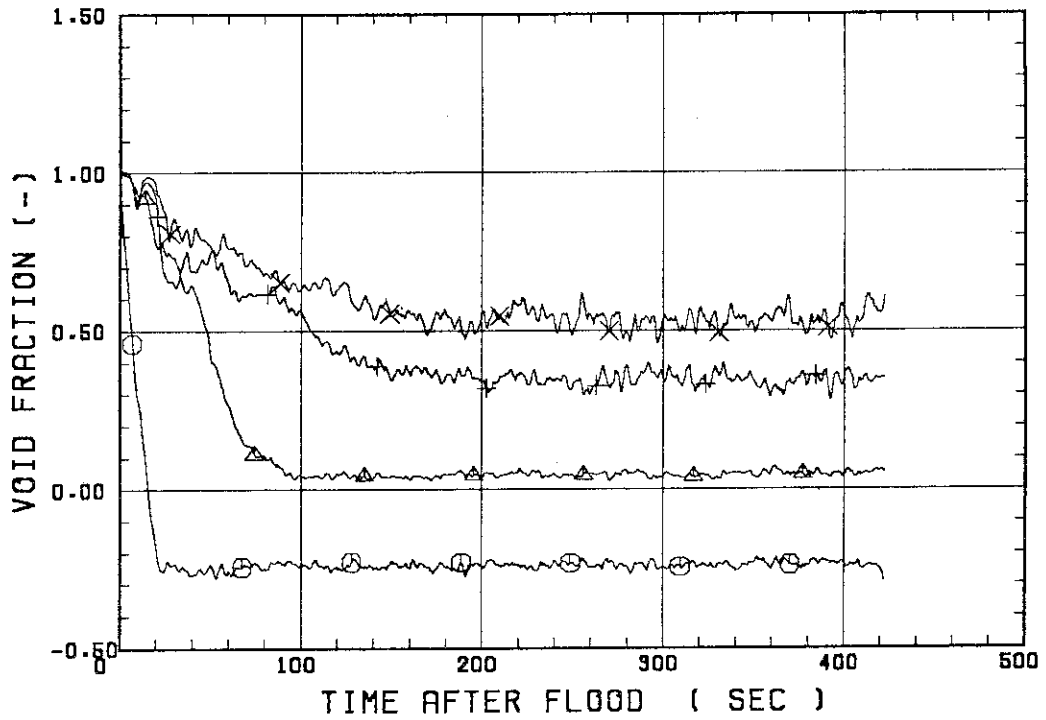
△--- DPT8B

+--- DP10



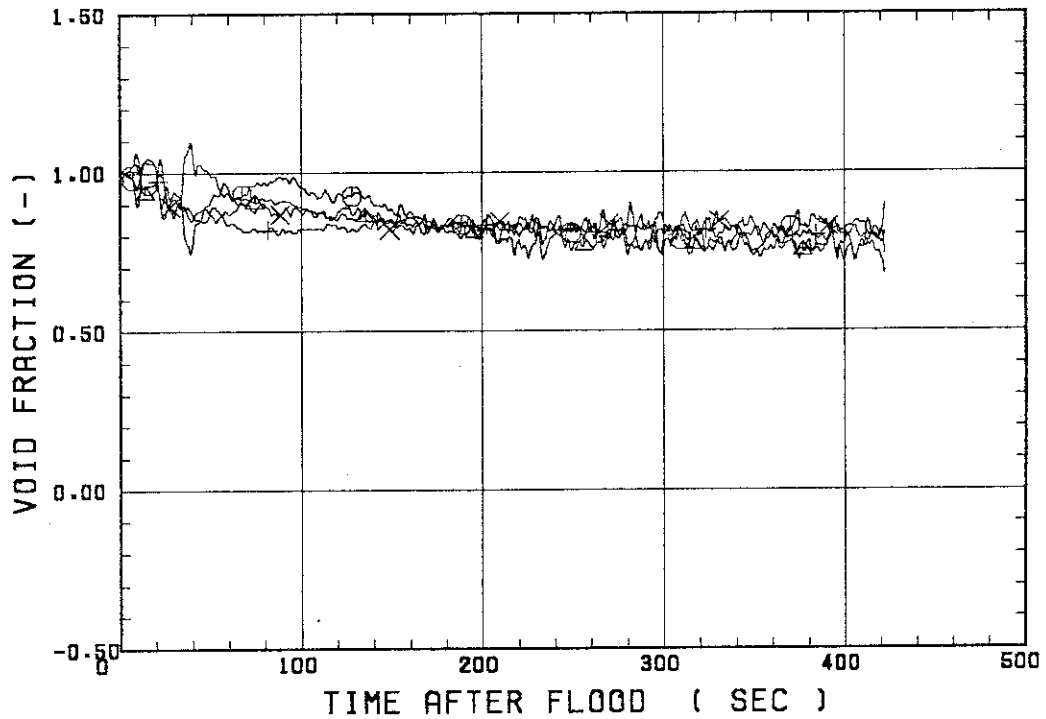
SMALL SCALE REFLOOD TEST
RUN 8308

○--- VDPT2 △--- VDPT4 +--- VDPT5
X--- VDPT6B



SMALL SCALE REFLOOD TEST
RUN 8308

○--- VDPT7 △--- VDPT8B +--- VDP10
X--- VDP12



 * RUN NO. 8309 *

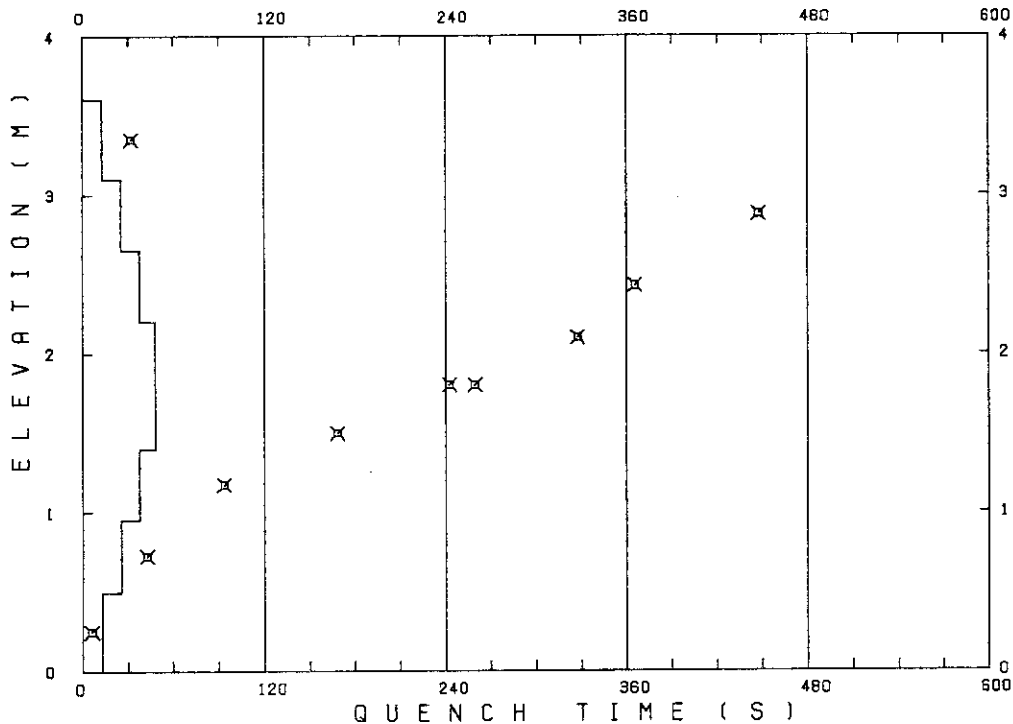
 TEST CONDITIONS

LINEAR PEAK POWER 1.8 KW/M
 SYSTEM PRESSURE 0.1 MPA
 INLET WATER TEMPERATURE 80 -C
 INJECTED WATER VELOCITY 4.0 CM/S

 TEMPERATURE PROFILE

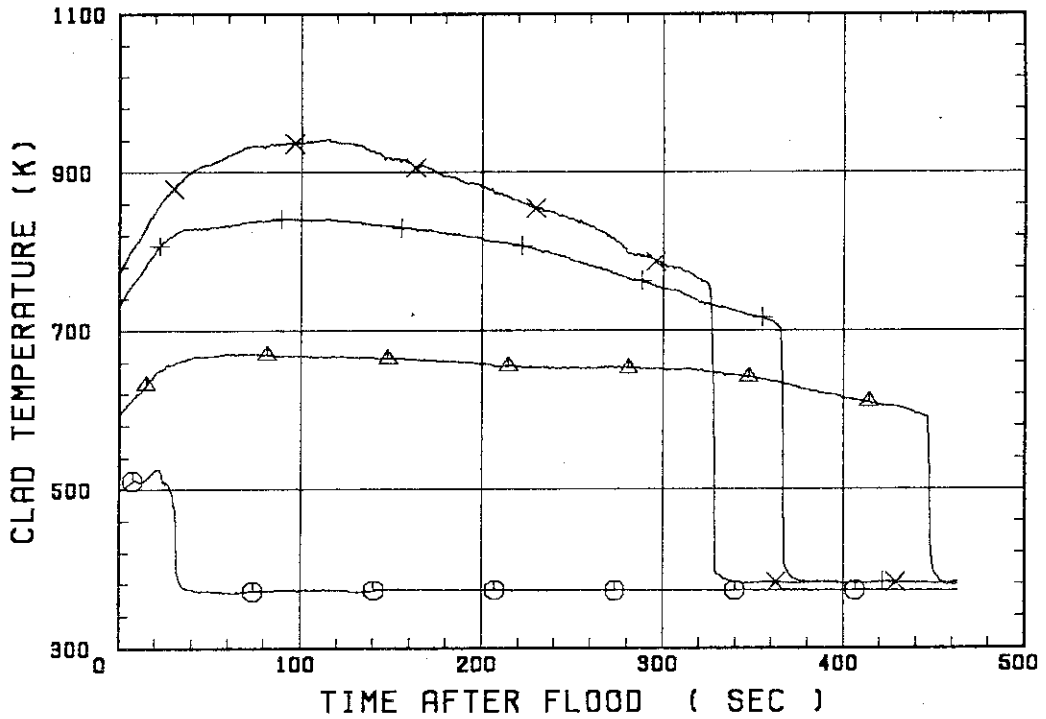
CH.NO.	SYMBOL	INITIAL TEMP. (.C)	TURNAROUND TIME (S)	TURNAROUND TEMP. (.C)	QUENCH TIME (S)	QUENCH TEMP. (.C)
1	TE1L	225	22.0	252	32.0	176
36	TA2	321	73.5	398	447.5	316
37	TA3	456	93.5	568	365.5	429
67	TC4U	494	115.5	668	327.5	446
68	TC4M	506	30.5	597	242.5	409
8	TS4M	560	41.5	668	259.5	380
69	TC4L	514	43.5	609	168.5	462
39	TA5	452	32.5	527	93.5	358
40	TA6	320	17.5	348	42.5	312
5	TE7	217	4.0	220	6.0	214

RUN NO. 8309



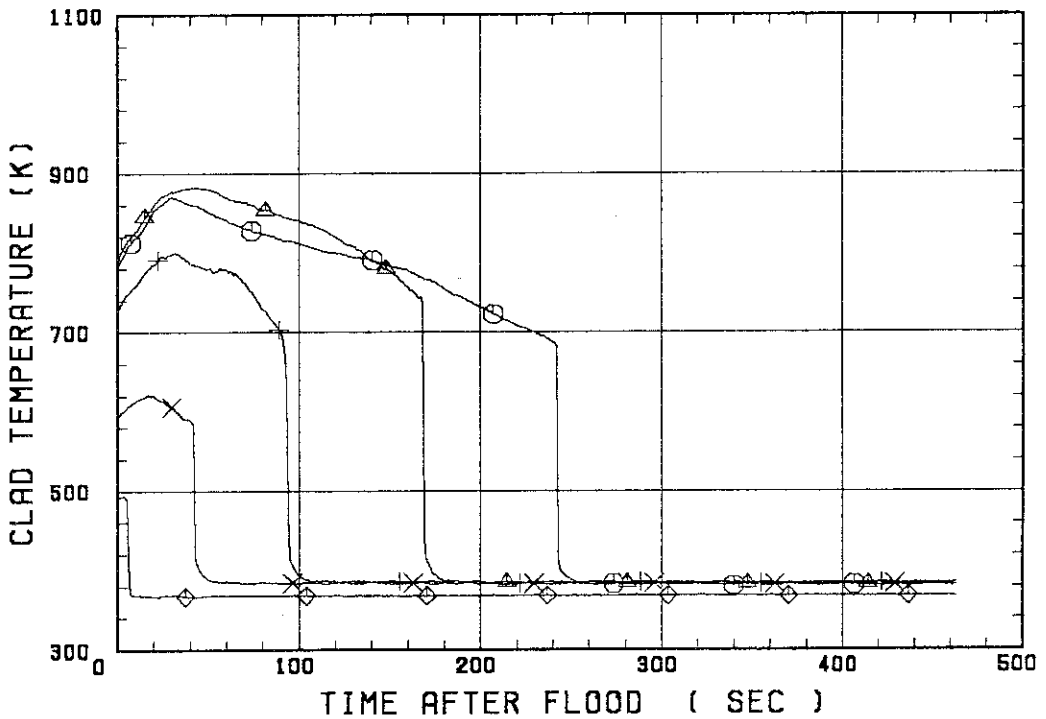
SMALL SCALE REFLOOD TEST
 RUN 8309

○--- TE1L ▲--- TA2 +--- TA3
 X--- TC4U

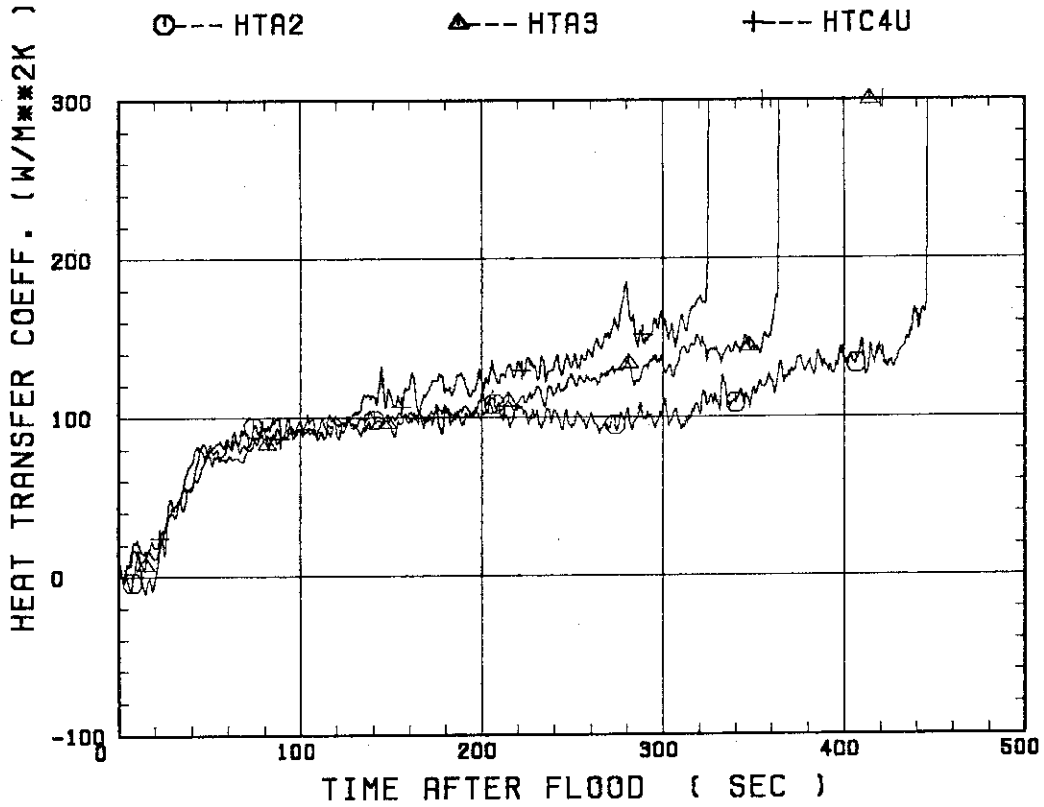


SMALL SCALE REFLOOD TEST
 RUN 8309

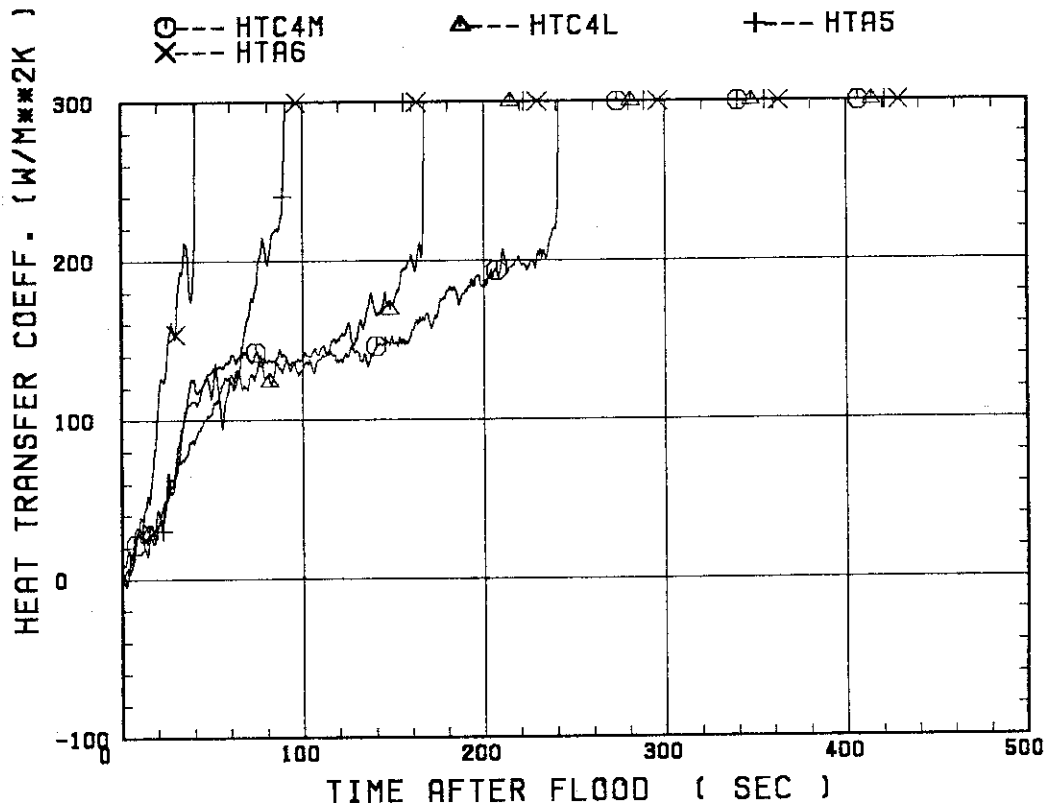
○--- TC4M ▲--- TC4L +--- TA5
 X--- TA6 ◆--- TE7



SMALL SCALE REFLOOD TEST
 RUN 8309

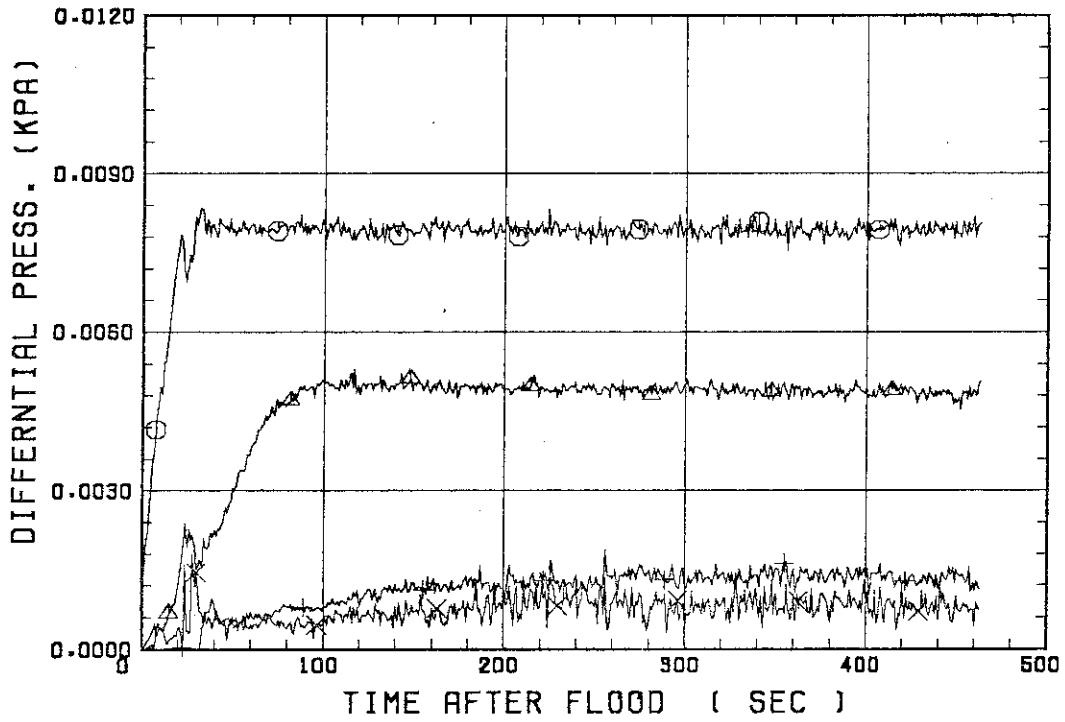


SMALL SCALE REFLOOD TEST
 RUN 8309



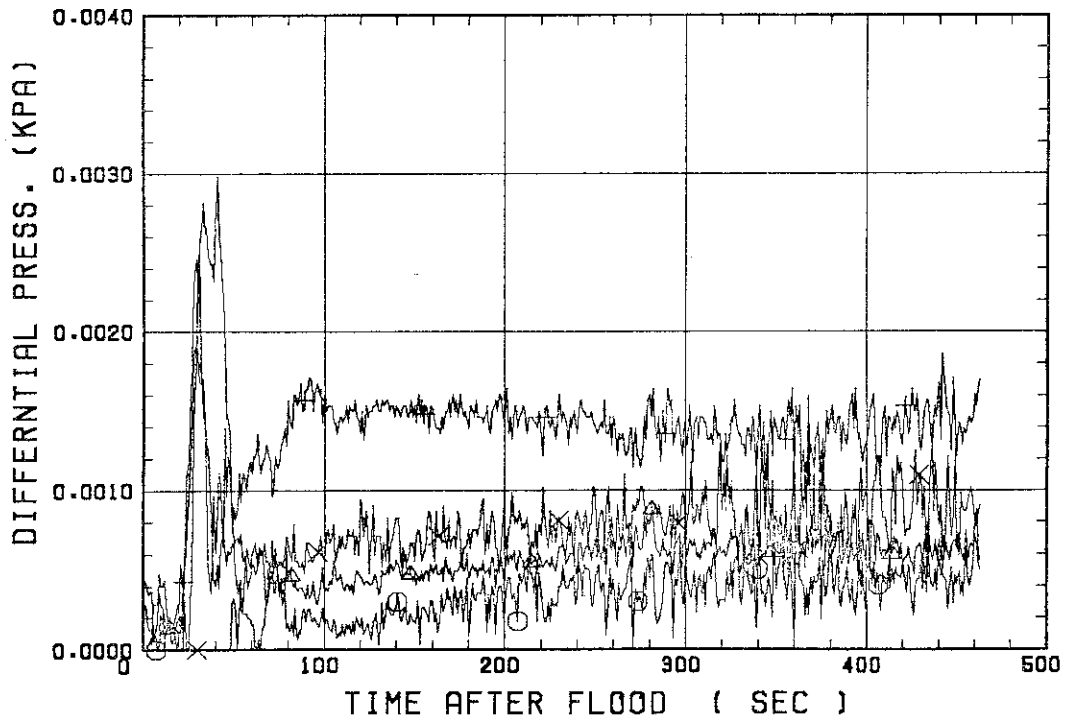
SMALL SCALE REFLOOD TEST
RUN 8309

○ --- DPT2 △ --- DPT4 + --- DPT5
X --- DPT6B



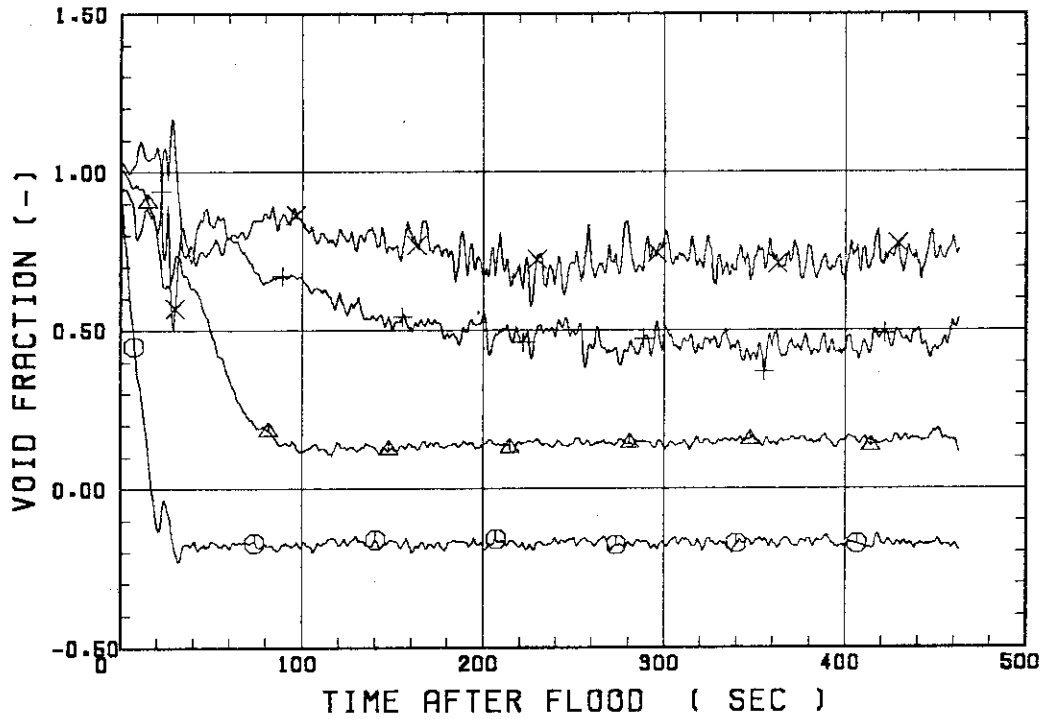
SMALL SCALE REFLOOD TEST
RUN 8309

○ --- DPT7 △ --- DPT8B + --- DP10
X --- DP12



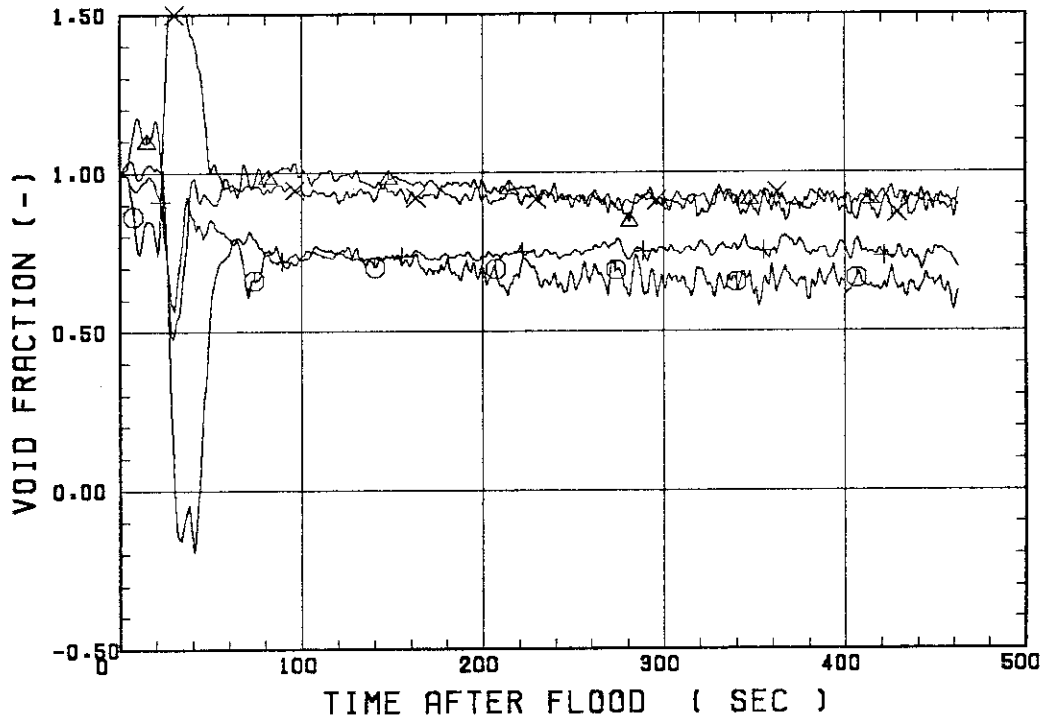
SMALL SCALE REFLOOD TEST
RUN 8309

○--- VDPT2 ▲--- VDPT4 +--- VDPT5
X--- VDPT6B



SMALL SCALE REFLOOD TEST
RUN 8309

○--- VDPT7 ▲--- VDPT8B +--- VDP10
X--- VDP12



 * RUN NO. 8311 *

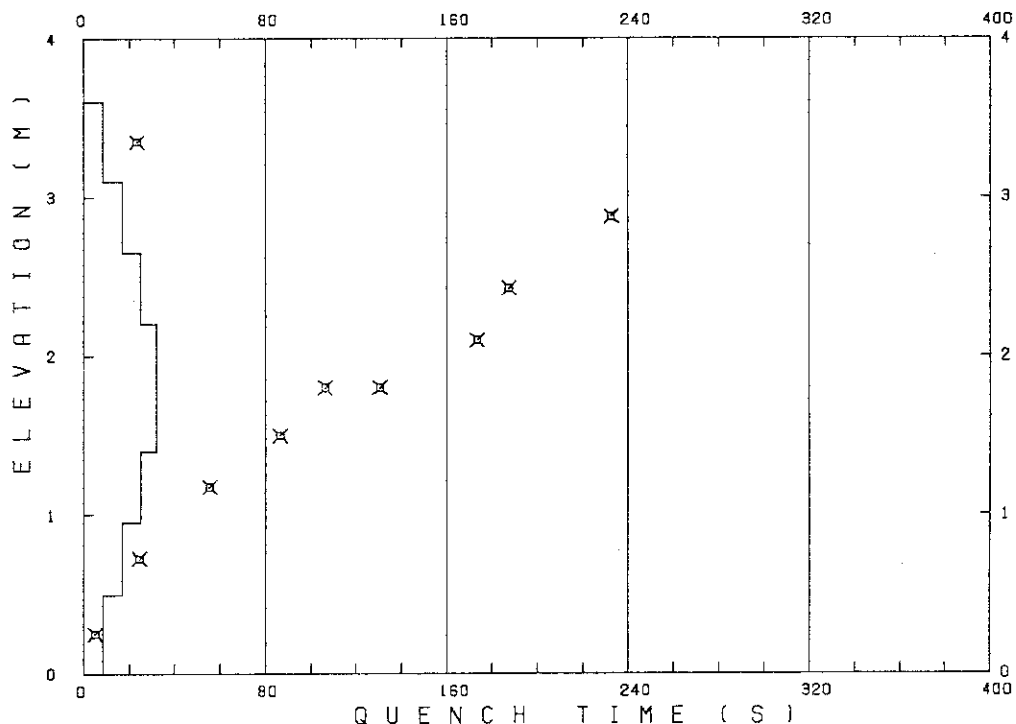
 TEST CONDITIONS

LINEAR PEAK POWER 1.8 KW/M
 SYSTEM PRESSURE 0.2 MPA
 INLET WATER TEMPERATURE 80 .C
 INJECTED WATER VELOCITY 4.0 CM/S

 TEMPERATURE PROFILE

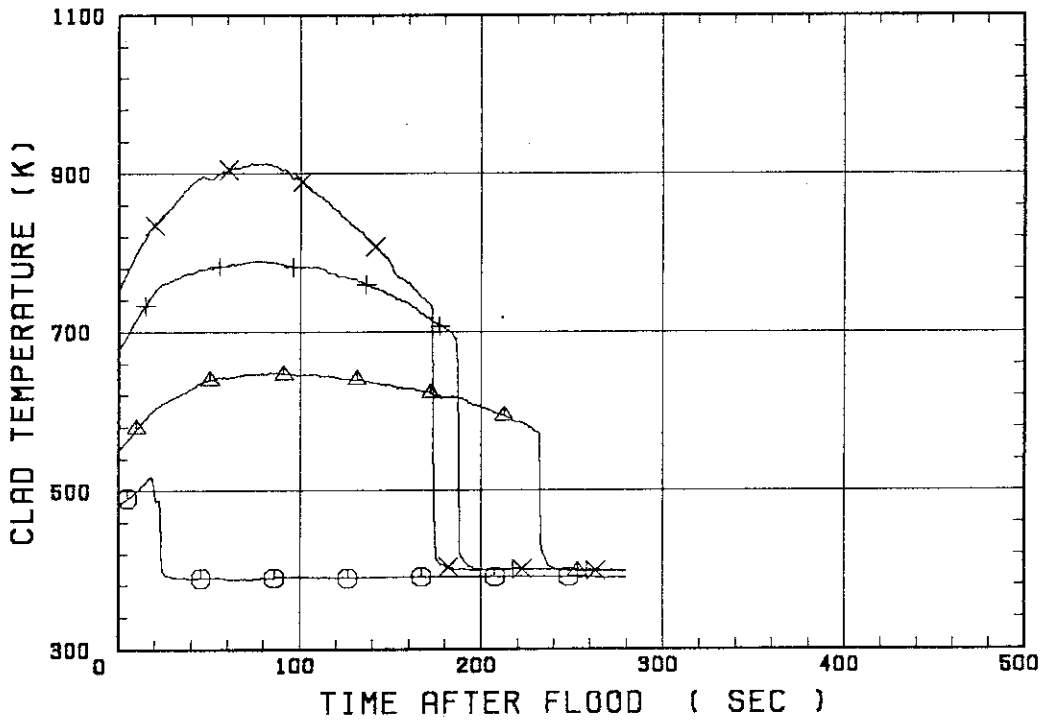
CH.NO.	SYMBOL	INITIAL TEMP. (.C)	TURNAROUND TIME (S)	TURNAROUND TEMP. (.C)	QUENCH TIME (S)	QUENCH TEMP. (.C)
1	TE1L	209	18.5	245	23.5	201
36	TA2	277	84.5	376	232.5	297
37	TA3	402	77.5	517	187.5	384
67	TC4U	476	73.5	640	173.5	455
68	TC4M	481	26.5	565	130.5	400
8	TS4M	593	32.5	632	106.5	425
69	TC4L	490	39.5	575	86.5	464
54	TR5	460	18.5	515	55.5	423
55	TR6	393	13.5	359	24.5	323
5	TE7	204	3.5	208	5.0	191

RUN NO. 8311



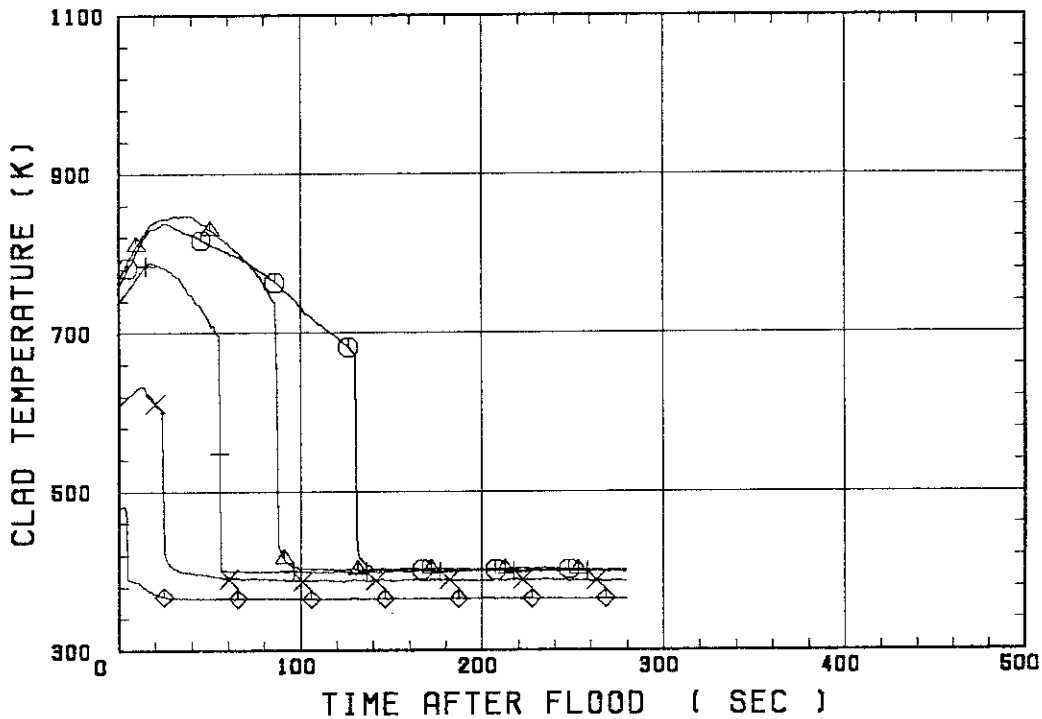
SMALL SCALE REFLOOD TEST
 RUN 8311

○--- TE1L △--- TA2 +--- TA3
 X--- TC4U

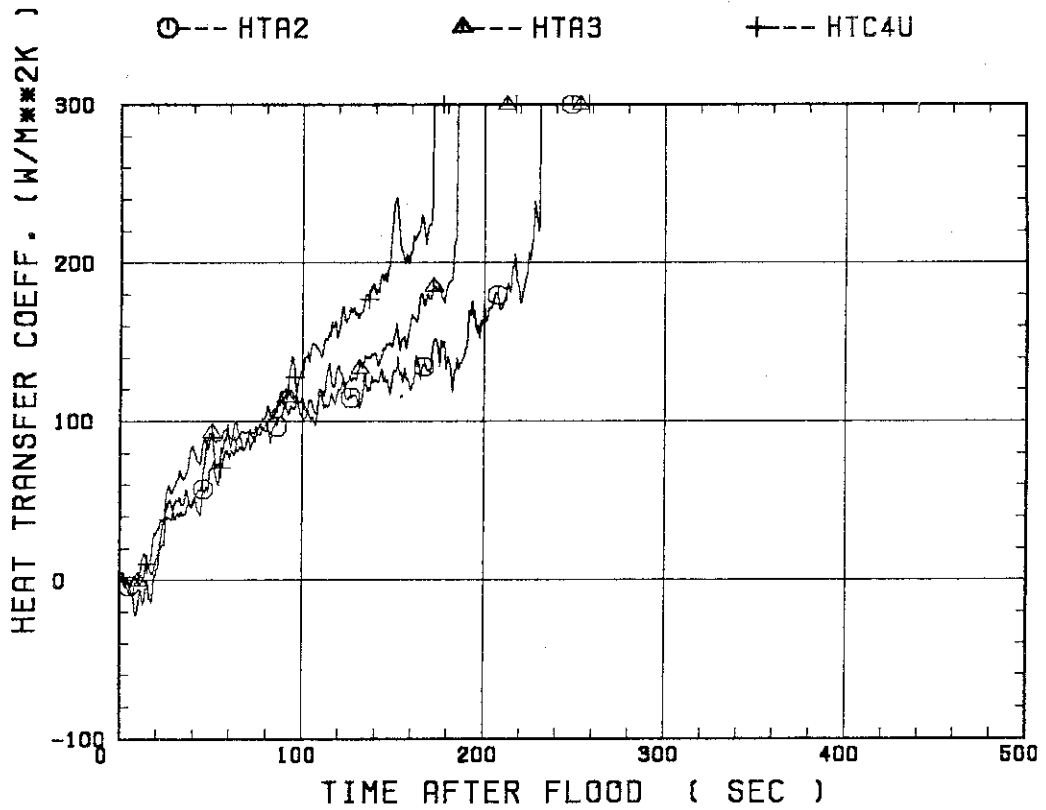


SMALL SCALE REFLOOD TEST
 RUN 8311

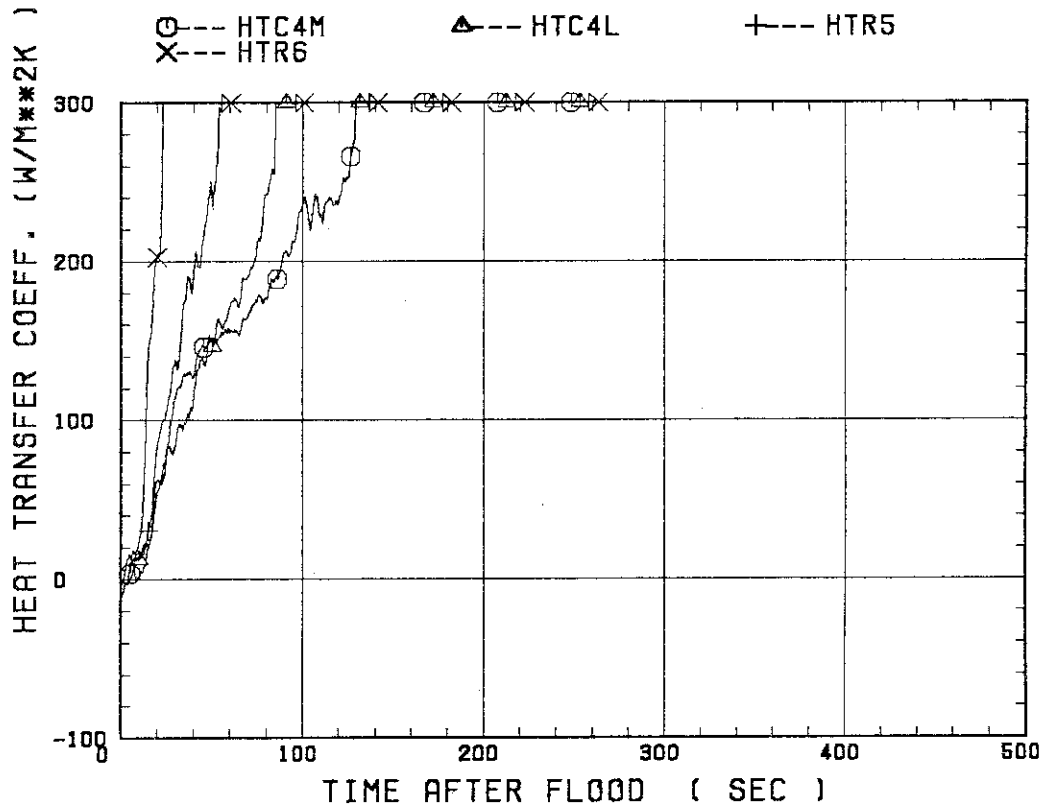
○--- TC4M △--- TC4L +--- TR5
 X--- TR6 ◇--- TE7



SMALL SCALE REFLOOD TEST
RUN 8311

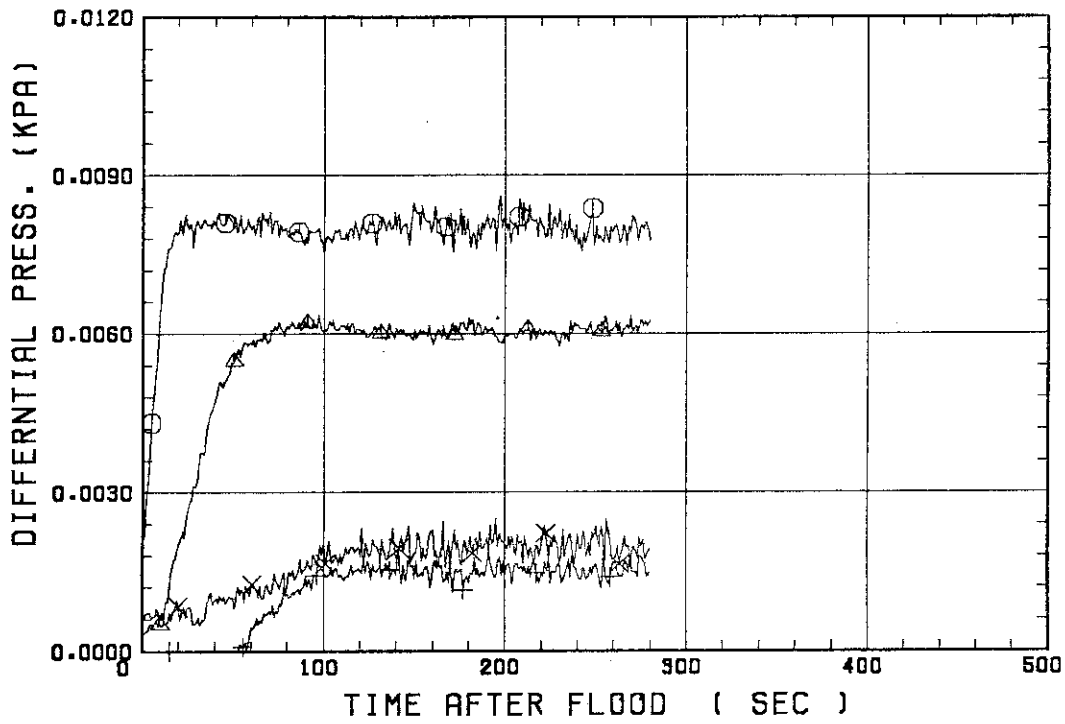


SMALL SCALE REFLOOD TEST
RUN 8311



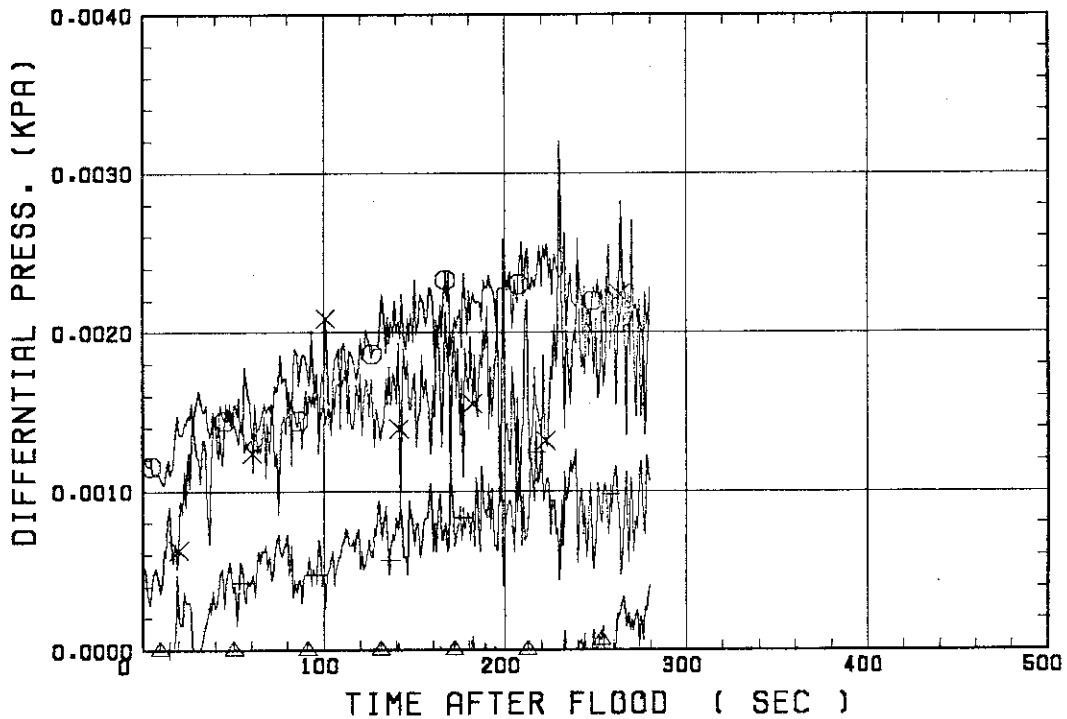
SMALL SCALE REFLOOD TEST
RUN 8311

○ --- DPT2 △ --- DPT4 + --- DPT5
X --- DPT6B



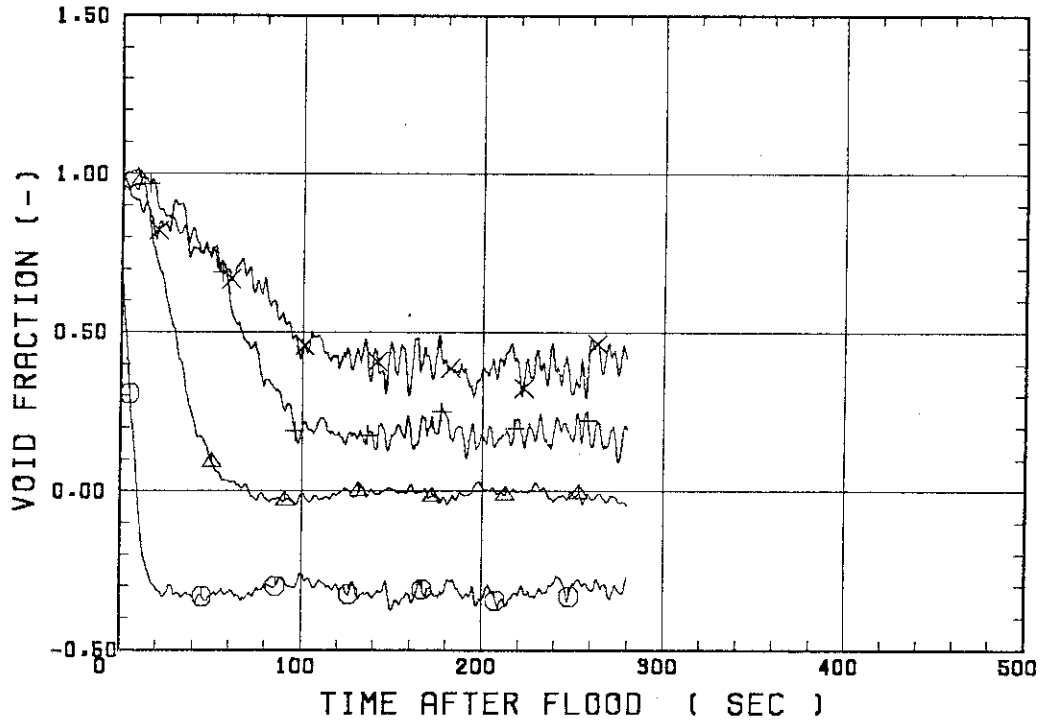
SMALL SCALE REFLOOD TEST
RUN 8311

○ --- DPT7 △ --- DPT8B + --- DP10
X --- DP12



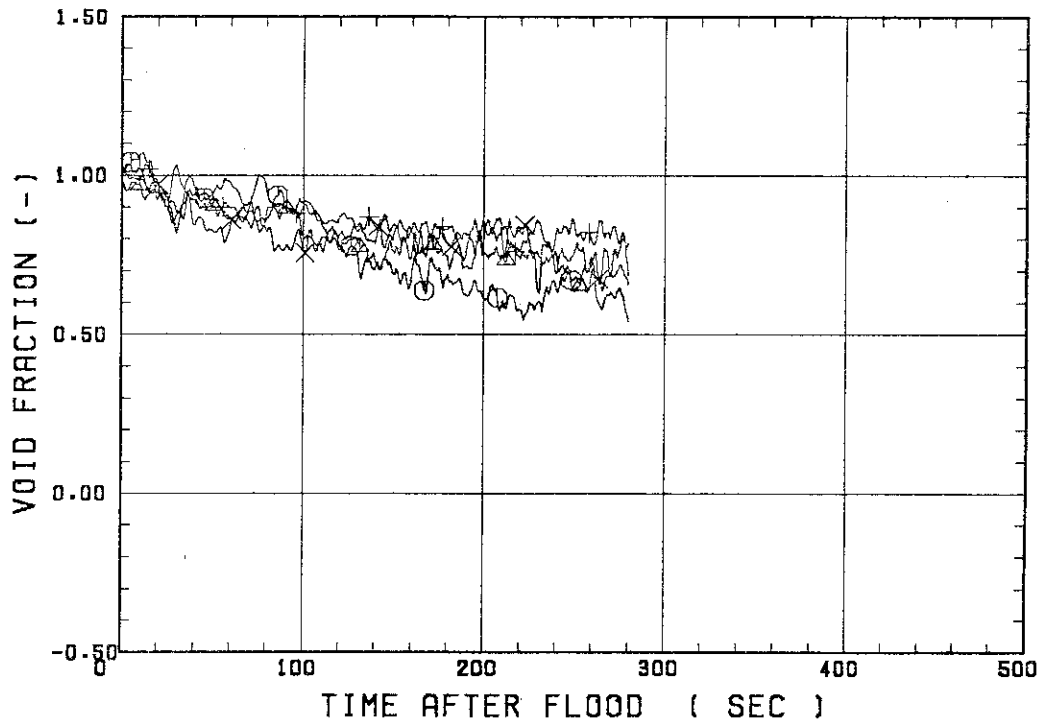
SMALL SCALE REFLOOD TEST
RUN 8311

○--- VDPT2 △--- VDPT4 +--- VDPT5
X--- VDPT6B



SMALL SCALE REFLOOD TEST
RUN 8311

○--- VDPT7 △--- VDPT8B +--- VDP10
X--- VDP12



 * RUN NO. 8312 *
 * *****

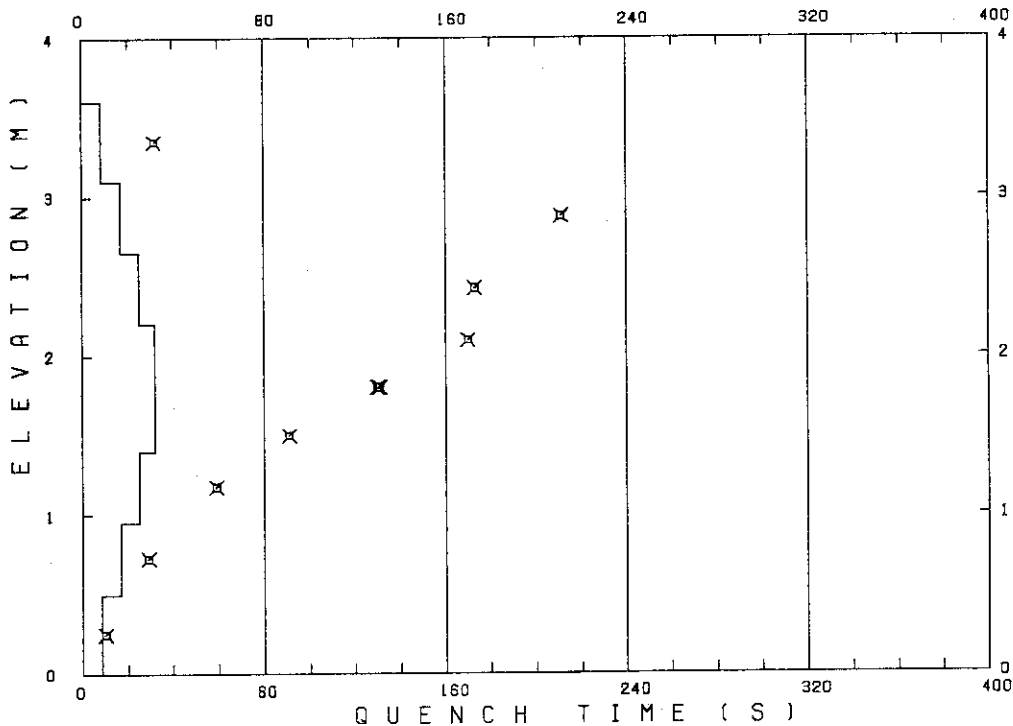
 TEST CONDITIONS

LINEAR PEAK POWER 1.6 KW/M
 SYSTEM PRESSURE 0.2 MPA
 INLET WATER TEMPERATURE 100 .C
 INJECTED WATER VELOCITY 4.0 CM/S

 TEMPERATURE PROFILE

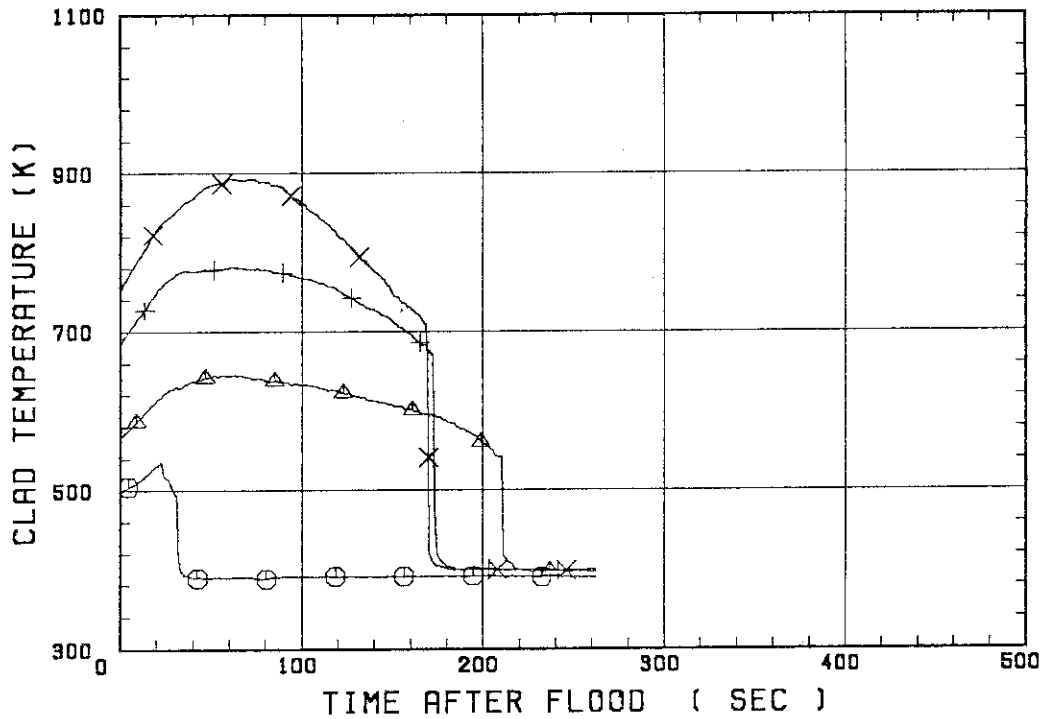
CH.NO.	SYMBOL	INITIAL TEMP. (.C)	TURNAROUND TIME (S)	TURNAROUND TEMP. (.C)	QUENCH TIME (S)	QUENCH TEMP. (.C)
1	TE1L	225	23.0	262	32.0	205
36	TA2	292	63.0	373	211.0	269
37	TA3	409	62.0	509	173.0	398
67	TC4U	475	73.0	620	170.0	392
68	TC4M	470	30.0	554	130.0	382
8	TS4M	524	34.5	623	131.0	350
69	TC4L	487	35.0	570	91.0	444
54	TR5	448	27.0	508	59.0	399
55	TR6	326	19.0	357	29.0	323
5	TE7	212	7.0	220	10.0	193

RUN NO. 8312



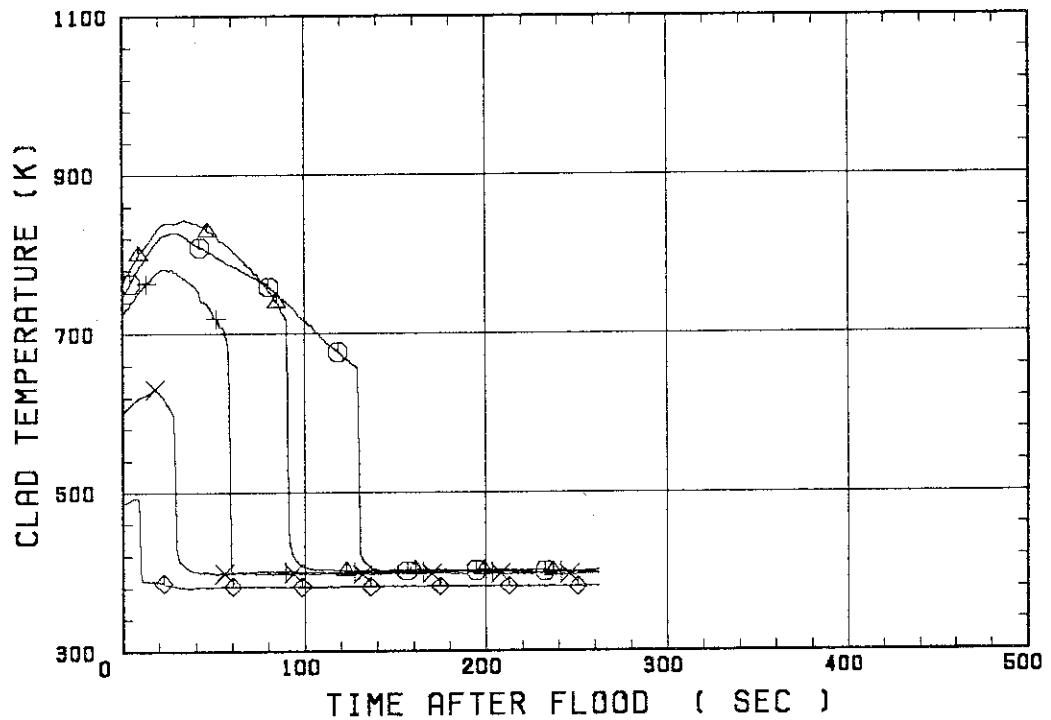
SMALL SCALE REFLOOD TEST
 RUN 8312

○--- TE1L △--- TR2 +--- TR3
 X--- TC4U

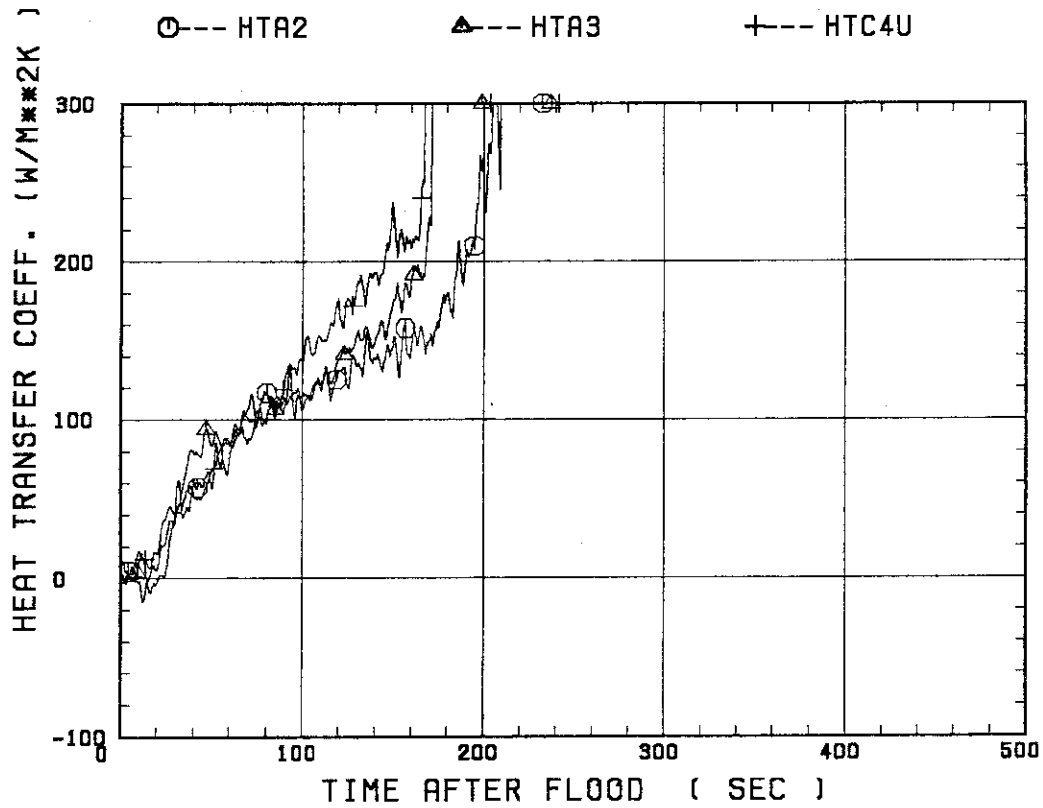


SMALL SCALE REFLOOD TEST
 RUN 8312

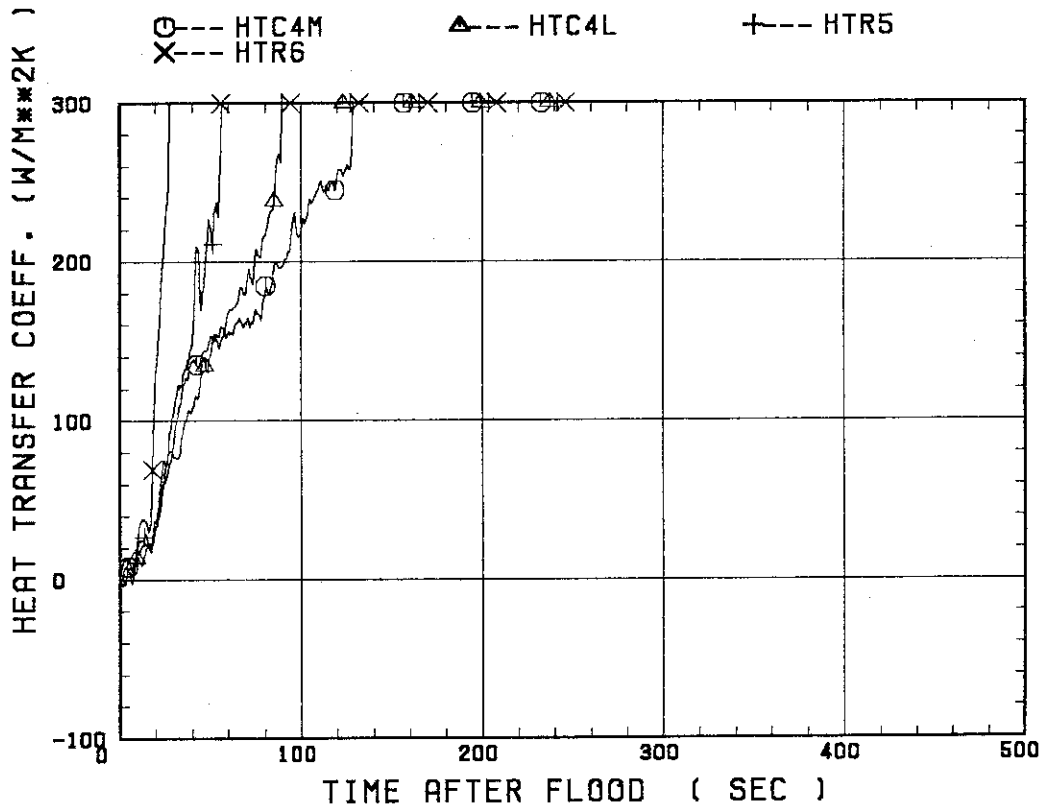
○--- TC4M △--- TC4L +--- TR5
 X--- TR6 ◇--- TE7



SMALL SCALE REFLOOD TEST
 RUN 8312

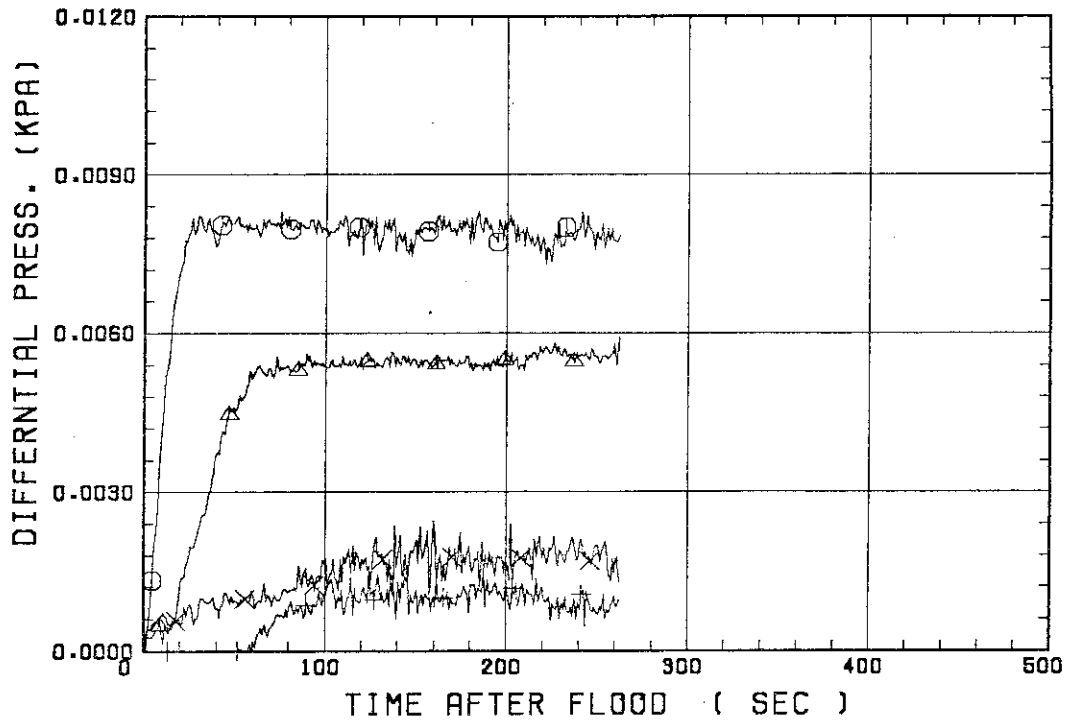


SMALL SCALE REFLOOD TEST
 RUN 8312



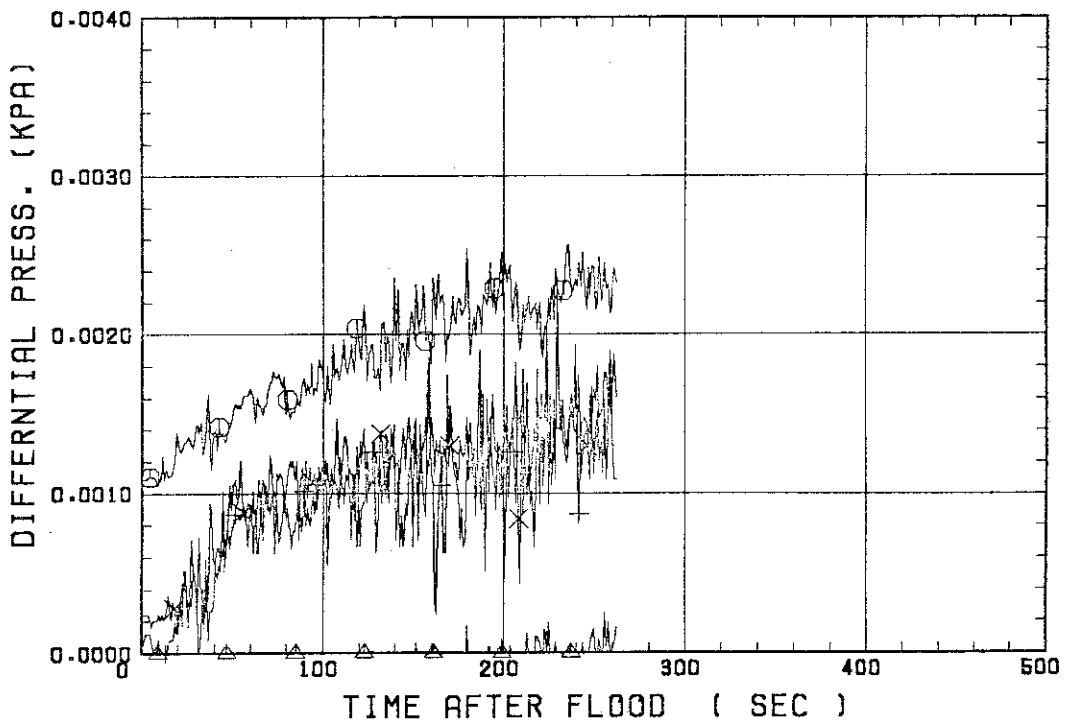
SMALL SCALE REFLOOD TEST
RUN 8312

○ --- DPT2 △ --- DPT4 + --- DPT5
X --- DPT6B



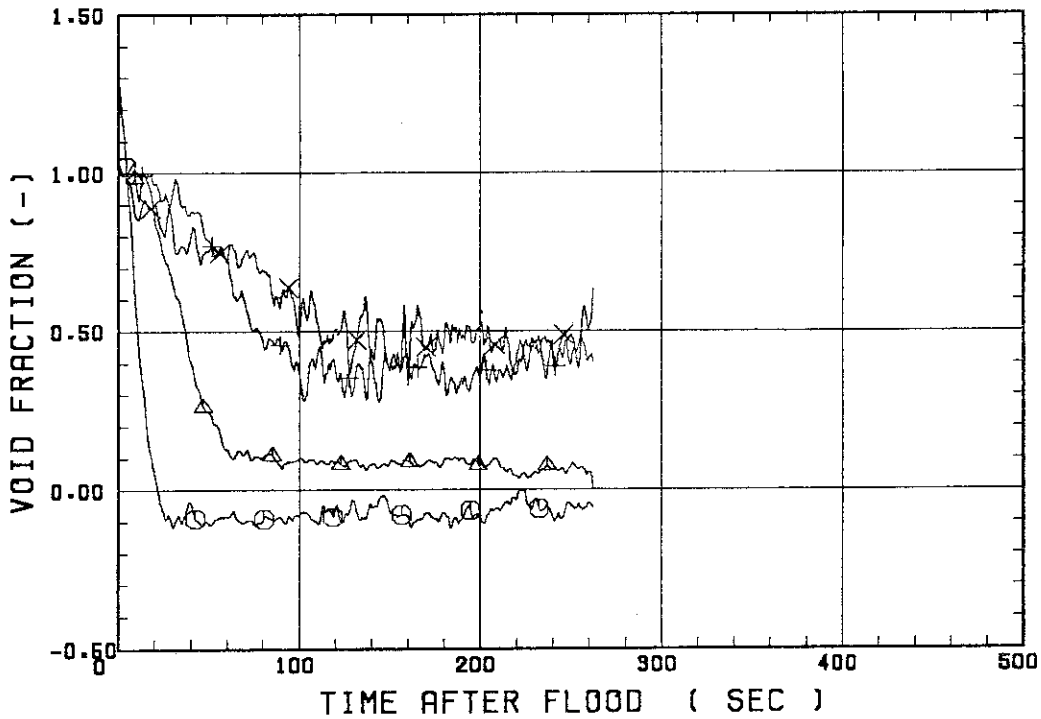
SMALL SCALE REFLOOD TEST
RUN 8312

○ --- DPT7 △ --- DPT8B + --- DP10
X --- DP12



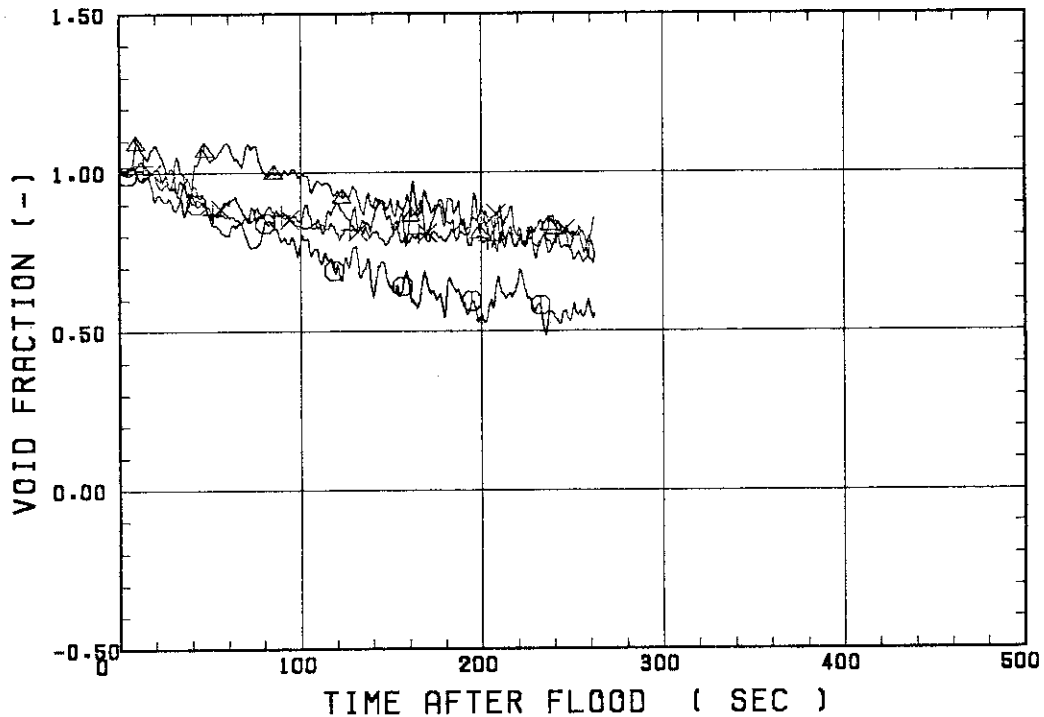
SMALL SCALE REFLOOD TEST
RUN 8312

○--- VDPT2 △--- VDPT4 +--- VDPT5
X--- VDPT6B



SMALL SCALE REFLOOD TEST
RUN 8312

○--- VDPT7 △--- VDPT8B +--- VDP10
X--- VDP12



 * RUN NO. 8313 *

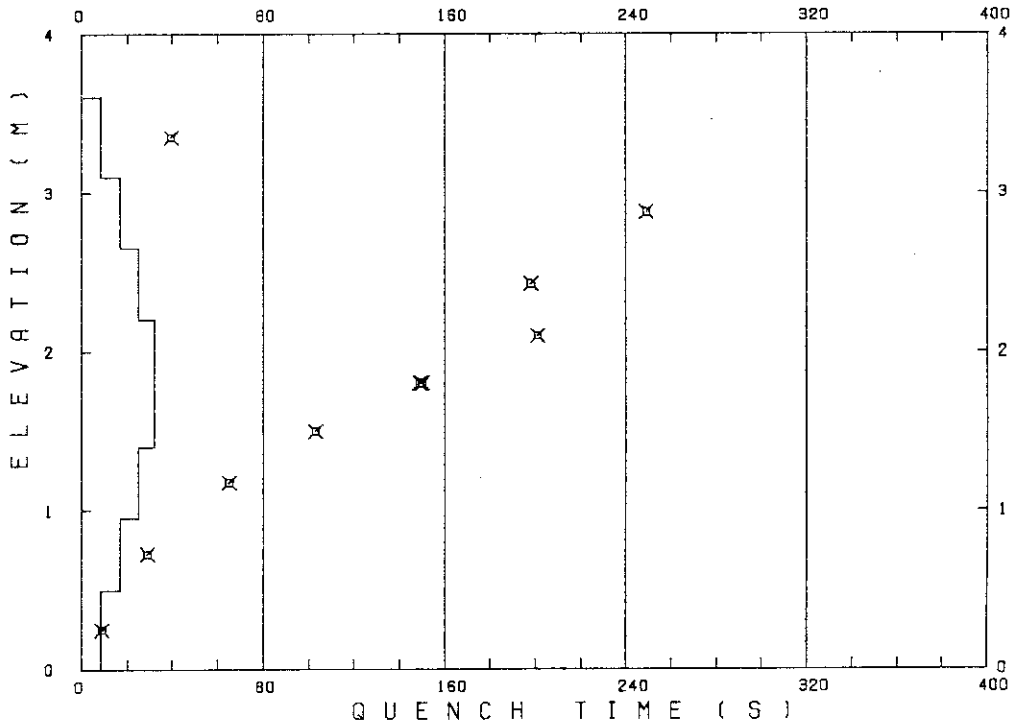
 TEST CONDITIONS

LINEAR PEAK POWER 1.8 KW/M
 SYSTEM PRESSURE 0.2 MPA
 INLET WATER TEMPERATURE 100 .C
 INJECTED WATER VELOCITY 3.9 CM/S

 TEMPERATURE PROFILE

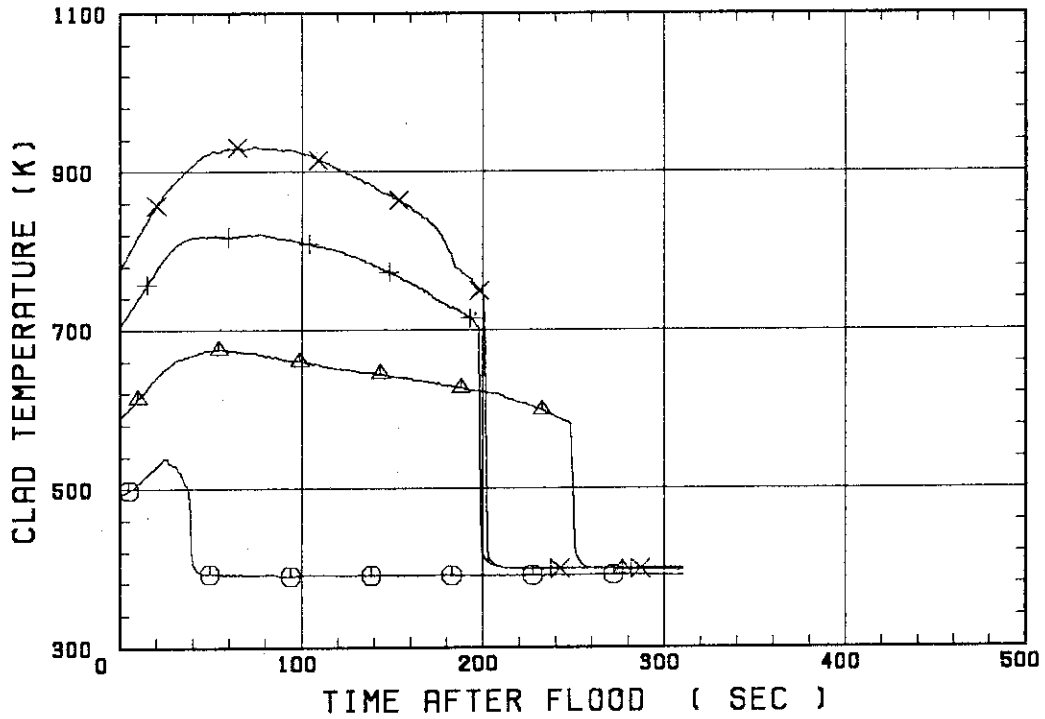
CH.NO.	SYMBOL	INITIAL TEMP. (.C)	TURNAROUND TIME (S)	TURNAROUND TEMP. (.C)	QUENCH TIME (S)	QUENCH TEMP. (.C)
1	TE1L	218	26.5	265	39.5	192
36	TA2	314	56.0	403	249.0	308
37	TA3	430	78.0	548	198.0	429
67	TC4U	500	75.0	658	201.0	465
68	TC4M	496	33.0	591	150.0	396
8	TS4M	532	36.5	661	149.0	349
69	TC4L	519	29.0	611	103.0	437
54	TR5	447	26.0	521	65.0	424
55	TR6	322	18.0	357	29.0	330
5	TE7	214	6.0	222	9.0	214

RUN NO. 8313



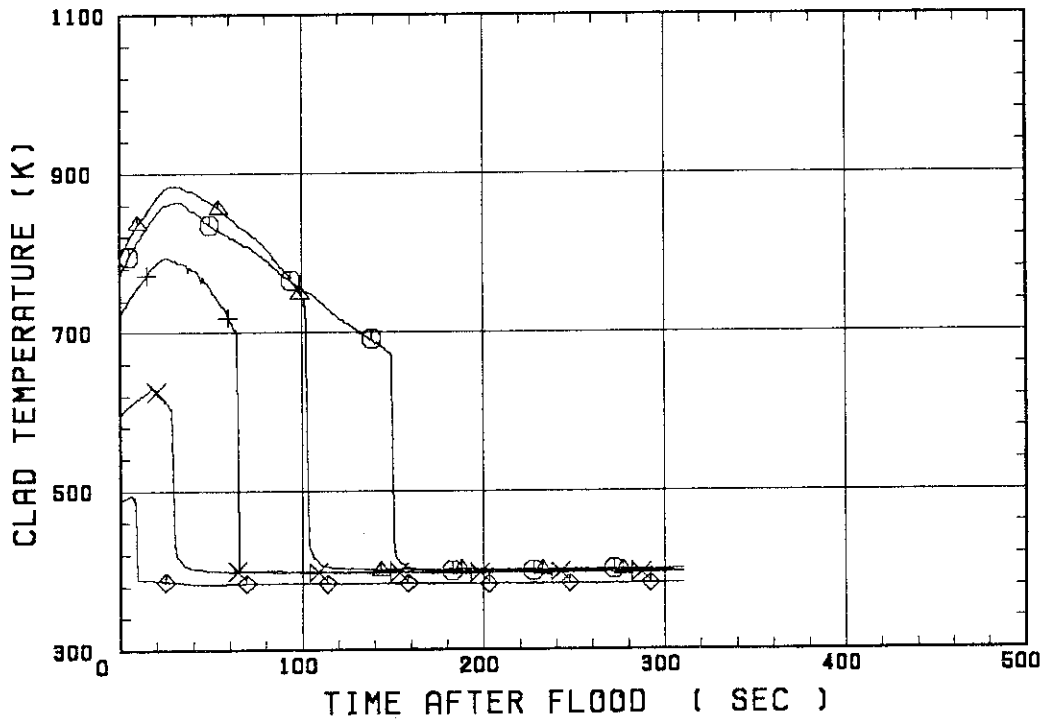
SMALL SCALE REFLOOD TEST
 RUN 8313

○--- TE1L △--- TA2 +--- TA3
 X--- TC4U

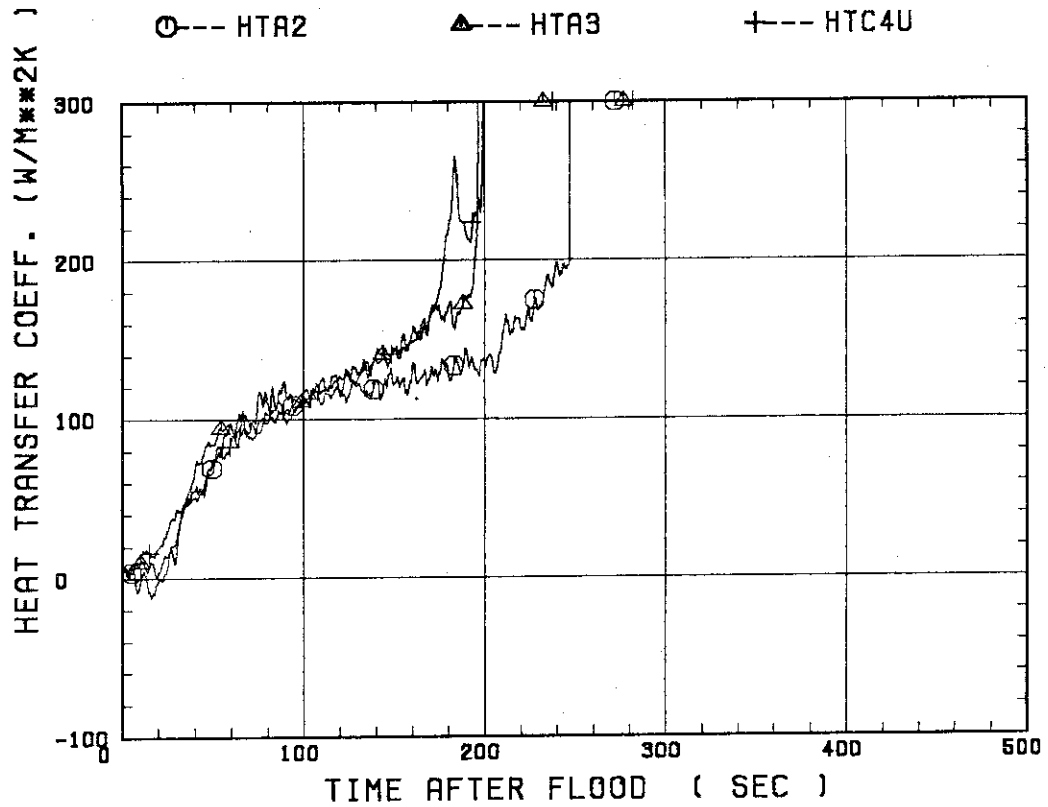


SMALL SCALE REFLOOD TEST
 RUN 8313

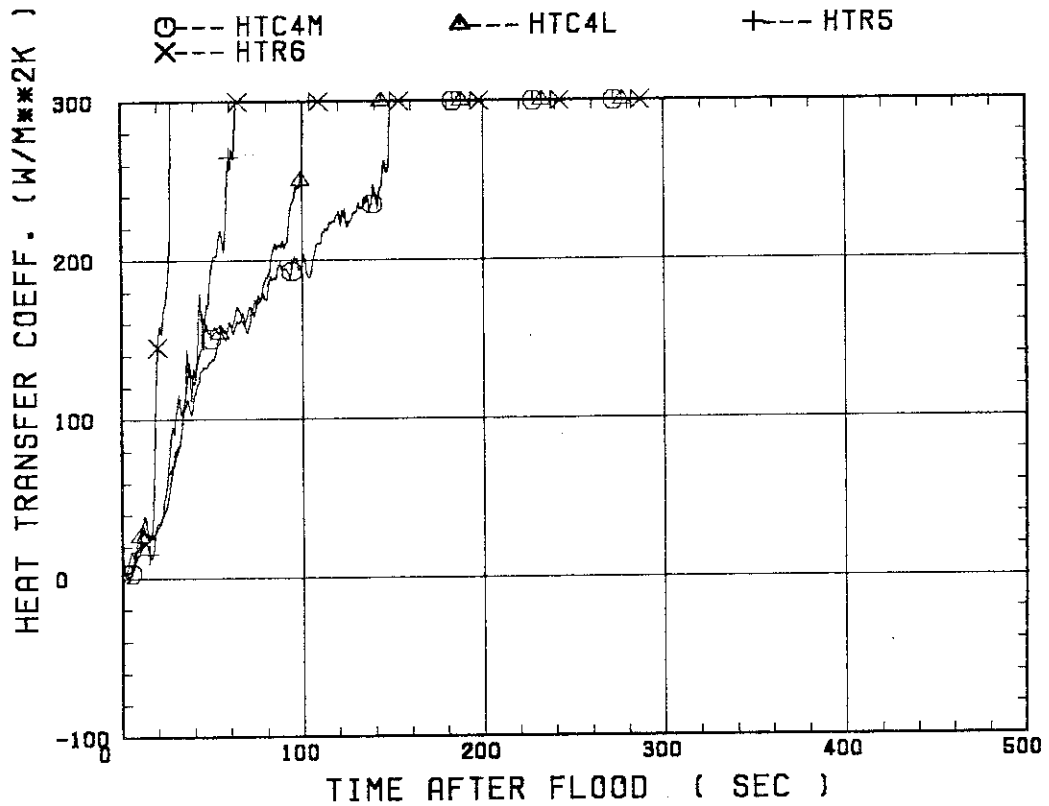
○--- TC4M △--- TC4L +--- TR5
 X--- TR6 ◆--- TE7



SMALL SCALE REFLOOD TEST
 RUN 8313

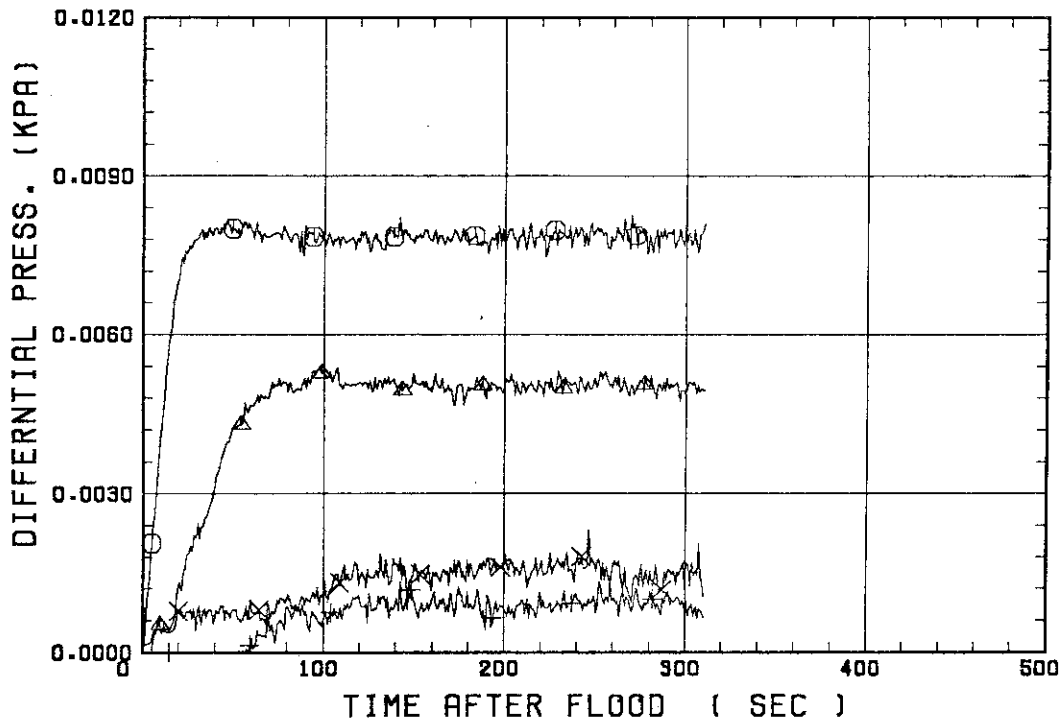


SMALL SCALE REFLOOD TEST
 RUN 8313



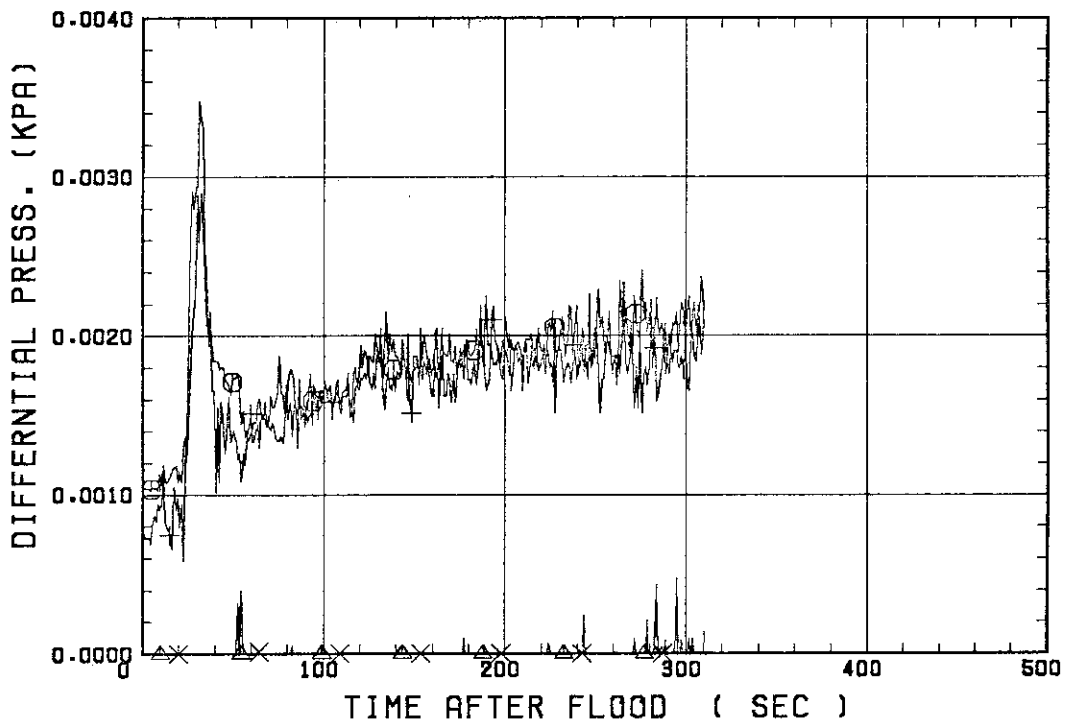
SMALL SCALE REFLOOD TEST
RUN 8313

○--- DPT2 ▲--- DPT4 +--- DPT5
X--- DPT6B



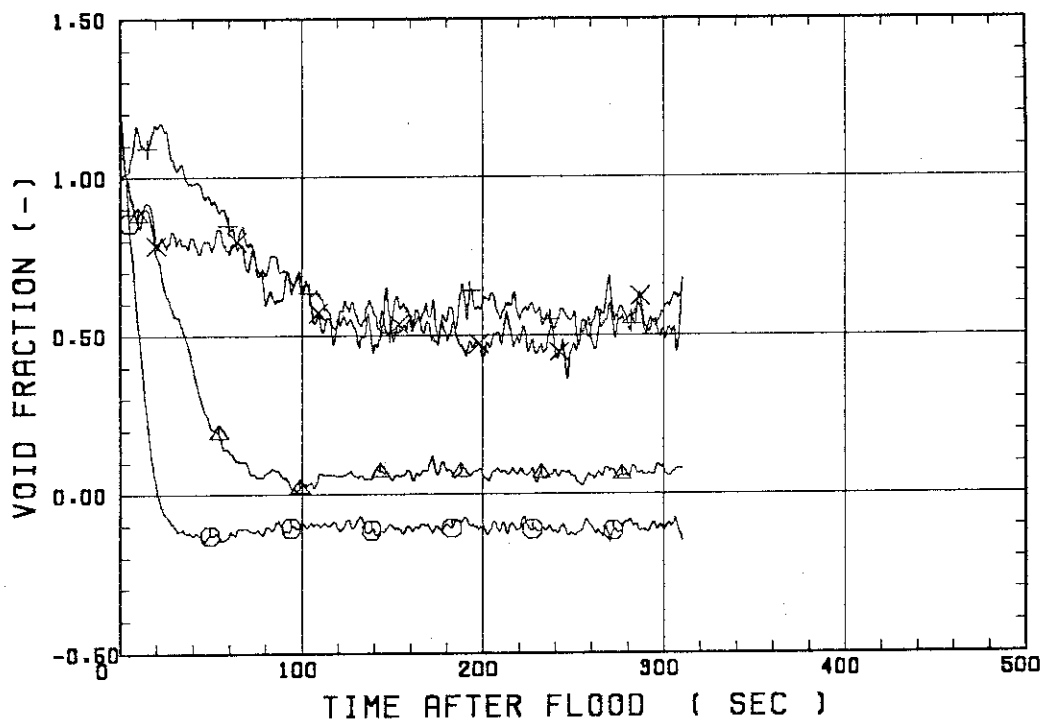
SMALL SCALE REFLOOD TEST
RUN 8313

○--- DPT7 ▲--- DPT8B +--- DP10
X--- DP12



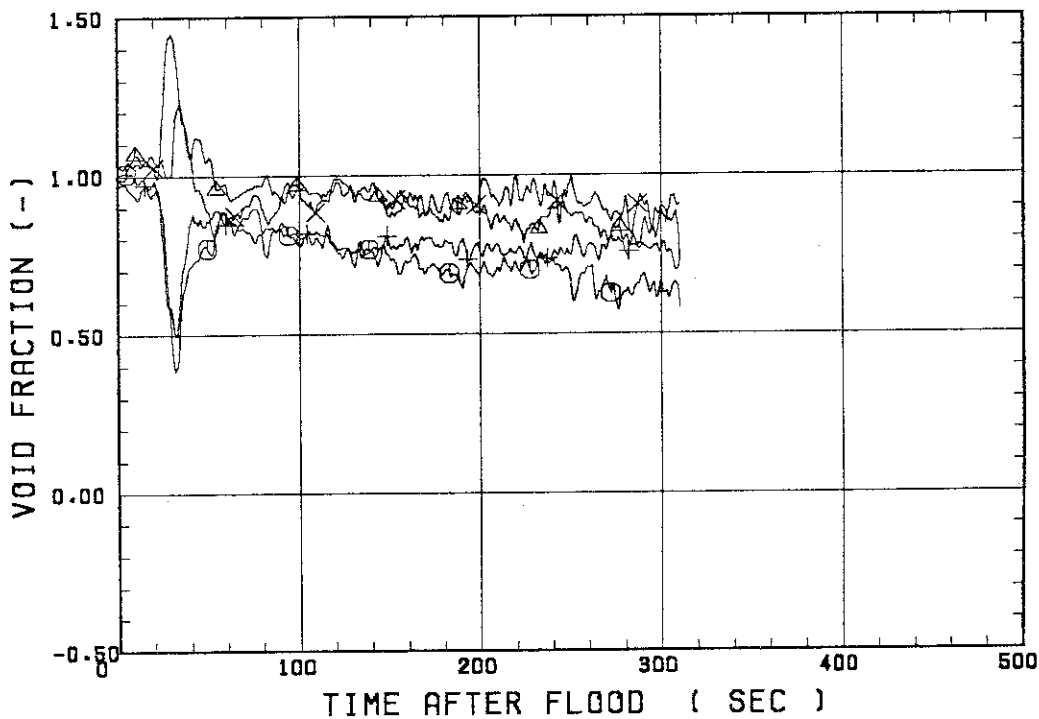
SMALL SCALE REFLOOD TEST
RUN 8313

○--- VDPT2 △--- VDPT4 +--- VDPT5
X--- VDPT6B



SMALL SCALE REFLOOD TEST
RUN 8313

○--- VDPT7 △--- VDPT8B +--- VDP10
X--- VDP12



 * RUN NO. 8314 *

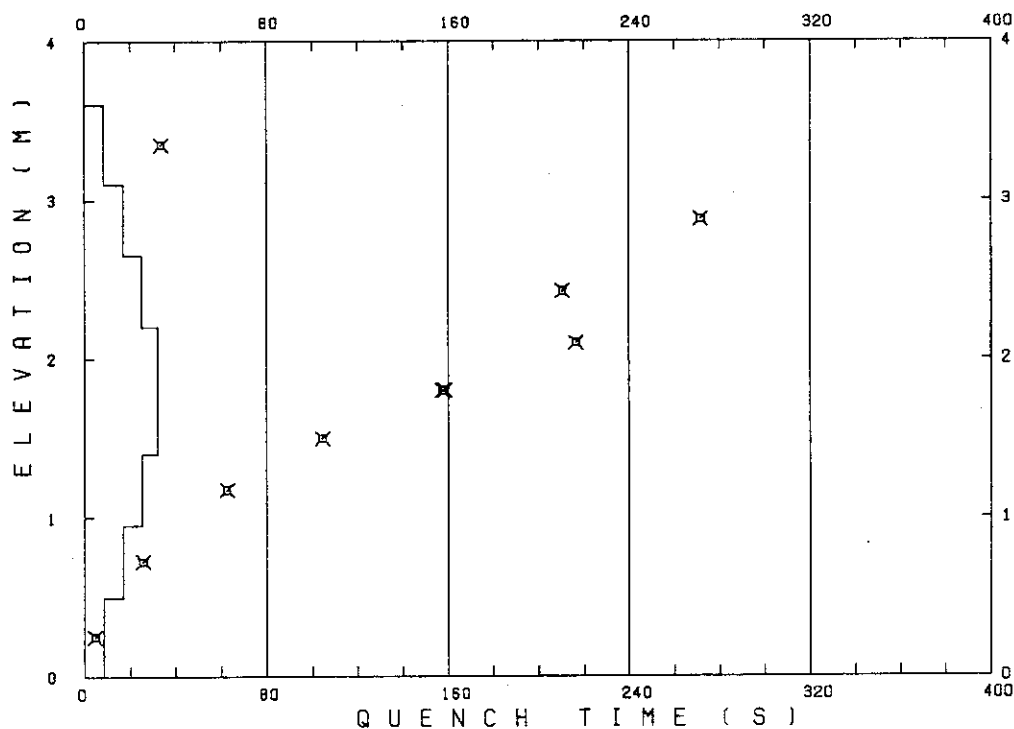
 TEST CONDITIONS

LINEAR PEAK POWER 2.0 KW/M
 SYSTEM PRESSURE 0.2 MPA
 INLET WATER TEMPERATURE 100 .C
 INJECTED WATER VELOCITY 3.9 CM/S

 TEMPERATURE PROFILE

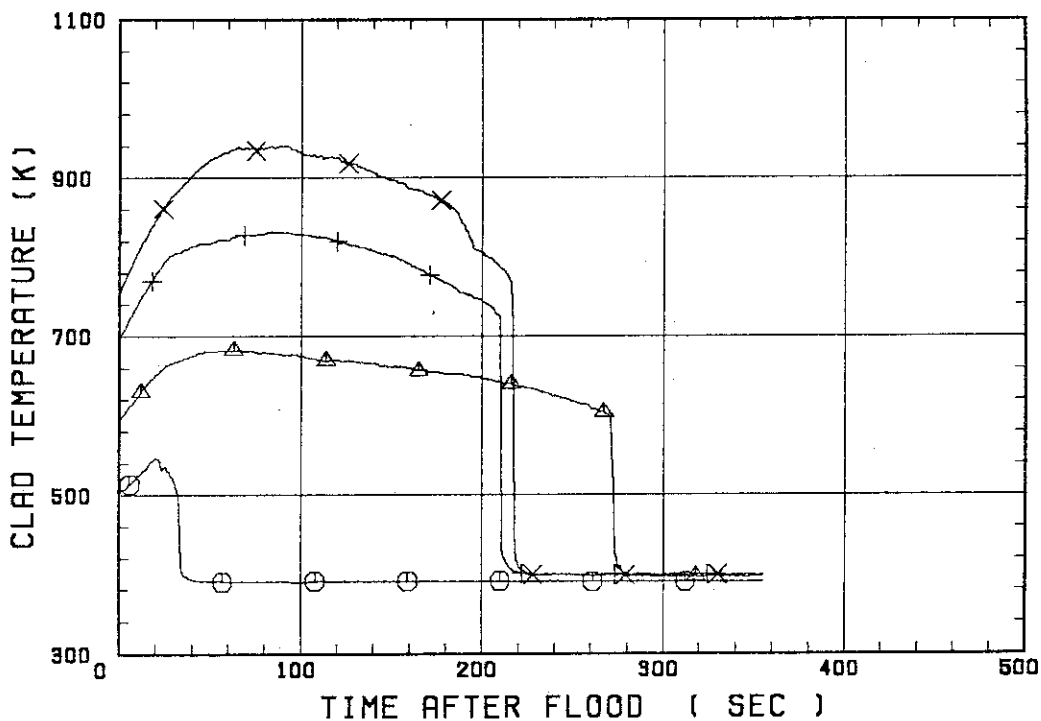
CH.NO.	SYMBOL	INITIAL TEMP. (.C)	TURNAROUND TIME (S)	TURNAROUND TEMP. (.C)	QUENCH TIME (S)	QUENCH TEMP. (.C)
1	TE1L	229	20.5	273	33.5	208
36	TA2	320	67.5	409	271.5	324
37	TA3	422	84.5	559	210.5	448
67	TC4U	478	91.5	667	216.5	493
68	TC4M	482	28.5	576	157.5	412
8	TS4M	535	34.0	659	158.5	363
69	TC4L	503	36.5	600	104.5	478
54	TR5	459	29.5	524	62.5	429
55	TR6	338	13.5	366	25.5	337
5	TE7	221	2.5	224	4.5	208

RUN NO. 8314



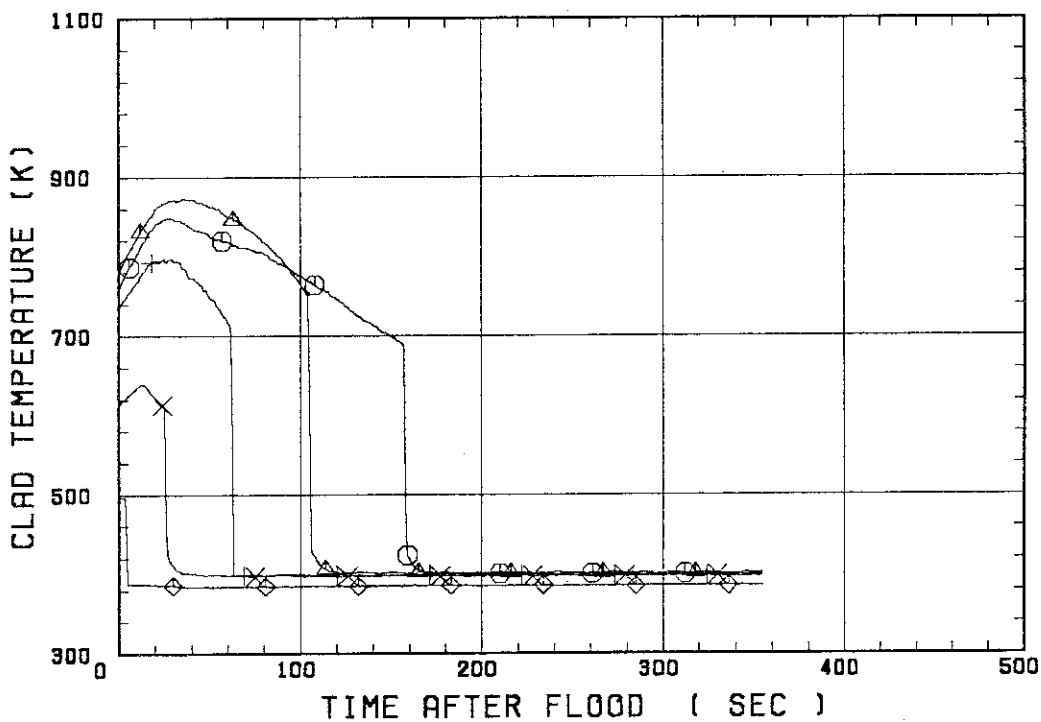
SMALL SCALE REFLOOD TEST
 RUN 8314

○ --- TE1L ▲ --- TA2 + --- TA3
 X --- TC4U

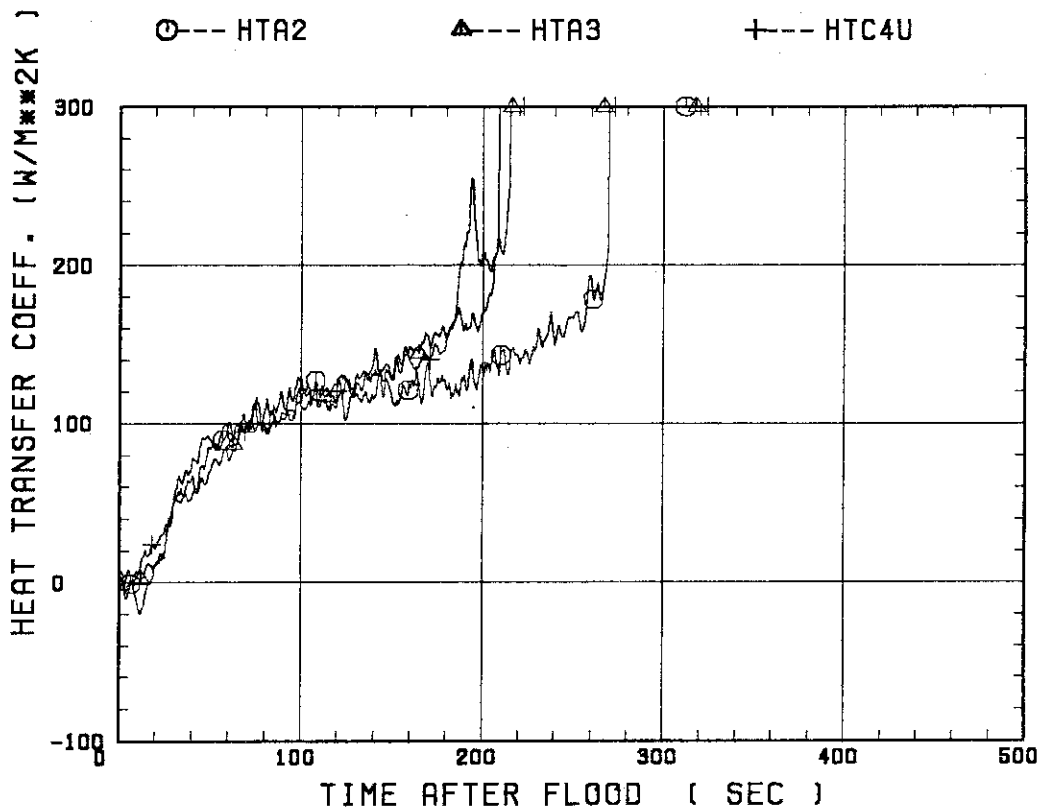


SMALL SCALE REFLOOD TEST
 RUN 8314

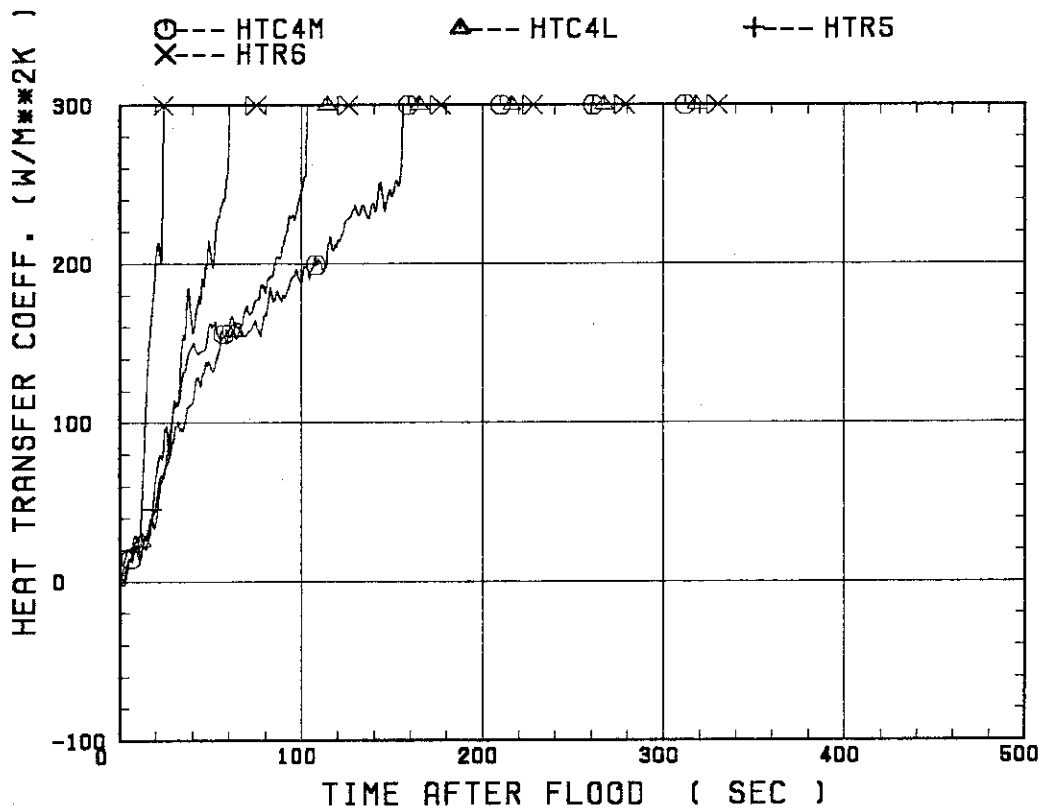
○ --- TC4M ▲ --- TC4L + --- TR5
 X --- TR6 ◆ --- TE7



SMALL SCALE REFLOOD TEST
 RUN 8314

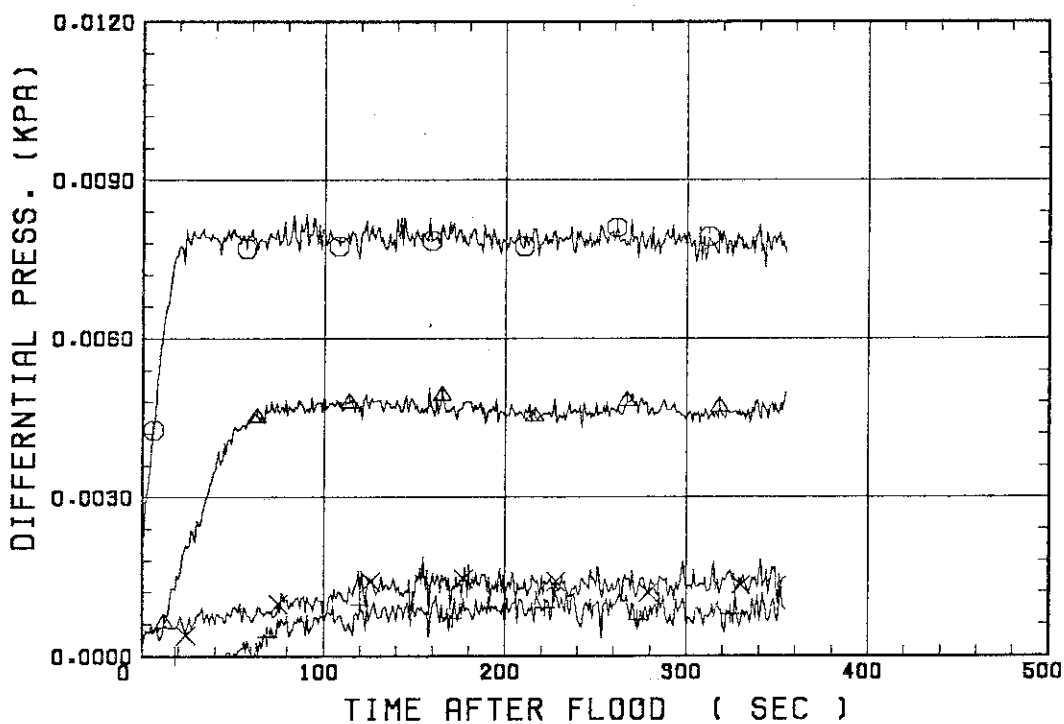


SMALL SCALE REFLOOD TEST
 RUN 8314



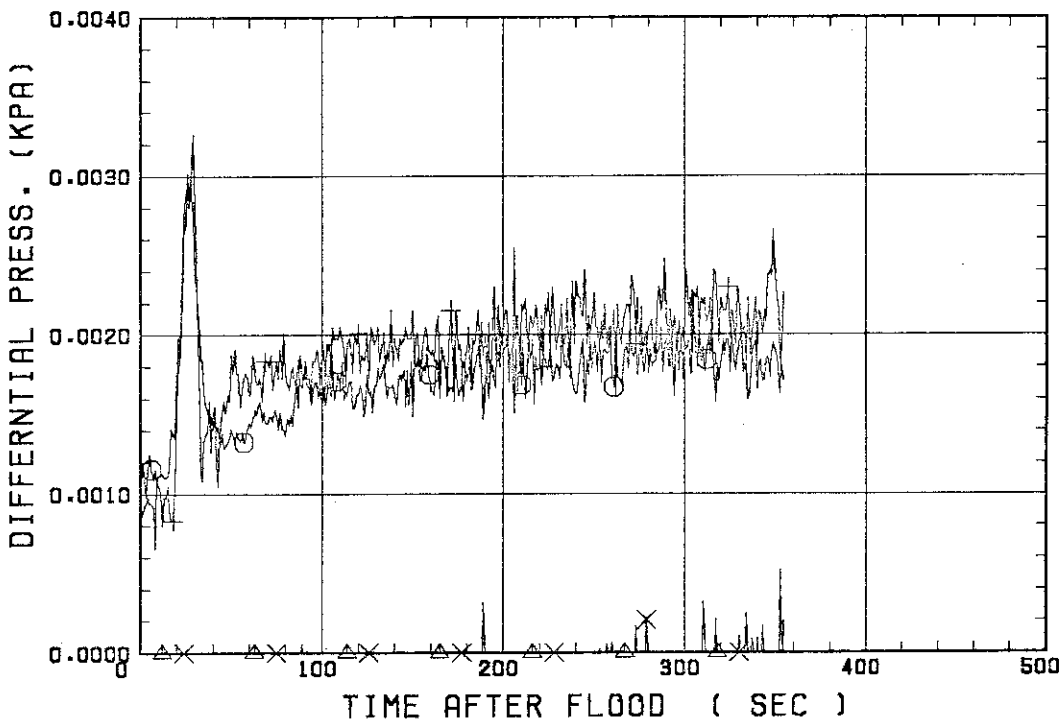
SMALL SCALE REFLOOD TEST
RUN 8314

○--- DPT2 ▲--- DPT4 +--- DPT5
X--- DPT6B



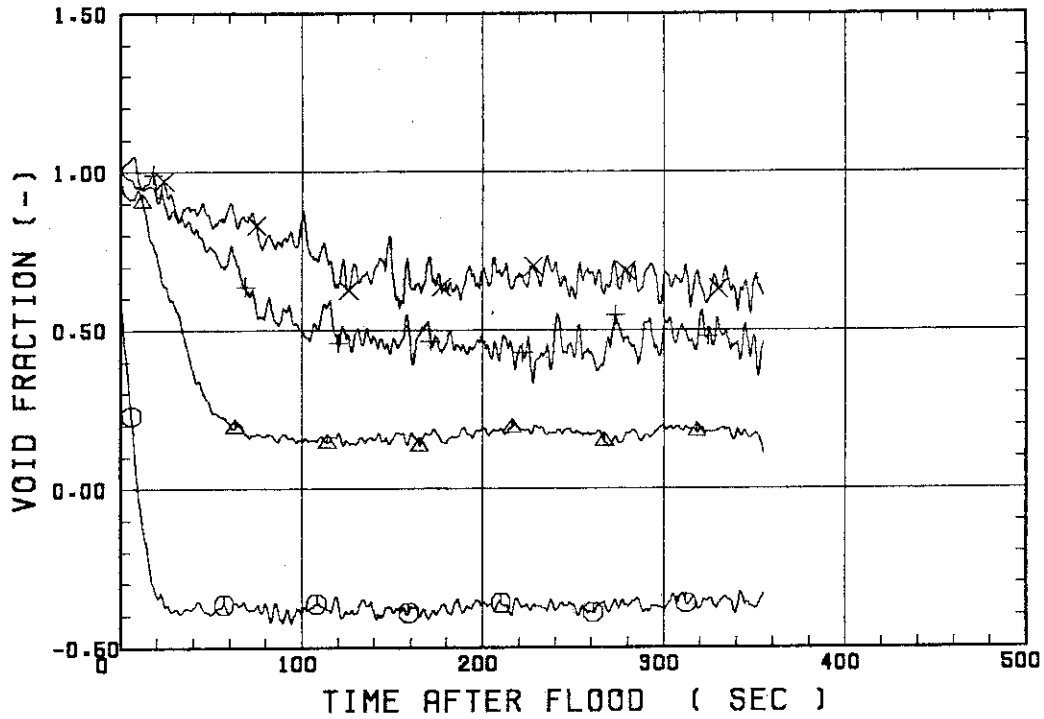
SMALL SCALE REFLOOD TEST
RUN 8314

○--- DPT7 ▲--- DPT8B +--- DP10
X--- DP12



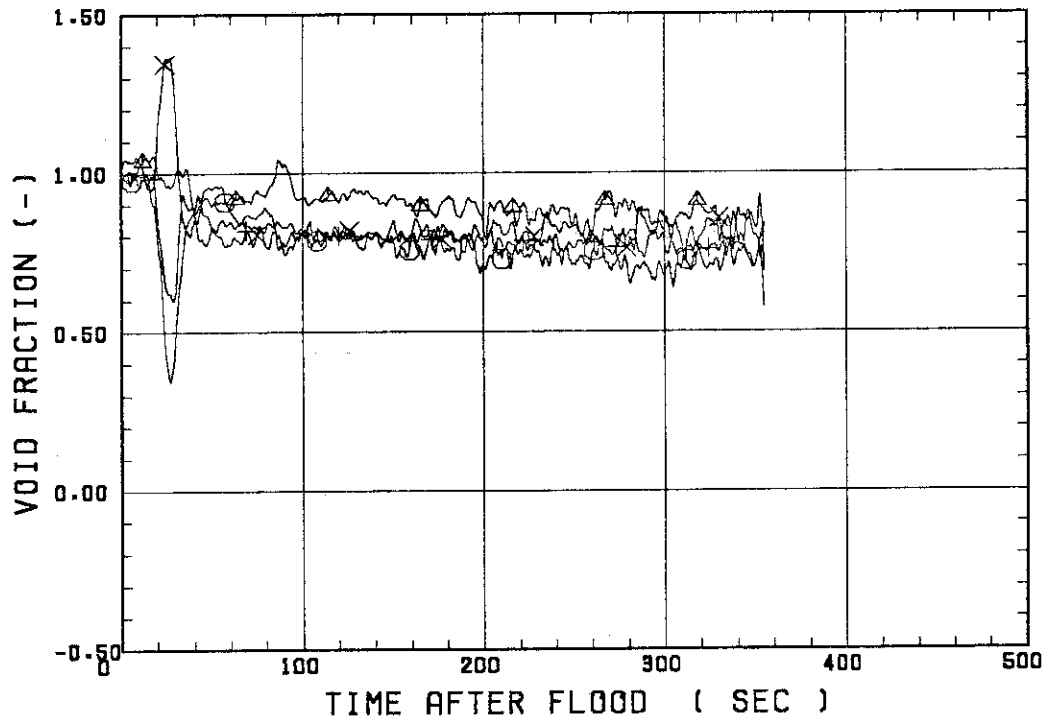
SMALL SCALE REFLOOD TEST
RUN 8314

○--- VDPT2 △--- VDPT4 +--- VDPT5
X--- VDPT6B



SMALL SCALE REFLOOD TEST
RUN 8314

○--- VDPT7 △--- VDPT8B +--- VDP10
X--- VDP12



 * RUN NO. 8316 *

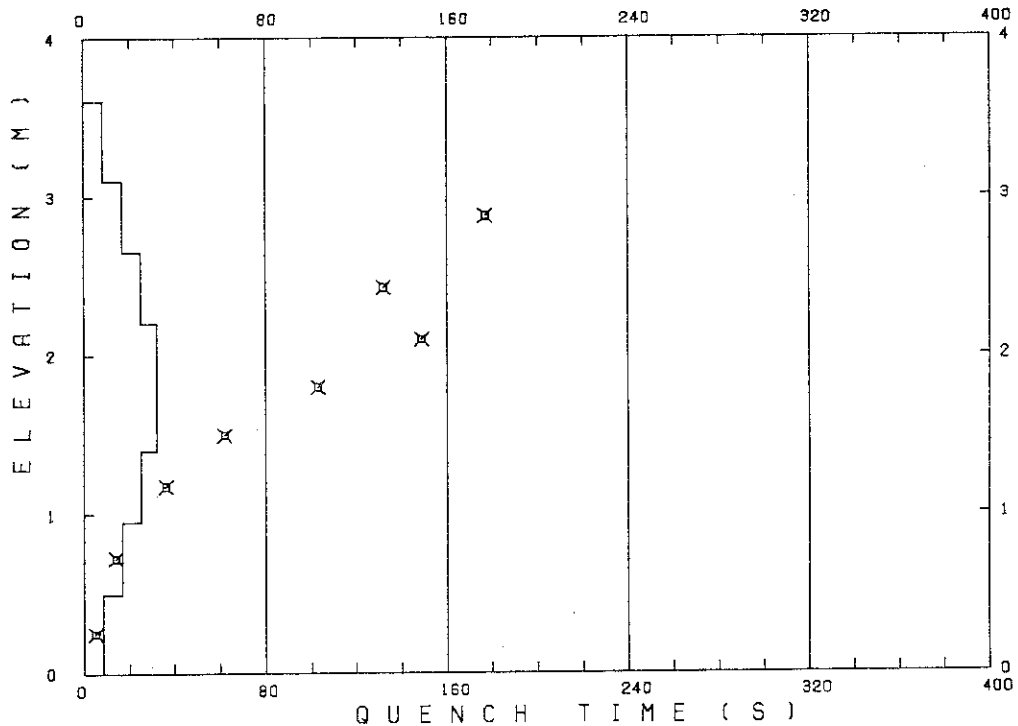
 TEST CONDITIONS

LINEAR PEAK POWER 1.8 KW/M
 SYSTEM PRESSURE 0.2 MPA
 INLET WATER TEMPERATURE 100 .C
 INJECTED WATER VELOCITY 4.1 CM/S

 TEMPERATURE PROFILE

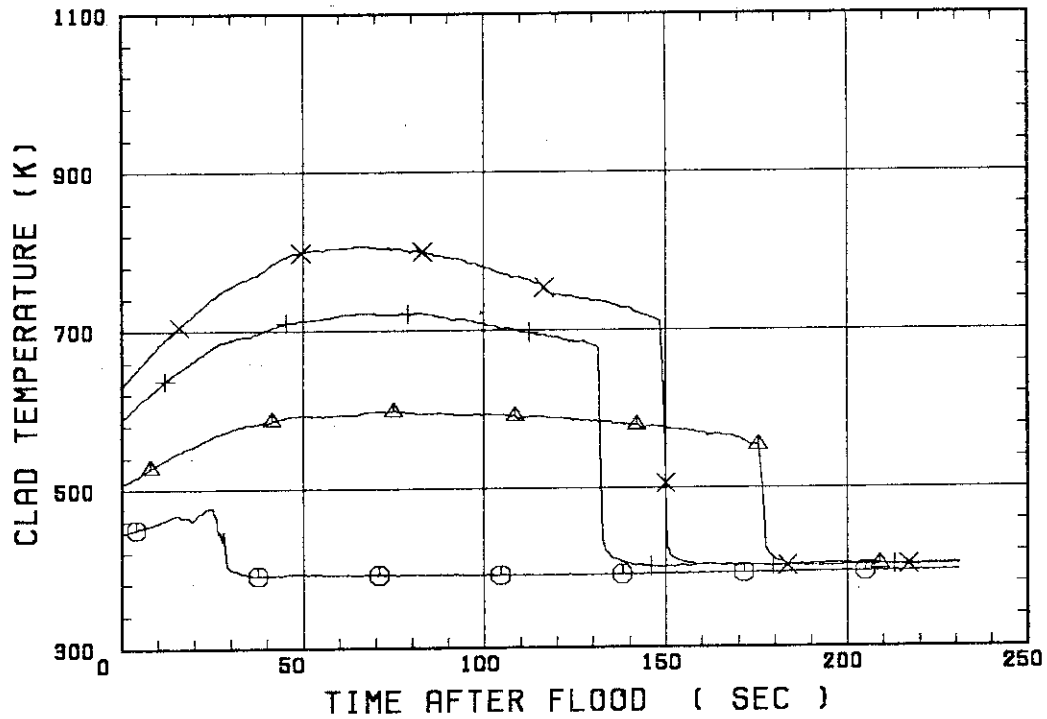
CH.NO.	SYMBOL	INITIAL TEMP. (.C)	TURNAROUND TIME (S)	TURNAROUND TEMP. (.C)	QUENCH TIME (S)	QUENCH TEMP. (.C)
1	TE1L	171	25.0	204		
36	TA2	232	76.0	325	177.0	239
37	TA3	313	82.0	449	132.0	404
67	TC4U	354	67.0	534	149.0	437
68	TC4M	358	41.0	460	103.0	383
69	TC4L	367	30.0	466	62.0	425
54	TR5	324	22.0	388	36.0	350
55	TR6	240	13.0	270	14.0	269
5	TE7	168	5.0	175	5.0	175

RUN NO. 8316



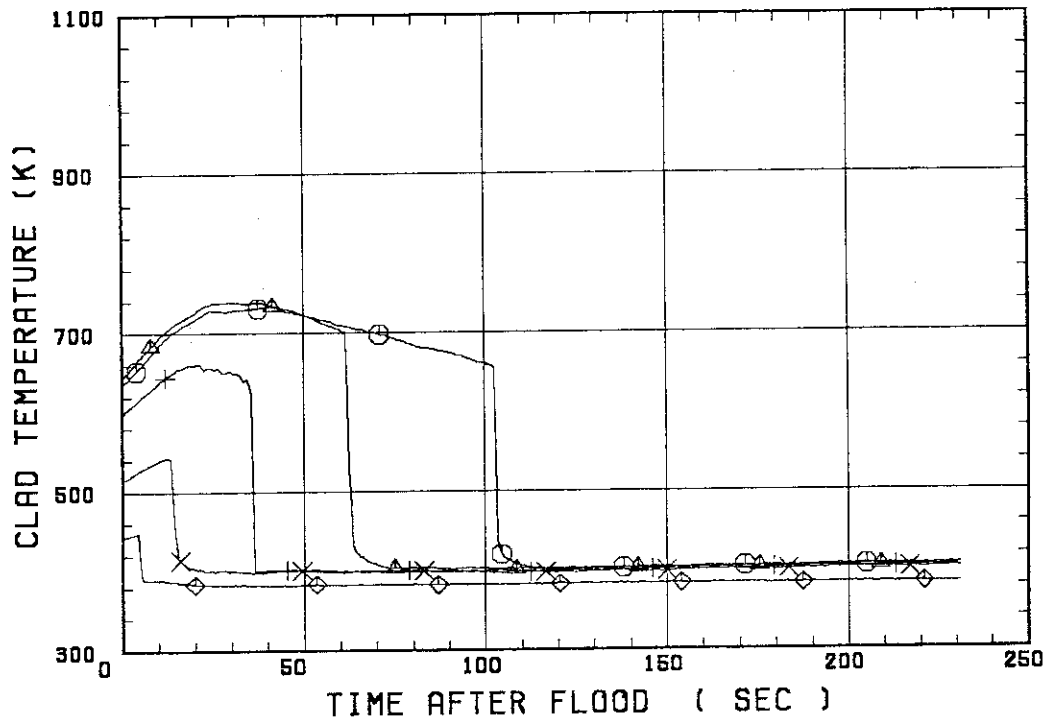
SMALL SCALE REFLOOD TEST
 RUN 8316

○--- TE1L △--- TA2 +--- TA3
 X--- TC4U

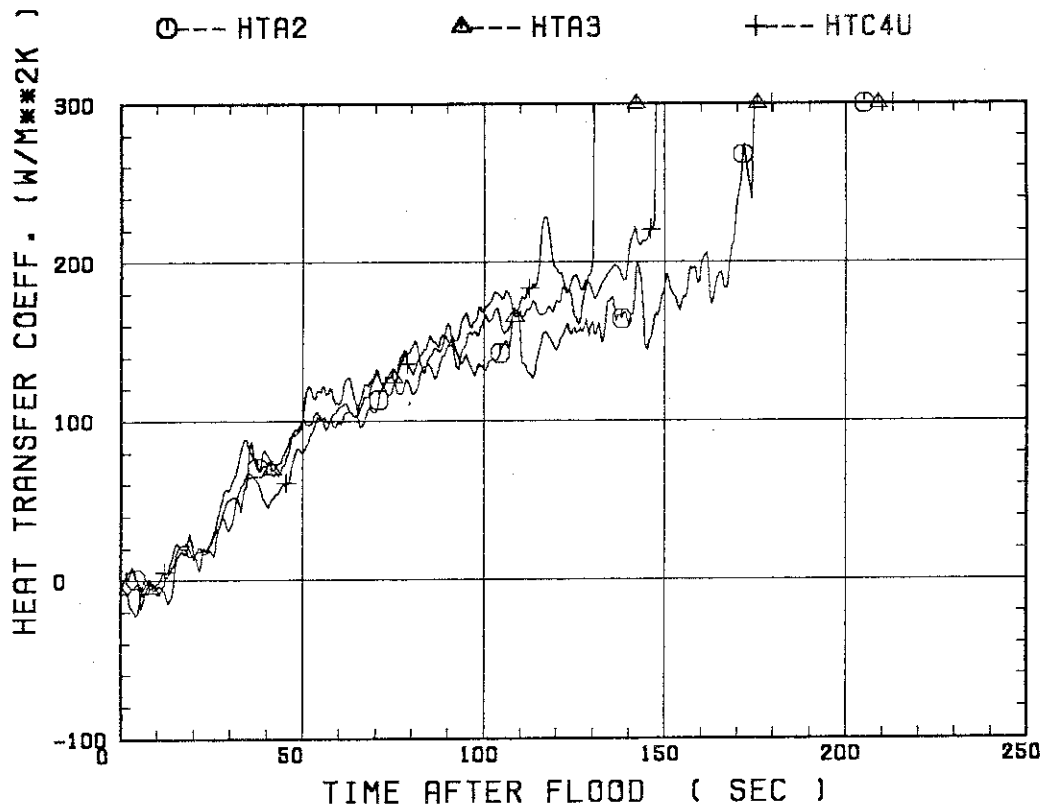


SMALL SCALE REFLOOD TEST
 RUN 8316

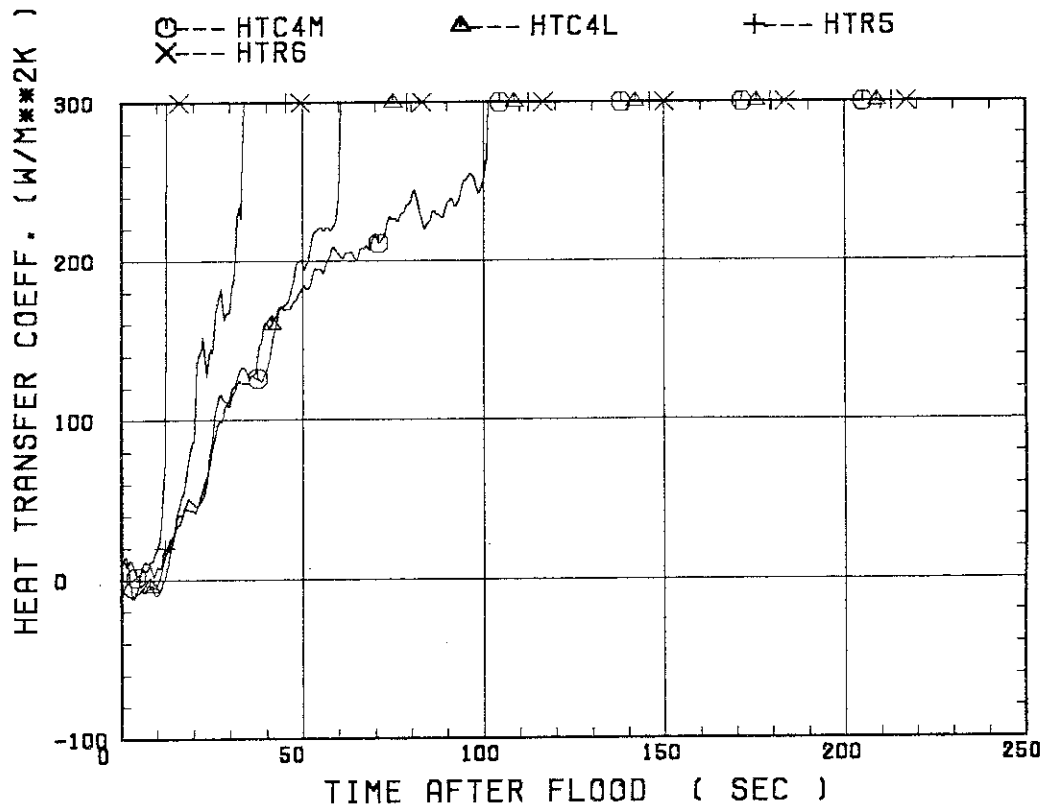
○--- TC4M △--- TC4L +--- TR5
 X--- TR6 ◇--- TE7



SMALL SCALE REFLOOD TEST
 RUN 8316

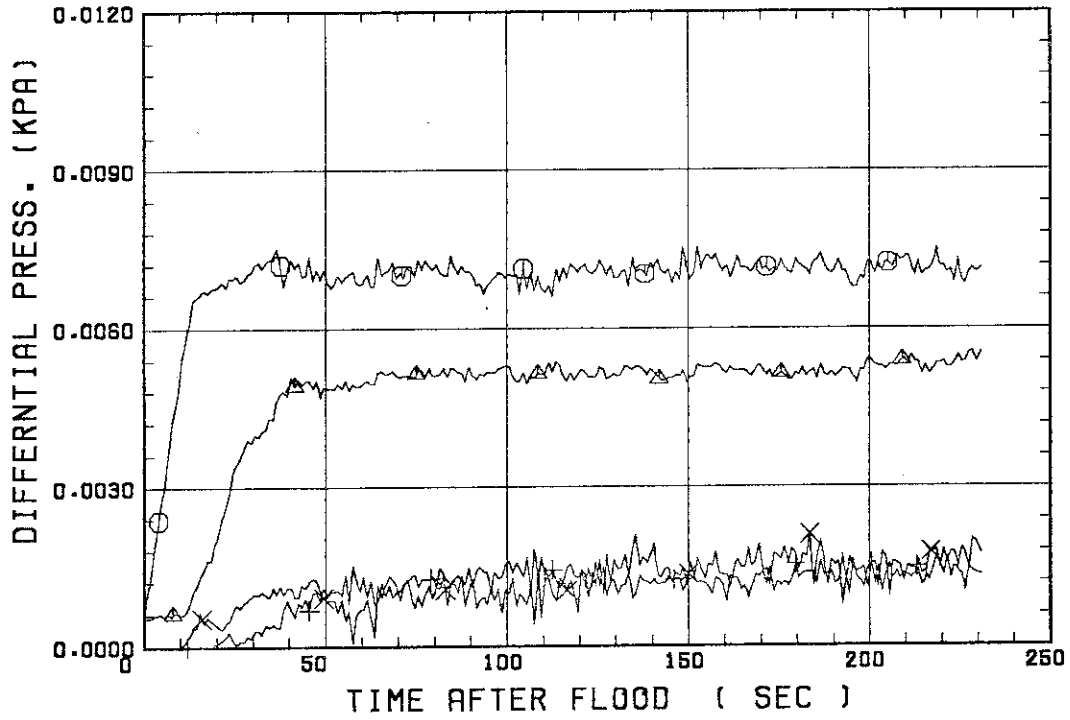


SMALL SCALE REFLOOD TEST
 RUN 8316



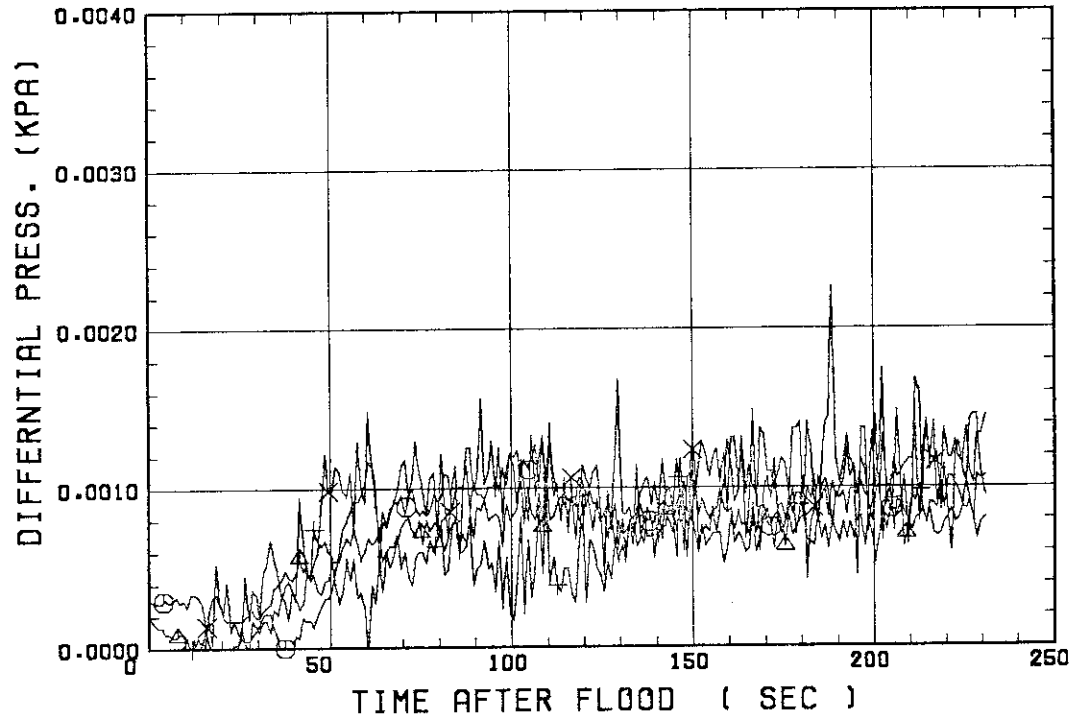
SMALL SCALE REFLOOD TEST
RUN 8316

○---DPT2 ▲---DPT4 +---DPT5
X---DPT6B



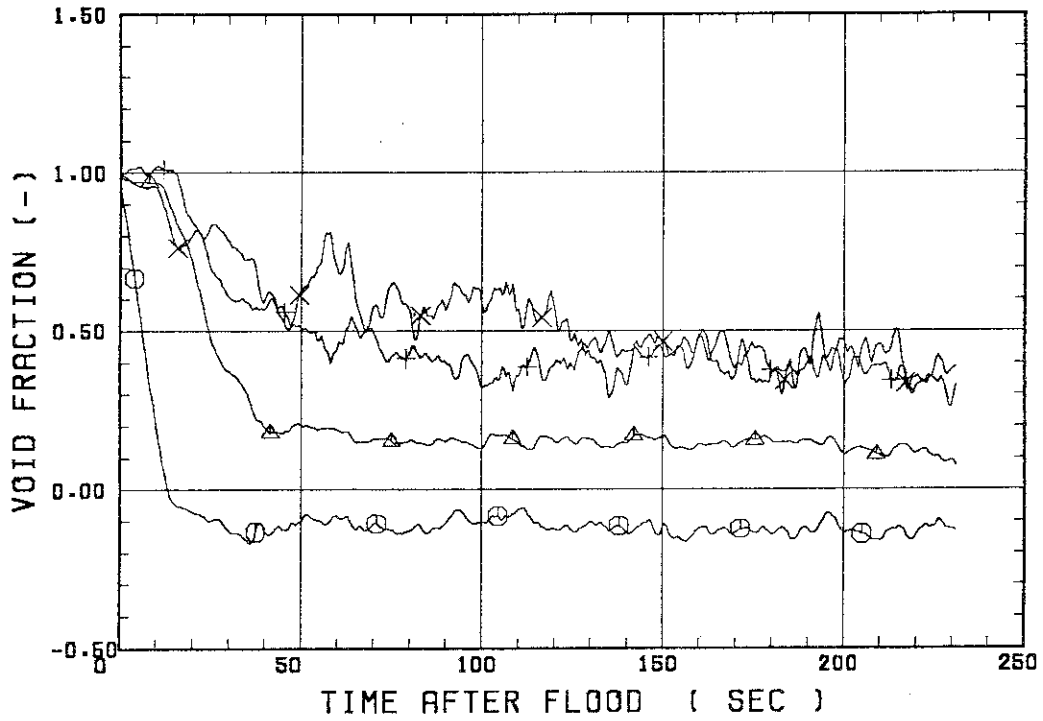
SMALL SCALE REFLOOD TEST
RUN 8316

○---DPT7 ▲---DPT8B +---DP10
X---DP12



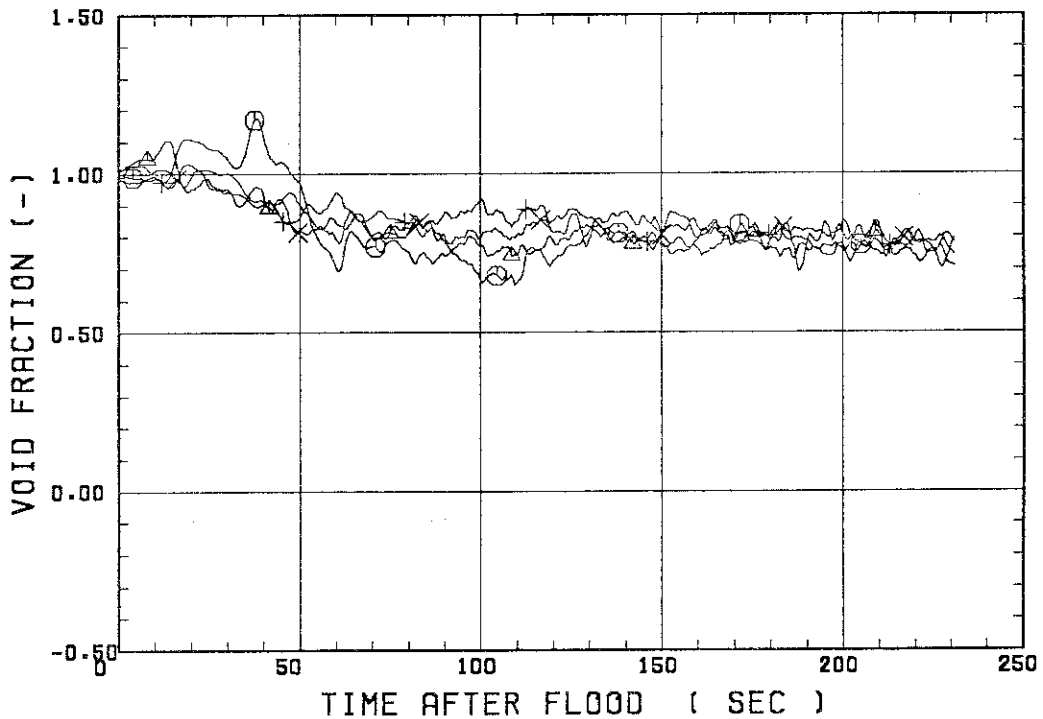
SMALL SCALE REFLOOD TEST
RUN 8316

○--- VDPT2 ▲--- VDPT4 +--- VDPT5
X--- VDPT6B



SMALL SCALE REFLOOD TEST
RUN 8316

○--- VDPT7 ▲--- VDPT8B +--- VDP10
X--- VDP12



 * RUN NO. 8317 *

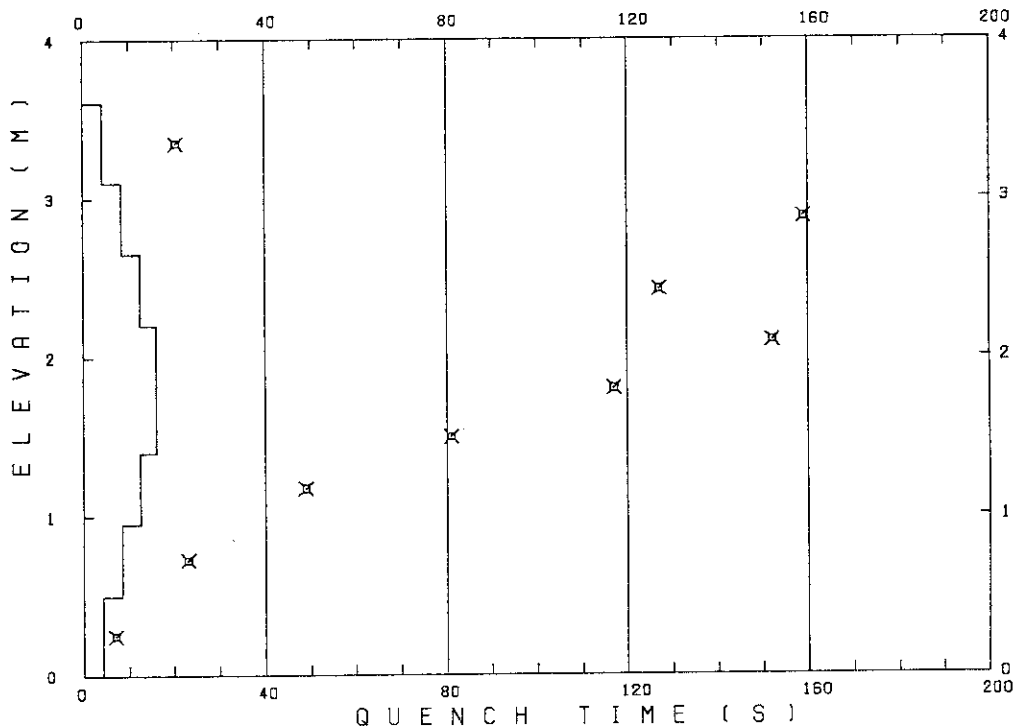
 TEST CONDITIONS

LINEAR PEAK POWER 1.8 KW/M
 SYSTEM PRESSURE 0.2 MPA
 INLET WATER TEMPERATURE 100 .C
 INJECTED WATER VELOCITY 6.0 CM/S

 TEMPERATURE PROFILE

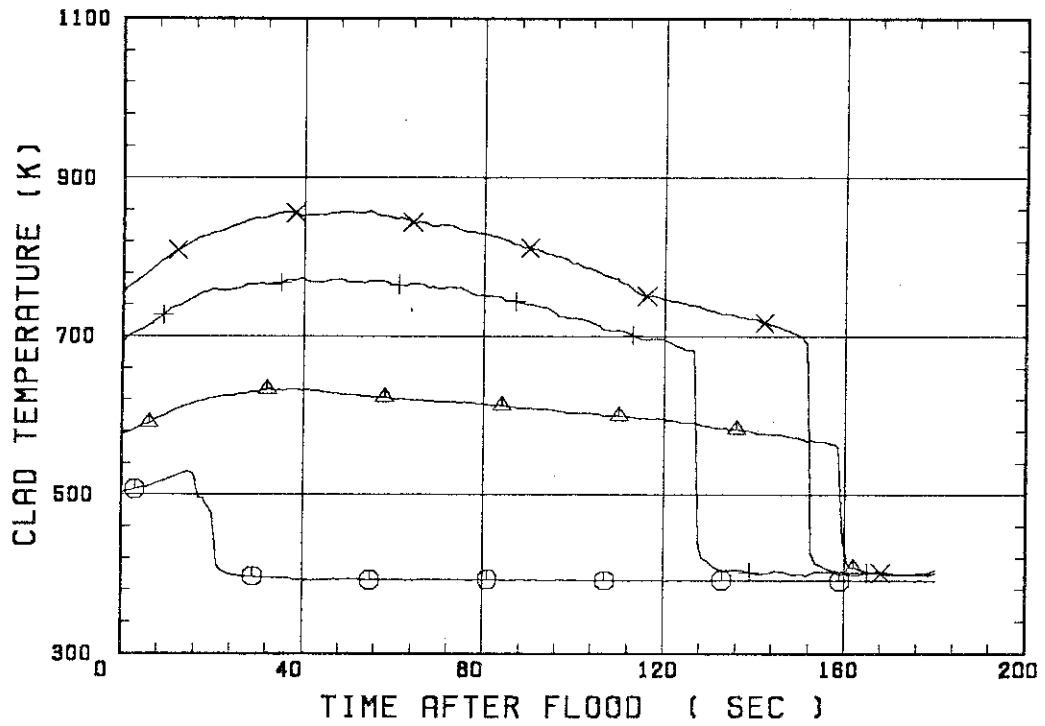
CH.NO.	SYMBOL	INITIAL TEMP. (.C)	TURNAROUND TIME (S)	TURNAROUND TEMP. (.C)	QUENCH TIME (S)	QUENCH TEMP. (.C)
1	TE1L	230	15.0	256	20.5	202
36	TA2	301	39.0	360	159.0	287
37	TA3	417	40.0	500	127.0	409
87	TC4U	481	55.0	585	152.0	417
68	TC4M	477	20.0	537	117.0	385
69	TC4L	498	18.0	559	81.0	411
54	TR5	448	15.0	495	49.0	403
55	TR6	329	13.0	353	23.0	323
5	TE7	194	5.5	200	7.0	196

RUN NO. 8317



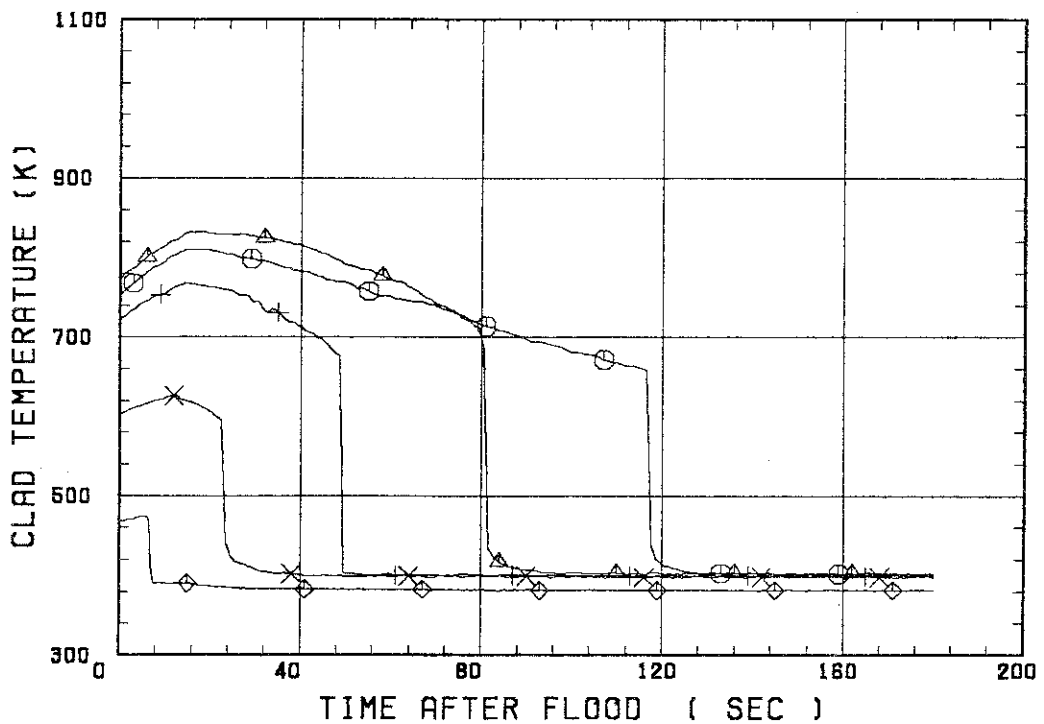
SMALL SCALE REFLOOD TEST
RUN 8317

○--- TE1L ▲--- TA2 +--- TA3
X--- TC4U

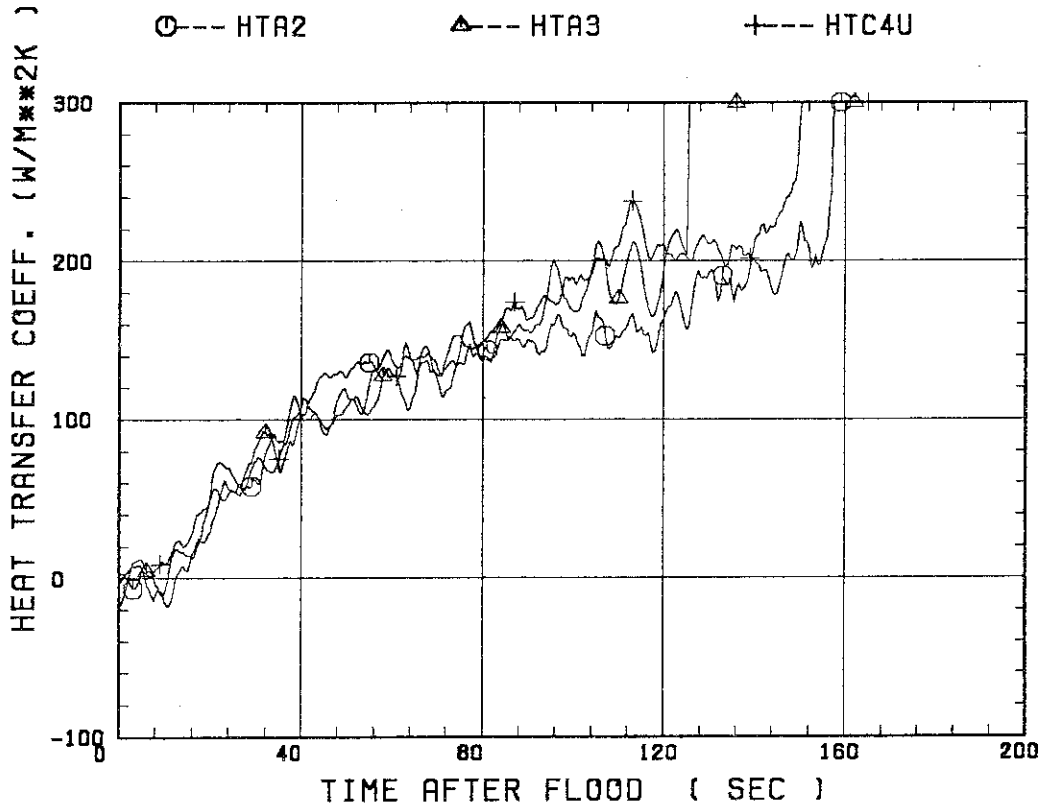


SMALL SCALE REFLOOD TEST
RUN 8317

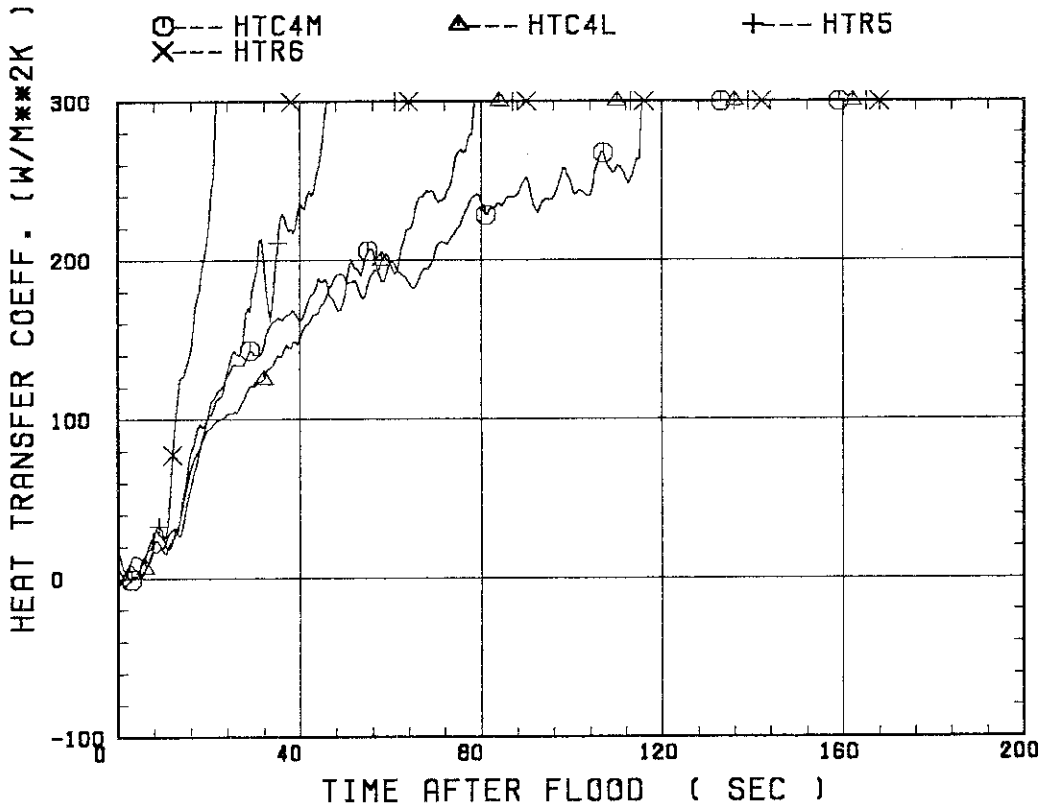
○--- TC4M ▲--- TC4L +--- TR5
X--- TR6 ◆--- TE7



SMALL SCALE REFLOOD TEST
 RUN 8317

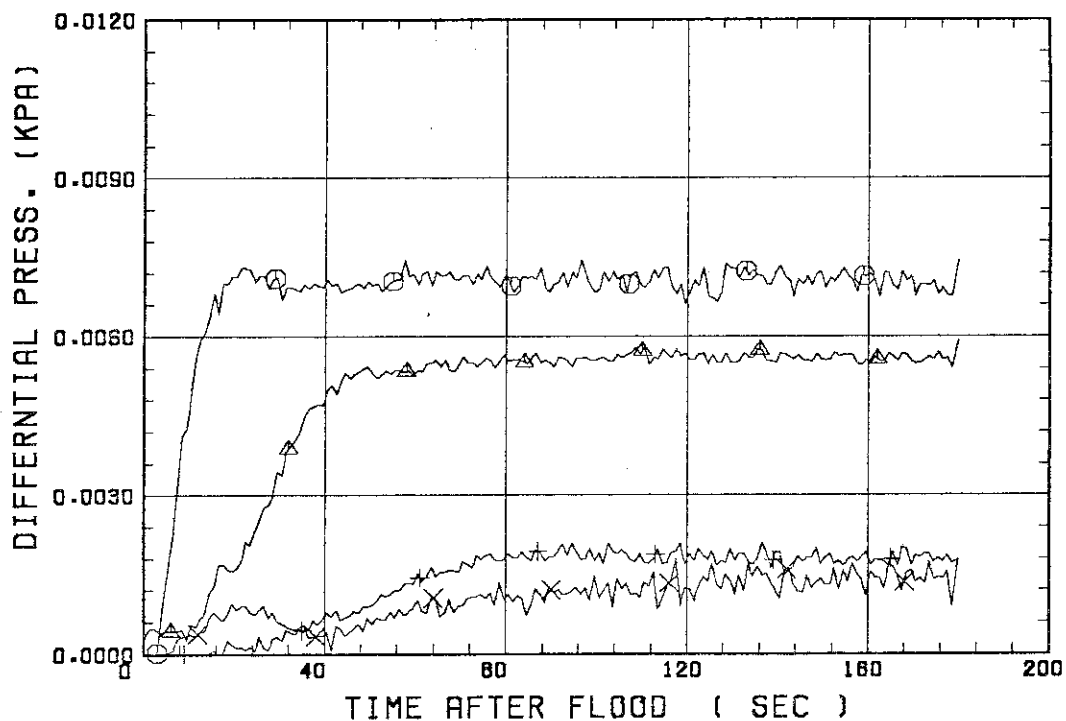


SMALL SCALE REFLOOD TEST
 RUN 8317



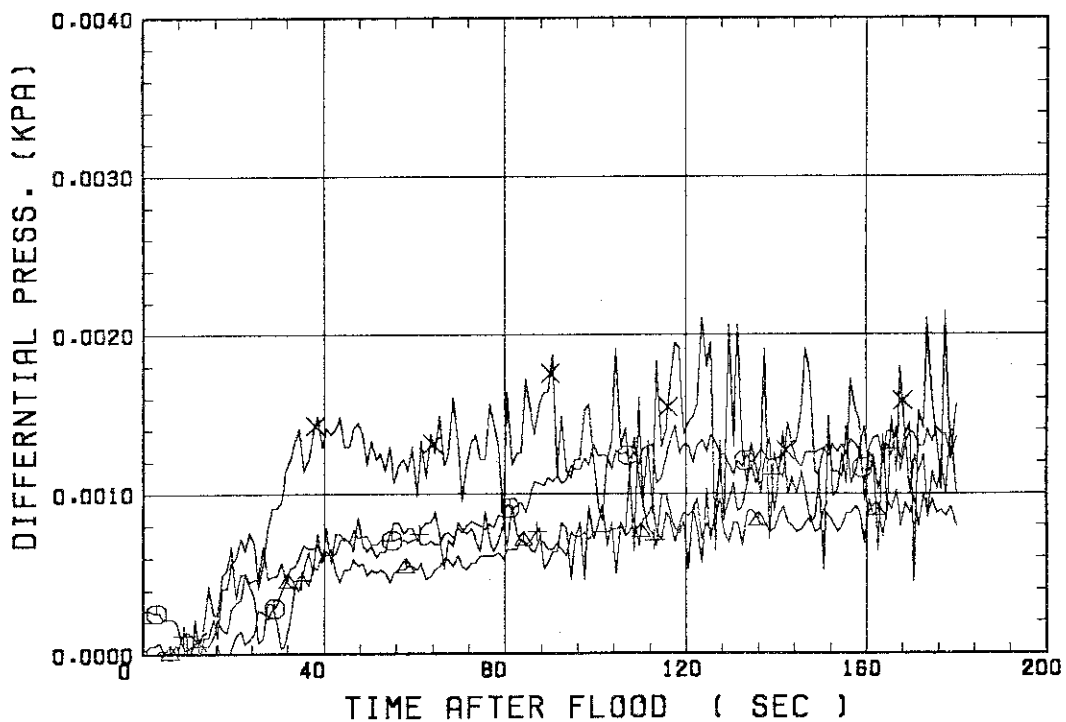
SMALL SCALE REFLOOD TEST
 RUN 8317

○ --- DPT2 △ --- DPT4 + --- DPT5
 X --- DPT6B



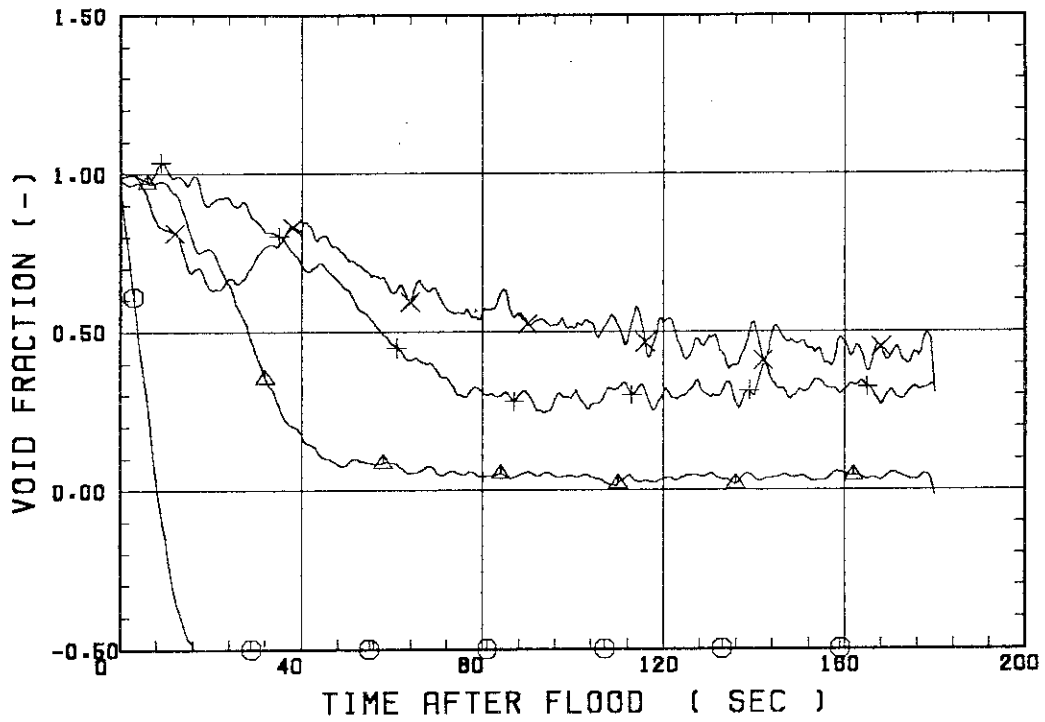
SMALL SCALE REFLOOD TEST
 RUN 8317

○ --- DPT7 △ --- DPT8B + --- DP10
 X --- DP12



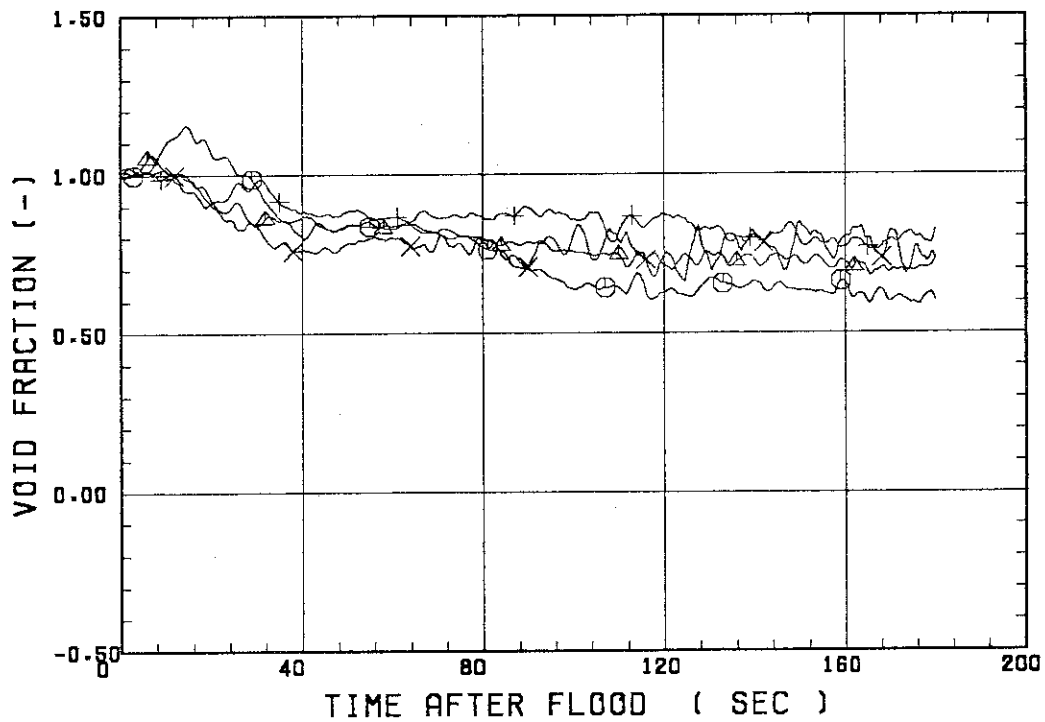
SMALL SCALE REFLOOD TEST
RUN 8317

○--- VDPT2 △--- VDPT4 +--- VDPT5
X--- VDPT6B



SMALL SCALE REFLOOD TEST
RUN 8317

○--- VDPT7 △--- VDPT8B +--- VDP10
X--- VDP12



 * RUN NO. 8318 *

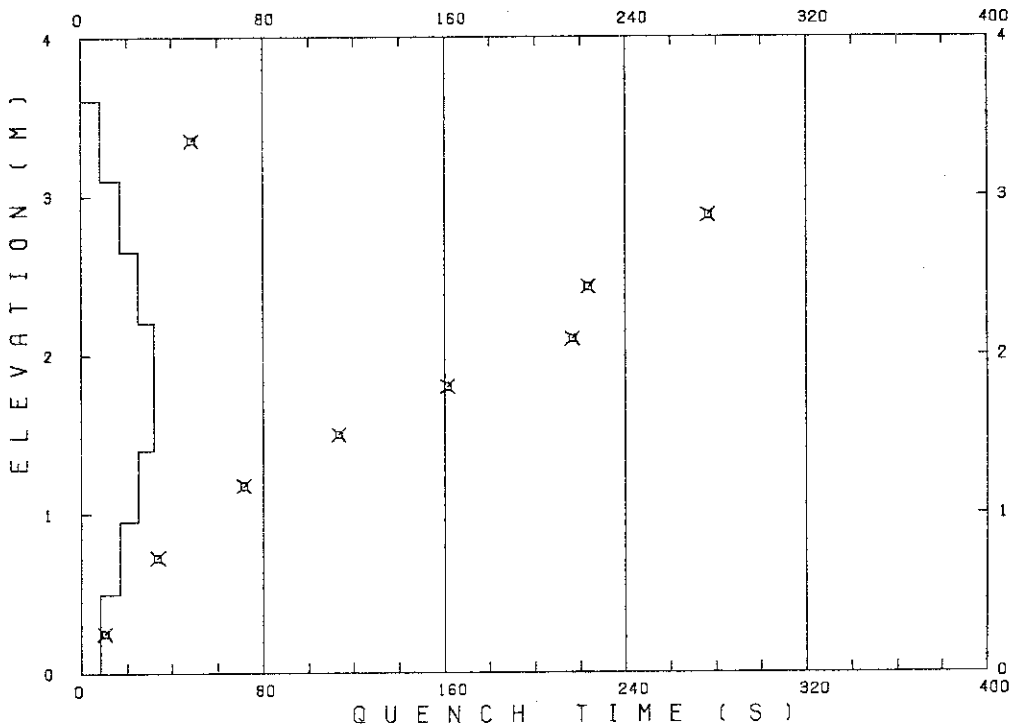
 TEST CONDITIONS

LINEAR PEAK POWER 1.8 KW/M
 SYSTEM PRESSURE 0.2 MPA
 INLET WATER TEMPERATURE 100 .C
 INJECTED WATER VELOCITY 3.1 CM/S

 TEMPERATURE PROFILE

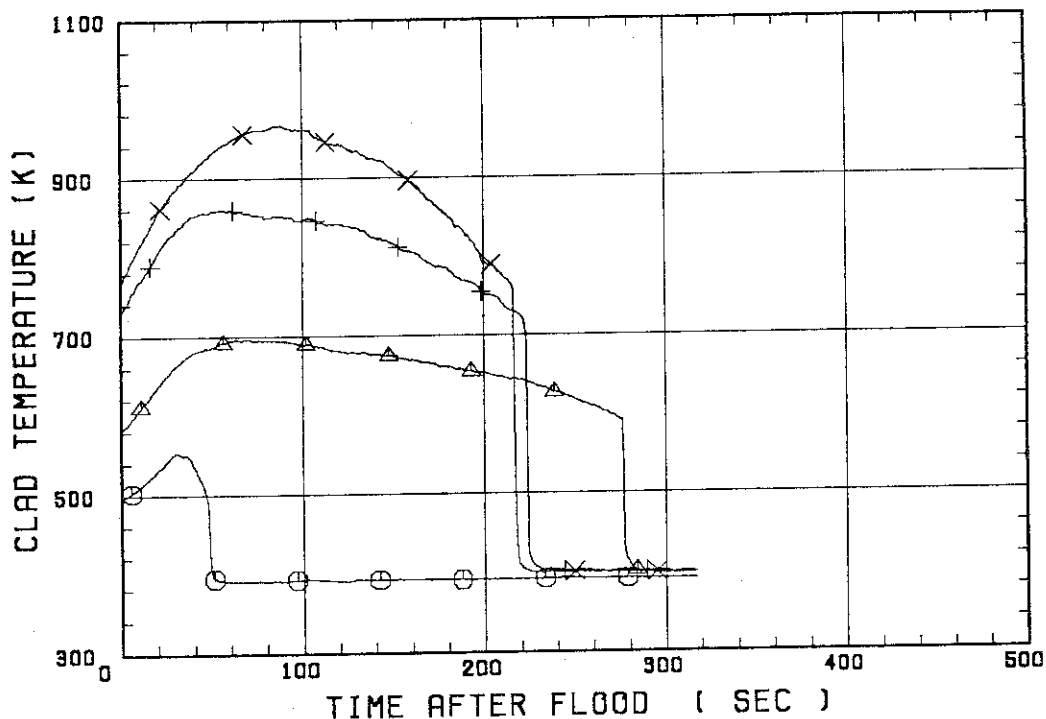
CH.NO.	SYMBOL	INITIAL TEMP. (.C)	TURNAROUND TIME (S)	TURNAROUND TEMP. (.C)	QUENCH TIME (S)	QUENCH TEMP. (.C)
1	TE1L	222	31.0	281	48.5	202
36	TA2	307	68.5	424	276.5	318
37	TA3	454	57.5	587	223.5	427
67	TC4U	490	88.5	694	216.5	482
68	TC4M	483	39.5	603	161.5	406
69	TC4L	504	43.5	621	113.5	453
54	TR5	449	32.5	536	71.5	438
55	TR6	320	21.5	364	33.5	330
5	TE7	212	7.0	221	10.5	213

RUN NO. 8318



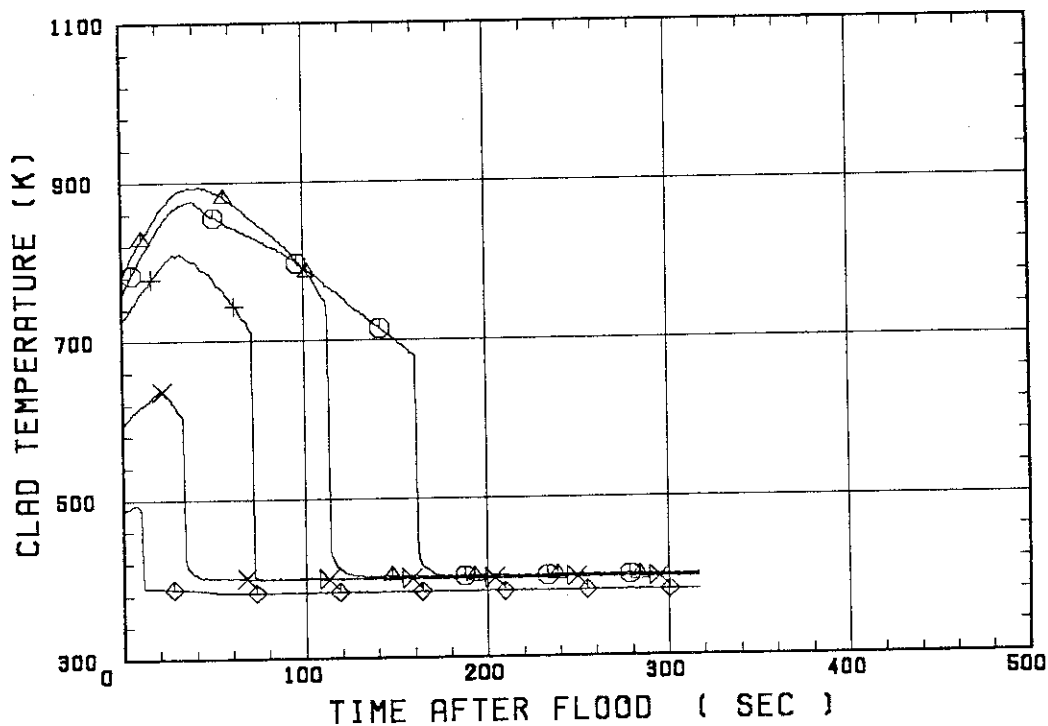
SMALL SCALE REFLOOD TEST
 RUN 8318

○ --- TE1L △ --- TA2 + --- TA3
 X --- TC4U

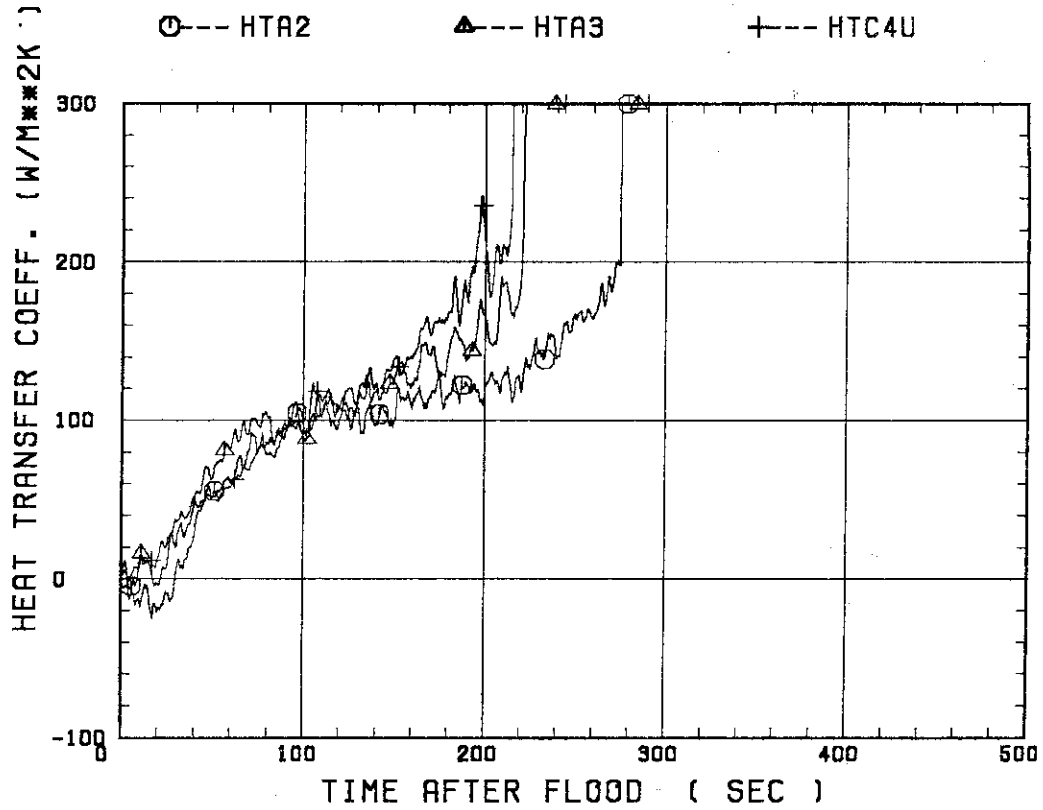


SMALL SCALE REFLOOD TEST
 RUN 8318

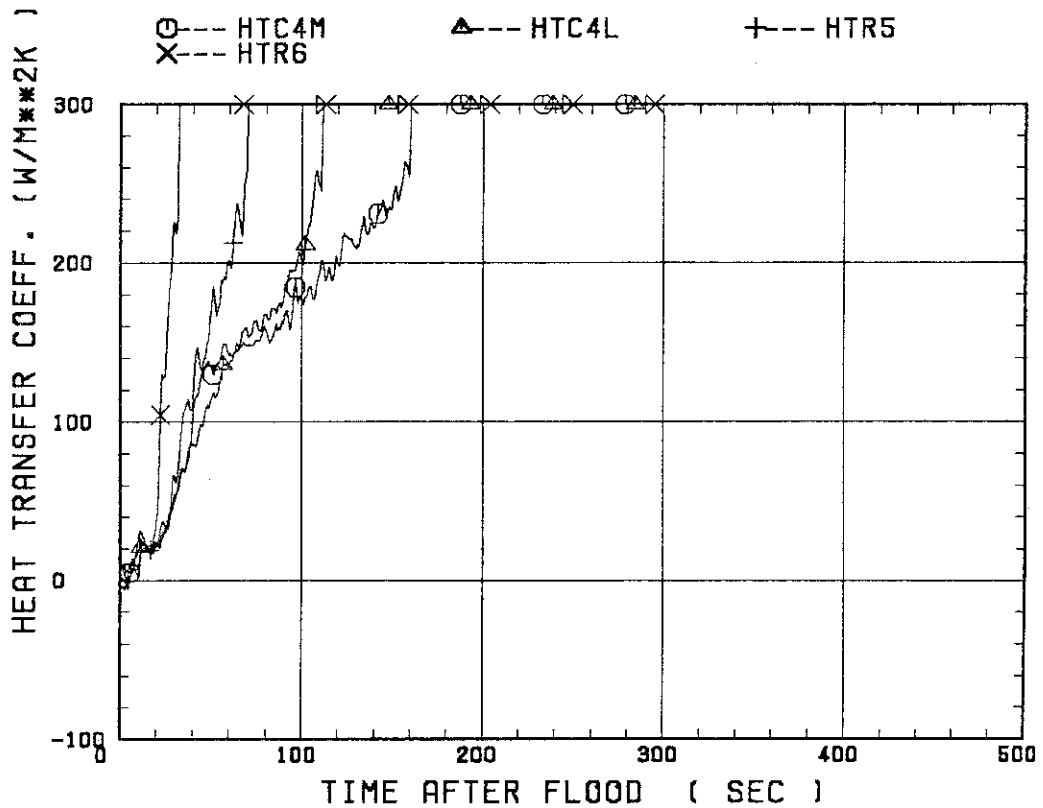
○ --- TC4M △ --- TC4L + --- TR5
 X --- TR6 ◇ --- TE7



SMALL SCALE REFLOOD TEST
RUN 8318

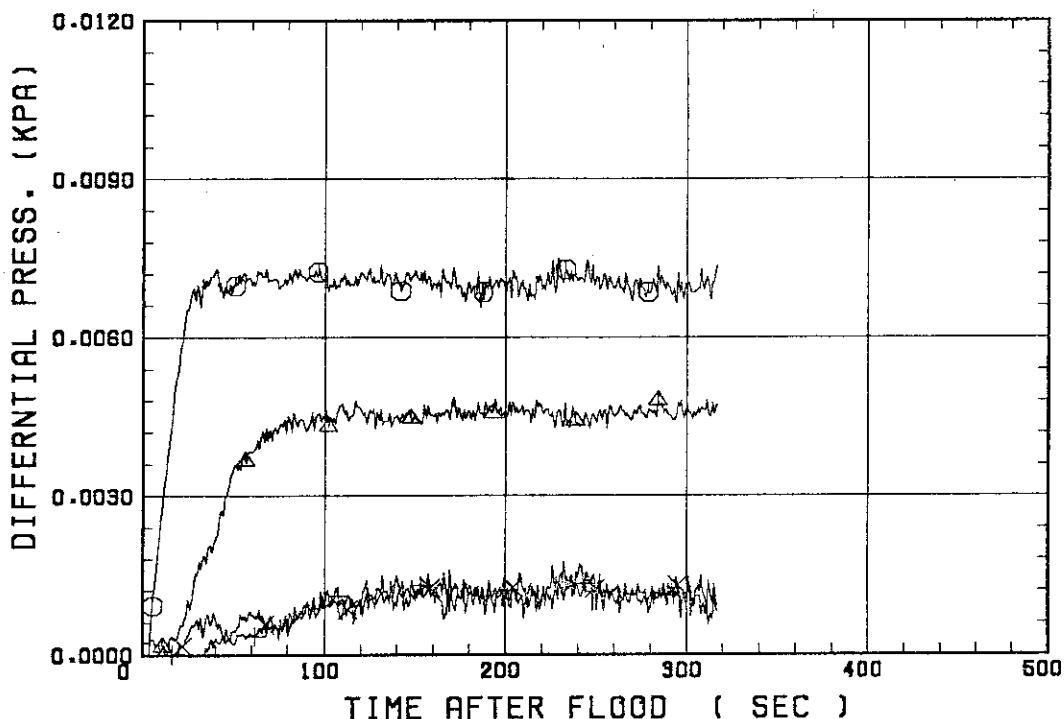


SMALL SCALE REFLOOD TEST
RUN 8318



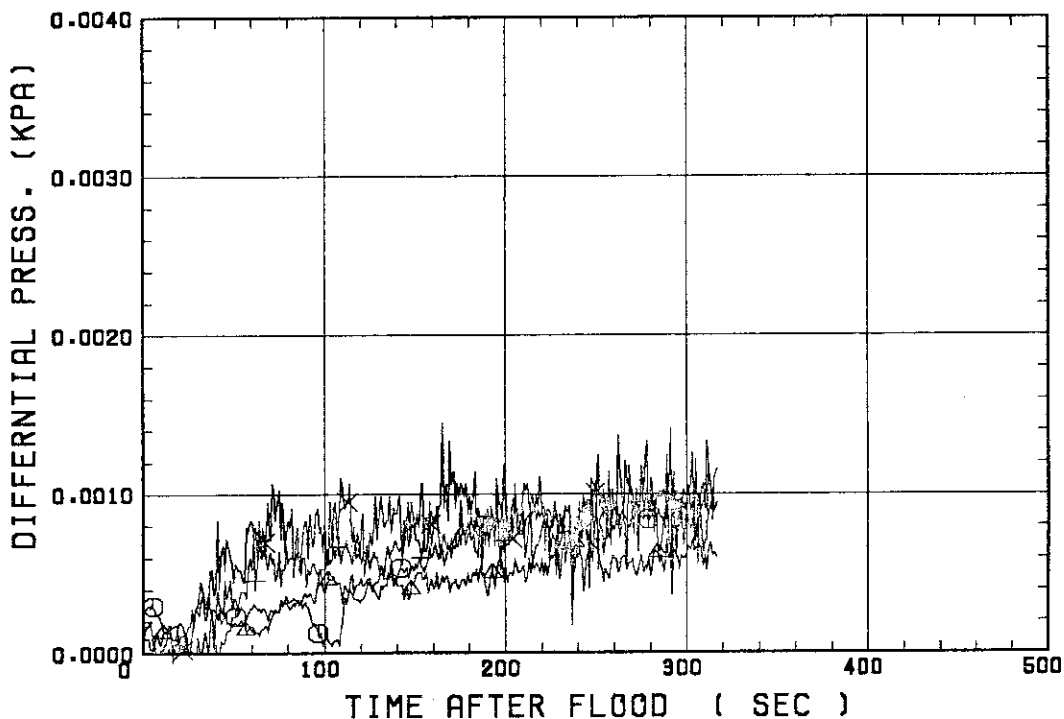
SMALL SCALE REFLOOD TEST
RUN 8318

○ --- DPT2 ▲ --- DPT4 + --- DPT5
X --- DPT6B



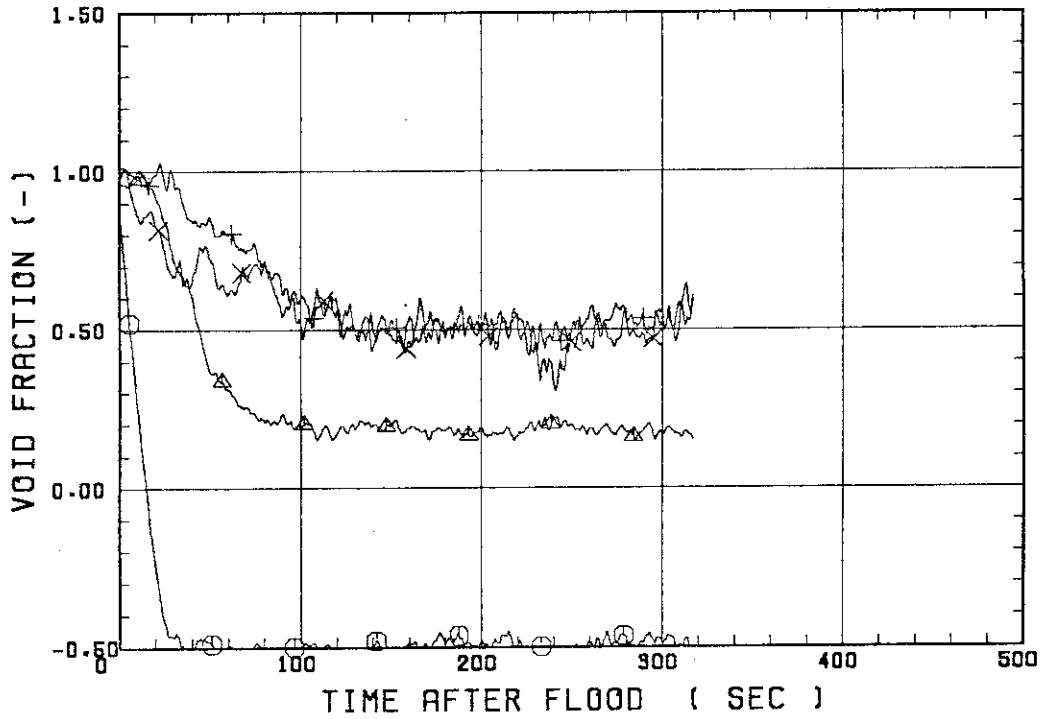
SMALL SCALE REFLOOD TEST
RUN 8318

○ --- DPT7 ▲ --- DPT8B + --- DP10
X --- DP12



SMALL SCALE REFLOOD TEST
RUN 8318

○ --- VDPT2 △ --- VDPT4 + --- VDPT5
X --- VDPT6B



SMALL SCALE REFLOOD TEST
RUN 8318

○ --- VDPT7 △ --- VDPT8B + --- VDP10
X --- VDP12

